Distribution Agreement

In presenting this thesis or dissertation as a partial fulfillment of the requirements for an advanced degree from Emory University, I hereby grant to Emory University and its agents the non- exclusive license to archive, make accessible, and display my thesis or dissertation in whole or in part in all forms of media, now or hereafter known, including display on the world wide web. I understand that I may select some access restrictions as part of the online submission of this thesis or dissertation. I retain all ownership rights to the copyright of the thesis or dissertation. I also retain the right to use in future works (such as articles or books) all or part of this thesis or dissertation.

Signature:

Ingrid K. Wilt Date

TOTAL SYNTHESIS AND BIOLOGICAL INVESTIGATIONS OF NATURAL PRODUCT INSPIRED ANTIMICROBIALS

By

Ingrid K. Wilt
Doctor of Philosophy

Chemistry

William M. Wuest, Ph.D.
Advisor

Dennis Liotta, Ph.D.
Committee Member

Huw M. L. Davies, Ph.D.
Committee Member

Accepted:

Kimberly Jacob Arriola, Ph.D.
Dean of the James T. Laney School of Graduate Schools

Date

TOTAL SYNTHESIS AND BIOLOGICAL INVESTIGATIONS OF NATURAL PRODUCT INSPIRED ANTIMICROBIALS

By

Ingrid K. Wilt

B.A., The Colorado College, 2017

Advisor: William M. Wuest, Ph.D.

An abstract of
A dissertation submitted to the Faculty of the
James T. Laney School of Graduate Studies of Emory University
in partial fulfillment of the requirements for the degree of
Doctor of Philosophy
in Chemistry
2022

Abstract

TOTAL SYNTHESIS AND BIOLOGICAL INVESTIGATIONS OF NATURAL PRODUCT INSPIRED ANTIMICROBIALS

By Ingrid K. Wilt

Natural products have a rich history of antimicrobial use. Chemodiversity and complexity of these structures often culminate in unique biological properties. Divergent and convergent synthetic approaches allow rapid diversification of natural product core scaffolds to evaluate the influence of structure on biological activity. The first chapter provides insight on antimicrobial development inspired by natural products, isolation of novel bioactive natural products, and synthetic approaches to generate compound libraries to evaluate key chemical moieties involved in microbial inhibition.

The second chapter describes the synthesis of phenolic bisabolanes isolated from deep sea sediment that display potent activity towards microbial pathogens. Despite structural similarities, these natural products are reported to have narrow spectrum bioactivity suggesting minor changes in structure can result in unique mechanisms of action. Initially, the chapter focuses on the synthesis of peniciaculin A, a natural product with reported species specific activity against the plant fungal pathogen *Alternaria brassicae.* Investigations of the unique reported bioactivity leveraging synthetic derivatives of the natural product suggest peniciaculin A may be inhibiting fungal growth as a ubiquinone mimic. Identification of a key transformation in the synthesis of peniciaculin A allowed for rapid generation of 1-hydroxyboivinianin A, a lactone derivative with reported species specific activity against aquatic bacteria *Vibrio harveyi*.

The third chapter explores the development of a common intermediate strategy for the synthesis of antifungal natural products, the purpurides. A key tricyclic intermediate was accessed through a tethered intramolecular Diels-Alder cycloaddition. The desired *trans* bicyclic system was synthesized via heterogeneous hydrogen atom transfer. Notably, heterogeneous catalysis provided solely *cis* isomer, invalidating previous reports of obtaining the *trans* isomer of analogous systems using this approach.

The fourth chapter investigates natural product metabolites as narrow spectrum antimicrobial agents. Epoxy isonitrile containing natural products demonstrate specific and potent antibacterial activity against gram-positive pathogens, in particular *Staphylococcus aureus.* This scaffold, however, is extremely labile under acidic and basic conditions, undergoing a Payne rearrangement to produce a stable epoxy ketone metabolite and releasing hydrogen cyanide. Toxicity associated with the release of hydrogen cyanide renders these molecules unusable as antibiotics. When compared to the activity of sodium cyanide *in vivo*, epoxy isonitriles, including amycomicin, aerocyandin, and YM-47515, were shown to be more potent. Thus, the epoxy isonitriles were thought to act as prodrugs, undergoing the Payne rearrangement to produce active epoxy ketone metabolites. These metabolites would not only reduce the toxicity of the parent compounds by eliminating the release of hydrogen cyanide, but could be accessed via a more facile synthetic route. We synthesized and performed biological assays with

epoxy ketone containing metabolites and identified that the epoxy isonitrile moiety is pertinent for biological activity. Serendipitously, we discovered an α,β-unsaturated epoxy ketone analogue that exhibited moderate activity against *S. aureus*.

The fifth chapter includes discussion of a subpopulation of bacteria, persisters. Diminished response to antibacterials is often exacerbated by the presence of persister or metabolically dormant populations of bacteria. Membrane perturbing small molecules have the potential to eliminate persister populations, but use has been limited due to the low selectivity of these compounds for bacterial over mammalian membranes. Bithionol, a previously approved anthelmintic drug, is shown to inhibit methicillin-resistant *Staphylococcus aureus* (MRSA) persister cells via disruption of the membrane lipid bilayer at nontoxic levels to mammalian cells. Investigation of the structure activity relationship of bithionol and its tendency to interact with bacterial membranes suggests bioactivity correlates with the ability to increase membrane fluidity. This work demonstrates that membrane perturbing small molecules can be selective antibacterial agents and further investigations of this mechanism of action is warranted.

TOTAL SYNTHESIS AND BIOLOGICAL INVESTIGATIONS OF NATURAL PRODUCT INSPIRED ANTIMICROBIALS

By

Ingrid K. Wilt

B.A., The Colorado College, 2017

Advisor: William M. Wuest, Ph.D.

A dissertation submitted to the Faculty of the
James T. Laney School of Graduate Studies of Emory University
in partial fulfillment of the requirements for the degree of
Doctor of Philosophy
in Chemistry
2022

Acknowledgements

"We will all, at some point, encounter hurdles to gaining access and entry, moving up and conquering self-doubt; but on the other side is the capacity to own opportunity and tell our own story" – Stacey Abrams

I would like to acknowledge my advisor, Prof. William Wuest, for teaching me the art of the sales-pitch and always keeping me on my toes. He has encouraged me to be involved in every aspect of the research process, from grant applications to project generation, and to be independent. My committee members, Prof. Dennis Liotta and Prof. Huw Davies, have provided feedback and encouragement during our annual meetings. I am inspired by Prof. Liotta's commitment to developing therapies to treat unmet medical needs and Prof. Davies' ability to build community and facilitate scientific discussion and collaboration. My work was greatly supported by the staff in the chemistry department, namely mass-spec assistance from Dr. Fred Strobel, crystallography data from Dr. John Basca, chemical orders and supplies and French toast from Steve Krebs, and safety advice from Todd Polly.

I would not be here today without the support of The Colorado College Department of Chemistry. My mentor Prof. Habiba Vaghoo, is the scientist and mentor I aspire to be. She has continued to fill the role of mentor throughout my Ph.D. and has provided unwavering support and encouragement. Her gift for teaching and mentorship is unmatched. Thank you for listening to me, believing in me, and continuing to advocate for me during this journey.

My first mentor in graduate school, Dr. Guillaume Ernouf, fostered my scientific curiosity, taught me how to navigate a research lab, and provided critical feedback for my growth as a chemist. I would also like to thank my first graduate student mentee, Adrian Demeritte, for his scientific insight and, at times, support. Adrian, I hope you can give yourself time to grow and find strength in asking for and accepting help. My first undergraduate mentee, Alex Kim, brought joy and curiosity to lab. Our time working together was cut short, but I am excited to see everything he will accomplish both in and out of the lab.

It has been lovely to share an office with several chemists who have served as mentors or fellow compatriots in this tumultuous life, including Dr. Guillaume Ernouf, Dr. Kelly Morrison, Ryan Allen, and Martina Golden. It is a unique privilege to be a part of Bill's first Emory Cohort and graduate alongside my peers. I am grateful for our shared experience and their continued support. The Wuest lab culture has changed significantly since I joined the lab in 2017, and I am thankful to all the individuals who've made it a more supportive community.

My friendships outside of lab brought me welcome distraction and joy. My peers in the Davies lab, including Yannick Boni and Dr. Bo Wei, and mentors in the department, Drs. Wenbin Liu and Ally Boyington, have always supported me, especially during times it was lacking in my own work environment. Coffee trips with Andrew Mahoney and Maizie Lee were the highlight of my week. Maizie deserves additional thanks for reviving breakfast club and voluntarily joining me for runs at 6 AM every Friday at Dancing Goats.

Finally, I would like to thank my friends and family outside of the lab. Most of my friends will never leave Colorado or Minnesota (who can blame them), but Alicia Danielsen made the trek to the south multiple times and her visits were always wonderful. My parents, Dr. Kristine Ensrud and Dr. Timothy Wilt, are two of my biggest inspirations. Dr. Ensrud has taught me how to craft a piece of writing to make it *sing* and to advocate for myself when others failed to do so. Dr. Wilt is my biggest fan. From his constant curiosity to his words of wisdom, my dad has taught me to find joy in life and remain true to who I am. To my sister, Grete Wilt, thank you for being my best friend and reminding me there's a life full of adventures outside the lab and convincing me to bring

Buddy to Atlanta. Our morning runs, Friday bagels, and Atlanta adventures will be cherished forever. I would also like to thank my grandma, Marie Wilt, who is no longer with us. She was the first person to truly believe in me and gave me confidence to continue my educational pursuits.

I am so thankful for the family my partner Aaron Bosse and I have built with our cat Loaf and dog Buddy. Thank you for helping me be silly, for pushing yourself to be an advocate for your community, and for supporting me during this journey. I am proud of the science you've accomplished but am most proud of the mentor and leader you've become. Finally, I'd like to thank my dog, Buddy. He has been a constant reminder that life has so much more to offer than the bench. I look forward to our outdoor adventures in the Northeast.

Table of contents

1. *Chapter 1. Introduction to natural product inspired antimicrobials* 1

1.1.Traditional medicine...1

1.2. Synthetic approaches to modern antimicrobials 1

1.3. Development of antimicrobial resistance...5

1.4. Approaches to combating antimicrobial resistance and development of novel therapies...8

1.4.1. Combination therapy and regulated use 8

1.4.2. Analogue design 8

1.4.3. Novel natural products..10

1.4.4. Wuest lab's approach to combating antimicrobial resistance..................13

1.4.4.1. Natural product inspired analogues...14

1.4.4.2. Repurposing 16

1.5. Conclusion 17

1.6. Chapter 1 references...18

2. *Chapter 2. Application of a key transformation for the synthesis of phenolic bisabolanes and biological investigations of their derivatives* 25

2.1. Introduction...25

2.1.1. Antifungal ubiquinone mimics 25

2.1.2. Antimicrobial phenolic bisabolanes 29

2.1.3. Previous synthetic approaches to phenolic bisabolanes 31

2.1.3.1. Aggarwal’s 1,2-migration 32

2.1.3.2.Gilheany’s asymmetric Grignard 33

2.1.3.3. Diastereoselective nucleophilic addition to chiral imidazolidinone ...34

2.1.3.4. Yajima’s synthesis of the peniciaculins..34

2.2. Results and discussion 35

2.2.1. 1,2-migration 35

2.2.2. Asymmetric Grignard 39

2.2.3. Chiral imidazolidinone 43

2.2.4. Analogue design and synthesis...54

2.2.4.1. Ethoxy-acrylate analogues 55

2.2.4.2. Ketone analogues 56

2.2.4.3. Diorcinol analogues...58

2.2.5. Application of key transformation for the synthesis of other phenolic bisabolanes..59

2.2.6. Antimicrobial bioactivity..66

2.3. Conclusion 68

2.4. Chapter 2 references...69

3. *Chapter 3. Leveraging core scaffold for the synthesis of amino acid-sesquiterpene conjugates and antimicrobial investigations of their derivatives* 73

3.1. Introduction 73

3.1.1. Development of antifungals for clinic use 73

3.1.2. Antimicrobial purpurides: a common intermediate in sight 77

3.1.3. Previous approaches to 6-6 trans bicycles 79

3.2. Results and discussion 82

3.2.1. Construction of common intermediate via intramolecular Diels-Alder cycloaddition 82

3.2.2. Building *trans* fused bicycle via HAT 83

3.2.3. Esterification 88

3.2.4. Analogue design 92

3.2.5. Preliminary biological investigations 94

3.3. Conclusion 95

3.4. Chapter 3 references 96

4. *Chapter 4. Synthesis and biological investigations of epoxy-isonitrile metabolites* 100

4.1. Introduction 100

4.1.1. Narrow spectrum antibiotics 100

4.1.2. Epoxy isonitrile containing natural products 101

4.2. Results and discussion 104

4.2.1. Synthesis of metabolites 104

4.2.2. Antimicrobial activity 106

4.3. Conclusion 109

4.4. Chapter 4 references 110

5. *Chapter 5. Membrane perturbing small molecules as novel antimicrobials* 112

5.1. Introduction...112

5.1.1. Persister cells 112

5.1.2. Membrane perturbation as a mechanism of action 115

5.1.3. Repurposing bithionol as a novel antimicrobial 116

5.2. Results and discussion 119

5.2.1. Synthesis of bithionol analogues 119

5.2.2. Antimicrobial activity...122

5.2.3. Mechanism of action 126

5.3. Conclusion 128

5.4. Chapter 5 references 128

6. *Chapter 6. Experimental details* 132

6.1. Supplementary figures, schemes, and tables 132

6.1.1. Chapter 2 132

6.1.2. Chapter 3 133

6.1.3. Chapter 4 133

6.2. Biology: general notes...136

6.3. Biology: Procedures and supplemental information 137

6.3.1. Chapter 4 IC_{50} assay curves 138

6.4. Chemistry: General notes 139

6.5. Chemistry: Synthesis procedures and characterization 140

6.5.1. Chapter 2 140

6.5.2. Chapter 3 194

6.5.3. Chapter 4 205

6.5.4. Chapter 5 208

6.6. Crystal analysis 213

6.7. SI references 233

7. *Appendix* 235

Table of Schemes

Scheme 2.1 1,2-migration 32

Scheme 2.2 Synthesis of tertiary alcohols using chiral imidazolidinones 34

Scheme 2.3 Retrosynthetic approach 1.0 to peniciaculin A 36

Scheme 2.4 Synthesis of substrate for 1,2-migration 36

Scheme 2.5 Retrosynthetic approach 2.0 to peniciaculin A 40

Scheme 2.6 Synthesis of model substrate for stereoselective Grignard addition 41

Scheme 2.7 Retrosynthetic approach 3.0 to peniciaculin A 43

Scheme 2.8 Reported Grignard addition 44

Scheme 2.9 Diastereoselective Grignard addition with peniciaculin core 44

Scheme 2.10 Synthesis of the carbon skeleton of peniciaculin A 49

Scheme 2.11 Synthesis of aryl bromide coupling partner 50

Scheme 2.12 Peniciaculin A end game 54

Scheme 2.13 Synthesis of ethoxy acrylate analogues 56

Scheme 2.14 Synthesis of diaryl ketone analogues 57

Scheme 2.15 Synthesis of triaryl ketone analogues 58

Scheme 2.16 Synthesis of diorcinol analogues 59

Scheme 2.17 Retrosynthetic approach to 1-hydroxyboivinianin A 60

Scheme 2.18 Proposed synthesis of *ent*-1-hydroxyboivinianin A 61

Scheme 2.19 Retrosynthetic approach 2.0 to 1-hydroxyboivinianin A 62

Scheme 2.20 Synthesis of 1-hydroxyboivinianin A 64

Scheme 2.21 Synthesis of linear acid 64

Scheme 3.1 Retrosynthesis of the purpurides..82

Scheme 3.2 Synthesis of common intermediate..83

Scheme 3.3 Complementary hydrogenation methodology...85

Scheme 3.4 Racemization and inactivation of N-acetyl-L-valine 90

Scheme 4.1 Payne rearrangement 103

Scheme 4.2 Synthesis of post-aerocyanidin and post-YM47515..105

Scheme 4.3 Synthesis of post-amycomicin 106

Scheme 5.1 Proposed alternative bridgehead analogues..121

Scheme 5.2 Synthesis of aryl analogues 122

Table of Figures

Figure 1.1 Antimicrobials derived from natural sources..........2

Figure 1.2 High throughput screen approach..........3

Figure 1.3 Bacterial cell..........3

Figure 1.4 Structure of fungal cell..........4

Figure 1.5 Antibiotics and resistance mechanisms..........7

Figure 1.6 Discovery of novel antibiotics through analogue design..........9

Figure 1.7 Analogue development to overcome antimicrobial resistance..........10

Figure 1.8 Novel culture techniques to identify antimicrobial small molecules..........12

Figure 1.9 Bioactive marine natural products..........13

Figure 1.10 Wuest lab's approach to developing novel antimicrobial agents..........14

Figure 1.11 Convergent and divergent synthetic strategies..........16

Figure 1.12 Repurposing drugs for antimicrobial use..........17

Figure 2.1 Ubiquinone oxidation states..........26

Figure 2.2 Succinate dehydrogenase inhibitors (SDHIs)..........27

Figure 2.3 Complex III inhibitors..........28

Figure 2.4 Examples of bioactive phenolic bisabolanes..........30

Figure 2.5 Proposed overlap of peniciaculin A with prototypical QoI scaffold..........31

Figure 2.6 Stereoselective Grignard addition..........33

Figure 2.7 Yajima and coworkers' synthesis of peniciaculin A..35

Figure 2.8 Proposed asymmetric transition state...42

Figure 2.9 Proposed model for diastereoselective nucleophilic addition 47

Figure 2.10 Analogue design for peniciaculin A 55

Figure 2.11 Spontaneous cyclization of the linear acid to 1-hydroxyboivinianin A 65

Figure 2.12 Key SAR findings from antifungal screen..66

Figure 3.1 Fungal cell wall and mechanism of action of antifungal small molecules 74

Figure 3.2 Prototypical structure of azoles...75

Figure 3.3 Prototypical structure of common antifungals used in the clinic..........................76

Figure 3.4 Structures of the purpurides 78

Figure 3.5 Common intermediate strategy to access amino acid-conjugated sesquiterpenoids 79

Figure 3.6 Biomimetic approaches to terpene synthesis..79

Figure 3.7 Modifications of commercially available terpenes 80

Figure 3.8 Diels-Alder cycloadditions in the synthesis of terpenes 81

Figure 3.9 Examples of heterogeneous hydrogenation to form trans terpenes......................84

Figure 3.10 Stereochemistry of hydrogenation product..86

Figure 3.11 Proposed SAR investigations of the purpurides 94

Figure 4.1 Narrow spectrum antibiotics in the clinic 101

Figure 4.2 Epoxy isonitrile narrow spectrum antibacterials 102

Figure 4.3 Known fatty acid biosynthesis inhibitors 104

Figure 5.1 Bacterial persistence..113

Figure 5.2 Time kill curves...114

Figure 5.3 Known membrane perturbers...116

Figure 5.4 Repurposed small molecules as antibiotics 118

Figure 5.5 Identification of bithionol 119

Figure 5.6 Analogue design 120

Figure 5.7 Synergism of bithionol with conventional antibiotics 124

Figure 5.8 Membrane fluidity...125

Figure 5.9 Proposed mechanism of action of bithionol 127

Table of Tables

Table 2.1 Optimization of the 1,2-migration 38

Table 2.2 Benzylic oxidation 39

Table 2.3 Activation of benzylic alcohol 46

Table 2.4 Optimization of key lithium-halogen exchange 48

Table 2.5 Diaryl ether coupling 53

Table 2.6 Optimization of hydrogenation in the synthesis of 1-hydroxyboivinianin A.........63

Table 2.7 Antifungal activity of phenolic bisabolanes and analogues..............................68

Table 3.1 Optimization of hydrogenation to obtain *trans* isomer 88

Table 3.2 Esterification screen...89

Table 3.3 Esterification of model substrate (−)-borneol...92

Table 3.4 Preliminary MIC data of pupuride intermediates 95

Table 4.1 MIC data of epoxy ketone metabolites and derivatives...................................107

Table 4.2 Bacterial growth inhibition of 4.13 and representative IC_{50} curves 109

Table 5.1 SAR of antibiotic activity and membrane fluidity of bithionol analogues...........123

Table of SI Schemes, Figures, and Tables

Figure S2.1 Copper iodide facilitated methoxy deprotection 132

Scheme S2.1 Ligand synthesis...132

Scheme S2.2 Synthesis of imidazolidinone 133

Scheme S3.1 Synthesis of racemic and optically enriched 2° alcohol...................................133

Table S4.1 Comparison of ^{1}H and ^{13}C NMR spectra of (+)-4.4 and the natural product ($CDCl_3$) 133

Table S4.2 Comparison of ^{1}H and ^{13}C NMR spectra of 4.6 and the natural product (CD_3OD) 134

Table S4.2 Comparison of ^{1}H and ^{13}C NMR spectra of (+)-4.5 and the natural product (CD_3OD) 135

List of Abbreviations

Ac acetyl

AIBN azobisisobutyronitrile

APCI atmospheric pressure chemical ionization

Ar aryl

Bn benzyl

Boc *tert*-butyloxycarbonyl

Bu butyl

CA community aquired

Cbz carboxybenzyl

CFU colony forming unit

DBU 1,8-diazabicycloundec-7-ene

1,2-DCE 1,2-dichloroethane

DCM dichloromethane

DIBAL-H diisobutylaluminum hydride

DIPEA *N,N*-diisopropylethylamine

DMAD dimethyl acetylenedicarboxylate

DMAP *N*,*N*-4-(dimethylamino)pyridine

DMF *N,N*-dimethylformamide

dppf 1,1'-bis(diphenylphosphino)ferrocene

d.r. diastereomeric ratio

EDG electron-donating group

ee enantiomeric excess

Et ethyl

equiv equivalents

ESI electrospray ionization

EWG electron-withdrawing group

Fmoc Fluorenylmethyloxycarbonyl

h hours

HA hospital acquired

HAT hydrogen atom transfer

HPLC high performance liquid chromatography

HRMS high-resolution mass spectrometry

HWE Horner-Wadsworth Emmons

IFI invasive fungal infection

IR infrared spectroscopy

L ligand

LAH lithium aluminum hydride

LDA lithium diisopropylamide

LLS longest linear sequence

MDK minimum duration of killing

Me methyl

MIC minimum inhibitory concentration

min minutes

mmol millimoles

MoA mechanism of action

MOM methoxymethyl

MRSA methicillin resistant *Staphylococcus aureus*

Ms mesyl

MS molecular sieves

NBS *N*-bromosuccinimide

NMR nuclear magnetic resonance

nr no reaction

OMe methoxy

PG protecting group

Ph phenyl

PKC persister killing concentration

Pr propyl

PTLC preparatory thin layer chromatography

PTSA *p*-toluenesulfonic acid

Q$_i$ quinone inside

Q$_o$ quinone outside

QiI quinone inside inhibitor

QoI quinone outside inhibitor

SAR structure activity relationship

SDH succinate dehydrogenase

SDHI succinate dehydrogenase inhibitor

SEM trimethylsilylethoxymethyl

TBAC tetrabutylammonium chloride

TBAF tetrabutylammonium fluoride

TBAI tetrabutylammonium iodide

TBS *tert*-butyldimethylsilyl

TEA triethylamine

temp temperature

Tf trifluoromethanesulfonyl

THF tetrahydrofuran

TIPS triisopropylsilyl

TLC thin layer chromatography

TMEDA *N*,*N*,*N’N’*-tetramethylethylenediamine

TS transition state

Chapter 1. Introduction to natural product inspired antimicrobials

1.1. Traditional medicine

Nature has provided individuals with a fundamental human right since the beginning of time: accessible and affordable health care. For thousands of years, healers from across the globe have developed therapies inspired and enabled by our natural world. Traditional healers indigenous to the Tamilnadu region of India, for example, have relied on the rich plant biodiversity of the region to treat ailments ranging from toothaches to fevers[1]. Many of these therapies have more recently been linked by researchers to antimicrobial activity. While *Aristolochia bracteolata* (audu thinna pali)[2] is traditionally used to treat skin burns, extracts from the leaves of another member of the genus, *Aristolochia indica* (isvara mulli), demonstrated activity in an antifungal assay against *Aspergillus fumigatus,* the most common invasive fungal infection in immunosuppressed individuals[3]. Furthermore, tetracycline, an antibiotic currently used to treat upper respiratory tract and skin infections and acne, has been found in human skeletal remains from ancient Sudanese Nubia dating back to 350-550 CE and from skeletal remains from the late Roman period from Dakhleh Oasis, Egypt. Intriguingly, documentation of infectious diseases were low in the Sudanese Nubian population and no traces of bone infection were detected in the bone specimens from Dakhleh Oasis[4]. The knowledge of these indigenous people, passed down generations, served as the foundation for modern medicine.

1.2. Synthetic approaches to modern antimicrobials

The "Golden Age" of modern antimicrobials began in the mid 20th century with the isolation of Penicillin G, a member of the β-lactam class of antibiotics characterized by the 4-membered β -lactam ring. The successful isolation of Penicillin G prompted a cascade of antimicrobial innovation from the mid-1940s to the 1960s[5]. Initially, antimicrobial agents were primarily derived from natural sources including streptomycin isolated in 1944[6] and vancomycin in the 1950s[7] (Figure **1.1**). As the quest for discovery continued, synthetic antimicrobials such as methicillin (1959)[8] and ampicillin (1961)[9] infiltrated the market.

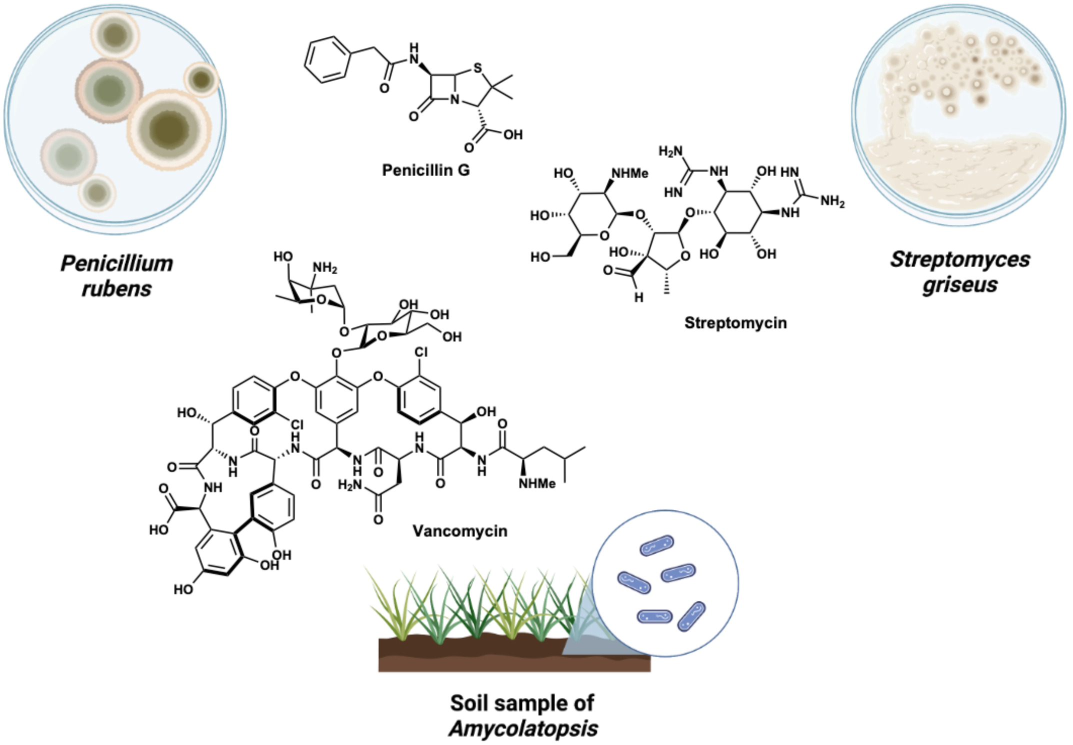

Figure 1.1. **Antimicrobials derived from natural sources.** Natural products at the beginning of the Golden Age were isolated from natural sources, mainly microbes. Figure constructed in Biorender.com.

A "screening" approach to find "magic bullet" drugs that selectively target disease-causing microbes was used as far back as 1904. Paul Ehrlich argued that chemists could create selective therapies and led an effort to develop a drug for the treatment of syphilis, a sexually transmitted infection caused by the spirochete *Treponema pallidium*[10]. At the time, syphilis was treated by inorganic mercury salts that were associated with serious and long-lasting adverse side effects. Ehrlich's lab synthesized and screened a total of 606 compounds in syphilis-infected rabbits and identified Salvarsan and Neosalvarsan, two of the most frequently prescribed drugs until the commercialization of penicillin in the 1940s[11] (Figure **1.2**). The screening approach popularized by Ehrlich has been used to identify numerous antimicrobial agents such as sulfa drugs developed by Klarer and Mietzsch[12], quinolones (ciprofloxacin)[13], and oxazolidinones (linezolid)[14].

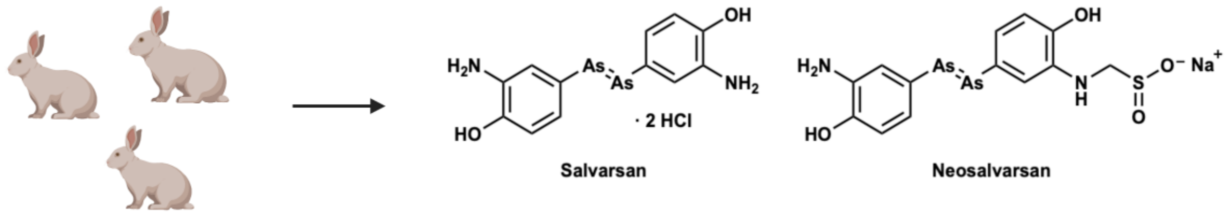
Salvarsan
Neosalvarsan
· 2 HCl

Figure 1.2. High throughput screen approach. High throughput screens have led to the identification of potent antimicrobials. Ehrlich developed two anti-syphilis compounds by using live bunny infection models. Figure constructed in Biorender.com.

There are several classes of antibiotics defined based on their mechanism of action currently used in the clinic including penicillins[15], tetracyclines[16], cephalosporins [17], quinolones[18], lincomycins[19], macrolides[20], sulfonamides[21], glycopeptides[22], aminoglycosides[23], and carbapenems[24]. These antibiotics target vital life processes for cellular growth and replication such as protein synthesis (*i.e.* aminoglycosides, tetracyclines, macrolides, lincosamides), cell wall synthesis (*i.e.* glycopeptides, β-lactams—cephalosporins, penicillins, carbapenems), folate

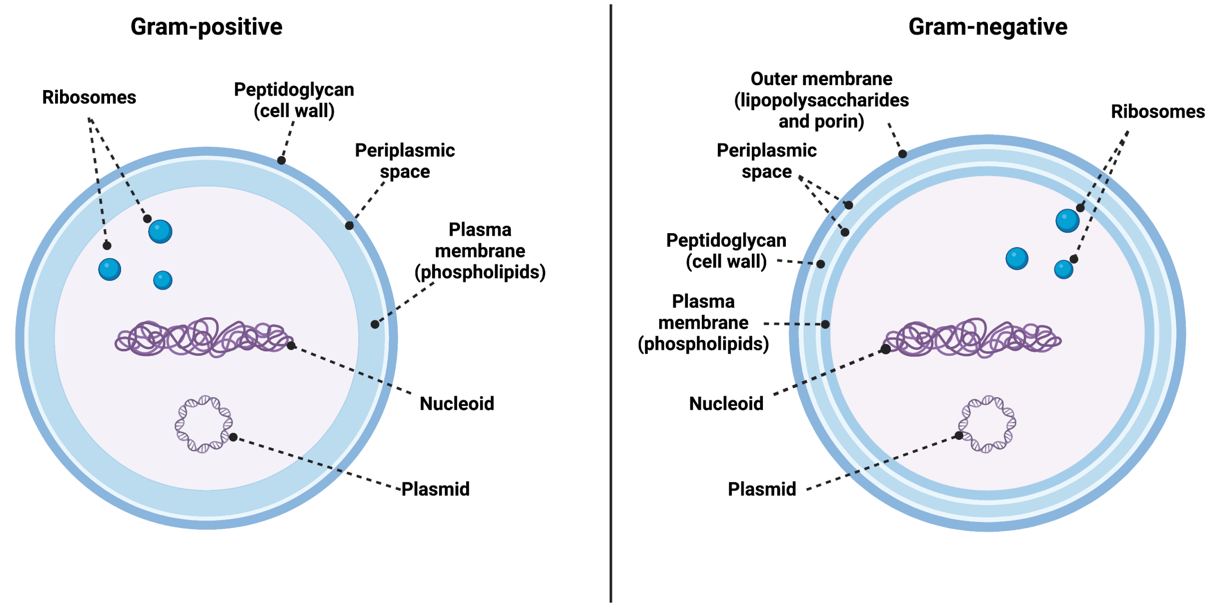
Gram-positive
Ribosomes
Peptidoglycan (cell wall)
Periplasmic space
Plasma membrane (phospholipids)
Nucleoid
Plasmid
Gram-negative
Outer membrane (lipopolysaccharides and porin)
Ribosomes
Periplasmic space
Peptidoglycan (cell wall)
Plasma membrane (phospholipids)
Nucleoid
Plasmid

Figure 1.3. Bacterial cell. Gram-positive bacteria are enveloped in a peptidoglycan cell wall and phospholipid plasma membrane (left). Gram-negative bacteria have an additional outer membrane made of lipopolysaccharides (right). Figure constructed in Biorender.com.

synthesis (*i.e.* trimethoprim, sulfonamides), and DNA replication (*i.e.* quinolones, rifamycins)[25-27]. Most antibacterials can also be classified as "broad spectrum" indicating activity against both gram-positive and gram-negative bacteria[28]. Notably, narrow spectrum activity against gram-positive pathogens is more common rather than gram-negative; in part, due to the additional outer membrane of gram-negative cells that prevents antibiotic penetration[29, 30] (Figure **1.3**).

Unlike bacteria, fungi are eukaryotic cells and share many of the same cellular pathways observed in mammalian cells (Figure **1.4**). Thus, developing antifungals that exhibit minimal mammalian toxicity is incredibly challenging and there are only a few classes of antifungal agents[31]. In clinical settings, all antifungals inhibit biosynthesis or disrupt the integrity of the cell wall[32-34]. In addition to inhibiting cell wall biosynthesis, fungicides used to treat phytopathogens in agricultural settings typically act as ubiquinone mimics, inhibiting ATP production and cellular respiration by binding to succinate dehydrogenase or cytochrome b in the electron transport chain[35, 36]. Over 60% of fungicide sales fall into these three classes: sterol biosynthesis inhibitors

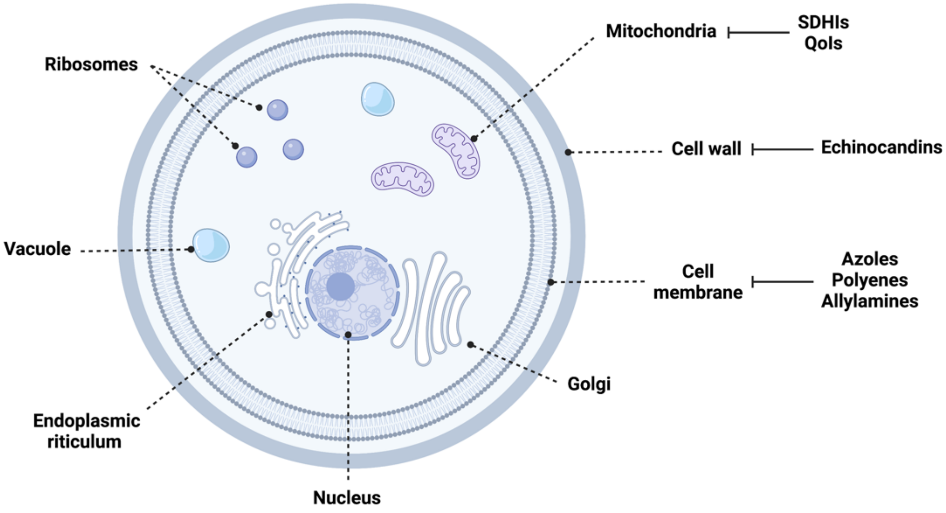

Figure 1.4. Structure of fungal cells. All clinically used antifungals inhibit cell wall or cell membrane integrity and biosynthesis, while agricultural antifungals disrupt cell membranes and mitochondrial respiration. Figure constructed in Biorender.com.

or azoles (14α-demethylase inhibitors), quinone outside inhibitors (QoIs), and succinate dehydrogenase inhibitors (SDHIs)[37].

1.3. Development of antimicrobial resistance

Although these small molecules have revolutionized the way in which infections are treated in both clinical and agricultural settings, microbes are capable of evading preexisting treatments via rapid phenotypic or genotypic changes under selective external pressure[38-41]. Evasion of antimicrobials has been documented long before the modern era of antibiotics and anthropogenic influence[42]. Microbes evolved in complex consortia, and, as a result, have developed defense and self-protection mechanisms in the form of antimicrobial small molecules (defense) and machinery to evade the toxic effects of said small molecules (self-protection)[43]. Evidence of microbes' innate ability to evade antimicrobial toxicity continues to be documented in the 21st century. For example, *Escherichia coli* isolated from soil in the remote regions of Alaska were found to encode resistance elements including β-lactamses[44], one of the culprits of β-lactam resistance[45]. Structure-based phylogeny of the identified β-lactamase suggests serine β-lactamases existed nearly 2 billion years ago. Thus, diversity in these enzymes is primarily a result of ancient evolution, not present antibiotic pressure[44].

Genotypic changes, or resistance, allow microbes to evade treatment by interfering with an antimicrobial agent's role within the cell (Figure **1.5**). The resistome can be broken down into two general categories: intrinsic resistance caused by changes to an organism's fundamental genome; and acquired resistance resulting from nonnative gene incorporation into a sensitive microbe via mobile genetic elements[46]. Intrinsic resistance can manifest as point mutations of a protein target to decrease small molecule binding[47], expression of novel efflux pumps[48] to remove the agent from the cell, or small molecule degradation[49], such as hydrolysis of the active pharmacophore by beta lactamases[50]. Acquired resistance can also evade drug action through similar mechanisms, but is ultimately the result of horizontal gene transfer, or the non-sexual interchange of genetic information between genomes[51]. This process can occur between bacteria of different species by three mechanisms: transformation—bacteria acquire DNA from their environment[52]; conjugation—DNA is directly transferred to another organism[53]; or transduction—DNA is moved from one cell to another by bacteriophages[54] (bacterial viruses). Horizontal gene transfer is not only responsible for the mobilization of resistance genes, but also genes that encode virulence factors[55]. These factors, such as biofilm, toxins, or siderophores, can provide organisms with a competitive advantage over other microbes and often render infections more resistant to treatment[56].

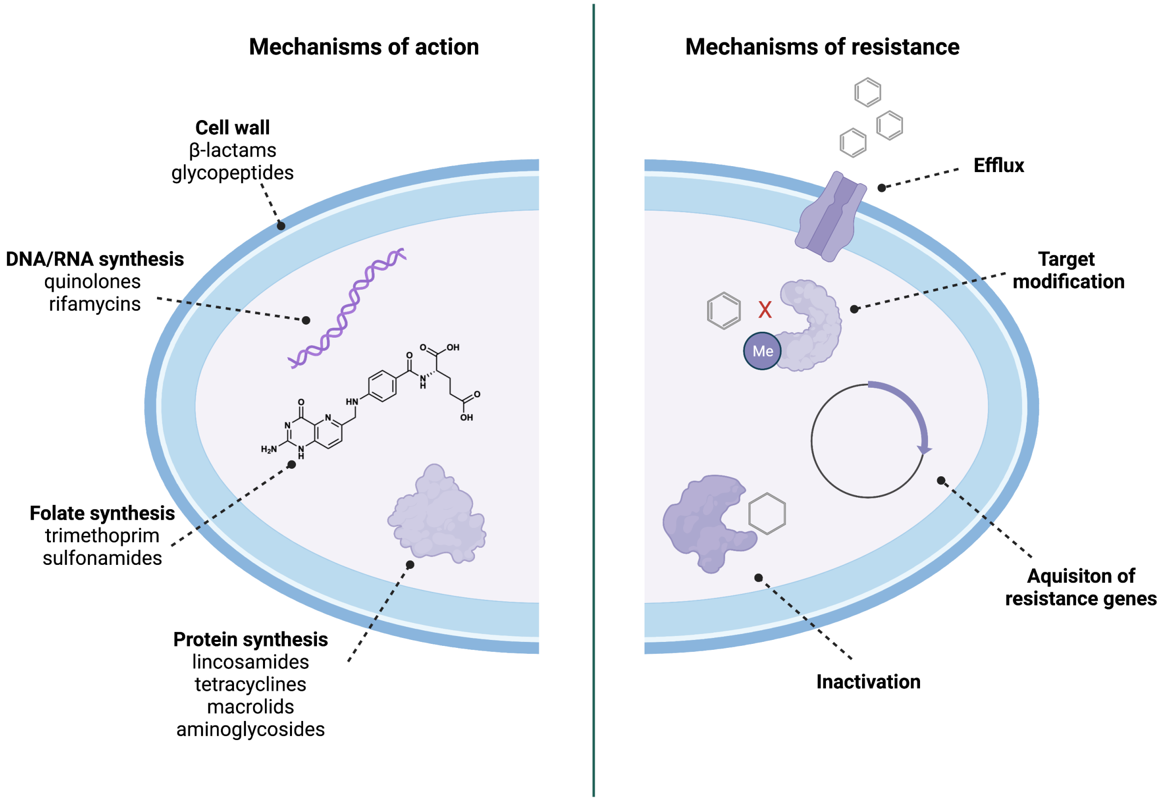
Mechanisms of action
Cell wall
β-lactams
glycopeptides
DNA/RNA synthesis
quinolones
rifamycins
Folate synthesis
trimethoprim
sulfonamides
Protein synthesis
lincosamides
tetracyclines
macrolids
aminoglycosides
Mechanisms of resistance
Efflux
Target modification
X
Me
Aquisiton of resistance genes
Inactivation

Figure 1.5. Antibiotics and resistance mechanisms. Clinically relevant antibiotics target vital life processes of bacteria. Microbes evade treatment through over expression of efflux pumps, target modification, and inactivation of antimicrobial agent. Resistance can evolve from selective pressure or can be acquired through horizontal gene transfer. Figure constructed in Biorender.com.

Resistance to an antimicrobial can occur through one or all of the mechanisms described above. The aminoglycosides class of antibiotics is a prime example of the multiple ways in which microbes can evade antimicrobial treatment and the challenges that exist in developing novel therapies to combat these resistance mechanisms. Bacterial resistance to the aminoglycosides results from a combination of efflux, target modification, and small molecule degradation. Many aminoglycosides are excised from the cell by multidrug efflux pumps such as AcrAd-TolC in *E. coli*[57, 58], AdeABC and AdeDE in *Acinetobacter baumannii*[59], and MexXY-OprM in *Pseudomonas aeruginosa*[60]. Although these efflux pumps are expressed at low levels in wild-type cells, mutation in repressor genes can result in overexpression. In *P. aeruginosa*, mutations in the repressor gene *mexZ* leading to overexpression of MexXY-OprM is a commonly acquired resistance mechanism[61, 62]. Target modification via enzyme-mediated methylation of a key nucleotide residue in the binding pocket of the ribosomal A-site[63, 64] (*i.e.* t-RNA binding site) can also confer resistance to aminoglycosides[65, 66]. Finally, the most impactful form of aminoglycoside resistance occurs through covalent modification of the small molecule scaffold. Multiple enzymes are capable of modifying the substrate and are encoded on mobile genetic elements present in both gram-negative and gram-positive bacteria, leading to acquired resistance[46].

1.4. Approaches to combating antimicrobial resistance and developing novel therapies

1.4.1. Combination therapy and regulated use

Several strategies to combat resistance and bolster our portfolio of existing antimicrobials have emerged[67]. Combination therapy to decrease exposure time and dosage to one antimicrobial may increase the longevity of many therapies[68, 69]. For example, to prevent resistance to fungicides in agricultural settings, it is recommended to alternate QoIs with fungicides possessing different mechanisms of action. As a rule of thumb, QoIs derived from the natural product strobilurin should make up no more than one-third of all fungicide applications during growing season and strictly regulated to two sequential and four total applications, including pre-mixes containing strobilurin[70].

1.4.2. Analogue design

For decades, researchers and clinicians, relied on chemical derivatization of known compounds to bolster the portfolio of available treatments. Analogue design of existing antimicrobial structures can allow the scaffolds to access new binding modes and potentially create higher affinity for mutated protein targets in resistant microbes[46]. One example of this strategy recently published in the literature by Mitcheltree and coworkers disclosed over 500 analogues of lincosamides, a class of antibiotics that inhibit protein synthesis by binding to bacterial ribosomes. Mitcheltree found one analogue, iboxamycin, circumvented many known resistance mechanisms in addition to demonstrating improved antibacterial activity[71] (Figure **1.6**).

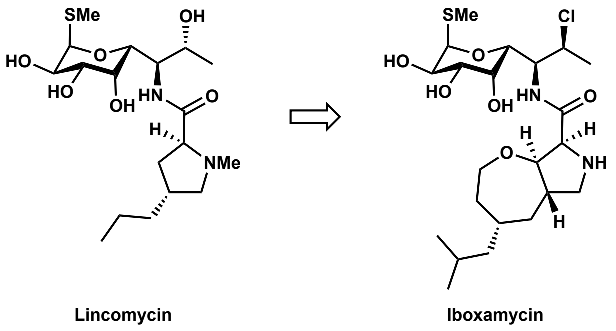

Figure 1.6. Discovery of novel antibiotics through analogue design. Modifications to the southern half of lincomycin produced an analogue, iboxamycin, that is capable of inhibiting resistant microbes.

Iboxamycin inhibited bacterial strains that express *erm* genes, which have been implicated in resistance mechanisms. Expression of *erm* genes produces enzymes that catalyze the methylation of a key nucleotide in the lincosamide binding site of bacterial ribosomes. Unlike other lincosamides, the crystal structure of iboxamycin bound to methylated ribosome suggest the modified nucleotide is displaced by the analogue, thus preventing resistance via this known mechanism[71]. Studies like this rely on flexibility of the designed synthetic route to generate a wide array of structural analogues and suggest that partial structural revision of a small molecule can overcome antimicrobial resistance.

Development of aminoglycoside analogues by Crich and co-workers also demonstrate the utility of this approach. Through the synthesis of several paromomycin derivatives, an apramycin-paromomycin hybrid was identified that minimized ototoxicity typically associated with aminoglycoside antibiotics and overcame aminoglycoside modifying enzyme resistance mechanisms. Reduced toxicity was primarily due to increased biding affinity for the prokaryotic ribosome over eukaryotic mitochondrial ribosomes, while evasion of resistance mechanisms was a result of key structural changes to the core scaffold[72]. Further structural optimization led to the production of two additional derivatives, 2'-*N*-alkyl-paromomycin[73] and propylamycin[74], that demonstrated increased selectivity for the prokaryotic ribosome and retained activity in the presence of clinically relevant aminoglycoside modifying enzymes (Figure **1.7**).

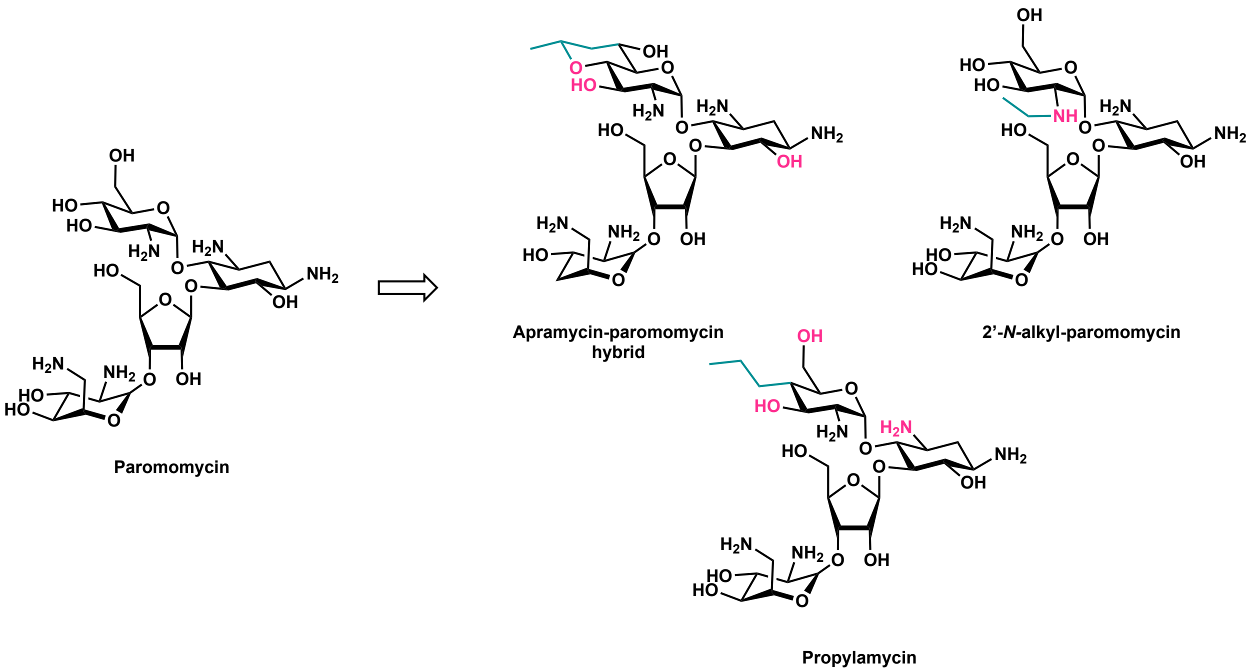

Figure 1.7. Analogue development to overcome antimicrobial resistance. Analogues of paromomycin prevent covalent modifications to aminoglycoside scaffold by aminoglycoside modifying enzymes thus evading bacterial resistance mechanisms. Changes to core scaffold shown in teal and sites where modification was prevented in magenta.

1.4.3. Novel natural products

Nature has proven a steadfast inspiration in the discovery of novel antimicrobial small molecules. New and repeated exploration of our environment, from deep ocean trenches to the geographical poles, has enabled scientists to identify and isolate potent and selective antimicrobial agents with intriguing chemical structures. Over 60% of antibiotics developed in the past 40 years are based on or derived from natural products[75]. Bioactive natural products have been predominately isolated from microorganisms, with 90% of natural product-derived commercial antibiotics isolated from the Actinobacteria phylum of bacteria[76]. Discovery of novel antimicrobial agents is impeded by several barriers, namely silent gene clusters, cultivation of organisms, and re-isolation of known compounds[75].

Researchers, however, have placed an emphasis on developing techniques to overcome these challenges. For example, co-cultivation of an antimicrobial producing microbe species in a multi-species environment can prompt expression of silent genes to produce antimicrobial metabolites as a self-defense mechanism[77, 78]. Advances in genetic engineering have also enabled silent gene expression to produce antimicrobial natural products via heterogeneous expression and promoter insertion to facilitate gene expression[79-81].

Advances in culturing techniques to support "unculturable" organisms has increased the possibility of isolating a novel antimicrobial agent from previously unexplored microbes. Using a multichannel device, the iChip[82, 83], Ling and co-workers were able to congruently isolate and grow uncultured bacteria. Each channel contains approximately one bacterial cell, and the entire device is covered with two semi-permeable membranes. This allows the iChip to be placed in the bacteria's natural environment (*e.g.* soil) where nutrients and growth factors from their surroundings can pass through the membranes while containing the population of microbes to the channel. Thus, bacteria unculturable by traditional lab techniques can produce enough viable cells *in situ* to be sustained *in vitro*. Using this technique, extracts from 10,000 unculturable isolates were screened against bacterial pathogen *Staphylococcus aureus;* extracts from β-proteobacteria *Eleftheria terrae* exhibited promising activity. Isolation of the active compound led to the discovery of teixobactin, a natural product with unique chemical features (Figure **1.8**). Teixobactin displays potent activity against gram-positive pathogens and negligible mammalian toxicity. Furthermore, teixobactin inhibits bacterial growth by disrupting cell wall biosynthesis by binding to a highly conserved motif of lipid II and lipid III. Excitingly, low risk of resistance to teixobactin is observed due to its highly conserved target. Thus, innate resistance mechanisms are likely nonexistent[82, 84, 85].

Beyond promoting silent gene expression and improved culture techniques, our natural world offers incredible opportunities to explore the production of novel bioactive natural products. Isolation of bioactive small molecules has predominately been achieved by investigating microbes and plant species from terrestrial/soil ecosystems[76]. Thus, there is untapped potential in the less explored, but equally beautiful regions of our planet such as the marine ecosystem which exists in stark contrast to its terrestrial counterpart. Although the marine ecosystem is known to produce natural products, such as cometin A and a class of chlorinated dihydroquinones, that display potent bioactivity against multiple microbial species, less than 2% of natural product samples are from the deep sea[86] (Figure **1.9**). The unique biodiversity of the minimally explored deep-sea marine environments contrasts the well explored terrestrial and soil ecosystems and suggests there is a surplus of chemodiversity waiting to be discovered. Increasing our sampling efforts in this less explored environment will inevitably lead to the discovery of novel antimicrobials.

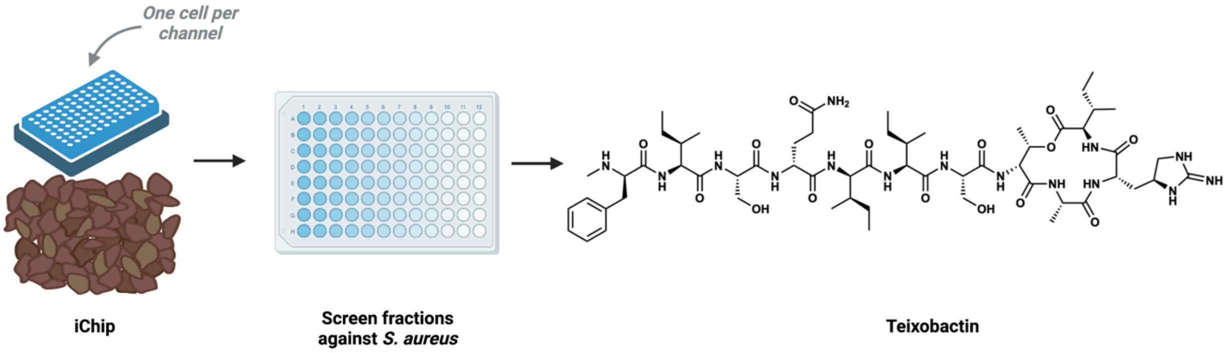

Figure 1.8. Novel culture techniques to identify antimicrobial small molecules. Isolation of teixobactin using novel culturing techniques. Figure was constructed in Biorender.com.

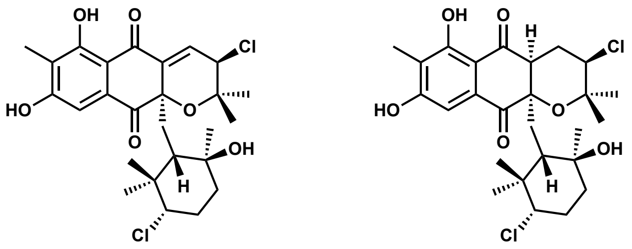

Dihydroquinones

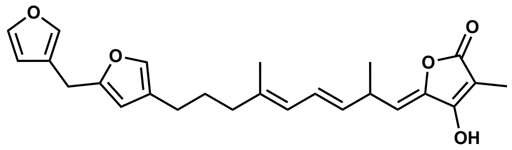

Cometin A

Figure 1.9. Bioactive marine natural products.

1.4.4. Wuest lab's approach to combating antimicrobial resistance

The Wuest lab has developed several strategies to combat emerging antimicrobial resistance focusing on total synthesis of natural products, medicinal chemistry efforts in analogue design, and *in vitro* investigations of the interactions of small molecules within the target microbe. Molecules of interest are typically identified based on unique antimicrobial properties such as species specific or narrow spectrum activity; potential to target a novel mechanism of action or overcome resistance through an explored pharmacophore or chemotype; or induction of an unexplained phenotype (*e.g.* disruption of biofilm or colony organization). Once synthesized, these molecules and derivatives are assayed against a panel of microbial pathogens to better elucidate their antimicrobial potential. Preliminary structure activity relationship (SAR) studies provide crucial information for the design of future analogues, including chemical probes for affinity-based protein profiling to identify protein targets or resistance selection assays to determine non-protein cellular targets. Identification of a mechanism of action (MoA) subsequently aids in rationale analogue design to create structures with higher affinity and potency for their microbial target.

Thus, a continuous feedback loop is created whereby biological findings inform future synthetic efforts and these efforts enable novel biological explorations (Figure **1.10**).

1.4.4.1. Natural product inspired analogues

Due to the high chemodiversity of natural products, we often seek inspiration from our natural world for the design of antimicrobial inhibitors. Syntheses must be amenable to analogue design to facilitate comprehensive biological studies. Diverted total synthesis, a concept introduced by Dr. Samuel Danishefsky in 2006[87], is a common strategy for construction of large libraries of compounds. This strategy relies on the late-stage diversification of either a natural product or common intermediate to build chemodiversity. Conversely, convergent synthesis allows for diversification of two or more complex intermediates prior to a key transformation that forms the molecular skeleton. Both approaches have been extensively exploited by the Wuest lab to design libraries of antimicrobial compounds.

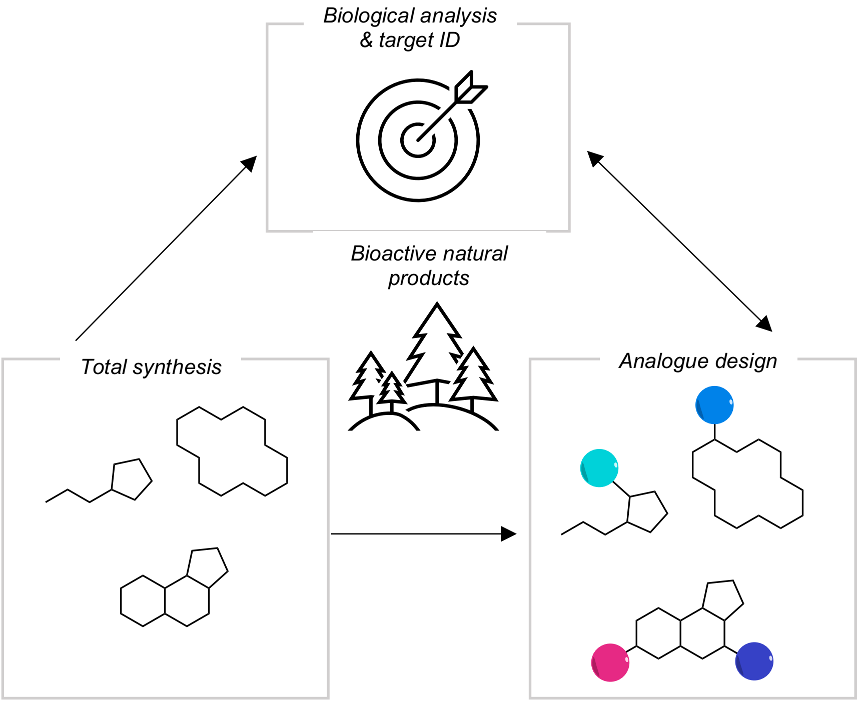

Figure 1.10. Wuest lab's approach to developing novel antimicrobial agents. Research in the Wuest lab is inspired by nature's production of potent antimicrobial small molecules. Designing flexible syntheses enables rapid analogue generation. Biological investigations guide future analogue design to develop more potent scaffolds and molecular probes for target identification.

Promysalin, a natural product isolated from the soil bacteria *Pseudomonas putida* and displaying species specific activity against *P. aeruginosa*, was synthesized in a convergent fashion in 2015 by the Wuest lab. Late-stage esterification joined two complex fragments to build the skeleton of promysalin[88] and enabled numerous generations of analogues, creating diversity through selection of alternate fragments[89] (*i.e.* carbon chains, proline substituents, salicylate derivatives, etc.) (Figure **1.11a**). This strategy also facilitated Yao minimalist probe installation for affinity-based protein profiling and identification of promysalin's target as succinate dehydrogenase (SDH)[90].

Alternatively, diverted synthesis was used in the Wuest lab's total synthesis of baulamycins, natural products isolated from marine organisms proposed to inhibit bacterial iron acquisition[91], to generate a panel of analogues. After testing synthetically acquired baulamycin A, our lab found that bioactivity was not iron dependent as the Sherman lab's isolation report had suggested in their isolation report, hinting at an alternative mechanism of action. Thus, a key terminal alkene intermediate was employed in a diverted fashion for late-stage cross metathesis with various side chains to probe the role of the alkyl chain in the newly proposed mechanism of action, membrane perturbation[92] (Figure **1.11b**).

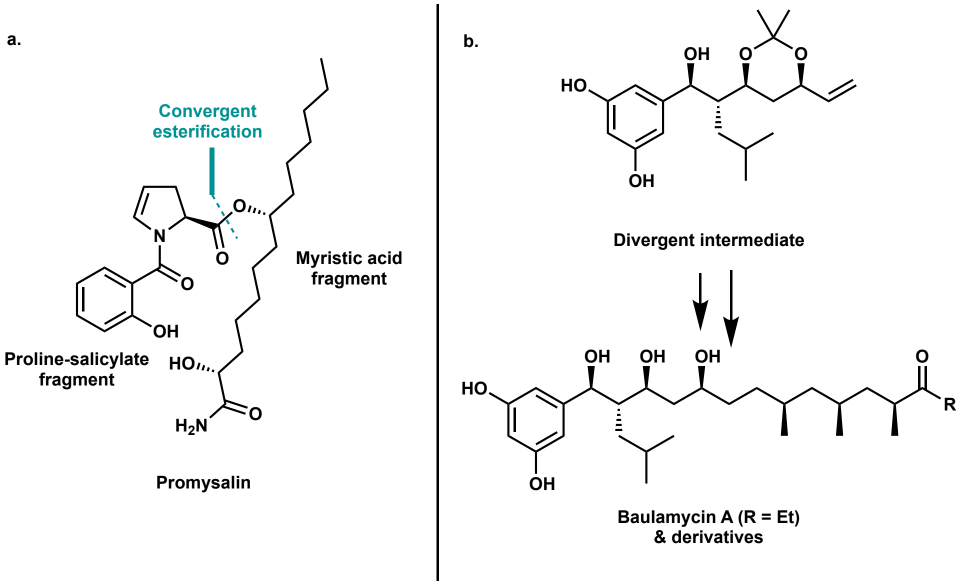
a.
Convergent esterification
Proline-salicylate fragment
Myristic acid fragment
Promysalin
b.
Divergent intermediate
Baulamycin A (R = Et) & derivatives

Figure 1.11. Convergent and divergent synthesis strategies. Wuest lab approach to total synthesis of natural products. a. Convergent synthesis of promysalin enabled analogue design and target identification. b. Divergent synthesis of baulamycin derivatives reassessed the proposed mechanism of action of this class of natural products.

1.4.4.2. Repurposing

The Wuest lab also takes a medicinal chemistry approach to identifying novel antimicrobial agents. Our collaboration with Drs. Mylonakis and Ausubel identified several promising antibacterial agents conceptualized from “repurposing” pharmaceuticals for use as antibiotics. By focusing on reassessing preapproved FDA drugs for antimicrobial activity, we eliminate the extended time and effort that is necessary to bring novel drugs from the bench to the bedside. Our lab has been involved in numerous efforts to repurpose molecules such as CD437[93], a synthetic retinoid, and nTZDpa[94], a nonthiazolidinedione peroxisome proliferator-activated receptor gamma partial agonist (*i.e.* antidiabetic) (Figure **1.12**). Both molecules demonstrate activity against resistant bacterial infections and hint at the untapped potential existing in our current portfolio of pharmaceuticals. Findings support reassessment and integration of known structures into clinical antimicrobial use.

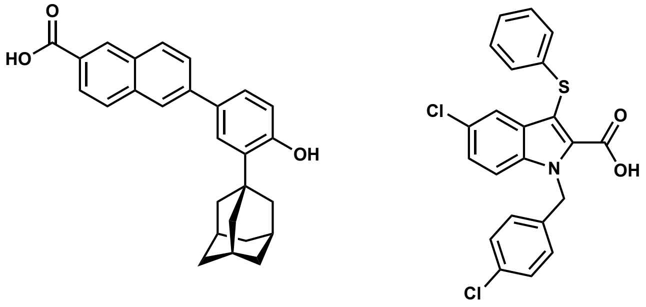

CD437 nTZDpa

Figure 1.12. Repurposing drugs for antimicrobial use. Medicinal chemistry scaffolds investigated by the Wuest lab.

1.5. Conclusion

Access to affordable, high quality health care as well as a sustainable nutritious food supply should be a fundamental right of all individuals. One approach towards achieving these twin goals is to efficiently and effectively develop new, safe, and affordable antimicrobials that can be used in clinical and agricultural settings through identification and isolation of natural products, total organic synthesis of new biologics, and repurposing of existing agents. This thesis will discuss projects that explored both total synthesis and medicinal chemistry approaches to combat microbial infections in agricultural and clinical settings. Although the Wuest lab has traditionally concentrated on antibacterial agents, this thesis focuses on a new sector of the lab specifically investigating antifungal natural products isolated from marine environments with applications in both agricultural and clinical settings. The primary focus was design and completion of total syntheses and analogue development of these bioactive natural products including phenolic bisabolanes and sesquiterpenoid amino acid conjugates. The phenolic bisabolanes, discussed in chapter 2, display potent activity against agriculturally relevant pathogen *Alternaria brassicae*, while sesquiterpenoid amino acids, discussed in chapter 3, exhibit activity against the clinically relevant pathogen *Candida albicans*. Both of these projects are original proposals that utilized a diverted synthesis strategy to build complexity and facilitate rapid analogue production. A portion of this work was also inspired by the Wuest's lab design of antibacterial agents. In chapter 4, the discussion includes the total synthesis of epoxy isonitrile metabolites that exhibit narrow spectrum gram-positive activity. Finally, chapter 5 describes a collaboration with Drs. Mylonakis and Ausubel in the repurposing and antibacterial mechanism of action studies of synthetic small molecule bithionol, a potent inhibitor of methicillin resistant *S. aureus* (MRSA).

References

1. Muthu, C.; Ayyanar, M.; Raja, N.; Ignacimuthu, S., Medicinal plants used by traditional healers in Kancheepuram district of Tamil Nadu, India. *J. Ethnobiol. Ethnomed.* **2006,** *2*, 43-43.
2. Mathew, L. S.; Peter, E. L.; Weisheit, A.; Tolo, C. U.; Deng, A. L.; Ogwang, P. E., Ethno medical knowledge and traditional use of Aristolochia bracteolata Lam. for malaria among local communities in Jubek State of South Sudan: A cross-sectional survey. *J. Ethnopharmacol.* **2021,** *279*, 114314.
3. Munuswamy, H.; Thirunavukkarasu, T.; Rajamani, S.; Elumalai, E. K.; Ernest, D., A review on antimicrobial efficacy of some traditional medicinal plants in Tamilnadu. *J. Acute Dis.* **2013,** *2* (2), 99-105.
4. Bassett Everett, J.; Keith Margaret, S.; Armelagos George, J.; Martin Debra, L.; Villanueva Antonio, R., Tetracycline-Labeled Human Bone from Ancient Sudanese Nubia (A.D. 350). *Science* **1980,** *209* (4464), 1532-1534.
5. Gould, K., Antibiotics: from prehistory to the present day. *J. Antimicrob. Chemother.* **2016,** *71* (3), 572-5.
6. Waksman, S. A.; Reilly, H. C.; Johnstone, D. B., Isolation of Streptomycin-producing Strains of Streptomyces griseus. *J. Bacteriol. Res.* **1946,** *52* (3), 393-397.
7. Levine, D. P., Vancomycin: a history. *Clin. Infect. Dis.* **2006,** *42 Suppl 1*, S5-12.
8. Enright, M. C.; Robinson, D. A.; Randle, G.; Feil, E. J.; Grundmann, H.; Spratt, B. G., The evolutionary history of methicillin-resistant Staphylococcus aureus (MRSA). *Proc. Natl. Acad. Sci. U.S.A.* **2002,** *99* (11), 7687-92.
9. Kaushik, D.; Mohan, M.; Borade, D. M.; Swami, O. C., Ampicillin: rise fall and resurgence. *J. Clin. Diagn. Res.* **2014,** *8* (5), ME01-3.
10. Strebhardt, K.; Ullrich, A., Paul Ehrlich's magic bullet concept: 100 years of progress. *Nat. Rev. Cancer* **2008,** *8* (6), 473-480.
11. Vernon, G., Learning from history: why we should remember the German University in Breslau (now Wroclaw). *Br. J. Gen. Pract.* **2018,** *68* (673), 380-381.
12. Gradmann, C., Book Review: The first miracle drugs: how the sulfa drugs transformed medicine. *Med. Hist.* **2008,** *52* (3), 416-417.
13. Emmerson, A. M.; Jones, A. M., The quinolones: decades of development and use. *J. Antimicrob. Chemother.* **2003,** *51 Suppl 1*, 13-20.

14. Hashemian, S. M. R.; Farhadi, T.; Ganjparvar, M., Linezolid: a review of its properties, function, and use in critical care. *Drug Des. Devel. Ther.* **2018,** *12*, 1759-1767.
15. Nathwani, D.; Wood, M. J., Penicillins. *Drugs* **1993,** *45* (6), 866-894.
16. Chopra, I.; Roberts, M., Tetracycline Antibiotics: Mode of Action, Applications, Molecular Biology, and Epidemiology of Bacterial Resistance. *Microbiol. Mol. Biol. Rev.* **2001,** *65* (2), 232-260.
17. Page, M. G. P., Cephalosporins in clinical development. *Expert Open. Invest. Drugs* **2004,** *13* (8), 973-985.
18. Andersson, M. I.; MacGowan, A. P., Development of the quinolones. *J. Antimicrob. Chemother.* **2003,** *51* (suppl_1), 1-11.
19. Umemura, E.; Wakiyama, Y.; Kumura, K.; Ueda, K.; Masaki, S.; Watanabe, T.; Yamamoto, M.; Hirai, Y.; Fushimi, H.; Yoshida, T.; Ajito, K., Synthesis of novel lincomycin derivatives and their in vitro antibacterial activities. *J. Antibiot. Res.* **2013,** *66* (3), 195-198.
20. Zhanel, G. G.; Dueck, M.; Hoban, D. J.; Vercaigne, L. M.; Embil, J. M.; Gin, A. S.; Karlowsky, J. A., Review of Macrolides and Ketolides. *Drugs* **2001,** *61* (4), 443-498.
21. Supuran, C. T., Special Issue: Sulfonamides. *Molecules* **2017,** *22* (10), 1642.
22. Butler, M. S.; Hansford, K. A.; Blaskovich, M. A. T.; Halai, R.; Cooper, M. A., Glycopeptide antibiotics: Back to the future. *J. Antibiot. Res.* **2014,** *67* (9), 631-644.
23. Serio Alisa, W.; Keepers, T.; Andrews, L.; Krause Kevin, M.; Bush, K., Aminoglycoside Revival: Review of a Historically Important Class of Antimicrobials Undergoing Rejuvenation. *EcoSal Plus* **2018,** *8* (1).
24. Kapoor, G.; Saigal, S.; Elongavan, A., Action and resistance mechanisms of antibiotics: A guide for clinicians. *J. Anaesthesiol. Clin. Pharmacol.* **2017,** *33* (3), 300-305.
25. Boyd, N. K.; Teng, C.; Frei, C. R., Brief Overview of Approaches and Challenges in New Antibiotic Development: A Focus On Drug Repurposing. *Front. Cell. Infect. Microbiol.* **2021,** *11*.
26. Kohanski, M. A.; Dwyer, D. J.; Collins, J. J., How antibiotics kill bacteria: from targets to networks. *Nat. Rev. Microbiol.* **2010,** *8* (6), 423-435.
27. Khameneh, B.; Iranshahy, M.; Soheili, V.; Fazly Bazzaz, B. S., Review on plant antimicrobials: a mechanistic viewpoint. *Antimicrob. Resist. Infect. Control* **2019,** *8* (1), 118.
28. Gerber, J. S.; Ross, R. K.; Bryan, M.; Localio, A. R.; Szymczak, J. E.; Wasserman, R.; Barkman, D.; Odeniyi, F.; Conaboy, K.; Bell, L.; Zaoutis, T. E.; Fiks, A. G., Association of Broad- vs Narrow-Spectrum Antibiotics With Treatment Failure, Adverse Events, and Quality of Life in Children With Acute Respiratory Tract Infections. *JAMA* **2017,** *318* (23), 2325-2336.
29. Peterson, E.; Kaur, P., Antibiotic Resistance Mechanisms in Bacteria: Relationships Between Resistance Determinants of Antibiotic Producers, Environmental Bacteria, and Clinical Pathogens. *Front. Microbiol.* **2018,** *9*, 2928.
30. Kong, J.; Wu, Z.-X.; Wei, L.; Chen, Z.-S.; Yoganathan, S., Exploration of Antibiotic Activity of Aminoglycosides, in Particular Ribostamycin Alone and in Combination With Ethylenediaminetetraacetic Acid Against Pathogenic Bacteria. *Front. Microbiol.* **2020,** *11*.
31. Scorzoni, L.; de Paula e Silva, A. C. A.; Marcos, C. M.; Assato, P. A.; de Melo, W. C. M. A.; de Oliveira, H. C.; Costa-Orlandi, C. B.; Mendes-Giannini, M. J. S.; Fusco-Almeida, A. M., Antifungal Therapy: New Advances in the Understanding and Treatment of Mycosis. *Front. Microbiol.* **2017,** *8*.

32. Ostrosky-Zeichner, L.; Casadevall, A.; Galgiani, J. N.; Odds, F. C.; Rex, J. H., An insight into the antifungal pipeline: selected new molecules and beyond. *Nat. Rev. Drug Discov.* **2010,** *9* (9), 719-27.
33. Li, X.; Hou, Y.; Yue, L.; Liu, S.; Du, J.; Sun, S., Potential Targets for Antifungal Drug Discovery Based on Growth and Virulence in Candida albicans. *Antimicrob. Agents Chemother.* *59* (10), 5885-5891.
34. Liu, N.; Tu, J.; Dong, G.; Wang, Y.; Sheng, C., Emerging New Targets for the Treatment of Resistant Fungal Infections. *J. Med. Chem.* **2018,** *61* (13), 5484-5511.
35. Musso, L.; Fabbrini, A.; Dallavalle, S., Natural Compound-derived Cytochrome bc1 Complex Inhibitors as Antifungal Agents. *Molecules* **2020,** *25* (19).
36. Brauer, V. S.; Rezende, C. P.; Pessoni, A. M.; De Paula, R. G.; Rangappa, K. S.; Nayaka, S. C.; Gupta, V. K.; Almeida, F., Antifungal Agents in Agriculture: Friends and Foes of Public Health. *Biomolecules* **2019,** *9* (10), 521.
37. Jorgensen, L. N.; Heick, T. M., Azole Use in Agriculture, Horticulture, and Wood Preservation - Is It Indispensable? *Front. Cell Infect. Microbiol.* **2021,** *11*, 730297.
38. Reygaert, W. C., An overview of the antimicrobial resistance mechanisms of bacteria. *AIMS Microbiol.* **2018,** *4* (3), 482-501.
39. Fauci, A. S.; Marston, H. D., The Perpetual Challenge of Antimicrobial Resistance. *JAMA* **2014,** *311* (18), 1853-1854.
40. Davey, P.; Sneddon, J.; Nathwani, D., Overview of strategies for overcoming the challenge of antimicrobial resistance. *Expert Rev. Clin. Pharmacol.* **2010,** *3* (5), 667-686.
41. Wagner, B.; Filice, G. A.; Drekonja, D.; Greer, N.; MacDonald, R.; Rutks, I.; Butler, M.; Wilt, T. J., Antimicrobial stewardship programs in inpatient hospital settings: a systematic review. *Infect. Control Hosp. Epidemiol.* **2014,** *35* (10), 1209-28.
42. Landecker, H., Antibiotic Resistance and the Biology of History. *Body Soc.* **2015,** *22* (4), 19-52.
43. Podolsky, S. H., The evolving response to antibiotic resistance (1945–2018). *Palgrave Commun.* **2018,** *4* (1), 124.
44. Allen, H. K.; Moe, L. A.; Rodbumrer, J.; Gaarder, A.; Handelsman, J., Functional metagenomics reveals diverse beta-lactamases in a remote Alaskan soil. *ISME J.* **2009,** *3* (2), 243-51.
45. Dever, L. A.; Dermody, T. S., Mechanisms of Bacterial Resistance to Antibiotics. *Arch. Intern. Med.* **1991,** *151* (5), 886-895.
46. Hobson, C.; Chan, A. N.; Wright, G. D., The Antibiotic Resistome: A Guide for the Discovery of Natural Products as Antimicrobial Agents. *Chem. Rev.* **2021,** *121* (6), 3464-3494.
47. Woodford, N.; Ellington, M. J., The emergence of antibiotic resistance by mutation. *Clin. Microbiol. Infect.* **2007,** *13* (1), 5-18.
48. Soto, S. M., Role of efflux pumps in the antibiotic resistance of bacteria embedded in a biofilm. *Virulence* **2013,** *4* (3), 223-229.
49. Wright, G. D., Bacterial resistance to antibiotics: enzymatic degradation and modification. *Adv. Drug Deliv. Rev.* **2005,** *57* (10), 1451-70.
50. He, Y.; Lei, J.; Pan, X.; Huang, X.; Zhao, Y., The hydrolytic water molecule of Class A beta-lactamase relies on the acyl-enzyme intermediate ES* for proper coordination and catalysis. *Sci. Rep.* **2020,** *10* (1), 10205.
51. Sun, D.; Jeannot, K.; Xiao, Y.; Knapp, C. W., Editorial: Horizontal Gene Transfer Mediated Bacterial Antibiotic Resistance. *Front. Microbiol.* **2019,** *10*.

52. Hasegawa, H.; Suzuki, E.; Maeda, S., Horizontal Plasmid Transfer by Transformation in Escherichia coli: Environmental Factors and Possible Mechanisms. *Front. Microbiol.* **2018,** *9*.
53. Sun, D., Pull in and Push Out: Mechanisms of Horizontal Gene Transfer in Bacteria. *Front. Microbiol.* **2018,** *9*.
54. Wang, G. H.; Sun, B. F.; Xiong, T. L.; Wang, Y. K.; Murfin, K. E.; Xiao, J. H.; Huang, D. W., Bacteriophage WO Can Mediate Horizontal Gene Transfer in Endosymbiotic Wolbachia Genomes. *Front. Microbiol.* **2016,** *7*.
55. Deng, Y.; Xu, H.; Su, Y.; Liu, S.; Xu, L.; Guo, Z.; Wu, J.; Cheng, C.; Feng, J., Horizontal gene transfer contributes to virulence and antibiotic resistance of Vibrio harveyi 345 based on complete genome sequence analysis. *BMC Genet.* **2019,** *20* (1), 761.
56. Mukherjee, S.; Bassler, B. L., Bacterial quorum sensing in complex and dynamically changing environments. *Nat. Rev. Microbiol.* **2019,** *17* (6), 371-382.
57. Anes, J.; McCusker, M. P.; Fanning, S.; Martins, M., The ins and outs of RND efflux pumps in Escherichia coli. *Front. Microbiol.* **2015,** *6*, 587.
58. Aires, J. R.; Nikaido, H., Aminoglycosides are captured from both periplasm and cytoplasm by the AcrD multidrug efflux transporter of Escherichia coli. *J. Bacteriol.* **2005,** *187* (6), 1923-9.
59. Coyne, S.; Courvalin, P.; Perichon, B., Efflux-mediated antibiotic resistance in Acinetobacter spp. *Antimicrob. Agents Chemother.* **2011,** *55* (3), 947-53.
60. Hocquet, D.; Vogne, C.; El Garch, F.; Vejux, A.; Gotoh, N.; Lee, A.; Lomovskaya, O.; Plesiat, P., MexXY-OprM efflux pump is necessary for a adaptive resistance of Pseudomonas aeruginosa to aminoglycosides. *Antimicrob. Agents Chemother.* **2003,** *47* (4), 1371-5.
61. Hay, T.; Fraud, S.; Lau, C. H.; Gilmour, C.; Poole, K., Antibiotic inducibility of the mexXY multidrug efflux operon of Pseudomonas aeruginosa: involvement of the MexZ anti-repressor ArmZ. *PLoS One* **2013,** *8* (2), e56858.
62. Poole, K., Pseudomonas aeruginosa: resistance to the max. *Front. Microbiol.* **2011,** *2*, 65.
63. Kotra Lakshmi, P.; Haddad, J.; Mobashery, S., Aminoglycosides: Perspectives on Mechanisms of Action and Resistance and Strategies to Counter Resistance. *Antimicrob. Agents Chemother.* **2000,** *44* (12), 3249-3256.
64. Francois, B.; Russell, R. J.; Murray, J. B.; Aboul-ela, F.; Masquida, B.; Vicens, Q.; Westhof, E., Crystal structures of complexes between aminoglycosides and decoding A site oligonucleotides: role of the number of rings and positive charges in the specific binding leading to miscoding. *Nucleic Acids Res.* **2005,** *33* (17), 5677-90.
65. Shcherbakov, D.; Akbergenov, R.; Matt, T.; Sander, P.; Andersson, D. I.; Bottger, E. C., Directed mutagenesis of Mycobacterium smegmatis 16S rRNA to reconstruct the in vivo evolution of aminoglycoside resistance in Mycobacterium tuberculosis. *Mol. Microbiol.* **2010,** *77* (4), 830-40.
66. Maus, C. E.; Plikaytis, B. B.; Shinnick, T. M., Molecular analysis of cross-resistance to capreomycin, kanamycin, amikacin, and viomycin in Mycobacterium tuberculosis. *Antimicrob. Agents Chemother.* **2005,** *49* (8), 3192-7.
67. Rogers Van Katwyk, S.; Hoffman, S. J.; Mendelson, M.; Taljaard, M.; Grimshaw, J. M., Strengthening the science of addressing antimicrobial resistance: a framework for planning, conducting and disseminating antimicrobial resistance intervention research. *Health Res. Policy Syst.* **2020,** *18* (1), 60.

68. Fischbach, M. A., Combination therapies for combating antimicrobial resistance. *Curr. Opin.* **2011,** *14* (5), 519-523.

69. Angst Daniel, C.; Tepekule, B.; Sun, L.; Bogos, B.; Bonhoeffer, S., Comparing treatment strategies to reduce antibiotic resistance in an in vitro epidemiological setting. *Proc. Natl. Acad. Sci. U.S.A.* **2021,** *118* (13), e2023467118.

70. Rosenzweig, N.; Atallah, Z. K.; Olaya, G.; Stevenson, W. R., Evaluation of QoI Fungicide Application Strategies for Managing Fungicide Resistance and Potato Early Blight Epidemics in Wisconsin. *Plant Dis.* **2008,** *92* (4), 561-568.

71. Mitcheltree, M. J.; Pisipati, A.; Syroegin, E. A.; Silvestre, K. J.; Klepacki, D.; Mason, J. D.; Terwilliger, D. W.; Testolin, G.; Pote, A. R.; Wu, K. J. Y.; Ladley, R. P.; Chatman, K.; Mankin, A. S.; Polikanov, Y. S.; Myers, A. G., A synthetic antibiotic class overcoming bacterial multidrug resistance. *Nature* **2021,** *599* (7885), 507-512.

72. Mandhapati, A. R.; Yang, G.; Kato, T.; Shcherbakov, D.; Hobbie, S. N.; Vasella, A.; Bottger, E. C.; Crich, D., Structure-Based Design and Synthesis of Apramycin-Paromomycin Analogues: Importance of the Configuration at the 6'-Position and Differences between the 6'-Amino and Hydroxy Series. *J. Am. Chem. Soc.* **2017,** *139* (41), 14611-14619.

73. Sati, G. C.; Sarpe, V. A.; Furukawa, T.; Mondal, S.; Mantovani, M.; Hobbie, S. N.; Vasella, A.; Bottger, E. C.; Crich, D., Modification at the 2'-Position of the 4,5-Series of 2-Deoxystreptamine Aminoglycoside Antibiotics To Resist Aminoglycoside Modifying Enzymes and Increase Ribosomal Target Selectivity. *ACS Infect. Dis.* **2019,** *5* (10), 1718-1730.

74. Matsushita, T.; Sati, G. C.; Kondasinghe, N.; Pirrone, M. G.; Kato, T.; Waduge, P.; Kumar, H. S.; Sanchon, A. C.; Dobosz-Bartoszek, M.; Shcherbakov, D.; Juhas, M.; Hobbie, S. N.; Schrepfer, T.; Chow, C. S.; Polikanov, Y. S.; Schacht, J.; Vasella, A.; Bottger, E. C.; Crich, D., Design, Multigram Synthesis, and in Vitro and in Vivo Evaluation of Propylamycin: A Semisynthetic 4,5-Deoxystreptamine Class Aminoglycoside for the Treatment of Drug-Resistant Enterobacteriaceae and Other Gram-Negative Pathogens. *J. Am. Chem. Soc.* **2019,** *141* (12), 5051-5061.

75. Miethke, M.; Pieroni, M.; Weber, T.; Bronstrup, M.; Hammann, P.; Halby, L.; Arimondo, P. B.; Glaser, P.; Aigle, B.; Bode, H. B.; Moreira, R.; Li, Y.; Luzhetskyy, A.; Medema, M. H.; Pernodet, J. L.; Stadler, M.; Tormo, J. R.; Genilloud, O.; Truman, A. W.; Weissman, K. J.; Takano, E.; Sabatini, S.; Stegmann, E.; Brotz-Oesterhelt, H.; Wohlleben, W.; Seemann, M.; Empting, M.; Hirsch, A. K. H.; Loretz, B.; Lehr, C. M.; Titz, A.; Herrmann, J.; Jaeger, T.; Alt, S.; Hesterkamp, T.; Winterhalter, M.; Schiefer, A.; Pfarr, K.; Hoerauf, A.; Graz, H.; Graz, M.; Lindvall, M.; Ramurthy, S.; Karlen, A.; van Dongen, M.; Petkovic, H.; Keller, A.; Peyrane, F.; Donadio, S.; Fraisse, L.; Piddock, L. J. V.; Gilbert, I. H.; Moser, H. E.; Muller, R., Towards the sustainable discovery and development of new antibiotics. *Nat. Rev. Chem.* **2021,** *5* (10), 726-749.

76. Schneider, Y. K., Bacterial Natural Product Drug Discovery for New Antibiotics: Strategies for Tackling the Problem of Antibiotic Resistance by Efficient Bioprospecting. *Antibiotics* **2021,** *10* (7).

77. Abrudan, M. I.; Smakman, F.; Grimbergen, A. J.; Westhoff, S.; Miller, E. L.; van Wezel, G. P.; Rozen, D. E., Socially mediated induction and suppression of antibiosis during bacterial coexistence. *Proc. Natl. Acad. Sci. U.S.A.* **2015,** *112* (35), 11054-9.

78. Granato, E. T.; Meiller-Legrand, T. A.; Foster, K. R., The Evolution and Ecology of Bacterial Warfare. *Curr. Biol.* **2019,** *29* (11), R521-R537.

79. Myronovskyi, M.; Rosenkranzer, B.; Nadmid, S.; Pujic, P.; Normand, P.; Luzhetskyy, A., Generation of a cluster-free Streptomyces albus chassis strains for improved heterologous expression of secondary metabolite clusters. *Metab. Eng.* **2018,** *49*, 316-324.
80. Gomez-Escribano, J. P.; Bibb, M. J., Engineering Streptomyces coelicolor for heterologous expression of secondary metabolite gene clusters. *Microb. Biotechnol.* **2011,** *4* (2), 207-15.
81. Komatsu, M.; Komatsu, K.; Koiwai, H.; Yamada, Y.; Kozone, I.; Izumikawa, M.; Hashimoto, J.; Takagi, M.; Omura, S.; Shin-ya, K.; Cane, D. E.; Ikeda, H., Engineered Streptomyces avermitilis host for heterologous expression of biosynthetic gene cluster for secondary metabolites. *ACS Synth. Biol.* **2013,** *2* (7), 384-96.
82. Lodhi, A. F.; Zhang, Y.; Adil, M.; Deng, Y., Antibiotic discovery: combining isolation chip (iChip) technology and co-culture technique. *Appl. Microbiol. Biotechnol.* **2018,** *102* (17), 7333-7341.
83. Kealey, C.; Creaven, C. A.; Murphy, C. D.; Brady, C. B., New approaches to antibiotic discovery. *Biotechnol. Lett.* **2017,** *39* (6), 805-817.
84. Ling, L. L.; Schneider, T.; Peoples, A. J.; Spoering, A. L.; Engels, I.; Conlon, B. P.; Mueller, A.; Schaberle, T. F.; Hughes, D. E.; Epstein, S.; Jones, M.; Lazarides, L.; Steadman, V. A.; Cohen, D. R.; Felix, C. R.; Fetterman, K. A.; Millett, W. P.; Nitti, A. G.; Zullo, A. M.; Chen, C.; Lewis, K., A new antibiotic kills pathogens without detectable resistance. *Nature* **2015,** *517* (7535), 455-9.
85. Wright, G., An irresistible newcomer. *Nature* **2015,** *517* (7535), 442-444.
86. Skropeta, D., Deep-sea natural products. *Nat. Prod. Rep.* **2008,** *25* (6), 1131-66.
87. Wilson, R. M.; Danishefsky, S. J., Small Molecule Natural Products in the Discovery of Therapeutic Agents: The Synthesis Connection. *J. Org. Chem.* **2006,** *71* (22), 8329-8351.
88. Steele, A. D.; Knouse, K. W.; Keohane, C. E.; Wuest, W. M., Total synthesis and biological investigation of (-)-promysalin. *J. Am. Chem. Soc.* **2015,** *137* (23), 7314-7.
89. Post, S. J.; Keohane, C. E.; Rossiter, L. M.; Kaplan, A. R.; Khowsathit, J.; Matuska, K.; Karanicolas, J.; Wuest, W. M., Target-Based Design of Promysalin Analogues Identifies a New Putative Binding Cleft in Succinate Dehydrogenase. *ACS Infect. Dis.* **2020,** *6* (6), 1372-1377.
90. Keohane, C. E.; Steele, A. D.; Fetzer, C.; Khowsathit, J.; Van Tyne, D.; Moynie, L.; Gilmore, M. S.; Karanicolas, J.; Sieber, S. A.; Wuest, W. M., Promysalin Elicits Species-Selective Inhibition of Pseudomonas aeruginosa by Targeting Succinate Dehydrogenase. *J. Am. Chem. Soc.* **2018,** *140* (5), 1774-1782.
91. Tripathi, A.; Schofield, M. M.; Chlipala, G. E.; Schultz, P. J.; Yim, I.; Newmister, S. A.; Nusca, T. D.; Scaglione, J. B.; Hanna, P. C.; Tamayo-Castillo, G.; Sherman, D. H., Baulamycins A and B, broad-spectrum antibiotics identified as inhibitors of siderophore biosynthesis in Staphylococcus aureus and Bacillus anthracis. *J. Am. Chem. Soc.* **2014,** *136* (4), 1579-86.
92. Steele, A. D.; Ernouf, G.; Lee, Y. E.; Wuest, W. M., Diverted Total Synthesis of the Baulamycins and Analogues Reveals an Alternate Mechanism of Action. *Org. Lett.* **2018,** *20* (4), 1126-1129.
93. Kim, W.; Zhu, W.; Hendricks, G. L.; Van Tyne, D.; Steele, A. D.; Keohane, C. E.; Fricke, N.; Conery, A. L.; Shen, S.; Pan, W.; Lee, K.; Rajamuthiah, R.; Fuchs, B. B.; Vlahovska, P. M.; Wuest, W. M.; Gilmore, M. S.; Gao, H.; Ausubel, F. M.; Mylonakis, E., A

new class of synthetic retinoid antibiotics effective against bacterial persisters. *Nature* **2018,** *556* (7699), 103-107.

94. Kim, W.; Steele, A. D.; Zhu, W.; Csatary, E. E.; Fricke, N.; Dekarske, M. M.; Jayamani, E.; Pan, W.; Kwon, B.; Sinitsa, I. F.; Rosen, J. L.; Conery, A. L.; Fuchs, B. B.; Vlahovska, P. M.; Ausubel, F. M.; Gao, H.; Wuest, W. M.; Mylonakis, E., Discovery and Optimization of nTZDpa as an Antibiotic Effective Against Bacterial Persisters. *ACS Infect. Dis.* **2018,** *4* (11), 1540-1545.

Chapter 2. Application of a key transformation for the synthesis of phenolic bisabolanes and biological investigations of their derivatives

Disclaimer: The project goals and hypothesis for peniciaculin A were originally developed independently by Ingrid K. Wilt. Further concept development has been provided by Adrian R. Demeritte. Ingrid K. Wilt completed the synthesis of the Aggarwal and Gilheany inspired methods described in the text and the ketone analogues derived from the latter route. Adrian R. Demeritte synthesized the diamine ligand following the procedure reported by Gilheany. Adrian R. Demerrite and Ingrid K. Wilt both optimized the diastereoselective nucleophilic addition route and have contributed equally to this work. Ingrid K. Wilt synthesized all compounds reported to **(−)-2.28** and Adrian R. Demeritte completed the final three steps. Only compounds synthesized by Ingrid K. Wilt are reported in the SI. Ingrid K. Wilt and Adrian R. Demeritte proposed the ethoxy acrylate analogues and Adrian R. Demeritte performed the synthesis. Adrian R. Demeritte completed the synthesis of the diorcinol analogue. Characterization of intermediates synthesized by Adrian R. Demeritte were not included. Ingrid K. Wilt independently designed and completed the synthesis of 1-hydroxyboivinianin A. Ingrid K. Wilt optimized growth conditions of *Vibrio harveyi* and ran preliminary biological assays. Collaborators at Corteva Agriscience screened a panel of compounds for herbicidal, insecticidal, and fungicidal activity. These results are reported in table **2.7**.

2.1. Introduction

2.1.1. Antifungal ubiquinone mimics

The agricultural industry, a pinnacle of society, relies on agrochemicals including pesticides, insecticides, herbicides, and fungicides to maximize crop yield and prevent the spread of disease. These chemicals are often designed to mimic and outcompete natural cofactors in the target organism such as ubiquinone. Ubiquinone (coenzyme Q) is involved in the electron transport chain (ETC) and facilitates aerobic mitochondrial respiration through redox cycling of three different states including fully oxidized ubiquinone, semiquinone ubisemiquinone, and fully reduced ubiquinol[1] (Figure **2.1**). Ubiquinone accepts electrons in complex II (succinate dehydrogenase) to facilitate interconversion of succinate and fumarate via reduction to ubiquinol. In complex III (cytochrome b), ubiquinol donates electrons to form ubiquinone and translocate protons[2]. Design of ubiquinone mimics to inhibit both complex II and III has led to successful production of potent crop protective agents[3].

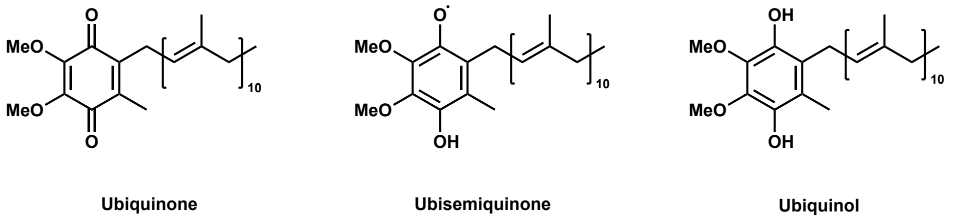

Ubiquinone **Ubisemiquinone** **Ubiquinol**

Figure 2.1. Ubiquinone oxidation states. Ubiquinone cycles through three redox states to enable one and two electron redox processes.

Succinate dehydrogenase inhibitors (SDHIs) bind to complex II and all 19 approved fungicides share a prototypical pharmacophore: a carboxyl "core" linked via amide bond to an aniline substituent[4] (Figure **2.2**). All cocrystal structures of SDH (porcine heart[5], avian[6], and *Escherichia coli*[7, 8]) suggest the carboxy core is buried deep within the ubiquinone binding site (Q-site). Thus, analogue efforts have been focused on modifications to the carboxy core to maximize biding affinities of SDHIs to the Q-site[9].

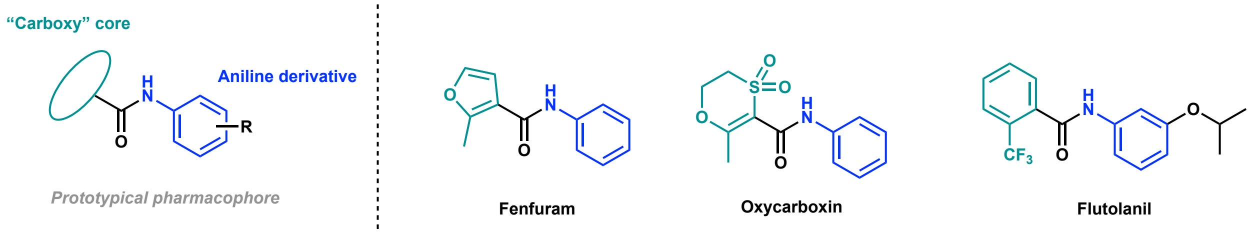

Figure 2.2. Succinate dehydrogenase inhibitors (SDHIs). Prototypical structure of SDHIs include a carboxy core and aniline derivative. Analogue design of these small molecules has focused on structural modifications to the carboxy core generating compounds such as fenfuram, oxycarboxin, and flutolanil.

Complex III inhibitors are divided into three classes based on binding location: quinone outside inhibitors (QOIs) bind to the ubiquinol oxidation (Q_O) site; quinone inside inhibitors (QiIs) to the ubiquinone reduction (Q_i) pocket; and dual inhibitors (PN) to both (Figure **2.3**). It is proposed these inhibitors may act by preventing water mediated proton transfer required to reduce ubiquinone[10]. Although only a small amount of QiIs and PNs have been identified (Figure **2.3a&b**), QoIs are the second most common fungicide in the global agricultural fungicide market (*i.e.* $2.7 billion in sales, manufacture, and use)[11]. QoIs were introduced in the 1990s inspired by the natural product strobulurin A, a small molecule isolated from small forest mushroom *Strobilurus tenacellus*. Unlike SDHIs, extensive analogue design of strobulurin has identified several pharmacophores that maintain QoI activity[12]. Pharmacophores such as ethoxy-acrylate, methoxy-acetamide, oximo-acetamide, methoxy-carbamate, oximo-acetate, dihydrodioxazine, and benzyl-carbamate can be found in QoIs currently used in agricultural settings and are all considered analogues of strobulurin[13]. One aspect that is maintained throughout all synthetic QoIs to date is a central linking ring that enhances UV stability compared to the linear polyene found in strobilurin A[14] (Figure **2.3c**). The extensive chemical diversity of QoIs is a central feature to their continued use as each pharmacophore can adopt unique binding modes within the Qo site.

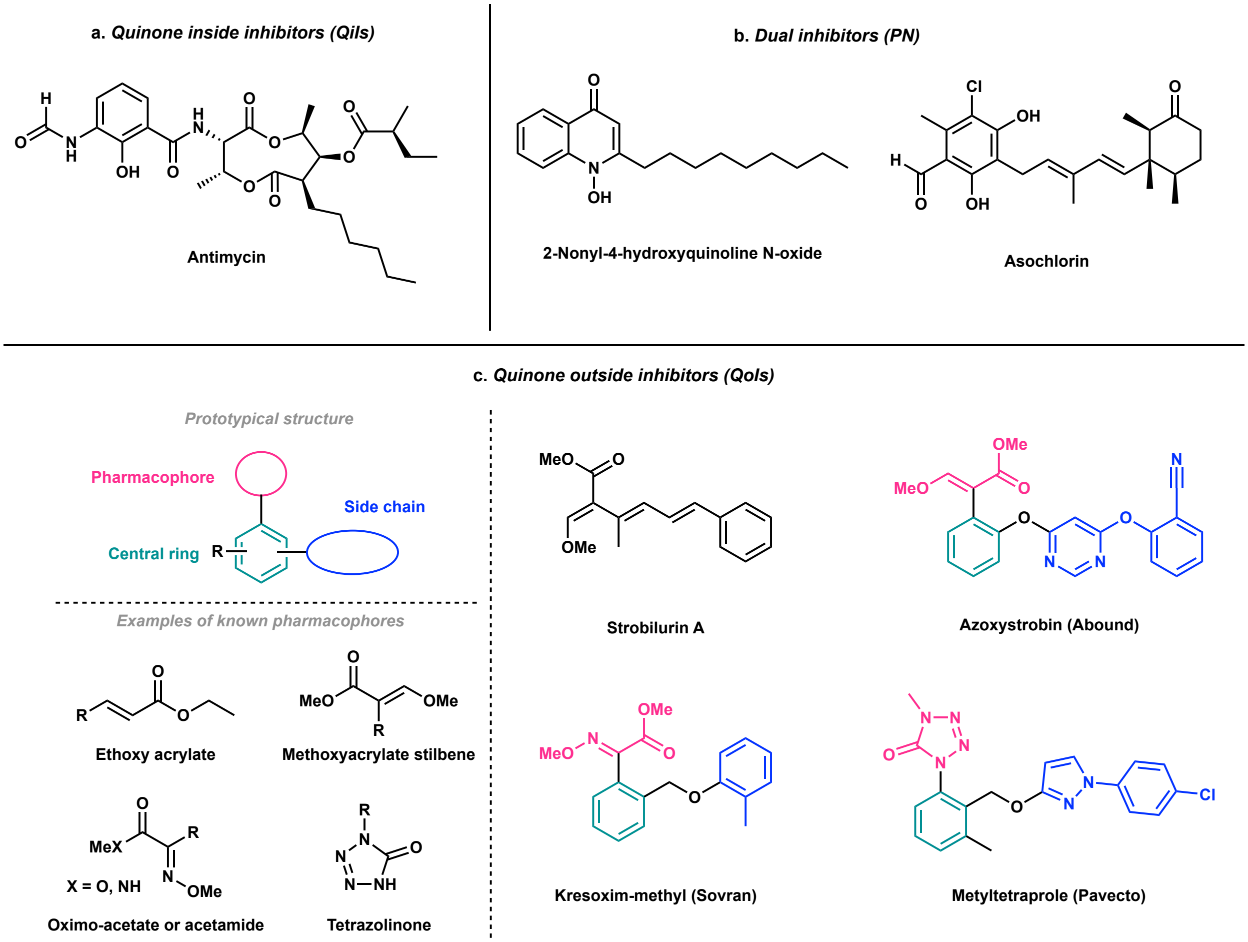
a. Quinone inside inhibitors (QiIs)
Antimycin
b. Dual inhibitors (PN)
2-Nonyl-4-hydroxyquinoline N-oxide
Asochlorin
c. Quinone outside inhibitors (QoIs)
Prototypical structure
Pharmacophore
Side chain
Central ring
Examples of known pharmacophores
Ethoxy acrylate
Methoxyacrylate stilbene
X = O, NH
Oximo-acetate or acetamide
Tetrazolinone
Strobilurin A
Azoxystrobin (Abound)
Kresoxim-methyl (Sovran)
Metyltetraprole (Pavecto)

Figure 2.3. Complex III inhibitors. Structural diversity of cytochrome b inhibitors. a. Antimycin binds to the quinone inside site and is the only known small molecule to bind to this site. b. Dual inhibitors bind to both the Qi and Qo sites. c. A prototypical structure of QoIs includes a pharmacophore attached via a central aryl ring to a n unsaturated/aryl side chain. Several pharmacophores can retain QoI activity, but can may accommodate different biding modes within the same binding pocket.

Despite the chemical diversity of QoIs, due to the site-specific mode of action, these scaffolds can lead to the development of fungicide resistance. Resistance is most commonly observed across fungal species as a single point mutation G143A in the Qo site of cytochrome *b*. Less common, however, in species such as *Alternaria solani* (early potato blight), amino acid substitution F129L renders many QoIs ineffective. These mutations disrupt the binding mode of most QoIs through additional steric interactions with the central ring[15]. Efforts to design complex

III inhibitors, however, with novel binding modes could be an excellent strategy to overcome emerging antifungal resistance[16].

One example of this strategy is the development of a novel class of QoIs, cyclic triazolinones, that are effective against wild-type and resistant mutant fungi[17]. By calculating binding free energy of metyltetraprole tetrazolinone (Pavecto) in wild-type and resistant mutant Q_o sites, Arakawa and coworkers suggest the novel QoI pharmacophore can compensate subtle changes in the Q_o site due to the additional steric hindrance between the methyl group of A143 by trading van der Waals interactions for Coulomb[18]. Pavecto paves the way for future studies investigating small molecule QoIs with novel pharmacophores as a strategy to overcome antifungal resistance. Furthermore, fungicides with narrow spectrum or species-specific activity remain less explored than broad spectrum agents and may facilitate better understanding of the heterogeneity that exists between fungal Q_o sites.

2.1.2. Antimicrobial phenolic bisabolanes

Synthetic chemists often look to nature to gain inspiration for the development of novel bioactive small molecules. Phenolic bisabolanes isolated from marine environments possess unique bioactivity and have the potential to expand chemotypes of known antimicrobial small molecules. Peniciaculin A (**(+)-2.1**), a phenolic bisabolane sesquiterpenoid isolated from *Penicillium aculeatum* SD-321 from marine sediment in the deep South China Sea, demonstrates potent and selective activity against the fungal pathogen *Alternaria brassicae* (MIC = 0.5 μg/mL)[19] (Figure **2.4**). Cruciferous vegetables are prone to fungal infections from *A. brassicae* causing premature wilting and dark spots. This leads to significant economic loss and depleted crop yield[20]. With the rapid evolution of fungal resistance to commonly used fungicides, there is dire need for novel inhibitors to combat developing resistance and economic loss due to *A. brassicae* and other fungal phytopathogens[21].

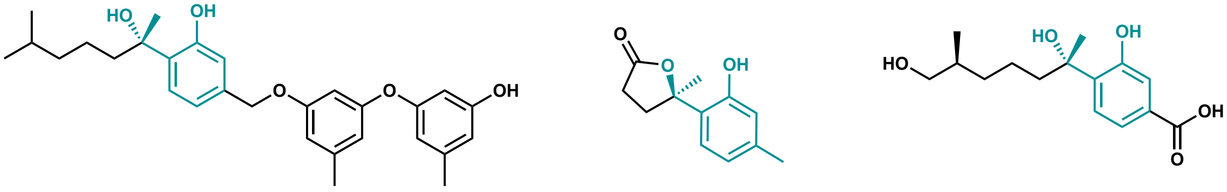

Peniciaculin A
(+)-2.1
MIC = 0.50 μg/mL A. *brassicae*

1-Hydroxyboivinianin A
(+)-2.2
MIC = 4.0 μg/mL V. *harveyi*

(7*S*,11*S*)-(+)-12-Hydroxysydonic acid
MIC = 0.5 μg/mL S. *aureus*
MIC = 0.5 μg/mL V. *parahaemolyticus*

Figure 2.4. Examples of bioactive phenolic bisabolanes.

Comparing the structure of peniciaculin A to known QoIs, similarities are evident. The structure can be broken into three regions including sidechain diaryl ether, central ring phenol, and unexplored pharmacophore alkyl sidechain containing the tertiary alcohol (Figure **2.5a**). Furthermore, preliminary binding site modeling comparing known QoI azoxystrobin and peniciaculin A suggest the phenol core of peniciaculin A interacts with key Phe128 residue in the Qo site and the biaryl fragment with Phe274, Phe276, and Tyr278, while the alkyl side chain may access an unexplored hydrophobic binding pocket, increasing potency against *A. brassicae* (Figure **2.5b**). Furthermore, the model suggests the central ring of peniciaculin A can accommodate an alternative binding mode than azoxystrobin. This unexplored binding mode may also confer activity against G143A mutant strains, as previously demonstrated by Pavecto[17, 18]. Synthesis of peniciaculin A and key derivatives will allow for biological investigations of this novel class of proposed QoIs and provide valuable insight on the development of novel pharmacophores to combat emerging antifungal resistance. Furthermore, the apparent species-specific antifungal activity of peniciaculin A may aid in elucidating how the heterogeneity of Qo sites between fungal species effects binding affinity to small molecules and the resulting dichotomy (*i.e.* G143A or F129L) of resistance development. Additionally, the phenol core of peniciaculin A is found in several co-isolates, including 1-hydroxyboivinianin A, a small molecule reported to have selective activity against a growing bacterial threat *Vibrio harveyi*[19]. Thus, we aimed to design a synthesis that could not only serve as a platform for analogue development of peniciaculin A, but that could also produce a multitude of phenolic bisabolane natural products with unique antimicrobial activity (Figure **2.4**).

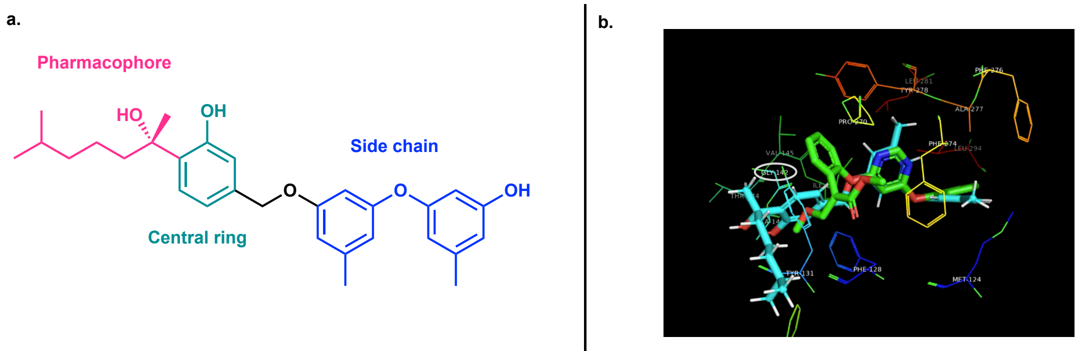

Proposed QoI features of 2.1

Qo binding site
Azoxystrobin modeled in green *Peniciaculin A modeled in cyan*

Figure 2.5. Proposed overlap of peniciaculin A with prototypical QoI scaffold. a. Proposed similarities between peniciaculin A and prototypical QoIs. b. Preliminary binding site model of peniciaculin A (cyan) and known QoI azoxystrobin (green) in the Qo site. Binding model created in Pymol with porcine Qo site. Relevant G residue is G142 in the computed model.

2.1.3. Previous approaches synthetic approaches to phenolic bisabolanes

The construction of the tertiary alcohol with high stereoselectivity was anticipated to be the most challenging aspect of the synthesis. Although many methods exist to form chiral tertiary alcohols, the continuous flow of methods published each year hints at the synthetic challenges associated with constructing such a stereocenter[22]. Of note, methods focused on acetophenone derivatives often lack diversity in substrate scope, specifically pertaining to *ortho* substituents and, if heteroatoms are included, protecting group choice[23-25]. Inspiration for the formation of benzylic tertiary alcohol in the synthesis of peniciaculin A was primarily derived from 1,2-migration methodology development by Aggarwal[26], enantioselective Grignard addition by Gilheany[27], and the use of a chiral imidazolidinone auxiliary explored by several groups such as Sakito and Ito[28-30].

2.1.3.1. Aggarwal's 1,2-migration

In 2012, Aggarwal and coworkers completed the synthesis of several phenolic bisabolanes to demonstrate the stereoretentive lithiation-borylation-1,2-migration methodology developed by the lab[26]. They showed it was possible to take an enantioenriched secondary carbamate, perform a stereorentenive lithiation followed by transmetallation with alkyl substituted pinacolatoboron and 1,2-migration to form borylated intermediates. Subsequent protodeborylation or oxidation resulted in the desired substituted benzylic stereocenters. Aggarwal presents examples of a phenolic bisabolane containing a tertiary alcohol ((*R*)-(+)-gossonorol) and several with ortho phenols ((R)-(–)-curcuphenol), but none that contain both a tertiary benzylic alcohol and ortho substituted phenol[26]. Additionally, the substrate scope only contained phenols with methoxy protecting groups. Thus, it was proposed the scope of this methodology could be expanded to more highly substituted aryl rings to form benzylic tertiary alcohols in the synthesis of peniciaculin A.

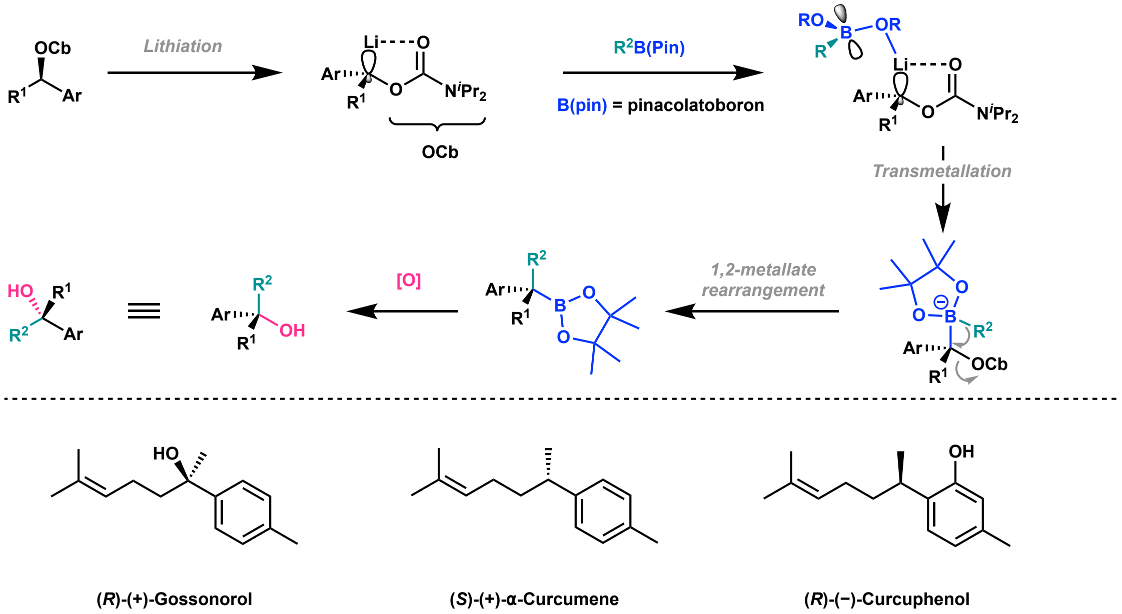
OCb
R¹
Ar
Lithiation
Li
O
Ar
R¹
O
N^iPr₂
OCb
R²B(Pin)
B(pin) = pinacolatoboron
RO
B
OR
R
Transmetallation
1,2-metallate rearrangement
O
B
R²
OCb
[O]
OH
HO
(R)-(+)-Gossonorol
(S)-(+)-α-Curcumene
(R)-(−)-Curcuphenol

Scheme 2.1. 1,2-migration. Aggarwal's lithiation-borylation-oxidation sequence rapidly builds complexity. Deprotonation alpha to the carbamate followed by subsequent lithiation facilitates transmetallation to form a C-B bond. Stereoretentive 1,2-metallate rearrangement forges a new C-C bond. Oxidation furnishes the desired tertiary benzylic alcohol.

2.1.3.2. Gilheany's asymmetric Grignard

In an alternative approach, the Gilheany lab developed asymmetric Grignard additions to form tertiary benzylic alcohols. Through rational design, a diamine tridentate ligand was identified and its stochiometric use allowed for the synthesis of tertiary alcohols with high enantiomeric excess (ee) (Figure **2.6**). Although stochiometric amounts of ligand were required to obtain high ee, Gilheany notes the ligand can easily be recovered from silica column on a small scale by elution with cyclohexane:EtOAc:triethylamine (5:4:1) and reused without erosion of ee. Furthermore, a formal synthesis of vitamin E was completed through stereoselective addition of methylmagnesium iodide to prochiral ketone[27]. Similar to Aggarwal's methodology, only methyl protected phenols could be found in the substrate scope. It was envisioned that this transformation could be used for late-stage formation of the tertiary alcohol and intermediates along the route could be assessed for biological activity to probe our novel pharmacophore hypothesis.

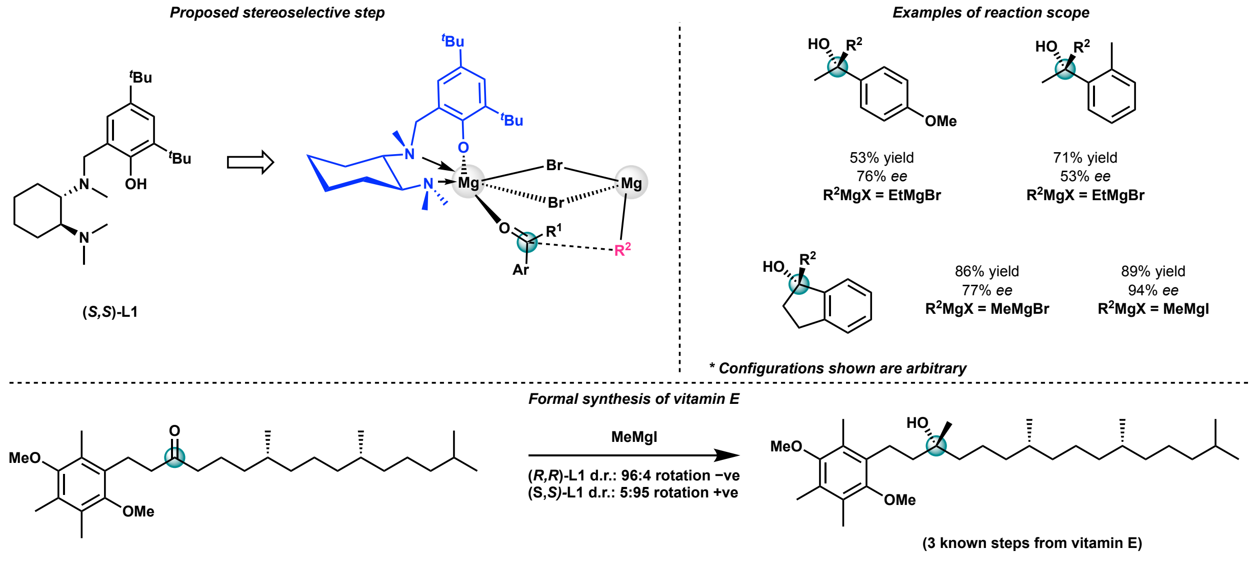

Proposed stereoselective step
tBu
tBu
N
OH
N
(S,S)-L1
tBu
tBu
O
N
N
Mg
Br
Br
Mg
O
R1
Ar
R2
Examples of reaction scope
HO R2
OMe
53% yield
76% ee
R2MgX = EtMgBr
HO R2
71% yield
53% ee
R2MgX = EtMgBr
HO R2
86% yield
77% ee
R2MgX = MeMgBr
89% yield
94% ee
R2MgX = MeMgI
* Configurations shown are arbitrary
Formal synthesis of vitamin E
MeO
O
OMe
MeMgI
(R,R)-L1 d.r.: 96:4 rotation −ve
(S,S)-L1 d.r.: 5:95 rotation +ve
MeO
HO
OMe
(3 known steps from vitamin E)

Figure 2.7. Stereoselective Grignard addition. Gilheany and coworkers developed tridentate ligands to explore stereoselective Grignard additions to acetophenone derivatives and completed a formal synthesis of vitamin E.

2.1.3.3. Diastereoselective nucleophilic addition to chiral imidazolidinone

Finally, there have been several investigations of the synthesis of phenolic bisabolanes using methodology inspired by the use of a chiral imidazolidinone to facilitate diastereoselective nucleophilic addition (Scheme **2.2**). First reports of the use of such imidazolidinones to form tertiary alcohols was provided by Sakito and coworkers[28] in the synthesis of marine antibiotic malyngolide. Ito and coworkers used a similar strategy in the asymmetric synthesis of two phenolic bisabolanes, (+)-curcutetraol and (+)-sydonol[29]. We envisioned incorporating these strategies in the synthesis of peniciaculin A, anticipating asymmetric nucleophilic addition would produce the desired tertiary alcohol in high ee. It was also speculated a more efficient route to access the alkyl sidechain than described by Ito and coworkers was possible through leveraging the reactivity of the homobenzylic aldehyde formed after aminal hydrolysis.

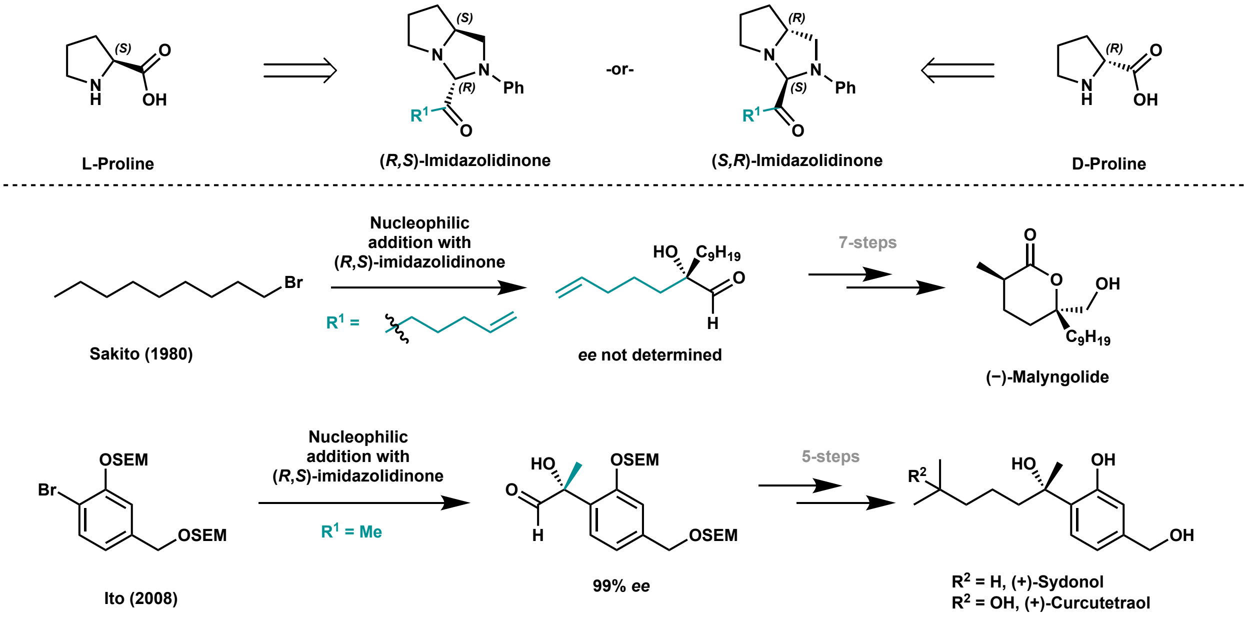
(S)
L-Proline
(S)
(R)
N
N
Ph
R^1
O
(R,S)-Imidazolidinone
-or-
(R)
(S)
R^1
(S,R)-Imidazolidinone
(R)
D-Proline
Br
Sakito (1980)
Nucleophilic addition with (R,S)-imidazolidinone
R^1 =
HO
C_9H_{19}
H
ee not determined
7-steps
OH
C_9H_{19}
(−)-Malyngolide
OSEM
Br
OSEM
Ito (2008)
Nucleophilic addition with (R,S)-imidazolidinone
R^1 = Me
HO
OSEM
H
OSEM
99% ee
5-steps
R^2
HO
OH
OH
R^2 = H, (+)-Sydonol
R^2 = OH, (+)-Curcutetraol

Scheme 2.2. Synthesis of tertiary alcohols using chiral imidazolidinones.

2.1.3.4. Yajima's synthesis of the peniciaculins

After we had sent our initial analogues of peniciaculin A to Corteva Agriscience for antifungal testing, Yajima and coworkers published a total synthesis of peniciaculin A and B. The route relies on a key Suzuki-Miyaura coupling between commercially available aryl iodide and boronic acid. Sharpless asymmetric dihydroxylation builds the benzylic tertiary alcohol. Subsequent activation and reductive olefination of the primary alcohol followed by cross metathesis builds the full alkyl side chain. Late stage diaryl ether incorporation via mesylation, chlorination, and displacement of benzylic alcohol installs the full carbon skeleton of peniciaculin A[31] (Figure **2.7**). No biological investigations or analogues were completed in the publication. Furthermore, no MoA nor similarities between peniciaculin A and QoIs was proposed. The route we developed described below in the results and discussion is highly amenable to analogue design and will probe key components of our QoI hypothesis that were unexplored in Yajima and coworkers' publication.

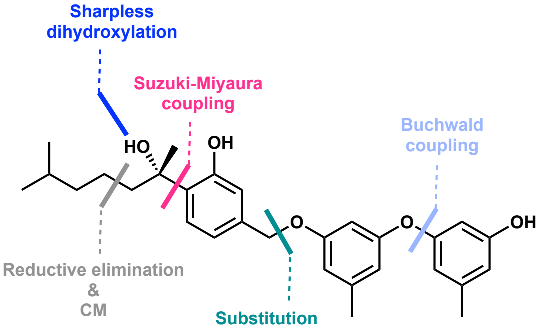

Figure 2.7. Yajima and coworkers' synthesis of peniciaculin A.

2.2. Results and discussion

2.2.1. 1,2-migration

Inspired by Aggarwal's use of a stereoretentive 1,2-migration to construct tertiary benzylic alcohols, an analogous transformation was proposed to build the core of peniciaculin A. Retrosynthetically, I envisioned breaking peniciaculin A into two fragments: the phenol core containing the tertiary alcohol; and a diaryl ether fragment derived from coupling of two orcinol synthons. Construction of the phenol core would be achieved via 1,2-migration to install the alkyl side chain and benzylic oxidation of commercially available 2-hydroxy-4-methylacetophenone (Scheme **2.3**).

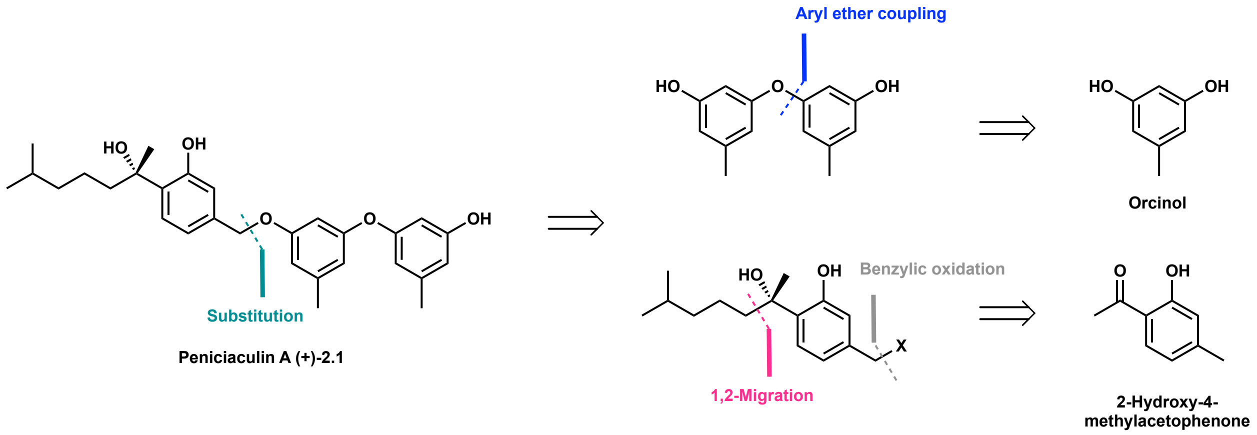
Aryl ether coupling
HO
OH
Orcinol
HO
OH
Substitution
Peniciaculin A (+)-2.1
HO
OH
Benzylic oxidation
X
1,2-Migration
O
OH
2-Hydroxy-4-methylacetophenone

Scheme 2.3. Retrosynthetic approach 1.0 to peniciaculin A.

The proposed route to peniciaculin A commenced with methyl protection and subsequent reduction of 2-hydroxy-4-methylacetophenone. Of note, an enantioselective route to peniciaculin A could be accomplished by performing a stereoselective Corey-Bakshi-Shibata (CBS) reduction of the ketone with (*S*)-(+)-2-methyl-CBS-oxazaborolidine, which would facilitate stereorentenive 1,2-migration. Carbamoylation primed the substrate to begin screening conditions for the proposed key step (Scheme **2.4**).

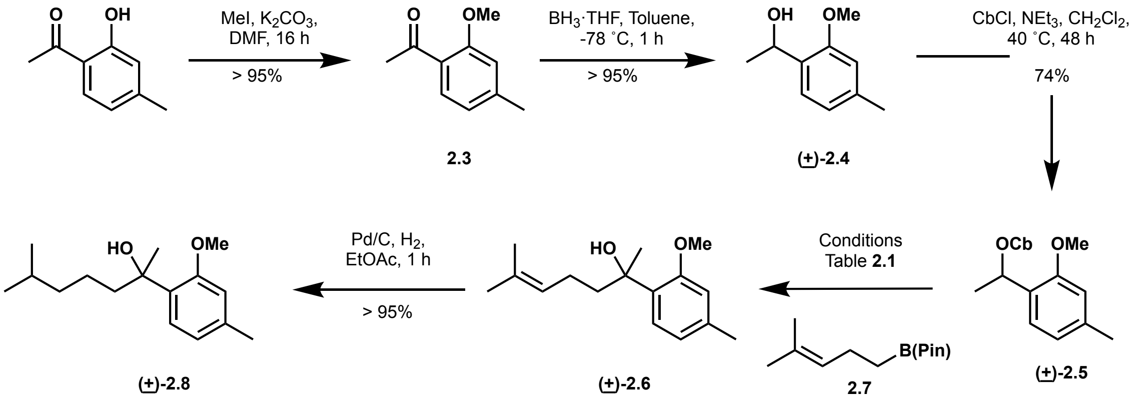
O
OH
MeI, K₂CO₃, DMF, 16 h
> 95%
O
OMe
2.3
BH₃·THF, Toluene, -78 °C, 1 h
> 95%
OH
OMe
(±)-2.4
CbCl, NEt₃, CH₂Cl₂, 40 °C, 48 h
74%
OCb
OMe
(±)-2.5
Conditions Table 2.1
B(Pin)
2.7
HO
OMe
(±)-2.6
Pd/C, H₂, EtOAc, 1 h
> 95%
HO
OMe
(±)-2.8

Scheme 2.4. Synthesis of substrate for 1,2-migration.

Standard conditions reported by Aggarwal were unsuccessful in producing the desired intermediate **(±)-2.6** (Table **2.1**, entries 1 & 2)[32, 33]. However, the addition of a Lewis acid, such as

$MgBr_2·OEt_2$ has been demonstrated in several cases to promote 1,2-migration[34, 35]. Furthermore, addition of CH_3OH at this time protonates any lithiated carbamate thus preventing racemization of the stereocenter[36]. With freshly prepared pinacol boronate ester and distilled Et_2O, the addition of $MgBr_2·OEt_2$ produced the desired tertiary alcohol in 4% yield (Table **2.1**, entry 3). Increasing the equivalents of $MgBr_2·OEt_2$ further increased the yield to 17% (Table **2.1**, entry 4). Allowing the reaction to stir overnight at room temperature after the addition of $MgBr_2·OEt_2$ appeared to be the optimal conditions, resulting in 30% yield of the tertiary alcohol (Table **2.1**, entry 5). Efforts to optimize the reaction further resulted in no change in yield and decomposition of the starting material.

Table 2.1. Optimization of the 1,2-migration.

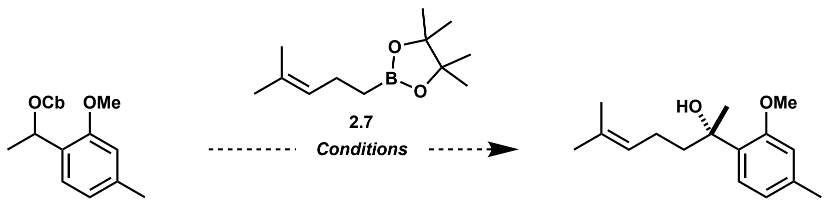

(±)-2.5

(±)-2.6

Entry	Conditions	Result
1	i. *S*-BuLi (1.06 equiv), Et_2O (0.25M), -78 ˚C, 15 min ii. 2.7 (1.2 equiv) 1.0M in Et_2O, -78 ˚C to rt, 2 h iii. 2M $NaOH_{(aq)}$ (4.2 equiv), H_2O_2 (4.2 equiv), THF (0.25M), 0˚C to rt, 2h	nr
2[a]	i. *S*-BuLi (1.3 equiv), Et_2O (0.25M), -78 ˚C, 15 min ii. 2.7[b] (1.5 equiv) 0.3M in Et_2O, -78 ˚C to rt, 1 h iv. 2M $NaOH_{(aq)}$ (4.2 equiv), H_2O_2 (4.2 equiv), THF (0.25M), 0˚C to rt, o/n	nr
3[a]	i. *S*-BuLi (1.3 equiv), Et_2O (0.25M), -78 ˚C, 15 min ii. 2.7[b] (1.5 equiv) 0.3M in Et_2O, -78 ˚C to rt, 1 h iii. $MgBr_2{\cdot}OEt_2$ (1.5 equiv) 0.30M in CH_3OH, 2h iv. 2M $NaOH_{(aq)}$ (7 equiv), H_2O_2 (11.8 equiv), THF (0.25M), 0˚C to rt, o/n	4% (11.4% BRSM)
4[a]	i. *S*-BuLi (1.3 equiv), Et_2O (0.25M), -78 ˚C, 15 min ii. 2.7[b] (1.5 equiv) 0.3M in Et_2O, -78 ˚C to rt, 1 h iii. $MgBr_2{\cdot}OEt_2$ (3.75 equiv) 0.30M in CH_3OH, 2h iv. 2M $NaOH_{(aq)}$ (7 equiv), H_2O_2 (11.8 equiv), THF (0.25M), 0˚C to rt, o/n	17%
5[a]	i. *S*-BuLi (1.3 equiv), Et_2O (0.25M), -78 ˚C, 15 min ii. 2.7[b] (1.5 equiv) 0.3M in Et_2O, -78 ˚C to rt, 1 h iii. $MgBr_2{\cdot}OEt_2$ (3.75 equiv) 0.30M in CH_3OH, o/n iv. 2M $NaOH_{(aq)}$ (7 equiv), H_2O_2 (11.8 equiv), THF (0.25M), 0˚C to rt, o/n	30%

[a]Diethyl ether was distilled from CaH and stored over 4Å MS
[b]Pinacol boronate **2.7** was prepared from 5-bromo-2-methylpent-2-ene

As mentioned prior, the substrate scope of the developed reaction only explored trisubstituted stereocenters with ortho methoxy groups or tetrasubstituted stereocenters, never both. Our results suggest incorporating more substituted substrates and obtaining high yields of the desired product may be a limitation of this reaction due to the steric interactions of the ortho methoxy group and pinacol boronate (scheme **2.1**). After successfully forming the key intermediate, benzylic oxidation of **(±)-2.8** was proposed. Despite extensive screening of conditions, only recovery or decomposition of starting material was observed (Table **2.2**). It is worth noting that utilizing a stereoinvertive method substituted the boronic ester for a borane developed by Aggarwal and coworkers may have increased the yield of the key step by preventing steric interactions between the *o*-methoxy and incoming pinacol boronate[32], but due to the unsuccessful benzylic oxidation, this method was not explored.

Table 1.2. Benzylic oxidation.

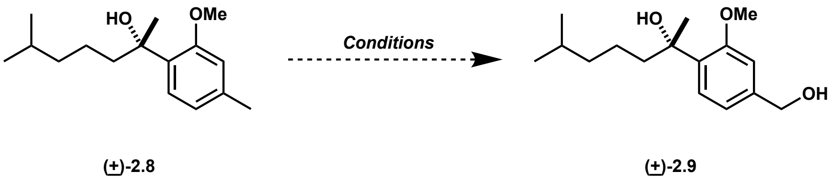

Entry	Conditions	Result
1	SeO_2, *t*-BuOOH	nr
2	$KMnO_4$	nr
3	PCC	nr
4	DDQ	nr
5	O_2, *s*-BuLi, EDTA	nr
6	KBr, oxone, NMO	nr
7	NBS, AIBN, *then* NaOH	Decomp

2.2.2. Asymmetric Grignard

As described by the Gilheany lab, using a stochiometric chiral diamine ligand[27], we proposed asymmetric Grignard addition would be a fruitful approach for late-stage installation of the tertiary alcohol. Retrosynthetically, we still envisioned breaking penciaculin A into a western and eastern half: the phenol core and diaryl ether. The alkyl side chain would now be installed via enolate addition of 2-hydroxy-4-methylacetophenone to an electrophilic carbon center (Scheme **2.5**). Methyl protecting groups were chosen for the free phenols to minimize steric hindrance ortho to the carbonyl involved in coordination of the magnesium-ligand complex during the asymmetric Grignard addition and allow for global deprotection as the proposed final step.

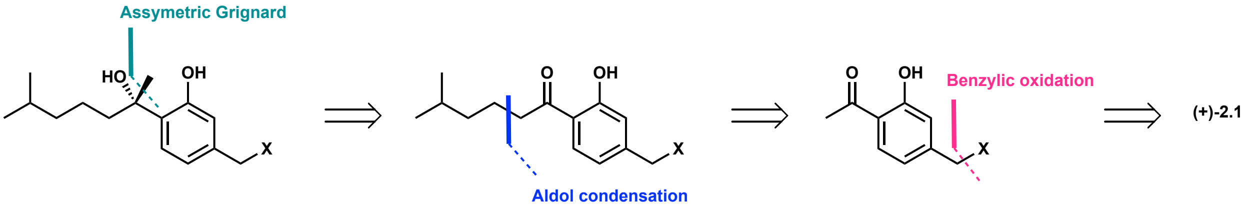

Scheme 2.5. Retrosynthetic approach 2.0 to peniciaculin A.

To explore the viability of the asymmetric Grignard addition, model substrate and truncated analogue **2.10** was synthesized commencing from **2.3**. Benzylic bromination followed by tetrabutylammonium bromide (TBAB) assisted displacement with monomethyl protected orcinol produced **2.12** in moderate yield. Aldol condensation of **2.12** with isovaleraldehyde followed by acid promoted elimination produced the full alkyl side chain in high yield. Reduction of the enone to the ketone was initially attempted with CuI and lithium aluminum hydride (LAH)[37]. Although disappearance of the enone peaks in the ^{1}H NMR of the major product suggested the desired 1,4-addition had occurred, only one methoxy peak at 3.8 ppm remained. It is likely that copper coordinated to the carbonyl and phenol in a 6-membered transition state, thus simultaneously facilitating nucleophilic iodine displacement of the methoxy protecting group and 1,4-reduction of the enone resulting in deprotection of the ortho phenol (SI **2.17**) (SI Figure **S2.1**). Using a bulky hydride source, L-selectride, chemoselective enone reduction was achieved in high yields to produce model substrate **2.10** (Scheme **2.6**).

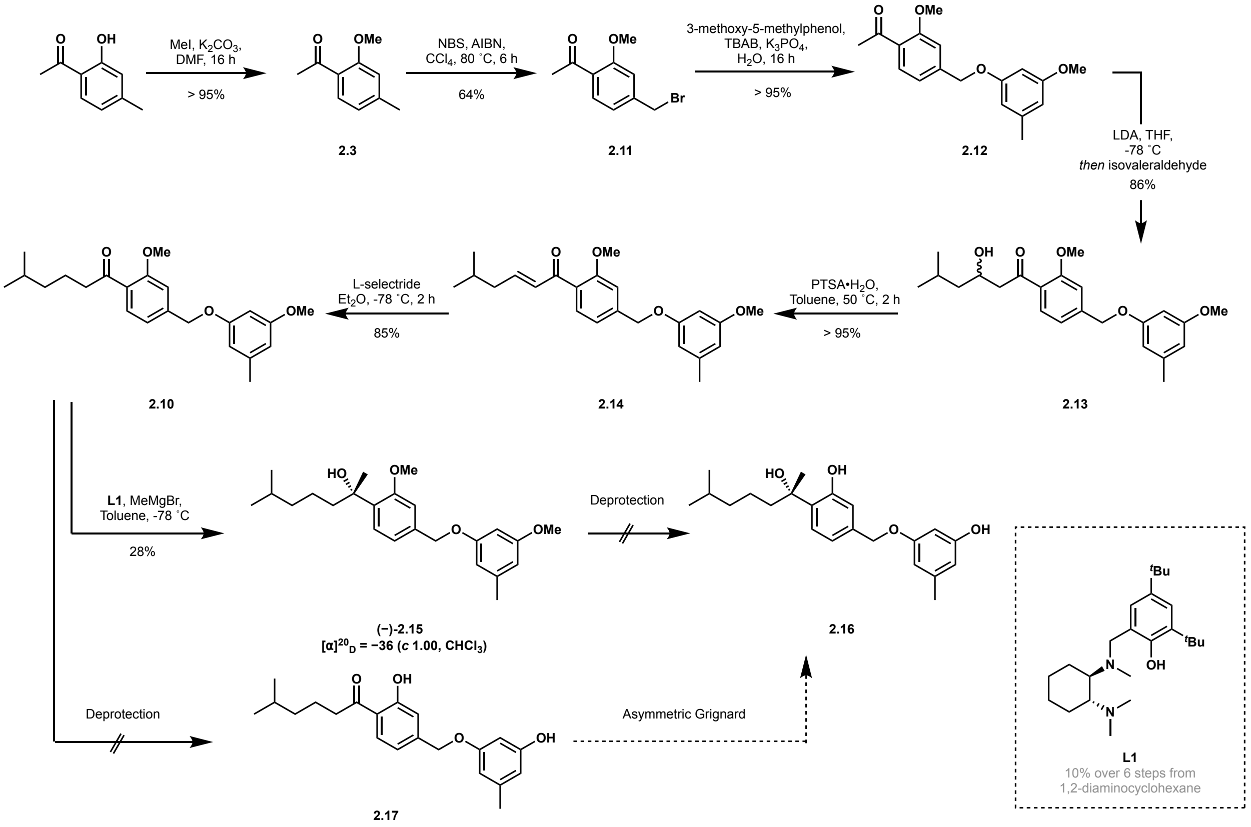
MeI, K2CO3, DMF, 16 h
> 95%
NBS, AIBN, CCl4, 80 °C, 6 h
64%
3-methoxy-5-methylphenol, TBAB, K3PO4, H2O, 16 h
> 95%
LDA, THF, -78 °C then isovaleraldehyde
86%
PTSA•H2O, Toluene, 50 °C, 2 h
> 95%
L-selectride Et2O, -78 °C, 2 h
85%
L1, MeMgBr, Toluene, -78 °C
28%
Deprotection
Deprotection
Asymmetric Grignard
2.3
2.11
2.12
2.13
2.14
2.10
(−)-2.15
[α]20D = −36 (c 1.00, CHCl3)
2.16
2.17
L1
10% over 6 steps from 1,2-diaminocyclohexane

Scheme 2.6. Synthesis of model substrate for stereoselective Grignard addition.

The asymmetric Grignard addition was performed with diamine ligand (**L1**) synthesized in 6 steps via reported procedure[27] (SI Scheme **S2.1**). The proposed transition state involves coordination of the ligand and carbonyl to the first equivalent of methylmagnesium bromide, which exists as a dimer with the second equivalent. The bulky *t*-Bu groups on the phenol ring block the bottom face of the magnesium complex, forcing the carbonyl to approach the nucleophile from the top face. The second equivalent then facilitates stereoselective *si*-face addition of the methyl nucleophile to the carbonyl. To obtain high stereoselectivity, it is critical for all components to coordinate to the magnesium center. Optically enriched tertiary alcohol was produced in low yield, predominately recovering starting material from the reaction likely due to the steric hindrance of the reacting carbonyl and controlled equivalents of methyl magnesium bromide to maintain good stereoselectivity[27]. Unfortunately attempts to perform the final deprotection led to decomposition of starting material and efforts to perform the deprotection prior to Grignard addition resulted in monodeprotection of the phenol core at low temperatures. This may be due to the electron withdrawing effects of the ortho carbonyl and electron dense orcinol fragment increasing or decreasing the electrophilicity of the respective methoxy groups. Increasing equivalents of BBr_3 or allowing the reaction to warm to 0 ˚C resulted in monodeprotection and simultaneous cleavage of the orcinol fragment to produce benzylic bromide (SI **2.18**). Furthermore, Gilheany notes bidentate ligands do not offer the same stereocontrol as tridentate ligands and incorporation of a solvent capable of chelating to the magnesium center (*i.e.* THF) results in no stereoselectivity[27]. Thus, attempting the transformation with unprotected ortho phenol would likely lead to erosion of stereoselectivity due to potential coordination of the phenol to the ligand-magnesium complex and subsequent ligand or carbonyl displacement (Figure **2.8**). To probe this hypothesis, the reaction was attempted with free phenol and observed no optical rotation for the isolated product. Although the enantioselective Grignard route was beginning to reach a roadblock, concurrent work on a third alternative route to peniciaculin A via diastereoselective

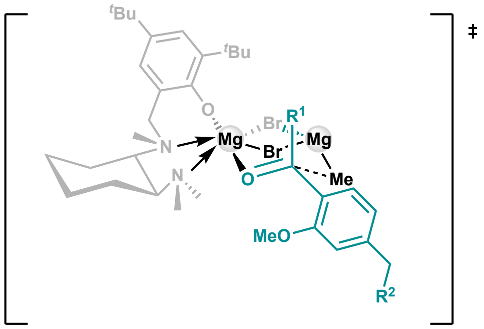

Figure 2.8 Proposed asymmetric transition state.

nucleophilic addition with a chiral imidazolidinone was encouraging and efforts were concentrated to optimize these transformations.

2.2.3. Chiral imidazolidinone

The previous syntheses of phenolic bisabolanes utilizing a diastereoselective nucleophilic addition with a chiral imidazolidinone required excess aryl bromide and suffered from irreproducible Grignard formations leading to inconsistent yields to generate the tertiary alcohol[29]. Thus, approaching this route, we aimed to optimize the key Grignard addition while maintaining flexibility to facilitate future analogue development. The retrosynthetic plan mirrored the previous routes, apart from the alkyl sidechain. We now envisioned deriving the side chain from a homologation and late-stage cross-metathesis from a key homobenzylic aldehyde and building the aldehyde from commercially available methyl 4-bromo-3-hydroxybenzoate (Scheme **2.7**).

Following Ito and coworker's described route to (+)-sydonol, we first explored the reported Grignard addition with known SEM protected substrate[29] (Scheme **2.8**). Chiral imidazolidinone (*R,S*) **(−)-2.20** was synthesized from *N*-Boc-*L*-proline in 5-steps[28, 30] or from commercially available (*S*)-(+)-2-(anilinomethyl)pyrrolidine in 2 steps[29] (SI scheme **S2.2**). Of note, the (*S,R*) enantiomer **(+)-2.20** was synthesized from *N*-Boc-*D*-proline following the same 5 step route. Initial attempts to reproduce Ito and coworkers' results[29] were of varying success obtaining a range of 0 to 60% yield of the homobenzylic aldehyde with respect to the limiting reagent, the imidazolidinone. The irreproducibility of the Grignard addition and requirement of excess aryl bromide (two equivalents) which underwent protodebromination upon protic quenching of the

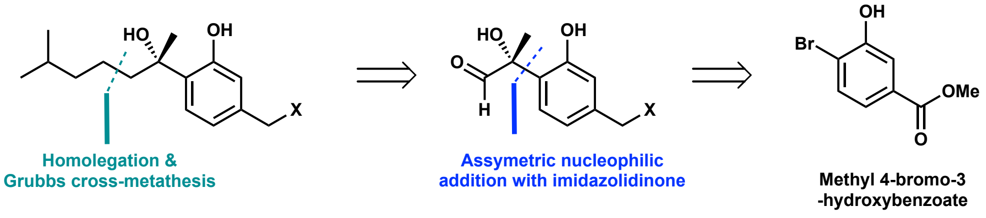

Scheme 2.7. Retrosynthetic approach 3.0 to peniciaculin A.

reaction suggested an alternative method for forming the aryl nucleophile would be necessary to complete a robust synthesis of peniciaculin A.

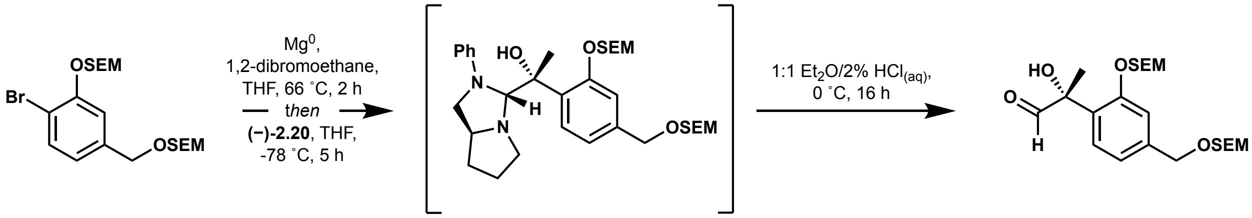
OSEM
Br
OSEM
Mg⁰,
1,2-dibromoethane,
THF, 66 ˚C, 2 h
then
(−)-2.20, THF,
-78 ˚C, 5 h
Ph
N
HO
N
H
OSEM
OSEM
1:1 Et₂O/2% HCl(aq),
0 ˚C, 16 h
HO
O
H
OSEM
OSEM

Scheme 2.8. Reported Grignard addition.

We were also anxious to explore methods for the installation of the diaryl ether fragment, a step previously unexplored in the synthesis of phenolic bisabolanes. We envisioned forming key intermediate **2.21** prior to aryl nucleophile formation as a platform for future analogue design (Scheme **2.9**). To differentiate the phenol from the benzylic alcohol and avoid potential dimerization of the aryl bromide, we began our synthesis with SEM protection of the phenol followed by reduction of the methyl ester to the benzylic alcohol. Although small scale DIBAL-H

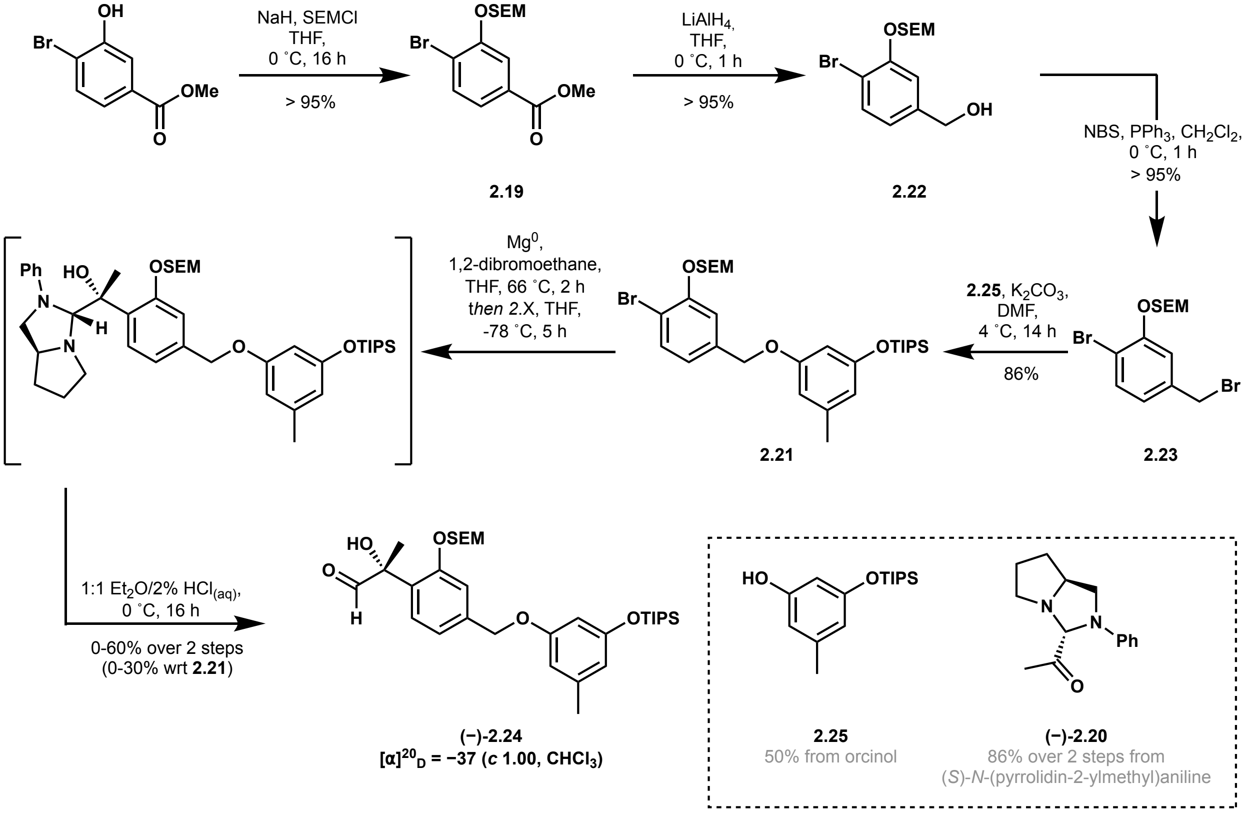
OH
Br
OMe
O
NaH, SEMCl
THF,
0 ˚C, 16 h
> 95%
OSEM
Br
OMe
O
2.19
LiAlH₄,
THF,
0 ˚C, 1 h
> 95%
OSEM
Br
OH
2.22
NBS, PPh₃, CH₂Cl₂,
0 ˚C, 1 h
> 95%
OSEM
Br
Br
2.23
2.25, K₂CO₃,
DMF,
4 ˚C, 14 h
86%
OSEM
Br
O
OTIPS
2.21
Mg⁰,
1,2-dibromoethane,
THF, 66 ˚C, 2 h
then 2.X, THF,
-78 ˚C, 5 h
Ph
N
HO
N
H
OSEM
O
OTIPS
1:1 Et₂O/2% HCl(aq),
0 ˚C, 16 h
0-60% over 2 steps
(0-30% wrt 2.21)
HO
O
H
OSEM
O
OTIPS
(−)-2.24
[α]²⁰D = −37 (c 1.00, CHCl₃)
HO
OTIPS
2.25
50% from orcinol
N
N
Ph
O
(−)-2.20
86% over 2 steps from
(S)-N-(pyrrolidin-2-ylmethyl)aniline

Scheme 2.9. Diastereoselective Grignard addition with peniciaculin A core.

reduction produced the benzylic alcohol **2.22** in near quantitative yield, reactions run on gram scale resulted in predominately SEM truncation. Slow addition of LAH to cooled reaction mixture and short reaction times, however, produced the desired benzylic alcohol with minimal SEM truncation. SEM truncation with DIBAL-H is likely due to the longer reaction times and increased temperature required for reduction compared to LAH, leading to the undesired truncation. From there, we attempted to directly install monoprotected orcinol via Mitsunobu displacement of the benzylic alcohol[38]. Although various diazodicarboxylates were screened, no displacement of the benzylic alcohol was observed (Table **2.3**, entry 1). Transforming the benzylic alcohol to a benzylic bromide was then attempted using standard Appel conditions[39] leading to SEM truncation (Table **2.3**, entry 2). SEM truncation may be occurring through a similar mechanism reported for the deprotection of MOM groups with CBr_4 and PPh_3[40], although deprotection typically requires elevated temperatures (refluxing methylene chloride) and *para* electron-withdrawing groups (EWG). Alternatively, slow addition of PBr_3 at low temperatures successfully furnished the benzylic bromide on small scale while avoiding SEM truncation (Table **2.3**, entry 3). Attempting to scale up the reaction, however, lead to solely SEM truncated product, potentially due to larger scale production of HBr (Table **2.3**, entry 4). Modifying Appel conditions using NBS as the electrophilic source of bromide was successful on both small and large scales in high yield with slow addition of a suspension of NBS in CH_2Cl_2 to the cooled reaction mixture (Table **2.3**, entries 5&6).

Table 2.3. Benzylic activation.

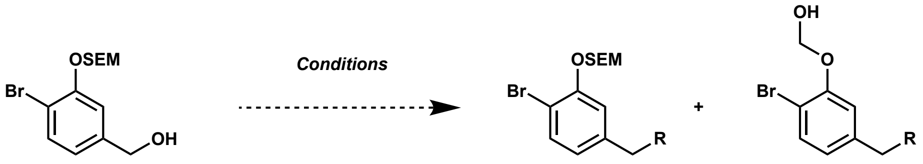

2.22 SEM truncation

Entry	R	Conditions	Scale	Result
1	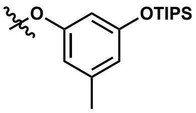	2.25, PPh_3, azodicarboxylate, THF	50 mg	nr
2	Br	CBr_4, PPh_3, CH_2Cl_2, 0 ˚C, 20 min	20 mg	SEM truncation
3	Br	PBr_3 (dropwise), CH_2Cl_2, 0 ˚C, 1 h	400 mg	70% yield
4	Br	PBr_3 (dropwise), CH_2Cl_2, 0 ˚C, 1 h	1 g	SEM truncation
5	Br	NBS (0.1M in CH_2Cl_2), PPh_3, CH_2Cl_2, 0 ˚C, 1 h	100 mg	>95% yield
6	Br	NBS (0.1M in CH_2Cl_2), PPh_3, CH_2Cl_2, 0 ˚C, 1 h	2 g	>95% yield

The benzylic bromide underwent subsequent substitution under basic conditions with monoTIPS protected orcinol. Although using monoTIPS protected orcinol would allow for selective TIPS deprotection in the presence of SEM protected phenol of the diaryl fragment for late stage diaryl ether coupling, it is moderately base sensitive. Thus, dimerization was observed leading to the formation of a triaryl intermediate upon potassium carbonate facilitated TIPS deprotection with standard reaction conditions. Shortening reaction time resulted in a mix of starting material, dimer, and desired product. Holding the reaction temperature at 4 ˚C using a stir plate in the refrigerator overnight prevented TIPS deprotection and dimerization, resulting in complete conversion of starting material to the desired product **2.21**.

We attempted to reproduce the conditions reported by Ito and coworkers to form **(−)-2.24** via Grignard formation and diastereoselective nucleophilic addition with imidazolidinone **(−)-2.20**[29]. Although we had minor success in producing the homobenzylic alcohol, yields were variable ranging from 0-60% with respect to the limiting reagent **2.21**. The conditions reported by Ito required 2 equivalents of aryl bromide. Therefore, our yields were in the range of 0-30% with respect to advanced intermediate **2.21**. Although we attempted optimization of Grignard formation through addition of 4Å MS, activation of Mg^0, freshly distilled solvent, and longer reaction times, we found protodebromination was always the predominant product and starting material was never recovered. Thus, we sought a more robust method to produce the desired aryl nucleophile to form the tertiary alcohol aiming to use the aryl bromide **2.21** as the limiting reagent.

Grignard nucleophiles can suffer from decreased nucleophilicity due to the more covalent nature of the Mg-C bond. Therefore, we proposed using a lithium halogen exchange to produce a lithiated species and increase the ionic character of the metal-C bond, in this case Li-C. We had previously experienced great success generating a benzaldehyde intermediate (**2.35**) using this strategy to develop simplified analogues of peniciaculin A. Of note, the SEM protecting group appeared to be non-interchangeable with other silyl or alkyl derived protecting groups for the lithium-halogen exchange. The main concern was diminished diastereoselectivity depending on the favored transition state of nucleophilic addition (Figure **2.9**). Desired *anti*-addition of the aryl

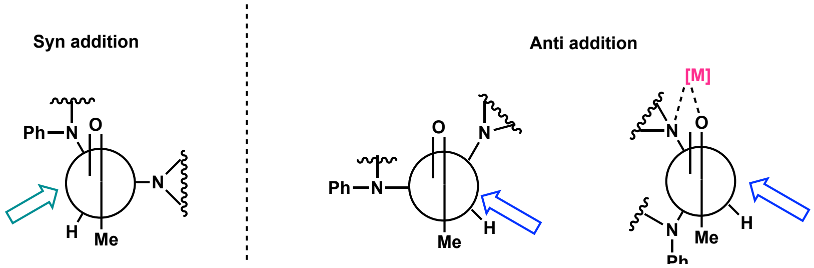

Figure 2.9. Proposed model for diastereoselective nucleophilic addition.

Grignard was promoted by chelation of the proline nitrogen and carbonyl with divalent Mg[30]. However, the same chelation is not possible using monovalent Li as a counterion.

With this in mind, optimization of the lithium-halogen exchange begun noting that if *syn*-addition was observed, the (*S, R*) enantiomer of the imidazolidinone could be used to set the desired tertiary alcohol stereocenter. Fortunately, comparing the optical rotations of **2.24** produced by both Grignard and lithium-halogen exchange, we observed anti-addition of the lithiated species due to the preferred Felkin-Ahn confirmation adopted by the imidazolidinone. We also aimed to use the aryl bromide **2.21** as the limiting reagent to avoid protodebromination of the valuable intermediate. Treatment of one equivalent of aryl bromide **2.21** at -78˚C with TMEDA followed by *n*-BuLi produced the desired lithiated species which then underwent reaction with the chiral imidazolidinone at -78˚C to form the benzylic tertiary alcohol (Table **2.4**, entry 1). Removing TMEDA resulted in no detectable product formation, likely due to decreased stability of the lithiated species (Table **2.4**, entry 2).

Table 2.4. Optimization of key lithium-halogen exchange.

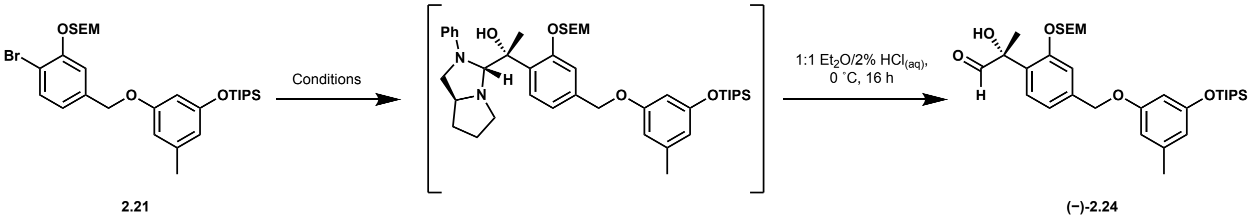

2.21

(−)-2.24
$[\alpha]^{20}_{D}$ = −39.0 (*c* 1.00, $CHCl_3$)

Entry	TMEDA	Mol Sieves	Electrophile	Time[a]	Yield (%)
1	Yes	No	Imidazolidinone (−)-2.20[b]	5 h	34
2	No	No	Imidazolidinone (−)-2.20[b]	5 h	Trace
3	Yes	Yes	Imidazolidinone (−)-2.20[b]	5 h	65
4	Yes	Yes	DMF	5 h	80
5	Yes	Yes	Imidazolidinone (−)-2.20[b]	18 h	76

[a]Reactions were stirred for 2 h at -78 ˚C prior to electrophile addition. Times recorded are reaction length after electrophile addition
[b]1.5 equiv of imidazolidinone was used for standard conditions. Increasing the equivalents of imidazolidinone did not imrpove yield

Despite the reproducibility of our results, we sought to investigate the source of protodebromination of the lithiated species. We found addition of crushed 4Å MS to remove any remaining H_2O led to a two-fold increase in the yield of the tertiary alcohol (Table **2.4**, entry 3). We continued to observe protodebromination product, however, and concluded this was likely due to slow and incomplete reaction of the nucleophile with the chiral imidazolidone as we'd obtained minimal protoderbromination using DMF as the electrophile (Table **2.4**, entry 4). Increasing reaction time to 18 hours at -78 ˚C further mitigated protodebromination leading to good yield of the desired product (Table **2.4**, entry 5). Hydrolysis of the aminal unmasked aldehyde **(−)-2.24** and investigations of the ee of this transformation are currently underway. The homobenzylic aldehyde was homologated to terminal alkene **(−)-2.26** using standard Wittig conditions. Subsequent Grubbs cross-metathesis with excess 4-methyl-1-pentene occurred at reflux in CH_2Cl_2. Careful separation with preparative thin layer chromatography (PTLC) efficiently recovered starting material and isolated desired product **(−)-2.27**. Selective TIPS deprotection at 0 ˚C furnished free phenol **(−)-2.28** primed for diaryl ether coupling (Scheme **2.10**).

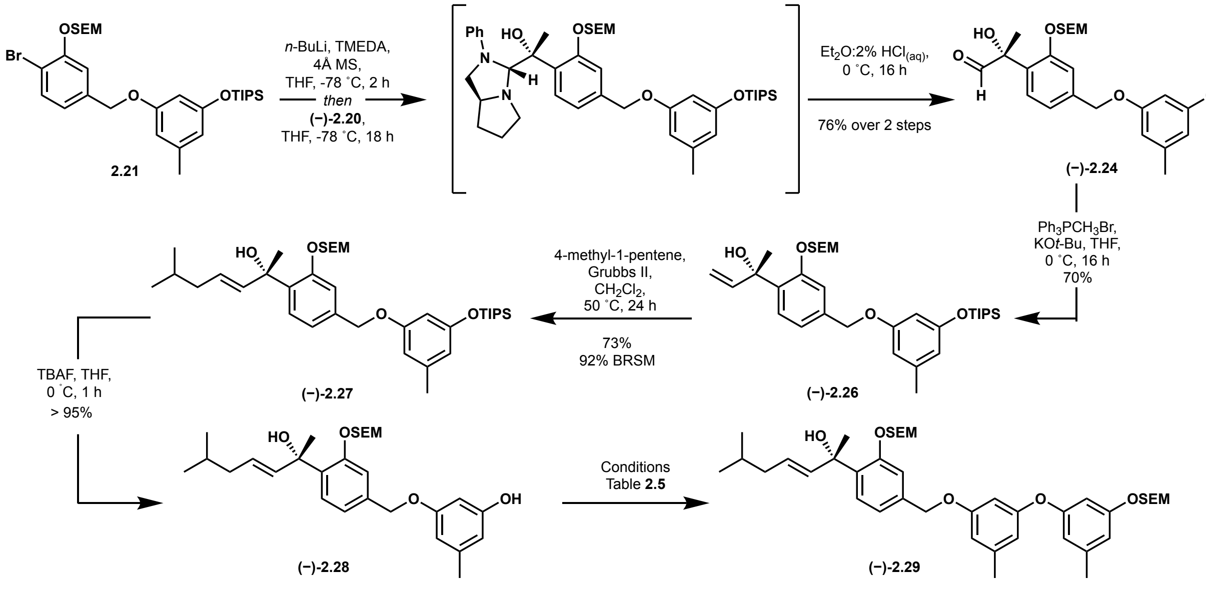
OSEM
Br
O
OTIPS
2.21
n-BuLi, TMEDA,
4Å MS,
THF, -78 ˚C, 2 h
then
(−)-2.20,
THF, -78 ˚C, 18 h
Ph
HO
N
N
H
Et₂O:2% HCl(aq),
0 ˚C, 16 h
76% over 2 steps
O
H
(−)-2.24
Ph₃PCH₃Br,
KOt-Bu, THF,
0 ˚C, 16 h
70%
(−)-2.26
4-methyl-1-pentene,
Grubbs II,
CH₂Cl₂,
50 ˚C, 24 h
73%
92% BRSM
(−)-2.27
TBAF, THF,
0 ˚C, 1 h
> 95%
OH
(−)-2.28
Conditions
Table 2.5
(−)-2.29

Scheme 2.10. Synthesis of the carbon skeleton of peniciaculin A.

Initially, a palladium catalyzed Buchwald coupling was proposed between free phenol and aryl halide equivalent[41] (Table **2.5**, entry 1). No success was observed with aryl triflate coupling partners, thus we decided to synthesize the more active aryl bromide. Although conversion of the aryl triflate to aryl bromide was attempted via Miyaura borylation followed by bromination with $CuBr_2$, $MgBr_2$[42], or Br_2 and PPh_3[43], both methods resulted in no reaction or decomposition of starting material. I also attempted conversion of orcinol directly to 3-bromo-5-methylphenol with PPh_3 and Br_2[44] or PBr_3[45] but observed decomposition of starting material. These transformations were likely inhibited by the electron dense orcinol ring and would require strong EWGs, such as a nitro substituent, to proceed. Adapting a procedure reported by Huang and coworkers, we transformed commercially available 3,5-dibromotoluene to 3-bromo-5-methylphenol in two steps[46]. A monolithium-halogen exchange using *t*-BuLi followed by addition of triisopropyl borate was performed to form the boronic acid **2.30**. Subsequent oxidation with KOH and H_2O_2 furnished phenol **2.31** in 76% yield over two-steps. Following SEM protection of the phenol, aryl bromide **2.32** was primed for optimization of the diaryl ether coupling (Scheme **2.11**).

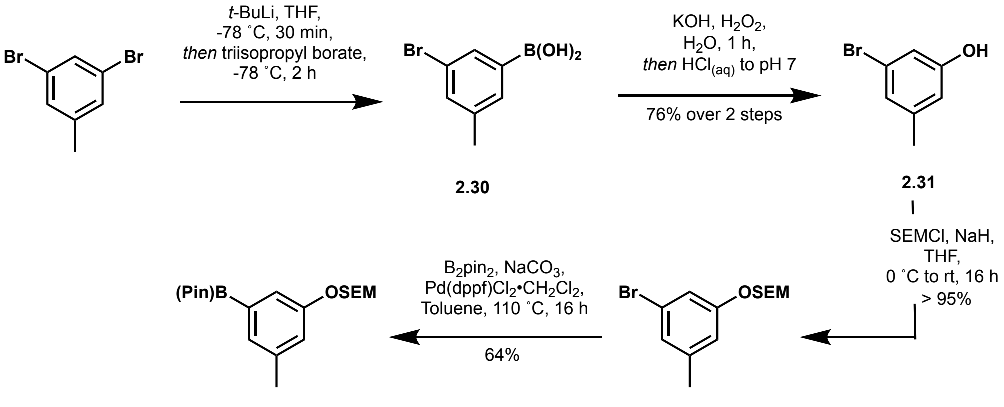
Br
Br
t-BuLi, THF,
-78 ˚C, 30 min,
then triisopropyl borate,
-78 ˚C, 2 h
Br
B(OH)₂
2.30
KOH, H₂O₂,
H₂O, 1 h,
then HCl(aq) to pH 7
76% over 2 steps
Br
OH
2.31
SEMCl, NaH,
THF,
0 ˚C to rt, 16 h
> 95%
Br
OSEM
2.32
B₂pin₂, NaCO₃,
Pd(dppf)Cl₂•CH₂Cl₂,
Toluene, 110 ˚C, 16 h
64%
(Pin)B
OSEM
2.33

Scheme 1.11. Synthesis of aryl bromide coupling partner.

Copper catalyzed Ullman type coupling with standard reported conditions resulted in decomposition of starting material[47] (Table **2.5**, entry 2). Utilizing Cs_2CO_3 to increase the solubility of the reaction intermediates and incorporation of a pyridine ligand (**L2**) to facilitate oxidative addition of proposed Cu(I) to the aryl bromide led to no reaction at lower temperatures and decomposition of starting material as temperature increased[48, 49] (Table **2.5**, entries 3&4). This is likely due to the electron dense coupling partners potentially slowing reductive elimination and thus the bond forming step of the Ullman type reaction[50].

Leveraging intermediate **2.32**, we were able to perform a successful palladium catalyzed Miyaura borylation with bis(pinacolato)diboron thus producing the aryl boronic ester **2.33** for a copper catalyzed Chan Lam coupling. We took inspiration from reports by the Watson group at Strathclyde University in collaboration with GlaxoSmithKline and the Stahl group at University of Wisconsin-Madison. Watson and coworkers noted several components that were key to the reaction success such as use of excess $B(OH)_3$ to complex pinacol to prevent formation of pinacol/copper complexes that shut down the copper catalyzed mechanism. Additionally, running the reaction under a dry air or O_2 atmosphere allows re-oxidation of Cu(I) to Cu(II), the active catalyst species[51, 52]. Faster oxidation of Cu(I) to Cu(II) can also be facilitated using an amine base or $B(OH)_3$ to prevent side reactions of the Cu(I) species. Although this methodology was successfully applied to the reaction design of a similar substrate (**2.50**), the reaction was unsuccessful for the natural product scaffold (Table **2.5**, entry 5).

Fortunately, Schutzenmeister and coworkers recently published a report on palladium catalyzed C-O bond couplings to synthesize anti-MRSA diaryl ethers derived from orcinol. A catalyst, ligand, and base screen were completed, and they noted choice of base was crucial to the success of the reaction. Their investigations suggest $K_3PO_4 \cdot H_2O$ may act as a hydroxide donor to deprotonate the phenol and facilitate bromide dissociation from Pd^{II}. Using an alternative Pd^0 source, phosphine ligand, or base led to no reaction or decomposition of the starting material[53].

Applying this reaction system to our coupling, we produced the desired C-O bond forming the full carbon skeleton of peniciaculin A (Table **2.5**, entry 6).

Table 2.5. Diaryl ether coupling.

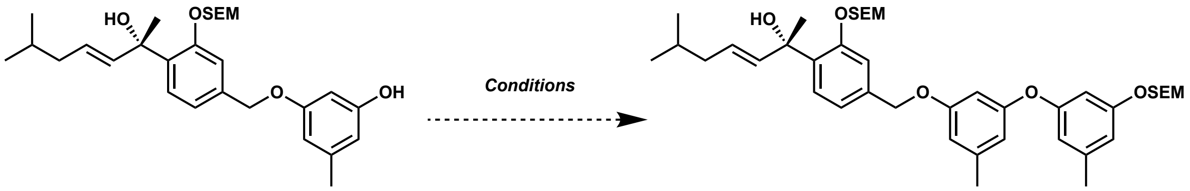
HO
OSEM
OH
Conditions
HO
OSEM
O
O
OSEM

2.28

2.29

Entry	Aryl halide coupling partner	Conditions	Result
1	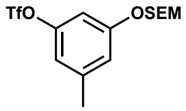	Pd(OAc)$_2$, Johnphos, K$_3$PO$_4$, toluene, 100 ˚C, 18 h	nr
2	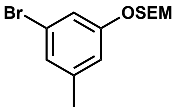	CuBr, KO*t*-Bu, DMSO, 120 ˚C, 16 h	Decomp
3	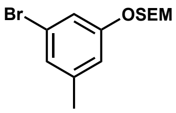	CuBr, L2[a], Cs$_2$CO$_3$, DMSO, 90 ˚C, 16 h	nr
4	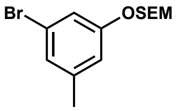	CuBr, L2[a], Cs$_2$CO$_3$, DMSO, 120 ˚C, 16 h	Decomp
5	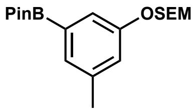	Cu(OAc)$_2$, B(OH)$_3$, 4Å MS, CH$_3$CN, 80 ˚C, 1.5 days	nr
6	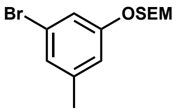	Pd$_2$(dba)$_3$, *t*-BuXPhos, K$_3$PO$_4$·H$_2$O, dioxane, 100 ˚C, 16 h	85%

[a] L2 = 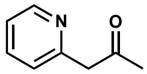

With the full triaryl fragment in hand, we performed a global SEM deprotection using excess TBAF and DBU, both dried over 4Å MS for 24 h prior to use, at 80 ˚C. Although truncation of SEM was a major challenge in optimizing the first steps of the synthesis, deprotection proceeded smoothly to produce **(−)-2.34**. We anticipated reduction of the olefin using standard conditions would likely result in cleavage of the entire eastern diaryl ether fragment via benzylic hydrogenation akin to traditional benzyl deprotection. Thus, we performed the final olefin hydrogenation with Lindlar catalyst and observed peaks correlating to peniciaculin A in the crude ^{1}H NMR. Work is ongoing to optimize the final hydrogenation (Scheme **2.12**).

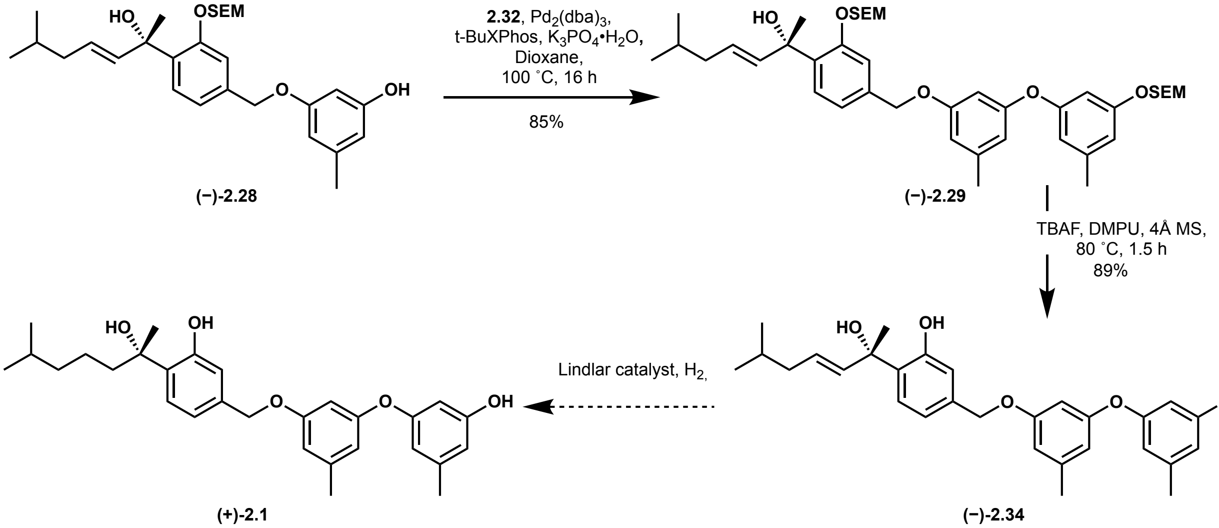
HO
OSEM
OH
(−)-2.28
2.32, Pd2(dba)3,
t-BuXPhos, K3PO4•H2O,
Dioxane,
100 °C, 16 h
85%
HO
OSEM
O
O
OSEM
(−)-2.29
TBAF, DMPU, 4Å MS,
80 °C, 1.5 h
89%
HO
OH
O
O
OH
(+)-2.1
Lindlar catalyst, H2,
HO
OH
O
O
OH
(−)-2.34

Scheme 2.12. Peniciaculin A end game.

2.2.4. Analogue design and synthesis

Analogue design of peniciaculin A was predominately based on systematic truncation of the orcinol components and modifications to the alkyl sidechain (Figure **2.10**). Existing QoIs consist of polyaromatic and highly conjugated systems[17]. Thus, we were curious if a truncated version of peniciaculin A could maintain activity while more closely mimicking structures of known fungicides such as picoxystrobin, kresoxim-methyl, or mandestrobin[14]. Furthermore, truncated analogues could be accessed in two steps less than triaryl derivatives and would eliminate the use a Pd coupling step and *t*-BuLi. We were also curious if the diaryl ether eastern fragment would demonstrate antifungal activity as antibacterial activity of such structures has been reported previously[53]. Finally, if peniciaculin A is mimicking ubiquinone as a QoI simplification of the alkyl side chain for a conjugated system may be tolerated.

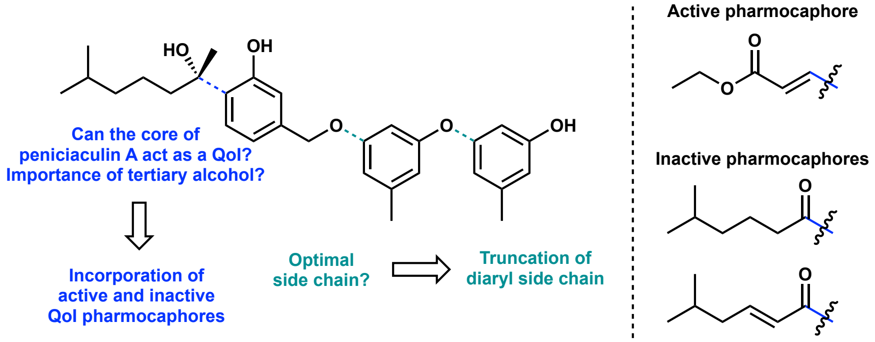
HO
OH
O
O
OH
Can the core of peniciaculin A act as a QoI? Importance of tertiary alcohol?
Incorporation of active and inactive QoI pharmocaphores
Optimal side chain?
Truncation of diaryl side chain
Active pharmocaphore
O
O
Inactive pharmocaphores
O
O

Figure 2.10. Analogue design for peniciaculin A.

2.2.4.1. Ethoxy acrylate analogues

To probe our hypothesis that peniciaculin A is acting as a QoI, we aimed to assess if the phenol and diorcinol fragment were mimicking the prototypical central ring and sidechain structure. By replacing the alkyl sidechain with known QoI pharmacophore, ethoxy-acrylate, we hypothesized analogues would maintain activity against *A. brassicae* and would likely demonstrate broad spectrum antifungal activity. Analogues were derived from **2.21** via lithium-halogen exchange of the aryl bromide and nucleophilic addition with DMF to form benzaldehyde **2.35**. Horner-Wadsworth Emmons (HWE) followed by global silyl deprotection produced a truncated ethoxy-acrylate analogue **2.37**. Selective TIPS deprotection of **2.37** followed by palladium catalyzed Buchwald coupling of aryl bromide and global SEM deprotection produced the full triaryl acrylate analogue **2.40** (Scheme **2.13**).

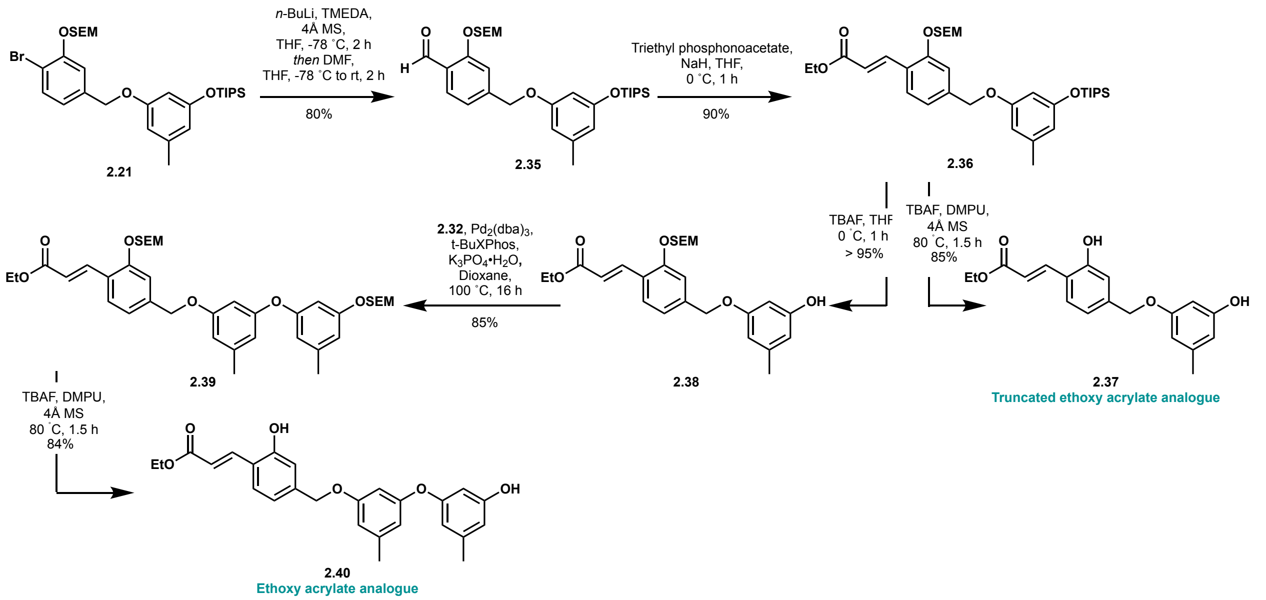
Br
OSEM
O
OTIPS
2.21
n-BuLi, TMEDA,
4Å MS,
THF, -78 °C, 2 h
then DMF,
THF, -78 °C to rt, 2 h
80%
H
O
OSEM
OTIPS
2.35
Triethyl phosphonoacetate,
NaH, THF,
0 °C, 1 h
90%
EtO
O
OSEM
OTIPS
2.36
TBAF, THF
0 °C, 1 h
> 95%
TBAF, DMPU,
4Å MS
80 °C, 1.5 h
85%
OH
OH
2.37
Truncated ethoxy acrylate analogue
2.32, Pd2(dba)3,
t-BuXPhos,
K3PO4•H2O,
Dioxane,
100 °C, 16 h
85%
2.38
2.39
OSEM
TBAF, DMPU,
4Å MS
80 °C, 1.5 h
84%
2.40
Ethoxy acrylate analogue

Scheme 2.13. Synthesis of ethoxy acrylate analogues.

2.2.4.2. Ketone analogues

Intermediates from the enantioselective Grignard route to peniciaculin A served as a platform for simplified alkyl side chains to probe our novel pharmacophore hypothesis, forming triaryl ketone and diaryl ketone and enone analogues. These analogues were proposed to demonstrate minimal bioactivity if the tertiary alcohol was indeed acting as a QoI pharmacophore as the simplified sidechains are not known to have QoI activity. Diaryl ketone analogues were synthesized following the initial route, replacing the methoxy protecting group of the orcinol fragment for benzyl (**2.46**). This allowed final global deprotection of the diaryl scaffold with BBr_3 to afford deprotected diaryl **2.45** and served as a model study for global deprotection of the full triaryl analogue (Scheme **2.14**).

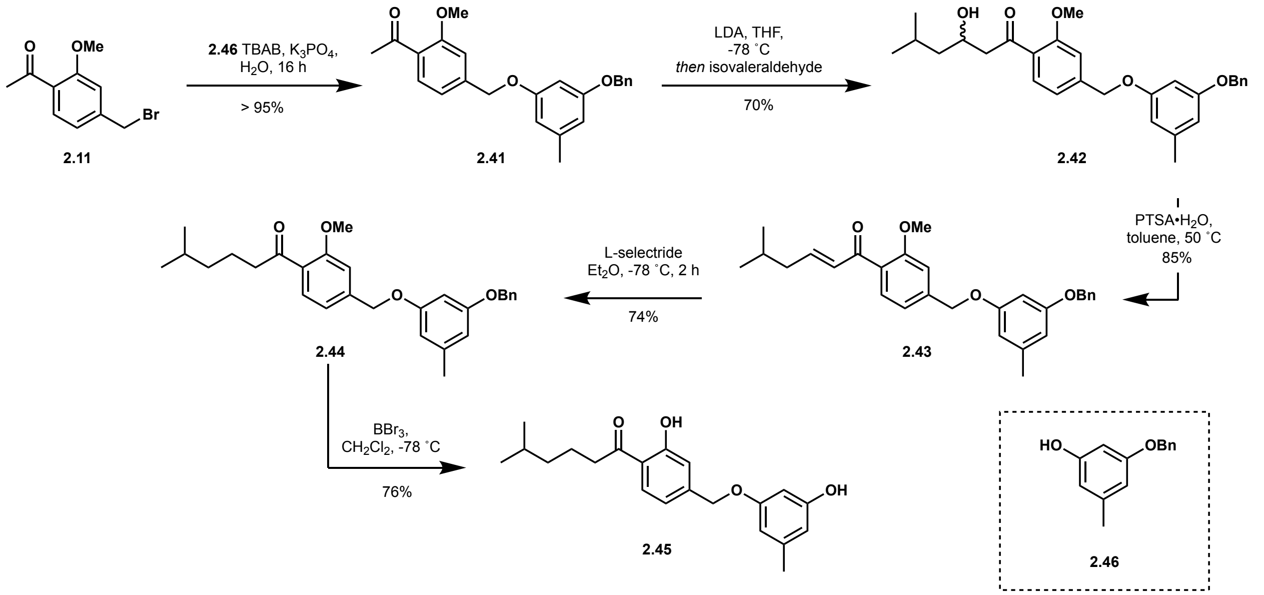
2.46 TBAB, K3PO4, H2O, 16 h
> 95%
LDA, THF, -78 ˚C then isovaleraldehyde
70%
PTSA•H2O, toluene, 50 ˚C
85%
L-selectride Et2O, -78 ˚C, 2 h
74%
BBr3, CH2Cl2, -78 ˚C
76%
2.11
2.41
2.42
2.43
2.44
2.45
2.46

Scheme 2.14. Synthesis of diaryl ketone analogues.

To produce triaryl analogues, monoTIPS protected orcinol was incorporated at the benzylic position of **2.11** via SN2 displacement of benzylic bromide. Following the initial route, aldol condensation with isovaleraldehyde resulted in enone **2.49**. TIPS deprotection produced enone analogue **2.50**. Chan-Lam coupling of free phenol **2.50** with aryl pinacol boronate **2.55** resulted in the full triaryl scaffold **2.51**. Although palladium catalyzed Buchwald coupling was also attempted with aryl bromide **2.32**, no desired product was isolated. Global deprotection of the methyl and benzyl groups was attempted to reveal the full triaryl enone analogue, however, only decomposition of starting material was observed. Final deprotection with BBr_3 at -78 ˚C after enone reduction by 1,4-addition with L-selectride, however, resulted in the desired triaryl ketone analogue **2.53** and monobenzyl deprotected triaryl **2.54** (Scheme **2.15**). Efforts to produce solely the global deprotected product **2.53** resulted in byproduct formation (*i.e.* benzyl ether cleavage and decomposition).

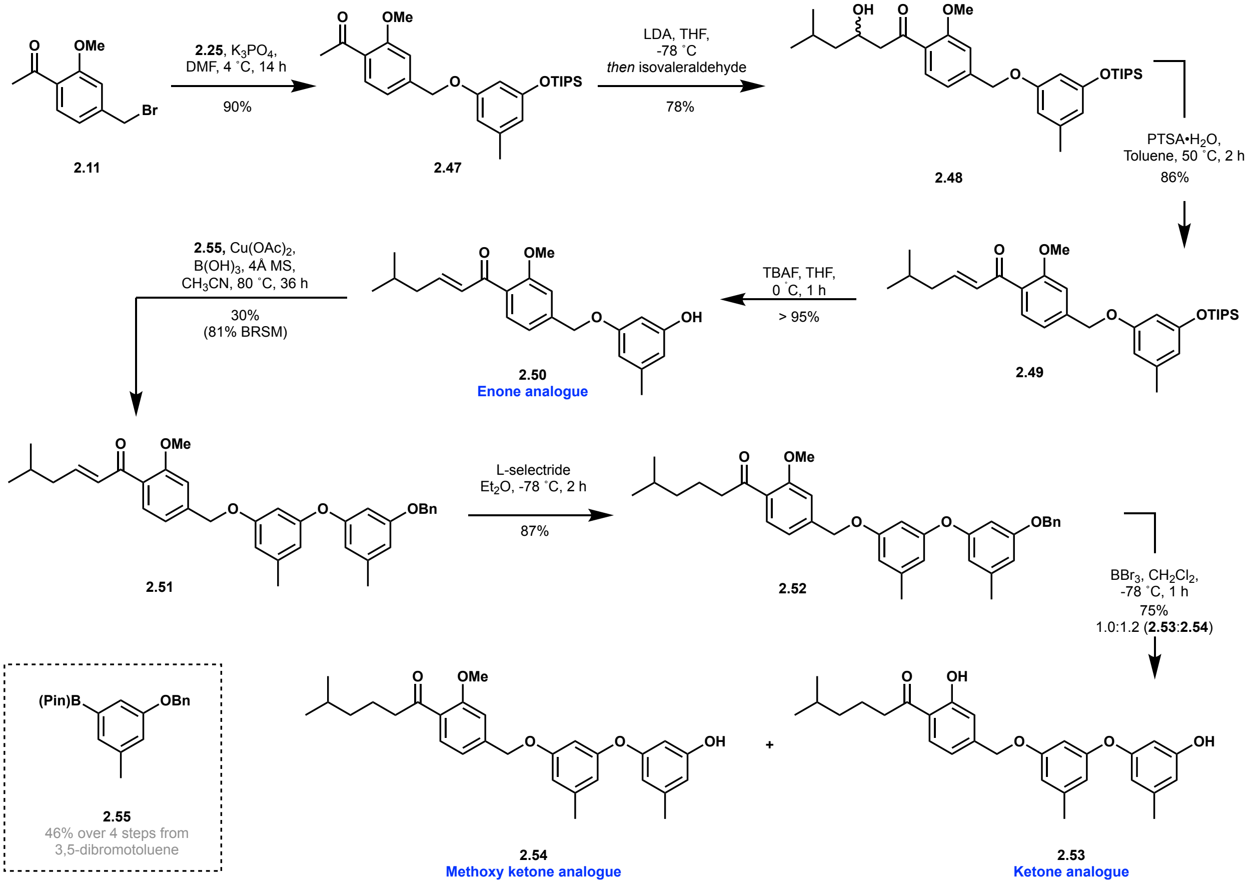

2.11
2.25, K3PO4, DMF, 4 °C, 14 h
90%
2.47
LDA, THF, -78 °C then isovaleraldehyde
78%
2.48
PTSA•H2O, Toluene, 50 °C, 2 h
86%
2.49
TBAF, THF, 0 °C, 1 h
> 95%
2.50
Enone analogue
2.55, Cu(OAc)2, B(OH)3, 4Å MS, CH3CN, 80 °C, 36 h
30%
(81% BRSM)
2.51
L-selectride Et2O, -78 °C, 2 h
87%
2.52
BBr3, CH2Cl2, -78 °C, 1 h
75%
1.0:1.2 (2.53:2.54)
(Pin)B
OBn
2.55
46% over 4 steps from 3,5-dibromotoluene
2.54
Methoxy ketone analogue
+
2.53
Ketone analogue
OMe
OTIPS
OH
Br

Scheme 2.15. Synthesis of triaryl ketone analogues.

2.2.4.3. Diorcinol analogues

Derivatives of dirocinol with substitution at one phenol exhibit potent antibacterial activity against MRSA[53] and we hypothesized similar activity may exist against fungal species. As these derivatives mimic the central ring and sidechain of QoIs, we were curious how omission of the pharmacophore and central ring would alter bioactivity. Thus, palladium catalyzed Buchwald coupling was performed on monobenzyl protected orcinol **2.46** with aryl bromide **2.32** followed by SEM deprotection to produce diaryl ether analogue **2.57**. With analogues in hand, we aimed to perform initial structure activity relationship evaluation of peniciaculin A in collaboration with Corteva Agriscience.

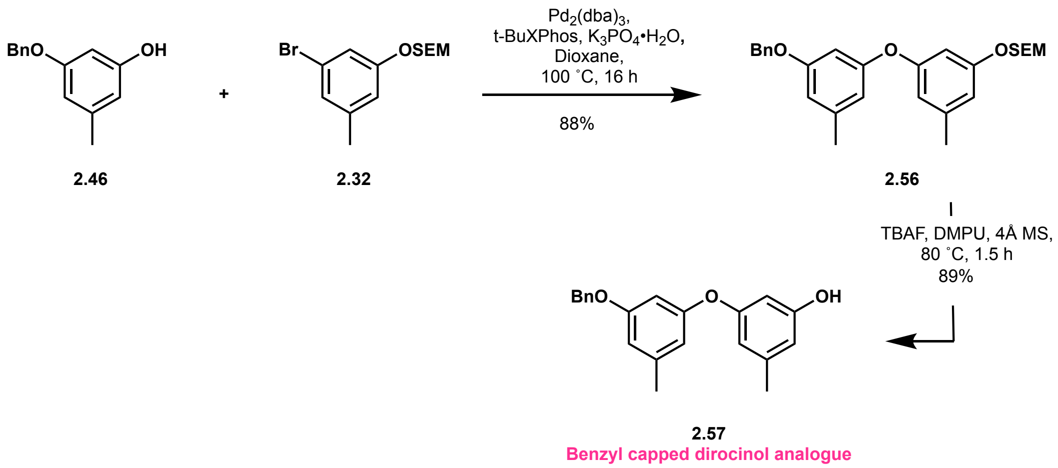

Scheme 2.16. Synthesis of diorcinol analogues.

2.2.5. Application of key transformation for the synthesis of other phenolic bisabolanes

Having completed the key step of the synthesis of peniciaculin A, we aimed to apply our optimized key transformation in the synthesis of other antimicrobial phenolic bisabolanes. We became interested in the synthesis of lactone containing phenolic bisabolane 1-hydroxyboivinianin A **(+)-2.2** due to its reported narrow spectrum activity against aquatic pathogen *Vibrio harveyi* (MIC = 4.0 μg/mL)[19]. *V. harveyi* is a gram-negative bacterium and is one of several bioluminescent species in the genus *Vibrio.* It is believed to be the primary cause of luminous vibriosis or "milky seas effect", in which great expanses of seawater translucently glow in various shades of blue. This phenomenon can occur on such a large scale it is even visible from satellites orbiting earth. The organism has also been critical in researchers' study and understanding of interspecies bacterial communication, known as quorum sensing[54].

Despite these intriguing attributes, pathogenic *V. harveyi* infections can lead to mass mortality in aquatic species, in particular in aquatic agricultural settings[55]. Human infections are also possible through consumption of undercooked seafood or exposure of an open wound while swimming. β-Lactams such as ampicillin and methicillin are used in clinical settings to treat *V. harveyi* infections[56]. With global warming causing rising ocean temperatures and decreasing water salinity, however, these infections are becoming more common and antibiotic resistance is likely to emerge[57]. Thus, paired with our optimized key transformation, the need for novel antibiotics made 1-hydroxyboivinianin A **(+)-2.2** an exciting target.

It was envisioned that 1-hydroxyboivinianin A **(+)-2.2** could be quickly accessed through a late-stage lactone formation from a linear precursor which could be further simplified to the homobenzylic aldehyde. From there, it was evident the homobenzylic aldehyde could be built via lithium-halogen exchange and nucleophilic addition with (*S*,*R*)-imidazolidinone **(+)-2.20** from commercially available 2-bromo-5-methylphenol (Scheme **2.17**). The proposed synthesis was 7-steps LLS. Unlike the (*R,S*)-imidazolidinone precursor (*S*)-(+)-2-(anilinomethyl)pyrrolidine, the (*S*,*R*) is not commercially available. Thus, optimization of the route was performed on *ent*-1-hydroxyboivinianin A **(−)-2.20** to avoid consumption of the more valuable (*S*,*R*)-imidazolidinone.

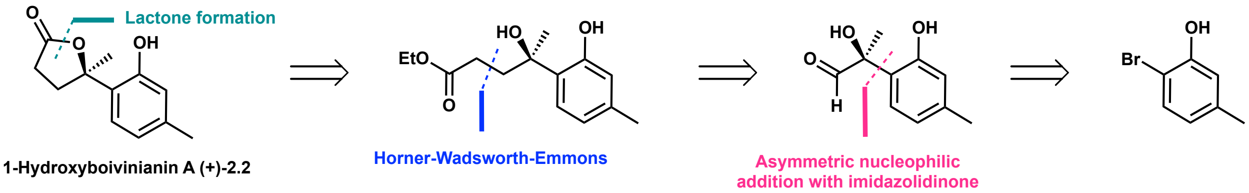

Lactone formation
O
O
OH
1-Hydroxyboivinianin A (+)-2.2
EtO
O
HO
OH
Horner-Wadsworth-Emmons
O
H
HO
OH
Asymmetric nucleophilic addition with imidazolidinone
Br
OH

Scheme 2.17. Retrosynthetic approach to 1-hydroxyboivinianin A.

In the synthesis of peniciaculin A, we'd experienced good yields for the lithium-halogen exchange using SEM as a phenol protecting group and observed no hemiacetal formation upon final deprotection. Thus, the synthesis began of *ent*-1-hydroxyboivinianin A **(−)-2.2** with SEM protection of 2-bromo-5-methylphenol. The substrate underwent subsequent lithium-halogen exchange and nucleophilic addition with imidazolidinone **(−)-2.20** followed by acidic hydrolysis to furnish the desired tertiary alcohol and homobenzylic aldehyde **(−)-2.59**. HWE reaction and olefin hydrogenation with Lindlar catalyst produced the linear precursor **(−)-2.61**. Initial attempts to perform an acid catalyzed lactone formation with PTSA·H_2O led to decomposition of the starting material. Under basic conditions, however, using excess LiOH, lactone **(−)-2.62** was formed in high yield. With the natural product in sight, the final SEM deprotection was performed using identical conditions to the final global SEM deprotection of peniciaculin A. New peaks appeared in the crude NMR, but they did not match the anticipated spectrum of *ent*-1-hydroxyboivinianin A. After purification, the ^{1}H NMR of the isolated product clearly showed two new peaks at 5.35 ppm and 5.17 ppm indicating SEM truncation to produce hemiacetal **(−)-2.63** (Scheme **2.18**). Although more promising results were found using less common deprotection conditions with $MgBr_2$[58], namely a mass hit for the desired product, it was anticipated that a change in protecting group strategy could expedite the synthesis of the desired natural product.

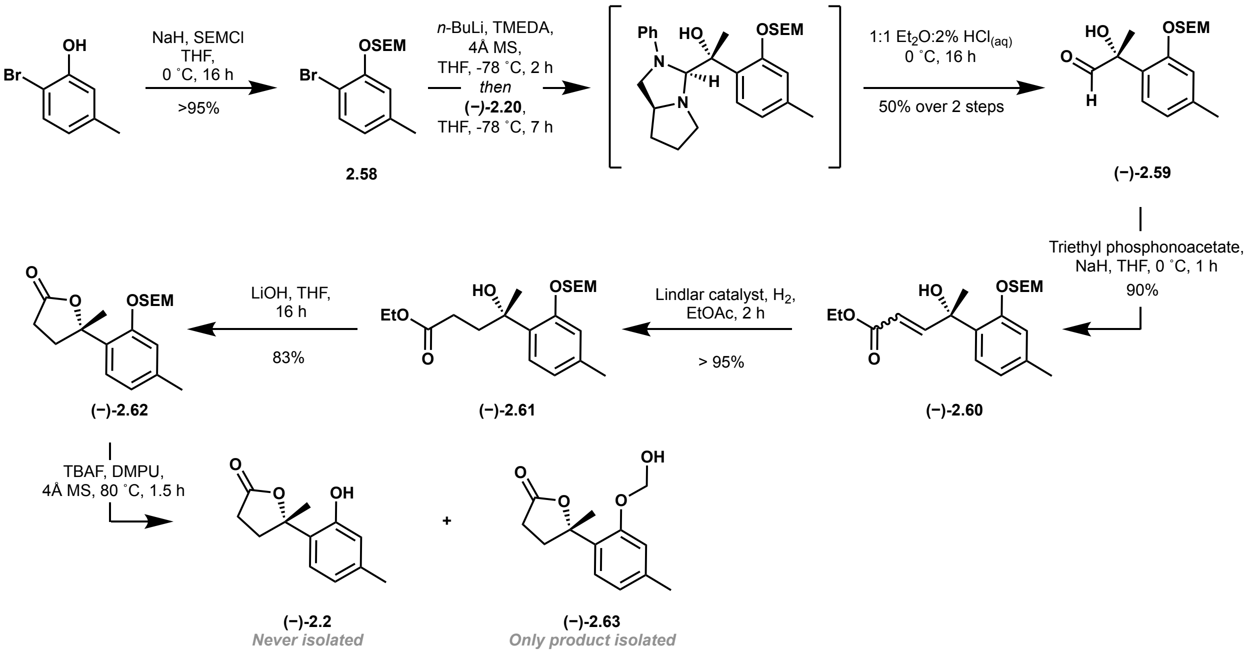

NaH, SEMCl THF, 0 °C, 16 h
>95%
2.58
n-BuLi, TMEDA, 4Å MS, THF, -78 °C, 2 h then (−)-2.20, THF, -78 °C, 7 h
1:1 Et2O:2% HCl(aq) 0 °C, 16 h
50% over 2 steps
(−)-2.59
Triethyl phosphonoacetate, NaH, THF, 0 °C, 1 h
90%
(−)-2.60
Lindlar catalyst, H2, EtOAc, 2 h
> 95%
(−)-2.61
LiOH, THF, 16 h
83%
(−)-2.62
TBAF, DMPU, 4Å MS, 80 °C, 1.5 h
(−)-2.2
Never isolated
(−)-2.63
Only product isolated

Scheme 2.18. Proposed synthesis of *ent*-1-hydroxyboivinianin A.

After careful consideration, it was reasoned that a benzyl protecting group could be removed in concert with olefin hydrogenation, thus reducing the step count from 7 to 6. Of note, previous explorations of alternative protecting groups in the synthesis of peniciaculin A demonstrated methoxy and other silyl phenol protecting groups were not compatible with the lithium halogen exchange, primarily leading to decomposition of starting material. It was envisioned, however, that the antibonding π^* orbitals of the benzyl protecting group could potentially stabilize the forming carbanion. Additionally, a proposed intramolecular HWE to form the lactone would reduce necessary purification steps (Scheme **2.19**).

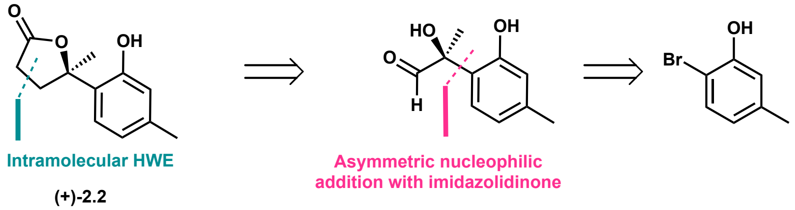

(+)-2.2

Scheme 2.19. Retrosynthetic approach 2.0 to 1-hydroxyboivinianin A.

Benzyl protection followed by lithium-halogen exchange and nucleophilic addition with imidazolidinone and hydrolysis of the aminal produced tertiary alcohol (+)-**2.65**. DCC coupling of (+)-**2.65** with diethylphosphonoacetic acid followed by treatment with NaH to produce the phosphonate carbanion resulted in intramolecular HWE with homobenzylic alcohol to form furanone (+)-**2.66**. Once again, the intermediate was one step away from the natural product and a final simultaneous benzyl deprotection and olefin hydrogenation was attempted with Pd/C. The isolated product, however, did not match the expected ^{1}H NMR, showing the benzylic methyl group as a doublet at 1.61 ppm. LCMS analysis indicated a mass of 208.11 g/mol suggesting benzyl ester cleavage to form the linear acid **2.68** occurred under the current deprotection conditions (Table **2.6**, entry 1).

Thus, optimization of conditions that would distinguish between benzyl deprotection and *p*-methylbenzyl ester cleavage was required. Benzyl groups are typically more susceptible to

Table 2.6. Optimization of hydrogenation in the synthesis of 1-hydroxyboivinianin A.

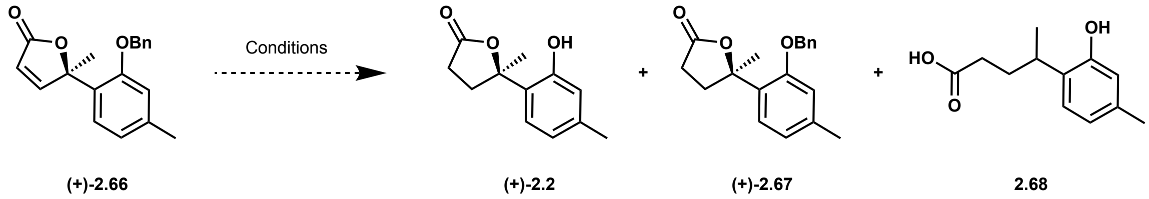

Entry	Catalyst	Solvent	Isolated product
1	10% Pd/C	EtOAc	2.68
2	Lindlar	EtOAc	(+)-2.67
3	Lindlar	1:1 EtOAc:EtOH	(+)-2.2 & (+)-2.67 (4:1)

reductive deprotections than *p*-methylbenzyl groups. Therefore, it was hypothesized that using a poisoned palladium catalyst to facilitate hydrogenation that we had previously used in the synthesis of peniciaculin A, Lindlar catalyst, could distinguish between the two benzyl groups. Hydrogenation with Lindlar catalyst in EtOAc performed olefin hydrogenation without lactone ring opening, but no benzyl deprotection was observed (Table **2.6**, entry 2). Switching to 1:1 EtOAc/EtOH to increase hydrogen solubility while maintaining solubility of furanone (+)-**2.66** produced the desired product in 2 h with minimal cleavage of lactone to acid **2.68** and formation of the benzyl protected lactone (+)-**2.67** (Table **2.6**, entry 3). With these conditions in hand, both the natural and unnatural enantiomers of 1-hydroxyboivinianin A were synthesized from (*S,R*)- and (*R,S*)-imidazolidinones respectively in 6 steps LLS and 42% overall yield (Scheme **2.20**). Both compounds were submitted for antimicrobial investigations at Corteva Agriscience.

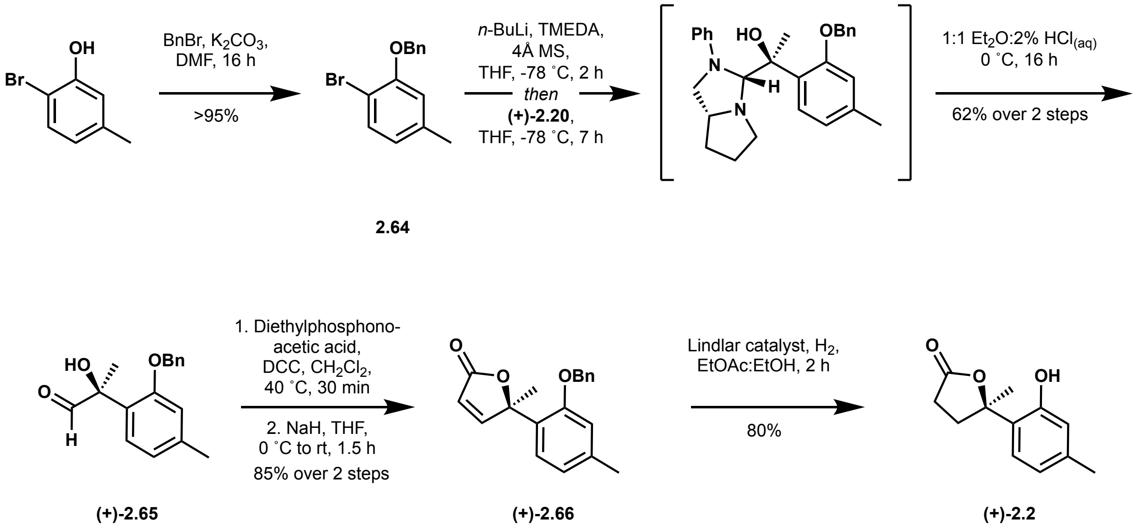
BnBr, K_2CO_3, DMF, 16 h
>95%
n-BuLi, TMEDA, 4Å MS, THF, -78 ˚C, 2 h then (+)-2.20, THF, -78 ˚C, 7 h
2.64
1:1 Et_2O:2% $HCl_{(aq)}$ 0 ˚C, 16 h
62% over 2 steps
1. Diethylphosphonoacetic acid, DCC, CH_2Cl_2, 40 ˚C, 30 min
2. NaH, THF, 0 ˚C to rt, 1.5 h
85% over 2 steps
Lindlar catalyst, H_2, EtOAc:EtOH, 2 h
80%
(+)-2.65
(+)-2.66
(+)-2.2

Scheme 2.20. Synthesis of 1-hydroxyboivinianin A.

Having obtained the natural product, we were curious to investigate the active species of the lactone—specifically whether the lactone was hydrolyzed *in vitro*. The synthesis of the linear species (+)-**2.** capitalized on the flexibility of the homobenzylic alcohol and initial route scouted for the synthesis of the natural product. It was envisioned that deriving **2.70** from benzyl protected substrate would enable a global deprotection and hydrogenation as a final step. HWE with homobenzylic aldehyde (+)-**2.65** and benzyl 2-(diethoxyphosphoryl)acetate proceeded in good

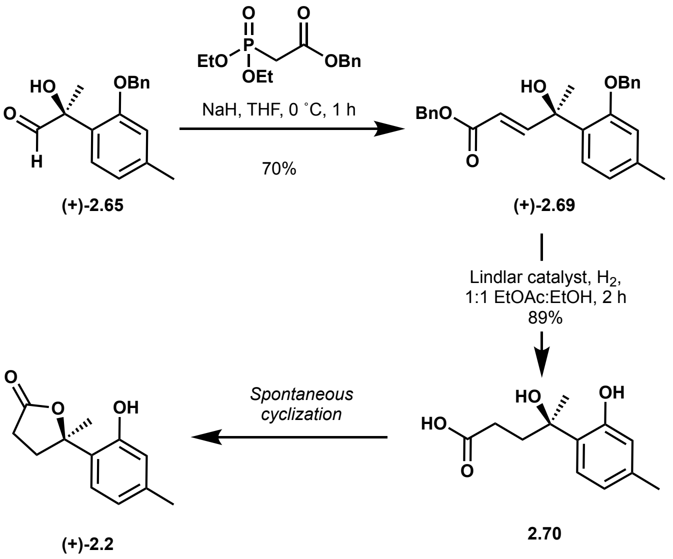
NaH, THF, 0 ˚C, 1 h
70%
(+)-2.65
(+)-2.69
Lindlar catalyst, H_2, 1:1 EtOAc:EtOH, 2 h
89%
Spontaneous cyclization
(+)-2.2
2.70

Scheme 2.21. Synthesis of linear acid.

yield to produce the benzyl protected unsaturated (+)-**2.69**. Subsequently, (+)-**2.69** was subjected to hydrogenation conditions optimized in the synthesis of 1-hydroxyboivinianin A (Scheme **2.21**).

Initial ^{1}H NMR and HRMS data suggested the desired acid **2.70** formed in very good yield. After analyzing the isolated material 5 hours after purification, however, a mixture of products was found (Figure **2.11**). Additional purification of the mixture was performed to isolate the linear acid **2.70** and an unknown compound. Through NMR characterization of the unknown compound, it was determined that the data matched that of 1-hydroxyboivinianin A **(+)-2.2**. Furthermore, HRMS and the optical rotation of the isolated compound supported this finding. This suggests the linear acid undergoes a spontaneous cyclization to form the natural product and the lactone is the active species *in vitro*.

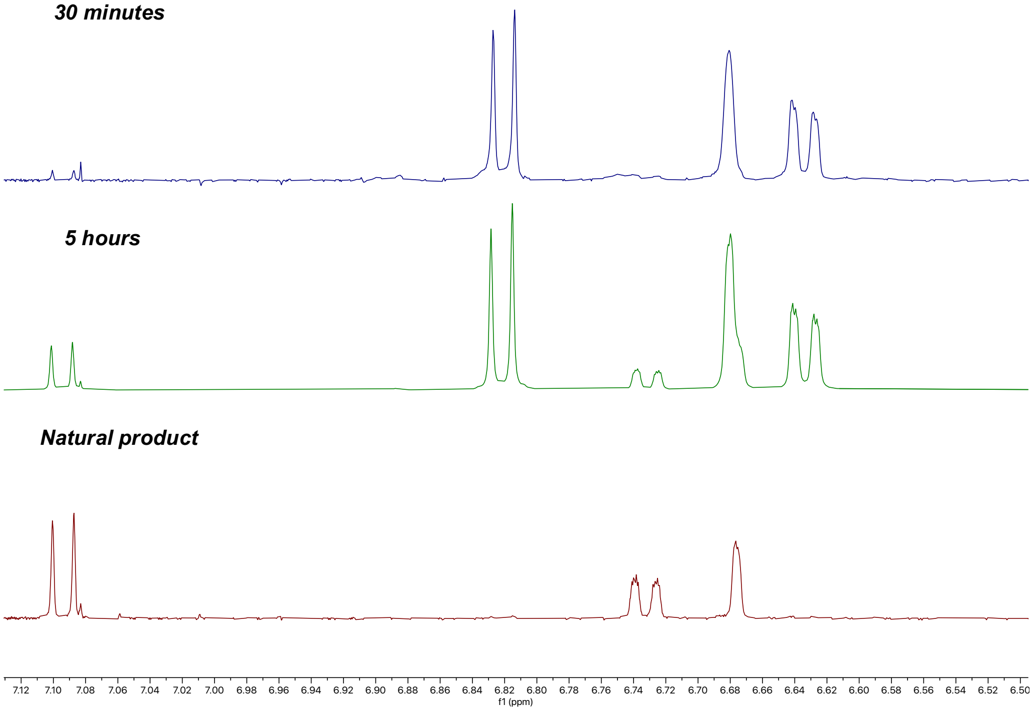

Figure 2.11. Spontaneous cyclization of the linear acid to form 1-hydroxyboivinianin A. Times reported after purification and isolation of the linear acid.

2.2.6. Antimicrobial bioactivity

A panel of analogues of peniciaculin A and both enantiomers of 1-hydroxyboivinianin A were tested for fungicidal, insecticidal, and herbicidal activity by Corteva Agriscience (Table **2.7**). Although Corteva was unable to test the compounds against *A. brassicae*, if analogues of peniciaculin A are acting as QoIs, they will likely exhibit broad-spectrum antifungal activity. That is indeed what we observed. As hypothesized, incorporating known pharmacophore ethoxy acrylate for analogues **2.37** and **2.40** resulted in activity against several fungal pathogens, suggesting the phenol core and diaryl fragment of peniciaculin A are mimicking the central ring and side chain portions of known QoIs, while the alkyl side chain is acting as the pharmacophore. Surprisingly, truncated ethoxy acrylate **2.37** demonstrated more potent activity than full triaryl **2.40** indicating truncating peniciaculin A may increase its proposed antifungal activity. Full and truncated ketone analogues **2.54**, **2.50**, and **2.45** exhibited minor antifungal activity, further supporting our hypothesis that the alkyl side chain is acting as a novel pharmacophore and is required for activity (Figure **2.12**).

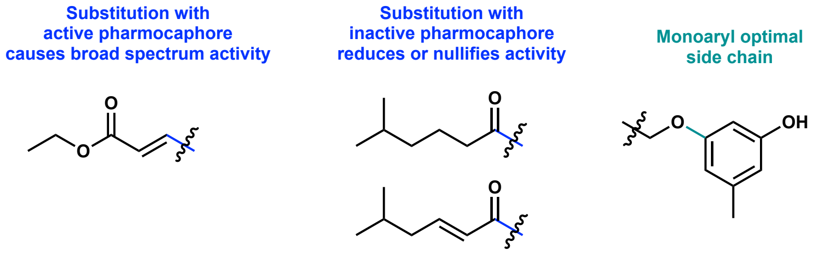
Substitution with
active pharmacophore
causes broad spectrum activity
Substitution with
inactive pharmacophore
reduces or nullifies activity
Monoaryl optimal
side chain
O
O
O
O
O
OH

Figure 2.12. Key SAR findings from antifungal testing.

Monobenzyl capped diaryl ether analogue **2.57** possessed potent antifungal activity against corn smut (*Ustilago maydis*) and rice blast (*Magnaporthe oryzae*). The broad-spectrum antimicrobial activity of this analogue may warrant further investigations to determine its mammalian toxicity profile and mechanism of action. Furthermore, minimal SAR has been completed to determine ideal mono phenol substitution of the diorcinol core and may aid in elucidating a possible MoA for these types of small molecules.

Finally, 1-hydroxyboivinianin A and its enantiomer demonstrated minor antifungal activity. Interestingly, the activity profile of each enantiomer was unique. This may be indicative of a specific enzyme target and warrants further investigations of the antibacterial activity of 1-hydroxyboivinianin A against reported target *V. harveyi* to confirm activity and elucidate a possible MoA. Additionally, testing 1-hydroxyboivinianin A and its enantiomer against a panel of microbial pathogens will allow us to better assess its reported narrow spectrum activity against *V. harveyi.* Future in house studies will test all analogues and natural products against gram-positive and negative bacteria and fungal pathogens including *A. brassicae*, *A. alternata*, and *A. solani* obtained from ATCC.

Table 2.7. Antifungal activity of phenolic bisabolanes and analogues.

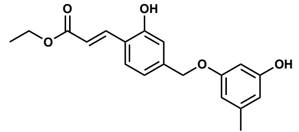

2.37

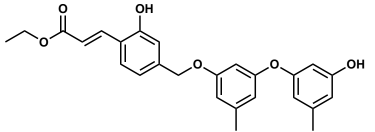

2.40

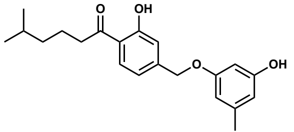

2.45

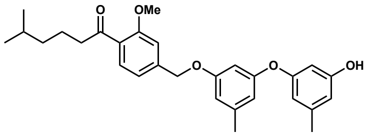

2.54

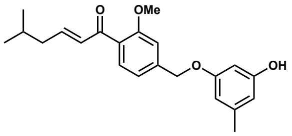

2.50

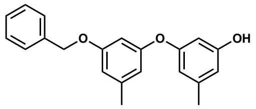

2.57

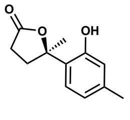

(+)-2.2

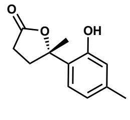

(−)-2.2

	Fungicidal data[a]							
	Corn smut	*Grey mold*	*Rice blast*	*Wheat leaf blotch*	*Pythium irregulare*	*Late blight of potatoes/tomatoes*	*Anthracnose of curcubits*	*Leaf spot of beet*
Compound	(USTIMA)	(BOTRCI)	(PYRIOR)	(SEPTTR)	(PYTHIR)	(MC4100)	(COLLA)	(CERCBE)
2.37	40	-	100	10	100	100	30	-
2.40	20	35	55	-	30	5	40	-
2.45	25	-	-	-	-	-	25	-
2.54	25	-	30	-	-	-	15	-
2.50	10	-	40	-	20	20	30	20
2.57	100	-	100	30	30	30	20	-
(+)-2.2	10	15	5	5	15	-	10	-
(−)-2.2	25	5	-	-	-	-	25	-

[a]Inhibition (%) at 5 ppm

2.3. Conclusion

Exploration of the synthesis of peniciaculin A led to the optimization of a key lithium halogen exchange to produce aryl nucleophile for diastereoselective nucleophilic addition with chiral imidazolidinone. This transformation has been leveraged in the total synthesis of phenolic bisabolane 1-hydroxyboivinianin A. Preliminary biological investigations supports our speculations that peniciaculin A is acting as a QoI with novel tertiary alcohol pharmacophore. Work in the immediate future will assess activity of peniciaculin A and analogues against strains of *Alternaria* and a panel of bacterial pathogens. Biological investigations of 1-hydroxyboivinianin A and its enantiomer suggest the small molecule may be interacting with a protein target. Activity against reported target *V. harveyi* will be completed in addition to a panel of fungal and bacterial pathogens.

References

1. Zhao, R. Z.; Jiang, S.; Zhang, L.; Yu, Z. B., Mitochondrial electron transport chain, ROS generation and uncoupling (Review). *Int. J. Mol. Med.* **2019,** *44* (1), 3-15.
2. Nohl, H.; Gille, L.; Staniek, K., The biochemical, pathophysiological, and medical aspects of ubiquinone function. *Ann. N. Y. Acad. Sci.* **1998,** *854*, 394-409.
3. Musso, L.; Fabbrini, A.; Dallavalle, S., Natural Compound-derived Cytochrome bc1 Complex Inhibitors as Antifungal Agents. *Molecules* **2020,** *25* (19).
4. Luo, B.; Ning, Y., Comprehensive Overview of Carboxamide Derivatives as Succinate Dehydrogenase Inhibitors. *J. Agric. Food Chem.* **2022,** *70* (4), 957-975.
5. Inaoka, D. K.; Shiba, T.; Sato, D.; Balogun, E. O.; Sasaki, T.; Nagahama, M.; Oda, M.; Matsuoka, S.; Ohmori, J.; Honma, T.; Inoue, M.; Kita, K.; Harada, S., Structural Insights into the Molecular Design of Flutolanil Derivatives Targeted for Fumarate Respiration of Parasite Mitochondria. *Int. J. Mol. Sci.* **2015,** *16* (7), 15287-308.
6. Huang, L. S.; Sun, G.; Cobessi, D.; Wang, A. C.; Shen, J. T.; Tung, E. Y.; Anderson, V. E.; Berry, E. A., 3-nitropropionic acid is a suicide inhibitor of mitochondrial respiration that, upon oxidation by complex II, forms a covalent adduct with a catalytic base arginine in the active site of the enzyme. *J. Biol. Chem.* **2006,** *281* (9), 5965-72.
7. Ruprecht, J.; Yankovskaya, V.; Maklashina, E.; Iwata, S.; Cecchini, G., Structure of Escherichia coli succinate:quinone oxidoreductase with an occupied and empty quinone-binding site. *J. Biol. Chem.* **2009,** *284* (43), 29836-46.
8. Ruprecht, J.; Iwata, S.; Rothery, R. A.; Weiner, J. H.; Maklashina, E.; Cecchini, G., Perturbation of the quinone-binding site of complex II alters the electronic properties of the proximal [3Fe-4S] iron-sulfur cluster. *J. Biol. Chem.* **2011,** *286* (14), 12756-65.
9. Yao, T. T.; Fang, S. W.; Li, Z. S.; Xiao, D. X.; Cheng, J. L.; Ying, H. Z.; Du, Y. J.; Zhao, J. H.; Dong, X. W., Discovery of Novel Succinate Dehydrogenase Inhibitors by the Integration of in Silico Library Design and Pharmacophore Mapping. *J. Agric. Food. Chem.* **2017,** *65* (15), 3204-3211.
10. Esser, L.; Yu, C.-A.; Xia, D., Structural basis of resistance to anti-cytochrome bc_1 complex inhibitors: implication for drug improvement. *Curr. Pharm. Des.* **2014,** *20* (5), 704-724.
11. Phillips, M. W. A., Agrochemical industry development, trends in R&D and the impact of regulation. *Pest Manag. Sci.* **2020,** *76* (10), 3348-3356.
12. Morton, V.; Staub, T., A Short History of Fungicides. *APSnet Feature Articles* **2008**.
13. Ding, S.; Halterman, D. A.; Meinholz, K.; Gevens, A. J., Distribution and Stability of Quinone Outside Inhibitor Fungicide Resistance in Populations of Potato Pathogenic Alternaria spp. in Wisconsin. *Plant Dis.* **2019,** *103* (8), 2033-2040.
14. Feng, Y.; Huang, Y.; Zhan, H.; Bhatt, P.; Chen, S., An Overview of Strobilurin Fungicide Degradation:Current Status and Future Perspective. *Front. Microbiol.* **2020,** *11*, 389.
15. Zeng, F.; Arnao, E.; Zhang, G.; Olaya, G.; Wullschleger, J.; Sierotzki, H.; Ming, R.; Bluhm, B. H.; Bond, J. P.; Fakhoury, A. M.; Bradley, C. A., Characterization of Quinone Outside Inhibitor Fungicide Resistance in Cercospora sojina and Development of Diagnostic Tools for its Identification. *Plant Dis.* **2015,** *99* (4), 544-550.

16. Zuccolo, M.; Kunova, A.; Musso, L.; Forlani, F.; Pinto, A.; Vistoli, G.; Gervasoni, S.; Cortesi, P.; Dallavalle, S., Dual-active antifungal agents containing strobilurin and SDHI-based pharmacophores. *Sci. Rep.* **2019,** *9* (1), 11377.

17. Matsuzaki, Y.; Yoshimoto, Y.; Arimori, S.; Kiguchi, S.; Harada, T.; Iwahashi, F., Discovery of metyltetraprole: Identification of tetrazolinone pharmacophore to overcome QoI resistance. *Bioorg. Med. Chem.* **2020,** *28* (1), 115211.

18. Arakawa, A.; Kasai, Y.; Yamazaki, K.; Iwahashi, F., Features of interactions responsible for antifungal activity against resistant type cytochrome bc1: A data-driven analysis based on the binding free energy at the atomic level. *PLoS One* **2018,** *13* (11), e0207673.

19. Li, X. D.; Li, X. M.; Xu, G. M.; Zhang, P.; Wang, B. G., Antimicrobial Phenolic Bisabolanes and Related Derivatives from Penicillium aculeatum SD-321, a Deep Sea Sediment-Derived Fungus. *J. Nat. Prod.* **2015,** *78* (4), 844-9.

20. Biswas, M.; Ghosh, T., Evaluation of Phyto-extracts, Biological Agents and Chemicals against the Development of Alternaria brassicae in vitro and in vivo. *European J. Med. Plants* **2018,** *22* (3), 1-9.

21. Vega, B.; Dewdney, M. M., Distribution of QoI Resistance in Populations of Tangerine-Infecting Alternaria alternata in Florida. *Plant Dis.* **2013,** *98* (1), 67-76.

22. Liu, Y.-L.; Lin, X.-T., Recent Advances in Catalytic Asymmetric Synthesis of Tertiary Alcohols via
Nucleophilic Addition to Ketones. *Adv. Synth. Catal.* **2019,** *361* (5), 876-918.

23. Fager, D. C.; Lee, K.; Hoveyda, A. H., Catalytic Enantioselective Addition of an Allyl Group to Ketones Containing a Tri-, a Di-, or a Monohalomethyl Moiety. Stereochemical Control Based on Distinctive Electronic and Steric Attributes of C-Cl, C-Br, and C-F Bonds. *J. Am. Chem. Soc.* **2019,** *141* (40), 16125-16138.

24. Osakama, K.; Nakajima, M., Asymmetric Direct 1,2-Addition of Aryl Grignard Reagents to Aryl Alkyl Ketones. *Org. Lett.* **2016,** *18* (2), 236-9.

25. Niu, S.; Zhang, H.; Xu, W.; Bagdi, P. R.; Zhang, G.; Liu, J.; Yang, S.; Fang, X., Access to enantioenriched compounds bearing challenging tetrasubstituted stereocenters via kinetic resolution of auxiliary adjacent alcohols. *Nat. Commun.*
2021, *12* (1), 3735.

26. Aggarwal, V. K.; Ball, L. T.; Carobene, S.; Connelly, R. L.; Hesse, M. J.; Partridge, B. M.; Roth, P.; Thomas, S. P.; Webster, M. P., Application of the lithiation–borylation reaction to the rapid and enantioselective synthesis of the bisabolane family of sesquiterpenes. *ChemComm* **2012,** *48* (74), 9230-9232.

27. Bieszczad, B.; Gilheany, D. G., Asymmetric Grignard Synthesis of Tertiary Alcohols through Rational Ligand Design. *Angew. Chem. Int. Ed.* **2017,** *56* (15), 4272-4276.

28. Sakito, Y.; Tanaka, S.; Asami, M.; Mukaiyama, T., AN ASYMMETRIC TOTAL SYNTHESIS OF A NEW MARINE ANTIBIOTIC-MALYNGOLIDE. *Chem. Lett.* **1980,** *9* (10), 1223-1226.

29. Zhang, C.; Ito, S.; Hosoda, N.; Asami, M., First asymmetric total synthesis of (+)-curcutetraol. *Tetrahedron Lett.* **2008,** *49* (16), 2552-2554.

30. O'Brien, P.; Warren, S., Synthesis of (R)- or (S)-diphenylphosphinoyl hydroxy aldehydes and 1,2-diols using Mukaiyama's bicyclic aminal methodology and Sharpless asymmetric dihydroxylation. *J. Chem. Soc. Perkin. Trans. I* **1996,** (17), 2129-2138.

31. Yajima, A.; Shirakawa, I.; Shiotani, N.; Ueda, K.; Murakawa, H.; Saito, T.; Katsuta, R.; Ishigami, K., Practical synthesis of aromatic bisabolanes: Synthesis of 1,3,5-bisabolatrien-7-ol, peniciaculin A and B, and hydroxysydonic acid. *Tetrahedron* **2021,** *92*, 132253.

32. Bagutski, V.; French, R. M.; Aggarwal, V. K., Full chirality transfer in the conversion of secondary alcohols into tertiary boronic esters and alcohols using lithiation-borylation reactions. *Angew. Chem. Int. Ed.* **2010,** *49* (30), 5142-5.

33. Nave, S.; Sonawane, R. P.; Elford, T. G.; Aggarwal, V. K., Protodeboronation of Tertiary Boronic Esters: Asymmetric Synthesis of Tertiary Alkyl Stereogenic Centers. *J. Am. Chem. Soc.* **2010,** *132* (48), 17096-17098.

34. Bagutski, V.; Elford, T. G.; Aggarwal, V. K., Synthesis of highly enantioenriched C-tertiary amines from boronic esters: application to the synthesis of igmesine. *Angew. Chem. Int. Ed.* **2011,** *50* (5), 1080-3.

35. Sonawane, R. P.; Jheengut, V.; Rabalakos, C.; Larouche-Gauthier, R.; Scott, H. K.; Aggarwal, V. K., Enantioselective construction of quaternary stereogenic centers from tertiary boronic esters: methodology and applications. *Angew. Chem. Int. Ed.* **2011,** *50* (16), 3760-3.

36. Scott, H. K.; Aggarwal, V. K., Highly enantioselective synthesis of tertiary boronic esters and their stereospecific conversion to other functional groups and quaternary stereocentres. *Chemistry* **2011,** *17* (47), 13124-32.

37. Ashby, E. C.; Lin, J. J.; Kovar, R., New and effective reagents for 1,4 reduction of .alpha.,.beta.-unsaturated ketones, LiAlH4-CuI and Its reactive species H2AlI. *J. Org. Chem.* **1976,** *41* (11), 1939-1943.

38. Swamy, K. C. K.; Kumar, N. N. B.; Balaraman, E.; Kumar, K. V. P. P., Mitsunobu and Related Reactions: Advances and Applications. *Chemical Reviews* **2009,** *109* (6), 2551-2651.

39. de Andrade, S. C. V.; de Mattos, C. S. M., New Reagents and Synthetic Approaches to the Appel Reaction. *Curr. Org. Synth.* **2015,** *12* (3), 309-327.

40. Peng, Y.; Ji, C.; Chen, Y.; Huang, C.; Jiang, Y., An Efficient and Selective Deprotecting Method for Methoxymethyl Ethers. *Cheminform.* **2011,** *36*, 4325-4330.

41. Burgos, C. H.; Barder, T. E.; Huang, X.; Buchwald, S. L., Significantly Improved Method for the Pd-Catalyzed Coupling of Phenols with Aryl Halides: Understanding Ligand Effects. *Angew. Chem. Int. Ed.* **2006,** *45* (26), 4321-4326.

42. Bedford, R. B.; Brenner, P. B.; Carter, E.; Gallagher, T.; Murphy, D. M.; Pye, D. R., Iron-Catalyzed Borylation of Alkyl, Allyl, and Aryl Halides: Isolation of an Iron(I) Boryl Complex. *Organometallics* **2014,** *33* (21), 5940-5943.

43. Kaku, T.; Matsunaga, N.; Ojida, A.; Tanaka, T.; Hara, T.; Yamaoka, M.; Kusaka, M.; Tasaka, A., 17,20-Lyase inhibitors. Part 4: Design, synthesis and structure–activity relationships of naphthylmethylimidazole derivatives as novel 17,20-lyase inhibitors. *Bioorg. Med. Chem.* **2011,** *19* (5), 1751-1770.

44. Pijper, D.; Jongejan, M. G. M.; Meetsma, A.; Feringa, B. L., Light-Controlled Supramolecular Helicity of a Liquid Crystalline Phase Using a Helical Polymer Functionalized with a Single Chiroptical Molecular Switch. *J. Am. Chem. Soc.* **2008,** *130* (13), 4541-4552.

45. Levin, J. I.; Chen, J. M.; Cole, D. C. Acetylenic Alpha-Amino Acid-Based Sulfonamide Hydroxamic Acid Tace Inhibitors. EP1144368 (A2), 2001/10/17/, 2001.

46. Huang, X.; He, W.; Peng, L.; Tang, L.; Wang, L.; Bai, Q. Preparation method of Venetoclax intermediate and product. CN109320516 (A), 2019/02/12/, 2019.

47. Yang, S.; Wu, C.; Ruan, M.; Yang, Y.; Zhao, Y.; Niu, J.; Yang, W.; Xu, J., Metal- and ligand-free Ullmann-type C–O and C–N coupling reactions promoted by potassium tert-butoxide. *Tetrahedron Lett.* **2012,** *53* (33), 4288-4292.

48. Zhang, Q.; Wang, D.; Wang, X.; Ding, K., (2-Pyridyl)acetone-promoted Cu-catalyzed O-arylation of phenols with aryl iodides, bromides, and chlorides. *J. Org. Chem.* **2009,** *74* (18), 7187-90.

49. Maiti, D.; Buchwald, S. L., Cu-catalyzed arylation of phenols: synthesis of sterically hindered and heteroaryl diaryl ethers. *J. Org. Chem.* **2010,** *75* (5), 1791-1794.

50. Lo, Q. A.; Sale, D.; Braddock, D. C.; Davies, R. P., Mechanistic and Performance Studies on the Ligand-Promoted Ullmann Amination Reaction. *ACS Catal.* **2017,** *8* (1), 101-109.

51. King, A. E.; Brunold, T. C.; Stahl, S. S., Mechanistic Study of Copper-Catalyzed Aerobic Oxidative Coupling of Arylboronic Esters and Methanol: Insights into an Organometallic Oxidase Reaction. *J. Am. Chem. Soc.* **2009,** *131* (14), 5044-5045.

52. King, A. E.; Ryland, B. L.; Brunold, T. C.; Stahl, S. S., Kinetic and Spectroscopic Studies of Aerobic Copper(II)-Catalyzed Methoxylation of Arylboronic Esters and Insights into Aryl Transmetalation to Copper(II). *Organometallics* **2012,** *31* (22), 7948-7957.

53. Boehlich, G. J.; de Vries, J.; Geismar, O.; Gudzuhn, M.; Streit, W. R.; Wicha, S. G.; Schutzenmeister, N., Total Synthesis of Anti-MRSA Active Diorcinols and Analogues. *Chemistry* **2020,** *26* (44), 9846-9850.

54. Defoirdt, T.; Boon, N.; Sorgeloos, P.; Verstraete, W.; Bossier, P., Quorum sensing and quorum quenching in Vibrio harveyi: lessons learned from in vivo work. *ISME J.* **2008,** *2* (1), 19-26.

55. Zhang, X. H.; He, X.; Austin, B., Vibrio harveyi: a serious pathogen of fish and invertebrates in mariculture. *Mar. Life Sci. Technol.* **2020**, 1-15.

56. Brehm, T. T.; Berneking, L.; Rohde, H.; Chistner, M.; Schlickewei, C.; Sena Martins, M.; Schmiedel, S., Wound infection with Vibrio harveyi following a traumatic leg amputation after a motorboat propeller injury in Mallorca, Spain: a case report and review of literature. *BMC Infect. Dis.* **2020,** *20* (1), 104.

57. Montanchez, I.; Kaberdin, V. R., Vibrio harveyi: A brief survey of general characteristics and recent epidemiological traits associated with climate change. *Mar. Environ. Res.* **2020,** *154*, 104850.

58. Vakalopoulos, A.; Hoffmann, H. M. R., Novel Deprotection of SEM Ethers: A Very Mild and Selective Method Using Magnesium Bromide. *Org. Lett.* **2000,** *2* (10), 1447-1450.

Chapter 3. Leveraging core scaffold for the synthesis of amino acid-sesquiterpene conjugates and antimicrobial investigations of their derivatives

Disclaimer: Ingrid K. Wilt independently developed the project goals, hypotheses, and future work. She also designed and completed all synthetic work described below. Martina Golden collected preliminary MIC data reported in Table **3.4**.

3.1. Introduction

3.1.1. Development of antifungals for clinical use

Since 3000 B.C.E., infectious diseases have been documented as a threat to human health. While ample availability of vaccines and antibacterial agents exist to manage viral and bacterial infections respectively, therapies for fungal disease remain widely unexplored[1, 2]. Compared to developing antibacterials, antifungals have several added challenges[3]. Namely, like mammalian cells, fungi are eukaryotic organisms. Thus, due to lack of differentiation between fungal and mammalian cellular processes, potential antifungal targets are diminished[4]. Additionally, fungal infections have historically been less common than bacterial resulting in less enthusiasm for development of novel therapies and diagnostic techniques[5]— the first antifungal drugs, fluconazole and itraconazole[6], were not introduced into the clinic until the early 1990s. The Global Action Fund for Fungal Infections (GAFFI), however, recently estimated 300 million people worldwide suffer from serious fungal infections each year and over 1.5 million of these individuals will die from fungal disease[7].

Treatment of fungal infections largely depends on the severity of infection. Infections can be classified as superficial (skin or mucous membranes) or invasive fungal infections (IFIs)[8]. Superficial infections are rarely life threatening and typically easily diagnosed. Treatment with topical antifungal agents can effectively eradicate superficial infections. IFIs, however, are challenging to recognize due to their nonspecific symptoms (*i.e.* fever and chills) often leading to misdiagnosis[9]. Improper diagnosis results in a high mortality rate of 50% due to incorrect or late intervention. IFIs require more aggressive treatments such as intravenous administration of antifungals for a minimum of two weeks[10].

Antifungal agents primarily inhibit fungal growth by disrupting biosynthesis or integrity of ergosterol, the key sterol component of fungal cell membranes, or cell wall biosynthesis (Figure **3.1**). Existing treatment for fungal human disease can be grouped into four main classes[11] based on their mechanism of action: azoles[12]; polyenes[13]; allylamines[14]; and echinocandins[15]. Azoles are the main class of antifungals used in and approved for the clinical settings[16].

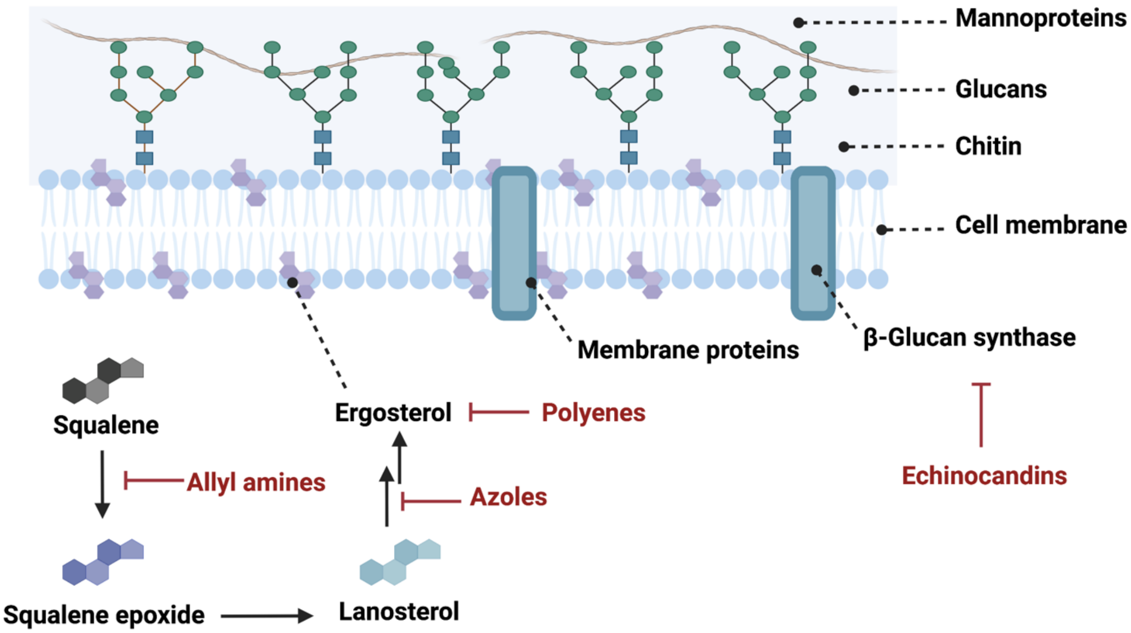
Mannoproteins
Glucans
Chitin
Cell membrane
Membrane proteins
β-Glucan synthase
Squalene
Ergosterol
Polyenes
Allyl amines
Azoles
Echinocandins
Squalene epoxide
Lanosterol

Figure 3.1. Fungal cell wall and mechanisms of antifungal small molecules. The figure was created in Biorender.com

The primary function of Azoles is to inhibit fungal cytochrome P450 enzyme, 14α-demethylase (Erg11), involved in the biosynthesis ergosterol[11]. This class of inhibitors is also widely used in the agricultural industry. Azoles can be broken down further into two sub classes: imidazoles and triazoles. Imidazoles (*i.e.* ketoconazole, miconazole, clotrimazole, and econazole) are solely used to treat superficial infections[17], while triazoles (i.e. fluconazole, itraconazole, voriconazole, and posaconazole) treat both superficial and IFIs[18]. Both subclasses share a common structural model containing two aromatic side chains, a linker, and a heme binding group (*i.e.* azole or imidazole) (Figure **3.2**). Due to their greater affinity for fungal over mammalian P450 enzymes, triazoles demonstrate an improved safety profile compared to imidazoles and can thus be used for IFIs[19].

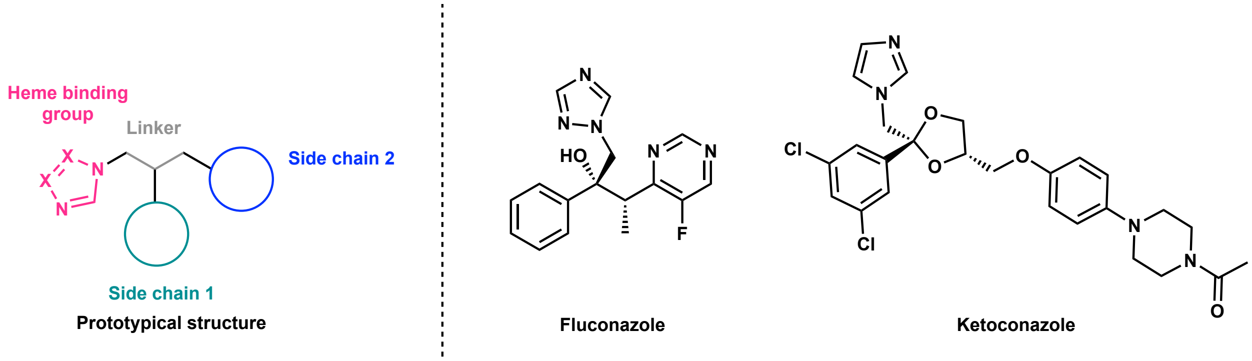

Prototypical structure

Fluconazole

Ketoconazole

Figure 3.2. Prototypical structure of azoles.

Polyenes, including amphotericin B (AMB), act by binding to membrane ergosterol and forming pores in the plasma membrane[20] (Figure **3.3a**). A similar mechanism of action is proposed for their antibacterial activity. Echinocandins disrupt fungal cell walls by binding to 1,3-β glucan synthase, an enzyme not found in mammalian cells, and thus exhibit minimal mammalian toxicity[19, 21]. All echinocandins are lipopeptides and the ones used in clinical settings contain cyclic hexapeptides with *N*-linked acyl lipid side chains (Figure **3.3b**). The final class, allylamines such as terbinafine, inhibit squalene epoxidase (monooxygenase), an enzyme necessary for the biosynthesis of ergosterol. Accumulation of toxic concentrations of squalene may play a role in the fungicidal activity of these drugs. Again, all allylamines share a prototypical structure including two aromatic side chains linked by a tertiary allylamine[22] (Figure **3.3c**).

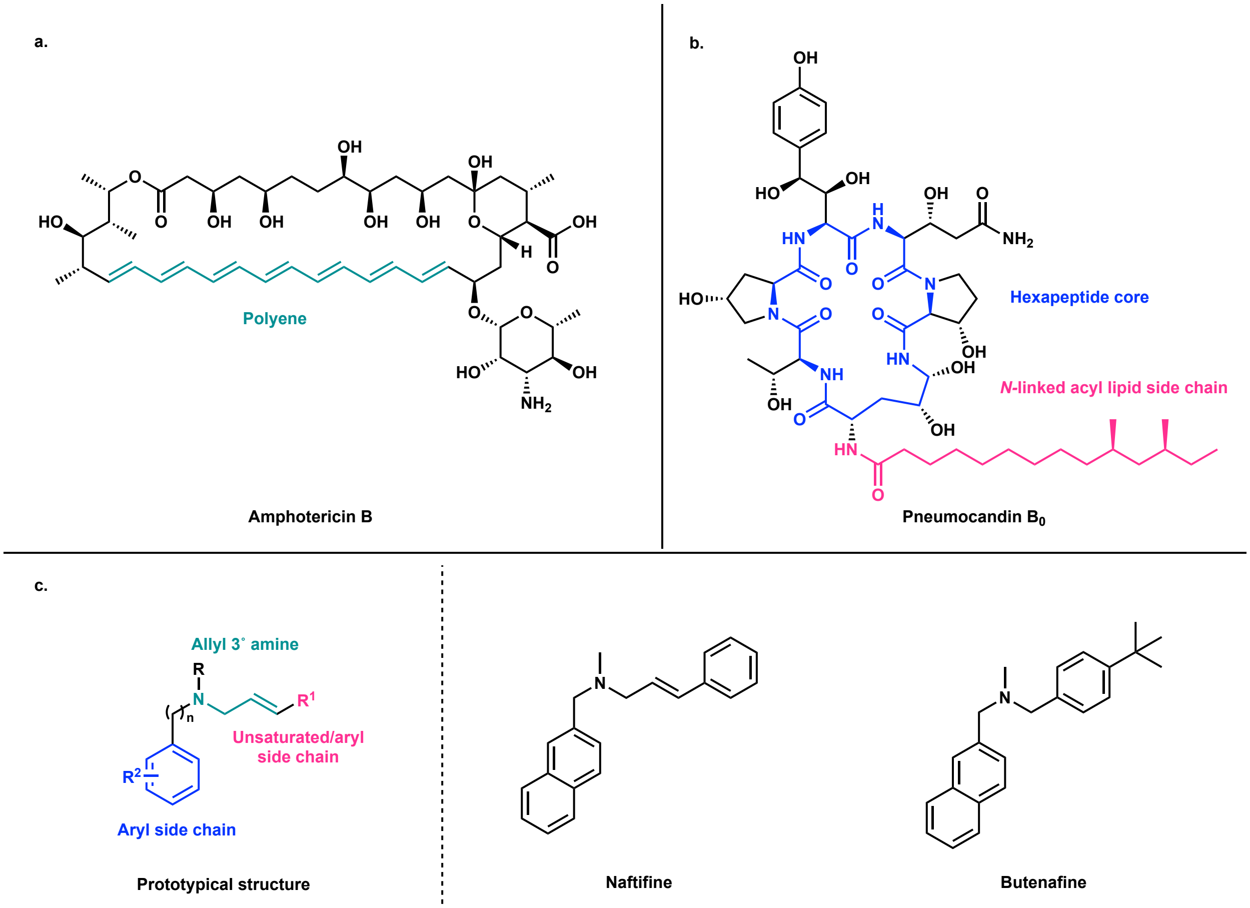
a.
Polyene
Amphotericin B
b.
Hexapeptide core
N-linked acyl lipid side chain
Pneumocandin B$_0$
c.
Allyl 3˚ amine
Unsaturated/aryl side chain
Aryl side chain
Prototypical structure
Naftifine
Butenafine

Figure 3.3. Prototypical structures of common antifungals used in the clinic. a. Polyenes, such as amphotericin B, contain long unsaturated and conjugated hydrocarbon chains. b. Echinocandins contain a hexapeptide core and *N*-linked acyl side chain. c. Allylamines are constructed from an aryl core, allyl 3˚ amine, and an unsaturated or aryl side chain.

Two of the main concerns regarding current clinical use of these fungicides is the increasing occurrence of fungal infections and emergence of resistance to existing treatments[23]. Of particular concern in both of these categories is the genus *Candida*. Invasive candidiasis infections are the leading cause of IFIs with 40-60% of cases from *C. albicans*. Although the preferred treatment option for *Candida* infections is fluconazole, azole resistance in most *Candida* species has also been identified in clinical samples ranging from 2.3 (*C. tropicalis*) to upwards of 96.6% (*C. krusei*) of the isolates tested[24]. Resistance to azoles is primarily a result of amino acid mutations in the predicted catalytic site of Erg11p[25], overexpression of the enzyme target ERG11 through mutations of gene regulators[26], overexpression of drug efflux pumps[27, 28], and inactivation of the *ERG3* gene which prevents accumulation of the toxic sterol 14α-methylergosta-8,24(28)-dien-3β,6α-diol caused by azole treatment[29].

Furthermore, some species, such as *C. auris*, have been linked to increasing number of overall global fungal infections with more multi drug resistant than susceptible infections recorded. Many researchers hypothesize this is due to increasing temperatures caused by global warming enhancing selective pressure for fungal species to become more adaptable to human body temperatures[30]. With our existing climate and limited portfolio of antifungals, there is dire need to develop novel antifungal agents that are selective for fungi over mammalian cells and expand upon the structural diversity of preexisting treatments. The structural complexity of natural products often lends itself to specific and potent activity and would provide an excellent opportunity to diversify and expand the current scope of antifungal agents. Discovery of structurally diverse selective antifungal agents has the potential to greatly impact the future of public health.

3.1.2. Antimicrobial purpurides: a common intermediate in sight

The purpurides are a unique class of small molecules isolated from marine organisms that possess an unusual drimane sesquiterpene-amino acid conjugate. Purpuride **(+)-3.1**, isolated in 1973, is the first example of a natural product to contain this unusual skeleton[31]. The purpurides demonstrate potent activity against the opportunistic pathogen *C. albicans* (1.3-3.3 μM) and negligible mammalian toxicity[32]. The complex structure of these small molecules is atypical of the four classes of antifungals previously described. Thus, the purpurides may be inhibiting fungal growth through a novel mechanism of action and/or enzyme target. Purpurides B **(+)-3.2** and C

(+)-3.3 also exhibit antibacterial activity against gram negative bacteria *Pseudomonas aeruginosa* (2.6 μM) and *Klebsiella aerogenes* (1.2-2.4 μM)[32], while recently isolated purpuride D **(+)-3.4** has reported activity against *E. coli* (20.5 μM)[33]. Due to similarities between bacterial and fungal cell walls, if the purpurides are targeting similar processes to elicit their antimicrobial effects in bacterial and fungal species, this may indicate cell wall disruption as a probable MOA[34]. Our lab has recently become interested in developing the chemical biology tools necessary to investigate natural product inspired antibacterial cell wall inhibitors (i.e. carolacton). The purpurides and analogues thereof may serve as another tool to explore new cell wall biosynthesis inhibitors and the confluence of cell wall antimicrobial agents.

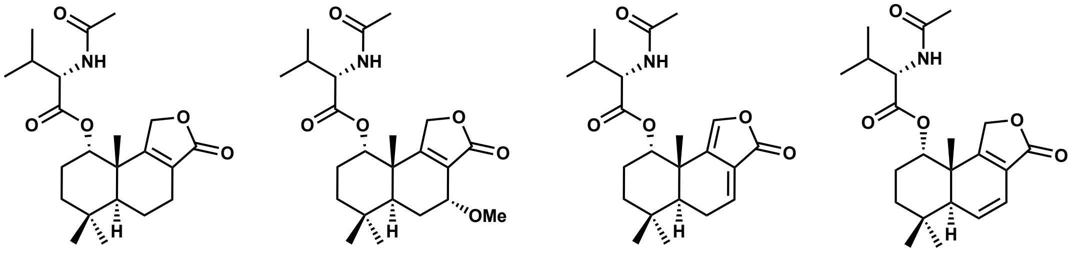

Purpuride (+)-3.1 **Purpuride B (+)-3.2** **Purpuride C (+)-3.3** **Purpuride D (+)-3.4**

Figure 3.4. Structures of the purpurides.

A plethora of synthetically unexplored bioactive natural products contain the tricyclic core found in the purpurides. Thus, the synthesis of the purpurides was designed to be amenable to late-stage diversification to allow access to natural products such as berkedrimanes (active against *C. albicans*)[35] and minioluteumides (unexplored antimicrobial activity)[36] (Figure **3.5**). It was proposed that a common intermediate could be quickly diversified to form 9 natural products through late-stage oxidation and elimination sequences. It was also envisioned that focusing analogue design on modifications to the amino-acid fragment to investigate possible probe placements for future affinity-based protein profiling to identify the protein target of this class of natural products in both bacterial and fungal species.

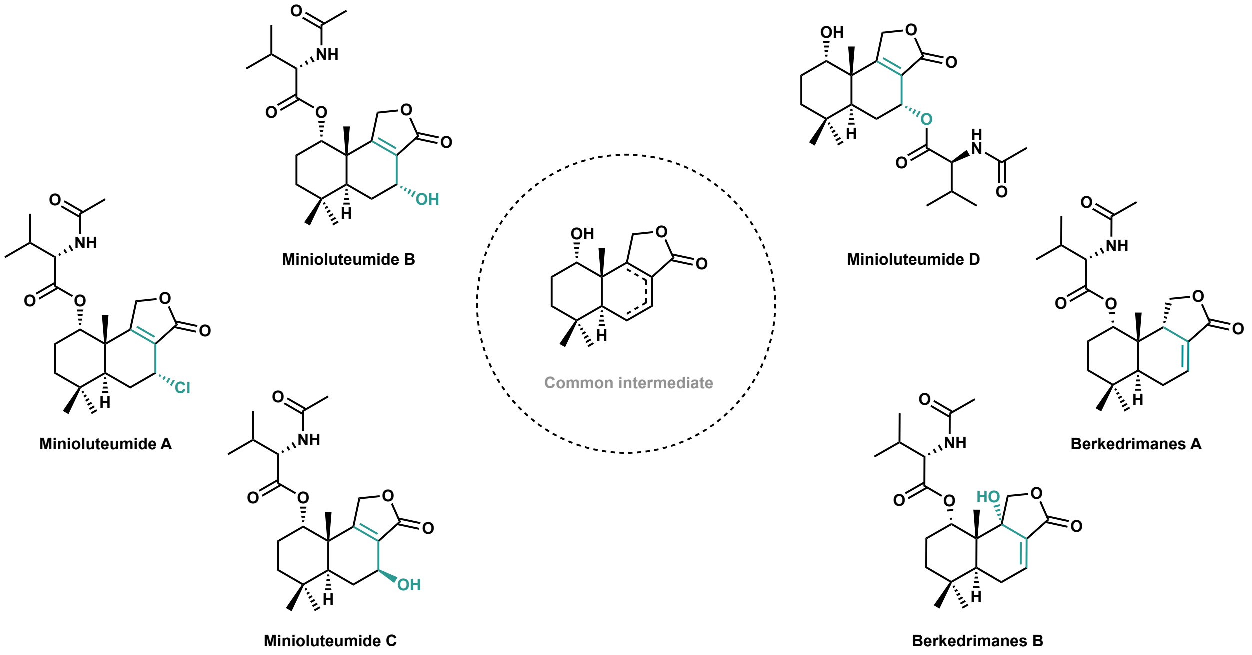
Minioluteumide B
Minioluteumide D
Common intermediate
Minioluteumide A
Berkedrimanes A
Minioluteumide C
Berkedrimanes B

Figure 3.5. Common intermediate strategy to access amino acid conjugated sesquiterpenoids.

3.1.3. Previous approaches to 6-6 trans bicycles

Over the past century, numerous approaches to *trans*-terpenes have been explored. Stereospecific Lewis acid promoted cyclization, mimicking known cyclase cationic cascades in biosynthetic pathways[37], has been used in the synthesis of natural products such as (+)-seclareolide[38] and key intermediates *en route* to more complex natural products[39] (Figure **3.6**). Although these approaches build complexity from feedstock chemicals, overall yields to form the desired intermediates are often low. Additionally, developing a route to perform a cascade for the

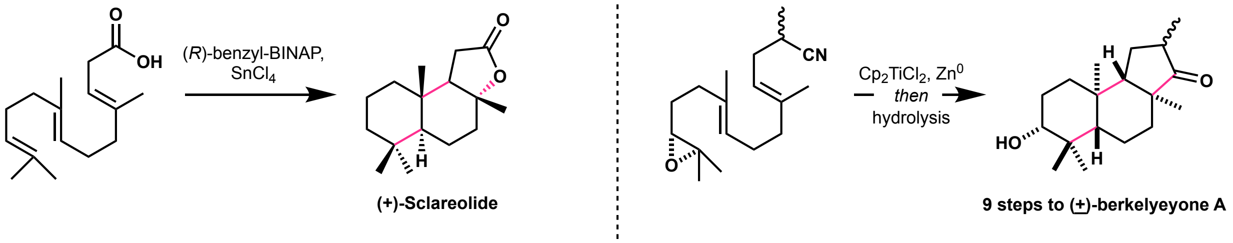
(R)-benzyl-BINAP, SnCl4
(+)-Sclareolide
Cp2TiCl2, Zn0
then
hydrolysis
9 steps to (±)-berkelyeyone A

Figure 3.6. Biomimetic approaches to terpene synthesis.

synthesis of the common intermediate to access the purpurides quickly outnumbered the steps proposed for alternative routes.

Chemical modification of commercially available terpenes with preexisting *trans* stereochemistry has led to the syntheses of molecules such as (+)-chlorolissoclimide from by Vanderwal and Alexanian, while biocatalytic modifications popularized by Hans Renata, have produced terpenes such as *N*-acetyl-polyveoline[40-42] (Figure **3.7**). However, Renata notably has yet to develop an enzymatic C-1 oxidation necessary for the synthesis of structures such as the purpurides. Discussions with his group have hinted at the challenges of developing such an enzyme through directed evolution. Thus, biocatalytic strategies to build a common intermediate for the synthesis of the purpurides seemed unlikely and a lengthy elimination, allylic oxidation, and reduction sequence would be required to furnish the C-1 hydroxy.

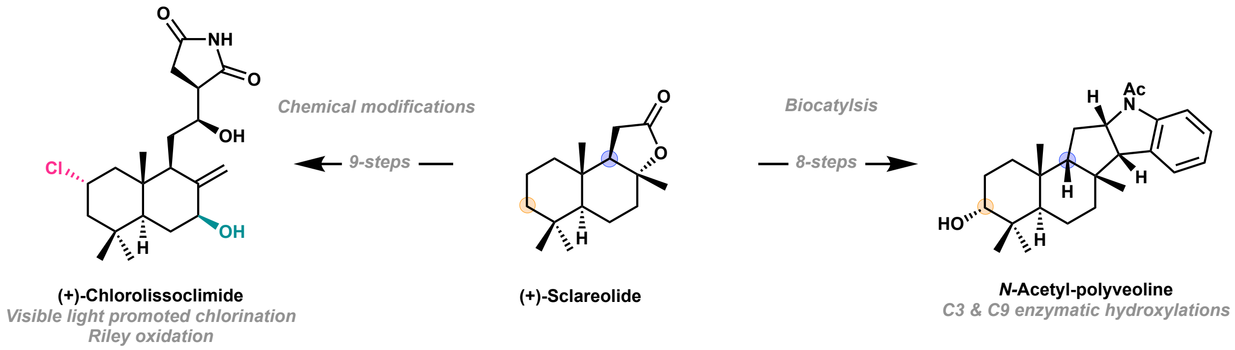
O
NH
O
OH
Cl
OH
H
Chemical modifications
9-steps
O
O
H
Biocatylsis
8-steps
H
Ac
N
H
H
HO
H
(+)-Chlorolissoclimide
Visible light promoted chlorination
Riley oxidation
(+)-Sclareolide
N-Acetyl-polyveoline
C3 & C9 enzymatic hydroxylations

Figure 3.7. Modification of commercially available terpenes.

Diels-Alder cycloadditions are another powerful tool to form 6-membered polycyclic systems. This approach has been used in Mori's synthesis of polygodial to build the carbon skeleton followed by reported heterogeneous hydrogenation to form the *trans* diastereomer[43]. Monica and coworkers synthesized 1(*R*)-hydroxypolygodial using a similar intermolecular diastereoselective Diels-Alder cycloaddition leveraging a bulky TBS protecting group at the C-1 hydroxy to force dienophile approach from the bottom face and produce the desired relative *cis* stereochemistry at C-1 and C-10[44] (Figure **3.8a**). It was envisioned that the purpurides could engage the hydroxy substituent at C-1 to facilitate an analogous diastereoselective Diels-Alder cycloaddition to build the 6-6 bicyclic core of the purpurides. Unfortunately, the reported reaction resulted in low yield of the desired diastereomer and challenging purification due to excess DMAD coeluting on silica column with the product. Furthermore, to produce the desired (*S*)-hydroxy of the purpurides at C-1 would require a redundant oxidation-reduction sequence of the (*R*) enantiomer required for the diastereoselective Diels-Alder.

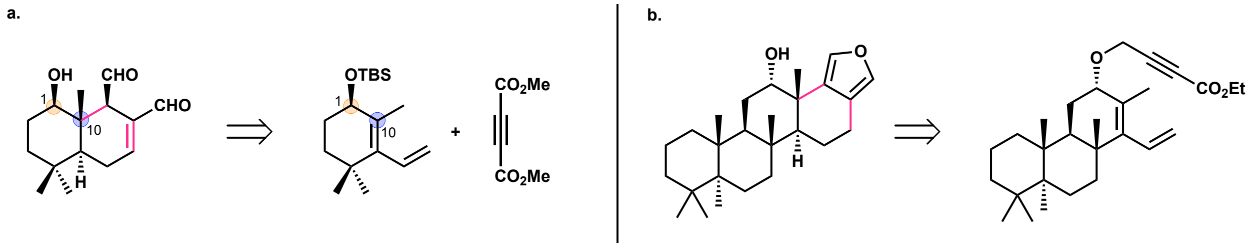

1(*R*)-Hydroxypolygodial

16-Deacetoxy-12-*epi*-scalarafuran

Figure 3.8. Diels-Alder cycloadditions in the synthesis of terpenes.

Alternatively, it was envisioned that an intramolecular Diels Alder cycloaddition could be employed to form the bicyclic core of the common intermediate through a tethered intermediate **(±)-3.7.** Although this approach has been fruitful in tetracyclic systems such as Abad and coworkers' synthesis of the scalarane skeleton[45] and Wang and coworkers' synthesis of 16-deacetoxy-12-*epi*-scalarafuran acetate[46], the synthesis of bicyclic systems remains mostly explored. This effort would capitalize on the inherent stereochemistry of the secondary alcohol at C-1 to set the relative stereochemistry at C-10. Both Abad and Wang had reported forming the *trans* stereoisomer through a standard heterogeneous hydrogenation of the resulting alkene with Pd/C. Thus, retrosynthetically, formation of the purpurides was proposed through final esterification of *trans* bicycle **(±)-3.5**. The desired *trans* isomer would be formed via late-stage hydrogenation and diversification of common intermediate **(±)-3.6.** Common intermediate **(±)-3.6** would be derived from intramolecular Diels-Alder cycloaddition of tethered intermediate **(±)-3.7** which was further simplified to known secondary alcohol **(±)-3.8** (4 known steps from α-ionone). The proposed synthesis could easily accommodate an enantioselective route by utilizing enantioenriched (−)-**3.8** (6 known steps from α-ionone)[44, 47] (Scheme **3.1**)

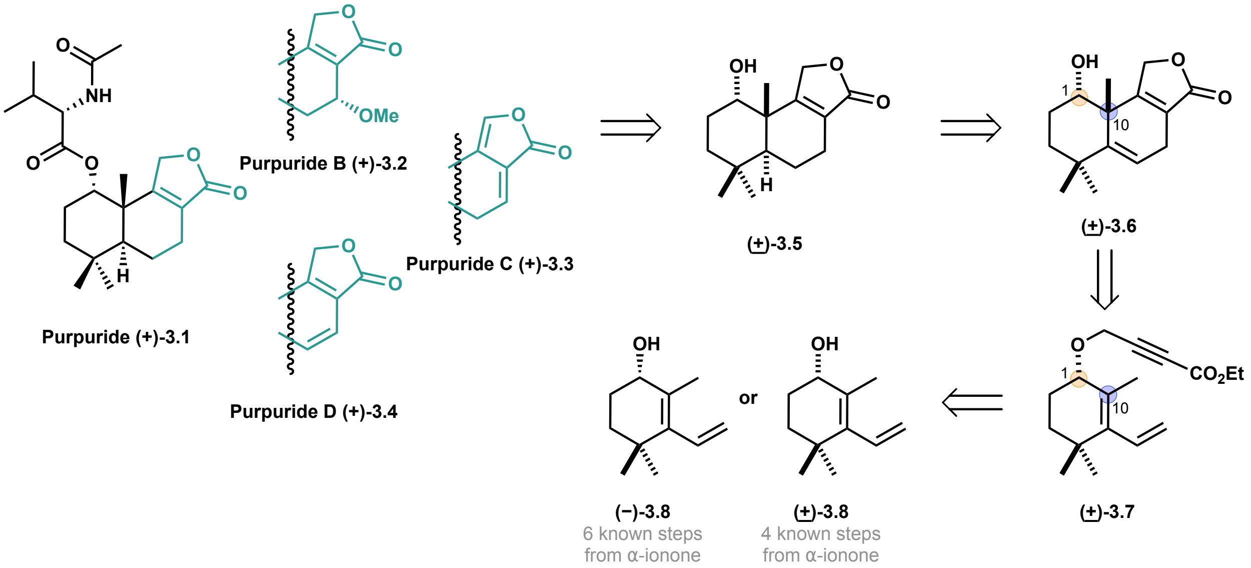
Purpuride (+)-3.1
Purpuride B (+)-3.2
Purpuride C (+)-3.3
Purpuride D (+)-3.4
(±)-3.5
(±)-3.6
1
10
(−)-3.8
6 known steps from α-ionone
or
(±)-3.8
4 known steps from α-ionone
(±)-3.7
OMe
CO2Et

Scheme 3.1. Retrosynthetic approach to the purpurides.

3.2. Results and discussion

3.2.1. Construction of common intermediate *via* intramolecular Diels-Alder cycloaddition

Construction of the precursor for the Diels-Alder cycloaddition began with 2° alcohol **(±)-3.8** synthesized in high yield from (±)-α-ionone in 4 known steps[44, 47]. The enantioselective route would be achieved through oxidation of **(±)-3.8** and stereoselective reduction of resulting ketone **3.9** with (*R*)-CBS or ruthenium catalyzed hydrogenation with dichloro[(R)-(+)-2,2'-bis(diphenylphosphino)-1,1'-binaphthyl][(1S,2S)-(-)-1,2-diphenylethylenediamine]ruthenium(II) ($RuCl_2$[(R)-binap, (S,S)-DPEN]) (SI scheme **S3.1**). Propargylation of the 2° alcohol followed by homologation proceeded in high yield to form the ethylynoate **(±)-3.7**. Subsequent Diels-Alder cycloaddition in refluxing toluene furnished the desired tricycle **(±)-3.11**. Although initial analysis of the crude ^{1}H NMR suggested moderate dr of 5:1, it was unclear how the *cis* C1-C10 stereoisomer formed given the ring strain of the proposed product. Further analysis suggests a major and minor unknown byproduct, not diastereomer, are forming that coelute on TLC and silica column corresponding to disappearance of the ethoxy protons. Studies are underway to identify the major byproduct. With tricycle **(±)-3.11** in hand, dihydrofuran ring cleavage was accomplished by treatment with Ac_2O and ZnI_2 to produce the common intermediate **(±)-3.6** (Scheme **3.2**). Although synthesis of several members of the purpuride family was originally proposed, intermediate **(±)-3.6** was carried forward in the synthesis of purpuride as a platform to optimize the final proposed hydrogenation and esterification.

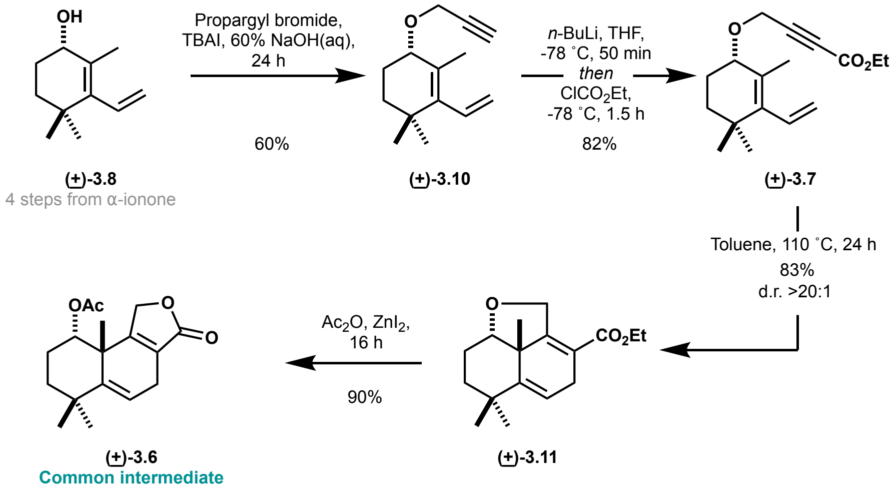
OH
Propargyl bromide,
TBAI, 60% NaOH(aq),
24 h
60%
O
n-BuLi, THF,
-78 °C, 50 min
then
ClCO2Et,
-78 °C, 1.5 h
82%
O
CO2Et
(±)-3.8
4 steps from α-ionone
(±)-3.10
(±)-3.7
Toluene, 110 °C, 24 h
83%
d.r. >20:1
OAc
O
O
Ac2O, ZnI2,
16 h
90%
O
CO2Et
(±)-3.6
Common intermediate
(±)-3.11

Scheme 3.2. Synthesis of common intermediate.

3.2.2. Building *trans* fused bicycle *via* HAT

In previous syntheses of terpenes, *trans* fused rings were reportedly accessed with moderate to high diastereoselectivity using standard or slightly modified heterogenous hydrogenation conditions from intermediates analogous to **(±)-3.6**[46-51] (Figure **3.9**). Reports also suggest chemoselective reduction of the more electron rich alkene. Thus, after obtaining intermediate **(±)-3.6**, the hydrogenation was performed with 5% Pd/C in methanol. Initial characterization suggested diastereomers formed in a 1:1.1 ratio (Table **3.1**, entry 1). After careful separation with PTLC, the products were identified as over hydrogenated **(±)-3.12** and what was believed to be *trans* **(±)-3.13**. To confirm relative stereochemistry, an NOE spectrum was obtained of **(±)-3.13**. The data, however, was inconclusive (Figure **3.10a**).

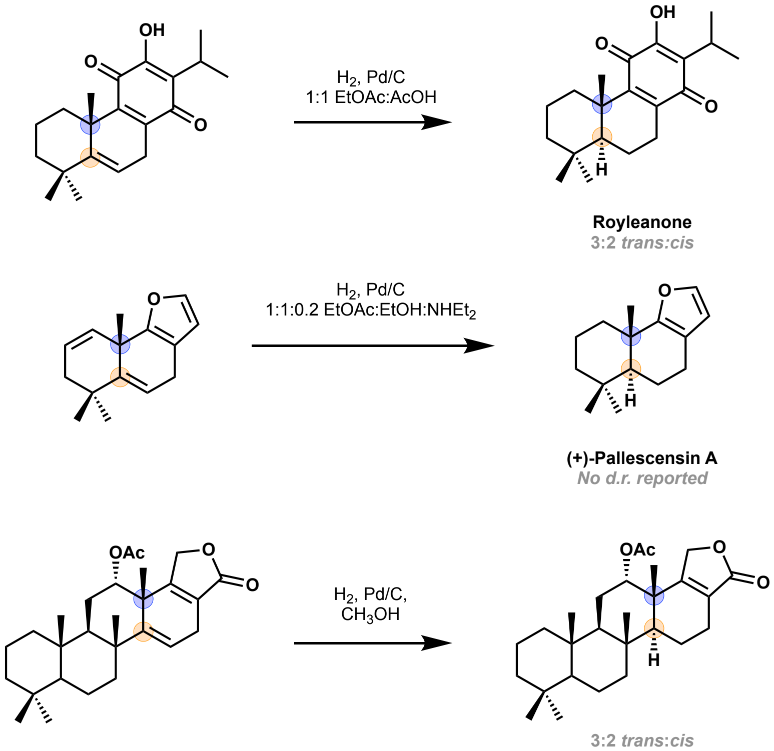
OH
O
O
H₂, Pd/C
1:1 EtOAc:AcOH
OH
O
O
H
Royleanone
3:2 trans:cis
O
H₂, Pd/C
1:1:0.2 EtOAc:EtOH:NHEt₂
O
H
(+)-Pallescensin A
No d.r. reported
OAc
O
O
H₂, Pd/C,
CH₃OH
OAc
O
O
H
3:2 trans:cis

Figure 3.9. Examples of heterogeneous hydrogenations to form *trans* terpenes.

To avoid over hydrogenation, an alternative method was sought out to reduce the more electron rich olefin, specifically homogeneous catalysis. The most used homogeneous catalysis system, Li in NH_3, is notorious for poor selectivity and would likely not be amenable to selective olefin reduction in the presence of the furanone. Shenvi and coworkers, however, have developed robust methodology for homogeneous Mn or Fe catalyzed reductive hydrogen atom transfer (HAT) of electron rich olefins. Importantly, they note preferential formation of the thermodynamically favored *trans* isomer over the kinetically favored *cis*. Additionally, they propose HAT is complimentary to Pd/C catalyzed heterogeneous hydrogenation of bicyclic systems[50, 52] (Scheme **3.3**).

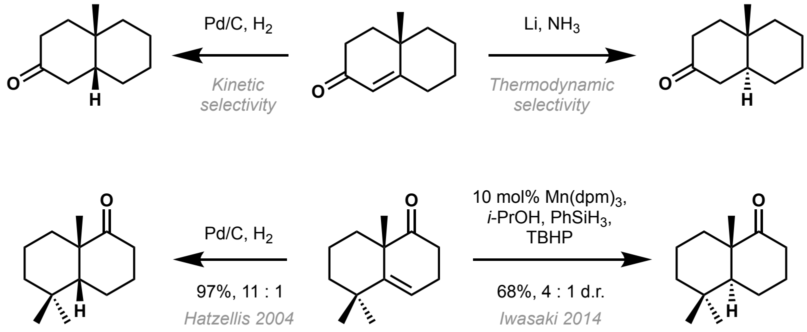
Pd/C, H_2
Kinetic selectivity
Li, NH_3
Thermodynamic selectivity
O
H
10 mol% $Mn(dpm)_3$, *i*-PrOH, $PhSiH_3$, TBHP
97%, 11 : 1
Hatzellis 2004
68%, 4 : 1 d.r.
Iwasaki 2014

Scheme 3.3. Complementary hydrogenation methodology to form the *cis* isomer under heterogeneous catalysis conditions and *trans* with homogeneous.

Skepticism began to arise that **(±)-3.13** was indeed the *trans* product. With no spectra to compare **(±)-3.13** to and inconclusive NOE data, it was reasoned that a crystal structure was the best method to determine the relative stereochemistry of **(±)-3.13**. Fortunately, single crystals were obtained and definitively assigned **(±)-3.13** as the *cis* isomer (Figure **3.10b**). This indicates that structures reported in previous syntheses using Pd/C to obtain *trans* isomers are likely incorrect and any biological findings from these studies may need to be reassessed.

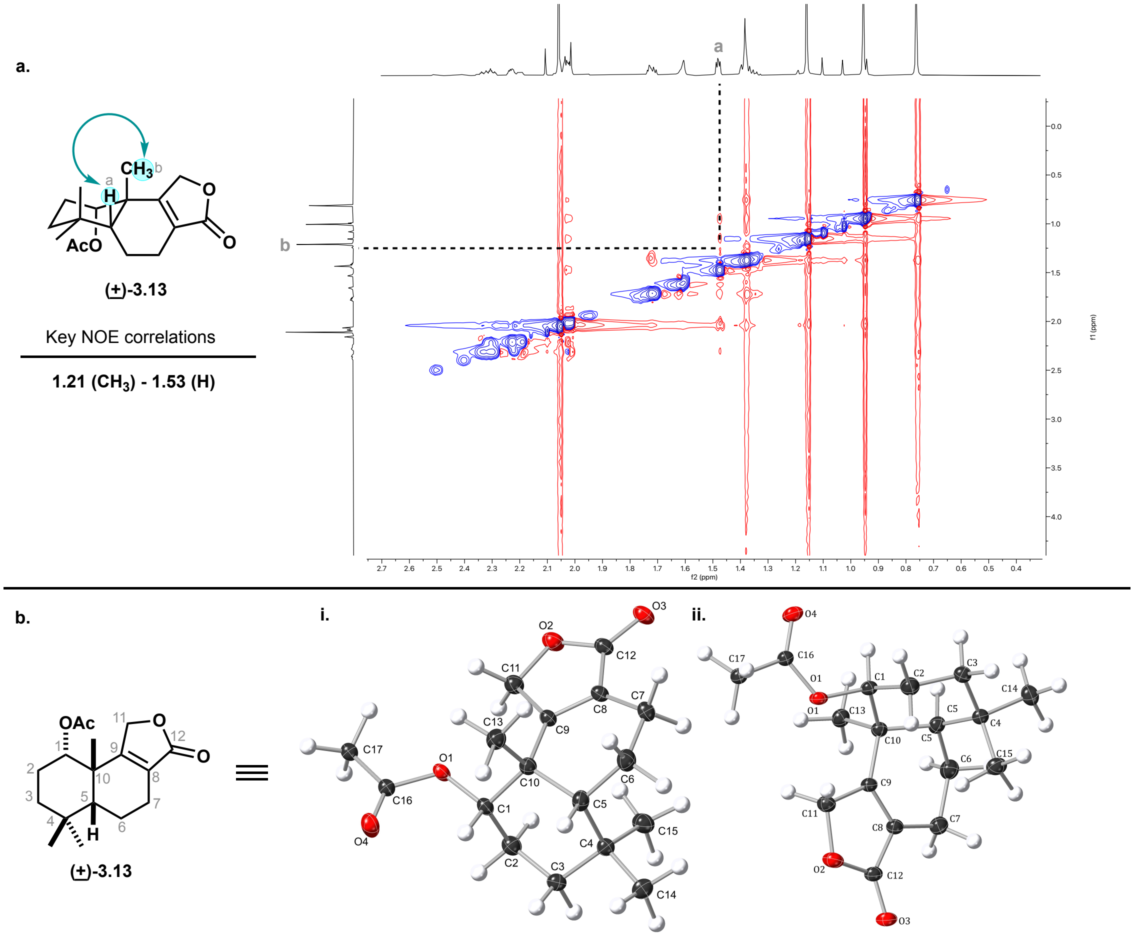

Figure 3.10. Stereochemistry of hydrogenation product. a. Expected key NOE correlation between axial proton (a) and methyl (b). NOE shows possible correlation between a and b. b. Single crystal structure of **(±)-3.13** shows *cis* configuration. A view of the molecular structure, atom C1 and C10 has *S* configuration and C5, *R* (i). A view of the molecular structure showing the chair conformation of the ring C1-C2-C3-C4-C5-C10. This ring is in a chair conformation with some twisting towards a half-chair conformation.

Proceeding with common intermediate **(±)-3.6**, I then began optimization of HAT to obtain the *trans* isomer. Unfortunately, determining d.r. from crude ^{1}H NMR or after filtering the material through a silica plug proved challenging due to traces of Mn(dpm)$_3$ and excess PhSiH$_3$ in the crude sample. Thus, all reactions required purification by silica column to analyze stereoselectivity and conversion. Applying standard reported conditions to **(±)-3.6**, the desired *trans* stereoisomer **(±)-3.14** was obtained in a 1.7:1.0 *trans:cis* isolated d.r. (Table **3.1**, entry 2).

Although the *trans* isomer was obtained, we wanted to investigate if the presence of free hydroxy would improve the diastereoselectivity of the HAT. Thus, a chemoselective acetate hydrolysis was performed with 10% KOH at 0 ˚C[53] to obtain **(±)-3.15.** Free hydroxy **(±)-3.15** was subjected to standard reaction conditions resulting in 6:1 *trans:cis* isolated d.r. (Table **3.1**, entry 3) indicating free hydroxy impacts selectivity of the HAT. Schowen[54] and others has suggested that alcoholic solvent can increase the hydridic character of the silane reductant via pentavalent silane formation[55]. Shenvi, however, observed a variety of silane-derived products by GCMS and instead suggest Ph(*i*-PrO)SiH_2 is a superior reductant[56]. In both cases, the presence of hydroxy groups can improve HAT and similar logic may explain the improved diastereoselectivity observed with **(±)-3.15**.

Although the HAT was reproducible on small scale (10-20 mg) to produce **(±)-3.17**, attempts to scale up (>50 mg) has resulted in incomplete conversion of starting material, fortunately without erosion of d.r. Resubjecting the crude material to standard conditions results in complete conversion of **(±)-3.15** to the hydrogenated product, indicating small scale conditions are not directly translatable to larger scale. Increased equivalents of reagents and time may be necessary to optimize large scale reactions. Current conditions, however, allow for minimal variation without completely stalling the reaction or eroding diastereoselectivity, thus impeding continued exploration of optimal conditions. Therefore, further optimization may be possible using more recently reported conditions by Shenvi involving Ph(*i*-PrO)SiH_2 as the stochiometric reductant. Shenvi and coworkers have demonstrated Ph(*i*-PrO)SiH_2 is more adaptable to changing reaction conditions such as solvent and temperature[56]. Thus, more extensive investigations using Ph(*i*-PrO)SiH_2 as alternative to $PhSiH_3$ may prove to be effective at larger scale conversion of **(±)-3.15** to **(±)-3.17** via HAT.

Table 3.2. Optimization of hydrogenation to obtain *trans* isomer.

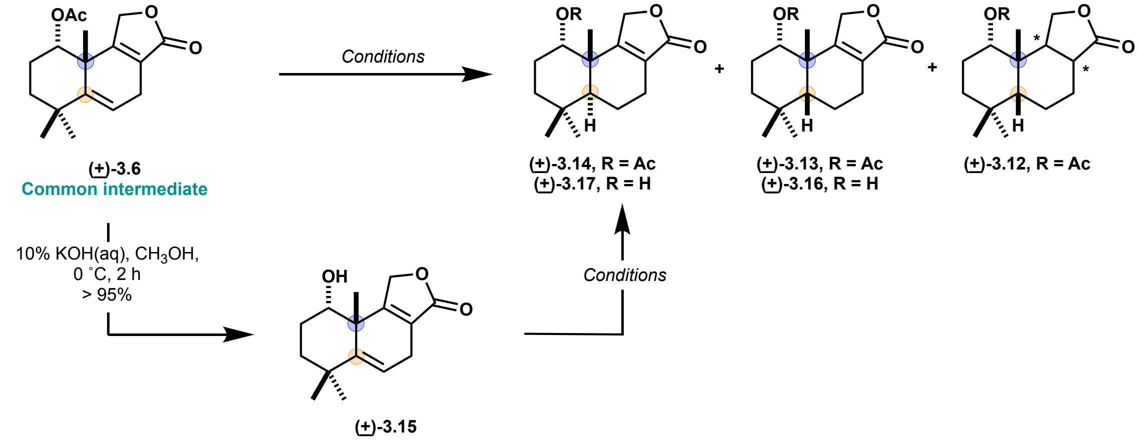
OAc
O
O
(±)-3.6
Common intermediate
Conditions
OR
H
+
(±)-3.14, R = Ac
(±)-3.17, R = H
(±)-3.13, R = Ac
(±)-3.16, R = H
*
(±)-3.12, R = Ac
10% KOH(aq), CH3OH,
0 ˚C, 2 h
> 95%
OH
(±)-3.15
Conditions

*Only one diastereomer isolated. Stereocenters are undetermined

Entry	R	Conditions	Product distrubution (*trans:cis:*over hydrogenation)[a]
1	Ac	5% Pd/C, H_2, CH_3OH, 12 h	—:1.1:1.0
2	Ac	$PhSiH_3$, TBHP, $Mn(dpm)_3$, *i*-PrOH, 83 ˚C, 2 h	1.7:1.0:—
3	H	$PhSiH_3$, TBHP, $Mn(dpm)_3$, *i*-PrOH, 83 ˚C, 3 h	6.0:1.0:—

[a] Isolated product distribution after silica column or PTLC purification

3.2.3. Esterification

With **(±)-3.17** in hand, we were anxious to explore the final esterification with *N*-acetyl-*L*-valine. I began by screening standard coupling conditions (Table **3.2**, entries 1-5). No product was detected by ^{1}H NMR or LC-MS. We were curious if *L*-valine was too sterically hindered to undergo coupling under standard conditions with **(±)-3.17**. Unfortunately, coupling with Fmoc protected *L*-leucine to produce an analogue mimicking the *L*-valine substitution produced no product (Table **3.2**, entry 6). Forming the acyl chloride was also unsuccessful in obtaining the product (Table **3.2**, entry 7). Yamaguchi and Shiina esterification were no more fruitful (Table **3.2**, entries 8-10).

Table 3.3. Esterification screen.

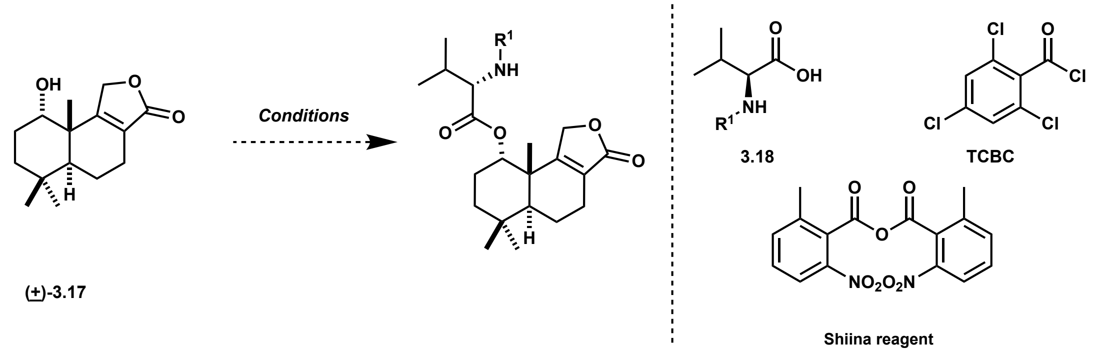

Entry	Coupling partner (R^1)	Conditions	Result
1	3.18 (acyl)	EDC, DMAP, CH_2Cl_2	nr
2	3.18 (acyl)	DCC, DMAP, THF	nr
3	3.18 (acyl)	DCC, NaH, THF	Decomp
4	3.18 (acyl)	DCC, HOBt, THF, 72 h	nr
5	3.18 (acyl)	HBTU, HOBt, NMM, CH_2Cl_2:DMF, 48 h	nr
6	*N*-Fmox-*L*-leucine	EDC, DMAP, CH_2Cl_2	nr
7	3.18 (acyl)	Oxalyl chloride, Et_3N, DMF, CH_2Cl_2	nr
8	3.18 (acyl)	TCBC, Et_3N, DMAP, toluene	nr
9	3.18 (acyl)	TCBC, Et_3N, DMAP, toluene, 80 °C	Decomp
10	3.18 (acyl)	Shiina reagent, Et_3N, DMAP, CH_2Cl_2	nr

Coupling with *N*-acyl-*L*-valine seemed impossible due to steric hindrance of the axial 2° alcohol, the acid coupling partner, and potential unproductive side reactions of *N*-acyl-*L*-valine. We believed we could optimize conditions to accommodate the steric hindrance of the axial 2° alcohol and acid coupling partner but were concerned about side reactivity of *N*-acyl-*L*-valine. Under standard coupling conditions, *N*-acetyl-*L*-valine undergoes azlactone formation akin to the first step of the Erlenmeyer-Plöchl azlactone amino acid synthesis resulting in racemization of the α-stereocenter via oxazole formation. Unreactive oxazole can then stall or inhibit esterification[57] (Scheme **3.4**). Using an alternative *N* substituent would be necessary to rescue the reaction and prevent racemization. Although this would add two steps to the proposed route (*i.e.* deprotection and acylation), it also provides flexibility for future analogue design and probe installation with the free amine. Additionally, I proposed commercially available (−)-borneol could act as a model substrate for the 2° alcohol of **(±)-3.17** to optimize the key esterification.

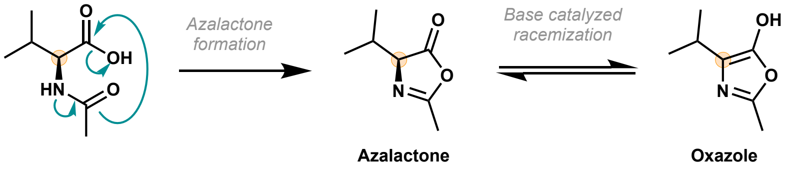

Scheme 3.4. Racemization and inactivation of *N*-acetyl-*L*-*valine.*

Coupling conditions were screened with (−)-borneol and Boc and Fmoc protected amine. Unsurprisingly, standard coupling conditions resulted in no reaction (Table **3.3**, entries 1-2). TBTU coupling and Shiina esterification resulted in trace products by LC-MS, but no product was observed by ^{1}H NMR or TLC (Table **3.3**, entries 3-4). Minor improvements were observed activating the acid as an acyl fluoride with TFFH and catalytic DMAP using Boc and Fmoc as amine protecting groups (Table **3.3**, entries 5-8). Acyl fluorides are often more water-stable and less susceptible to base-promoted oxazolone or ketene formation than their acyl-chloride counterparts. Thus, racemization through either the formation of oxazolone or ketene intermediates *via* fluoride displacement is less common and harsher conditions can be tolerated[58]. Unfortunately, increasing equivalents and time of reaction didn't appear to increase yield and attempts to isolate the esterified product by mass guided HPLC purification and silica column were unsuccessful. Investigations of acyl fluorides suggest stabilization or isolation of the acyl fluoride intermediate may improve yield. Thus, stabilization using benzyltriphenylphosphonium dihydrogentrifluoride (PTF) will be attempted in the future to optimize this transformation.

Nanjo and coworkers developed a hypervalent iodine catalyzed decarboxylative coupling of α-ketoacids with various amines and alcohols to produce amide and ester linkages respectively. Importantly, racemization is not observed[59]. Synthesis of *N*-Boc protected-*L*-valine-α-ketoacid following the procedure reported by Thuaud and coworkers was very low yielding[60], but nevertheless using 1.5 equiv of hypervalent iodine and α-ketoacid produced the desired product in trace amounts (Table **3.3**, entry 9). Increasing the equivalents to 5 appeared to increase product formation by LCMS analysis (Table **3.3**, entry 10). Mass guided purification, however, was unsuccessful in isolating the product. Coupling with Fmoc and Cbz protected α-ketoacid will be attempted in the future to more closely mimic substrates reported by Nanjo.

Table 4.3. Esterification of model substrate (−)-borneol.

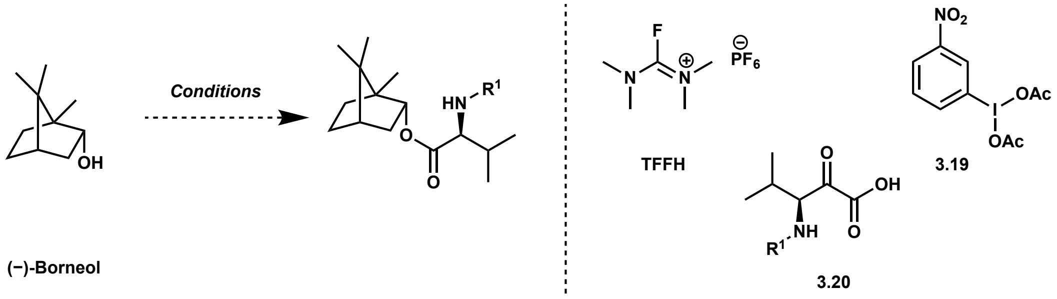

Entry	Coupling partner (R^1)	Conditions	Result[a]
1	3.18 (Boc)	EDC, DMAP, CH_2Cl_2	nr
2	3.18 (Boc)	DCC, DMAP, THF	nr
3	3.18 (Boc)	TBTU, Et_3N, CH_2Cl_2	Trace
4	3.18 (Fmoc)	Shiina reagenet, Et_3N, DMAP, CH_2Cl_2	Trace
5	3.18 (Boc)	TFFH, DIPEA, CH_2Cl_2, 80 ˚C, 24 h	Trace
6	3.18 (Boc)	TFFH, DIPEA, DMAP, CH_2Cl_2, 80 ˚C, 24 h	Trace
7	3.18 (Boc)	TFFH, DIPEA, DMAP, CH_2Cl_2, 80 ˚C, 48 h	Trace
8	3.18 (Fmoc)	TFFH, DIPEA, DMAP, CH_2Cl_2, 80 ˚C, 24 h	Trace
9	3.20 (Boc)	3.19, CH_2Cl_2	Trace
10[b]	3.20 (Boc)	3.19, CH_2Cl_2	>5%

[a]Product was detected by direct-injection for LRMS and ^1H NMR
[b]5 equiv of **3.20** (Boc) and **3.19**

3.2.4. Analogue design

Analogues of the purpurides are designed to probe how the amino acid fragment influences specificity and activity (Figure **3.11**). Initial biological investigations of intermediate **(+)-3.1** suggest the hydrolyzed compound is inactive against microbial species[32]. External studies have also demonstrated cytotoxicity of the hydrolyzed product indicating the amino acid fragment may play a role in facilitating selective inhibition of fungal and bacterial cells over mammalian[61]. Thus, proposed analogues will incorporate various structural modifications including linear and branched acyl chains and "simplified" amino acids (*i.e.* glycine, alanine, and β-*L*-valine). Although coupling with *L*-valine has proven challenging, esterification of axial 2° alcohols has been demonstrated with less sterically crowded acid substrates[62]. Therefore, changing the acid coupling partner from *L*-valine to a less sterically crowded substrate will not only probe the importance of the structural component, but may also facilitate successful esterification of the 2° alcohol.

Additionally, modifications to the furanone ring were proposed based on precedence of highly electrophilic species acting as covalent inhibitors[63]. These analogues would probe potential covalent interactions of the furanone with a protein target through hetero-Michael (*i.e.* sulfa or oxa) addition to the enone. To explore the prospect of a covalent protein-small molecule interaction, fully saturated analogues will be synthesized. Specifically, if the furanone is critical for activity, saturated analogues should demonstrate minimal inhibitory activity compared to the natural products. Further analysis can be completed to determine if covalent interactions are occurring and may provide valuable insight into probe design (*i.e.* diazirine may be unnecessary) for future proteomic experiments.

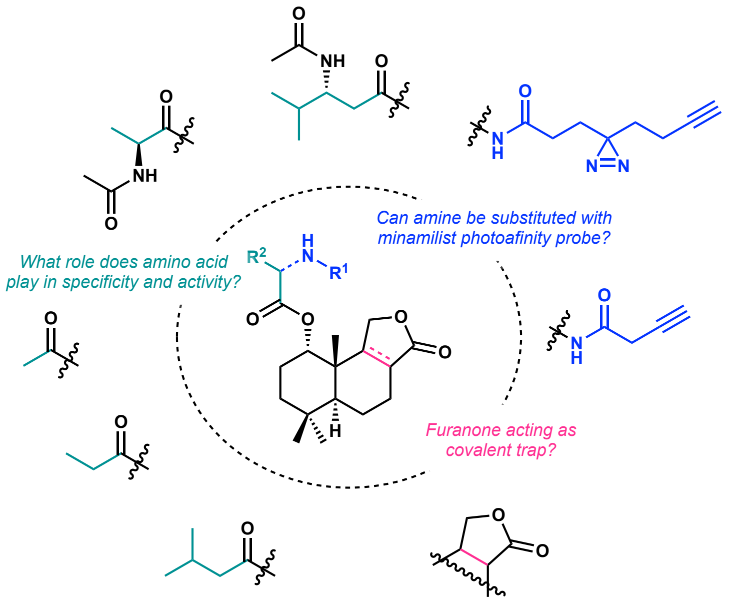
What role does amino acid play in specificity and activity?
Can amine be substituted with minamilist photoafinity probe?
Furanone acting as covalent trap?
R2
R1
NH
N=N
O
H

Figure 3.11. Proposed SAR investigations of the purpurides.

3.2.5. Preliminary biological investigations

Preliminary biological investigations were completed to explore antibacterial activity of free hydroxyl intermediates. Both *cis* and *trans* diastereomers as well as over hydrogenated intermediates were tested. Acyl capped intermediates were also explored to probe the necessity of the *N*-acetyl-*L*-valine moiety for activity. None of the hydroxy intermediates tested demonstrated activity against *S. aureus* nor *P. aeruginosa* suggesting the ester is not acting as a prodrug, undergoing hydrolysis to produce the active hydroxy component (Table **3.4**). Additionally, acyl capped intermediates were inactive against both strains of bacteria indicating the amino acid moiety, or an extended acyl chain may be critical for activity. Future studies will investigate the activity of these intermediates against *C. albicans* to determine if similar SAR trends are observed between fungal and bacterial species.

Table 3.4. Microbial Minimum Inhibitory Concentrations of Purpuride Intermediates.

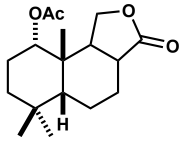

(±)-**3.12**

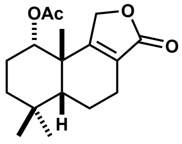

(±)-**3.13**

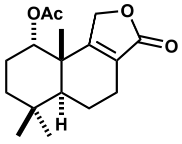

(±)-**3.14**

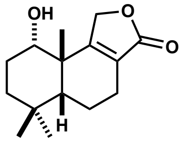

(±)-**3.16**

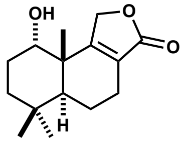

(±)-**3.17**

	MIC[a],[b] (μM)	
	S. aureus (MSSA)	*P. aeruginosa*
Compound	(Newman)	(PAO1)
(±)-**3.12**	-	-
(±)-**3.13**	-	-
(+)-**3.14**	-	-
(±)-**3.16**	-	-
(−)-**3.17**	-	-

[a]Levofloxacin was used as a positive control, [b]All assays were realized in triplicate

3.3. Conclusion

Common intermediate **(±)-3.6** was synthesized in 4 steps from known 2° alcohol. Key transformations, including intramolecular Diels-Alder cycloaddition and HAT were developed to produce the desired diastereomer of the purpurides core in high yield with good isolated d.r. Efforts to complete the final esterification between 2° alcohol and *L*-valine is ongoing. Primary focus will be on optimizing the protecting group of the α-keto acid for hypervalent iodine(III) mediated esterification and methods to stabilize acyl fluoride formation for coupling with TFFH. Synthesis of other members of the purpurides is also underway, specifically optimizing allylic oxidation of **(±)-3.6** to provide a common intermediate for the synthesis of purpuride B and minioluteumides A-D. Although no antibacterial activity was demonstrated by intermediates tested against *S. aureus* and *P. aeruginosa*, future studies of these intermediates with *C. albicans* and the synthesized natural products against a panel of pathogens will be completed.

References

1. Rodrigues, M. L.; Nosanchuk, J. D., Fungal diseases as neglected pathogens: A wake-up call to public health officials. *PLoS Negl. Trop. Dis.* **2020,** *14* (2), e0007964.
2. Brandt, M. E.; Park, B. J., Think fungus–prevention and control of fungal infections. *Emerg. Infect. Dis.* **2013,** *19* (10), 1688-9.
3. Almeida, F.; Rodrigues, M. L.; Coelho, C., The Still Underestimated Problem of Fungal Diseases Worldwide. *Front. Microbiol.* **2019,** *10*.
4. Litvintseva, A. P.; Brandt, M. E.; Mody, R. K.; Lockhart, S. R., Investigating fungal outbreaks in the 21st century. *PLoS Pathog.* **2015,** *11* (5), e1004804.
5. Brown, G. D.; Denning, D. W.; Gow, N. A.; Levitz, S. M.; Netea, M. G.; White, T. C., Hidden killers: human fungal infections. *Sci. Transl. Med.* **2012,** *4* (165), 165rv13.
6. Maertens, J. A., History of the development of azole derivatives. *Clin. Microbiol. Infect.* **2004,** *10 Suppl 1*, 1-10.
7. Vallabhaneni, S.; Mody, R. K.; Walker, T.; Chiller, T., The Global Burden of Fungal Diseases. *Infect. Dis. Clin. North Am.* **2016,** *30* (1), 1-11.
8. von Lilienfeld-Toal, M.; Wagener, J.; Einsele, H.; Cornely, O. A.; Kurzai, O., Invasive Fungal Infection. *Dtsch. Artzebl. Int.* **2019,** *116* (16), 271-278.
9. Webb, B. J.; Ferraro, J. P.; Rea, S.; Kaufusi, S.; Goodman, B. E.; Spalding, J., Epidemiology and Clinical Features of Invasive Fungal Infection in a US Health Care Network. *Open Forum Infect. Dis.* **2018,** *5* (8), ofy187.
10. Kumar, L.; Verma, S.; Bhardwaj, A.; Vaidya, S.; Vaidya, B., Eradication of superficial fungal infections by conventional and novel approaches: a comprehensive review. *Artif. Cells Nanomed. Biotechnol.* **2014,** *42* (1), 32-46.
11. Johnson, L. B.; Kauffman, C. A., Voriconazole: a new triazole antifungal agent. *Clin. Infect. Dis.* **2003,** *36* (5), 630-7.
12. Georgopapadakou, N. H.; Walsh, T. J., Antifungal agents: chemotherapeutic targets and immunologic strategies. *Antimicrob. Agents Chemother.* **1996,** *40* (2), 279-291.
13. Chandrasekar, P., Management of invasive fungal infections: a role for polyenes. *J. Antimicrob. Chemother.* **2011,** *66* (3), 457-465.
14. Bezemer, J. M.; van der Ende, J.; Limpens, J.; de Vries, H. J. C.; Schallig, H. D. F. H., Safety and efficacy of allylamines in the treatment of cutaneous and mucocutaneous leishmaniasis: A systematic review. *PLoS ONE* **2021,** *16* (4), e0249628.
15. Grover, N. D., Echinocandins: A ray of hope in antifungal drug therapy. *Indian J. Pharmacol.* **2010,** *42* (1), 9-11.
16. Shafiei, M.; Peyton, L.; Hashemzadeh, M.; Foroumadi, A., History of the development of antifungal azoles: A review on structures, SAR, and mechanism of action. *Bioorg. Chem.* **2020,** *104*, 104240.
17. Holt, R. J., Topical pharmacology of imidazole antifungals. *J. Cutan. Pathol.* **1976,** *3* (1), 45-59.
18. Peyton, L. R.; Gallagher, S.; Hashemzadeh, M., Triazole antifungals: a review. *Drugs Today (Barc)* **2015,** *51* (12), 705-18.
19. Boucher, H. W.; Groll, A. H.; Chiou, C. C.; Walsh, T. J., Newer systemic antifungal agents : pharmacokinetics, safety and efficacy. *Drugs* **2004,** *64* (18), 1997-2020.

20. Serhan, G.; Stack, C. M.; Perrone, G. G.; Morton, C. O., The polyene antifungals, amphotericin B and nystatin, cause cell death in Saccharomyces cerevisiae by a distinct mechanism to amphibian-derived antimicrobial peptides. *Ann. Clin. Microbiol. Antimicrob.* **2014,** *13*, 18.

21. Denning, D. W., Echinocandin antifungal drugs. *Lancet* **2003,** *362* (9390), 1142-1151.

22. Stütz, A.; Georgopoulos, A.; Granitzer, W.; Petranyi, G.; Berney, D., Synthesis and structure-activity relationships of naftifine-related allylamine antimycotics. *J. Med. Chem.* **1986,** *29* (1), 112-25.

23. Fisher, M. C.; Henk, D. A.; Briggs, C. J.; Brownstein, J. S.; Madoff, L. C.; McCraw, S. L.; Gurr, S. J., Emerging fungal threats to animal, plant and ecosystem health. *Nature* **2012,** *484* (7393), 186-94.

24. Whaley, S. G.; Berkow, E. L.; Rybak, J. M.; Nishimoto, A. T.; Barker, K. S.; Rogers, P. D., Azole Antifungal Resistance in Candida albicans and Emerging Non-albicans Candida Species. *Front. Microbiol.* **2016,** *7*, 2173.

25. Xiang, M. J.; Liu, J. Y.; Ni, P. H.; Wang, S.; Shi, C.; Wei, B.; Ni, Y. X.; Ge, H. L., Erg11 mutations associated with azole resistance in clinical isolates of Candida albicans. *FEMS Yeast Res.* **2013,** *13* (4), 386-93.

26. Dunkel, N.; Liu, T. T.; Barker, K. S.; Homayouni, R.; Morschhauser, J.; Rogers, P. D., A gain-of-function mutation in the transcription factor Upc2p causes upregulation of ergosterol biosynthesis genes and increased fluconazole resistance in a clinical Candida albicans isolate. *Eukaryot. Cell* **2008,** *7* (7), 1180-90.

27. Coste, A.; Selmecki, A.; Forche, A.; Diogo, D.; Bougnoux, M. E.; d'Enfert, C.; Berman, J.; Sanglard, D., Genotypic evolution of azole resistance mechanisms in sequential Candida albicans isolates. *Eukaryot. Cell* **2007,** *6* (10), 1889-904.

28. Selmecki, A.; Gerami-Nejad, M.; Paulson, C.; Forche, A.; Berman, J., An isochromosome confers drug resistance in vivo by amplification of two genes, ERG11 and TAC1. *Mol. Microbiol.* **2008,** *68* (3), 624-41.

29. Morio, F.; Pagniez, F.; Lacroix, C.; Miegeville, M.; Le Pape, P., Amino acid substitutions in the Candida albicans sterol Delta5,6-desaturase (Erg3p) confer azole resistance: characterization of two novel mutants with impaired virulence. *J. Antimicrob. Chemother.* **2012,** *67* (9), 2131-8.

30. Casadevall, A.; Kontoyiannis, D. P.; Robert, V., On the Emergence of Candida auris: Climate Change, Azoles, Swamps, and Birds. *mBio* **2019,** *10* (4).

31. King, T. J.; Roberts, J. C.; Thompson, D. J., Studies in mycological chemistry. Part XXX and last. Isolation and structure of purpuride, a metabolite of Penicillium purpurogenum stoll. *J. Chem. Soc. Perkin Trans. 1* **1973,** (0), 78-80.

32. Wang, H.; Wang, Y.; Liu, P.; Wang, W.; Fan, Y.; Zhu, W., Purpurides B and C, two new sesquiterpene esters from the aciduric fungus Penicillium purpurogenum JS03-21. *Chem. Biodivers.* **2013,** *10* (7), 1185-92.

33. Kaleem, S.; Ge, H.; Yi, W.; Zhang, Z.; Wu, B., Isolation, structural elucidation, and antimicrobial evaluation of the metabolites from a marine-derived fungus Penicillium sp. ZZ1283. *Nat. Prod. Res.* **2021,** *35* (15), 2498-2506.

34. Zhao, W.; Fernando, L. D.; Kirui, A.; Deligey, F.; Wang, T., Solid-state NMR of plant and fungal cell walls: A critical review. *Solid State Nucl. Magn. Reson.* **2020,** *107*, 101660.

35. Stierle, D. B.; Stierle, A. A.; Girtsman, T.; McIntyre, K.; Nichols, J., Caspase-1 and -3 inhibiting drimane sesquiterpenoids from the extremophilic fungus Penicillium solitum. *J. Nat. Prod.* **2012,** *75* (2), 262-6.

36. Ngokpol, S.; Suwakulsiri, W.; Sureram, S.; Lirdprapamongkol, K.; Aree, T.; Wiyakrutta, S.; Mahidol, C.; Ruchirawat, S.; Kittakoop, P., Drimane Sesquiterpene-Conjugated Amino Acids from a Marine Isolate of the Fungus Talaromyces minioluteus (Penicillium Minioluteum). *Mar. Drugs* **2015,** *13* (6), 3567-80.

37. Baunach, M.; Franke, J.; Hertweck, C., Terpenoid biosynthesis off the beaten track: unconventional cyclases and their impact on biomimetic synthesis. *Angew. Chem. Int. Ed.* **2015,** *54* (9), 2604-26.

38. Upar, K. B.; Mishra, S. J.; Nalawade, S. P.; Singh, S. A.; Khandare, R. P.; Bhat, S. V., Efficient enantioselective synthesis of (+)-sclareolide and (+)-tetrahydroactinidiolide: chiral LBA-induced biomimetic cyclization. *Tetrahedron Asymmetry* **2009,** *20* (14), 1637-1640.

39. Hung, K.; Hu, X.; Maimone, T. J., Total synthesis of complex terpenoids employing radical cascade processes. *Nat. Prod. Rep.* **2018,** *35* (2), 174-202.

40. Li, F.; Renata, H., A Chiral-Pool-Based Strategy to Access trans-syn-Fused Drimane Meroterpenoids: Chemoenzymatic Total Syntheses of Polysin, N-Acetyl-polyveoline and the Chrodrimanins. *J. Am. Chem. Soc.* **2021,** *143* (43), 18280-18286.

41. Li, J.; Li, F.; King-Smith, E.; Renata, H., Merging chemoenzymatic and radical-based retrosynthetic logic for rapid and modular synthesis of oxidized meroterpenoids. *Nat. Chem.* **2020,** *12* (2), 173-179.

42. Zhang, X.; King-Smith, E.; Dong, L.-B.; Yang, L.-C.; Rudolf Jeffrey, D.; Shen, B.; Renata, H., Divergent synthesis of complex diterpenes through a hybrid oxidative approach. *Science* **2020,** *369* (6505), 799-806.

43. Mori, K.; Watanabe, H., Synthesis of both the enantiomers of polygodial, an insect antifeedant sesouiterpene. *Tetrahedron* **1986,** *42* (1), 273-281.

44. Della Monica, C.; Della Sala, G.; Izzo, I.; De Petrocellis, L.; di Marzo, V.; Spinella, A., Enantioselective synthesis of 1-(R)-hydroxypolygodial and its 9α epimer, 1-(R)-hydroxyisotadeonal. *Tetrahedron* **2007,** *63* (29), 6866-6873.

45. Abad, A.; Agulló, C.; C. Cuñat, A.; Carmen Llosá, M., Stereoselective construction of the tetracyclic scalarane skeleton from carvone. *ChemComm* **1999,** (5), 427-428.

46. Wang, Z.-L.; Zhang, Z.-G.; Li, H.-C.; Deng, W.-P., Concise stereoselective synthesis of marine sesterterpene, 16-deacetoxy-12-epi-scalarafuran acetate and its 14-epimer via intramolecular Diels–Alder addition. *Tetrahedron* **2011,** *67* (36), 6939-6943.

47. Della Monica, C.; Della Sala, G.; D'Urso, D.; Izzo, I.; Spinella, A., Enantioselective synthesis of 1(R)-hydroxypolygodial. *Tetrahedron Lett.* **2005,** *46* (23), 4061-4063.

48. Carreño, M. C.; García Ruano, J. L.; Toledo, M. A., Enantioselective synthesis of (+)-royleanone from sulfinyl quinones. *Chemistry* **2000,** *6* (2), 288-91.

49. Zeng, F.; Arnao, E.; Zhang, G.; Olaya, G.; Wullschleger, J.; Sierotzki, H.; Ming, R.; Bluhm, B. H.; Bond, J. P.; Fakhoury, A. M.; Bradley, C. A., Characterization of Quinone Outside Inhibitor Fungicide Resistance in Cercospora sojina and Development of Diagnostic Tools for its Identification. *Plant Dis.* **2015,** *99* (4), 544-550.

50. Hatzellis, K.; Pagona, G.; Spyros, A.; Demetzos, C.; Katerinopoulos, H. E., Correction of the Structure of a New Sesquiterpene from Cistus creticus ssp. creticus. *J. Nat. Prod.* **2004,** *67* (12), 1996-2001.

51. Paquette, L. A.; Maleczka, R. E., Enantioselective construction of natural (+)-pallescensin A. A sigmatropic pathway to furanosesquiterpenes. *J. Org. Chem.* **1992,** *57* (26), 7118-7122.

52. Iwasaki, K.; Wan, K. K.; Oppedisano, A.; Crossley, S. W.; Shenvi, R. A., Simple, chemoselective hydrogenation with thermodynamic stereocontrol. *J. Am. Chem. Soc.* **2014,** *136* (4), 1300-3.

53. Abad, A.; Agulló, C.; Cuñat, A. C.; García, A. B.; Giménez-Saiz, C., Synthetic studies on the preparation of oxygenated spongiane diterpenes from carvone. *Tetrahedron* **2003,** *59* (48), 9523-9536.

54. O'Donnell, K.; Bacon, R.; Chellappa, K. L.; Schowen, R. L.; Lee, J. K., Catalytic mode, solvent isotope effects, and transition-state structure in hydride expulsion from silicon. *J. Am. Chem. Soc.* **1972**.

55. Revunova, K.; Nikonov, G. I., Base-Catalyzed Hydrosilylation of Ketones and Esters and Insight into the Mechanism. *Chem. Eur.* **2014,** *20* (3), 839-845.

56. Obradors, C.; Martinez, R. M.; Shenvi, R. A., Ph(i-PrO)SiH2: An Exceptional Reductant for Metal-Catalyzed Hydrogen Atom Transfers. *J. Am. Chem. Soc.* **2016,** *138* (14), 4962-4971.

57. De Jersey, J.; Zerner, B., Spontaneous and enzyme-catalyzed hydrolysis of saturated oxazolinones. *Biochemistry* **1969,** *8* (5), 1967-1974.

58. Due-Hansen, M. E.; Pandey, S. K.; Christiansen, E.; Andersen, R.; Hansen, S. V. F.; Ulven, T., A protocol for amide bond formation with electron deficient amines and sterically hindered substrates. *Org. Biomol. Chem.* **2016,** *14* (2), 430-433.

59. Nanjo, T.; Kato, N.; Takemoto, Y., Oxidative Decarboxylation Enables Chemoselective, Racemization-Free Esterification: Coupling of alpha-Ketoacids and Alcohols Mediated by Hypervalent Iodine(III). *Org. Lett.* **2018,** *20* (18), 5766-5769.

60. Thuaud, F.; Rohrbacher, F.; Zwicky, A.; Bode, J. W., Incorporation of Acid-Labile Masking Groups for the Traceless Synthesis of C-Terminal Peptide α-Ketoacids. *Org. Lett.* **2016,** *18* (15), 3670-3673.

61. Ma, M.; Ge, H.; Yi, W.; Wu, B.; Zhang, Z., Bioactive drimane sesquiterpenoids and isocoumarins from the marine-derived fungus Penicillium minioluteum ZZ1657. *Tetrahedron Lett.* **2020,** *61* (7).

62. Wang, Y.; Nagai, T.; Watanabe, I.; Hagiwara, K.; Inoue, M., Total Synthesis of Euonymine and Euonyminol Octaacetate. *J. Am. Chem. Soc.* **2021,** *143* (49), 21037-21047.

63. Johnson, D. S.; Weerapana, E.; Cravatt, B. F., Strategies for discovering and derisking covalent, irreversible enzyme inhibitors. *Future Med. Chem.* **2010,** *2* (6), 949-64.

Chapter 4. Synthesis and biological investigations of epoxy-isonitrile metabolites

Disclaimer: This work was adapted from the following publication with permission from all authors: Epoxy isonitriles, a unique class of antibiotics: synthesis of their metabolites and biological investigations[1]

Dr. Guillaume Ernouf designed the project and synthesized *post*-amycomicin and *post*-aerocyanidin. Ingrid K. Wilt synthesized Cinchona alkaloid catalysts and elongated analogue *post*-YM4750. Dr. Guillaume Ernouf and Ingrid K. Wilt completed MIC assays and IC_{50} curves.

4.1. Introduction

4.1.1. Narrow spectrum antibiotics

Scientists have explored numerous campaigns to combat emerging antimicrobial resistance. “Narrow spectrum” antibiotics with species-specific inhibitory activity may play an important role in these efforts. In theory, by eliminating only pathogenic bacteria, narrow spectrum therapies allow the commensal (nonharmful) bacteria to remain. These commensals not only serve a critical function in maintaining host health but provide competition to prevent developing resistant and pathogenic strains from gaining capital in the host microbiome[2]. Although the concept of narrow spectrum antibiotics is not a novel strategy for combating resistance, these therapies are far less common than broad spectrum. The development of narrow spectrum treatments is stymied by numerous challenges, namely sluggish advancements in diagnostic techniques to rapidly characterize the causative species, polymicrobial infections, and identifying and enrolling suitable patient populations for clinical trials[3].

Despite these challenges, the development of narrow spectrum antibiotics has recently seen success with two new antibiotics approved for clinical use: Fidaxomicin (dificid) and sarecycline (seysara) (Figure **4.1**). Dificid, a tiacumicin macrocyclic antibiotic, treats gram-positive *Clostridium difficile*-associated diarrhea by binding to the “switch regions” of bacterial RNA polymerase and preventing the unwinding of DNA required to initiate transcription. In a meta-analysis of resistant *C. difficile* derived from human stool samples, Sholeh and coworkers found that only 1 out of 1184 clinical isolates demonstrated fidaxomicin resistance based on the breakpoint dosage of ≥8 µg/mL[4]. Seysara also demonstrates selective gram-positive activity. Clinically, it's used in the treatment of acne caused by *Cutibacterium acnes.* The small molecule is a member of the tetracycline class of antibiotics and inhibits bacterial growth by binding to the 30S and 50S subunit of microbial ribosomes to inhibit protein synthesis. Although resistance to other tetracyclines with broad-spectrum antibacterial activity is well documented, *in vitro* testing suggests seysara resistance due to spontaneous genome mutations is infrequent (*i.e.* 10^{-10} at 4-8 x MIC)[5]. Although difficid and seysara have demonstrated excellent clinical practicality, additional interest lies in developing narrow spectrum small molecules with novel MOAs.

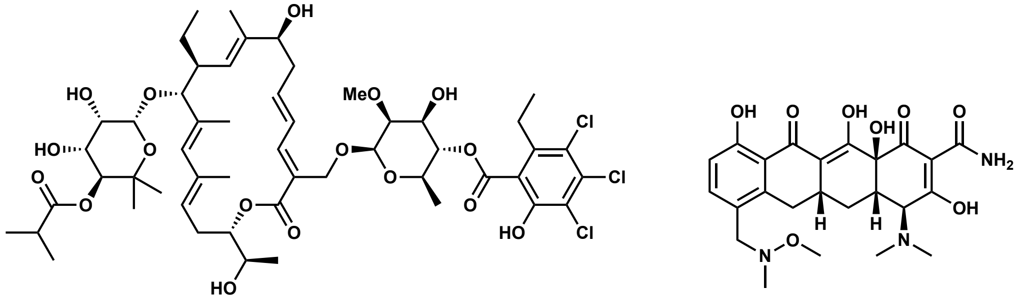

Dificid

Seysara

Figure 4.1. Narrow spectrum antibiotics in the clinic. Difficid is prescribed for the treatment of *C. difficile* and seysara for *C. acnes*.

4.1.2. Epoxy isonitrile containing natural products

As previously described, selective or narrow spectrum antibacterial agents may prove a successful method for combating emerging bacterial resistance. Ideally, these treatments would eliminate selective pressure needed for developing resistance by only killing pathogenic bacteria and allowing commensal organisms to survive. Although researchers have noted the potent antimicrobial activity of epoxy isonitrile natural products, the structural complexity of this moiety has prevented in-depth investigations of this class of compounds. In 1987, the epoxy isonitrile containing aerocyanidin[6] (**4.1**) was isolated exhibiting a highly potent profile against gram-positive pathogens. An elongated derivative of aerocyanidin, YM-47515[7] (**4.2**), was isolated a decade later, and very recently, Clardy and coworkers, during a co-culture bacterial assay with *Streptomyces* 84 *coelicolor* M145, identified amycomicin (**4.3**) which displays potent bactericidal effects in *S. aureus*[8] (Figure **4.2**).

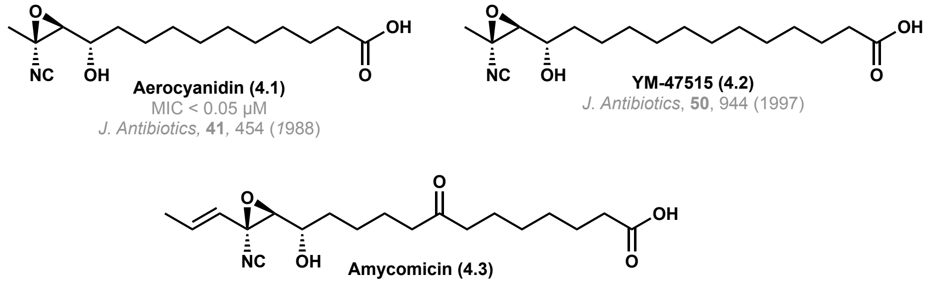

Aerocyanidin (4.1)
MIC < 0.05 µM
J. Antibiotics, **41**, 454 (1988)

YM-47515 (4.2)
J. Antibiotics, **50**, 944 (1997)

Amycomicin (4.3)
MIC = 0.03 µM
Proc. Natl. Acad. Sci., **40**, 10124 (2018)

Figure 4.2. Epoxy isonitrile narrow spectrum antibacterials. Aerocyanidin, YM-47515, and amycomicin display potent activity against gram-positive pathogen *S. aureus*.

Despite potent activity, the potential for *in vivo* release of toxic hydrogen cyanide via Payne rearrangement of the epoxy isonitrile scaffold renders these small molecules undesirable for use as pharmaceuticals (Scheme **4.1**). Upon comparison to inorganic cyanide, however, aerocyanidin exhibited more potent activity, suggesting the epoxy isonitrile scaffold may be acting as a prodrug[6]. If the epoxy isonitrile scaffold is acting as a prodrug, administering only the rearranged epoxy ketone metabolite would eliminate bacterial infections, while reducing toxicity by preventing the release of hydrogen cyanide *in vivo*.

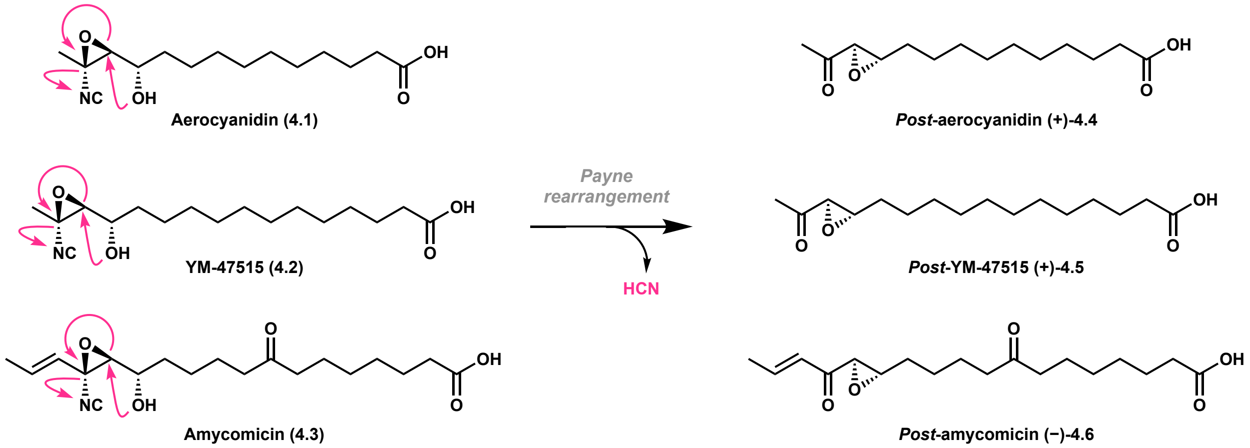

Scheme 4.1. Payne rearrangement. Epoxy isonitrile containing natural products can undergo a Payne rearrangement to produce stable epoxy ketone metabolites and release cyanide.

Furthermore, Clardy and coworkers. recently discovered that by supplementing growth media with exogenous oleic acids, *S. aureus* can overcome amycomicin inhibition. This suggests amycomicin may be targeting fatty acid biosynthesis. Additionally, overexpression of FabH in *S. aureus*, a key enzyme in fatty acid biosynthesis, resulted in a fourfold increase in the MIC against amycomicin, while the overexpression of other Fab proteins was inconsequential. This indicates FabH is likely the target of amycomicin[8]. Fortunately, targeting lipid biosynthesis is of particular interest to researchers for developing antibacterial agents as metabolism of fatty acids is often unique to each species of bacteria thus insinuating a specific or narrow spectrum mode of action for these epoxy ketone natural products[9]. Lipid biosynthesis has continued to gain traction as a potential antibacterial target and is the known target of several natural products such as cerulenin[10], a covalent inhibitor of FabB/F, and phomallenic acid C[11]. Additionally, CG400549[12] and Afabicin (FabI)[13] are currently in development to fight MRSA, providing further precedence for targeting this pathway with narrow spectrum antibiotics (Figure **4.3**). To date, however, FabH remains an underexplored antibacterial target. Thus, investigations of epoxy isonitrile derivatives may aid in the development of antibiotics with novel MoAs.

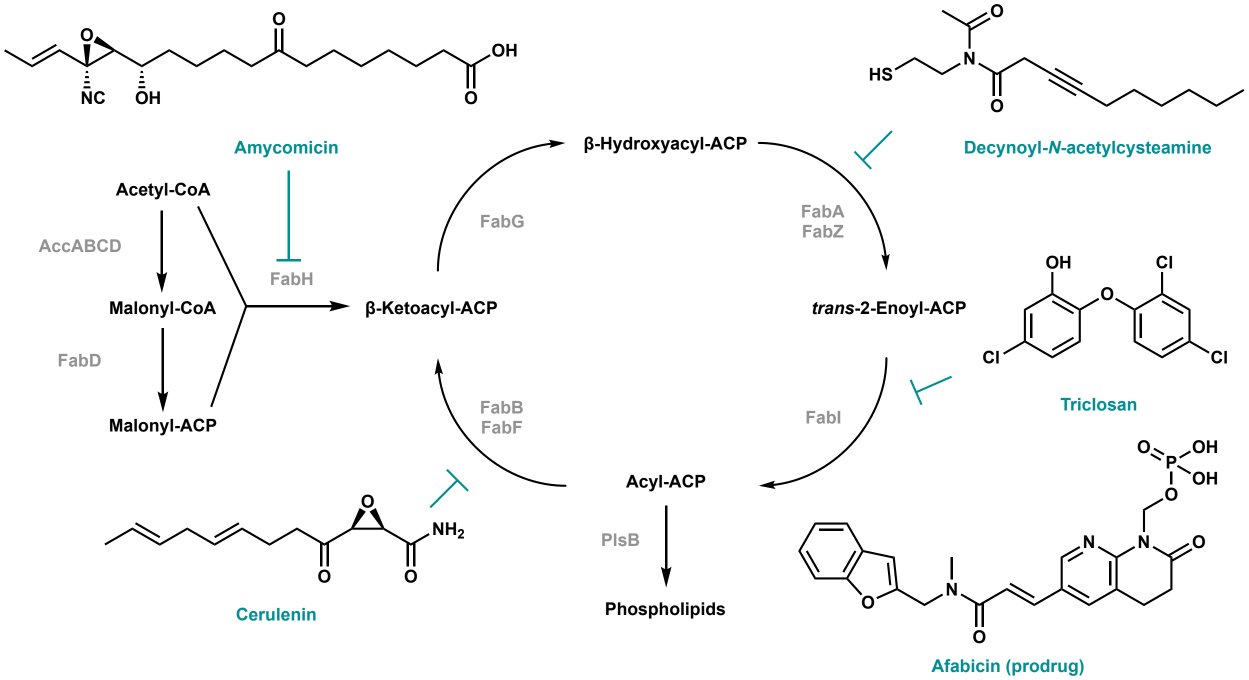
Amycomicin
Decynoyl-*N*-acetylcysteamine
Acetyl-CoA
AccABCD
Malonyl-CoA
FabD
Malonyl-ACP
FabH
β-Ketoacyl-ACP
FabG
β-Hydroxyacyl-ACP
FabA
FabZ
trans-2-Enoyl-ACP
Triclosan
FabI
Acyl-ACP
FabB
FabF
PlsB
Phospholipids
Cerulenin
Afabicin (prodrug)

Figure 4.1. Known fatty acid biosynthesis inhibitors.

4.2. Results and discussion

4.2.1. Synthesis of metabolites

Post-aerocyanidin (+)-**4.4** and *post*-YM-47515 (+)-**4.5** were prepared in three steps from known intermediates **4.7**[14] and **4.8**[15] respectively. Subsequent cross-metathesis with methyl vinyl ketone (MVK) and Grubbs M204 catalyst[16] resulted in α,β-unsaturated ketones in high yield. Subsequent treatment with an amine base and hydrogen peroxide produced racemic substrates **(±)-4.11** and **(±)-4.12** (condition A). Cinchona primary amine catalyst was used to facilitate stereoselective epoxide formation to generate key intermediates **(+)-4.11** and **(+)-4.12** (condition B)[17, 18].

Hydrolysis of the resulting methyl ester with lithium hydroxide proceeded in moderate yield to produce *post*-aerocyanidin **(+)-4.4**. Attempts to improve the yield by performing the hydrolysis with sodium hydroxide resulted in slow reaction time and partial degradation of the epoxy ketone. For the elongated analogue, *post*-YM47515, lithium hydroxide produced the desired acid in low yield. Thus, a milder enzymatic hydrolysis was performed with pig liver esterase (PLE)[19] in a 1:9 mixture of acetone in pH 7 buffer at 37 °C furnishing *post*-YM47515 **(+)-4.5** in high yield (Scheme **4.2**).

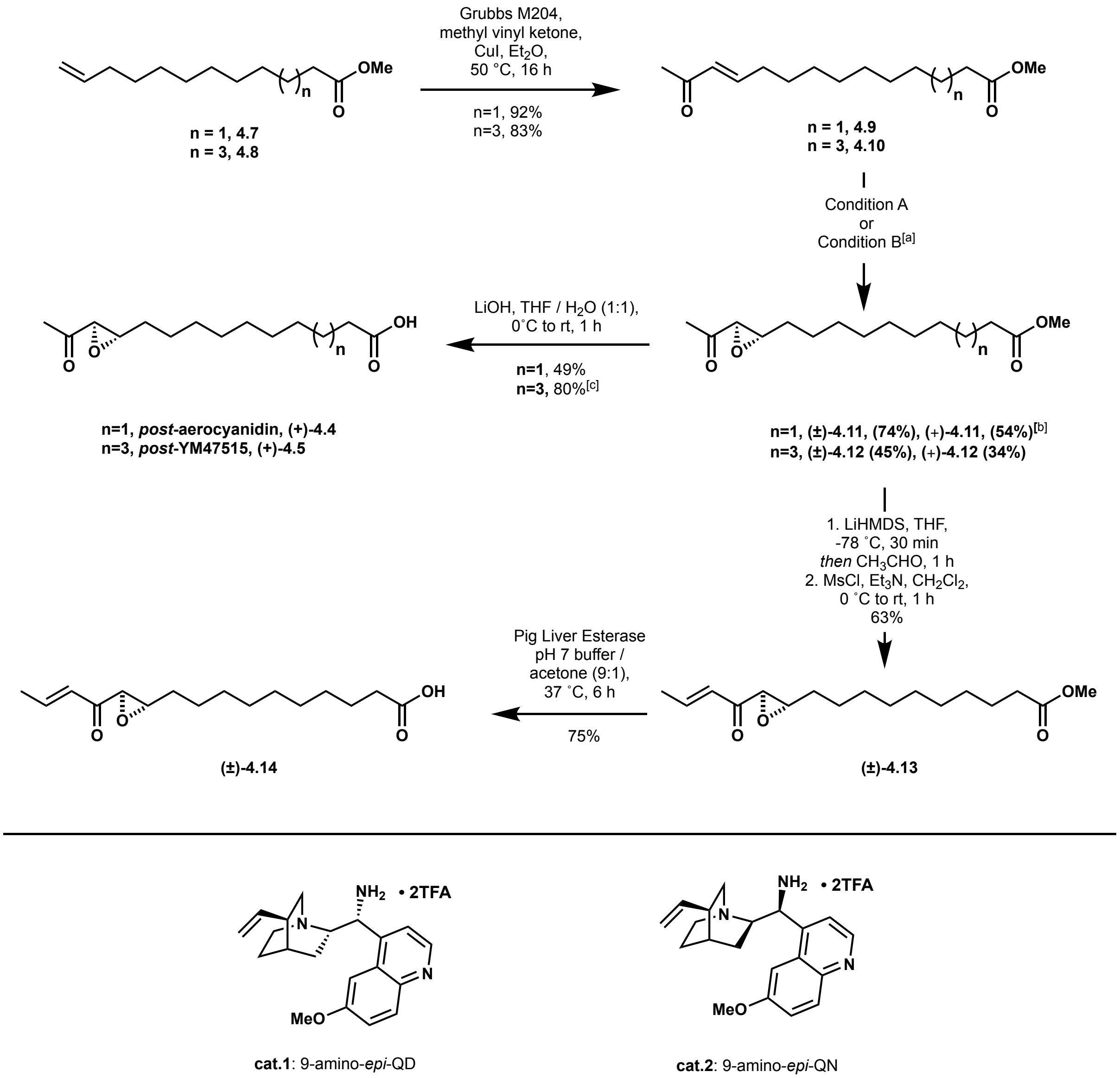
OMe
n
O
n = 1, 4.7
n = 3, 4.8
Grubbs M204,
methyl vinyl ketone,
CuI, Et$_2$O,
50 °C, 16 h
n=1, 92%
n=3, 83%
OMe
O
n
O
n = 1, 4.9
n = 3, 4.10
Condition A
or
Condition B[a]
OMe
O
O
n
O
n=1, (±)-4.11, (74%), (+)-4.11, (54%)[b]
n=3, (±)-4.12 (45%), (+)-4.12 (34%)
LiOH, THF / H$_2$O (1:1),
0°C to rt, 1 h
n=1, 49%
n=3, 80%[c]
OH
O
O
n
O
n=1, post-aerocyanidin, (+)-4.4
n=3, post-YM47515, (+)-4.5
1. LiHMDS, THF,
-78 °C, 30 min
then CH$_3$CHO, 1 h
2. MsCl, Et$_3$N, CH$_2$Cl$_2$,
0 °C to rt, 1 h
63%
OMe
O
O
O
(±)-4.13
Pig Liver Esterase
pH 7 buffer /
acetone (9:1),
37 °C, 6 h
75%
OH
O
O
O
(±)-4.14
NH$_2$ • 2TFA
N
N
MeO
cat.1: 9-amino-epi-QD
NH$_2$ • 2TFA
N
N
MeO
cat.2: 9-amino-epi-QN

Scheme 4.2. **Synthesis of *post*-aerocyanidin and *post*-YM47515**. [a]Condition A: H_2O_2 in H_2O, *t*-$BuNH_2$, CH_3OH, 0 °C to rt, 16 h. Condition B: Cat. 1, H_2O_2 in H_2O, dioxane, 50 °C, 16 h. Same conditions were used with cat. 2. [b] **(−)-4.13** was synthesized with cat 2. [c] Hydrolysis was performed with PLE since LiOH resulted in poor yield.

To investigate the synthetic feasibility of *post*-amycomicin **(–)-4.6**, we envisioned transforming intermediate **(±)-4.12** to enone **(±)-4.14**. Aldolization of **(±)-4.12** with acetalaldehyde and lithium bis(trimethylsilyl)amide (LiHMDS) produced a diastereomeric mixture of alcohols (1:1). Subsequent treatment with methanesulfonyl chloride in the presence of triethyl amine resulted in elimination of the alcohol and production of enone **(±)-4.13**. Attempts to hydrolyze the methyl ester with hydroxide sources resulted in degradation of the substrate. Thus, milder enzymatic conditions with PLE[19] were utilized to afford enone **(±)-4.14** (Scheme **4.2**).

With model product enone **(±)-4.14** in hand, synthesis of *post*-amycomicin **(–)-4.6** proceeded via Negishi coupling between acyl chloride (derived from suberic acid monomethyl ester) and hex-5-enylzinc bromide in the presence of tetrakis(triphenylphosphine)palladium[20] to produce ketone **(±)-4.16**. Subsequent cross-metathesis and epoxidation produced methyl ketone **(±)-4.17**. Epoxidation with condition A formed epoxy ketone **(±)-4.18** in good yield. Following the same procedure optimized for model substrate **(±)-4.14**, **(±)-4.18** underwent aldol condensation followed by enzymatic hydrolysis to afford *post*-amycomicin **(±)-4.6** in moderate yield (Scheme **4.3**).

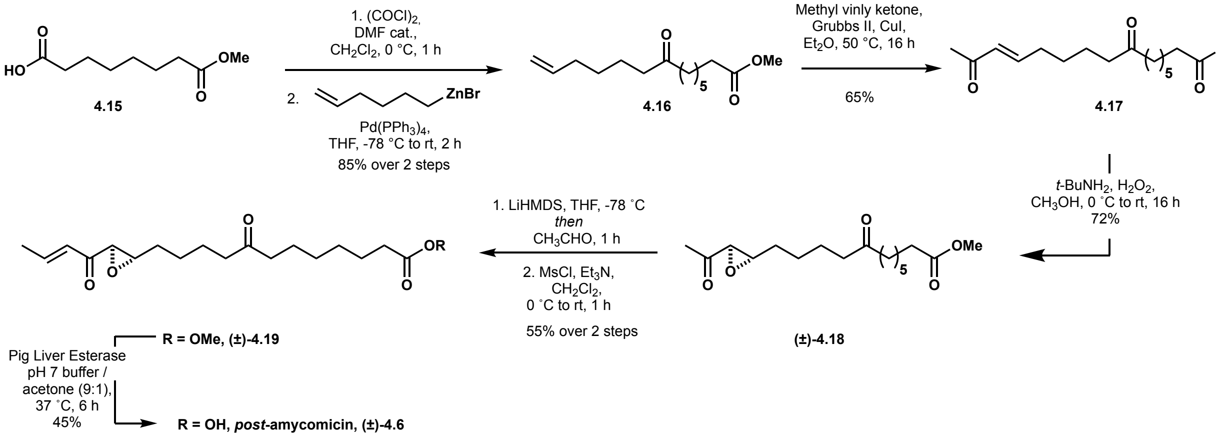
HO
OMe
4.15
1. (COCl)₂, DMF cat., CH₂Cl₂, 0 °C, 1 h
2. ZnBr
Pd(PPh₃)₄, THF, -78 °C to rt, 2 h
85% over 2 steps
4.16
5
Methyl vinly ketone, Grubbs II, CuI, Et₂O, 50 °C, 16 h
65%
4.17
t-BuNH₂, H₂O₂, CH₃OH, 0 °C to rt, 16 h
72%
(±)-4.18
1. LiHMDS, THF, -78 °C then CH₃CHO, 1 h
2. MsCl, Et₃N, CH₂Cl₂, 0 °C to rt, 1 h
55% over 2 steps
OR
R = OMe, (±)-4.19
Pig Liver Esterase pH 7 buffer / acetone (9:1), 37 °C, 6 h
45%
R = OH, post-amycomicin, (±)-4.6

Scheme 4.3. Synthesis of *post*-amycomicin.

4.2.2. Antimicrobial activity

Having obtained all rearranged products, we began screening the metabolites for activity against a panel of bacteria. We tested compounds against *S. aureus* to investigate our pro-drug hypothesis and unfortunately found none of the rearranged products exhibited notable activity.

Clardy and coworkers published an additional study at this time disclosing the activity of amycomycin. They demonstrated that as pH of the media increases, amycomycin's antibacterial effect diminishes and activity is completely abolished at a pH ≥ 8[8]. This suggests that as the pH increases, amycomycin is undergoing the Payne rearrangement to produce the inactive epoxy ketone **(−)-4.6** and is consistent with our results.

We subsequently tested intermediates in our synthesis for antibacterial activity against gram-positive and gram-negative bacteria. Interestingly, we found **(±)-4.13** was active against community-acquired methicillin-resistant *S. aureus* (CA-MRSA) and hospital-acquired methicillin-resistant *S. aureus* (HA-MRSA), admittedly with modest MICs (Table **4.1**). Notably, the methyl ester and epoxy enone were essential in preserving efficacy as carboxylic acid **(±)-4.14** and methyl ketone **(±)-4.11** were inactive within the concentration range tested.

Table 4.1. MIC data of epoxy ketone metabolites and derivatives.

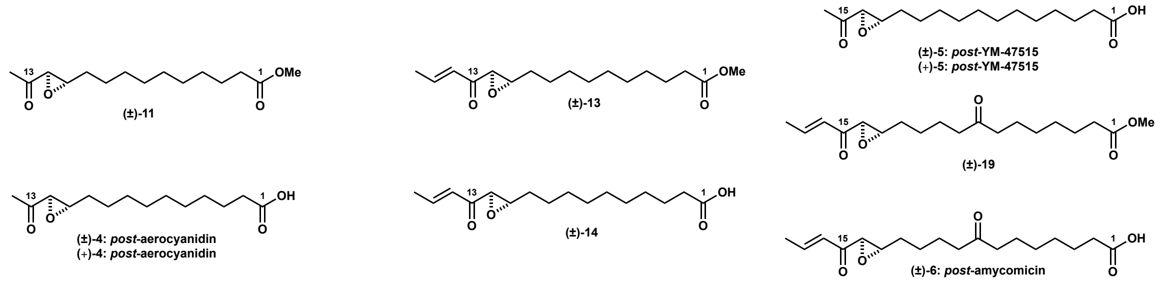
13
1
OMe
O
O
O
(±)-11
13
1
OMe
O
O
O
(±)-13
15
1
OH
O
O
O
(±)-5: post-YM-47515
(+)-5: post-YM-47515
15
1
OMe
O
O
O
O
(±)-19
13
1
OH
O
O
O
(±)-4: post-aerocyanidin
(+)-4: post-aerocyanidin
13
1
OH
O
O
O
(±)-14
15
1
OH
O
O
O
O
(±)-6: post-amycomicin

	MIC[a],[b],[c] (μM)						
	S. aureus (CA-MRSA)	*S. aureus* (HA-MRSA)	*S. aureus* (MSSA)	*E. faecalis*	*B. subtilis*	*E. coli*	*P. aeruginosa*
Compound	(USA300)	(ATCC 33592)	(Newman)	(ATCC 51575)	(ATCC 6633)	(MC4100)	(PAO1)
(±)-**11**	>500	-	-	-	-	-	-
(±)-4: *post*-aerocyanidin	>500	-	-	-	-	-	-
(+)-4: *post*-aerocyanidin	>500	-	-	-	-	-	-
(±)-13	**250**	**250**	**250**	**250**	>500	>500	**250**
(−)-13	**125**	**250**	**125**	**250**	-	-	**250**
(+)-**13**	**250**	**250**	**250**	**250**	-	-	**250**
(±)-14	>500	-	-	-	-	-	-
(±)-5: *post*-YM-47515	>500	-	-	-	-	-	-
(−)-5: *post*-YM-47515	>500	-	-	-	-	-	-
(±)-**19**	>500	-	-	-	-	-	-
(±)-6: *post*-amycomicin	>500	-	-	-	-	-	-

[a] Quaternary ammonium cation (12,3,2,3,12) was used as a postive control
[b] These assays were realized in triplicate and over 16 h
[c] Media was buffered to maintain a pH = 7

We were curious if one enantiomer of **(±)-4.13** was more bioactive and synthesized both **(−)-4.13** and **(+)-4.13** using catalyst 1 or 2 of the Cinchona primary amine catalysts[17, 18] respectively (Scheme **4.2**). Subsequently, we measured the IC_{50} of **4.13** against several gram-positive (*S. aureus, Enterococcus faecalis, Bacillus subtilis*) and gram-negative (*Escherichia coli*, *P. aeruginosa*) strains. In all cases, **(−)-4.13** was the most active compound (Table **4.2**). This may be indicative that growth inhibition is occurring through interaction of **(−)-4.13** with a protein target. Although **(−)-4.13** possesses chemotype similarities to known FabB/FabF inhibitor cerulenin, further assays are necessary to determine if **(−)-4.13** is targeting the fatty acid cycle or is acting through a novel MoA. Supplementing the growth media with exogenous oleic acids to rescue growth and probe our hypothesis that **(−)-4.13** may be interacting with a protein in the fatty acid cycle was attempted, but results were inconclusive.

Table 4.2. Bacterial growth inhibition of 4.13 and representative IC$_{50}$ curves. Representative IC$_{50}$ curves shown.

	IC$_{50}$ (µg/mL)				
Compound	*S. aureus* (CA-MRSA)	*S. aureus* (HA-MRSA)	*S. aureus* (MSSA)	*E. faecalis*	*P. aeruginosa*
	(USA300)	(ATCC 33592)	(Newman)	(ATCC 51575)	(PAO1)
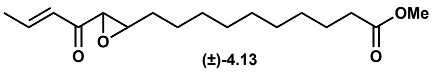 (±)-4.13	29	43	32	53	51
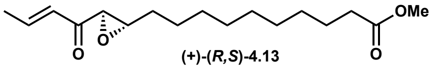 (+)-(*R*,*S*)-4.13	32	46	35	52	55
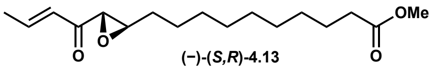 (−)-(*S*,*R*)-4.13	20	36	27	50	34

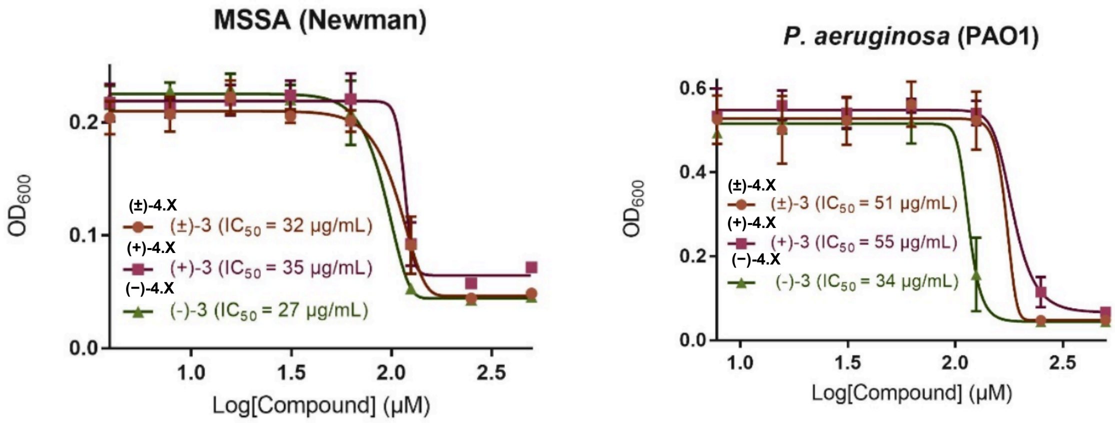

4.3. Conclusion

Herein describes the first total synthesis of epoxy ketone natural product metabolites. We demonstrated the metabolites are inactive against *S. aureus*, suggesting the epoxy ketone does not act as a prodrug and the scaffold is necessary for antibacterial activity. Furthermore, the scaffold may be necessary for selectivity against gram-positive pathogens as intermediate **(−)-4.13** demonstrated moderate activity against gram-positive and gram-negative bacteria.

Serendipitously, we discovered that α,β-unsaturated epoxy ketone **(±)-4.13** exhibits activity against a broad spectrum of bacteria and identified **(−)-4.13** as the more potent enantiomer.

References

1. Ernouf, G.; Wilt, I. K.; Zahim, S.; Wuest, W. M., Epoxy Isonitriles, A Unique Class of Antibiotics: Synthesis of Their Metabolites and Biological Investigations. *ChemBioChem* **2018,** *19* (23), 2448-2452.
2. Melander, R. J.; Zurawski, D. V.; Melander, C., Narrow-Spectrum Antibacterial Agents. *Medchemcomm.* **2018,** *9*, 12-21.
3. Alm, R. A.; Lahiri, S. D., Narrow-Spectrum Antibacterial Agents-Benefits and Challenges. *Antibiotics* **2020,** *9* (7).
4. Sholeh, M.; Krutova, M.; Forouzesh, M.; Mironov, S.; Sadeghifard, N.; Molaeipour, L.; Maleki, A.; Kouhsari, E., Antimicrobial resistance in Clostridioides (Clostridium) difficile derived from humans: a systematic review and meta-analysis. *Antimicrob. Resist. Infect. Control* **2020,** *9* (1), 158.
5. Del Rosso, J. Q., SARECYCLINE AND THE NARROW-SPECTRUM TETRACYCLINE CONCEPT: Currently Available Data and Potential Clinical Relevance in Dermatology. *J. Clin. Aesthet. Dermatol.* **2020,** *13* (10), 45-48.
6. Parker, W. L.; Rathnum, M. L.; Johnson, J. H.; Wells, J. S.; Principe, P. A.; Sykes, R. B., Aerocyanidin, a new antibiotic produced by Chromobacterium violaceum. *J. Antibiot.* **1988,** *41* (4), 454-60.
7. Sugawara, T.; Tanaka, A.; Imai, H.; Nagai, K.; Suzuki, K., YM-47515, a novel isonitrile antibiotic from Micromonospora echinospora subsp. echinospora. *J. Antibiot.* **1997,** *50* (11), 944-8.
8. Pishchany, G.; Mevers, E.; Ndousse-Fetter, S.; Horvath, D. J., Jr.; Paludo, C. R.; Silva-Junior, E. A.; Koren, S.; Skaar, E. P.; Clardy, J.; Kolter, R., Amycomicin is a potent and specific antibiotic discovered with a targeted interaction screen. *Proc. Natl. Acad. Sci. U.S.A.* **2018,** *115* (40), 10124-10129.
9. Heath, R. J.; White, S. W.; Rock, C. O., Lipid biosynthesis as a target for antibacterial agents. *Prog. Lipid Res.* **2001,** *40* (6), 467-497.
10. Price, A. C.; Choi, K. H.; Heath, R. J.; Li, Z.; White, S. W.; Rock, C. O., Inhibition of beta-ketoacyl-acyl carrier protein synthases by thiolactomycin and cerulenin. Structure and mechanism. *J. Biol. Chem.* **2001,** *276* (9), 6551-9.
11. Young, K.; Jayasuriya, H.; Ondeyka, J. G.; Herath, K.; Zhang, C.; Kodali, S.; Galgoci, A.; Painter, R.; Brown-Driver, V.; Yamamoto, R.; Silver, L. L.; Zheng, Y.; Ventura, J. I.; Sigmund, J.; Ha, S.; Basilio, A.; Vicente, F.; Tormo, J. R.; Pelaez, F.; Youngman, P.; Cully, D.; Barrett, J. F.; Schmatz, D.; Singh, S. B.; Wang, J., Discovery of FabH/FabF inhibitors from natural products. *Antimicrob. Agents Chemother.* **2006,** *50* (2), 519-26.
12. Yum, J. H.; Kim, C. K.; Yong, D.; Lee, K.; Chong, Y.; Kim, C. M.; Kim, J. M.; Ro, S.; Cho, J. M., In vitro activities of CG400549, a novel FabI inhibitor, against recently isolated clinical staphylococcal strains in Korea. *Antimicrob. Agents Chemother.* **2007,** *51* (7), 2591-3.
13. Wittke, F.; Vincent, C.; Chen, J.; Heller, B.; Kabler, H.; Overcash, J. S.; Leylavergne, F.; Dieppois, G., Afabicin, a First-in-Class Antistaphylococcal Antibiotic, in the Treatment of

Acute Bacterial Skin and Skin Structure Infections: Clinical Noninferiority to Vancomycin/Linezolid. *Antimicrob. Agents Chemother. 64* (10), e00250-20.
14. O'Brien, P. M.; Sliskovic, D. R.; Picard, J. A.; Lee, H. T.; Purchase, C. F., 2nd; Roth, B. D.; White, A. D.; Anderson, M.; Mueller, S. B.; Bocan, T.; Bousley, R.; Hamelehle, K. L.; Homan, R.; Lee, P.; Krause, B. R.; Reindel, J. F.; Stanfield, R. L.; Turluck, D., Inhibitors of acyl-CoA:cholesterol O-acyltransferase. synthesis and pharmacological activity of (+/-)-2-dodecyl-alpha-phenyl-N-(2,4,6-trimethoxyphenyl)-2H-tetrazole-5- acetamide and structurally related tetrazole amide derivatives. *J. Med. Chem.* **1996,** *39* (12), 2354-66.
15. Gao, Y.; Shan, Q.; Liu, J.; Wang, L.; Du, Y., The first convergent total synthesis of penarolide sulfate A2, a novel alpha-glucosidase inhibitor. *Org. Biomol. Chem.* **2014,** *12* (13), 2071-9.
16. Voigtritter, K.; Ghorai, S.; Lipshutz, B. H., Rate enhanced olefin cross-metathesis reactions: the copper iodide effect. *J. Org. Chem.* **2011,** *76* (11), 4697-702.
17. Lifchits, O.; Mahlau, M.; Reisinger, C. M.; Lee, A.; Fares, C.; Polyak, I.; Gopakumar, G.; Thiel, W.; List, B., The cinchona primary amine-catalyzed asymmetric epoxidation and hydroperoxidation of alpha,beta-unsaturated carbonyl compounds with hydrogen peroxide. *J. Am. Chem. Soc.* **2013,** *135* (17), 6677-93.
18. Reisinger, C. M.; Wang, X.; List, B., Catalytic asymmetric hydroperoxidation of alpha,beta-unsaturated ketones: an approach to enantiopure peroxyhemiketals, epoxides, and aldols. *Angew. Chem. Int. Ed.* **2008,** *47* (42), 8112-5.
19. Tamm, C., Pig liver esterase catalyzed hydrolysis: Substrate specificity and stereoselectivity. *Pure Appl. Chem.* **1992,** *64* (8), 1187-1191.
20. Grey, R. A., A palladium-catalyzed synthesis of ketones from acid chlorides and organozinc compounds. *J. Org. Chem.* **1984,** *49* (12), 2288-2289.

Chapter 5. Membrane perturbing small molecules as novel antimicrobials

Disclaimer: This work was adapted from three publications with permission from all authors:

1. A selective membrane-targeting repurposed antibiotic with activity against persistent methicillin-resistant *Staphylococcus aureus*[1]

2. Using membrane perturbing small molecules to target chronic persistent infections[2]

3. Hijacking the bacterial circuitry processes via chemical "hot-wiring": an under-explored avenue for therapeutic development[3]

Analogue synthesis was completed by Ingrid K. Wilt, Dr. Taylor Hari, and Dr. Andrew Steele. With guidance from Dr. Taylor Hari, Ingrid K. Wilt synthesized the thiol containing analogues described in the biological assays and independently developed the recrystallization protocols crucial for purification of analogues. Biological investigations were completed by Dr. Wooseong Kim. Molecular dynamics simulations were completed by Dr. Guijin Zou and experimental details can be found in the literature[1].

5.1. Introduction

5.1.1. Persister cells

Bacteria evade antibiotic treatment through numerous mechanisms. Although resistance is often discussed when developing novel antibiotics, populations of bacterial tolerance is a less explored mechanism contributing to the loss of activity of antibiotics. While resistance is a result of genotypic changes that can increase an antibiotic's MIC, tolerance is described as a temporary evasion or delay of death in the presence of bactericidal antibiotics without change in MIC[4, 5].

Prolonged antibiotic treatment, instead of increased dosage, is required to treat these infections. Tolerance is a consequence of slowed growth and decreased metabolism of an entire population of bacteria induced by environmental stress (*e.g.* antibiotics). A subcategory of tolerance, persistence, occurs through a phenotypic change of a subpopulation of bacteria that can survive antibiotic treatment regardless of dosage. These subpopulations compose <1% of most bacterial cultures, but external pressures, such as environmental cues or antibiotics, can induce higher levels of persistence in wild type populations[6]. Like tolerant populations, persister cells are often referred to as “dormant” or “metabolically inactive”[5]. Therefore, traditional antibiotic treatments that target growth dependent processes or metabolically active targets are rendered ineffective against persister populations. Furthermore, persister cells can revert to a metabolically active phenotype once these pressures are removed resulting in chronic and reoccurring infections[7] (Figure **5.1**).

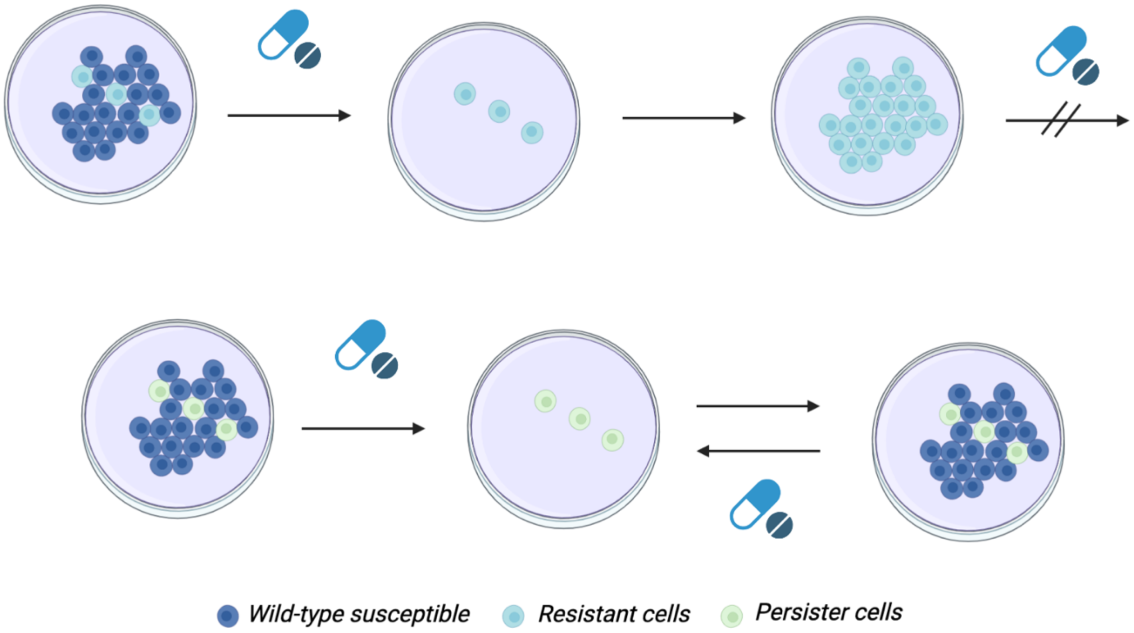

Figure 5.1. Bacterial persistence. Antibiotics kill wild type cells and leave resistant cells to repopulate the microbiome. Continued antibiotic treatment cannot eradicate infection (top). Persister subpopulations survive antibiotic treatment and once the external pressure is relieved, repopulate the host with wild-type bacteria. Reapplication of treatment will kill susceptible cells, but persister subpopulations may remain leading to reoccurring infections (bottom). Figure created in BioRender.com.

Time kill assays are typically performed to determine the type of population present (Figure **5.2**). Persistance can be identified based on a population's time-kill curve and minimum duration for killing (MDK)[8]. A population of persister cells has a "biphasic" killing curve. While susceptible populations will produce a fast, linear curve, tolerant populations exhibit slow and linear killing times as a result of "delayed" death. Communities with persisters cells will demonstrate a steep curve resulting from initial death of susceptible cells followed by a plateau in killing kinetics from survival of persister cells[8, 9]. More in depth analyses using microfluidics, flow cytometry, and DNA and RNA sequencing have also attempted to elucidate phenotypic features that may differentiate persister cells from wild-type and tolerant populations such as slowed growth or uptake of exogenous nutrients[10-13].

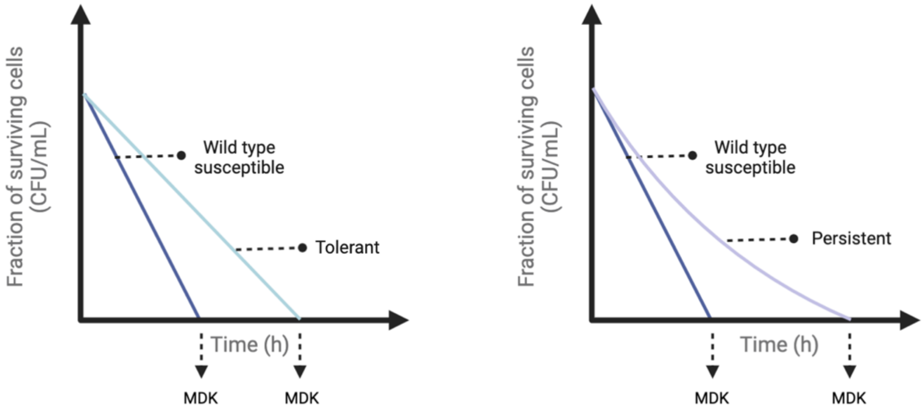

Figure 5.2. Time kill curves. Time kill curves for wild type antibiotic susceptible versus tolerant populations (left) and wild type antibiotic susceptible versus persistent (right). MDK for tolerant and persistent populations is greater than susceptible. Figure created in BioRender.com.

There is a critical lack of therapeutics capable of treating infections caused by nongrowing persister forms of bacterial infections. Investigators have proposed developing antibiotics that target different factors (*i.e.* genes, proteins, *etc.*) that appear to play a role in triggering the persistence phenotype[14-20]. The primary challenge with developing therapeutics, however, is reduced production of uptake machinery on the outer membrane rendering antibiotics that require active uptake into the cell to access their target process ineffective. Furthermore, resistance to antibiotics with specific protein or genomic targets occurs rapidly and could lead to resistant-persistent infections (*e.g.* MRSA persisters)[21]. Thus, researchers have proposed disrupting cell membrane integrity through membrane perturbation may be effective at eradicating persister populations while mitigating resistance development[22].

5.1.2. Membrane perturbation as a mechanism of action

Membrane perturbing antibacterials are often overlooked due to low selectivity for bacterial versus mammalian membranes. There are, however, several membrane perturbing drugs on the market such as nisin[23, 24], daptomycin[25], polymyxin B[26], and colistin[27] (Figure **5.3**). Membrane targeting agents typically execute their killing power in two different ways: depolarization or permeabilization of the membrane[22, 28, 29]. Depolarization disrupts the electronic gradient of bacterial membranes through the formation of ion-conducting pores that increase ion permeability and act as ion carriers. This culminates in dysregulation of the proton motive force thus stalling ATP production and transport across the cell membrane[30]. Membrane permeabilization occurs through the formation of small pores or interference with membrane integrity resulting in leakage of cellular components including cell machinery and nutrients. This ultimately causes cell death[31]. Intriguingly, increased permeabilization allows small molecules, including antibiotics, that typically require active uptake mechanisms, to passively enter the cell. Hence, membrane perturbing small molecules have been shown to eradicate persisters as well as render these populations susceptible to antibiotic treatment[32].

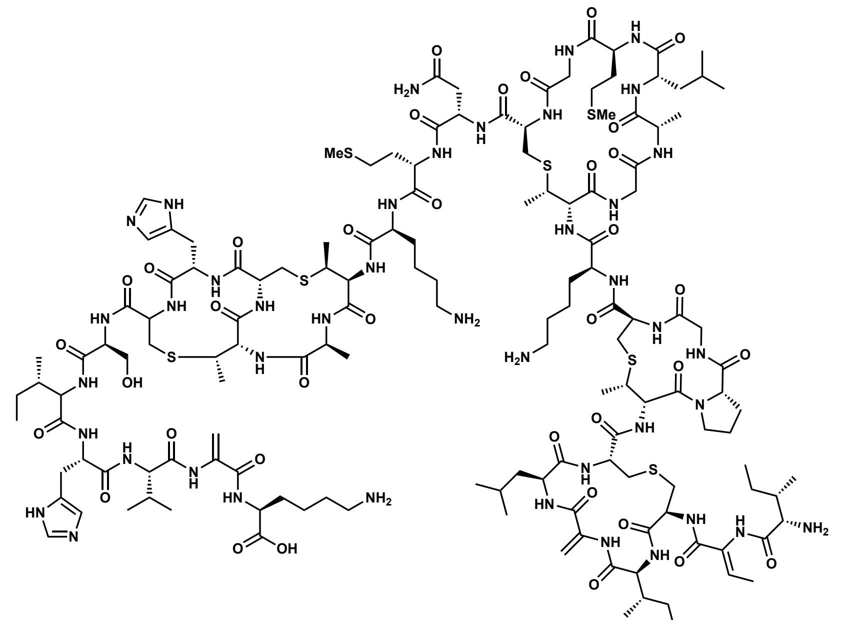

Nisin

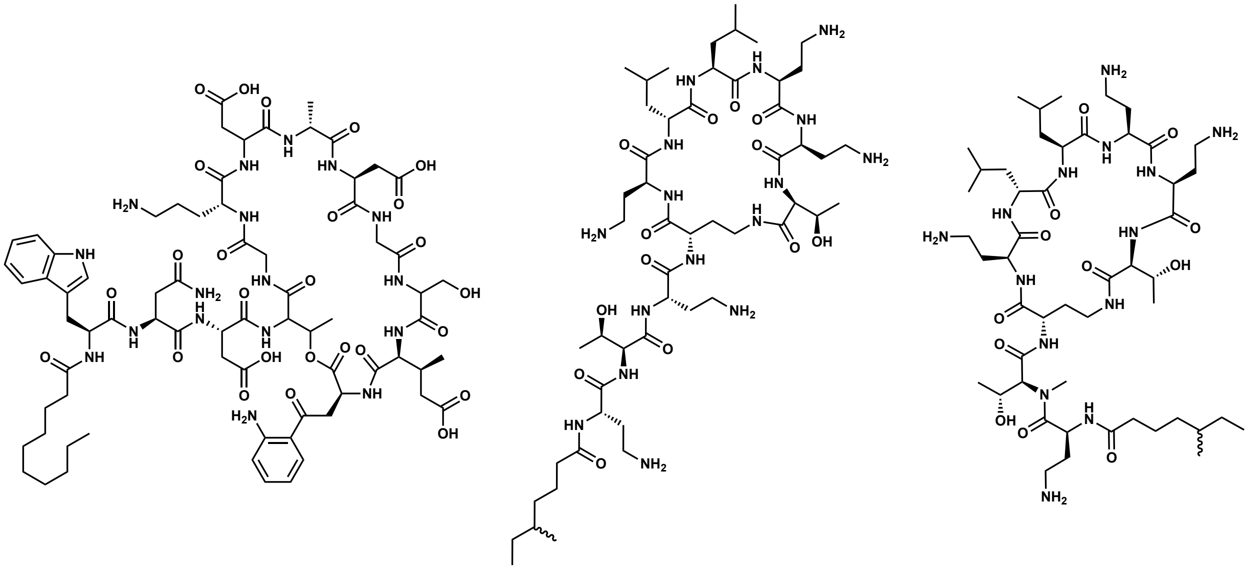

Daptomycin **Colistin** **Polymixin B**

Figure 5.3. Known membrane perturbers. Clinically relevant small molecules that disrupt bacterial growth through membrane perturbation.

5.1.3. Repurposing bithionol as a novel antimicrobial

Repurposing—identifying a new use for existing drugs—has gained traction in recent years for the discovery of new therapies. High throughput screens (HTS) of FDA approved therapies have enabled many of these efforts for "rediscovery" of therapeutics with novel antimicrobial potential. Utilizing the free-living nematode *C. elegans*, Mylonakis and Ausubel demonstrate a HTS that simultaneously tests a library of compounds for bioactivity and toxicity to determine the best drug candidates for repurposing[33-35]. Our collaborations with the Mylonakis and Ausubel labs have led to the identification of several drugs that possess potent antibacterial activity via membrane perturbation including CD437[33], a synthetic retinoid, and nTZDpA[35], an antidiabetic (Figure **5.4a**). Preliminary studies with these small molecules hint at a common mechanism of action whereby the polar regions interact with the positive phospholipid heads of the membrane followed by subsequent nonpolar aryl group intercalation into the cell membrane resulting in membrane disruption and cell death[33, 34] (Figure **5.4b**). Therapeutics to treat parasitic infections (anthelmintic) also often exhibit antimicrobial properties via bacterial membrane disruption. Both anthelmintic niclosamide and oxyclozanide were shown to have MICs of 0.5 and 0.2 µg/mL respectively in a study completed in 2015 against *S. aureus* clinical isolates, although niclosamide was shown to be toxic at these levels in *C. elegan* models[36] (Figure **5.4c**).

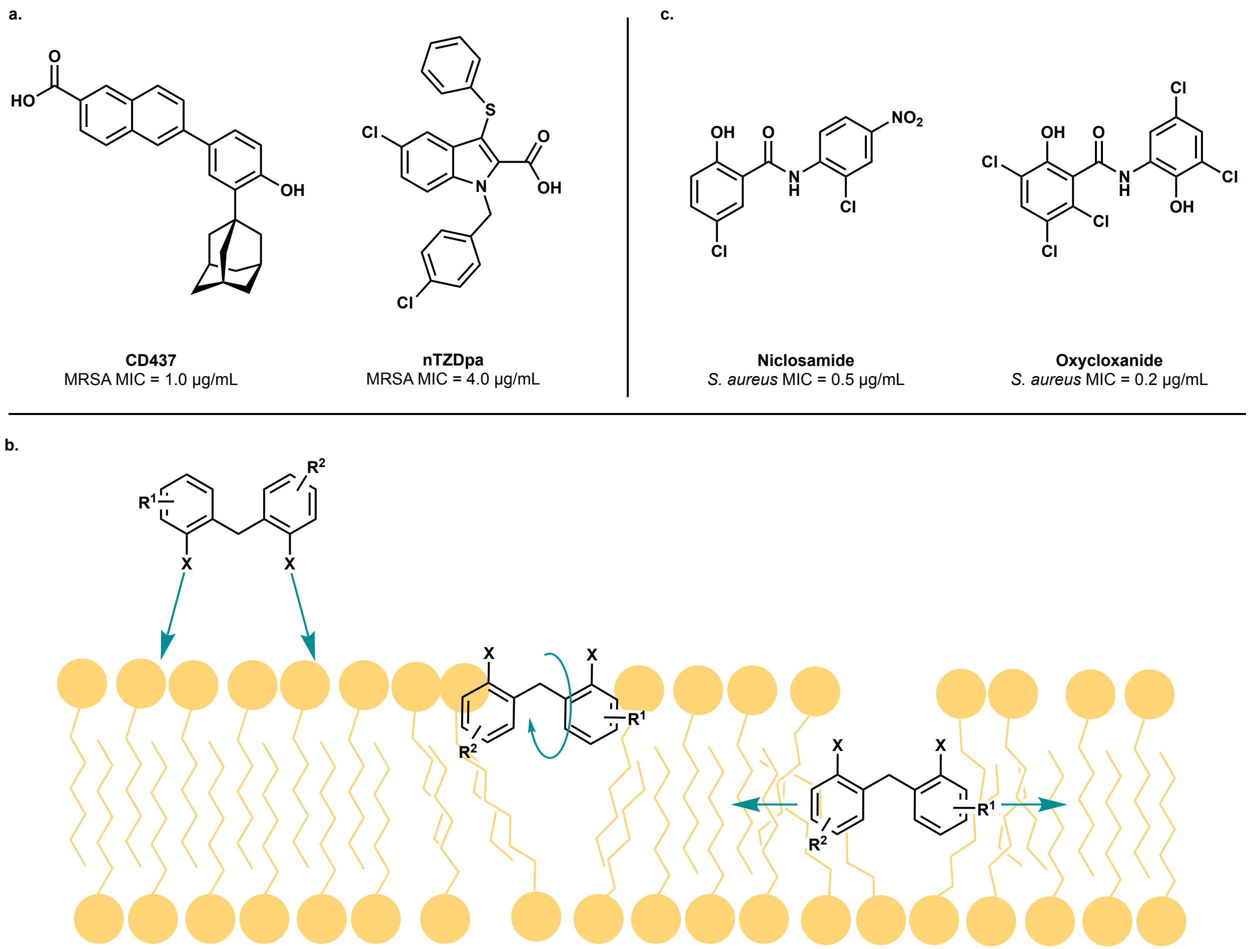
a.
CD437
MRSA MIC = 1.0 µg/mL
nTZDpa
MRSA MIC = 4.0 µg/mL
c.
Niclosamide
S. aureus MIC = 0.5 µg/mL
Oxycloxanide
S. aureus MIC = 0.2 µg/mL
b.
X
R1
R2

Figure 5.4. Repurposed small molecules as antibacterials. a. CD437 and nTZDpa were identified by Drs. Mylonakis and Ausubel as potent inhibitors of MRSA. b. Proposed mechanism of action membrane perturbation. c. Anthilmetic small molecules niclosamide and oxycloxane demonstrate antibacterial activity.

More recently, bithionol (**5.1**), an anthelmintic biaryl symmetrical small molecule used to treat tapeworm infection in equine, was identified in a *C. elegans* HTS (Figure **5.5a**) by our collaborators Drs. Ausubel and Mylonakis as a potent inhibitor of gram-positive bacteria, specifically *S. aureus* MW2 (MRSA) persister cells. Bithionol induced morphology changes of MRSA persister membranes (Figure **5.5b**) and inhibited both planktonic and biofilm persisters in a dose-dependent manner with a persister killing concentration (PKC) of 32 µg/mL (Figure **5.5c**). Importantly, bithionol exhibited low toxicity in *C. elegans* suggesting the small molecule is capable of selectively permeabilizing bacterial cells in the presence of eukaryotic organisms. To further explore this proposed mechanism of action, I aimed to synthesize a library of bithionol analogues to evaluate SAR while my collaborators conducted molecular dynamic simulations and biological assays.

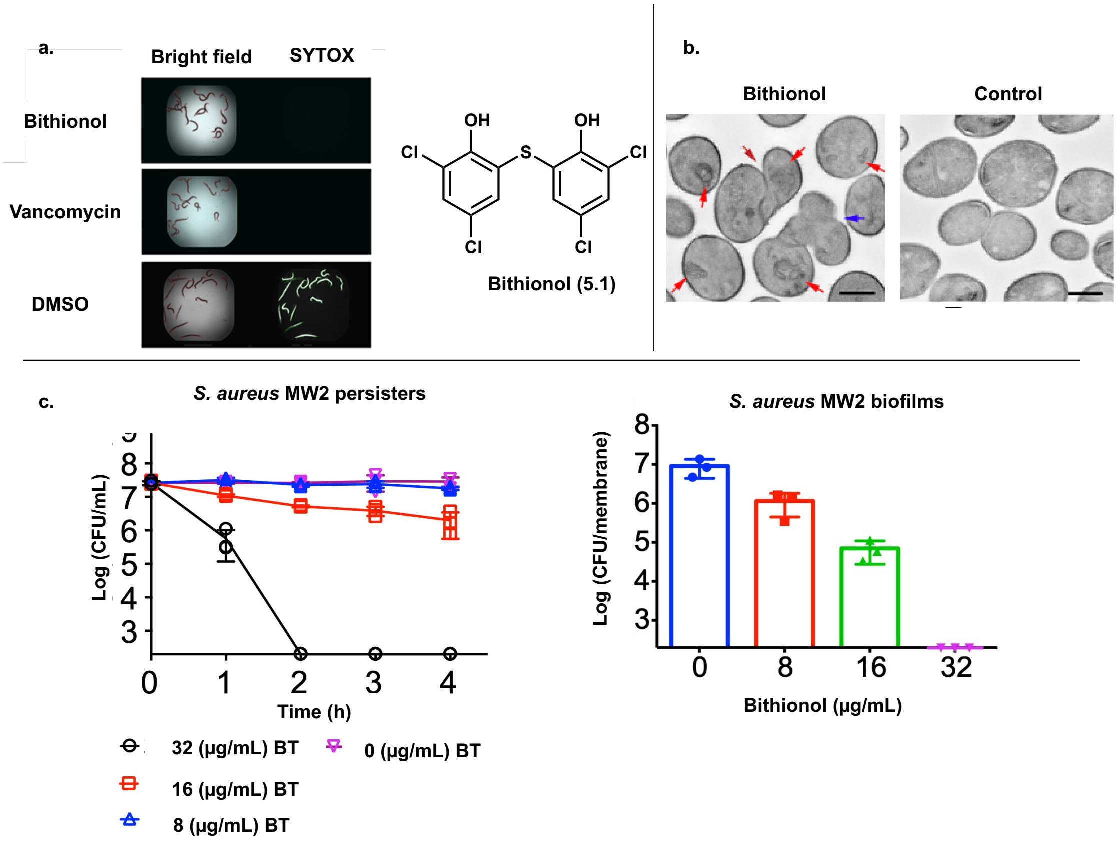

Figure 5.5. Identification of bithionol. a. Bithionol was identified in a *C. elegans* HTS as an inhibitor of MRSA growth. b. Transmission electron microscopy (TEM) images of bithionol inducing morphological changes to the cell membrane. Formation of intracellular mesosome-like structures indicated with red arrows, abnormal cell division brown, and cell lysis with blue. Cells were treated with 10 μg/mL bithionol or 0.1% DMSO (control) for 2 h. (Scale bars, 500 nm) c. Viability of MRSA MW2 cells in stationary-phase (left) or biofilm (right) measured by colony forming units (CFUs). The data points on the *x*-axis are below the level of detection (2 x 10^2 CFU/mL, or 2 x 10^2 CFU/membrane. Individual data points (n = 3 biologically independent samples) are shown; error bars represent means ± SD.

5.2. Results and discussion

5.2.1. Synthesis of bithionol analogues

To evaluate the SAR of bithionol, Dr. Steele, Dr. Hari, and I proposed several analogues. Alternative bridgeheads, such as N, O, and C, were proposed to elucidate the importance of the thiol linkage. Sulfones and sulfoxides would also be synthesized to further probe the thiol bridgehead. Methoxy capping of the phenols was designed to interrogate potential interactions between bithionol and the phospholipid heads of the bacterial membrane. Finally, we were interested in incorporating various aryl substituents to investigate factors contributing to membrane intercalation (Figure **5.6**).

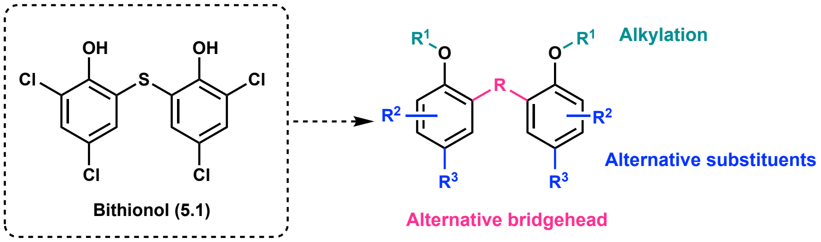

Figure 5.6. Analogue design. Bithionol analogue development was focused on probing the influence of structure on membrane intercalation.

Attempts were made to synthesize three aryl linkers including an amine, ketone, and ether bridgehead. Although Dr. Steele completed the synthesis of the amine bridgehead, preliminary bioactivity data suggested it was less active than bithionol and did not warrant further investigations. Synthesis of the other alternate bridgeheads by Dr. Taylor Hari proved challenging. Formation of the ketone bridgehead from methoxy amine intermediate were unsuccessful (Scheme **5.1**). In addition, progress towards the ether bridgehead was fruitless and resulted in protodehalogenation of aryl iodide in all cases.

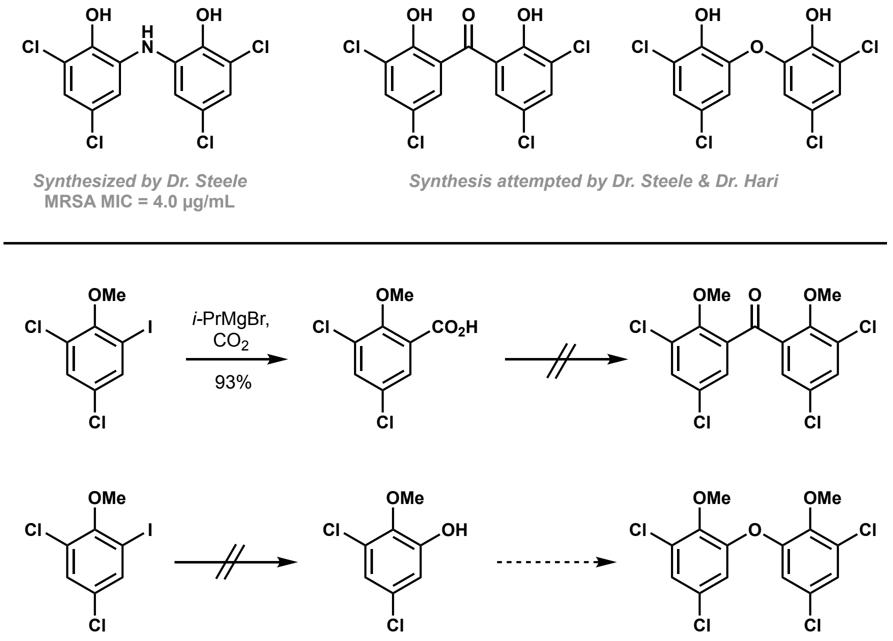
Synthesized by Dr. Steele
MRSA MIC = 4.0 μg/mL
Synthesis attempted by Dr. Steele & Dr. Hari
i-PrMgBr, CO2
93%

Scheme 5.1. Proposed alternative bridgehead analogues. Synthesis of bridgehead analogues attempted by Drs. Steele and Hari.

Synthesis of bithionol analogues utilizing the thiol bridgehead, however, were of great success. We began the synthesis of these analogues from a variety of commercially available substituted phenols via a Friedel-crafts sulfonylation to join two aryl rings using aluminum trichloride and sulfonyl chloride. Purification of intermediates initially performed with silica column resulted in low yields and impure product. Due to the crystalline nature of these intermediates, we were able to develop a robust recrystallization protocol from boiling toluene to produce sulfoxide intermediates. Subsequent reduction with zinc in acetic acid produced the thiol containing analogs. Again, silica column was an ineffective means of purification. Recrystallization of crude product was accomplished with boiling methylene chloride to produce sulfides **5.1-5.8** in moderate yields for biological evaluation (Scheme **5.2**).

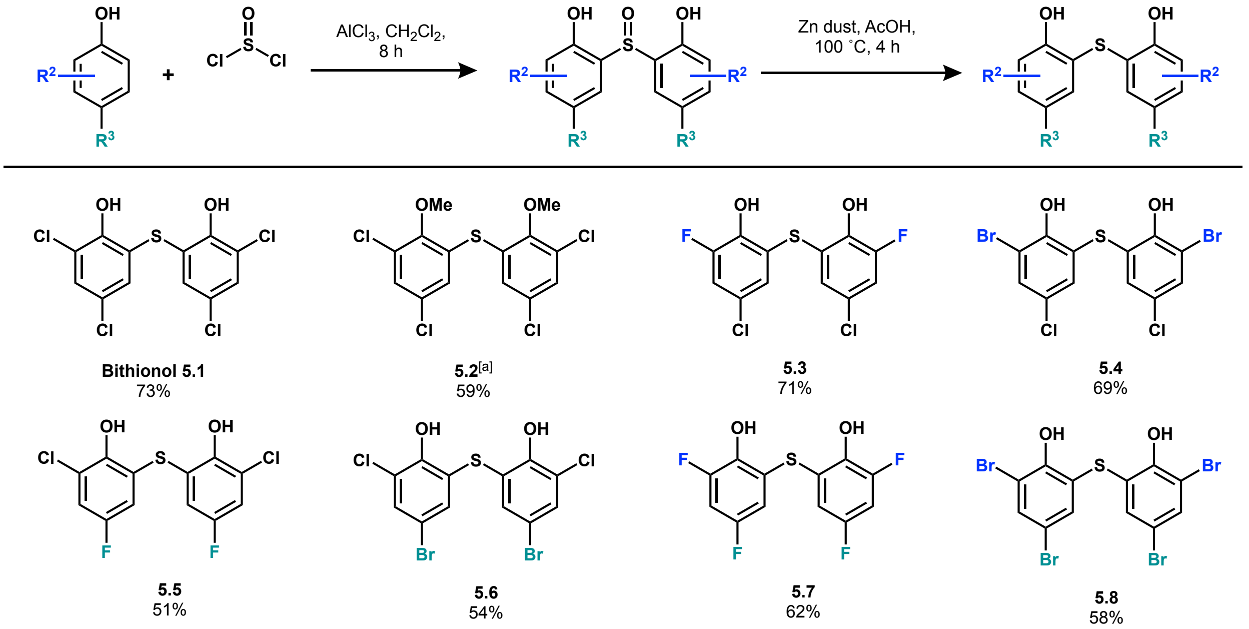

Scheme 5.2. Synthesis of aryl analogues. Aryl analogues of bithionol were synthesized in 2 steps from commercially available aryl halides. [a]**5.2** was synthesized in 3 steps, performing a phenol methylation of bithionol with dimethyl sulfate in 81%.

5.2.2. Antimicrobial activity

To further test our proposed mechanism of action and obtain additional insights into the effects of functional groups on the potency of bithionol, we conducted structure–activity relationship (SAR) studies by using a commercially available sulfoxide bithionol analogue, Bitin-S[37], as well as with 7 of the newly synthesized analogs (Table **5.1**). Bitin-S and synthetic bithionol methoxy analogue BT-OMe **5.2** were used to assess the effect of membrane binding affinity on antimicrobial and membrane activity. Additional hydrophilic interactions provided by the polar sulfoxide group of Bitin-S were shown to reduce antimicrobial activity (MIC 8 µg/mL) and decrease membrane disruption. Capping the phenols of bithionol to produce two methoxy groups diminished polarity (**5.2**) and abolished both antimicrobial and membrane activity. These results suggest the phenolic hydroxyl groups are critical for antimicrobial activity, likely forming a crucial polar interaction with the polar phosphonate heads of the membrane[35].

To probe the role of compound size and resulting polarization of the inserted molecule to perturb the membrane, we substituted alternative halogens for chlorine. Replacement of chlorine with fluorine resulted in reduced membrane and antimicrobial activities as seen with compounds BT-*o*F (**5.3**), BT-*p*F (**5.5**), and BT-*op*F (**5.7**), whereas substitution with bromine showed similar membrane and antimicrobial activities as bithionol as demonstrated by BT-*o*Br (**5.4**) and BT-*p*Br (**5.5**). The polarity of the C-F bond in the fluoro derivatives may increase the hydrophilicity of the aryl rings, thus decreasing membrane permeability. Although substituting chlorine for bromine at both the *ortho* and *para* positions may increase membrane perturbation, diminished activity of BT-*op*Br (**5.8**) suggests these substituents likely disrupt initial membrane association and penetration. This was further supported by our collaborator's computational analysis of the bromine derivatives showing an increased energy barrier for membrane perturbation of BT-*op*Br **5.8**.

Table 5.1. SAR of antibiotic activity and membrane fluidity of bithionol analogues.

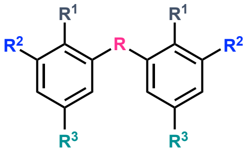

Cmpd	R	R1	R2	R3	MIC	PKC	MP	MFI
Bithionol	S	OH	Cl	Cl	1	32	Yes	Yes
Bitin-S	SO	OH	Cl	Cl	8	>64	Yes	No
BT-OMe	S	OMe	Cl	Cl	>64	>64	No	No
BT-*o*F	S	OH	F	Cl	2	>64	Yes	No
BT-*o*Br	S	OH	Br	Cl	1	32	Yes	Yes
BT-*p*F	S	OH	Cl	F	2	>64	Yes	No
BT-*p*Br	S	OH	Cl	Br	1	32	Yes	Yes
BT-*op*F	S	OH	F	F	8	>64	No	No
BT-*op*Br	S	OH	Br	Br	1	32	Yes	Yes

MIC, minimum inhibitory concentration (in micrograms per milliliter); PKC, persister killing concentration (in micrograms per milliliter) required to kill 5 x 10^7 CFU/mL MRSA persister cells below the limit of detection; MP, membrane permeabilization (determined based on SYTOX Green fluorescence intensity); MFI, membrane fluidity increase (determined based on Laurdan GP measurement).

Our collaborators also conducted synergism studies with bithionol and gentamicin, an antibiotic that exhibits nephrotoxicity[38] but is used to treat severe chronic MRSA infections and has been shown to work in synergy with membrane perturbing synthetic retinoids[33]. Although bithionol did not demonstrate excellent persister killing ability at low doses (*i.e.* 8 µg/mL), synergism studies found that combination therapy at the same does with 2 µg/mL of gentamicin led to complete eradication of MRSA persister cells. Maintaining the concentration of bithionol at 8 µg/mL and increasing gentamicin to 16 µg/mL completely cleared populations of biofilm persisters. In murine thigh infection models, used to mimic deep-seated chronic infections[39], treatments of solely bithionol at 30 mg/kg did not significantly reduce colony forming units (CFUs). Combination treatment of 30 mg/kg bithionol and 30 mg/kg gentamicin, however, resulted in 90% infection clearance (Figure **5.7**). Hepatic and renal toxicity of bithionol were also evaluated in these murine models by tracking serum levels of alanine aminotransferase (ALT) and blood urea nitrogen (BUN). Although combinations of vancomycin and gentamicin significantly increase BUN levels, the combination of bithionol and gentamicin increased neither. This suggests

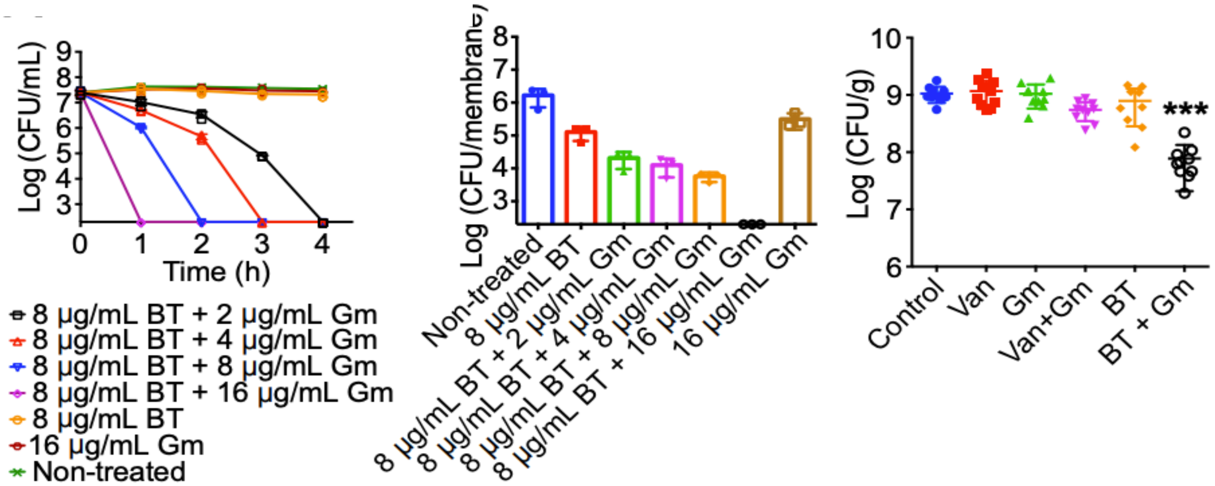

Figure 5.7. **Synergism of bithionol with convential antibiotics.** Bithionol (BT) demonstrates synergism with gentamicin (Gm) against MRSA persisters *in vitro* and *in vivo.* Stationary phase (left) or biofilm (middle) MRSA MW2 infections responded in a does dependent manner to treatment with combination of BT and Gm. CFUs were measured by serial dilution and plating on TSA plates. Assays were realized in triplicate (n = 3). (Right) MRSA MW2 infected mice (n = 10) were treated with control (5% Killophor + 5% ethanol, intraperitoneal (i.p.)), vancomycin (Van) (30 mg/kg, i.p.), gentamicin (Gm) (30 mg/kg, subcutaneous (s.c.)), bithionol (30 mg/kg, i.p.), or a combination of vancomycin (30 mg/kg, i.p.) or bithionol (30 mg/kg, i.p.) with gentamicin (30 mg/kg, s.c.) every 12 h for 3 d at 24 h post infection. The mice were euthanized at 12 h after the last treatment. Thighs were excised and homogenized to measure CFU. Statistical differences between control and treatment groups were measured by 1-way ANOVA and post hoc Tukey test (****P* < 0.001).

bithionol and its analogues are selective membrane disruptors, targeting bacterial membranes while leaving mammalian cell membranes unscathed.

Next, bithionol and analogues were investigated by our collaborators as membrane permeators. Previous SAR studies of membrane permeabilizers suggest that compounds can intercalate into the membrane without effecting the viability of MRSA persister cells. The SAR studies of our investigation demonstrated that some compounds that permeabilize MRSA persister cell membranes to SYTOX Green, such as Bitin-S, BT-*o*F, or BT-*p*F, do not kill them (Table **5.1**). Of the analogues synthesized, there appears to be a correlation between ability to increase membrane fluidity and activity against MRSA persister cells (Figure **5.8,** Table **5.1**)**.** These results were also observed with known membrane perturber nTZDpA and 11 nTZDpa analogues. Correlation between PKC and amount of induced membrane fluidity measured by Laurdan GP for bithionol, nTZDpa, and their analogues was also observed. These findings indicate membrane fluidity may be used as a biophysical indicator of antipersister bioactivity[40].

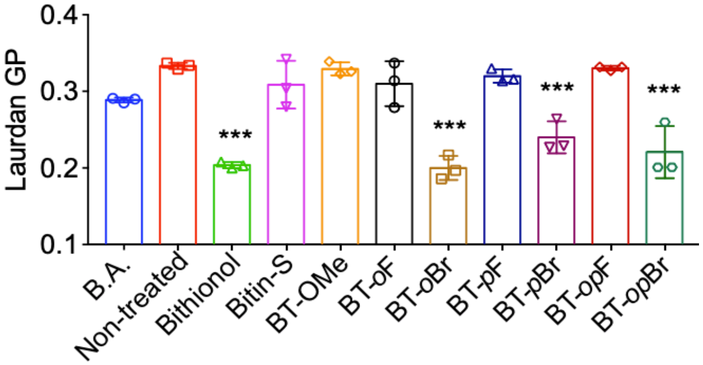

Figure 5.8. Membrane fluidity. Bithionol and other membrane perturbing analogues increase membrane fluidity of MRSA cells measured by Laurdan GP. Membrane fluidizer benzyl alcohol (B.A.; 50 mM) was used as a positive control. Individual data points (n =3 biologically independent samples) are shown; error bars represent means ± SD.

5.2.3. Mechanism of action

Computational modeling through molecular dynamic (MD) studies obtained through our collaboration with the Mylonakis lab provided additional support for our SAR and SYTOX-green data and suggests a mode of action for bithionol and its analogues (Figure **5.9a**). The polar phenol is hypothesized to initiate primary interactions with the amphiphilic phospholipid bilayer through hydrogen bonding, specifically with the hydrophilic phosphate heads. Methoxy caping of the phenol (**5.2**) completely eradicated activity supporting this proposed interaction. Subsequent incorporation of the non-polar aryl ring into the hydrophobic fatty-acid chain region leads to permeation and disruption of the membrane[40, 41] (Figure **5.9b**). The *ortho* and *para* chlorine moieties likely play a crucial role in lipid bilayer perturbation. In agreement with these findings, substituting chlorine for fluorine resulted in diminished antimicrobial activity. Thus, the MD simulations, supported by SAR data, demonstrate the two key elements for membrane activity are initial binding to the membrane surface via hydrophilic interactions of the phenols and membrane perturbation facilitated by the chlorinated aryl rings. Once bithionol is integrated into the bacterial cell, it may possess a secondary unidentified mode of action. Further studies, however, are necessary to probe a possible secondary target.

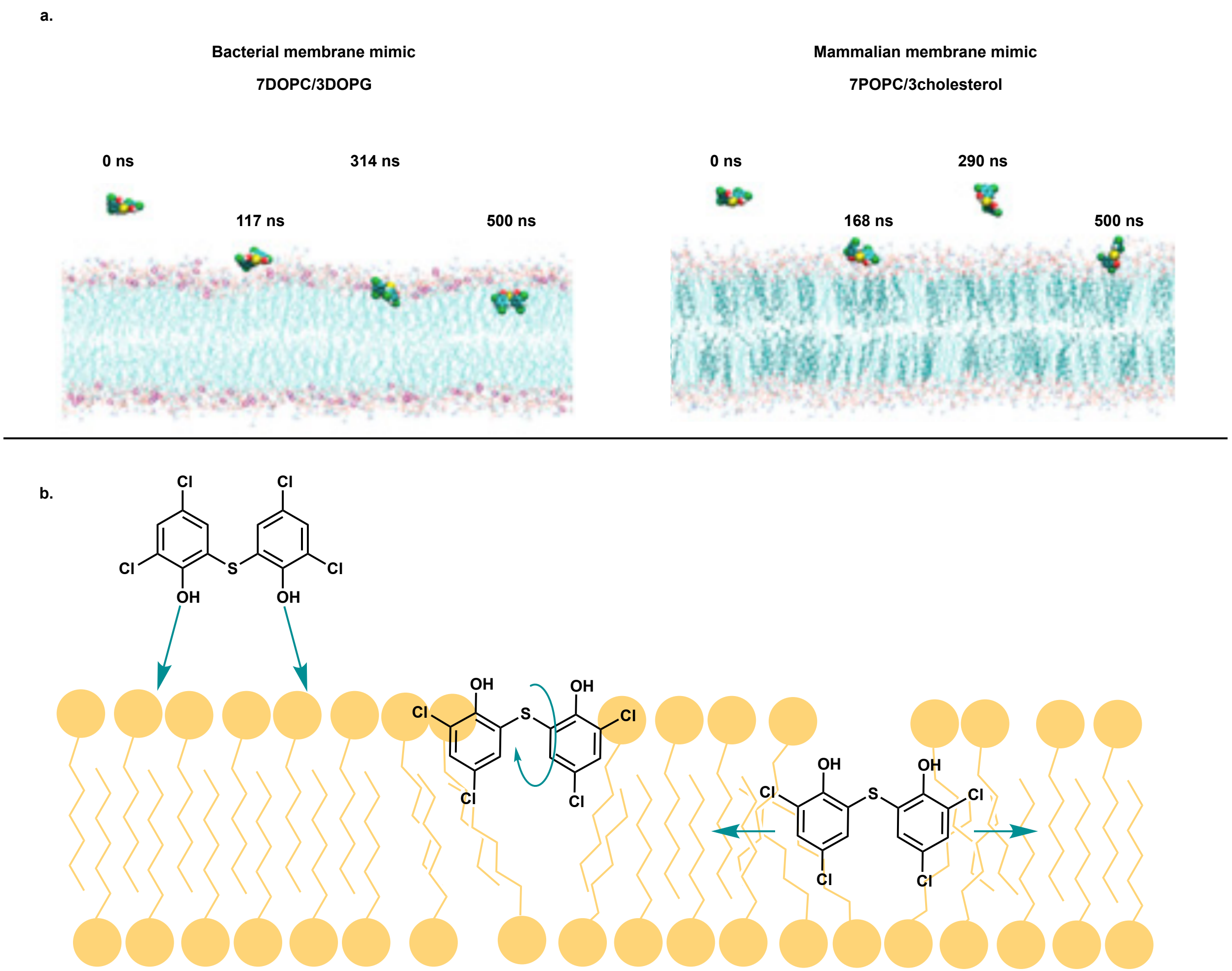

Figure 5.9. Proposed mechanism of action of bithionol. a. Bacterial membrane modeled with MD simulations (left). A ratio of 7 : 3 1,2-dioleoyl-sn-glycero-3-phosphocholine (DOPC) / 1,2-dioleoyl-sn-glycero-3-phospho(1'-rac-glycerol) (DOPG) to simulate negatively charged *S. aureus* membranes. Bithionol permeates membrane analogous to top figure. MD simulation of simplified mammalian cell membrane composed of zwitterionic lipid 1,2-palmitoyl-oleoyl-*sn*-glycero-3-phosphocholine (POPC) mixed with cholesterol (right). Simulations with a ratio of 7 : 3 POPC/cholesterol demonstrate bithionol fails to penetrate bilayer. b. Polar phenols make initial contact with outer phospholipid heads followed by intercalation of nonpolar aryl rings into the membrane. Disruption of the membrane increases membrane fluidity and facilitating permeability of other small molecules into the cell.

MD calculations to mimic mammalian cell membranes also provided insight into the lack of observed mammalian toxicity and high antibacterial specificity of bithionol. These studies suggest higher cholesterol content in mammalian cells prevents membrane perturbation and minimizes toxicity[42]. This data offers further evidence that membrane perturbers can act as selective antibacterial agents and design of these inhibitors warrant further investigations.

5.3. Conclusion

Bithionol and its analogues demonstrated activity against MRSA persister cells. In addition, SYTOX-green assays and synergism with known antibiotics suggests the primary mode of action of bithionol and derivatives is cell membrane disruption. Although cell membrane disrupters often show broad membrane activity, bithionol exhibited selectivity for bacterial cells with minimal hemolysis of mammalian red blood cells. Furthermore, bithionol was shown to reduce MRSA infections in murine models when treated in combination with gentamicin. This suggests bithionol may be a promising candidate for repurposing as an antibiotic, specifically when used in combination with preexisting antibiotic treatments.

References

1. Kim, W.; Zou, G.; Hari, T. P. A.; Wilt, I. K.; Zhu, W.; Galle, N.; Faizi, H. A.; Hendricks, G. L.; Tori, K.; Pan, W.; Huang, X.; Steele, A. D.; Csatary, E. E.; Dekarske, M. M.; Rosen, J. L.; Ribeiro, N. Q.; Lee, K.; Port, J.; Fuchs, B. B.; Vlahovska, P. M.; Wuest, W. M.; Gao, H.; Ausubel, F. M.; Mylonakis, E., A selective membrane-targeting repurposed antibiotic with activity against persistent methicillin-resistant Staphylococcus aureus. *Proc. Natl. Acad. Sci. U.S.A.* **2019,** *116* (33), 16529-16534.
2. Schrank, C. L.; Wilt, I. K.; Monteagudo Ortiz, C.; Haney, B. A.; Wuest, W. M., Using membrane perturbing small molecules to target chronic persistent infections. *RSC Med. Chem.* **2021,** *12* (8), 1312-1324.
3. Wilt, I. K.; Hari, T. P. A.; Wuest, W. M., Hijacking the Bacterial Circuitry of Biofilm Processes via Chemical "Hot-Wiring": An Under-explored Avenue for Therapeutic Development. *ACS Infect. Dis.* **2019,** *5* (6), 789-795.
4. Lewis, K., Persister cells. *Annu. Rev. Microbiol.* **2010,** *64*, 357-72.
5. Brauner, A.; Fridman, O.; Gefen, O.; Balaban, N. Q., Distinguishing between resistance, tolerance and persistence to antibiotic treatment. *Nat. Rev. Microbiol.* **2016,** *14* (5), 320-30.
6. Van den Bergh, B.; Fauvart, M.; Michiels, J., Formation, physiology, ecology, evolution and clinical importance of bacterial persisters. *FEMS Microbiol. Rev.* **2017,** *41* (3), 219-251.
7. Fisher, R. A.; Gollan, B.; Helaine, S., Persistent bacterial infections and persister cells. *Nat. Rev. Microbiol.* **2017,** *15* (8), 453-464.
8. Balaban, N. Q.; Helaine, S.; Lewis, K.; Ackermann, M.; Aldridge, B.; Andersson, D. I.; Brynildsen, M. P.; Bumann, D.; Camilli, A.; Collins, J. J.; Dehio, C.; Fortune, S.; Ghigo, J. M.; Hardt, W. D.; Harms, A.; Heinemann, M.; Hung, D. T.; Jenal, U.; Levin, B. R.; Michiels, J.; Storz, G.; Tan, M. W.; Tenson, T.; Van Melderen, L.; Zinkernagel, A.,

Definitions and guidelines for research on antibiotic persistence. *Nat. Rev. Microbiol.* **2019,** *17* (7), 441-448.

9. Tuomanen, E.; Durack, D. T.; Tomasz, A., Antibiotic tolerance among clinical isolates of bacteria. *Antimicrob. Agents Chemother.* **1986,** *30* (4), 521-527.

10. Allison, K. R.; Brynildsen, M. P.; Collins, J. J., Heterogeneous bacterial persisters and engineering approaches to eliminate them. *Curr. Opin. Microbiol.* **2011,** *14* (5), 593-8.

11. Goormaghtigh, F.; Van Melderen, L., Single-cell imaging and characterization of Escherichia coli persister cells to ofloxacin in exponential cultures. *Sci. Adv.* *5* (6), eaav9462.

12. Roostalu, J.; Joers, A.; Luidalepp, H.; Kaldalu, N.; Tenson, T., Cell division in Escherichia coli cultures monitored at single cell resolution. *BMC Microbiol.* **2008,** *8*, 68.

13. Shah, D.; Zhang, Z.; Khodursky, A.; Kaldalu, N.; Kurg, K.; Lewis, K., Persisters: a distinct physiological state of E. coli. *BMC Microbiol.* **2006,** *6*, 53.

14. Defraine, V.; Fauvart, M.; Michiels, J., Fighting bacterial persistence: Current and emerging anti-persister strategies and therapeutics. *Drug Resist. Updat.* **2018,** *38*, 12-26.

15. Keren, I.; Shah, D.; Spoering, A.; Kaldalu, N.; Lewis, K., Specialized persister cells and the mechanism of multidrug tolerance in Escherichia coli. *J. Bacteriol.* **2004,** *186* (24), 8172-80.

16. Rownicki, M.; Lasek, R.; Trylska, J.; Bartosik, D., Targeting Type II Toxin-Antitoxin Systems as Antibacterial Strategies. *Toxins* **2020,** *12* (9).

17. Mohiuddin, S. G.; Hoang, T.; Saba, A.; Karki, P.; Orman, M. A., Identifying Metabolic Inhibitors to Reduce Bacterial Persistence. *Front. Microbiol.* **2020,** *11*, 472.

18. Alumasa, J. N.; Manzanillo, P. S.; Peterson, N. D.; Lundrigan, T.; Baughn, A. D.; Cox, J. S.; Keiler, K. C., Ribosome Rescue Inhibitors Kill Actively Growing and Nonreplicating Persister Mycobacterium tuberculosis Cells. *ACS Infect. Dis.* **2017,** *3* (9), 634-644.

19. Orman, M. A.; Brynildsen, M. P., Establishment of a method to rapidly assay bacterial persister metabolism. *Antimicrob. Agents Chemother.* **2013,** *57* (9), 4398-409.

20. Marques, C. N.; Morozov, A.; Planzos, P.; Zelaya, H. M., The fatty acid signaling molecule cis-2-decenoic acid increases metabolic activity and reverts persister cells to an antimicrobial-susceptible state. *Appl. Environ. Microbiol.* **2014,** *80* (22), 6976-91.

21. Silver, L. L., Challenges of antibacterial discovery. *Clin. Microbiol. Rev.* **2011,** *24* (1), 71-109.

22. Hurdle, J. G.; O'Neill, A. J.; Chopra, I.; Lee, R. E., Targeting bacterial membrane function: an underexploited mechanism for treating persistent infections. *Nat. Rev. Microbiol.* **2011,** *9* (1), 62-75.

23. Ruhr, E.; Sahl, H. G., Mode of action of the peptide antibiotic nisin and influence on the membrane potential of whole cells and on cytoplasmic and artificial membrane vesicles. *Antimicrob. Agents Chemother.* **1985,** *27* (5), 841-845.

24. Prince, A.; Sandhu, P.; Ror, P.; Dash, E.; Sharma, S.; Arakha, M.; Jha, S.; Akhter, Y.; Saleem, M., Lipid-II Independent Antimicrobial Mechanism of Nisin Depends On Its Crowding And Degree Of Oligomerization. *Sci. Rep.* **2016,** *6*, 37908.

25. Miller, W. R.; Bayer, A. S.; Arias, C. A., Mechanism of Action and Resistance to Daptomycin in Staphylococcus aureus and Enterococci. *Cold Spring Harb. perspect. med.* **2016,** *6* (11).

26. Zavascki, A. P.; Goldani, L. Z.; Li, J.; Nation, R. L., Polymyxin B for the treatment of multidrug-resistant pathogens: a critical review. *J. Antimicrob. Chemother.* **2007,** *60* (6), 1206-15.

27. Bialvaei, A. Z.; Samadi Kafil, H., Colistin, mechanisms and prevalence of resistance. *Curr. Med. Res. Opin.* **2015,** *31* (4), 707-21.
28. McAuley, S.; Huynh, A.; Czarny, T. L.; Brown, E. D.; Nodwell, J. R., Membrane activity profiling of small molecule B. subtilis growth inhibitors utilizing novel duel-dye fluorescence assay. *Medchemcomm.* **2018,** *9* (3), 554-561.
29. Mingeot-Leclercq, M.-P.; Décout, J.-L., Bacterial lipid membranes as promising targets to fight antimicrobial resistance, molecular foundations and illustration through the renewal of aminoglycoside antibiotics and emergence of amphiphilic aminoglycosides. *Medchemcomm.* **2016,** *7* (4), 586-611.
30. Epand, R. M.; Walker, C.; Epand, R. F.; Magarvey, N. A., Molecular mechanisms of membrane targeting antibiotics. *Biochim. Biophys. Acta* **2016,** *1858* (5), 980-7.
31. Te Winkel, J. D.; Gray, D. A.; Seistrup, K. H.; Hamoen, L. W.; Strahl, H., Analysis of Antimicrobial-Triggered Membrane Depolarization Using Voltage Sensitive Dyes. *Front. Cell Dev. Biol.*
2016, *4*, 29.
32. Benarroch, J. M.; Asally, M., The Microbiologist's Guide to Membrane Potential Dynamics. *Trends Microbiol.* **2020,** *28* (4), 304-314.
33. Kim, W.; Zhu, W.; Hendricks, G. L.; Van Tyne, D.; Steele, A. D.; Keohane, C. E.; Fricke, N.; Conery, A. L.; Shen, S.; Pan, W.; Lee, K.; Rajamuthiah, R.; Fuchs, B. B.; Vlahovska, P. M.; Wuest, W. M.; Gilmore, M. S.; Gao, H.; Ausubel, F. M.; Mylonakis, E., A new class of synthetic retinoid antibiotics effective against bacterial persisters. *Nature* **2018,** *556* (7699), 103-107.
34. Kim, W.; Conery, A. L.; Rajamuthiah, R.; Fuchs, B. B.; Ausubel, F. M.; Mylonakis, E., Identification of an Antimicrobial Agent Effective against Methicillin-Resistant Staphylococcus aureus Persisters Using a Fluorescence-Based Screening Strategy. *PLoS One* **2015,** *10* (6), e0127640.
35. Kim, W.; Steele, A. D.; Zhu, W.; Csatary, E. E.; Fricke, N.; Dekarske, M. M.; Jayamani, E.; Pan, W.; Kwon, B.; Sinitsa, I. F.; Rosen, J. L.; Conery, A. L.; Fuchs, B. B.; Vlahovska, P. M.; Ausubel, F. M.; Gao, H.; Wuest, W. M.; Mylonakis, E., Discovery and Optimization of nTZDpa as an Antibiotic Effective Against Bacterial Persisters. *ACS Infect. Dis.* **2018,** *4* (11), 1540-1545.
36. Rajamuthiah, R.; Fuchs, B. B.; Conery, A. L.; Kim, W.; Jayamani, E.; Kwon, B.; Ausubel, F. M.; Mylonakis, E., Repurposing salicylanilide anthelmintic drugs to combat drug resistant Staphylococcus aureus. *PLoS One* **2015,** *10* (4), e0124595.
37. Meshi, T.; Yoshikawa, M.; Sato, Y., Metabolic fate of bis(3,5-dichloro-2-hydroxyphenyl)-sulfoxide (bithionol sulfoxide). *Biochem. Pharmacol.* **1970,** *19* (4), 1351-61.
38. Liu, C.; Bayer, A.; Cosgrove, S. E.; Daum, R. S.; Fridkin, S. K.; Gorwitz, R. J.; Kaplan, S. L.; Karchmer, A. W.; Levine, D. P.; Murray, B. E.; M, J. R.; Talan, D. A.; Chambers, H. F.; Infectious Diseases Society of, A., Clinical practice guidelines by the infectious diseases society of america for the treatment of methicillin-resistant Staphylococcus aureus infections in adults and children. *Clin. Infect. Dis.* **2011,** *52* (3), e18-55.
39. Conlon, B. P.; Nakayasu, E. S.; Fleck, L. E.; LaFleur, M. D.; Isabella, V. M.; Coleman, K.; Leonard, S. N.; Smith, R. D.; Adkins, J. N.; Lewis, K., Activated ClpP kills persisters and eradicates a chronic biofilm infection. *Nature* **2013,** *503* (7476), 365-70.
40. Wu, Y.; Bai, J.; Zhong, K.; Huang, Y.; Qi, H.; Jiang, Y.; Gao, H., Antibacterial Activity and Membrane-Disruptive Mechanism of 3-p-trans-Coumaroyl-2-hydroxyquinic Acid, a

Novel Phenolic Compound from Pine Needles of Cedrus deodara, against Staphylococcus aureus. *Molecules* **2016,** *21* (8).

41. Saeloh, D.; Tipmanee, V.; Jim, K. K.; Dekker, M. P.; Bitter, W.; Voravuthikunchai, S. P.; Wenzel, M.; Hamoen, L. W., The novel antibiotic rhodomyrtone traps membrane proteins in vesicles with increased fluidity. *PLoS Pathog.* **2018,** *14* (2), e1006876.

42. Bramkamp, M.; Lopez, D., Exploring the existence of lipid rafts in bacteria. *Microbiol. Mol. Biol. Rev.* **2015,** *79* (1), 81-100.

6. Chapter 6. Experimental details1822

6.1 Supplementary figures, schemes, and tables

6.1.1. Chapter 2

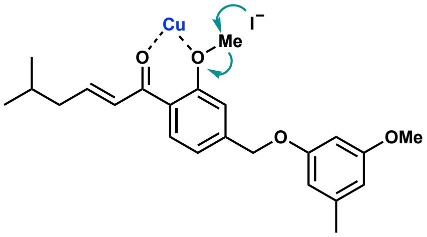
Cu
Me
I⁻
O
O
O
OMe

Figure S2.1. Copper iodide facilitated methoxy deprotection.

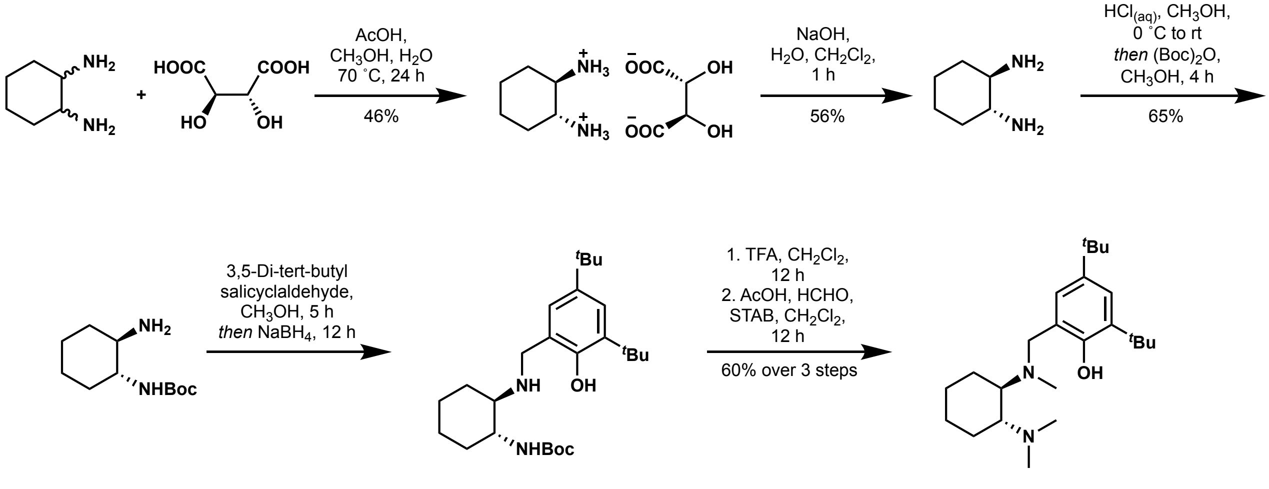
NH2
NH2
+
HOOC
COOH
HO
OH
AcOH,
CH3OH, H2O
70 °C, 24 h
46%
NH3
NH3
OOC
OOC
OH
OH
NaOH,
H2O, CH2Cl2,
1 h
56%
NH2
NH2
HCl(aq), CH3OH,
0 °C to rt
then (Boc)2O,
CH3OH, 4 h
65%
NH2
NHBoc
3,5-Di-tert-butyl
salicycladehyde,
CH3OH, 5 h
then NaBH4, 12 h
tBu
tBu
NH
OH
NHBoc
1. TFA, CH2Cl2,
12 h
2. AcOH, HCHO,
STAB, CH2Cl2,
12 h
60% over 3 steps
tBu
tBu
N
OH
N

L1

Scheme S2.1. Ligand synthesis.

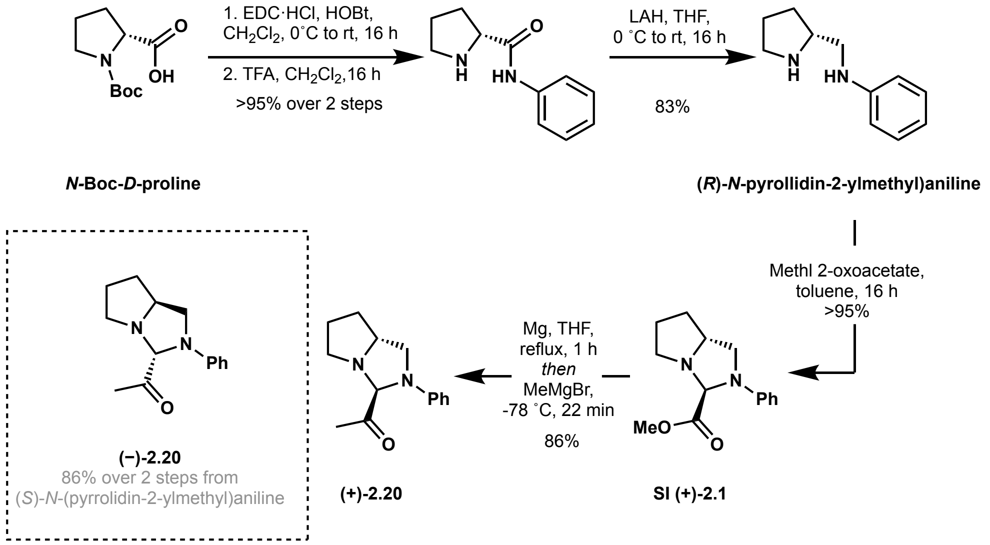
1. EDC·HCl, HOBt,
CH2Cl2, 0˚C to rt, 16 h
2. TFA, CH2Cl2,16 h
>95% over 2 steps
LAH, THF,
0 ˚C to rt, 16 h
83%
N-Boc-D-proline
(R)-N-pyrollidin-2-ylmethyl)aniline
Methl 2-oxoacetate,
toluene, 16 h
>95%
Mg, THF,
reflux, 1 h
then
MeMgBr,
-78 ˚C, 22 min
86%
(−)-2.20
86% over 2 steps from
(S)-N-(pyrrolidin-2-ylmethyl)aniline
(+)-2.20
SI (+)-2.1

Scheme S2.2. Synthesis of imidazolidinone.

6.1.2. Chapter 3

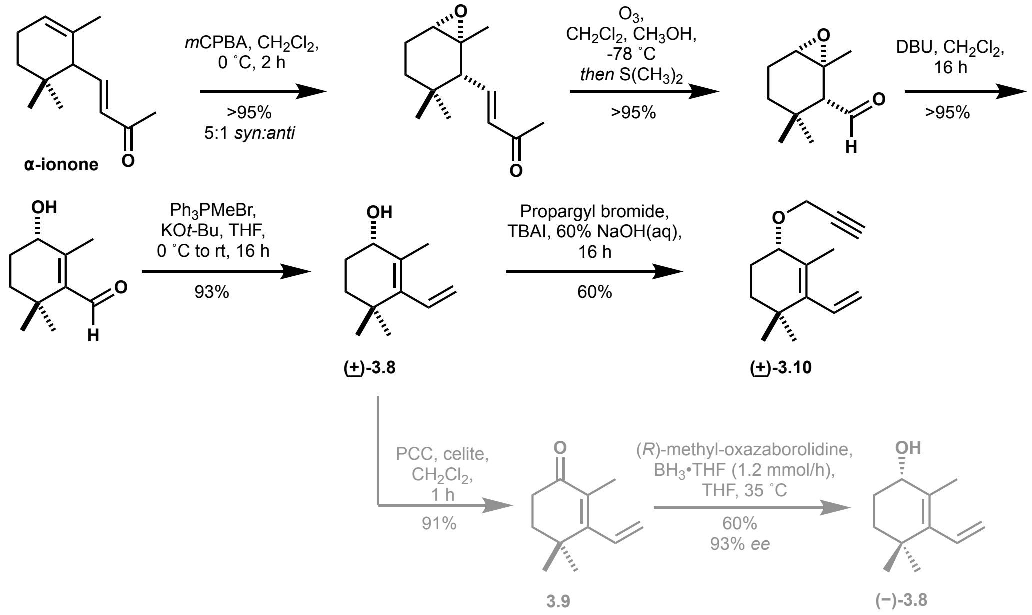
mCPBA, CH2Cl2,
0 ˚C, 2 h
>95%
5:1 syn:anti
α-ionone
O3,
CH2Cl2, CH3OH,
-78 ˚C
then S(CH3)2
>95%
DBU, CH2Cl2,
16 h
>95%
Ph3PMeBr,
KOt-Bu, THF,
0 ˚C to rt, 16 h
93%
(+)-3.8
Propargyl bromide,
TBAI, 60% NaOH(aq),
16 h
60%
(+)-3.10
PCC, celite,
CH2Cl2,
1 h
91%
3.9
(R)-methyl-oxazaborolidine,
BH3•THF (1.2 mmol/h),
THF, 35 ˚C
60%
93% ee
(−)-3.8

Scheme S3.1. Synthesis of racemic and optically enriched 2˚ alcohol.

6.1.3. Chapter 4

Table S4.1. Comparison of ^{1}H and ^{13}C NMR spectra of (+)-**4.4** and the natural product (CDCl$_3$).

	δ_H			δ_C	
	Natural (400 MHz)	**Synthetic (600 MHz)**		**Natural**	**Synthetic (600 MHz)**

1	-	-		-[a]	179.2
2	2.35, t (7.5)	2.35, t (7.5)			34.0
3	-[a]	1.70–1.21			31.9–24.8
4					
5					
6					
7					
8					
9					
10					
11	3.07, ddd (6.0, 5.0, 2.1)	3.07, ddd (6.1, 5.0, 2.0)			58.2
12	3.18, d (1.8)	3.18, d (2.0)			60.1
13	-	-			206.4
14	2.06, s	2.06, s			24.5

[a] Not reported

Table S4.2. Comparison of ^{1}H and ^{13}C NMR spectra of **4.6** and the natural product (CD_3OD).

	δ_H			δ_C	
	Natural (600 MHz)	**Synthetic (600 MHz)**		**Natural (600 MHz)**	**Synthetic (600 MHz)**
1	-	-		177.0	177.9
2	2.27, t (7.4)	2.30, t (7.4)		34.8	35.1
3	1.60, m	1.68–1.60, m		25.6	26.0

4	1.34, m	1.41–1.29, m		29.5	29.9
5	1.31, m	1.41–1.29, m		29.9	30.0
6	1.56, m	1.60–1.54, m		24.4	24.7
7	2.45, t (7.4)	2.48, t (7.5)		43.1	43.4
8	-	-		212.9	213.7
9	2.49, t (7.2)	2.51, t (7.4)		42.8	43.1
10	1.61, m	1.68–1.60, m		24.1	24.4
11	1.46, m	1.53–1.44, m		26.1	26.4
12	1.62, m 1.69, m	1.75–1.68, m 1.68–1.60, m		32.3	32.6
13	3.03, ddd (11.1, 4.9, 2.0)	3.05, app t (5.3)		59.2	59.7
14	3.51, d (2.0)	3.54, s		58.6	59.3
15	-	-		196.9	197.2
16	6.30, dq (15.8, 1.7)	6.33, d (15.8)		127.6	128.0
17	7.14, dq (15.8, 6.9)	7.15, dq (13.9, 6.9)		147.1	147.3
18	1.94, dd (6.9, 1.7)	1.96, d (6.9)		18.4	18.7

Table S4.3. Comparison of ^{1}H and ^{13}C NMR spectra of (+)-**4.5** and the natural product (CD_3OD).

	δ_H			δ_C	
	Natural (500 MHz)	**Synthetic (600 MHz)**		**Natural (500 MHz)**	**Synthetic (600 MHz)**
1	-[a]	-		179.0	177.9
2	2.24, t (7.7)	2.27, t (7.4)		36.0	35.1

3	1.59, m	1.60, m		26.5	26.1
4	1.30, m	1.43, m		30.5	30.56
5	1.28-1.67	1.16-1.43		26.9-30.8	26.9-30.63
6					
7					
8					
9					
10					
11					
12	1.57, m	1.60, m		32.9	32.9
13	3.11, td (5.5, 1.8)	3.12, ddd (6.4, 3.6, 1.8)		59.5	59.4
14	3.23 d (1.8)	3.24, d (1.8)		60.9	60.8
15	-[a]	-		208.0	208.0
16	2.06, s	2.06, s		24.8	24.8

6.2 Biology: General notes

Bacterial strains and culture conditions: *P. aeruginosa* PA01 was a gift from Prof. George O'Toole (Dartmouth Medical School). CA-MRSA (USA300) and MSSA (Newman) were a gift from Dr. Bettina Buttaro (Lewis Katz school of Medicine at Temple). *E. faecalis* (ATCC 51575) and HA-MRSA (ATCC 33592) were purchased from American Type Culture Collection (ATCC). Bacterial cultures were grown from direct inoculation of freezer stocks into LB media, incubating overnight at 37 °C, and diluted 5 µL of culture in liquid LB media (5 mL). Growth curves were obtained at least when using a strain for the first time to determine typical OD values at during each growth stage and to get a gauge on the rate of growth. If strains will be used in assays together, direct comparisons are made to ensure growth curves are similar or that procedures are modified appropriately. OD readings are taken at 600 nm, unless noted otherwise, and all OD readings were done with a SpectraMax 190 or SpectraMax iD3 plate reader.

6.3 Biology: Procedures and supplemental information

Minimum inhibitory concentration (MIC). Compounds were serially diluted two-fold from stock solutions to yield twelve test concentrations. Overnight cultures were diluted to ca. 10^6 cfu/mL in MH media and regrown to exponential phase as determined by optical density recorded at 600 nm (OD600). All cultures were diluted again to ca. 10^6 cfu/mL in MH media (CLSI Standards)[37] and 100 µL were inoculated into each well of a U-bottom 96-well plate (BD Biosciences, BD 351177) containing 100 µL of compound solution. Plates were incubated statically at 37°C for 24 h upon which time wells were evaluated visually for bacterial growth. The MIC was determined as the lowest concentration of compound resulting in no bacterial growth visible to the naked eye, based on the majority of three independent experiments. Aqueous DMSO controls were conducted as appropriate for each compound.

IC_{50} Assay Procedures: Overnight cultures of the indicated bacteria were diluted 1:100 in fresh LB media, and regrown at 37 °C with 200 rpm shaking. When the cultures reached mid-log phase, bacteria were diluted to a concentration of 0.004 using the following equation: (x µL O/N)(OD reading) = (0.004)(volume needed) and 100 µL was inoculated into each well of a 96-well plate (Corning ® 96-well clear bottom plates), which contained 100 µL of serially diluted compound. Compound serial dilutions were done starting from a 10 mM stock solution in DMSO, which was diluted with LB media to arrive at the desired final concentration. 96-well plates were grown statically at 37 °C for 16 hours, upon which time the OD at 595 nm was measured using a plate reader. IC_{50} values were calculated by fitting the OD readings in triplicate from separate O/N cultures vs. concentration with a 5-parameter-logistic model. The MIC value reflects the lowest concentration where no growth was visualized, and each assay was performed in triplicate

6.3.1. Chapter 4 IC_{50} assay curves

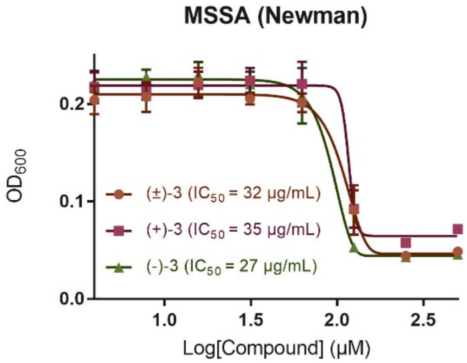
MSSA (Newman)

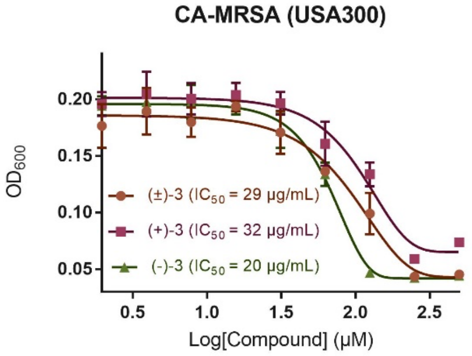
CA-MRSA (USA300)

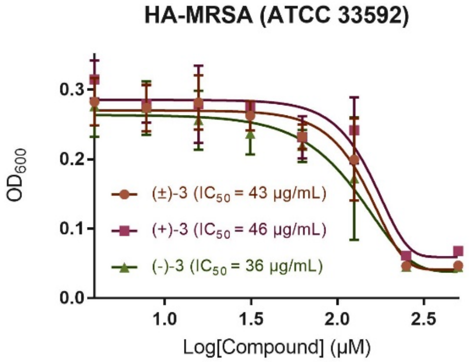
HA-MRSA (ATCC 33592)

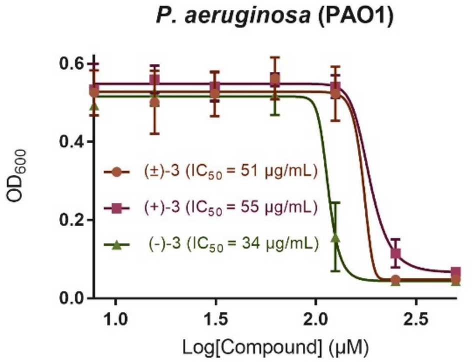
P. aeruginosa (PAO1)

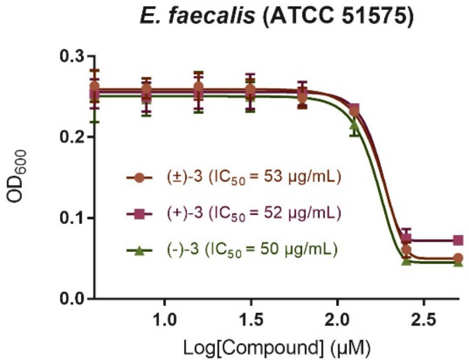
E. faecalis (ATCC 51575)

6.4 Chemistry: General notes

NMR spectra: NMR spectra were recorded using the following spectrometers: Bruker Avance 600 (600/150 MHz), Varian Inova 600 (600/150 MHz), Varian Inova 500 (500/125 MHz), Varian Inova 400 (400/100 MHz), VNMR 400 (400/100 MHz), or Mercury 300 (300/75 MHz). Chemical shifts are quoted in ppm relative to tetramethylsilane and with the indicated solvent as an internal reference (proton NMRs: $CDCl_3$ = 7.26; $(CD_3)_2CO$ = 2.05; D_2O = 4.79; $(CD_3)_2SO$ = 2.50; CD_3OD = 3.31). The following abbreviations are used to describe signal multiplicities: s (singlet), d (doublet), t (triplet), q (quartet), m (multiplet), br (broad), dd (doublet of doublets), dt (doublet of triplets), etc.

Mass spectra: Accurate mass spectra were recorded on a Thermo LTQ-FTMS using either APCI or ESI techniques.

Infrared spectra: Infrared spectra were obtained using a Thermo Nicolet Nexus 670 FTIR spectrophotometer.

Specific rotation: Specific rotation measurements were made with a 1 dm path length using a Perkin Elmer 341 Polarimeter with a sodium lamp set to 589 nm.

Reaction setup, monitoring, and purification: Non-aqueous reactions were performed under an atmosphere of argon, in flame-dried glassware, with HPLC-grade solvents purified on a Pure Process Technology purification system. Amine bases were freshly distilled from CaH_2 before use. All other chemicals were used as received from Oakwood, TCI America, Sigma-Aldrich, Alfa Aesar, AK Scientific, Enamine, or Strem. Brine refers to a saturated aqueous solution of sodium chloride. Reactions were monitored via thin-layer chromatography (TLC) using EMD Millipore TLC silica gel aluminum plates with $KMnO_4$, vanillin, *p*-anisaldehyde, or ninhydrin stain. Purification via column chromatography refers to purification on a Biotage Isolera flash chromatography purification system using a silica gel column and an increasing gradient of ethyl acetate in hexanes, diethyl ether in hexanes, or methanol in dichloromethane. Compounds that underwent biological testing were assessed for purity via analytical HPLC using an Agilent Technologies 1200 Series HPLC instrument and an acetonitrile in water solvent system with 0.1% formic acid.

6.5 Chemistry: synthesis procedures and characterization

6.5.1. Chapter 2

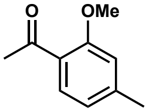

1-(2-methoxy-4-methylphenyl)ethan-1-one (2.3).

In a flame dried flask equipped with Teflon coated metal stir bar was added potassium carbonate (8.3 g, 60 mmol, 3 equiv) in anhydrous *N,N*-dimethylformamide (1M). To this suspension was slowly added 2’-hydroxy-4’-methylacetophenone (3 g, 20 mmol, 1 equiv). The reaction was stirred for 15 minutes prior to addition of iodomethane (3.75 mL, 60 mmol, 1 equiv) and then stirred overnight under an argon atmosphere. The reaction was quenched with aqueous 1N HCl and extracted with three portions of ethyl acetate. The combined organic layers were washed with five portions of brine, dried over anhydrous sodium sulfate, and concentrated *in vacuo*. The product was purified with silica column chromatography with a gradient of 0-15% ethyl acetate in hexanes and isolated as a white amorphous powder (3.2 g, >98% yield). The product was visualized on TLC with UV light. This compound is known in the literature[1].

^{1}H NMR (400 MHz, $CDCl_3$): δ 7.68 (d, *J* = 7.9 Hz, 1H), 6.81 (d, *J* = 9.3 Hz, 1H), 6.76 (s, 1H), 3.90 (s, 3H), 2.59 (s, 3H), 2.38 (s, 3H).

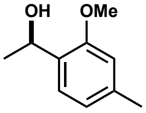

1-(2-methoxy-4-methylphenyl)ethan-1-ol ((±)-2.4)

This compound is known in the literature and was synthesized following reported procedure. A flame dried round bottom flask was charged with **2.3** (1 equiv) in anhydrous toluene (0.1M). The solution was cooled to -78 ˚C followed by addition of 1M BH_3·THF in toluene (1 equiv). The reaction was monitored by TLC and quenched with aqueous once all starting material had been consumed. The aqueous layer was extracted with three portions of diethyl ether and the combined organic layers were washed with brine, dried over anhydrous sodium sulfate, and concentrated *in vacuo*. The product was isolated as an amorphous white powder (mg, 96 % yield) and used without further purification[2].

^{1}H NMR (400 MHz, $CDCl_3$) δ 7.23 (d, *J* = 7.6 Hz, 1H), 6.79 (d, *J* = 6.7 Hz, 1H), 6.71 (s, 1H), 5.07 (q, *J* = 6.5 Hz, 1H), 3.85 (s, 4H), 2.37 (s, 4H), 1.50 (d, *J* = 6.6 Hz, 3H).

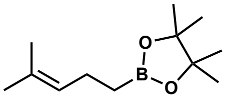

4,4,5,5-tetramethyl-2-(4-methylpent-3-en-1-yl)-1,3,2-dioxaborolane (2.7)

(4-Methylpent-3-enyl)magnesium bromide (0.5 M in THF, 1.0 equiv) prepared from 5-bromo-2-methylpent-e-ene was added to a dry schlenk tube under argon along with anhydrous tetrahydrofuran and this was cooled to -78 ˚C. Trimethylborate (1.2 equiv) was added and the mixture was stirred for 15 minutes at -78 ˚C before it was warmed to room temperature and stirred for 1.5 h. The mixture was then cooled to 0 ˚C and 5 ml of 3N HCl was added. The reaction mixture was warmed to room temperature and stirred for 10 minutes. The mixture was extracted with three portions of diethyl ether, dried over anhydrous magnesium sulfate, filtered and concentrated *in vacuo*. The crude boronic acid was then dissolved in a 4:1 mixture of pentane:Et_2O (50 ml) and to this was added pinacol (0.71 g, 6 mmol, 1.2 equiv). The reaction was stirred for 48 h, then diluted with petroleum ether and washed several times with water. The organic layer was dried over anhydrous magnesium sulfate, filtered and concentrated to provide desired boronic ester (92%). The title compound is known and matched reported spectra[3].

^{1}H NMR (400 MHz, $CDCl_3$) δ 5.11 (m, 1H), 2.13 – 2.02 (m, 2H), 1.65 (s, 3H), 1.59 (s, 3H), 1.23 (d, *J* = 1.5 Hz, 12H), 0.87 – 0.76 (m, 2H).

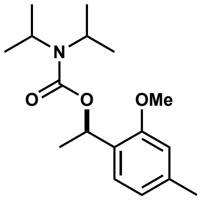

1-(2-methoxy-4-methylphenyl)ethyl diisopropylcarbamate ((±)-2.5)

This compound is known in the literature and was synthesized following reported procedure.

To a flame dried flask under was added **(±)-2.4** (1 equiv) to a solution of *N,N*-diisopropylcarbamoyl chloride (1.2 equiv) and triethyl amine (1.2 equiv) in anhydrous methylene chloride (0.5M) and heated to reflux for 48 h. The reaction mixture was cooled to room temperature and water was added. The organic phase was separated and the aqueous phase extracted with methylene chloride. The organic phases were combined, dried over anhydrous magnesium sulfate, and concentrated *in vacuo.* Purfiction by silica column chromatography (10% ethyl acetate in hexanes) afforded the title compound as an amorphous white powder (74% yield). The title compound is known and matched reported spectra[2].

^{1}H NMR (600 MHz, $CDCl_3$): δ 7.22 (d, *J* = 7.7 Hz, 1H), 6.76 (d, *J* = 7.0 Hz, 1H), 6.67 (s, 1H), 6.13 (q, *J* = 6.5 Hz, 1H), 3.81 (s, 3H), 2.33 (s, 3H), 1.61 (s, 1H), 1.48 (d, *J* = 6.5 Hz, 2H), 1.20 (d, *J* = 6.9 Hz, 12H).

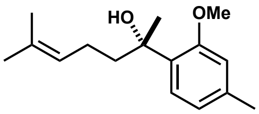

2-(2-methoxy-4-methylphenyl)-6-methylhept-5-en-2-ol ((±)-2.5)

To a flame dried flask equipped with Teflon coated metal stir bar was added **(±)-2.5** (50 mg, 0.17 mmol, 1 equiv) in anhydrous diethyl ether (0.25M) distilled over CaH onto 4Å MS. The solution was cooled to -78 ˚C and *s*-BuLi (0.3M in cyclohexane, 750 µL, 0.22 mmol, 1.3 equiv) was added dropwise to ensure reaction temperature remained under -70 ˚C. The reaction was stirred for 15 minutes before dropwise addition of a solution of **2.3** (54 mg, 0.25 mmol, 1.5 equiv) in anhydrous diethyl ether (0.3M). Stirring was continued for 1 hour at -78 ˚C, at which time $MgBr_2 \cdot OEt_2$ (200 mg, 0.75 mmol, 3.75 equiv) in 750 µL of methanol was added. The solution was allowed to warm to room temperature and stirred overnight. The reaction was diluted with BHT stabilized tetrahydrofuran (0.15M) and cooled to 0 ˚C. An aqueous solution of 2M NaOH (600 µL, 1.2 mmol, 7 equiv) followed by H_2O_2 (30% (w/w) in H_2O, 200 µL, 2.0 mmol, 11.8 equiv) were added slowly and the reaction was stirred overnight, allowing to warm to room temperature. The reaction was diluted with 2.5 mL of water and extracted with three portions of diethyl ether. The combined organic layers were washed with brine, dried over anhydrous magnesium sulfate, and concentrated *in vacuo*. Purification was completed with silica column chromatography with a gradient of 0-30% ethyl acetate in hexanes and the product was isolated as a yellow oil (13 mg, 30 % yield). The product was visualized on TLC with UV light and after heat activation with $KMnO_4$. The compound was characterized by ^1H NMR[4, 5].

R_f = 0.35 (2:1 hexanes:ethyl acetate)

^{1}H NMR (400 MHz, $CDCl_3$) δ 7.20 (d, *J* = 7.7 Hz, 1H), 6.77 (d, *J* = 7.0 Hz, 1H), 6.70 (s, 1H), 5.14 – 5.00 (m, 1H), 3.86 (s, 3H), 2.35 (s, 3H), 1.73 (m, 1H), 1.69 (m, 1H), 1.66 (m, 1H), 1.62 (m, 1H), 1.56 (s, 3H), 1.50 (d, *J* = 6.5 Hz, 6H), 1.26 (s, 3H).

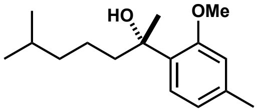

2-(2-methoxy-4-methylphenyl)-6-methylheptan-2-ol ((±)-2.8)

To a vial were added **2.5** (30 mg, 0.12 mmol, 1 equiv) and 10 wt.% Pd/C (1.3 mg, mmol, 10 mol%) in ethyl acetate (0.2M). The vial was purged with argon then 5 times with hydrogen. The solution was stirred for 1 hour at room temperature then filtered over celite and concentrated *in vacuo*. The product was obtained without further purification as a yellow oil (30 mg, >98% yield) and characterized ^{1}H and ^{13}C NMR. The title compound is known and matched reported spectra.

R$_f$ = 0.58 (4:1 hexanes:ethyl acetate)

^{1}H NMR (400 MHz, CDCl$_3$) δ 7.13 (d, *J* = 7.7 Hz, 1H), 6.75 (d, *J* = 7.7 Hz, 1H), 6.73 (s, 1H), 3.87 (s, 1H), 2.33 (s, 3H), 1.96 – 1.70 (m, 2H), 1.54 (s, 3H), 1.48 (dq, *J* = 13.1, 6.6 Hz, 1H), 1.32 – 1.17 (m, 2H), 1.17 – 1.08 (m, 2H), 0.82 (dd, *J* = 6.6, 0.7 Hz, 6H).

^{13}C NMR (100 MHz, CDCl$_3$) δ 187.44, 138.04, 126.74, 121.51, 112.42, 75.18, 55.43, 42.67, 39.53, 27.99, 27.55, 27.53[a], 22.77[a], 22.74, 22.42.

[a]Peaks reported at 27.53, and 22.77 were unable to be selected on mnova.

ν$_{max}$/cm^{-1} (film): 3463, 2951, 2867, 1465, 1251.

HRMS: APCI (*m/z*) calcd for C$_{16}$H$_{25}$O [M+H$^+$]: 233.18999, found 233.18937.

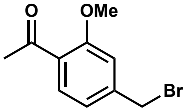

1-(4-(bromomethyl)-2-methoxyphenyl)ethan-1-one (2.11)

In a flame dried flask equipped with Teflon coated metal stir bar were added **2.3** (2 g, 12.1 mmol, 1 equiv), *N*-bromosuccinimide (2.4 g, 14.6 mmol, 1.2 equiv), and 2,2-azobis(2-methylpropionitrile) (108 mg, 0.61 mmol, 5 mol%) in tetrachloromethane (0.17M) under an argon atmosphere. An oven dried reflux condenser was fitted to the flask and the solution was stirred at reflux for six hours. The reaction was cooled to room temperature, filtered, and washed with aqueous 1N HCl and a saturated aqueous solution of sodium bicarbonate. The organic layer was dried over anhydrous sodium sulfate and concentrated *in vacuo*. The product was purified by silica column chromatography using 0-10% ethyl acetate in hexanes as an eluent and isolated as an amorphous off-white powder (1.97 g, 60%

yield). Visualization of the product on TLC was performed with UV light and after heat activation with $KMnO_4$.

R_f = 0.47 (4:1 hexanes:ethyl acetate)

^{1}H NMR (400 MHz, $CDCl_3$): δ 7.71 (d, *J* = 8.7 Hz, 1H), 6.99 (d, *J* = 8.4 Hz, 0H), 6.96 (s, 2H), 4.45 (s, 2H), 2.62 (s, 3H).

^{13}C NMR (151 MHz, $CDCl_3$): δ 199.45, 158.67, 143.51, 131.11, 128.19, 121.06, 113.02, 64.37, 32.73, 32.18, 14.86.

ν_{max}/cm^{-1} (film): 2980, 2935, 2898, 1671, 1606.

HRMS: APCI (*m/z*) calcd for $C_{10}H_{10}O_2$ [M-H$^+$]: 240.98587, found 240.98599.

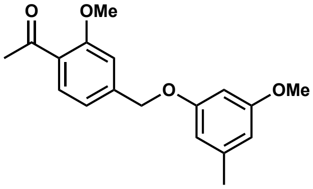

1-(2-methoxy-4-((3-methoxy-5-methylphenoxy)methyl)phenyl)ethan-1-one (2.12)

In a flask open to air were added **2.11** (300 mg, 1.23 mmol, 1.2 equiv), 3-methyoxy-5-methylphenol (138 mg, 1 mmol, 1 equiv), tetrabutylammonium chloride (370 mg, 1 mmol, 1 equiv), and potassium phosphate tribasic (318 mg, 1.5 mmol, 1.5 equiv) in deionized water (0.25M). The suspension was stirred overnight at room temperature. The reaction was concentrated *in vacuo* to remove solvent and then diluted with methylene chloride. The resulting suspension was washed with aqueous 1N HCl. The organic layer was dried over anhydrous sodium sulfate and concentrated *in vacuo*. The product was purified with silica column chromatography with a gradient of 0-15% ethyl acetate in hexanes and isolated as an off-white amorphous powder (308 mg, >98% yield). Visualization on TLC was performed with UV light and after heat activation with vanillin. The product stains red in vanillin.

R_f = 0.65 (4:1 hexanes:ethyl acetate)

^{1}H NMR (600 MHz, CDCl$_3$): δ 7.75 (d, *J* = 7.9 Hz, 1H), 7.05 (s, 1H), 7.03 (d, *J* = 7.9 Hz, 0H), 6.41 (s, 1H), 6.37 (s, 1H), 6.35 (s, 1H), 5.05 (s, 2H), 3.93 (s, 3H), 3.77 (s, 3H), 2.61 (s, 3H), 2.30 (s, 3H).

^{13}C NMR (151 MHz, CDCl$_3$): δ 199.8, 161.0, 159.8, 159.5, 143.7, 140.7, 131.2, 127.8, 119.4, 110.4, 108.1, 107.9, 98.7, 69.6, 55.9, 55.6, 32.2, 22.2.

ν_{max}/cm^{-1} (film): 2998, 2940, 2839, 1671, 1608.

HRMS: APCI (*m/z*) calcd for $C_{18}H_{21}O_4$ [M+H$^+$]: 301.14344, found 301.14312.

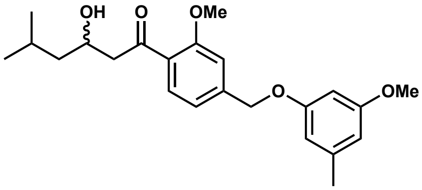

3-hydroxy-1-(2-methoxy-4-((3-methoxy-5-methylphenoxy)methyl)phenyl)-5-methylhexan-1-one ((±)-2.13)

In a flame dried flask equipped with a Teflon coated metal stir bar was added **2.12** (200 mg, 0.66 mmol, 1 equiv) in anhydrous tetrahydrofuran (0.1M) under an argon atmosphere. The reaction was cooled to -78˚C and lithium diisopropylamide (1M in 1:1 tetrahydrofuran : hexanes, 730 µL, 0.73 mmol, 1.1 equiv) was added slowly. The solution was stirred for 1 hour at -78 ˚C, then isovaleraldehyde (77 µL, 0.73 mmol, 1.1 equiv) was added. The reaction was stirred for an additional 1.5 hours at -78˚C. The ice bath was removed, and the reaction was quickly quenched with aqueous pH = 7 phosphate buffer. Allowing the reaction to warm past -78˚C results in addition at the benzylic position. Extraction of the aqueous layer was performed with three portions of ethyl acetate. The combined organic layers were washed with brine, dried over anhydrous sodium sulfate, and concentrated *in vacuo*. The product was purified with silica column chromatography with a gradient of 0-15% ethyl acetate in hexanes and isolated as a low melting point amorphous yellow solid (198 mg, 77% yield). Visualization of the product on TLC was performed with UV light and after heat activation with vanillin. The product stains purple in vanillin.

R$_f$ = 0.27 (4:1 hexanes:ethyl acetate).

^{1}H NMR (600 MHz, CDCl$_3$): δ 7.76 (d, *J* = 7.8 Hz, 1H), 7.05 (s, 1H), 7.06 – 7.02 (m, 1H), 6.40 (d, *J* = 0.8 Hz, 1H), 6.37 (d, *J* = 0.7 Hz, 1H), 6.35 (t, *J* = 2.0 Hz, 1H), 5.05 (s, 2H), 4.28 – 4.21 (m, 1H), 3.92 (s, 3H), 3.77 (s, 3H), 3.27 (d, *J* = 3.3 Hz, 1H), 3.21 (dd, *J* = 18.1, 2.3 Hz, 1H), 3.01 (dd, *J* = 18.1, 9.3 Hz, 1H), 2.31 (s, 3H), 1.85 (dddd, *J* = 13.3, 12.1, 8.7, 6.6 Hz, 1H), 1.57 – 1.52 (m, 1H), 1.25 – 1.16 (m, 1H), 0.94 (dd, *J* = 6.6, 3.7 Hz, 6H).

^{13}C NMR (151 MHz, CDCl$_3$): δ 202.84, 160.80, 159.59, 159.38, 143.98, 140.55, 130.88, 127.14, 119.29, 110.24, 107.97, 107.71, 98.52, 69.38, 66.24, 55.74, 55.41, 50.99, 45.80, 24.53, 23.54, 22.23, 22.01.

ν_{max}/cm^{-1} (film): 3521, 2954, 2868, 1664, 1608.

HRMS: APCI (*m/z*) calcd for $C_{23}H_{31}O_5$ [M+H$^+$]: 387.2166, found 387.21638.

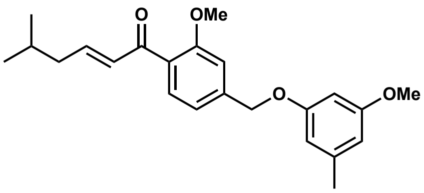

(*E*)-1-(2-methoxy-4-((3-methoxy-5-methylphenoxy)methyl)phenyl)-5-methylhex-2-en-1-one (2.14)

In a flame dried vial equipped with Teflon coated metal stir bar was added **(±)-2.13** (210 mg, 0.54 mmol, 1 equiv) and *p*-toluenesulfonic acid monohydrate (155 mg, 0.82 mmol, 1.5 equiv) in anhydrous toluene (0.15M) under an argon atmosphere. The vial was quickly sealed and heated to 50 ˚C for 2.5 hours. The reaction was cooled to room temperature, diluted with hexanes, filtered over celite, and concentrated *in vacuo* resulting in a yellow oil. The product was purified with silica column chromatography with a gradient of 0-15% ethyl acetate in hexanes and isolated as a yellow oil (171 mg, 86% yield). Visualization on TLC was performed with UV light and after heat activation with vanillin. The product stained brown in vanillin.

R$_f$ = 0.44 (4:1 hexanes:ethyl acetate).

^{1}H NMR (600 MHz, CDCl$_3$): δ 7.51 (d, *J* = 8.0 Hz, 1H), 7.05 – 7.02 (m, 2H), 6.87 – 6.80 (m, 1H), 6.65 (dt, *J* = 15.5, 1.3 Hz, 1H), 6.41 (s, 1H), 6.38 – 6.33 (m, 2H), 5.05 (s, 2H), 3.87 (s, 3H), 3.77 (s, 3H), 2.31 (s, 3H), 2.15 (ddd, *J* = 7.4, 6.8, 1.4 Hz, 2H), 1.78 (hept, *J* = 6.7 Hz, 1H), 0.94 (d, *J* = 6.7 Hz, 6H).

^{13}C NMR (151 MHz, CDCl$_3$): δ 193.42, 160.79, 159.70, 158.27, 148.15, 142.14, 140.50, 131.80, 130.56, 128.78, 119.32, 110.25, 107.97, 107.69, 98.51, 69.62, 55.80, 55.40, 42.02, 28.06, 22.57, 22.00.

ν_{max}/cm^{-1} (film): 2955, 2924, 2869, 1660, 1609.

HRMS: APCI (*m/z*) calcd for $C_{23}H_{29}O_4$ [M+H$^+$]: 369.20604, found 369.20615.

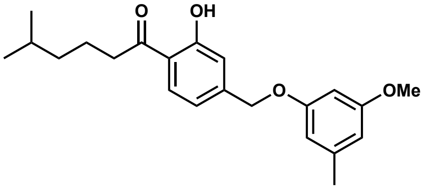

1-(2-hydroxy-4-((3-methoxy-5-methylphenoxy)methyl)phenyl)-5-methylhexan-1-one (2.17)

In a flame dried vial equipped with Teflon coated metal stir bar was added a solution of lithium aluminum hydride (1.4 mg, 36 μmol, 2 equiv) in anhydrous tetrahydrofuran (0.2M) to copper iodide (27 mg, 140 μmol, 8 equiv) at 0 ˚C under an atmosphere of argon. The suspension was stirred for at least 3 minutes prior to the addition of **2.14** (6.6 mg, 18 μmol, 1 equiv) in anhydrous tetrahydrofuran (0.1M). The temperature was maintained at 0 ˚C for 1 hour, then the reaction was quenched with an aqueous saturated solution of potassium sodium tartrate. The biphasic mixture was extracted with three portions of diethyl ether, dried over anhydrous magnesium sulfate, and concentrated *in vacuo*. The product was purified with silica column chromatography with a gradient of 0-15% ethyl acetate in hexanes and isolated as a yellow oil (4.2 mg, 64% yield). Visualization on TLC was performed with UV light and after heat activation with vanillin. Product stained red in vanillin.

R_f = 0.60 (4:1 hexanes:ethyl acetate)

^{1}H NMR (600 MHz, $CDCl_3$): δ 12.47 (s, 1H), 7.76 (d, *J* = 8.2 Hz, 1H), 7.04 (d, *J* = 1.8 Hz, 1H), 6.95 (dd, *J* = 8.2, 1.6 Hz, 1H), 6.37 (ddd, *J* = 14.7, 1.7, 0.8 Hz, 2H), 6.33 (t, *J* = 2.0 Hz, 1H), 5.03 (s, 1H), 3.77 (s, 3H), 2.99 – 2.92 (m, 2H), 2.30 (s, 3H), 1.79 – 1.70 (m, 2H), 1.64 – 1.59 (m, 1H), 1.32 – 1.23 (m, 2H), 0.91 (d, *J* = 6.7 Hz, 6H).

^{13}C NMR (151 MHz, $CDCl_3$): δ 206.76, 162.85, 160.78, 159.53, 146.37, 140.51, 130.49, 118.78, 117.24, 116.57, 107.91, 107.74, 98.47, 69.00, 55.40, 38.72, 38.64, 28.04, 22.65, 22.56, 22.00.

ν_{max}/cm^{-1} (film): 3280, 2954, 2869, 1641, 1595.

HRMS: APCI (*m/z*) calcd for $C_{22}H_{29}O_4$ [M+H$^+$]: 357.20604, found 357.20586.

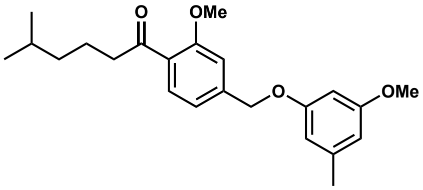

1-(2-methoxy-4-((3-methoxy-5-methylphenoxy)methyl)phenyl)-5-methylhexan-1-one (2.10)

In a flame dried flask under an argon atmosphere was added **2.14** (150 mg, 0.41 mmol, 1 equiv) in anhydrous diethyl ether (0.1M). The solution was cooled to -78 ˚C in a dry ice-acetone bath and L-selectride (1M in tetrahydrofuran, 0.41 mL, 0.41 mmol, 1 equiv) was added dropwise. The reaction was stirred for 1 hour at -78 ˚C, then the ice bath was removed. The reaction was quenched immediately with a saturated aqueous solution of ammonium chloride. The resulting biphasic mixture was extracted with three portions of diethyl ether and the combined organic layers were dried over anhydrous magnesium sulfate and concentrated *in vacuo* resulting in a yellow oil. The product was purified with silica column chromatography with a gradient of 0-15% ethyl acetate in hexanes and isolated as a yellow oil (129 mg, 85% yield). Visualization on TLC was performed with UV light and after heat activation with vanillin. The product stained orange-brown in vanillin.

R_f = 0.62 (4:1 hexanes:ethyl acetate)

^{1}H NMR (600 MHz, $CDCl_3$): δ 7.67 (d, *J* = 7.7 Hz, 1H), 7.04 (s, 1H), 7.02 (d, *J* = 7.7 Hz, 1H), 6.41 (s, 1H), 6.36 (s, 1H), 6.35 (s,10H), 5.04 (s, 2H), 3.91 (s, 3H), 3.77 (s, 3H), 2.99 – 2.89 (m, 2H), 2.30 (s, 2H), 1.72 – 1.63 (m, 1H), 1.56 (dt, *J* = 13.3, 6.7 Hz, 1H), 1.25 – 1.17 (m, 1H), 0.88 (d, *J* = 6.6 Hz, 6H).

^{13}C NMR (151 MHz, $CDCl_3$) δ 203.0, 160.7, 159.6, 158.7, 142.8, 140.5, 130.6, 128.2, 119.3, 110.1, 107.9, 107.6, 98.5, 77.3, 77.1, 76.9, 69.5, 55.6, 55.4, 55.3, 44.1, 38.8, 28.0, 28.0, 22.7, 22.4, 22.0.

ν_{max}/cm^{-1} (film): 2953, 2868, 2843, 1672, 1608.

HRMS: APCI (*m/z*) calcd for $C_{23}H_{31}O_4$ [M+H$^+$]: 371.22169, found 371.22145.

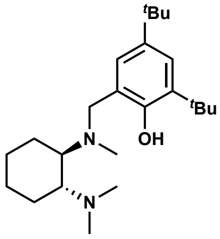

2,4-di-*tert*-butyl-6-((((1*R*,2*R*)-2-(dimethylamino)cyclohexyl)(methyl)amino)methyl)phenol (L_1)

The title compound was prepared via literature procedure in 6 steps and matched reported spectra. Tert-butyl (1*R*,2*R*)-2-aminocyclohexylcarbamate (1.0 eq) was dissolved in methanol (15 vol.) and 3,5-di-tert-butyl-2-hydroxybenzaldehyde (1.0 eq.) was added to the solution. The mixture was stirred for 5 hours and then solid sodium borohydride (2.0 eq.) was added slowly. The mixture was stirred for another 12 hours and quenched with an aqueous solution of sodium bicarbonate (10 vol.). The product was extracted with diethyl ether (3 x 20 vol.) and the organic phase was washed with water (3 x 20 vol.). The solvent was removed *in vacuo* to yield a crude product which was dissolved in CH_2Cl_2/TFA (1:2, 10 vol.) and stirred for 12 hours. The mixture was basified with concentrated KOH to pH 12 (with cooling) and the product was extracted with diethyl ether (3 x 20 vol.) and washed with water (3 x 20 vol.) and dried over anhydrous sodium sulfate. The solvent was removed *in vacuo* to yield solids, which were dissolved in methylene chloride (20 vol.). Acetic acid (glacial, 0.5 vol.) was added, followed by formaldehyde (aq., 37%, 2.0 vol.) and STAB (6.0 eq.). The mixture was stirred for 12 hours at room temperature, quenched with an aqueous solution of sodium bicarbonate (10 vol.). The product was extracted with diethyl ether (3 x 15 vol.) and washed with water (3 x 15 vol.). The solvent was removed *in vacuo* to yield a crude ligand **L1**. The product was purified by silica column chromatography, using cyclohexane:ethyl acetate mixture (80:20) as an eluent and recrystallized from hot IPA/water (2:1) to yield a purified ligand **L1**. The title compound is known and matched reported spectra[6].

^{1}H NMR (600 MHz, Chloroform-*d*): δ 7.18 (d, $J = 2.4$ Hz, 1H), 6.83 (d, $J = 2.4$ Hz, 1H), 3.92 (d, $J = 12.8$ Hz, 1H), 3.20 (s, 1H), 2.52 (td, $J = 10.8, 3.3$ Hz, 2H), 2.25 (s, 6H), 2.20 (s, 3H), 2.03 – 1.97 (m, 2H), 1.84 – 1.76 (m, 2H), 1.42 (s, 9H), 1.28 (s, 9H), 1.21 – 1.11 (m, 4H).

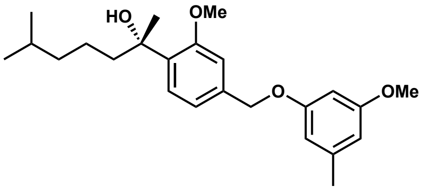

(*S*)-2-(2-methoxy-4-((3-methoxy-5-methylphenoxy)methyl)phenyl)-6-methylheptan-2-ol ((−)-2.15)

In a flame dried vial under an argon atmosphere was added **L₁** (25 mg, 67 µmol, 1 equiv) in anhydrous toluene (0.2M). A solution of **2.10** (25 mg, 67 µmol, 1 equiv) was then added to the reaction in anhydrous toluene (0.4M) and stirred for 5 minutes at room temperature. The solution was cooled to -78 ˚C with a dry ice-acetone bath and methylmagnesium bromide (0.42M in 6 : 1 toluene : diethyl ether prepared from 3M solution of methylmagnesium bromide in diethyl ether, 0.34 mL, 140 µmol, 2.1 equiv) was added dropwise. The reaction was stirred for 1 hour at -78 ˚C and determined to be incomplete by TLC (4:1 hexanes:ethyl acetate). Stirring for an additional hour at -78 ˚C resulted in no change. An additional equivalent of methylmagnesium bromide (0.16 mL, 67 µM, 1 equiv) was added and the reaction was stirred for another hour at -78 ˚C. The ice bath was removed and the reaction was quenched immediately with 2-propanol:water (3:1) and diluted with hexane. The solution was allowed to warm to room temperature before quenching with a saturated aqueous solution of ammonium chloride. The aqueous layer was extracted with three portions of hexanes and the combined organic layers were washed with water (3x) and brine (3x) and dried over anhydrous magnesium sulfate, and concentrated *in vacuo*. To separate the ligand from the crude mixture, the residue was diluted with hexanes and a few drops of glacial acetic acid were added. The solution was filtered through a 2 cm Pasteur pipette silica plug, washing with 5 mL of hexanes:ethyl acetate (1:1). The fraction collected after filtration contained the desired product and was concentrated *in vacuo*. The product was purified with silica column chromatography with a gradient of 0-10% ethyl acetate in hexanes and was isolated as a low melting point amorphous off-white powder (7.2 mg, 28% yield). Visualization on TLC was performed with UV light and after heat activation with vanillin—product stained brown.

The ligand was recovered from the silica plug by rinsing with 10 mL of cyclohexane:ethyl acetate : triethylamine (5:4:1).

R_f = 0.39 (4:1 hexanes:ethyl acetate)

^{1}H NMR (400 MHz, $CDCl_3$) δ 7.28 (d, *J* = 8.3 Hz, 1H), 6.99 (d, *J* = 6.7 Hz, 2H), 6.42 (s, 1H), 6.36 (s, 2H), 5.00 (s, 2H), 3.90 (s, 3H), 3.77 (s, 3H), 2.31 (s, 3H), 1.95 – 1.76 (m, 2H), 1.49 (dt, *J* = 13.1, 6.6 Hz, 1H), 1.28 (s, 3H), 1.22 – 1.16 (m, 2H), 1.16 – 1.08 (m, 2H), 0.82 (d, *J* = 6.6 Hz, 6H).

^{13}C NMR (151 MHz, $CDCl_3$): δ 160.7, 159.9, 157.2, 140.4, 137.1, 134.8, 127.0, 120.0, 110.6, 107.9, 107.5, 98.4, 75.2, 69.8, 55.5, 55.3, 42.4, 39.4, 31.8, 29.7, 27.9, 27.4, 22.7, 22.3.

ν_{max}/cm^{-1} (film): 3558, 2951, 2931, 1595, 1501.

HRMS: APCI (*m/z*) calcd for $C_{24}H_{35}O_4$ [M+H$^+$]: 387.25299, found 387.25248.

$[\alpha]^{20}_D = -36$ (*c* = 1, chloroform)

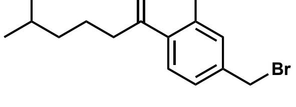

1-(4-(bromomethyl)-2-hydroxyphenyl)-5-methylhexan-1-one (2.18)

In a flame dried vial under an argon atmosphere was added **2.10** (20 mg, 53 µmol, 1 equiv) in anhydrous methylene chloride 0.1M. The solution was cooled to -78 ˚C prior to drop-wise addition of boron tribromide (1M in methylene chloride, 160 µL, 160 µmol, 3 equiv). The reaction was stirred for 1 hour at -78 ˚C[a] then allowed to warm to 0 ˚C. After stirring for 1 hour, the reaction was quenched with water and extracted with three portions of dichloromethane. The combined organic layers were dried over anhydrous magnesium sulfate and concentrated *in vacuo*. The product was purified with silica column chromatography with a gradient of 0-15% ethyl acetate in hexanes and isolated as an orange amorphous powder (13.8 mg, 87% yield). Visualization of the product on TLC was performed with UV light. The product did not stain in vanillin.

[a]Maintaining -78 ˚C for the duration of the reaction resulted in monomethyl deprotection to produce **2.17**

R_f = 0.53 (4:1 hexanes:ethyl acetate)

^{1}H NMR (600 MHz, $CDCl_3$): δ 12.45 (s, 1H), 7.74 (d, *J* = 8.3 Hz, 1H), 6.99 (d, *J* = 1.8 Hz, 1H), 6.92 (dd, *J* = 8.2, 1.8 Hz, 1H), 4.40 (s, 2H), 2.97 – 2.92 (m, 2H), 1.77 – 1.69 (m, 2H), 1.59 (dp, *J* = 13.3, 6.6 Hz, 1H), 1.30 – 1.23 (m, 2H), 0.90 (d, *J* = 6.6 Hz, 6H).

^{13}C NMR (151 MHz, $CDCl_3$): δ 206.61, 162.66, 146.07, 130.66, 119.65, 119.06, 118.87, 38.76, 38.59, 32.01, 28.02, 22.63, 22.44.

ν_{max}/cm^{-1} (film): 2953, 2927, 2900, 2868, 1639.

HRMS: APCI (*m/z*) calcd for $C_{14}H_{20}O_2Br$ [M+H$^+$]: 299.06433, found 299.06412.

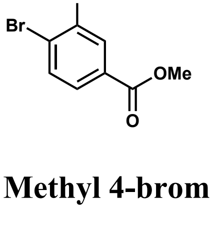

Methyl 4-bromo-3-((2-(trimethylsilyl)ethoxy)methoxy)benzoate (2.19)

To a suspension of NaH (60% dispersion in mineral oil, 520 mg, 13 mmol, 1.5 equiv) in anhydrous tetrahydrofuran (0.8M) at 0˚C was added a solution of methyl 4-bromo-3-hydroxybenzoate (2.00 g, 8.66 mmol, 1 equiv) in anhydrous THF (1.3M). The reaction was stirred under an argon atmosphere and allowed to war to room temperature. After one hour, the reaction was cooled to 0˚C and 2-(trimethylsilyl)ethoxymethyl chloride (2.3 mL, 13 mmol, 1.5 equiv) was added. The solution was stirred overnight and allowed to warm to room temperature. The reaction was quenched with a saturated aqueous solution of ammonium chloride and extracted with three portions of ethyl acetate. The combined organic layers were washed with bring, dried over anhydrous magnesium sulfate, and concentrated resulting in a yellow oil (3.1 g, >98% yield). The product was used without further purification and visualized on TLC with UV light and after heat activation with $KMnO_4$.

R_f = 0.69 (7:3 hexanes:ethyl acetate)

^{1}H NMR: (600 MHz, $CDCl_3$): δ 7.79 (d, *J* = 1.9 Hz, 1H), 7.61 (d, *J* = 8.2 Hz, 1H), 7.55 (dd, *J* = 8.2, 1.9 Hz, 1H), 3.90 (s, 3H), 3.84 – 3.79 (m, 2H), 1.00 – 0.92 (m, 2H), -0.00 (s, 9H).

^{13}C NMR (101 MHz, $CDCl_3$): δ 166.42, 153.97, 133.46, 130.66, 124.00, 118.64, 116.67, 93.60, 67.02, 52.48, 18.07, -1.28, -1.30, -1.32, -1.34.

ν_{max}/cm^{-1} (film): 2952, 2924, 1723, 1577, 1289.

HRMS: APCI (*m/z*) calcd for $C_{14}H_{20}O_4BrSi$ [M-H$^+$]: 359.03197, found 359.03276.

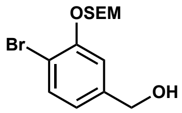

(4-bromo-3-((2-(trimethylsilyl)ethoxy)methoxy)phenyl)methanol (2.22)

A solution of **2.19** (3.1 g, 8.58 mmol, 1 equiv) in anhydrous tetrahydrofuran (0.28M) in a flame dried flask under an argon atmosphere was cooled to 0 ˚C. Lithium aluminum hydride (489 mg, 12.9 mmol, 1.5 equiv) was added in 50 mg portions over 15 minutes. The reaction was stirred for an additional 30 minutes at 0 ˚C then reverse quenched over an iced statured aqueous solution of potassium sodium tartrate. The solution was transferred to a separatory funnel and allowed to separate into two layers. The aqueous layer was extracted with five portions of ethyl acetate. The combined organic layers were washed with bring, dried over anhydrous magnesium sulfate, and concentrated *in vacuo*. The product was purified with silica column chromatography with a gradient of 0-30% ethyl acetate in hexanes and isolated as a yellow oil (2.83 g, >98% yield). Visualization on TLC was performed with UV light and after heat activation with $KMnO_4$.

R$_f$ = 0.59 (3:2 hexanes:ethyl acetate)

^{1}H NMR (500 MHz, $CDCl_3$): δ 7.50 (d, *J* = 8.1 Hz, 1H), 7.17 (d, *J* = 1.9 Hz, 1H), 6.88 (ddd, *J* = 8.1, 1.6, 1.0 Hz, 1H), 5.30 (s, 2H), 4.63 (s, 2H), 3.85 – 3.75 (m, 2H), 1.00 – 0.86 (m, 2H), -0.00 (s, 9H).

^{13}C NMR (126 MHz, $CDCl_3$) δ 154.12, 141.89, 133.43, 121.36, 114.71, 111.87, 93.58, 66.88, 64.82, 18.14, -1.29.

ν_{max}/cm^{-1} (film): 3364, 2951, 1247, 989, 831.

HRMS: APCI (*m/z*) calcd for $C_{13}H_{20}O_3BrSi$ [M-H$^+$]: 331.003706, found 331.03685.

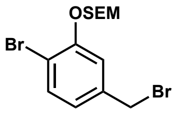

(2-((2-bromo-5-(bromomethyl)phenoxy)methoxy)ethyl)trimethylsilane (2.23)

In a flame dried flask equipped with a Teflon coated metal stir bar were added **2.22** (2.38 g, 7.14 mmol, 1 equiv) and triphenylphosphine (2.80 g, 10.7 mmol, 1.5 equiv) in anhydrous methylene chloride (0.1M) at 0 ˚C under an argon atmosphere. The solution was stirred for 5 minutes followed by slow addition of a suspension of *N*-bromosuccinimide (1.90 g, 10.7 mmol, 1.5 equiv) in anhydrous methylene chloride (0.2M) over 40 minutes. After addition of NBS, the resulting amber solution was stirred for an additional 1 hour at 0 ˚C. The reaction was quenched with water, immediately turning the solution dark purple. The biphasic mixture was transferred to a separatory funnel and allowed to separate. The aqueous layer was extracted with three portions of ethyl acetate.

The combined organic layers were washed with brine, dried over anhydrous sodium sulfate, and concentrated *in vacuo*. The product was purified with silica column chromatography with a gradient of 0-5% ethyl acetate in hexanes and was isolated as a yellow oil (2.7 g, 95% yield). Visualization on TLC was performed with UV light and after heat activation with $KMnO_4$.

R_f = 0.73 (7:3 hexanes:ethyl acetate)

^{1}H NMR (600 MHz, $CDCl_3$) δ 7.50 (d, *J* = 8.1 Hz, 1H), 7.20 (d, *J* = 2.0 Hz, 1H), 6.92 (dd, *J* = 8.1, 2.1 Hz, 1H), 5.31 (s, 2H), 4.42 (s, 2H), 3.86 – 3.78 (m, 2H), 1.03 – 0.88 (m, 2H), 0.01 (s, 9H).

^{13}C NMR (151 MHz, $CDCl_3$) δ 154.23, 138.55, 133.69, 123.57, 116.74, 113.02, 93.70, 66.95, 32.79, 18.14, -1.25, -1.27.

ν_{max}/cm^{-1} (film): 2952, 2896, 1481, 1247, 831.

HRMS: APCI (*m/z*) calcd for $C_{13}H_{19}O_2Br_2Si$ [M-H$^+$]: 392.95156, found 392.95281.

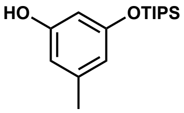

3-methyl-5-((triisopropylsilyl)oxy)phenol (2.25)

The product was prepared following literature procedure and characterization matched the reported spectra.[7]

To a solution of orcinol (1 equiv) in CH2Cl2 (0.2M) was added imidazole (1.5 equiv) and TIPS-Cl (1 equiv). After stirring at room temperature for 12 h, the reaction mixture was washed with a saturated aqueous solution of sodium bicarbonate, dried over anhydrous sodium sulfate, and concentrated *in vacuo*. The residue was purified by column chromatography (silica, hexanes/ethyl acetate gradient elution) to yield a colorless viscous oil (50% yield).

^{1}H NMR (600 MHz, $CDCl_3$): δ 6.29 (d, *J* = 0.7 Hz, 1H), 6.25 – 6.22 (m, 1H), 6.20 (d, *J* = 2.3 Hz, 1H), 2.23 (s, 3H), 1.28 – 1.19 (m, 3H), 1.09 (d, *J* = 7.4 Hz, 12H), 1.06 (d, *J* = 1.1 Hz, 6H).

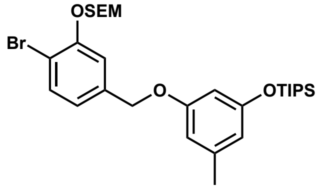

(3-((4-bromo-3-((2-(trimethylsilyl)ethoxy)methoxy)benzyl)oxy)-5 methylphenoxy)triisopropylsilane (2.21)

In a flame dried vial, a solution of **2.22** (1.18 g, 3.20 mmol, 1 equiv) in anhydrous *N,N*-dimethylformamide (0.8M) was cooled to 0 ˚C under an argon atmosphere. Potassium carbonate (530 mg, 3.84 mmol, 1.2 equiv) and **2.25** (900 mg, 3.20 mmol, 1 equiv) were added successively. The vial was sealed and moved to a stir plate inside the fridge at 4 ˚C. The reaction was stirred overnight in the fridge, then quenched with a saturated aqueous solution of ammonium chloride and diluted with ethyl acetate. The aqueous layer was extracted with three portions of ethyl acetate. The combined organic layers were washed with five portions of brine, dried over anhydrous sodium sulfate, and concentrated *in vacuo*. The product was purified was purified with silica column chromatography with a gradient of 0-10% hexanes in ethyl acetate and isolated as a yellow oil (1.64 g, 86% yield). Visualization on TLC was performed with UV light and after heat activation with vanillin—the starting material doesn't stain, while the product stains orange.

R_f = 0.81 (7:3 hexanes:ethyl acetate)

^{1}H NMR (600 MHz, $CDCl_3$): δ 7.52 (d, *J* = 8.1 Hz, 1H), 7.22 (s, 1H), 6.94 (d, *J* = 8.1 Hz, 1H), 6.39 (s, 1H), 6.33 (s, 1H), 6.26 (s, 1H), 5.30 (s, 2H), 4.94 (s, 2H), 3.84 – 3.78 (m, 2H), 2.26 (s, 3H), 1.24 – 1.15 (m, 2H), 1.07 (d, *J* = 7.2 Hz, 18H), 0.99 – 0.90 (m, 3H), 0.00 (s, 9H).

^{13}C NMR (151 MHz, $CDCl_3$): δ 159.36, 157.00, 154.17, 140.08, 138.17, 133.42, 121.84, 115.06, 113.88, 112.09, 108.68, 103.99, 93.65, 69.31, 66.84, 21.82, 18.10, 18.06, 12.75, -1.25, -1.28.

ν_{max}/cm^{-1} (film): 2946, 2894, 2866, 1589, 1162.

HRMS: APCI (*m/z*) calcd for $C_{29}H_{38}O_4BrSi_2$ [M+H$^+$]: 595.2269, found 595.22715.

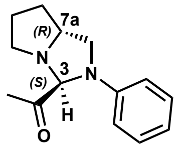

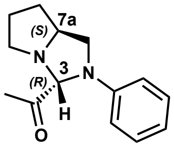

1-((3*S*,7a*R*)-2-phenylhexahydro-1*H*-pyrrolo[1,2-*c*]imidazol-3-yl)ethan-1-one ((+)-2.20) and 1-((3*R*,7a*S*)-2-phenylhexahydro-1*H*-pyrrolo[1,2-*c*]imidazol-3-yl)ethan-1-one ((−)-2.20)

(+)-2.20 was prepared following literature precedent in 5-steps from *N*-Boc-*D*-proline and **(−)-2.20** was prepared following an identical route in 5-steps from *N*-Boc-*L*-proline or 2-steps from (*S*)-(+)-2-(anilinomethyl)pyrrolidine[8, 9].

A solution of methoxycarbonyl aminal (**(*R,S*)-SI 2.1** for the synthesis of **(−)-2.20** and **(*S,R*)-SI 2.1** for the synthesis of **(+)-2.20**) (246 mg, 1.0 mmol, 1 equiv) in anhydrous tetrahydrofuran (0.1M) was added to anhydrous magnesium chloride (106 mg, 1.1 mmol, 1.1 equiv) dried prior to use at 100 ˚C for 1 h under vacuum through a syringe and the mixture was refluxed for 1 h. Then, the reaction mixture was cooled to -78 ˚C, and a diethyl ether solution (3M) of methylmagnesium bromide (660 µL, 2 mmol, 2 equiv) was added dropwise. The reaction was stirred at -78 ˚C for 22 minutes, then quenched with a saturated aqueous solution of ammonium chloride. The solution was warmed to room temperature and extracted with three portions of diethyl ether. The combined organic layers were washed with water and brine, dried over anhydrous sodium sulfate, and concentrated *in vacuo*. The title compound was purified by silica column chromatography with a gradient of 0-10% ethyl acetate in hexanes and isolated as a red oil (200 mg, 86% yield). The product matched reported spectra[9].

$[\alpha]^{20}_{D} = +20.5$ (*c* 1.00, chloroform) (*S,R*)

$[\alpha]^{20}_{D} = -21.4$ (*c* 1.00, chloroform) (*R,S*)

^{1}H NMR (600 MHz, $CDCl_3$) δ 7.22 (dd, *J* = 8.7, 7.3 Hz, 2H), 6.76 (t, *J* = 7.3 Hz, 1H), 6.49 (d, *J* = 7.5 Hz, 2H), 4.39 (s, 1H), 3.94 (qd, *J* = 7.0, 4.7 Hz, 1H), 3.79 (dd, *J* = 8.5, 7.1 Hz, 1H), 3.22 (ddd, *J*

= 10.1, 7.2, 5.1 Hz, 1H), 3.14 (dd, *J* = 8.5, 6.6 Hz, 1H), 2.84 (dt, *J* = 10.1, 7.4 Hz, 1H), 2.13 (s, 3H), 1.94 (dddt, *J* = 10.6, 8.3, 7.2, 5.3 Hz, 1H), 1.90 – 1.82 (m, 1H), 1.73 (dddd, *J* = 12.8, 8.3, 7.1, 4.7 Hz, 1H).

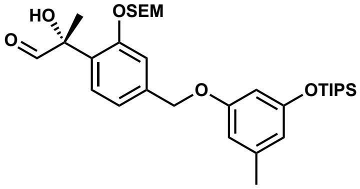

(*R*)-2-hydroxy-2-(4-((3-methyl-5-((triisopropylsilyl)oxy)phenoxy)methyl)-2-((2-(trimethylsilyl)ethoxy)methoxy)phenyl)propanal ((−)-2.24)

In a flame dried flask equipped with Teflon coated metal stir bar were added **2.21** (800 mg, 1.34 mmol, 1.00 equiv) and crushed freshly activated 4Å MS (134 mg) in anhydrous tetrahydrofuran (0.14M) under an argon atmosphere. The solution was cooled to -78˚C in a dry-ice acetone bath. TMEDA (240 µL, 1.67 mmol, 1.25 equiv) followed by 2.4M *n*-BuLi in hexane (700 µL, 1.67 mmol, 1.25 equiv) were added slowly and the resulting solution was stirred for two hours at -78˚C. A solution of (−)-**2.20** (463 mg, 2.01 mmol, 1.5 equiv) in anhydrous tetrahydrofuran (0.5M) was then added to the reaction and stirred at -78˚C for an additional seven hours. The reaction was quenched with saturated aqueous solution of ammonium chloride and extracted with three portions of diethyl ether. The combined organic layers were washed once with water and once with brine, then dried over anhydrous magnesium sulfate and concentrated *in vacuo*. The crude intermediate was transferred to a flask equipped with Teflon coated metal stir bar and dissolved in diethyl ether (0.1M). The solution was cooled to 0˚C in a Styrofoam cooler filled with ice. An aqueous solution of 2% HCl was added dropwise, and the reaction was stirred overnight in the sealed cooler at 0˚C. The reaction was diluted with water and diethyl ether and transferred to a separatory funnel and extracted with three portions of diethyl ether. The combined organic layers were washed with water and brine, then dried over anhydrous magnesium sulfate and concentrated. The product was purified with silica column chromatography using a 0-100% gradient of diethyl ether in hexanes and was isolated as a yellow oil (600 mg, 76% yield) Product was visualized on TLC after heat activation with $KMnO_4$.

Characterization with ^{1}H NMR, LRMS, and OR were completed, but due to the instability of the homobenzylic aldehyde, ^{13}C NMR was not obtained.

Product unstable in chloroform. Obtained proton, OR, and HRMS for characterization.

R_f = 0.44 (7:3 hexanes:ethyl acetate)

^{1}H NMR (600 MHz, Chloroform-d): δ 9.79 (d, J = 0.6 Hz, 1H), 7.51 (d, J = 7.9 Hz, 1H), 7.20 (d, J = 1.5 Hz, 1H), 7.11 (ddd, J = 7.9, 1.6, 0.8 Hz, 1H), 6.39 (ddd, J = 2.2, 1.4, 0.7 Hz, 1H), 6.32 (ddt, J = 2.1, 1.4, 0.7 Hz, 1H), 6.28 (dt, J = 2.8, 1.4 Hz, 1H), 5.27 – 5.21 (m, 2H), 4.03 (s, 2H), 3.76 – 3.66 (m, 2H), 2.25 (s, 3H), 1.67 (s, 3H), 1.25 – 1.16 (m, 3H), 1.07 (d, J = 7.4 Hz, 18H), 0.96 – 0.92 (m, 2H), 0.00 (s, 9H).

ν_{max}/cm^{-1} (film): 2946, 2893, 2866, 1736, 1589.

HRMS: APCI (*m/z*) calcd for $C_{32}H_{53}O_6Si_2$ [M+H$^+$]: 549.33752, found 589.33744.

$[\alpha]_D^{20} = -39$ (*c* 1.00, chloroform)

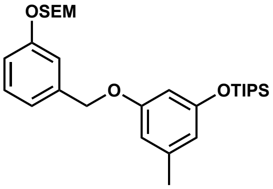

Triisopropyl(3-methyl-5-((3-((2-(trimethylsilyl)ethoxy)methoxy)benzyl)oxy)phenoxy)silane

The compound was characterized by ^{1}H NMR and HRMS.

R_f = 0.83 (7:3 hexanes:ethyl acetate)

^{1}H NMR (600 MHz, Chloroform-d): δ 7.32 – 7.24 (m, 1H), 7.12 – 7.09 (m, 1H), 7.04 (ddd, J = 7.3, 1.5, 0.8 Hz, 1H), 6.99 (ddd, J = 8.1, 2.5, 0.8 Hz, 1H), 6.41 (dq, J = 2.2, 0.7 Hz, 1H), 6.32 (tt, J = 1.3, 0.7 Hz, 1H), 6.30 (t, J = 2.2 Hz, 1H), 5.23 (s, 2H), 4.98 (s, 2H), 3.76 (ddt, J = 8.5, 7.1, 1.5 Hz, 2H), 2.26 (s, 2H), 1.30 – 1.15 (m, 3H), 1.08 (d, J = 7.3 Hz, 18H), 0.96 (ddt, J = 8.5, 7.1, 1.7 Hz, 2H), 0.00 (s, 9H).

HRMS: APCI (*m/z*) calcd for $C_{29}H_{49}O_4Si_2$ [M+H$^+$]: 517.31773, found 517.31664.

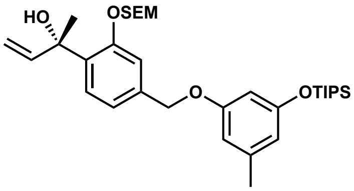

(*S*)-2-(4-((3-methyl-5-((triisopropylsilyl)oxy)phenoxy)methyl)-2-((2-(trimethylsilyl)ethoxy)methoxy)phenyl)but-3-en-2-ol ((−)-2.26)

In a flame dried flask under argon was added methyltriphenylphosphonium bromide (804 mg, 2.25 mmol, 2.5 equiv) in anhydrous tetrahydrofuran (0.1M). The solution was cooled to 0 ˚C, then potassium tert-butoxide (275 mg, 2.47 mmol, 2.75 equiv) was added resulting in an immediate color change from colorless to orange. The ylide was formed over 2 hours at 0 ˚C. A solution of **(−)-2.24** (530 mg, 0.90 mmol, 1 equiv) was then added in anhydrous tetrahydrofuran (0.19M) and the reaction stirred overnight, slowly warming to room temperature. The reaction was quenched with a saturated aqueous solution of ammonium chloride. The layers were allowed to separate and extracted with three portions of ethyl acetate. The combined organic layers were washed with brine, dried over anhydrous sodium sulfate, and concentrated *in vacuo*. The product was purified with silica column chromatography with a gradient of 0-15% ethyl acetate in hexanes and isolated as a yellow oil (370 mg, 70% yield). Visualization on TLC was performed with UV light and after heat activation with vanillin—product stains dark purple.

R_f = 0.81 (7:3 hexanes:ethyl acetate)

^{1}H NMR (600 MHz, $CDCl_3$): δ 7.33 (d, *J* = 8.0 Hz, 1H), 7.22 (d, *J* = 1.7 Hz, 1H), 7.04 (dd, *J* = 7.9, 1.8 Hz, 1H), 6.40 (s, 1H), 6.32 (s, 1H), 6.29 (t, *J* = 2.4 Hz, 1H), 5.78 (dt, *J* = 15.5, 1.4 Hz, 1H), 5.52

(dt, *J* = 15.6, 7.2 Hz, 1H), 4.96 (s, 2H), 3.80 – 3.71 (m, 2H), 2.26 (s, 3H), 1.25 – 1.17 (m, 2H), 1.07 (d, *J* = 7.3 Hz, 12H), 0.87 (dd, *J* = 6.6, 3.5 Hz, 3H), 0.00 (s, 9H).

^{13}C NMR (151 MHz, $CDCl_3$): δ 159.60, 156.99, 155.35, 140.01, 137.94, 137.71, 134.54, 127.03, 126.98, 120.74, 113.85, 113.74, 108.62, 103.97, 93.29, 74.58, 69.60, 66.94, 41.76, 28.53, 28.08, 22.51, 22.47, 21.82, 18.14, 18.07, 12.77, 12.76, -1.26.

ν_{max}/cm^{-1} (film): 2954, 2867, 2155, 2021, 1591.

HRMS: APCI (*m/z*) calcd for $C_{33}H_{55}O_5Si_2$ [M+H$^+$]: 587.35825, found 587.35895.

$[\alpha]^{20}_D = -3.75$ (*c* 0.24, chloroform)

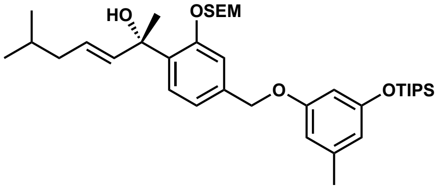

(*S*,*E*)-6-methyl-2-(4-((3-methyl-5-((triisopropylsilyl)oxy)phenoxy)methyl)-2-((2-(trimethylsilyl)ethoxy)methoxy)phenyl)hept-3-en-2-ol ((−)-2.27)

In a flame dried vial under argon combined **(−)-2.26** (160 mg, 0.27 mmol, 1 equiv), 4-methyl-1-pentene (340 µL, 2.7 mmol, 10 equiv), and Grubbs catalyst M204 (23 mg, 0.027 mmol, 10 mol%) in anhydrous methylene chloride. The solution was purged with argon for 10 minutes, then the vial was sealed and heated to 50 ˚C for 48 hours. The reaction was cooled to room temperature and quenched with a saturated aqueous solution of ammonium chloride. The aqueous layer was extracted with three portions of ethyl acetate, which were subsequently washed with brine and filtered over celite. The filtrate was dried over anhydrous sodium sulfate and concentrated *in vacuo* resulting in a brown residue. Purification was performed twice with PTLC using a mobile phase of 7:3 hexanes : ethyl acetate to isolate the desired product as a yellow oil (128 mg, 73% yield). The product was visualized on TLC with UV light and after heat activation with vanillin—the product stains light purple. The title compound was characterized by ^{1}H NMR and telescoped through to the deprotection, which was cleanly purified from remaining terminal alkene.

R$_f$ = 0.83 (7:3 hexanes:ethyl acetate)

^{1}H NMR (600 MHz, cdcl$_3$): δ 7.34 (dt, *J* = 7.8, 3.2 Hz, 1H), 7.24 – 7.21 (m, 1H), 7.07 – 7.01 (m, 1H), 6.41 (d, *J* = 3.4 Hz, 1H), 6.35 – 6.26 (m, 2H), 5.78 (dq, *J* = 15.5, 2.1 Hz, 1H), 5.53 (ddq, *J* = 15.3, 7.6, 3.4 Hz, 1H), 5.28 (s, 2H), 4.97 (s, 2H), 3.83 – 3.70 (m, 2H), 2.26 (s, 3H), 1.94 – 1.88 (m, 2H), 1.67 (s, 3H), 1.28 – 1.16 (m, 5H), 1.08 (dt, *J* = 7.1, 3.2 Hz, 18H), 0.97 (tq, *J* = 8.2, 3.2 Hz, 3H), 0.87 (dq, *J* = 6.5, 3.3 Hz, 6H), 0.01 (s, 9H).

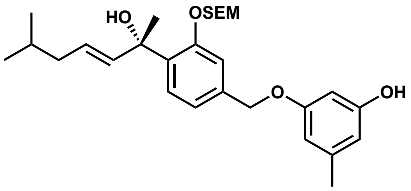

(*S*,*E*)-3-((4-(2-hydroxy-6-methylhept-3-en-2-yl)-3-((2-(trimethylsilyl)ethoxy)methoxy)benzyl)oxy)-5-methylphenol ((−)-2.28)

To a flame dried vial under argon was added **(−)-2.27** (75 mg, 0.11 mmol, 1 equiv) in anhydrous tetrahydrofuran (0.2M). The solution was cooled to 0 ˚C and tetrabutylammonium fluoride (1M in THF, 130 µL, 0.13 mmol, 1.1 equiv) was added. After 1 hour, the reaction was quenched with aqueous saturated ammonium chloride and extracted with three portions of ethyl acetate. The combined organic layers were washed with brine, dried over anhydrous sodium sulfate, and concentrated *in vacuo*. The product was purified with silica column chromatography with a gradient of 0-20% ethyl acetate in hexanes and isolated as an amorphous low melting point white powder (53 mg, >98% yield). Visualization on TLC was performed with UV light and after heat activation with vanillin—the product stains plum.

R$_f$ = 0.43 (7 : 3 hexanes : ethyl acetate)

^{1}H NMR (600 MHz, Chloroform-d): δ 7.35 (d, J = 7.9 Hz, 1H), 7.21 (s, 1H), 7.02 (d, J = 7.9 Hz, 1H), 6.36 (s, 1H), 6.25 (d, J = 16.7 Hz, 2H), 5.80 – 5.76 (m, 1H), 5.56 – 5.49 (m, 1H), 5.29 (s, 2H), 4.87 – 4.74 (m, 2H), 4.37 (s, 1H), 3.82 – 3.70 (m, 2H), 2.25 (s, 3H), 1.91 (t, J = 7.0 Hz, 2H), 1.68 (s, 3H), 1.63 – 1.56 (m, 1H), 1.00 – 0.94 (m, 2H), 0.89 – 0.84 (m, 6H), -0.01 (d, J = 1.1 Hz, 9H).

^{13}C NMR: (126 MHz, $CDCl_3$): δ 155.36, 144.95, 141.07, 140.71, 137.91, 137.62, 127.19, 127.08, 120.96, 114.12, 109.06, 108.44, 99.34, 93.33, 77.41, 77.16, 76.91, 74.80, 69.65, 67.04, 41.76, 28.54, 28.05, 22.50, 22.47, 21.72, 18.21, -1.27.

ν_{max}/cm^{-1} (film): 3321.80, 2953.19, 2924.35, 2898.3, 2868.89, 1594.93, 1248.77, 1148.00

HRMS: APCI (*m/z*) calcd for $C_{28}H_{41}O_6Si$ [M-H$^+$]: 486.28015, found 485.27147.

$[\alpha]^{20}_D = -0.4$ (*c* 0.14, chloroform)

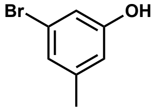

3-bromo-5-methylphenol (2.31)

The title compound was prepared following a procedure adapted from Zhao and coworkers in two steps from 3,5-dibromotoluene. In a flame dried flask equipped with Teflon coated metal stir bar was added 3,5-dibromotoluene (1.08 g, 4.34 mmol, 1 equiv) in anhydrous tetrahydrofuran (0.2M) under an argon atmosphere. The solution was cooled to -78 ˚C and *t*-BuLi (1.6M in hexanes, 3 mL, 4.8 mmol, 1.1 equiv) was slowly added. The reaction was stirred for 1 hour at -78 ˚C then triisopropyl borate (1.2 mL, 5.2 mmol, 1.2 equiv) was added. The solution was stirred for an additional 3 hours at -78 ˚C. An aqueous solution of ammonium chloride was added at -78 ˚C to quench the reaction, then the dry ice-acetone bath was removed and the solution was allowed to warm to room temperature, stirring overnight. The solution was transferred to a separatory funnel and the aqueous layer was extracted with three portions of ethyl acetate. The combined organic layers were washed with brine, dried over anhydrous sodium sulfate, and concentrated *in vacuo*. The boronic acid was carried through crude to the next step without characterization. Hydrolysis of the boronic acid was performed by transferring the crude boronic acid **2.30** (884 mg, 4.11 mmol, 1 equiv) to a round bottom flask open to air. Aqueous 0.5M NaOH (16.4 mL, 8.22 mmol, 2 equiv) and hydrogen peroxide (30% w/w) (2 mL, 20.6 mmol, 5 equiv) were then added sequentially. The reaction was stirred for 1 hour, then brough to a pH = 7 with aqueous 1N HCl. The aqueous solution was extracted with three portions of ethyl acetate and the combined organic layers were washed with brine, dried over anhydrous sodium sulfate, and concentrated *in vacuo*. The product was purified with silica column chromatography with a gradient of 0-50% ethyl acetate in hexanes and isolated as an amorphous red powder (580 mg, 76% yield over two steps). Visualization on TLC was performed with UV light and after heat activation with $KMnO_4$. The product matched reported spectra[10].

^{1}H NMR: (500 MHz, $CDCl_3$) δ 6.91 (dq, *J* = 1.5, 0.7 Hz, 1H), 6.82 (tt, *J* = 1.7, 0.6 Hz, 1H), 6.58 (ddt, *J* = 2.2, 1.4, 0.7 Hz, 1H), 2.28 (q, *J* = 0.6 Hz, 3H).

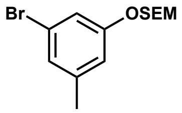

(2-((3-bromo-5-methylphenoxy)methoxy)ethyl)trimethylsilane (2.32)

To a suspension of NaH (60% dispersion in mineral oil, 186 mg, 4.65 mmol, 1.5 equiv) in anhydrous tetrahydrofuran (0.8M) at 0˚C was added a solution of **2.31** (580 mg, 3.10 mmol, 1 equiv) in anhydrous THF (1.3M). The reaction immediately turned blue and was stirred under an argon atmosphere. The solution was allowed to war to room temperature, turning brown. After one hour, the reaction was cooled to 0˚C and 2-(trimethylsilyl)ethoxymethyl chloride (820 µL, 4.65 mmol, 1.5 equiv) was added. The solution was stirred overnight and allowed to warm to room temperature. The reaction was quenched with a saturated aqueous solution of ammonium chloride and extracted with three portions of diethyl ether. The combined organic layers were washed with bring, dried over anhydrous sodium sulfate, and concentrated resulting in a yellow oil (979 mg, >98% yield). The product was used without further purification and visualized on TLC with UV light and after heat activation with $KMnO_4$.

R_f = 0.80 (7:3 hexanes:ethyl acetate)

^{1}H NMR (500 MHz, Chloroform-d) δ 7.02 (td, J = 2.2, 0.6 Hz, 1H), 6.96 (tt, J = 1.5, 0.7 Hz, 1H), 6.78 (ddt, J = 2.2, 1.5, 0.7 Hz, 1H), 5.18 (d, J = 0.6 Hz, 2H), 3.76 – 3.71 (m, 2H), 2.29 (t, J = 0.7 Hz, 2H), 0.99 – 0.93 (m, 2H), 0.00 (d, J = 0.6 Hz, 9H).

^{13}C NMR: (126 MHz, $CDCl_3$) δ 158.20, 141.16, 125.64, 122.47, 116.76, 115.95, 93.04, 66.53, 21.41, 18.18, -1.28.

ν_{max}/cm^{-1} (film): 2952.59, 2922.79, 2898.26, 1248.27, 1089.19, 1017.17, 856.30

HRMS: APCI (*m/z*) calcd for $C_{13}H_{20}BrO_2Si$ [M-H$^+$]: 316.04942, found 315.04155.

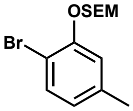

(2-((2-bromo-5-methylphenoxy)methoxy)ethyl)trimethylsilane (2.58)

To a suspension of NaH (60% dispersion in mineral oil, 513 mg, 12.8 mmol, 1.2 equiv) in anhydrous tetrahydrofuran (0.8M) at 0˚C was added a solution of 2-bromo-5-methylphenol (2.00 g, 10.7 mmol, 1 equiv) in anhydrous THF (1.3M). The reaction was stirred under an argon atmosphere and allowed to war to room temperature. After one hour, the reaction wa cooled to 0˚C and 2-(trimethylsilyl)ethoxymethyl chloride (2.27 mL, 12.8 mmol, 1.2 equiv) was added. The solution was stirred overnight and allowed to warm to room temperature. The reaction was quenched with a saturated aqueous solution of ammonium chloride and extracted with three portions of ethyl acetate. The combined organic layers were washed with bring, dried over anhydrous magnesium sulfate, and concentrated resulting in a yellow oil (3.38 g, >98% yield). The product was used without further purification and visualized on TLC with UV light and after heat activation with $KMnO_4$. This compound will not be published and was not characterized by HRMS.

R_f = 0.73 (4:1 hexanes:ethyl acetate)

^{1}H NMR (600 MHz, $CDCl_3$): δ 7.39 (d, *J* = 8.0 Hz, 1H), 6.99 (s, 1H), 6.70 (d, *J* = 8.1 Hz, 1H), 3.82 (m, 2H), 2.30 (s, 3H), 0.97 (m, 2H), 0.07 – 0.02 (m, 2H), 0.01 (s, 9H).

^{13}C NMR: (151 MHz, $CDCl_3$): δ 153.78, 138.81, 132.94, 123.89, 117.21, 109.53, 93.59, 66.72, 21.42, 18.14, -1.29.

ν_{max}/cm^{-1} (film): 2952, 2922, 1582, 1483, 832.

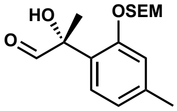

(*R*)-2-hydroxy-2-(4-methyl-2-((2-(trimethylsilyl)ethoxy)methoxy)phenyl)propanal ((−)-2.59)

In a flame dried flask equipped with Teflon coated metal stir bar were added **2.58** (317 mg, 1.00 mmol, 1.00 equiv) and crushed freshly activated 4Å MS (100 mg) in anhydrous tetrahydrofuran (0.14M) under an argon atmosphere. The solution was cooled to -78˚C in a dry-ice acetone bath. TMEDA (190 µL, 1.25 mmol, 1.25 equiv) followed by 2M *n*-BuLi in hexane (600 µL, 1.25 mmol, 1.25 equiv) were added slowly and the resulting solution was stirred for two hours at -78˚C. A solution of **(−)-2.20** (345 mg, 1.50 mmol, 1.5 equiv) in anhydrous tetrahydrofuran (0.5M) was then added to the reaction and stirred at -78˚C for an additional seven hours. The reaction was quenched with saturated aqueous solution of ammonium chloride and extracted with three portions of diethyl ether. The combined organic layers were washed once with water and once with brine, then dried over anhydrous magnesium sulfate and concentrated *in vacuo*. The crude intermediate was transferred to a flask equipped with Teflon coated metal stir bar and dissolved in diethyl ether (0.1M). The solution was cooled to 0˚C in a Styrofoam cooler filled with ice. An aqueous solution of 2% HCl was added dropwise, and the reaction was stirred overnight in the sealed cooler at 0˚C.

The reaction was diluted with water and diethyl ether and transferred to a separatory funnel and extracted with three portions of diethyl ether. The combined organic layers were washed with water and brine, then dried over anhydrous magnesium sulfate and concentrated. The product was purified with silica column chromatography using a 0-20% gradient of diethyl ether in hexanes and was isolated as a yellow oil (152 mg, 49% yield) Product was visualized on TLC after heat activation with $KMnO_4$. This compound will not be published and was not characterized by HRMS. Characterization with ^{1}H NMR and OR were completed, but due to the instability of the homobenzylic aldehyde, ^{13}C NMR was not obtained.

R$_f$ = 0.69 (4:1 hexanes:ethyl acetate)

^{1}H NMR (600 MHz, cdcl$_3$): δ 9.76 (s, 1H), 7.36 (d, *J* = 7.9 Hz, 1H), 6.97 (d, *J* = 0.8 Hz, 1H), 6.87 (ddd, *J* = 7.9, 1.6, 0.8 Hz, 1H), 5.24 (d, *J* = 7.0 Hz, 1H), 5.20 (d, *J* = 7.0 Hz, 1H), 3.81 – 3.59 (m, 2H), 2.34 (s, 3H), 1.65 (s, 3H), 1.00 – 0.93 (m, 2H), 0.00 (s, 9H).

$[\alpha]^{20}_D = -15.3$ (*c* 1.00, chloroform)

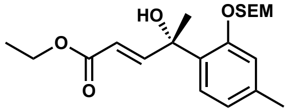

Ethyl (*S*,*E*)-4-hydroxy-4-(4-methyl-2-((2-(trimethylsilyl)ethoxy)methoxy)phenyl)pent-2-enoate ((−)-2.60)

To a flame dried flask equipped with Teflon coated metal stir bar under an argon atmosphere were added 95% triethyl phosphonoacetate (224 mg, 1.00 mmol, 2.6 equiv) in anhydrous tetrahydrofuran (0.4M). The solution was cooled to 0˚C. Sodium hydride (60% dispersion in mineral oil, 40 mg, 1 mmol, 2.6 equiv) was added and the reaction was stirred for 15 minutes. A solution of aldehyde **(−)-2.59** in anhydrous THF (0.3M) was slowly added to the reaction. The ice bath was removed, and the reaction was stirred at room temperature for one hour. The reaction was quenched with an aqueous solution of ammonium chloride and extracted with three portions of ethyl acetate. The combined organic layers were washed with brine, dried over anhydrous magnesium sulfate, and concentrated *in vacuo*. The product was purified with silica column chromatography with a gradient of 0-20% ethyl acetate in hexanes and was isolated as a yellow oil (134 mg, 90% yield). Product was visualized on TLC with UV light and after heat activation with vanillin. This compound will not be published and was not characterized by HRMS.

R_f = 0.42 (4:1 hexanes:ethyl acetate).

^{1}H NMR (600 MHz, $CDCl_3$): δ 7.22 (d, *J* = 7.9 Hz, 1H), 7.20 (d, *J* = 15.6 Hz, 1H), 7.01 (d, *J* = 0.9 Hz, 1H), 6.84 (ddd, *J* = 7.9, 1.7, 0.8 Hz, 1H), 5.96 (d, *J* = 15.6 Hz, 1H), 5.29 (d, *J* = 7.0 Hz, 1H), 5.25 (d, *J* = 7.0 Hz, 1H), 4.18 (q, *J* = 7.1 Hz, 2H), 3.82 – 3.64 (m, 2H), 2.35 (s, 3H), 1.72 (s, 3H), 1.29 (t, *J* = 7.1 Hz, 3H), 0.97 (ddd, *J* = 8.9, 7.0, 1.5 Hz, 2H), 0.02 (s, 9H).

^{13}C NMR (151 MHz, $CDCl_3$): δ 167.06, 155.01, 154.59, 139.50, 129.56, 126.35, 122.73, 118.03, 115.71, 93.13, 74.19, 67.01, 60.47, 27.04, 21.42, 18.13, 14.39, -1.30.

ν_{max}/cm^{-1} (film): 2956, 2924, 1717, 1248, 837.

$[\alpha]^{20}_{D} = -2.04$ (*c* 0.23, chloroform)

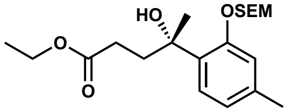

Ethyl(*S*)-4-hydroxy-4-(4-methyl-2-((2-(trimethylsilyl)ethoxy)methoxy)phenyl)pentanoate ((−)-2.61)

In a vial open to air combined **(−)-2.60** (120 mg, 0.315 mmol, 1 equiv) and Lindlar catalyst (4 mg, 9 µmol, 3 mol%) in ethyl acetate (0.25M). The reaction was flushed with argon then purged five times with hydrogen. The reaction was stirred for two hours at room temperature then filtered over celite and concentrated. The product was isolated as a yellow oil (118 mg, 98% yield) and used without further purification. Product was visualized on TLC with UV light and after heat activation with vanillin. This compound will not be published and was not characterized by HRMS.

R$_f$ = 0.43 (7:3, hexanes:ethyl acetate)

^{1}H NMR (600 MHz, CDCl$_3$): δ 7.23 (d, *J* = 7.9 Hz, 1H), 6.97 (s, 0H), 6.79 (ddd, *J* = 7.9, 1.7, 0.8 Hz, 1H), 5.29 (d, *J* = 1.0 Hz, 2H), 4.06 (q, *J* = 7.1 Hz, 2H), 3.80 – 3.74 (m, 3H), 2.64 – 2.56 (m, 1H), 2.52 – 2.41 (m, 1H), 2.40 – 2.33 (m, 1H), 2.13 (ddd, *J* = 13.4, 9.0, 6.4 Hz, 1H), 1.21 (t, *J* = 7.1 Hz, 3H), 1.00 – 0.95 (m, 2H), 0.00 (s, 9H).

^{13}C NMR (151 MHz, CDCl$_3$): δ 174.58, 154.63, 138.48, 131.44, 126.81, 122.45, 115.37, 92.93, 74.36, 66.84, 60.47, 36.76, 30.09, 28.05, 21.32, 18.13, 14.32, -1.30.

ν$_{max}$/cm^{-1} (film): 3512, 2953, 1780, 1733, 1247.

LRMS: ESI (*m/z*) calcd for $C_{20}H_{35}O_5Si$ [M+H$^+$]: 381.2019, found 381.202.

$[\alpha]^{20}_D = -14.7$ (*c* 1.00, chloroform)

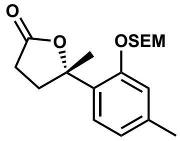

(*S*)-5-methyl-5-(4-methyl-2-((2-(trimethylsilyl)ethoxy)methoxy)phenyl)dihydrofuran-2(3*H*)-one ((−)-2.62)

In a flame dried flask equipped with Teflon coated metal stir bar were added **(−)-2.61** (30 mg, 0.078 mmol, 1 equiv) and LiOH (5.6 mg, 0.24 mmol, 3 equiv) in anhydrous tetrahydrofuran (3mM). The reaction was stirred overnight under an argon atmosphere. The reaction was filtered over cotton, rinsing with ethyl acetate and concentrated. The product was purified with silica column chromatography with a gradient of 0-20% ethyl acetate in hexanes and isolated as a yellow oil (22 mg, 83% yield). The product was visualized on TLC with UV light and after heat activation with vanillin. This compound will not be published and was not characterized by HRMS.

R$_f$ = 0.59 (7:3, hexanes:ethyl acetate)

^{1}H NMR (500 MHz, CDCl$_3$): δ 7.34 (d, *J* = 7.9 Hz, 1H), 6.98 (d, *J* = 0.7 Hz, 1H), 6.80 (ddd, *J* = 7.9, 1.6, 0.8 Hz, 1H), 3.75 (dd, *J* = 9.1, 7.5 Hz, 2H), 2.65 – 2.55 (m, 2H), 2.52 – 2.39 (m, 2H), 2.33 (s, 3H), 1.75 (s, 3H), 1.00 – 0.95 (m, 2H), 0.08 – 0.00 (m, 2H), 0.00 (s, 9H).

^{13}C NMR (101 MHz, CDCl$_3$): δ 177.14, 153.17, 139.30, 129.47, 125.43, 122.13, 115.10, 92.50, 86.96, 66.67, 34.71, 29.08, 27.16, 21.43, 18.08, -1.30.

ν_{max}/cm^{-1} (film): 2952, 17778, 1246, 1061, 836.

LRMS: ESI (*m/z*) calcd for $C_{18}H_{29}O_4Si$ [M+H$^+$]: 337.1757, found 337.176.

$[\alpha]^{20}_D = -1.6$ (*c* 1.00, chloroform)

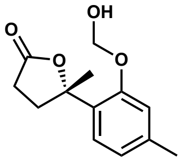

(*S*)-5-(2-(hydroxymethoxy)-4-methylphenyl)-5-methyldihydrofuran-2(3*H*)-one ((−)-2.63)

In a flame dried vial under an argon atmosphere were added **2.X** (6.7 mg, 0.02 mmol, 1 equiv), DBU (320 µL, 2.5 mmol, 125 equiv), and TBAF (1M in THF, 320 µL, 0.32 mmol, 16 equiv). Prior to the reaction, DBU was dried over 4Å MS for 24 hours. The solution was heated to 80 ˚C for 1.5 hours. The reaction was cooled to room temperature and quenched with a saturated aqueous solution of ammonium chloride. The layers were allowed to separate and extracted with three portions of diethyl ether. The combined organic layers were washed twice with water, twice with brine, dried over anhydrous magnesium sulfate, and concentrated *in vacuo*. Crude ^{1}H NMR analysis indicated formation of the title compound. This compound will not be published and was not characterized by HRMS.

R$_f$ = 0.41 (19:1 methylene chloride:methanol)

^{1}H NMR (500 MHz, cdcl$_3$): δ 6.96 (d, *J* = 7.7 Hz, 1H), 6.76 (dt, *J* = 1.6, 0.6 Hz, 1H), 6.70 (ddd, *J* = 7.7, 1.7, 0.7 Hz, 1H), 5.34 (q, *J* = 1.4 Hz, 1H), 5.17 (q, *J* = 1.0 Hz, 1H), 3.27 – 3.22 (m, 1H), 2.93 (s, 3H), 2.72 – 2.66 (m, 1H), 2.56 (ddd, *J* = 7.5, 6.8, 0.7 Hz, 2H), 2.30 (s, 3H).

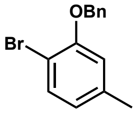

2-(benzyloxy)-1-bromo-4-methylbenzene (2.64)

In a flame dried flask under an argon atmosphere were added 2-bromo-5-methylphenol (1 g, 5.34 mmol, 1 equiv) in anhydrous *N,N*-dimethylformamide (0.8M). The solution was cooled to 0 ˚C, then potassium carbonate (812 mg, 5.88 mmol, 1.1 equiv) and benzyl bromide (700 µL, 5.88 mmol, 1.1 equiv) were added in that order. The reaction was stirred overnight and allowed to warm to room temperature. The suspension was filtered and the filtrate quenched with aqueous 1N HCl. The aqueous phase was extracted with three portions of diethylether and the combined organic layers were washed with water, with five portions of brine, dried over anhydrous magnesium sulfate, and concentrated *in vacuo*. The title compound was obtained as a yellow oil (1.48 g, >98% yield) without further purification. The product matched published spectra[11].

^{1}H NMR (600 MHz, $CDCl_3$): δ 7.53 – 7.47 (m, 2H), 7.45 – 7.37 (m, 3H), 7.36 – 7.30 (m, 1H), 6.78 (s, 1H), 6.68 (d, *J* = 8.0 Hz, 1H), 5.14 (s, 2H), 2.30 (s, 3H).

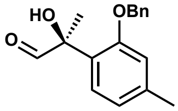

(*S*)-2-(2-(benzyloxy)-4-methylphenyl)-2-hydroxypropanal ((+)-2.65)

In a flame dried flask equipped with Teflon coated metal stir bar were added **2.64** (223 mg, 0.80 mmol, 1.00 equiv) and crushed freshly activated 4Å MS (80 mg) in anhydrous tetrahydrofuran (0.14M) under an argon atmosphere. The solution was cooled to -78˚C in a dry-ice acetone bath. TMEDA (150 µL, 1.0 mmol, 1.25 equiv) followed by 2.5 M *n*-BuLi in hexane (400 µL, 1.0 mmol, 1.25 equiv) were added slowly and the resulting solution was stirred for two hours at -78˚C. A solution of **(+)-2.20** (278 mg, 1.21 mmol, 1.5 equiv) in anhydrous tetrahydrofuran (0.5M) was then added to the reaction and stirred at -78˚C for an additional seven hours. The reaction was quenched with saturated aqueous solution of ammonium chloride and extracted with three portions of diethyl ether. The combined organic layers were washed once with water and once with brine, then dried over anhydrous magnesium sulfate and concentrated *in vacuo*. The crude intermediate was transferred to a flask equipped with Teflon coated metal stir bar and dissolved in diethyl ether (0.1M). The solution was cooled to 0˚C in a Styrofoam cooler filled with ice. An aqueous solution of 2% HCl was added dropwise, and the reaction was stirred overnight in the sealed cooler at 0˚C. The reaction was diluted with water and diethyl ether and transferred to a separatory funnel and extracted with three portions of diethyl ether. The combined organic layers were washed with water and brine, then dried over anhydrous magnesium sulfate and concentrated. The product was purified with silica column chromatography using a 0-20% gradient of diethyl ether in hexanes and was isolated as a yellow oil (131 mg, 61% yield) Product was visualized on TLC after heat activation with $KMnO_4$. The benzyl protected substate proved to be more stable than SEM, thus ^{13}C NMR was obtained for the title compound.

R_f = 0.63 (7:3 hexanes:ethyl acetate)

^{1}H NMR (400 MHz, $CDCl_3$): δ 9.78 (s, 1H), 7.47 – 7.32 (m, 6H), 6.85 (ddd, *J* = 7.8, 1.6, 0.8 Hz, 1H), 6.80 (s, 1H), 5.07 (d, *J* = 2.8 Hz, 2H), 2.35 (s, 3H), 1.64 (s, 3H).

^{13}C NMR (151 MHz, $CDCl_3$): δ 202.19, 155.53, 140.35, 136.09, 128.96, 128.53, 127.87, 127.39, 126.48, 122.34, 113.24, 78.39, 70.80, 21.74, 21.62.

ν_{max}/cm^{-1} (film): 2922, 2091, 1731, 1502, 1286.

HRMS: APCI (*m/z*) calcd for $C_{17}H_{17}O_3$ [M-H$^+$]: 269.11832, found 269.11825.

$[\alpha]^{20}_D$ = +62.2 (*c* 1.00, chloroform)

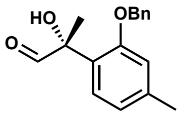

(*R*)-2-(2-(benzyloxy)-4-methylphenyl)-2-hydroxypropanal ((−)-2.65)

The title compound was prepared following the procedure for the synthesis of **(−)-2.65** using **(−)-2.20**. Obtained as a yellow oil (40 mg, 58% yield).

$[\alpha]^{20}_{D} = -60.3$ (*c* 1.00, chloroform)

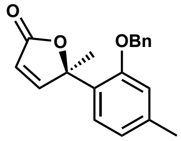

***(R*)-5-(2-(benzyloxy)-4-methylphenyl)-5-methylfuran-2(5*H*)-one ((+)-2.66)**

In a flame dried vial were added DCC (36 mg, 0.176 mmol, 2 equiv) and 2-(diethoxyphosphoryl)acetic acid (25 µL, 0.176 mmol, 2 equiv) to a stirring solution of **(+)-2.65** (24 mg, 0.088 mmol, 1 equiv) in anhydrous methylene chloride (0.1M) under an argon atmosphere. The vial was sealed and heated to reflux for 30 minutes. The reaction was cooled to room temperature and filtered over celite. The filtrate was concentrated *in vacuo*. The resulting residue was transferred with 0.5 mL anhydrous tetrahydrofuran to a stirring suspension of NaH (60% disperion in mineral oil, 7 mg, 0.176 mmol, 2 equiv) in anhydrous tetrahydrofuran (0.18M) at 0 ˚C. The reaction was stirred for 15 minutes at 0 ˚C, then the ice bath was removed and stirring was continued for 90 minutes. The solution was quenched with water and extracted with three portions of ethyl acetate. The combined organic layers were washed with brine, dried over anhydrous sodium sulfate, and concentrated *in vacuo*. The crude residue was purified by silica column chromatography with an eluent of 0-20% ethyl acetate in hexanes. The title compound was obtained as an off-white amorphous powder (22 mg, 85% yield) and visualized on TLC with UV light and after heat activation with $KMnO_4$.

R_f = 0.52 (7:3 hexanes:ethyl acetate)

^{1}H NMR (600 MHz, $CDCl_3$): δ 8.02 (d, *J* = 5.6 Hz, 1H), 7.47 (d, *J* = 8.3 Hz, 1H), 7.45 – 7.34 (m, 5H), 6.81 (d, *J* = 5.7 Hz, 2H), 5.87 (d, *J* = 5.6 Hz, 1H), 5.11 (q, 2H), 2.34 (s, 3H), 1.79 (s, 3H).

^{13}C NMR (151 MHz, $CDCl_3$): δ 172.57, 160.49, 154.55, 139.87, 136.47, 129.01, 128.53, 127.83, 125.85, 125.81, 122.23, 118.55, 112.97, 89.07, 70.58, 25.51, 21.55.

ν_{max}/cm^{-1} (film): 2923, 2037, 1763, 1257, 1104.

HRMS: APCI (*m/z*) calcd for $C_{19}H_{19}O_3$ [M+H$^+$]: 295.13287, found 295.1332.

$[\alpha]^{20}_D = +232$ (*c* 1.00, chloroform)

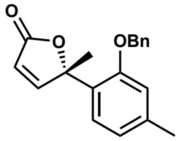

***(S)*-5-(2-(benzyloxy)-4-methylphenyl)-5-methylfuran-2(5*H*)-one ((−)-2.66)**

The title compound was prepared following the procedure for the synthesis of **(+)-2.66**. Obtained as an amorphous off-white powder (8.9 mg, 84% yield).

$[\alpha]^{20}_D = -142$ (*c* 0.5, chloroform)

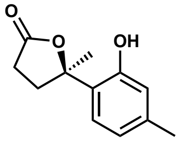

(*R*)-5-(2-hydroxy-4-methylphenyl)-5-methyldihydrofuran-2(3*H*)-one ((+)-2.2)

To a vial equipped with Teflon coated metal stir bar were added **(+)-2.66** (10 mg, 0.03 mmol, 1 equiv) and Lindlar catalyst (5 mg, 0.012 mmol, 40 mol%) to a 1 mL 1:1 solution of ethyl acetate:ethanol. The reaction was purged with argon, then purged 5 times with hydrogen and stirred at room temperature under a hydrogen atmosphere for 3 hours. The hydrogen balloon was removed and the reaction was filtered over celite and concentrated *in vacuo*. The title compound was purified on silica column chromatography using an eluent of 0-50% diethyl ether in hexanes and isolated as an off-white amorphous powder (4.95 mg, 80% yield). Visualization on TLC was performed with UV light and after heat activation with $KMnO_4$.

R$_f$ = 0.34 (1:1 hexanes:diethyl ether)

^{1}H NMR (600 MHz, CDCl$_3$): δ 7.09 (d, *J* = 7.9 Hz, 1H), 6.73 (ddd, *J* = 7.9, 1.7, 0.8 Hz, 1H), 6.68 (d, *J* = 1.0 Hz, 1H), 6.03 (s, 1H), 2.76 – 2.64 (m, 2H), 2.58 – 2.51 (m, 1H), 2.46 (ddd, *J* = 12.0, 8.7, 6.3 Hz, 1H), 2.29 (d, *J* = 0.7 Hz, 3H), 1.74 (s, 3H).

^{13}C NMR (151 MHz, CDCl$_3$): δ 175.96, 152.80, 139.77, 126.15, 125.34, 121.48, 118.14, 87.99, 34.50, 28.66, 27.75, 21.02.

ν$_{max}$/cm^{-1} (film): 3257, 2916, 2186, 1586, 1097.

HRMS: APCI (*m/z*) calcd for $C_{12}H_{15}O_3$ [M+H$^+$]: 207.10157, found 207.10169.

$[\alpha]^{20}_D$ = +27.0 (*c* 0.50, chloroform)

$[\alpha]^{20}_D$ = +25.8 (*c* 0.49, chloroform, lit)[12]

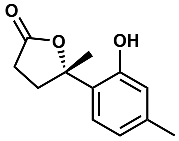

(*S*)-5-(2-hydroxy-4-methylphenyl)-5-methyldihydrofuran-2(3*H*)-one ((−)-2.1)

The title compound was prepared following the procedure for the synthesis of **(+)-2.1**. Obtained as an off-white amorphous powder (5.03 mg, 80% yield)

$[\alpha]^{20}_D$ = −26.1 (*c* 0.50, chloroform)

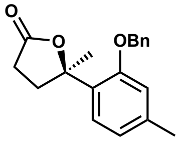

(*R*)-5-(2-(benzyloxy)-4-methylphenyl)-5-methyldihydrofuran-2(3*H*)-one ((+)-2.67)

Isolated as an amorphous off-white powder (1.6 mg, 18% yield).

R$_f$ = 0.71 (1:1 hexanes:diethyl ether)

^{1}H NMR (600 MHz, $CDCl_3$): δ 7.42 (d, *J* = 4.4 Hz, 3H), 7.40 – 7.35 (m, 2H), 6.82 (s, 1H), 6.80 (d, *J* = 8.7 Hz, 1H), 5.09 (s, 2H), 2.66 – 2.49 (m, 2H), 2.46 – 2.36 (m, 2H), 2.41 – 2.19 (m, 3H), 1.74 (s, 3H).

^{13}C NMR (151 MHz, $CDCl_3$): δ 177.13, 154.55, 139.24, 136.75, 129.56, 128.85, 128.30, 127.68, 125.57, 121.56, 113.18, 87.01, 70.34, 34.65, 29.04, 27.20, 21.50.

ν_{max}/cm^{-1} (film): 2927, 1774, 1290, 1243, 1065.

HRMS: APCI (*m/z*) calcd for $C_{19}H_{21}O_3$ [M+H$^+$]: 297.14852, found 297.14894.

$[\alpha]^{20}_D$ = +19.8 (*c* 0.25, chloroform)

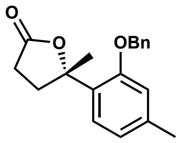

(*S*)-5-(2-(benzyloxy)-4-methylphenyl)-5-methyldihydrofuran-2(3*H*)-one ((−)-2.67)

Isolated as an amorphous white powder (1.5 mg, 17% yield).

$[\alpha]^{20}_D$ = −20.4 (*c* 0.25, chloroform)

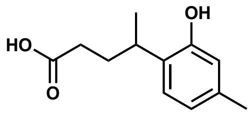

4-(2-hydroxy-4-methylphenyl)pentanoic acid (2.68)

The title compound was isolated as an amorphous off-white powder.

^{1}H NMR (400 MHz, $CDCl_3$): δ 7.03 (d, *J* = 7.7 Hz, 1H), 6.72 (dd, *J* = 7.8, 1.8 Hz, 1H), 6.64 (d, *J* = 1.0 Hz, 1H), 3.08 (h, *J* = 6.9 Hz, 1H), 2.42 – 2.30 (m, 2H), 2.27 (s, 3H), 1.91 (dq, *J* = 14.4, 7.2 Hz, 1H), 1.78 (dq, *J* = 13.8, 6.8 Hz, 1H), 1.27 (d, *J* = 7.0 Hz, 3H).

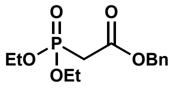

benzyl 2-(diethoxyphosphoryl)acetate

This is a known compound and was prepared according to literature procedure. The spectra matched published data[13].

Triethylphosphonoacetic acid (1 equiv) was dissolved in methanol (0.5M) and cesium carbonate (0.5 equiv) was added. The mixture was stirred for 2 hours under an argon atmosphere. The mixture was concentrated and dissolved in DMF (0.5M) and cooled to 0 ˚C. Benzyl bromide (1.2 equiv) was added and the mixture was warmed to room temperature and stirred overnight. The reaction was diluted with ethyl acetate and washed with water and brine. The organic layer was dried over anhydrous magnesium sulfate and concentrated *in vacuo.* The title compound was purified by silica column chromatograph (50-66% ethyl acetate in hexnes) and isolated as a colorless oil (75%).

^{1}H NMR (600 MHz, cdcl$_3$): δ 7.40 – 7.28 (m, 5H), 5.17 (d, *J* = 6.9 Hz, 2H), 4.17 – 4.07 (m, 4H), 3.00 (dd, *J* = 21.5, 6.5 Hz, 2H), 1.33 – 1.21 (m, 6H).

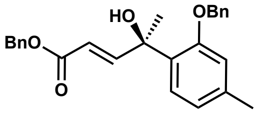

benzyl (*R*,*E*)-4-(2-(benzyloxy)-4-methylphenyl)-4-hydroxypent-2-enoate ((+)-2.69)

To a flame dried vial under an argon atmosphere was benzyl 2-(diethoxyphosphoryl)acetate added (43 mg, 150 µmol, 2 equiv) to a suspension of NaH (60% dispersion in mineral oil, 6 mg, 150 µL, 2 equiv) in anhydrous tetrahydrofuran (0.1M) at 0 ˚C. The solution was stirred for 30 minutes at 0 ˚C, then (+)-**2.65** (20 mg, 74 µmol, 1 equiv) was added in 0.5 mL anhydrous tetrahydrofuran. The reaction was warmed to room temperature and monitored by TLC. After 30 minutes, the reaction was quenched with water and extracted with three portions of diethyl ether. The combined organic layers were dried over anhydrous sodium sulfate and concentrated *in vacuo* resulting in a clear oil. The crude material was purified on silica column chromatography with an eluent of 0-20% ethyl acetate in hexanes. The product was isolated as a clear oil (21 mg, 70% yield) and visualized on TLC with UV light and after heat activation with vanillin—stained red.

R$_f$ = 0.68 (7:3 hexanes:ethyl acetate)

^{1}H NMR (500 MHz, CDCl$_3$, mixture of E/Z isomers): δ 7.39 – 7.28 (m, 5H), 7.23 – 7.18 (m, 1H), 6.84 – 6.76 (m, 2H), 5.87 (dd, *J* = 21.5, 15.6 Hz, 1H), 5.23 – 5.12 (m, 1H), 5.12 – 5.00 (m, 2H), 2.33 (s, 3H), 1.67 (s, 3H).

^{13}C NMR (101 MHz, CDCl$_3$): δ 166.90, 156.21, 155.17, 139.49, 136.18, 135.93, 129.26, 128.92, 128.69, 128.55, 128.40, 128.34, 128.02, 128.00, 126.46, 122.07, 117.91, 113.45, 74.15, 70.72, 66.31, 26.82, 21.52.

ν$_{max}$/cm^{-1} (film): 3524, 2923, 2853, 1715, 1274.

HRMS: APCI (*m/z*) calcd for $C_{26}H_{25}O_3$ [M+H$^+$]: 385.17982, found 385.17908.

$[\alpha]^{20}_D$ = +3.9 (*c* 0.34, chloroform)

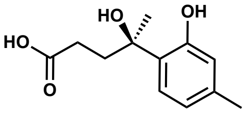

(*R*)-4-hydroxy-4-(2-hydroxy-4-methylphenyl)pentanoic acid (2.70)

To a vial equipped with Teflon coated metal stir bar were added (+)-**2.69** (10 mg, 25 μmol, 1 equiv) and Lindlar catalyst (0.5 mg, 1 μmol, 40 mol%) to a 1 mL 1:1 solution of ethyl acetate:ethanol. The reaction was purged with argon, then purged 5 times with hydrogen and stirred at room temperature under a hydrogen atmosphere for 3 hours. The hydrogen balloon was removed and the reaction was filtered over celite and concentrated *in vacuo*. The title compound was purified by PTLC with an eluent of 1:1 hexanes:ethyl acetate (1% acetic acid) and isolated as an off-white amorphous powder (5mg, 89% yield). Visualization on TLC was performed with UV light and after heat activation with vanillin—stained red.

R$_f$ = 0.16 (1:1 hexanes:ethyl acetate (1% acetic acid))

^{1}H NMR (600 MHz, $CDCl_3$) δ 6.82 (d, *J* = 7.9 Hz, 1H), 6.68 (s, 1H), 6.63 (dd, *J* = 8.4, 1.6 Hz, 1H), 2.55 – 2.42 (m, 2H), 2.35 – 2.28 (m, 1H), 2.27 (s, 3H), 2.20 – 2.12 (m, 1H), 1.64 (s, 3H).

HRMS: APCI (*m/z*) calcd for $C_{12}H_{15}O_4$ [M-H$^+$]: 223.09758, found 223.09709.

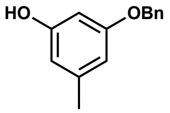

3-(benzyloxy)-5-methylphenol (2.46)

To a suspension of orcinol (1 equiv) and potassium carbonate (2 equiv) in DMF is added benzyl bromide (0.9 equiv) dropwise at room temperature. The mixture was stirred for 12 hours then diluted with water and extracted with ethyl acetate. The organic layers were dried over anhydrous sodium sulfate and concentrated *in vacuo.* The title compound was purified by silica column chromatography (46%). This compound is known and spectra matched literature reports. The title compound is known and matched reported spectra[14].

^{1}H NMR (600 MHz, $CDCl_3$): δ 7.42-7.33 (m, 5H), 6.41 (s, 1H), 6.30 (s, 1H), 6.27 (s, 1H), 5.02 (s, 2H), 2.27 (s, 3H).

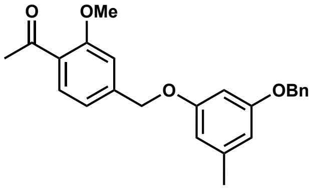

Benzyl protected diaryl (2.1)

In a flask open to air were added **2.11** (200 mg, 0.82 mmol, 1.2 equiv), **2.46** (146 mg, 0.68 mmol, 1 equiv), tetrabutylammonium bromide (222 mg, 0.68 mmol, 1 equiv), and potassium phosphate tribasic (212 mg, 1 mmol, 1.5 equiv) in deionized water (0.25M). The suspension was stirred overnight at room temperature. The reaction was concentrated *in vacuo* to remove solvent and then diluted with methylene chloride. The resulting suspension was washed with aqueous 1N HCl. The organic layer was dried over anhydrous sodium sulfate and concentrated *in vacuo*. The product was purified with silica column chromatography with a gradient of 0-15% ethyl acetate in hexanes and isolated as an off-white amorphous powder (256 mg, >98% yield). Visualization on TLC was performed with UV light and after heat activation with vanillin. The product stains red in vanillin.

R_{f} = 0.43 (4:1 hexanes:ethyl acetate)

^{1}H NMR (600 MHz, $CDCl_3$): δ 7.75 (d, *J* = 7.9 Hz, 1H), 7.47 – 7.28 (m, 5H), 7.04 (s, 1H), 7.01 (d, *J* = 9.4 Hz, 1H), 5.04 (s, 2H), 5.02 (s, 2H), 3.92 (s, 3H), 2.61 (s, 3H), 2.30 (s, 3H).

^{13}C NMR (151 MHz, $CDCl_3$): δ 199.7, 160.2, 159.9, 159.6, 143.7, 140.7, 137.3, 131.1, 128.9, 128.33, 127.9, 119.4, 110.4, 108.8, 108.6, 99.6, 70.3, 69.7, 55.9, 32.1, 22.2.

ν_{max}/cm^{-1} (film): 2063, 2922, 1670, 1592, 1148.

HRMS: APCI (*m/z*) calcd for $C_{24}H_{25}O_4$ [M+H^{+}]: 377.17474, found 377.1746.

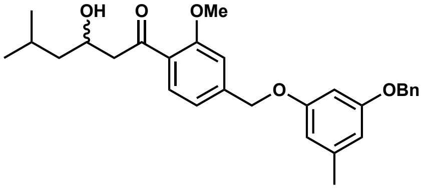

1-(4-((3-(benzyloxy)-5-methylphenoxy)methyl)-2-methoxyphenyl)-3-hydroxy-5-methylhexan-1-one (2.42)

In a flame dried flask equipped with a Teflon coated metal stir bar was added **2.41** (470 mg, 1.25mmol, 1 equiv) in anhydrous tetrahydrofuran (0.2M) under an argon atmosphere. The reaction was cooled to -78˚C and lithium diisopropylamide (1.0M in 1:1 tetrahydrofuran : hexanes, 1.37 mL, 1.37 mmol, 1.1 equiv) was added slowly. The solution was stirred for 1 hour at -78 ˚C, then isovaleraldehyde (150 µL, 1.27 mmol, 1.1 equiv) was added. The reaction was stirred for an additional 1.5 hours at -78˚C. The ice bath was removed, and the reaction was quickly quenched with aqueous pH = 7 phosphate buffer. Allowing the reaction to warm past -78˚C results in addition at the benzylic position. Extraction of the aqueous layer was performed with three portions of ethyl acetate. The combined organic layers were washed with brine, dried over anhydrous sodium sulfate, and concentrated *in vacuo*. The product was purified with silica column chromatography with a gradient of 0-15% ethyl acetate in hexanes and isolated as a low melting point amorphous yellow solid (405 mg, 70% yield). Visualization of the product on TLC was performed with UV light and after heat activation with vanillin. The product stains orange in vanillin.

R$_f$ = 0.22 (4:1 hexanes:ethyl acetate)

^{1}H NMR (600 MHz, $CDCl_3$) δ 7.75 (d, *J* = 7.8 Hz, 1H), 7.45 – 7.35 (m, 4H), 7.35 – 7.29 (m, 1H), 7.04 (s, 1H), 7.03 (d, *J* = 9.4 Hz, 1H), 6.46 (s, 1H), 6.42 (s, 2H), 5.05 (s, 2H), 5.02 (s, 2H), 4.32 – 4.21 (m, 1H), 3.91 (s, 3H), 3.21 (dd, *J* = 18.2, 2.5 Hz, 2H), 3.01 (dd, *J* = 18.0, 9.3 Hz, 1H), 1.86 (dtd, *J* = 8.6, 7.0, 3.9 Hz, 1H), 1.56 (ddd, *J* = 14.1, 8.9, 5.4 Hz, 1H), 1.23 (ddd, *J* = 13.3, 8.5, 4.4 Hz, 1H), 0.95 (dd, *J* = 6.7, 2.8 Hz, 6H).

^{13}C NMR (151 MHz, $CDCl_3$): δ 202.78, 160.07, 159.63, 159.37, 143.97, 140.57, 137.08, 130.85, 128.72, 128.71, 128.11, 127.63, 127.28, 119.29, 110.27, 108.66, 108.46, 99.44, 70.15, 69.43, 66.33, 55.74, 51.02, 45.90, 24.58, 23.53, 22.27, 21.98.

ν_{max}/cm^{-1} (film): 3509, 2954, 1664, 1594, 1150.

HRMS: APCI (*m/z*) calcd for $C_{29}H_{35}O_5$ [M+H$^+$]: 463.2479, found 463.24792.

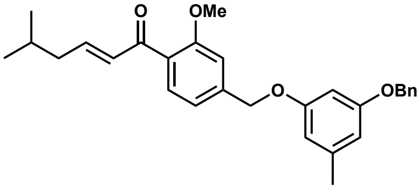

(*E*)-1-(4-((3-(benzyloxy)-5-methylphenoxy)methyl)-2-methoxyphenyl)-5-methylhex-2-en-1-one (2.43)

In a flame dried vial equipped with Teflon coated metal stir bar was added **2.42** (175 mg, 0.37 mmol, 1 equiv) and *p*-toluenesulfonic acid monohydrate (108 mg, 0.56 mmol, 1.5 equiv) in anhydrous toluene (0.15M) under an argon atmosphere. The vial was quickly sealed and heated to 50 ˚C for 2.5

hours. The reaction was cooled to room temperature, diluted with hexanes, filtered over celite, and concentrated *in vacuo* resulting in a yellow oil. The product was purified with silica column chromatography with a gradient of 0-15% ethyl acetate in hexanes and isolated as a yellow oil (140 mg, 85% yield). Visualization on TLC was performed with UV light and after heat activation with vanillin. The product stained brown in vanillin.

R$_f$ = 0.53 (4:1 hexanes:ethyl acetate).

^{1}H NMR (600 MHz, CDCl$_3$): δ 7.51 (d, *J* = 8.1 Hz, 1H), 7.42 (d, *J* = 7.0 Hz, 2H), 7.38 (dd, *J* = 8.5, 6.7 Hz, 2H), 7.32 (t, *J* = 7.2 Hz, 1H), 7.02 (d, *J* = 6.3 Hz, 1H), 6.83 (dt, *J* = 15.2, 7.5 Hz, 1H), 6.65 (dd, *J* = 15.5, 1.3 Hz, 1H), 6.45 (d, *J* = 9.7 Hz, 2H), 6.44 (s, 1H), 5.04 (s, 2H), 5.02 (s, 2H), 3.86 (s, 3H), 2.30 (s, 3H), 2.17 – 2.12 (m, 1H), 1.79 (hept, *J* = 6.7 Hz, 1H), 1.60 – 1.56 (m, 3H), 1.26 (t, *J* = 7.1 Hz, 1H), 0.94 (d, *J* = 6.6 Hz, 6H).

^{13}C NMR (151 MHz, CDCl$_3$): δ 193.35, 160.07, 159.75, 158.32, 148.01, 142.19, 140.53, 137.12, 131.85, 130.56, 128.87, 128.72, 128.10, 127.64, 119.32, 110.30, 108.63, 108.47, 99.44, 70.15, 69.68, 55.83, 42.03, 28.08, 22.57, 21.99.

ν_{max}/cm^{-1} (film): 2956, 1661, 1594, 1497, 1151.

HRMS: APCI (*m/z*) calcd for $C_{29}H_{33}O_4$ [M+H$^+$]: 445.23724, found 445.23748.

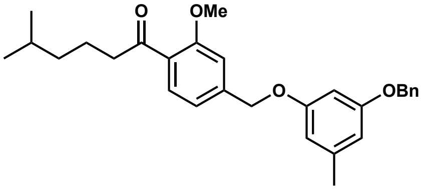

1-(4-((3-(benzyloxy)-5-methylphenoxy)methyl)-2-methoxyphenyl)-5-methylhexan-1-one (2.44)

In a flame dried flask under an argon atmosphere was added **2.43** (280 mg, 0.63 mmol, 1 equiv) in anhydrous diethyl ether (0.1M). The solution was cooled to -78 ˚C in a dry ice-acetone bath and L-selectride (1M in tetrahydrofuran, 630 µL, 0.63 mmol, 1 equiv) was added dropwise. The reaction was stirred for 1 hour at -78 ˚C, then the ice bath was removed. The reaction was quenched immediately with a saturated aqueous solution of ammonium chloride. The resulting biphasic mixture was extracted with three portions of diethyl ether and the combined organic layers were dried over anhydrous magnesium sulfate and concentrated *in vacuo* resulting in a yellow oil. The product was purified with silica column chromatography with a gradient of 0-15% ethyl acetate in hexanes and isolated as a yellow oil (208 mg, 74% yield). Visualization on TLC was performed with UV light and after heat activation with vanillin. The product stained orange-brown in vanillin.

R_f = 0.59 (4:1 hexanes:ethyl acetate)

^{1}H NMR (600 MHz, $CDCl_3$): δ 7.67 (d, *J* = 7.8 Hz, 1H), 7.44 – 7.41 (m, 2H), 7.40 – 7.37 (m, 2H), 7.35 – 7.31 (m, 1H), 7.02 (s, 1H), 7.01 (d, *J* = 7.8 Hz, 1H), 6.44 (d, *J* = 14.2 Hz, 2H), 6.43 (s, 1H), 5.04 (s, 2H), 5.02 (s, 2H), 3.90 (s, 3H), 2.96 – 2.91 (m, 2H), 2.30 (s, 3H), 1.70 – 1.63 (m, 2H), 1.55 (dt, *J* = 13.3, 6.6 Hz, 1H), 1.27 – 1.17 (m, 2H), 0.88 (d, *J* = 6.7 Hz, 6H).

^{13}C NMR (151 MHz, $CDCl_3$): δ 203.02, 160.00, 159.65, 158.79, 142.83, 140.54, 137.03, 130.69, 128.73, 128.20, 128.12, 127.66, 119.28, 110.17, 108.52, 108.36, 99.31, 70.09, 69.51, 55.69, 44.14, 38.82, 28.06, 22.71, 22.41, 22.01.

ν_{max}/cm^{-1} (film): 2952, 2868, 1672, 1593, 1150.

HRMS: APCI (*m/z*) calcd for $C_{29}H_{35}O_4$ [M+H$^+$]: 447.25299, found 447.25282.

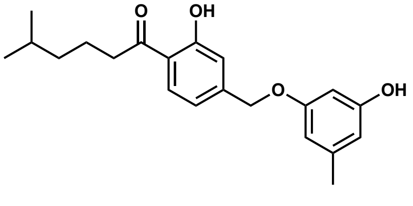

1-(2-hydroxy-4-((3-hydroxy-5-methylphenoxy)methyl)phenyl)-5-methylhexan-1-one (2.45)

In a flame dried vial under an argon atmosphere was added **2.44** (10 mg, 20 µmol, 1 equiv) in anhydrous methylene chloride 0.1M. The solution was cooled to -78 ˚C prior to drop-wise addition of boron tribromide (1M in methylene chloride, 60 µL, 60 µmol, 2.5 equiv). The reaction was stirred for 1 hour at -78 ˚ then quenched with water and extracted with three portions of dichloromethane.

The combined organic layers were dried over anhydrous magnesium sulfate and concentrated *in vacuo*. The product was purified with silica column chromatography with a gradient of 0-50% ethyl acetate in hexanes and isolated as an orange amorphous powder (5.2 mg, 76% yield). Visualization of the product on TLC was performed with UV light and after heat activation with vanillin— the product stained orange in vanillin.

R$_{f}$ = 0.29 (4:1 hexanes:ethyl acetate)

^{1}H NMR (600 MHz, $CDCl_3$): δ 12.46 (s, 1H), 7.76 (dd, *J* = 8.1, 2.2 Hz,1), 7.03 (s, 1H), 6.94 (d, *J* = 8.3 Hz, 1H), 6.38 (s,12H), 6.27 (d, *J* = 6.7 Hz, 2H), 5.02 (s, 2H), 2.99 – 2.92 (m, 2H), 2.27 (s, 3H), 1.75 (p, *J* = 7.7 Hz, 2H), 1.30-1.26 (m, 3H), 0.91 (dd, *J* = 6.6, 2.0 Hz, 6H).

^{13}C NMR (151 MHz, $CDCl_3$): δ 206.59, 162.77, 159.60, 156.48, 146.19, 140.76, 130.35, 118.71, 117.05, 116.42, 109.17, 108.22, 99.47, 68.93, 38.59, 27.91, 22.50, 22.45, 21.60.

ν$_{max}$/cm^{-1} (film): 3396, 2917, 2158, 1641, 1597.

HRMS: APCI (*m/z*) calcd for $C_{21}H_{27}O_4$ [M-H$^+$]: 343.19039, found 343.19063.

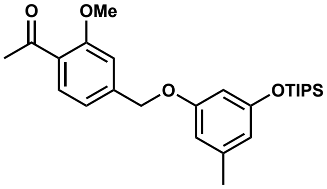

1-(2-methoxy-4-((3-methyl-5-((triisopropylsilyl)oxy)phenoxy)methyl)phenyl)ethan-1-one (2.47)

In a flame dried vial, a solution of **2.11** (100 mg, 0.36 mmol, 1 equiv) in anhydrous *N,N*-dimethylformamide (0.8M) was cooled to 0 ˚C under an argon atmosphere. Potassium carbonate (60 mg, 0.43 mmol, 1.2 equiv) and **2.25** (101 mg, 0.36 mmol, 1 equiv) were added successively. The vial was sealed and moved to a stir plate inside the fridge at 4 ˚C. The reaction was stirred overnight in the fridge, then quenched with a saturated aqueous solution of ammonium chloride and diluted with ethyl acetate. The aqueous layer was extracted with three portions of ethyl acetate. The combined organic layers were washed with five portions of brine, dried over anhydrous sodium sulfate, and concentrated *in vacuo*. The product was purified was purified with silica column chromatography with a gradient of 0-10% hexanes in ethyl acetate and isolated as a yellow oil (143 mg, 90% yield). Visualization on TLC was performed with UV light and after heat activation with vanillin—the starting material doesn't stain, while the product stains orange.

R_f = 0.61 (4:1 hexanes:ethyl acetate)

^{1}H NMR (600 MHz, $CDCl_3$): δ 7.75 (d, *J* = 7.9 Hz, 1H), 7.03 (s, 1H), 7.02 – 6.98 (m, 1H), 6.40 (s, 1H), 6.33 (s, 1H), 6.27 (dt, *J* = 2.3, 1.2 Hz, 1H), 5.04 (s, 2H), 3.91 (s, 3H), 2.61 (s, 3H), 1.22 – 1.15 (m, 3H), 1.06 (d, *J* = 7.4 Hz, 18H).

^{13}C NMR (151 MHz, $CDCl_3$): δ 199.56, 159.41, 159.28, 157.06, 143.76, 140.21, 130.92, 127.54, 119.04, 114.00, 110.07, 108.73, 103.98, 69.39, 55.66, 32.04, 21.82, 18.04, 18.02, 12.74.

ν_{max}/cm^{-1} (film): 2943, 2866, 1675, 1609, 1463.

HRMS: APCI (*m/z*) calcd for $C_{26}H_{39}O_4Si$ [M+H$^+$]: 443.26121, found 443.26049.

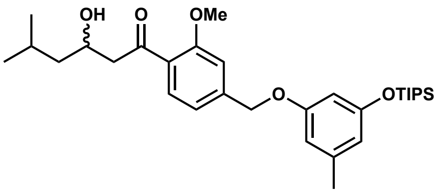

3-hydroxy-1-(2-methoxy-4-((3-methyl-5-((triisopropylsilyl)oxy)phenoxy)methyl)phenyl)-5-methylhexan-1-one (2.48)

In a flame dried flask equipped with a Teflon coated metal stir bar was added **2.47** (590 mg, 1.33 mmol, 1 equiv) in anhydrous tetrahydrofuran (0.2M) under an argon atmosphere. The reaction was cooled to -78˚C and lithium diisopropylamide (0.5M in 1:1 tetrahydrofuran : hexanes, 3 mL, 1.5 mmol, 1.1 equiv) was added slowly. The solution was stirred for 1 hour at -78 ˚C, then isovaleraldehyde (160 µL, 1.5 mmol, 1.1 equiv) was added. The reaction was stirred for an additional 1.5 hours at -78˚C. The ice bath was removed, and the reaction was quickly quenched with aqueous pH = 7 phosphate buffer. Allowing the reaction to warm past -78˚C results in addition at the benzylic position. Extraction of the aqueous layer was performed with three portions of ethyl acetate. The combined organic layers were washed with brine, dried over anhydrous sodium sulfate, and concentrated *in vacuo*. The product was purified with silica column chromatography with a gradient of 0-15% ethyl acetate in hexanes and isolated as a low melting point amorphous yellow solid (549 mg, 78% yield). Visualization of the product on TLC was performed with UV light and after heat activation with vanillin. The product stains purple in vanillin.

R$_f$ = 0.49 (7:3 hexanes:ethyl acetate)

^{1}H NMR (600 MHz, CDCl$_3$) δ 7.75 (d, *J* = 7.8 Hz, 1H), 7.03 (d, *J* = 8.5 Hz, 2H), 6.40 (s, 1H), 6.34 (s, 1H), 6.27 (t, *J* = 2.3 Hz, 1H), 5.04 (s, 2H), 4.25 (dddd, *J* = 9.0, 6.6, 4.3, 2.3 Hz, 1H), 3.90 (s, 3H), 3.21 (dd, *J* = 18.0, 2.4 Hz, 1H), 3.00 (dd, *J* = 18.1, 9.2 Hz, 1H), 2.26 (s, 3H), 1.85 (dddd, *J* = 13.5, 6.6, 5.6, 1.2 Hz, 1H), 1.57 – 1.52 (m, 1H), 1.25 – 1.15 (m, 4H), 1.07 (d, *J* = 7.3 Hz, 18H), 0.94 (dd, *J* = 6.6, 3.3 Hz, 6H).

^{13}C NMR (151 MHz, CDCl$_3$): δ 202.75, 159.41, 159.30, 157.11, 144.24, 140.24, 130.86, 127.16, 119.19, 114.08, 110.17, 108.77, 104.05, 69.37, 66.31, 55.71, 51.01, 45.88, 24.58, 23.53, 22.26, 21.81, 18.05, 12.78.

ν$_{max}$/cm^{-1} (film): 3515, 2946, 2866, 1608, 1165.

HRMS: APCI (*m/z*) calcd for $C_{31}H_{49}O_5Si$ [M+H$^+$]: 529.33438, found 529.3334.

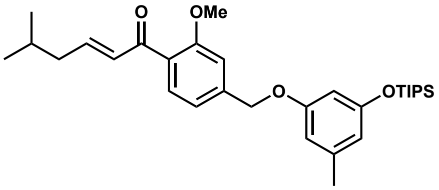

(*E*)-1-(2-methoxy-4-((3-methyl-5-((triisopropylsilyl)oxy)phenoxy)methyl)phenyl)-5-methylhex-2-en-1-one (2.49)

In a flame dried vial equipped with Teflon coated metal stir bar was added **2.48** (415 mg, 0.78 mmol, 1 equiv) and *p*-toluenesulfonic acid monohydrate (224 mg, 1.18 mmol, 1.5 equiv) in anhydrous toluene (0.15M) under an argon atmosphere. The vial was quickly sealed and heated to 50 ˚C for 2.5

hours. The reaction was cooled to room temperature, diluted with hexanes, filtered over celite, and concentrated *in vacuo* resulting in a yellow oil. The product was purified with silica column chromatography with a gradient of 0-15% ethyl acetate in hexanes and isolated as a yellow oil (171 mg, 86% yield). Visualization on TLC was performed with UV light and after heat activation with vanillin. The product stained brown in vanillin.

R$_f$ = 0.57 (4:1 hexanes:ethyl acetate)

^{1}H NMR (600 MHz, CDCl$_3$): δ 7.51 (d, *J* = 8.1 Hz, 1H), 7.10 – 6.95 (m, 2H), 6.84 (dt, *J* = 15.1, 7.4 Hz, 1H), 6.66 (dt, *J* = 15.5, 1.3 Hz, 1H), 6.40 (d, *J* = 0.8 Hz, 1H), 6.34 (d, *J* = 0.7 Hz, 1H), 6.29 (t, *J* = 2.2 Hz, 1H), 5.04 (s, 2H), 3.85 (s, 3H), 2.26 (s, 3H), 2.15 (ddd, *J* = 7.4, 6.8, 1.4 Hz, 2H), 1.79 (dp, *J* = 13.4, 6.7 Hz, 1H), 1.25 – 1.16 (m, 3H), 1.07 (d, *J* = 7.4 Hz, 18H), 0.94 (d, *J* = 6.7 Hz, 6H).

^{13}C NMR (151 MHz, CDCl$_3$): δ 193.25, 159.43, 158.36, 157.10, 147.88, 142.44, 140.18, 131.82, 130.59, 128.77, 119.22, 114.00, 110.19, 108.76, 104.07, 69.60, 55.79, 42.03, 28.08, 22.57, 21.81, 18.06, 12.79.

ν$_{max}$/cm^{-1} (film): 2946, 2867, 1610, 1463, 1164.

HRMS: APCI (*m/z*) calcd for $C_{31}H_{47}O_4Si$ [M+H$^+$]: 511.32381, found 511.32308.

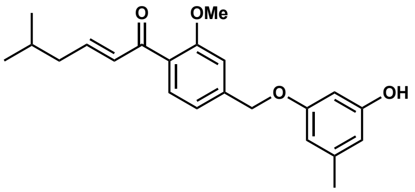

(*E*)-1-(4-((3-hydroxy-5-methylphenoxy)methyl)-2-methoxyphenyl)-5-methylhex-2-en-1-one (2.50)

To a flame dried vial under argon was added **2.49** (340 mg, 0.66 mmol, 1 equiv) in anhydrous tetrahydrofuran (0.2M). The solution was cooled to 0 ˚C and tetrabutylammonium fluoride (1M in THF, 800 µL, 0.79 mmol, 1.2 equiv) was added. After 1 hour, the reaction was quenched with aqueous saturated ammonium chloride and extracted with three portions of ethyl acetate. The combined organic layers were washed with brine, dried over anhydrous sodium sulfate, and concentrated *in vacuo*. The product was purified with silica column chromatography with a gradient of 0-20% ethyl acetate in hexanes and isolated as an amorphous low melting point white powder (228 mg, >98% yield). Visualization on TLC was performed with UV light and after heat activation with vanillin—the product stains plum.

R$_{f}$ = 0.40 (7:3 hexanes:ethyl acetate)

^{1}H NMR (600 MHz, CDCl$_3$): δ 7.51 (d, *J* = 8.1 Hz, 1H), 7.04 – 6.98 (m, 2H), 6.84 (dt, *J* = 15.2, 7.4 Hz, 1H), 6.65 (dt, *J* = 15.5, 1.4 Hz, 1H), 6.39 (t, *J* = 0.7 Hz, 1H), 6.29 (d, *J* = 1.6 Hz, 2H), 5.03 (s, 2H), 3.86 (s, 3H), 2.27 (s, 3H), 2.15 (ddd, *J* = 7.3, 6.7, 1.4 Hz, 2H), 1.79 (dp, *J* = 13.3, 6.7 Hz, 1H), 0.94 (d, *J* = 6.7 Hz, 6H).

^{13}C NMR (151 MHz, CDCl$_3$): δ 193.50, 159.88, 158.34, 156.78, 148.21, 142.24, 140.83, 131.82, 130.57, 128.81, 119.28, 110.28, 109.32, 108.33, 99.64, 69.64, 55.82, 42.04, 31.08, 28.08, 22.57, 21.74.

ν$_{max}$/cm^{-1} (film): 3354, 2955, 1655, 1612, 1148.

HRMS: APCI (*m/z*) calcd for $C_{22}H_{27}O_4$ [M+H$^+$]: 255.19039, found 355.19022.

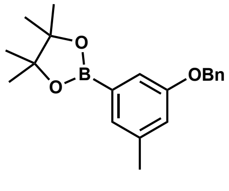

2-(3-(benzyloxy)-5-methylphenyl)-4,4,5,5-tetramethyl-1,3,2-dioxaborolane (2.55)

The title compound was prepared in two steps following an adapted patent procedure from **2.31**. A mixture of 3-romo-5-methylphenol (1 equiv), benzyl bromide (1.1 equiv) and potassium carbonate (3 equiv) in acetone (0.2M) were heated under reflux for 2 hours. The reaction mixture was cooled to room temperature and acidified with 2N hydrochloric acid. The aqueous layer was extracted with ethyl acetate and the organic layer was washed with brine, dried over anhydrous magnesium sulfate and concentrated *in vacuo* to afford a red oil. The crude mixture was transferred to a flame dried vial under an argon atmosphere and bis(pinacolato)diboron (3 equiv), $NaCO_3$ (4 equiv), and $Pd(dppf)Cl_2 \cdot CH_2Cl_2$ (10 mol%) were added in anhydrous toluene (0.12M). The vial was sealed, and the solution was heated to reflux for 16 h. The mixture was diluted with ethyl acetate and washed with water. The organic layer was dried over anhydrous sodium sulfate and concentrated *in vacuo*. The residue was purified by silica column chromatography to afford a sticky yellow oil (60% yield). The title compound is commercially available from Acela Pharmatech LLC and Anichem Inc. and matched reported characterization.

^{1}H NMR (600 MHz, Chloroform-*d*): δ 7.48 – 7.43 (m, 1H), 7.43 – 7.37 (m, 1H), 7.36 – 7.31 (m, 1H), 7.29 – 7.25 (m, 1H), 6.96 – 6.91 (m, 1H), 5.08 (s, 2H), 2.34 (s, 3H), 1.35 (s, 12H).

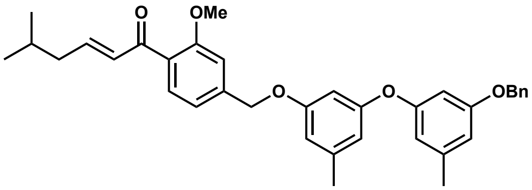

(*E*)-1-(4-((3-(3-(benzyloxy)-5-methylphenoxy)-5-methylphenoxy)methyl)-2-methoxyphenyl)-5-methylhex-2-en-1-one (2.51)

To a flame dried vial equipped with Teflon coated metal stir bar were added **2.50** (200 mg, 0.56 mmol, 2 equiv), **2.55** (91 mg, 0.28 mmol, 1 equiv), boric acid (35 mg, 0.56 mmol, 2 equiv), copper(II) acetate (51 mg, 0.28 mmol, 1 equiv), and 4Å MS (100 mg) in anhydrous acetonitrile under a dry air atmosphere. The vial was sealed and heated to reflux for 72 hours. The solution was cooled to room temperature, diluted with methylene chloride, and filtered over celite. The filtrate was washed with brine, dried over anhydrous magnesium sulfate, and concentrated *in vacuo*. The title compound was purified on silica column chromatography with a gradient of 0-20% ethyl acetate in hexanes and isolated as a clear yellow oil (47 mg, 30% yield). The product was visualized on TLC with UV light and after heat activation with vanillin—stained purple.

R_f = 0.78 (7:3 hexanes:ethyl acetate)

^{1}H NMR (600 MHz, $CDCl_3$): δ 7.51 (d, *J* = 8.1 Hz, 1H), 7.46 – 7.34 (m, 6H), 7.32 (tdd, *J* = 7.2, 4.2, 2.6 Hz, 1H), 7.01 (d, *J* = 5.1 Hz, 1H), 6.84 (dt, *J* = 15.0, 7.4 Hz, 1H), 6.65 (dt, *J* = 15.5, 1.4 Hz, 1H), 6.56 (d, *J* = 7.1 Hz, 1H), 6.45 (d, *J* = 8.0 Hz, 2H), 6.41 (s, 1H), 6.31 – 6.24 (m, 1H), 5.02 (d, *J* = 2.8 Hz, 2H), 5.00 (s, 2H), 3.86 (s, 3H), 2.29 (s, 3H), 2.27 (s, 3H), 2.15 (td, *J* = 7.1, 1.4 Hz, 2H), 1.79 (dp, *J* = 13.4, 6.7 Hz, 1H), 0.94 (d, *J* = 6.7 Hz, 6H).

^{13}C NMR (151 MHz, $CDCl_3$): δ 193.39, 160.02, 159.73, 158.32, 158.24, 148.11, 141.97, 140.78, 137.16, 136.95, 131.82, 130.58, 128.72, 128.14, 128.06, 127.68, 127.60, 119.37, 112.70, 112.45, 110.83, 110.81, 110.35, 109.01, 108.36, 103.16, 99.60, 70.20, 70.09, 69.73, 55.83, 42.03, 31.08, 28.08, 22.56, 21.82.

ν_{max}/cm^{-1} (film): 2955, 2922, 1599, 1462, 1153.

HRMS: APCI (*m/z*) calcd for $C_{36}H_{39}O_5$ [M+H$^+$]: 551.2792, found 551.2803.

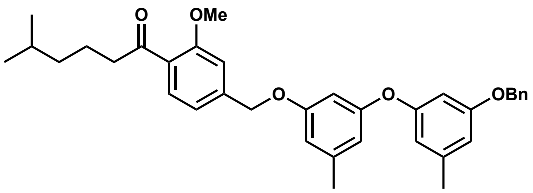

1-(4-((3-(3-(benzyloxy)-5-methylphenoxy)-5-methylphenoxy)methyl)-2-methoxyphenyl)-5-methylhexan-1-one (2.52)

In a flame dried flask under an argon atmosphere was added **2.51** (57 mg, 0.10 mmol, 1 equiv) in anhydrous diethyl ether (0.1M). The solution was cooled to -78 ˚C in a dry ice-acetone bath and L-selectride (1M in tetrahydrofuran, 110 µL mL, 0.10 mmol, 1 equiv) was added dropwise. The reaction was stirred for 1 hour at -78 ˚C, then the ice bath was removed. The reaction was quenched immediately with a saturated aqueous solution of ammonium chloride. The resulting biphasic mixture was extracted with three portions of diethyl ether and the combined organic layers were dried over anhydrous magnesium sulfate and concentrated *in vacuo* resulting in a yellow oil. The product was purified with silica column chromatography with a gradient of 0-15% ethyl acetate in hexanes and isolated as a yellow oil (48 mg, 87% yield). Visualization on TLC was performed with UV light and after heat activation with vanillin. The product stained orange-brown in vanillin.

R$_f$ = 0.50 (7:3 hexanes:ethyl acetate)

^{1}H NMR (600 MHz, CDCl$_3$) δ 7.66 (d, *J* = 7.8 Hz, 1H), 7.48 – 7.35 (m, 5H), 7.34 – 7.29 (m, 1H), 7.02 (s, 1H), 7.01 (d, *J* = 7.8 Hz, 1H), 6.56 (d, *J* = 9.9 Hz, 2H), 6.45 (s, 2H), 6.44 (s, 1H), 5.02 (s, 2H), 5.00 (s, 2H), 3.90 (s, 3H), 2.93 (t, 2H), 2.29 (s, 6H), 1.67 (p, *J* = 7.6 Hz, 2H), 1.57 (hept, *J* = 6.6 Hz, 1H), 1.25 – 1.20 (m, 2H), 0.89 (d, *J* = 6.6 Hz, 6H).

^{13}C NMR (151 MHz, CDCl$_3$) δ 202.94, 160.02, 159.71, 158.80, 158.24, 158.15, 142.62, 140.86, 140.78, 136.95, 130.69, 128.72, 128.71, 128.36, 128.14, 127.68, 127.60, 119.36, 112.72, 112.44, 110.82, 110.27, 103.15, 103.11, 70.19, 69.63, 55.71, 44.13, 38.85, 29.85, 28.06, 22.70, 22.42, 21.81.

ν$_{max}$/cm^{-1} (film): 2581, 2454, 1796, 1591, 968.

HRMS: APCI (*m/z*) calcd for $C_{36}H_{41}O_5$ [M+H$^+$]: 553.29485, found 553.29554.

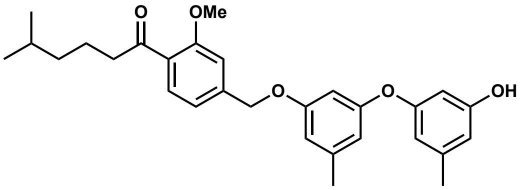

1-(4-((3-(3-hydroxy-5-methylphenoxy)-5-methylphenoxy)methyl)-2-methoxyphenyl)-5-methylhexan-1-one (2.54)

In a flame dried vial under an argon atmosphere was added **2.52** (20 mg, 36 μmol, 1 equiv) in anhydrous methylene chloride 0.1M. The solution was cooled to -78 ˚C prior to drop-wise addition of boron tribromide (1M in methylene chloride, 110 μL, 108 μmol, 3 equiv). The reaction was stirred for 1 hour at -78 ˚C then allowed to warm to 0 ˚C. After stirring for 1 hour, the reaction was quenched with water and extracted with three portions of dichloromethane. The combined organic layers were dried over anhydrous magnesium sulfate and concentrated *in vacuo*. The product was purified with PTLC with an eluent of 1:1 hexanes:diethyl ether. and isolated as an off-white low melting point solid (7.7 mg, 46% yield). Visualization of the product on TLC was performed with UV light and after heat activation with vanillin—both products stained orange.

R$_f$ = 0.60 (7:3 hexanes:ethyl acetate)

^{1}H NMR (600 MHz, CDCl$_3$): δ 7.63 (d, *J* = 7.8 Hz, 1H), 7.00 (s, 1H), 6.98 (d, *J* = 8.5 Hz, 1H), 6.55 (s, 1H), 6.46 (s, 1H), 6.40 (s, 3H), 6.24 (t, *J* = 2.3 Hz, 1H), 5.02 (s, 2H), 3.89 (s, 3H), 2.93 (t, 2H), 2.30 (s, 3H), 2.26 (s, 3H), 1.70 – 1.64 (m, 2H), 1.56 (dp, *J* = 13.3, 6.7 Hz, 1H), 1.25 – 1.19 (m, 2H), 0.88 (d, *J* = 6.6 Hz, 6H).

^{13}C NMR (151 MHz, CDCl$_3$): δ 203.32, 159.61, 158.75, 158.27, 158.16, 156.67, 142.64, 141.09, 140.89, 130.61, 128.42, 119.38, 112.84, 112.30, 111.38, 111.07, 110.25, 103.59, 103.21, 69.71, 55.73, 44.12, 38.85, 29.85, 28.07, 22.70, 22.42, 21.80, 21.60.

ν_{max}/cm^{-1} (film): 2921, 2144, 1973, 1586, 1156.

HRMS: APCI (*m/z*) calcd for $C_{29}H_{35}O_5$ [M+H$^+$]: 463.2470, found 463.24823.

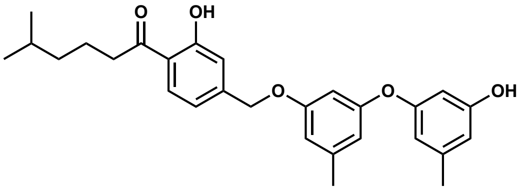

1-(2-hydroxy-4-((3-(3-hydroxy-5-methylphenoxy)-5-methylphenoxy)methyl)phenyl)-5-methylhexan-1-one (2.53)

The product was isolated as an off-white low melting point solid (8.6 mg, 53% yield).

R$_f$ = 0.61 (7:3 hexanes:ethyl acetate)

^{1}H NMR (600 MHz, CDCl$_3$): δ 12.50 (s, 1H), 7.75 (d, *J* = 8.2 Hz, 1H), 7.01 (d, *J* = 1.6 Hz, 1H), 6.93 (dd, *J* = 8.3, 1.6 Hz, 1H), 6.53 (t, *J* = 1.7 Hz, 1H), 6.45 (t, *J* = 1.6 Hz, 1H), 6.43 – 6.38 (m, 3H), 6.26 (t, *J* = 2.3 Hz, 1H), 5.01 (s, 2H), 2.95 (t, *J* = 7.5 Hz, 2H), 2.29 (s, 3H), 2.26 (s, 3H), 1.75 (tt, *J* = 10.8, 6.7 Hz, 2H), 1.62-1.59 (m, 1H), 1.29 – 1.26 (m, 2H), 0.91 (d, *J* = 6.6 Hz, 6H).

^{13}C NMR (151 MHz, $CDCl_3$) δ 206.77, 162.76, 159.43, 158.22, 158.07, 156.65, 146.13, 141.17, 140.93, 130.50, 118.87, 117.40, 116.75, 112.86, 112.26, 111.33, 111.05, 103.47, 103.11, 69.13, 38.73, 38.68, 28.05, 22.64, 22.56, 21.79, 21.60.

ν_{max}/cm^{-1} (film): 3373, 2925, 2170, 1787, 1156.

HRMS: APCI (*m/z*) calcd for $C_{28}H_{33}O_5$ [M+H$^+$]: 449.23225, found 449.23211.

6.5.2. Chapter 3

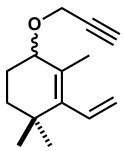

1,3,3-Trimethyl-6-(prop-2-yn-1-yloxy)-2-vinylcyclohex-1-ene (3.10)

The title compound is known and was prepared from α-ionone by literature procedure in 5 steps in 48% overall yield[15].

To a stirring solution of 2° alcohol (1 equiv) and propargyl bromide (80% in toluene, 10 equiv) was added TBAI (0.5 equiv). An aqueous solution of 60% NaOH was added dropwise and the reaction was stirred vigorously at room temperatue for 24 hours. The solution was reversed quenched over ice water and extracted with three portions of diethyl ether. The combined organic layers were washed with brine, dried over anhydrous sodium sulfate, and concentrated *in vacuo.* The title compound was purified by silica column chromatography (0-20% ethyl acetate in hexanes) to afford a yellow oil (60% yield). The spectra matched literature data[15].

^{1}H NMR (600 MHz, $CDCl_3$): δ 6.18 (ddt, *J* = 17.7, 11.4, 1.2 Hz, 1H), 5.28 (dd, *J* = 11.4, 2.5 Hz, 1H), 5.02 (dd, *J* = 17.8, 2.5 Hz, 1H), 4.25 (dd, *J* = 15.9, 2.4 Hz, 1H), 4.16 (dd, *J* = 15.9, 2.4 Hz, 1H), 3.83 (t, *J* = 4.3 Hz, 1H), 2.40 (t, *J* = 2.4 Hz, 1H), 1.84 – 1.80 (m, 1H), 1.79 (s, 3H), 1.75 (tdd, *J* = 13.8, 4.5, 3.1 Hz, 1H), 1.65 (ddd, *J* = 13.1, 11.4, 3.4 Hz, 1H), 1.35 (dddd, *J* = 13.0, 6.6, 3.1, 0.7 Hz, 1H), 1.01 (s, 3H), 0.98 (s, 3H).

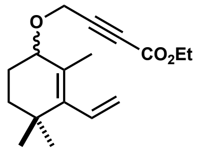

Ethyl 4-((2,4,4-trimethyl-3-vinylcyclohex-2-en-1-yl)oxy)but-2-ynoate ((±)-3.7)

In a flame dried flask under an argon atmosphere was added **(±)-3.10** (520 mg, 2.55 mmol, 1 equiv) in anhydrous tetrahydrofuran (0.04M). The solution was cooled to -78 ˚C and *n*-BuLi (2.2M in hexanes, 1.4 mL, 3.06 mmol, 1.2 equiv) was added dropwise. The reaction immediately turned purple and was stirred for 50 minutes at -78 ˚C. Ethyl chloroformate (300 µL, 3.06 mmol, 1.2 equiv) was added. The resulting dark red solution was stirred for an additional 1 hour at -78 ˚C, then allowed to warm to room temperature at which point the reaction was quenched with an aqueous saturated solution of ammonium chloride. The resulting biphasic mixture was extracted with three portions of diethyl ether and the combined organic layers were dried over anhydrous sodium sulfate and concentrated *in vacuo* resulting in a yellow oil. The title compound was purified by silica column chromatography with an eluent of 0-5% ethyl acetate in hexanes and isolated as a yellow oil (570 mg, 82% yield). The product was visualized on TLC with UV light and after heat activation with vanillin.

$\mathbf{R_{f}}$ = 0.72 (3:1 hexanes:ethyl acetate)

^{1}H NMR (600 MHz, $CDCl_3$)[a]: δ 6.18 (ddq, *J* = 17.8, 11.4, 1.2 Hz, 1H), 5.29 (ddd, *J* = 11.4, 5.9, 2.5 Hz, 1H), 5.02 (ddd, *J* = 17.8, 2.5, 1.4 Hz, 1H), 4.36 (d, *J* = 16.9 Hz, 1H), 4.29 (d, *J* = 16.9 Hz, 1H), 4.24 (q, *J* = 7.1 Hz, 2H), 3.83 (t, *J* = 4.2 Hz, 1H), 1.79 (s, 3H), 1.69 – 1.60 (m, 1H), 1.43 – 1.39 (m, 1H), 1.38 – 1.33 (m, 1H), 1.31 (t, *J* = 7.1 Hz, 3H), 1.28 – 1.24 (m, 1H), 1.01 (s, 3H), 0.98 (s, 3H).

^{13}C NMR (151 MHz, $CDCl_3$)[b]: δ 166.44, 161.78, 153.39, 149.25, 143.96, 143.55, 135.00, 134.86, 127.57, 127.20, 120.53, 120.23, 119.20, 119.05, 84.32, 84.20, 62.22, 56.19, 56.02, 39.14, 34.44, 34.34, 34.32, 28.85, 27.01, 26.97, 25.83, 23.52, 23.50, 23.49, 18.60, 18.58, 14.27, 14.14.

ν_{max}/cm^{-1} (film): 2958, 2933, 2933, 1710, 1256.

HRMS: APCI (*m/z*) calcd for $C_{17}H_{25}O_3$ [M+H$^+$]: 277.17982, found 277.17979.

[a]Peaks in ^{1}H-NMR spectrum split due to presence of O-ynoate rotamers. Compound **(±)-3.7** was unstable to high temperature NMR

[b]Peaks in ^{13}C-NMR spectrum split due to presence of rotamers. Compound **(±)-3.7**was unstable to high temperature NMR

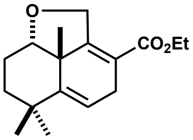

Ethyl(2a^1*S*,8a*S*)-2a^1,6,6-trimethyl-2a^1,4,6,7,8,8a-hexahydro-2*H*-naphtho[1,8-*bc*]furan-3-carboxylate ((±)-3.11)

To a flame dried pressure tube equipped with Teflon coated metal stir bar was added **(±)-3.7** (475 mg, 1.72 mmol, 1 equiv) in toluene (0.12M). Toluene was dried over 4Å MS for 48 hours and degassed prior to use. The solution was degassed for 10 minutes, then the tube was sealed and heated to reflux for 24 hours. The reaction was cooled to room temperature and concentrated *in vacuo* resulting in a yellow residue. The title compound was purified by column chromatography with a gradient of 0-10% ethyl acetate in hexanes (400 mg, 84% yield, d.r. > 20:1).

R$_{f}$ = 0.48 (4:1 hexanes:ethyl acetate)

^{1}H NMR (600 MHz, cdcl$_3$): δ 5.77 (dd, *J* = 6.4, 1.7 Hz, 1H), 4.85 (ddd, *J* = 16.0, 3.3, 1.1 Hz, 1H), 4.68 (ddd, *J* = 16.0, 3.8, 1.0 Hz, 1H), 4.20 (qd, *J* = 7.1, 4.1 Hz, 2H), 4.04 (dd, *J* = 10.5, 4.9 Hz, 1H), 3.30 (ddt, *J* = 20.9, 6.4, 1.1 Hz, 1H), 2.73 (dtd, *J* = 20.9, 3.6, 1.7 Hz, 1H), 1.79 (dq, *J* = 13.1, 4.8 Hz, 1H), 1.51 – 1.39 (m, 3H), 1.30 (t, *J* = 7.1 Hz, 3H), 1.18 (d, *J* = 1.9 Hz, 6H), 1.13 (s, 3H).

^{13}C NMR (151 MHz, CDCl$_3$) δ 166.44, 161.78, 149.25, 120.53, 120.22, 84.19, 68.80, 60.58, 48.71, 35.53, 34.58, 32.81, 30.63, 27.46, 26.62, 25.07, 14.50.

ν$_{max}$/cm^{-1} (film): 2960, 2932, 2863, 1708, 1268 .

HRMS: APCI (*m/z*) calcd for $C_{17}H_{25}O_3$ [M+H$^+$]: 277.17982, found 277.17979.

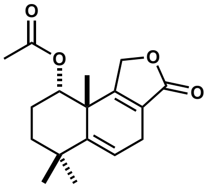

(9*S*,9a*S*)-6,6,9a-Trimethyl-3-oxo-1,3,4,6,7,8,9,9a-octahydronaphtho[1,2-*c*]furan-9-yl acetate ((±)-3.6)

In a flame dried flask under an argon atmosphere were added **(±)-3.11** (260 mg, 0.94 mmol, 1 equiv) and ZnI_2 (381 mg, 1.19 mmol, 1.27 equiv) in acetic acid (0.18M). The solution was stirred overnight at room temperature, then poured over iced water and extracted with three portions of diethyl ether. The combined organic layers were washed with a saturated aqueous solution of sodium bicarbonate (5X) and brine, dried over anhydrous sodium sulfate, and concentrated *in vacuo*. The title compound was purified by silica column chromatography with an eluent of 0-30% ethyl acetate in hexanes and isolated as an off-white amorphous powder (246 mg, 90% yield). The product was visualized on TLC by UV light and after heat activation with $KMnO_4$.

R_f = 0.33 (7:3 hexanes:ethyl acetate)

^{1}H NMR (600 MHz, $CDCl_3$): δ 5.89 (dd, *J* = 4.8, 2.6 Hz, 1H), 4.82 (ddd, *J* = 16.7, 3.4, 1.5 Hz, 1H), 4.51 (dt, *J* = 16.7, 2.6 Hz, 1H), 2.98 (dddd, *J* = 22.4, 4.6, 2.8, 1.5 Hz, 1H), 2.83 (ddt, *J* = 22.4, 3.4, 2.5 Hz, 1H), 2.15 – 2.07 (m, 1H), 1.98 (s, 3H), 1.83 (dtd, *J* = 15.2, 4.0, 3.0 Hz, 1H), 1.65 (td, *J* = 13.9, 4.1 Hz, 1H), 1.43 (s, 3H), 1.35 (dddd, *J* = 13.6, 4.0, 3.0, 0.8 Hz, 1H), 1.25 (s, 3H), 1.22 (s, 3H).

^{13}C NMR (151 MHz, $CDCl_3$): δ 173.55, 170.63, 164.71, 143.98, 124.00, 119.25, 74.96, 68.70, 41.76, 35.77, 34.25, 32.81, 30.60, 27.03, 22.58, 22.45, 21.32.

ν_{max}/cm^{-1} (film): 2944, 2869, 1759, 1736, 1242.

HRMS: APCI (*m/z*) calcd for $C_{17}H_{23}O_4$ [M+H$^+$]: 291.15909, found 291.15895.

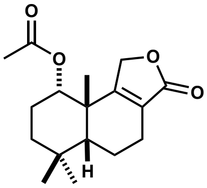

(5a*R*,9*S*,9a*S*)-6,6,9a-Trimethyl-3-oxo-1,3,4,5,5a,6,7,8,9,9a-decahydronaphtho[1,2-*c*]furan-9-yl acetate ((±)-3.13)

A vial under an argon atmosphere was charged with **(±)-3.6** (100 mg, 0.35 mmol, 1 equiv) and 5% Pd/C (292 mg) in methanol (0.024M). The reaction was purged with hydrogen and stirred under a hydrogen atmosphere at room temperature for 12 hours. The reaction was filtered over celite and concentrated *in vacuo.* The crude mixture was purified by PTLC with a 1:1 hexanes:ethyl acetate eluent. The tile compound was isolated as an amorphous white powder (53 mg, 52% yield) and was visualized on TLC with UV light—notably the title compound did not stain in vanillin.

R_f = 0.20 (1:1 hexanes:diethyl ether);

^{1}H NMR (600 MHz, $CDCl_3$): δ 5.00 – 4.87 (m, 1H), 4.75 – 4.70 (m, 1H), 2.42 – 2.30 (m, 1H), 2.30 – 2.22 (m, 1H), 2.11 (s, 3H), 2.10 – 2.07 (m, 1H), 1.82 – 1.74 (m, 1H), 1.66 (m, 1H), 1.53 (dd, *J* = 5.2, 3.1 Hz, 1H), 1.48 – 1.36 (m, 2H), 1.21 (s, 3H), 1.01 (s, 3H), 0.81 (s, 3H).

^{13}C NMR (151 MHz, $CDCl_3$) δ 173.87, 169.79, 164.13, 127.05, 79.80, 71.03, 49.04, 41.13, 34.40, 32.27, 28.72, 25.76, 21.30, 18.60, 17.61.

Key NOESY correlations: 1.21(CH_3)-1.53 (H)

ν_{max}/cm^{-1} (film): 2948, 2868, 1740, 1672, 1234.

HRMS: APCI (*m/z*) calcd for $C_{17}H_{25}O_4$ [M+H$^+$]: 293.17474, found 293.17413.

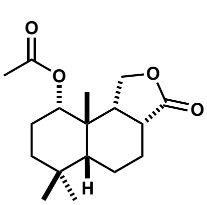

(3a*R*,5a*R*,9*S*,9a*S*,9b*R*)-6,6,9a-Trimethyl-3-oxododecahydronaphtho[1,2-*c*]furan-9-yl acetate ((±)-3.12)

The tile compound was isolated as an amorphous white powder (48 mg, 47% yield) and was visualized on TLC after heat activation with vanillin—the compound stained blue.

R_f = 0.22 (1:1 hexanes:diethyl ether)

^{1}H NMR (600 MHz, $CDCl_3$): δ 4.81 (dd, *J* = 6.5, 3.4 Hz, 1H), 4.42 (ddd, *J* = 9.6, 4.8, 1.5 Hz, 1H), 4.33 – 4.26 (m, 1H), 2.55 (dt, *J* = 7.5, 6.2 Hz, 1H), 2.45 (td, *J* = 7.9, 4.9 Hz, 1H), 2.06 (s, 3H), 2.01 (dd, *J* = 12.4, 5.9 Hz, 1H), 1.87 – 1.73 (m, 2H), 1.73 – 1.64 (m, 2H), 1.53 (ddd, *J* = 13.8, 10.5, 3.6 Hz, 1H), 1.46 (dddd, *J* = 12.3, 8.5, 6.0, 2.9 Hz, 1H), 1.23 – 1.16 (m, 2H), 1.15 (s, 3H), 1.08 (s, 3H), 0.99 (s, 3H).

^{13}C NMR (151 MHz, $CDCl_3$) δ 178.96, 170.83, 67.95, 49.40, 44.66, 38.96, 38.50, 34.24, 32.45, 32.05, 24.94, 21.59, 21.53, 21.34.

ν_{max}/cm^{-1} (film): 2955, 2858, 1774, 1736, 1375, 1235.

HRMS: APCI (*m/z*) calcd for $C_{17}H_{27}O_4$ $[M+H^+]$: 295.19039, found 295.18988.

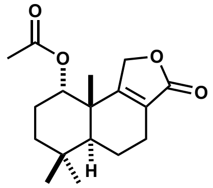

(5a*S*,9*S*,9a*S*)-6,6,9a-trimethyl-3-oxo-1,3,4,5,5a,6,7,8,9,9a-decahydronaphtho[1,2-*c*]furan-9-yl acetate ((±)-3.14)

In a flame dried vial under argon was added **(±)-3.6** (14.7 mg, 0.05 mmol, 1 equiv) in anhydrous 2-proponal (0.1M). Prior to use, 2-proponal was dried for 72 hours over 4Å MS and distileed over CaH (10% w/v). Once **(±)-3.6** was completely dissolved, phenylsilane (6 μL, 0.05 mmol, 1 equiv) and tert-butyl hydroeroxide (5M in decane, 15 μL, 0.075 mmol, 1.5 equiv) were added and the solution was degassed with argon for 10 minutes. Subsequently Tris(2,2,6,6-tetramethyl-**3**,5-

heptanedionato)manganese(III) (6 mg, 0.01 mmol, 20 mol%) was added and the reaction was degassed for no more than 30 seconds. The vial was sealed and heated to reflux for 2 hours. After 2 hours, the solution was cooled to room temperature and concentrated *in vacuo*. The concentrate was directly loaded onto a silica column for purification and eluted with 50-100% diethyl ether in hexanes. Both the *trans* and *cis* products were obtained as amorphous white powders (*trans:* 9.3 mg, 63%; *cis:* 5.4 mg, 37%; 1.7:1.0 isolated d.r.). The product was visualized on TLC with UV light and after heat activation with $KMnO_4$. Only the *cis* isomer was visible by UV light.

R_f = 0.25 (1:1 hexanes:diethyl ether)

^{1}H NMR (600 MHz, $CDCl_3$): δ 4.90 (t, *J* = 2.8 Hz, 1H), 4.70 (dt, *J* = 16.8, 2.8 Hz, 1H), 4.43 (ddd, *J* = 16.8, 3.7, 1.4 Hz, 1H), 2.46 – 2.37 (m, 1H), 2.23 – 2.15 (m, 1H), 2.04 (s, 3H), 1.95 (ddd, *J* = 13.3, 5.3, 2.1 Hz, 2H), 1.81 – 1.76 (m, 2H), 1.62 – 1.59 (m, 1H), 1.32 (ddd, *J* = 13.8, 4.2, 2.5 Hz, 1H), 1.23 (s, 3H), 1.01 (s, 3H), 0.95 (s, 3H).

^{13}C NMR (151 MHz, $CDCl_3$): δ 174.28, 170.54, 167.50, 125.81, 74.06, 68.18, 45.16, 40.76, 35.15, 33.22, 32.88, 22.45, 21.52, 21.47, 21.43, 21.41, 17.89.

ν_{max}/cm^{-1} (film): 2924, 2855, 1757, 1738, 1240.

HRMS: APCI (*m/z*) calcd for $C_{17}H_{25}O_4$ [M+H$^+$]:

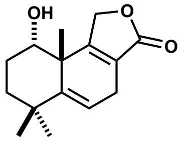

(9*S*,9a*S*)-9-hydroxy-6,6,9a-trimethyl-4,6,7,8,9,9a-hexahydronaphtho[1,2-*c*]furan-3(1*H*)-one ((±)-3.15)

In a vial open to air was added **(±)-3.6** (14.9 mg, 0.05 mmol, 1 equiv) in methanol (0.08M) and the solution was cool to 0 ˚C. An aqueous 10% potassium hydroxide solution (410 μL, 0.75 mmol, 15 equiv) was added dropwise and the solution was stirred at 0 ˚C for 2 hours. The reaction was diluted with water and quenched with aqueous 1N HCl. The solution was extracted with three portions of diethyl ether and the combined organic layers were dried over anhydrous sodium sulfate and concentrated *in vacuo* resulting in an off-white amorphous powder. The title compound was purified on silica column chromatography eluting with 50-100% diethyl ether in hexanes and isolated as an off-white amorphous powder (12.2 mg, >98% yield). The product was visualized on TLC with UV light and after heat activation with $KMnO_4$.

R_f = 0.31 (100% diethyl ether)

^{1}H NMR (600 MHz, $CDCl_3$): δ 5.96 (dd, *J* = 4.9, 2.6 Hz, 1H), 5.00 (dt, *J* = 16.3, 2.5 Hz, 1H), 4.87 (ddd, *J* = 16.3, 3.3, 1.4 Hz, 1H), 3.81 (s, 1H), 2.97 (dd, *J* = 22.3, 1.5 Hz, 1H), 2.82 (dd, *J* = 22.2, 2.7 Hz, 1H), 2.24 – 2.13 (m, 1H), 1.78 – 1.67 (m, 2H), 1.39 (s, 3H), 1.38 – 1.33 (m, 1H), 1.23 (s, 3H), 1.21 (s, 3H).

^{13}C NMR (151 MHz, $CDCl_3$): δ 173.90, 166.36, 143.91, 143.89, 123.77, 123.75, 121.00, 120.97, 72.54, 69.36, 43.64, 35.87, 33.63, 32.82, 32.80, 30.38, 26.96, 25.37, 22.56.

ν_{max}/cm^{-1} (film):

HRMS: APCI (*m/z*) calcd for $C_{15}H_{21}O_3$ [M+H$^+$]: 249.14852, found 249.14868.

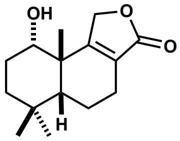

(5a*R*,9*S*,9a*S*)-9-hydroxy-6,6,9a-trimethyl-4,5,5a,6,7,8,9,9a-octahydronaphtho[1,2-*c*]furan-3(1*H*)-one ((±)-3.16)

The title compound was prepared following the hydrolysis procedure for the synthesis of **(±)-3.6**; **(±)-3.13** (19.5 mg, 0.07 mmol, 1 equiv), aqueous 10% KOH (600 µL, 1.05 mmol, 15 equiv) in methanol (0.08M), yielded the title compound (17.4 mg, >98% yield) as an amorphous off-white solid. The product was visualized on TLC after heat activation with $KMnO_4$.

R_f = 0.65 (100% diethyl ether)

^{1}H NMR (600 MHz, CDCl$_3$): δ 5.04 – 4.92 (m, 2H), 3.55 (dd, *J* = 11.8, 3.9 Hz, 1H), 2.36 (dtt, *J* = 18.6, 9.2, 2.9 Hz, 1H), 2.27 (ddt, *J* = 16.3, 8.5, 2.8 Hz, 1H), 2.08 (dddd, *J* = 15.3, 9.1, 7.1, 2.8 Hz, 2H), 1.71 – 1.64 (m, 1H), 1.48 (dd, *J* = 12.6, 2.7 Hz, 1H), 1.46 – 1.39 (m, 2H), 1.34 (s, 3H), 0.99 (s, 3H), 0.80 (s, 3H).

^{13}C NMR (151 MHz, CDCl$_3$): δ 174.51, 165.55, 126.48, 78.65, 71.98, 48.94, 42.63, 40.34, 34.67, 32.58, 29.58, 29.23, 22.82, 18.80, 17.74.

ν_{max}/cm^{-1} (film): 3459, 2924, 2854, 1731, 1461.

HRMS: APCI (*m/z*) calcd for $C_{15}H_{23}O_3$ [M+H$^+$]: 251.16417, found 251.16347.

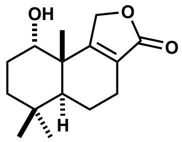

(5a*S*,9*S*,9a*S*)-9-hydroxy-6,6,9a-trimethyl-4,5,5a,6,7,8,9,9a-octahydronaphtho[1,2-*c*]furan-3(1*H*)-one ((±)-3.17)

In a flame dried vial under argon was added **(±)-3.15** (21.4 mg, 0.07 mmol, 1 equiv) in anhydrous 2-proponal (0.1M). Prior to use, 2-proponal was dried for 72 hours over 4Å MS and distileed over CaH (10% w/v). Once **(±)-3.15** was completely dissolved, phenylsilane (10 µL, 0.07 mmol, 1 equiv) and tert-butyl hydroeroxide (5M in decane, 20 µL, 0.105 mmol, 1.5 equiv) were added and the solution was degassed with argon for 10 minutes. Subsequently Tris(2,2,6,6-tetramethyl-**3**,5-heptanedionato)manganese(III) (8.5 mg, 0.014 mmol, 20 mol%) was added and the reaction was degassed for no more than 30 seconds. The vial was sealed and heated to reflux for 2 hours. After 3 hours, the solution was cooled to room temperature and concentrated *in vacuo*. The concentrate was directly loaded onto a silica column for purification and eluted with 50-100% diethyl ether in hexanes. Both the *trans* and *cis* products were obtained as amorphous white powders (*trans:* 17.1 mg, 83%; *cis:* 2.7 mg, 13%; 6.3:1.0 isolated d.r.) and visualized on TLC after heat activation with KMnO$_4$.

R$_f$ = 0.63 (100% diethyl ether)

^{1}H NMR (600 MHz, CDCl$_3$): δ 4.97 (ddd, *J* = 16.5, 3.7, 1.5 Hz, 1H), 4.75 (dt, *J* = 16.4, 2.7 Hz, 1H), 2.44 – 2.35 (m, 1H), 2.18 (dddd, *J* = 18.0, 11.6, 7.2, 3.3 Hz, 1H), 2.06 (tdd, *J* = 14.7, 4.4, 2.3 Hz, 1H), 1.93 (dd, *J* = 13.5, 7.0 Hz, 1H), 1.74 (dd, *J* = 12.7, 2.0 Hz, 1H), 1.69 (td, *J* = 14.1, 4.2 Hz, 1H), 1.62 – 1.59 (m, 1H), 1.39 (d, *J* = 4.5 Hz, 1H), 1.32 (ddd, *J* = 13.8, 4.7, 3.0 Hz, 1H), 1.17 (s, 3H), 1.00 (s, 3H), 0.93 (s, 3H).

^{13}C NMR (151 MHz, CDCl$_3$): δ 174.75, 169.22, 125.22, 71.65, 68.84, 43.99, 41.85, 34.49, 33.21, 33.08, 26.00, 21.82, 21.37, 17.87.

ν$_{max}$/cm^{-1} (film): 3468, 2940, 2872, 1735, 1137.

HRMS: APCI (*m/z*) calcd for $C_{15}H_{23}O_4$ [M+H$^+$]: 251.16417, found 251.16444.

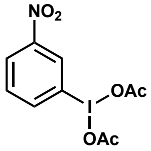

(3-Nitrophenyl)-λ^3-iodanediyl diacetate (3.19)

The title compound is known and was prepared following literature procedure. To a stirring solution of 3-nitroiodobenze (1 g, 4 mmol, 1 equiv) in acetonitrile (0.5M) was added 13.4 mL of sodium hypochlorite (5% w/v) followed by dropwise addition of 8 mL concentrated hydrochloric acid. The reaction was stirred at room temperature for 90 minutes resulting in a yellow suspension. The solid was collected by filtration and washed with water (3 x 2 mL) and hexanes (3 x 2 mL) and dried under reduced pressure resulting in a sparkly yellow solid (1.25 g, 98% yield). Dichloro(3-nitrophenyl)-λ^3-iodane was carried forward without characterization. In a flame dried flask under an argon atmosphere were added dichloro(3-nitrophenyl)-λ^3-iodane (1.25 g, 3.9 mmol, 1 equiv) and anhydrous sodium acetate (640 mg, 7.8 mmol, 1 equiv) in anhydrous acetonitrile (0.5M). The reaction was stirred overnight at room temperature. The suspension was filtered over a pad of celite and concentrated *in vacuo*. The title compound was isolated after recrystallization from 1:1 acetic acid:hexane as an off-white powder (1.05 g, 73% yield) and matched reported spectra[16].

^{1}H NMR (400 MHz, $CDCl_3$): δ 8.94 (t, *J* = 1.9 Hz, 1H), 8.44 (ddd, *J* = 8.3, 2.2, 1.0 Hz, 1H), 8.39 (ddd, *J* = 8.0, 1.7, 1.0 Hz, 1H), 7.72 (t, *J* = 8.1 Hz, 1H), 2.04 (s, 6H).

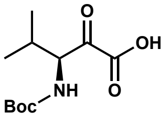

(*S*)-3-((*Tert*-butoxycarbonyl)amino)-4-methyl-2-oxopentanoic acid (3.20)

The title compound is known and was prepared following literature procedure[17]. Boc amino acid (1.00 equiv) was dissolved in dry *N,N*-dimethylformamide (0.1 M) and cooled to 0 °C. NEt^{i}Pr2 (3.00 equiv) and T3P (50 % w/w in ethyl acetate; 1.00 equiv) were successively added and the mixture was stirred for 5 min before the addition of 1-cyanomethyl-tetrahydrothiophenium bromide (1.00 equiv). The reaction was stirred for 1 h at 0 °C. The mixture was diluted with CH2Cl2 and washed with saturated aqueous sodium bicarbonate (3x150 mL), water (3x100 mL) and brine. The organic layer was dried over anhydrous sodium sulfate and concentrated *in vacuo* to give the desired product, which was used without further purification in the next step.

Boc-(*S*)-AA Cyanosulfurylide (1.00 equiv) was dissolved in THF/H_2O (2:1, 40.0 mM) and Oxone (1.50 equiv) was added in one portion. The suspension was stirred for 90 minutes. The mixture was diluted with ethyl acetate and separated. The organic layer was washed with saturated aqueous ammonium chloride (100 mL). The aqueous phase was extracted with ethyl acetate (3x50 mL). The combined organic layers were washed with brine, dried over anhydrous sodium sulfate and concentrated *in vacuo*. The crude product was used in the next step without further purification and matched reported characterization[18].

6.5.3. Chapter 4

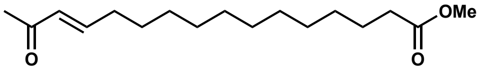

Methyl (*E*)-15-oxohexadec-13-enoate (4.10). In a flame dried flask equipped with a metal stir bar were added methyl tetradec-13-enoate **4.8** (83.0 mg, 0.345 mmol, 1 equiv) in diethyl ether (0.5M), methyl vinyl ketone (0.09 mL, 1.04 mmol, 3 equiv), Grubbs Catalyst, 2nd Generation (5.8 mg, 6.9 µmol, 2 mol %), and CuI (2.00 mg, 0.01 mmol, 3 mol %). The solution was stirred under argon at room temperature overnight, quenched with a saturated aqueous solution of ammonium chloride and extracted with three portions of ethyl acetate. The combined organic layers were washed with brine, dried over anhydrous magnesium sulfate, and concentrated *in vacuo*. The resulting brown residue was purified *via* column chromatography resulting in 80.0 mg of a yellow oil (83% yield).

^{1}H NMR (400 MHz, CDCl$_3$): δ 6.78 (td, J = 15.0, 6.8 Hz, 1H), 6.04 (d, J = 15.9 Hz, 1H), 3.64 (s, 3H), 2.27 (t, J = 7.0 Hz, 2H), 2.22 (s, 3H), 2.22 (m, 2H), 1.67–1.52 (m, 2H), 1.49–1.36 (m, 2H), 1.32–1.06 (m, 14H)

^{13}C NMR (100 MHz, CDCl$_3$): δ 198.9, 174.4, 148.8, 131.4, 51.5, 34.2, 32.6, 29.60, 29.56, 29.49, 29.45, 29.32, 29.26, 29.22, 28.2, 26.9, 25.0

HRMS: ESI (*m/z*) calcd for $C_{17}H_{31}O_3$ [M+H$^+$]: 283.22677, found 283.22663.

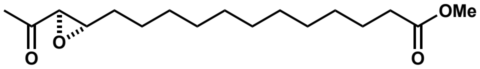

Methyl 12-((2*S,3*R**)-3-acetyloxiran-2-yl)dodecanoate ((±)-4.12)**. To a stirred solution of alkene **4.10** (104 mg, 0.36 mmol, 1 equiv) and *tert*-butylamine (2.6 mg, 0.04 mmol, 1 mol %) in methanol (2.5 mL) at 0 ˚C were slowly added 30% by weight hydrogen peroxide (0.20 mL, 1.8 mmol, 5 equiv). The solution was allowed to warm to room temperature and stirred overnight. The reaction was quenched with a 1:1 mixture of saturated aqueous sodium thiosulfate and aqueous sodium bicarbonate and extracted with three portions of dichloromethane. The combined organic layers were dried over anhydrous magnesium sulfate and concentrated *in vacuo*. The resulting solid was purified *via* column chromatography resulting in 48 mg of a white solid (45% yield).

^{1}H NMR (400 MHz, $CDCl_3$): δ 3.63 (s, 3H), 3.15 (d, J = 1.9 Hz, 1H), 3.04 (m, 1H), 2.27 (t, J = 7.6 Hz, 2H), 2.03 (s, 3H), 1.67–1.48 (m, 2H), 1.48–1.35 (m, 4H), 1.28–1.16 (m, 14H)

^{13}C NMR (100 MHz, $CDCl_3$): δ 206.0, 174.3, 59.9, 58.0, 51.4, 34.0, 31.7, 29.7, 29.44, 29.38, 29.37, 29.34, 29.2, 29.1, 25.7, 24.9, 24.3

HRMS: ESI (*m/z*) calcd for $C_{17}H_{31}O_3$ [M+H$^+$]: 299.22169, found 299.22170.

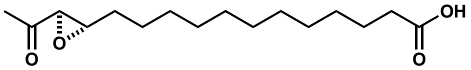

12-((2*S,3*R**)-3-acetyloxiran-2-yl)dodecanoic acid ((±)-4.5)**. Methyl ester **4.10** (24 mg, 0.08 mmol, 1 equiv) was dissolved in a mixture of 0.2 mL of acetone and 1.8 mL phosphate buffer (pH=7). Pig liver enzyme (PLE E3019-3.5KU–Aldrich) (10 mg) was added and the cloudy white suspension was stirred at 37 ˚C for 3 hours. The suspension was diluted with brine, extracted with three portions of ethyl acetate, dried over anhydrous magnesium sulfate, and concentrated *in vacuo*. The resulting white solid was purified *via* column chromatography (9 mg, 40% yield).

^{1}H NMR (600 MHz, $CDCl_3$): δ 3.18 (d, J = 1.8 Hz, 1H), 3.10-3.03 (m, 1H), 2.34 (t, J = 7.5 Hz, 2H), 2.06 (s, 3H), 1.73–1.37 (m, 6H), 1.37–1.19 (m, 14H)

^{13}C NMR (150 MHz, $CDCl_3$): δ 206.4, 179.7, 60.1, 58.3, 34.1, 31.9, 29.8, 29.6, 29.54, 29.49, 29.4, 29.3, 29.2, 25.1, 24.8, 24.5

HRMS ESI (*m/z*) calcd for $C_{16}H_{29}O_4$ [M+H$^+$]: 285.20604, found 285.20586.

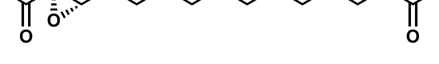

Methyl 12-((2*S*,3*R*)-3-acetyloxiran-2-yl)dodecanoate ((+)-4.12). 9-amino-*epi*-Quinidine (35 mg, 0.12 mmol, 30 mol %) was added to a solution of trifluoroacetic acid (67.8 mg, 0.6 mmol, 1.5 equiv) in 2 mL of dioxane. Alkene **4.10** (112 mg, 0.4 mmol, 1 equiv) was added and the solution was stirred at 50 ˚C. After 15 minutes, 30% by weight sodium hydroxide (0.1 mL, 0.6 mmol, 1.5 equiv) were added and the solution was stirred overnight. The reaction was quenched with a saturated aqueous solution of ammonium chloride and extracted with three portions of ethyl acetate. The combined organic layers were dried over anhydrous magnesium sulfate and concentrated *in vacuo*. To the resulting white solid were added 2 mL anhydrous methanol and 1 M solution of sodium methoxide in methanol (0.4 mL, 0.4 mmol, 1 equiv). After two hours, the reaction was quenched with a saturated aqueous solution of ammonium chloride and extracted with three portions of ethyl acetate. The combined organic layers were dried over anhydrous magnesium sulfate and concentrated *in vacuo*. Purification was performed by column chromatography resulting in 40.3 mg of a low melting point off-white solid (40 mg, 34% yield).

$[\alpha]_D^{20}$ = +14.5 (*c* 1.00, $CHCl_3$)

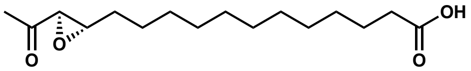

12-((2*S*,3*R*)-3-acetyloxiran-2-yl)dodecanoic acid ((+)-4.5). Methyl ester (+)-**4.12** (20 mg, 0.07 mmol, 1 equiv) was dissolved in a mixture of 0.2 mL of acetone and 1.8 mL phosphate buffer (pH=7). Pig liver enzyme (PLE E3019-3.5KU–Aldrich) (10 mg) were added and the cloudy white suspension was stirred at 37 ˚C for 3 hours. The suspension was diluted with brine, extracted with ethyl acetate, dried over anhydrous magnesium sulfate, and concentrated *in vacuo*. The resulting low melting point white solid was purified *via* column chromatography (16 mg, 80% yield).

^{1}H NMR (600 MHz, CD_3OD): δ 3.24 (d, *J* = 1.9 Hz, 1H), 3.12 (ddd, *J* = 6.4, 3.6, 1.8 Hz, 2H), 2.27 (t, *J* = 7.4 Hz, 2H), 2.06 (s, 3H), 1.51–1.75 (m, 6H), 1.42-1.52 (m, 2H), 1.16-1.43 (m, 12H)

^{13}C NMR (150 MHz, CD_3OD): δ 208.0 177.9, 60.8, 59.4, 35.1, 32.9, 30.63, 30.60, 30.57, 30.56, 30.41, 30.38, 30.24, 26.9, 26.1, 24.8

$[\alpha]_D^{20}$ = +3.3 (*c* 0.28, MeOH)

6.5.4. Chapter 5

Experimental procedures and physical data of compounds. To a flame-dried round-bottom flask charged with a Teflon-coated stir bar and $AlCl_3$ (1.0 equiv.), was diluted in CH_2Cl_2 (0.5 M) under inert atmosphere and left to stir. Substituted phenol (1.0 equiv.) was added portion-wise at 0 ºC, followed by slow addition of thionyl chloride (1.0 equiv.) over 30 minutes. The mixture was warmed to ambient temperature and monitored by TLC (35% EtOAc in hexanes). Upon consumption of starting materials, the reaction mixture was poured into ice water and separated with EtOAc. The combined organic layers were washed with brine, dried ($MgSO_4$), filtered, and concentrated *in vacuo* to yield crude sulfoxide product. Crystallization was achieved from boiling toluene and was checked by direct-injection for LRMS in negative ion mode. Sulfoxide material was carried through to the next step without additional characterization.

To a round-bottom flask charged with a Teflon-coated stir bar and sulfoxide material from the previous step (1.0 equiv.), was diluted in glacial acetic acid (0.1 M). Zinc dust (10.0 equiv.) was added to the mixture under inert atmosphere and left to stir. The reaction was refluxed at 100 ºC for 4 hours and monitored by TLC (35% EtOAc in hexanes). Upon completion, the reaction mixture was cooled to ambient temperature and passed through a plug of celite. The resulting solution was diluted in EtOAc and washed with a saturated solution of sodium bicarbonate (2×). The combined organic layers were further washed with water (3×), and brine (3×), dried ($MgSO_4$), filtered, and concentrated *in vacuo* to yield crude sulfide product. Crude product was diluted in a solution of methanol and CH_2Cl_2 (1:1) and checked by direct-injection for LRMS in negative ion mode. Crystallization was achieved from boiling CH_2Cl_2 and subjected for characterization.

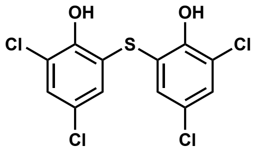

6,6'-thio-bis-(2,4-dichlorophenol) (**bithionol, 5.1**): Crystallization was achieved from hot CH_2Cl_2 to yield 3.75 g (10.5 mmol) of a white crystalline powder in 73% yield over two steps.

m.p. = 184-186 ºC.

^{1}H NMR (400 MHz, $(CD_3)_2CO$): δ 9.08 (s, 2H), 7.45 (dd, J = 4.9, 2.5 Hz, 2H), 7.13 (dd, J = 4.8, 2.5 Hz, 2H) ppm

^{13}CNMR (125 MHz, $(CD_3)_2CO$): δ 151.91, 131.24, 130.09, 125.53, 124.05, 122.78 ppm

ν_{max}/cm^{-1} (film): 3391, 3338 cm^{-1}

HRMS (ESI– TOF) *m/z*: calculated for $C_{12}H_5Cl_4O_2S$ [$(M - H)^-$] 352.87698, observed 352.87690 (Δ = 0.08 mmu).

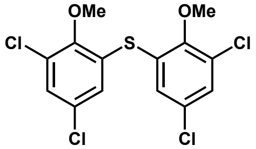

bis-(3,5-Dichloro-2-methoxyphenyl)-sulfane (**5.2**): To a solution of bithionol (100 mg, 0.280 mmol, 1.0 equiv.) in DMF (0.3 M) was added K_2CO_3 (165 mg, 1.19 mmol, 4.25 equiv.) and Me_2SO_4 (94 µL, 0.980 mmol, 3.5 equiv.). The resulting mixture was stirred overnight at room temperature and monitored by TLC (35% EtOAc in hexanes). Upon completion, the reaction was quenched water and separated from EtOAc (3×). The combined organic layers were washed with water (2×) and brine (3×), dried ($MgSO_4$), filtered, and concentrated *in vacuo* to afford clear, pale yellow oil. Purification by column chromatography (silica gel, 20% EtOAc in hexanes) yielded 87 mg (81%) of **9** as clear, colorless oil.

^{1}H NMR (400 MHz, $(CD_3)_2CO$): δ 7.51 (d, J = 2.2 Hz, 2H), 7.15 (d, J = 2.2 Hz, 2H), 3.90 (s, 6H) ppm.

ν_{max}/cm^{-1} (film): 3070, 2937 cm^{-1}

HRMS: (ESI+ TOF) *m/z*: calculated for $C_{14}H_{11}O_2Cl_4S$ [$(M + H)^+$] 382.92284, observed 382.92295 (Δ = 0.11 mmu)

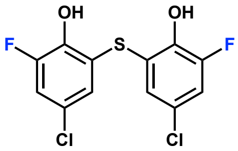

6,6'-thio-bis-(4-chloro-2-fluorophenol) (**5.3**): Isolated 170 mg (0.525 mmol) of a white powder in 65% yield over two steps (recrystallization solvent, CH_2Cl_2).

m.p. = 159-161 ºC.

^{1}H NMR (400 MHz, $(CD_3)_2CO$): δ 8.61 (br s, 2H), 7.27 (dd, J = 8.1, 3.0 Hz, 2H), 6.92 (dd, J = 8.3, 3.0 Hz, 2H) ppm

ν_{max}/cm^{-1} (film): 3301 cm^{-1}, 3081 cm^{-1}

HRMS (ESI– TOF) *m/z*: calculated for $C_{12}H_5Cl_2F_2O_2S$ [(M – H)$^-$] 320.93609, observed 320.93612 (Δ = 0.03 mmu).

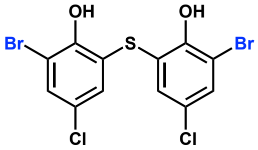

6,6'-thio-bis-(2-bromo-4-chlorophenol) (**5.4**): Isolated 325 mg (0.730 mmol) off-white powder in 69% yield over two steps (recrystallization solvent, CH_2Cl_2).

m.p. = 178-180 ºC**.**

^{1}H NMR (400 MHz, $(CD_3)_2CO$): δ 8.92 (br s, 2H), 7.59 (d, J = 2.1 Hz, 2H), 7.18 (d, J = 1.3 Hz, 2H) ppm

ν_{max}/cm^{-1} (film): 3355, 3064 cm^{-1}

HRMS: (ESI– TOF) *m/z*: calculated for $C_{12}H_5Br_2Cl_2O_2S$ [(M – H)$^-$] 440.77595, observed 440.77607 (Δ = 0.12 mmu).

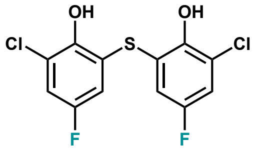

6,6'-thio-bis-(2-chloro-4-fluorophenol) (**5.5**): Isolated 225 mg (0.696 mmol) of an off-white powder in 51% yield over two steps (recrystallization solvent, CH_2Cl_2).

m.p. = 140-142 ºC

^{1}H NMR (400 MHz, $(CD_3)_2CO$): δ 8.64 (br s, 2H), 7.25 (dd, J = 8.1, 3.0 Hz, 2H), 6.90 (dd, J = 8.3, 3.0 Hz, 2H) ppm

ν_{max}/cm^{-1} (film): 3340 cm^{-1}

HRMS: (ESI– TOF) *m/z*: calculated for $C_{12}H_5Cl_2F_2O_2S$ [(M – H)$^-$] 320.93609, observed 320.93608 (Δ = 0.01 mmu).

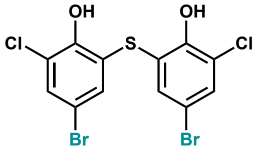

6,6'-thio-bis-(4-bromo-2-chlorophenol) (**5.6**): Isolated 249 mg (0.560 mmol) of a pale lavender powder (54% yield over two steps) (recrystallization solvent, CH_2Cl_2).

m.p. = 200-202 ºC

^{1}H NMR (400 MHz, $(CD_3)_2CO$): δ 7.46 (s, 2H), 7.36 (s, 2H) ppm

ν_{max}/cm^{-1} (film): 3063 cm^{-1}

HRMS: (ESI– TOF) *m/z*: calculated for $C_{12}H_5Br_2Cl_2O_2S$ [(M – H)$^-$] 440.77595, observed 440.77643 (Δ = 0.48 mmu)

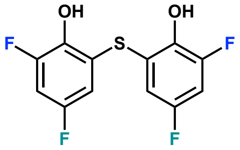

6,6'-thio-bis-(2,4-difluorophenol) (**5.7**): Isolated 163 mg (0.558 mmol) of a beige powder in 52% yield over two steps (recrystallization solvent, CH_2Cl_2).

m.p. = 127-130 ºC

^{1}H NMR (400 MHz, $(CD_3)_2CO$): δ 8.99 (s, 2H), 7.06 (ddd, J = 10.6, 8.5, 3.0 Hz, 2H), 6.75 (ddd, J = 8.6, 3.0, 1.9 Hz, 2H) ppm

ν_{max}/cm^{-1} (film): 3317, 3091 cm^{-1}

HRMS: (ESI– TOF) *m/z*: calculated for $C_{12}H_5F_4O_2S$ [$(M - H)^-$] 288.99519, observed 288.99519 (Δ = 0.00 mmu)

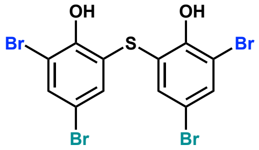

6,6'-thio-bis-(2,4-dibromophenol) (**5.8**): Isolated 67.6 mg (0.151 mmol) of an off-white powder in 58% yield over two steps (recrystallization solvent, CH_2Cl_2).

m.p. = 164-166 ºC

^{1}H NMR (400 MHz, $(CD_3)_2CO$) (rotamers): δ 9.36 (br, s, 2H), 7.29-7.25 (m, 2H), 6.99-7.00 (m, 2H) ppm

ν_{max}/cm^{-1} (film): 3364, 3057, 2921 cm^{-1}

HRMS: (ESI– TOF) *m/z*: calculated for $C_{12}H_5Br_4O_2S$ [$(M - H)^-$] 528.67492, observed 528.67482 (Δ = 0.10 mmu)

6.6 Crystal analysis

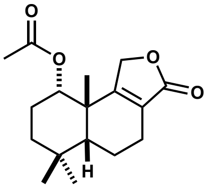

(5a*R*,9*S*,9a*S*)-6,6,9a-Trimethyl-3-oxo-1,3,4,5,5a,6,7,8,9,9a-decahydronaphtho[1,2-*c*]furan-9-yl acetate ((±)-3.13)

Submitted by: **Ingrid Wilt**

Solved by: **John Bacsa, Ingrid Wilt**

***R_1*=4.74%**

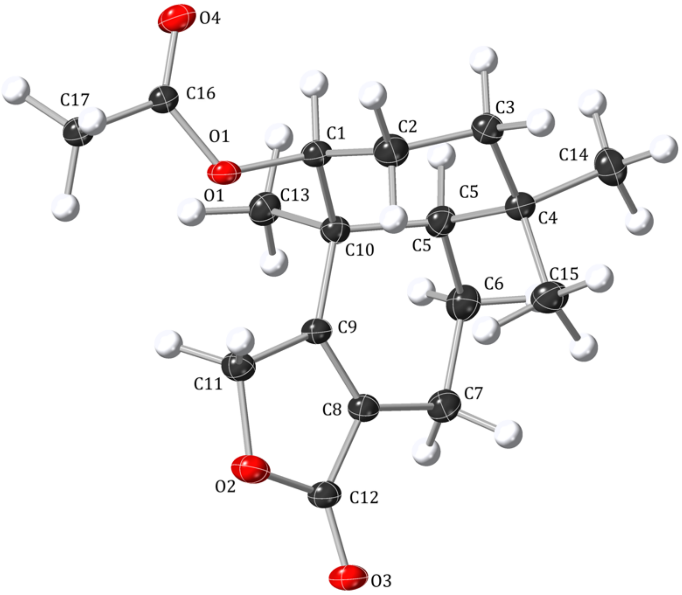
O4
C17
C16
O1
C1
C2
C3
C14
O1
C13
C10
C5
C5
C4
C15
C6
C9
C11
C8
C7
O2
C12
O3

Experimental. Single colorless plate-shaped crystals of **(±)-3.13** were used as supplied. A suitable crystal with dimensions 0.54 × 0.30 × 0.10 mm^3 was selected and mounted on a loop with paratone on a XtaLAB Synergy S diffractometer. The crystal was kept at a constant T = 101(1) K during data collection. The structure was solved with the **ShelXT** (Sheldrick, 2015) solution program using iterative methods and by using **Olex2** 1.5-alpha (Dolomanov et al., 2009) as the graphical interface. The model was refined with **olex2.refine** 1.5-alpha (Bourhis et al., 2015) using full matrix least squares minimisation on $\boldsymbol{F^2}$.

Crystal Data. $C_{17}H_{24}O_4$, M_r = 292.378, orthorhombic, $P2_12_12_1$ (No. 19), a = 6.5421(3) Å, b = 8.9749(4) Å, c = 25.7971(10) Å, $a = b = g = 90^{\circ}$, V = 1514.67(11) Å^3, T = 101(1) K, Z = 4, Z' = 1, m(Cu K_a) = 0.729, 14963 reflections measured, 2874 unique (R_{int} = 0.0455) which were used in all calculations. The final wR_2 was 0.1420 (all data) and R_1 was 0.0474 (I≥2 s(I)).

Compound	**(±)-3.13**
Formula	$C_{17}H_{24}O_4$
$D_{calc.}$/ g cm^{-3}	1.282
m/mm^{-1}	0.729
Formula Weight	292.378
Color	colorless
Shape	plate-shaped
Size/mm^3	0.54×0.30×0.10
T/K	101(1)
Crystal System	orthorhombic
Flack Parameter	-0.12(8)
Hooft Parameter	-0.12(8)
Space Group	$P2_12_12_1$
a/Å	6.5421(3)
b/Å	8.9749(4)
c/Å	25.7971(10)
a/°	90
b/°	90
g/°	90
V/Å^3	1514.67(11)
Z	4
Z'	1
Wavelength/Å	1.54184

Radiation type	Cu K_a
$Q_{min}/^{\circ}$	3.43
$Q_{max}/^{\circ}$	72.46
Measured Refl's.	14963
Indep't Refl's	2874
Refl's I≥2 *s*(I)	2778
R_{int}	0.0455
Parameters	207
Restraints	28
Largest Peak	0.4214
Deepest Hole	-0.2136
GooF	1.0503
wR_2 (all data)	0.1420
wR_2	0.1412
R_1 (all data)	0.0485
R_1	0.0474

Structure Quality Indicators

Reflections:

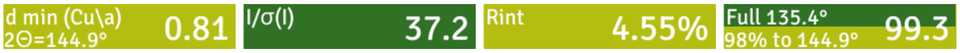

d min (Cu\a) 2Θ=144.9° 0.81	I/σ(I) 37.2	Rint 4.55%	Full 135.4° 98% to 144.9° 99.3

Refinement:

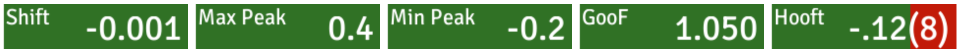

Shift -0.001	Max Peak 0.4	Min Peak -0.2	GooF 1.050	Hooft -.12(8)

A colourless plate-shaped-shaped crystal with dimensions 0.54 × 0.30 × 0.10 mm^3 was mounted on a loop with paratone. Data were collected using a XtaLAB Synergy, Dualflex, HyPix diffractometer equipped with an Oxford Cryosystems low-temperature device operating at T = 101(1) K.

Data were measured using *w* scans with Cu K$_a$ radiation. The diffraction pattern was indexed and the total number of runs and images was based on the strategy calculation from the program CrysAlisPro 1.171.41.116a (Rigaku OD, 2021). The maximum resolution that was achieved was *Q* = 72.46° (0.81 Å).

The unit cell was refined using CrysAlisPro 1.171.41.116a (Rigaku OD, 2021) on 3592 reflections, 24% of the observed reflections.

Data reduction, scaling and absorption corrections were performed using CrysAlisPro 1.171.41.116a (Rigaku OD, 2021). The final completeness is 99.07 % out to 72.46° in *Q*. A numerical absorption correction based on gaussian integration over a multifaceted crystal model was performed using CrysAlisPro 1.171.41.116a (Rigaku Oxford Diffraction, 2021). An empirical absorption correction using spherical harmonics, implemented in SCALE3 ABSPACK scaling algorithm was also applied. The absorption coefficient *m* of this material is 0.729 mm^{-1} at this wavelength (*l* = 1.54184Å) and the minimum and maximum transmissions are 0.311 and 1.000.

The structure was solved and the space group $P2_12_12_1$ (# 19) determined by the ShelXT (Sheldrick, 2015) structure solution program using using iterative methods and refined by full matrix least squares minimisation on $\boldsymbol{F}^2$ using version of **olex2.refine** 1.5-alpha (Bourhis et al., 2015). Most hydrogen atom positions were calculated geometrically and refined using the riding model, but some hydrogen atoms were refined freely.

Refinement was by using NoSpherA2, an implementation of non-spherical atom-form-factors (F. Kleemiss, H. Puschmann, O. Dolomanov, S.Grabowsky - https://doi.org/10.1039/D0SC05526C – 2020). NoSpherA2 implementation of HAR makes use of tailor-made aspherical atomic form factors calculated from a Hirshfeld-partitioned electron density (ED) not from spherical-atom form factors. The ED was calculated from a Gaussian basis set single determinant SCF wavefunction from DFT using selected functionals for a fragment of this crystal. The following options were used: SOFTWARE: ORCA PARTITIONING: NoSpherA2 INT ACCURACY: Normal METHOD: PBE BASIS SET: def2-TZVP CHARGE: 0 MULTIPLICITY: 1 DATE: 2021-09-29_15-42-12

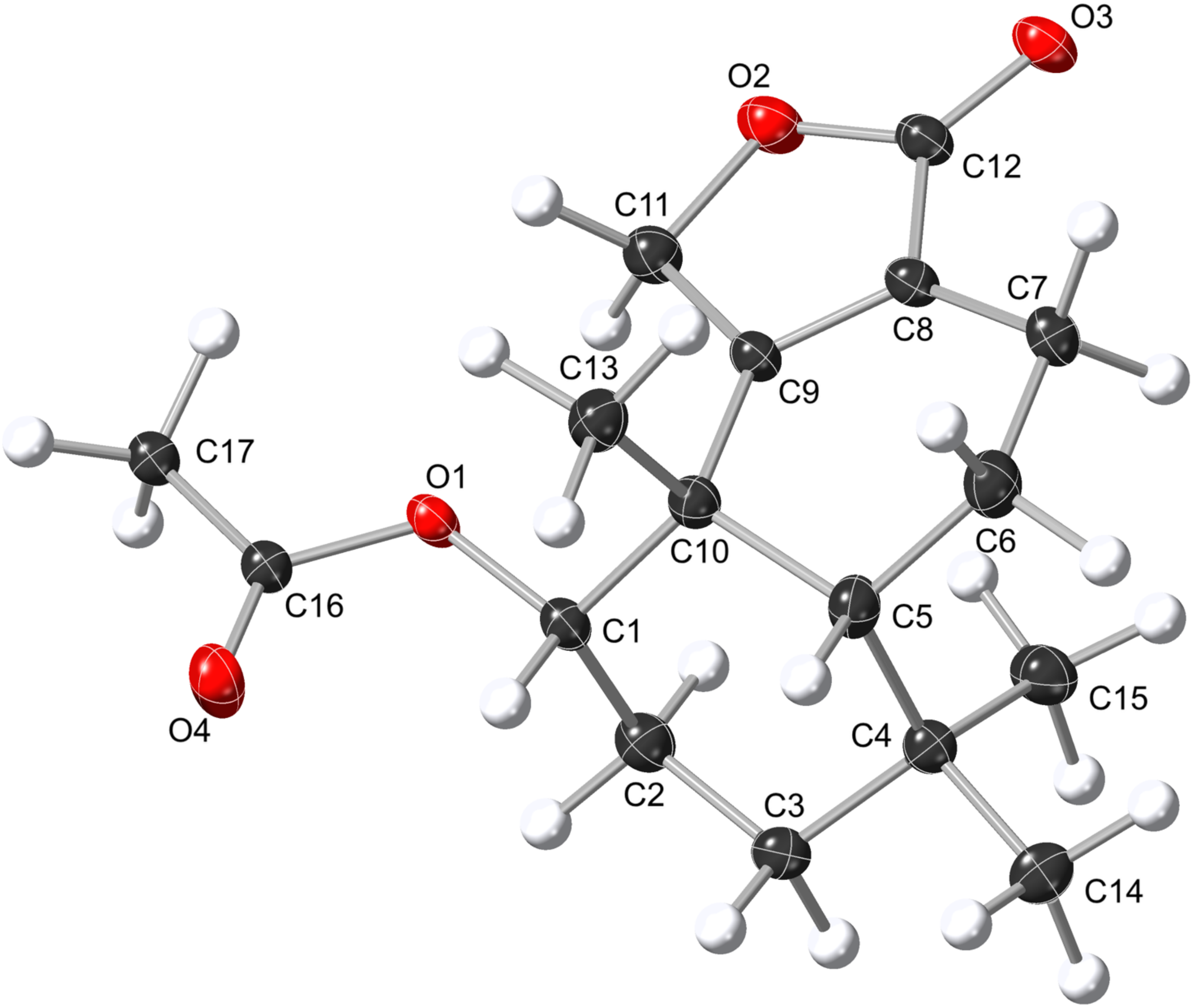
O3
O2
C12
C11
C7
C8
C13
C9
C17
O1
C6
C10
C16
C5
C1
C15
O4
C4
C2
C3
C14

Figure 2: A view of the molecular structure, atom C1 and C10 has S configuration and C5, R.

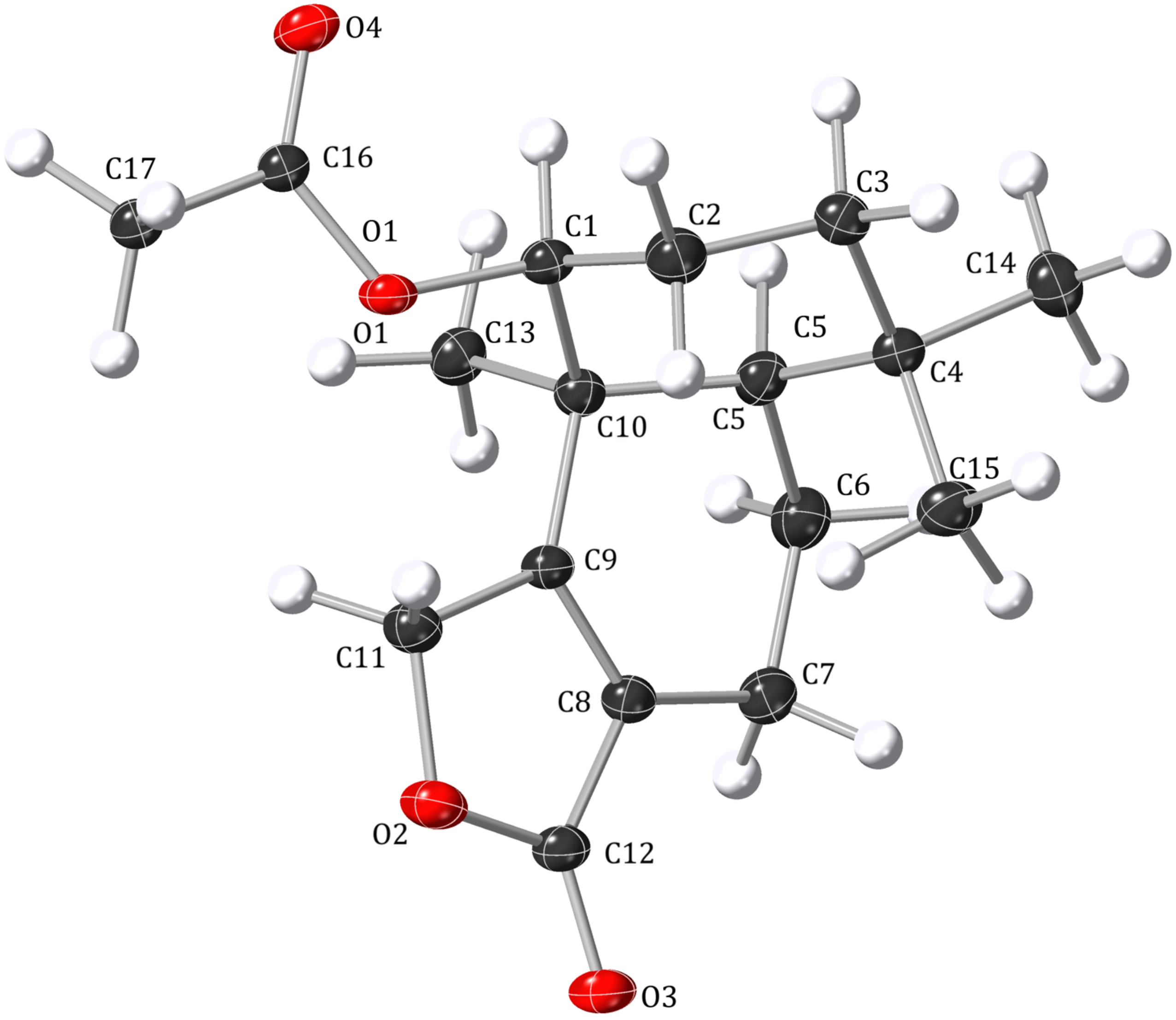
O4
C16
C17
O1
C1
C2
C3
C14
O1
C13
C5
C4
C10
C5
C15
C6
C9
C11
C7
C8
O2
C12
O3

Figure 3: A view of the molecular structure showing the chair conformation of the ring C1-C2-C3-C4-C5-C10. This ring is in a chair conformation with some twisting towards a half-chair conformation.

Data Plots: Diffraction Data

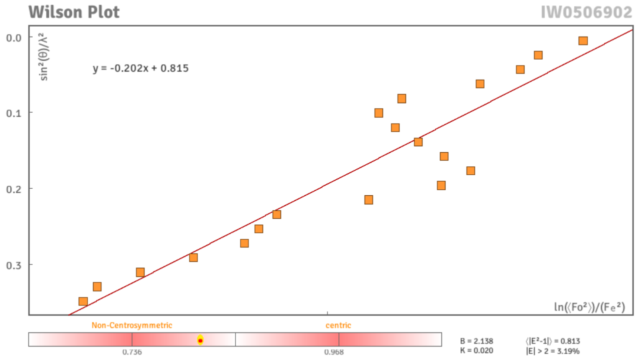

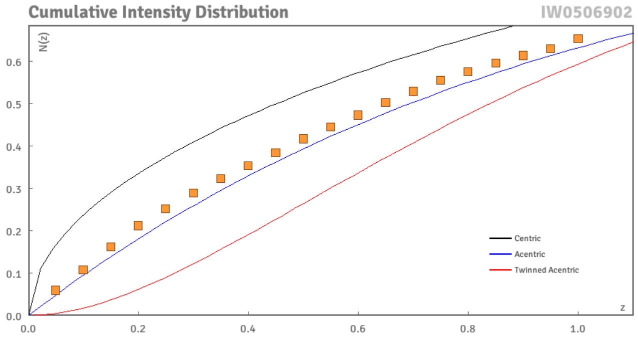

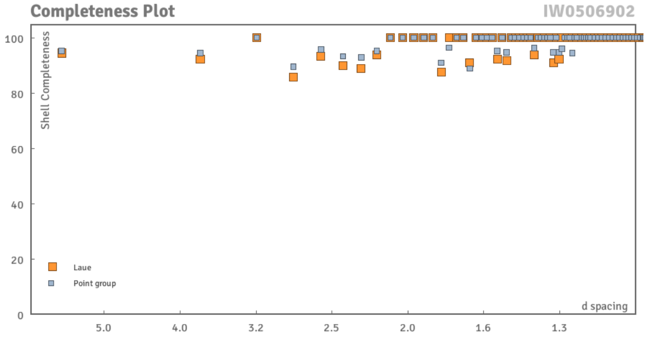

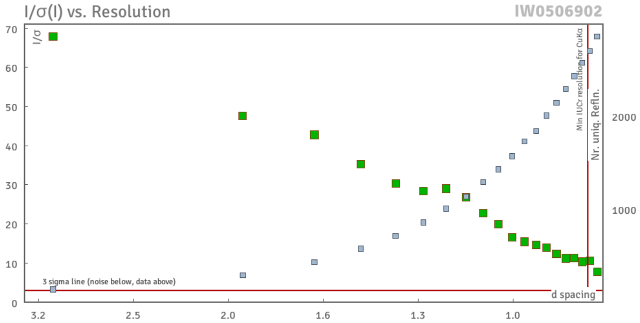

Data Plots: Refinement and Data

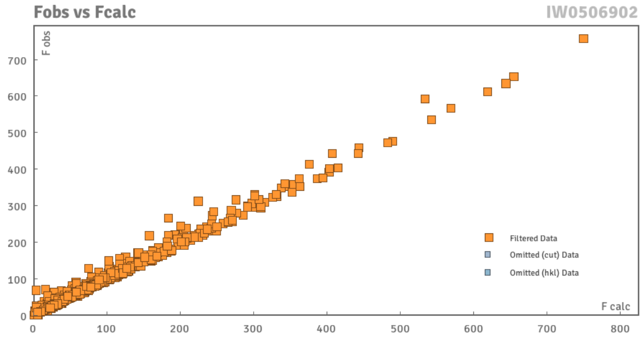

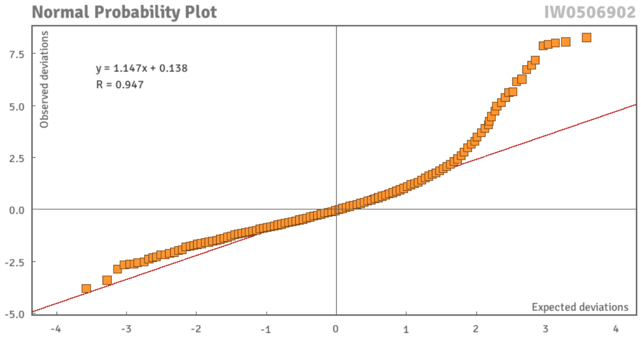

Reflection Statistics

Total reflections (after filtering)	14963	Unique reflections	2877
Completeness	0.96	Mean I/*s*	24.14
hkl_{max} collected	(6, 10, 31)	hkl_{min} collected	(-7, -10, -30)
hkl_{max} used	(7, 10, 31)	hkl_{min} used	(-7, 0, 0)
Lim d_{max} collected	100.0	Lim d_{min} collected	0.77
d_{max} used	12.9	d_{min} used	0.81
Friedel pairs	1928	Friedel pairs merged	0
Inconsistent equivalents	3	R_{int}	0.0455
R_{sigma}	0.0269	Intensity transformed	0
Omitted reflections	0	Omitted by user (OMIT hkl)	17
Multiplicity	(3201, 1949, 1106, 502, 222, 125, 63, 24, 5)	Maximum multiplicity	19
Removed systematic	0	Filtered off (Shel/OMIT)	0

absences

Table 1: Fractional Atomic Coordinates (×10^4) and Equivalent Isotropic Displacement Parameters ($Å^2$×10^3) for **IW0506902**. U_{eq} is defined as 1/3 of the trace of the orthogonalised U_{ij}.

Atom	**x**	**y**	**z**	$\mathbf{U_{eq}}$
O2	428(2)	6417.7(19)	2547.4(6)	26.3(4)
O3	1700(3)	4934(2)	1925.7(6)	30.7(4)
O1	1302(2)	7230.8(18)	4118.6(5)	21.1(4)
O4	2105(3)	8224(2)	4893.7(6)	33.6(5)
C11	914(3)	6770(3)	3079.9(8)	21.9(5)
C14	5499(5)	1678(3)	4108.3(10)	36.9(6)
C9	2713(3)	5799(3)	3208.1(8)	17.3(4)
C10	3924(3)	5758(2)	3702.9(8)	17.9(4)
C1	2633(3)	5962(3)	4193.3(8)	19.6(5)
C2	1322(4)	4625(3)	4333.3(9)	25.4(5)
C3	2715(4)	3302(3)	4422.0(9)	26.4(5)
C4	3944(4)	2868(3)	3937.4(8)	23.6(5)
C5	5148(3)	4261(3)	3733.8(9)	21.6(5)
C6	6315(4)	3971(3)	3223.3(10)	26.0(5)
C7	5022(4)	4013(3)	2723.1(9)	26.4(5)
C8	3248(3)	5054(3)	2776.9(8)	20.3(5)
C12	1796(4)	5404(3)	2364.6(8)	22.1(5)
C13	5433(4)	7079(3)	3686.5(9)	23.4(5)
C16	1102(3)	8231(3)	4502.6(8)	19.9(4)

Atom	x	y	z	***U**$_{eq}$*
C17	-547(4)	9332(3)	4376.2(8)	21.9(5)
C15	2513(4)	2138(3)	3538.4(9)	30.9(6)

Table 2: Anisotropic Displacement Parameters (×10^4) for **IW0506902**. The anisotropic displacement factor exponent takes the form: $-2p^{2}[h^{2}a^{*2} \times U_{11}+ \ldots +2hka^{*} \times b^{*} \times U_{12}]$

Atom	U_{11}	U_{22}	U_{33}	U_{23}	U_{13}	U_{12}
O2	27.6(9)	33.5(9)	17.8(7)	3.2(7)	-4.3(7)	0.3(7)
O3	47.2(10)	30.4(10)	14.4(8)	-2.3(8)	-4.2(7)	-2.1(7)
O1	24.8(8)	26.2(8)	12.4(7)	6.0(7)	-2.0(6)	-2.7(6)
O4	43.2(10)	33.5(10)	24.0(9)	12.9(8)	-13.1(8)	-11.5(8)
C11	20.3(10)	25.8(12)	19.6(10)	3.4(9)	-2.6(8)	-0.5(9)
C14	56.5(17)	26.5(13)	27.7(12)	12.9(13)	-1.1(12)	2.7(11)
C9	18.1(10)	20.0(10)	13.7(10)	0.2(8)	-0.3(8)	-1.2(8)
C10	17.8(10)	18.4(10)	17.6(10)	-0.1(8)	-1.4(8)	-1.1(8)
C1	23.5(10)	21.0(11)	14.4(10)	2.2(9)	0.3(8)	-2.0(9)
C2	28.3(12)	27.0(12)	20.8(11)	2.2(10)	4.5(9)	-0.2(9)
C3	38.7(13)	21.8(12)	18.8(11)	-0.4(10)	0.6(10)	1.4(9)
C4	34.5(12)	19.2(11)	17.2(10)	1.1(10)	-3.0(9)	-1.5(9)
C5	21.2(10)	20.3(11)	23.3(11)	3.5(8)	-3.9(8)	-4.0(9)
C6	24.0(11)	26.8(12)	27.2(12)	5.8(10)	2.8(9)	-2.9(10)
C7	35.1(13)	25.5(12)	18.8(11)	5.3(10)	5.9(9)	-2.5(10)

Atom	U_{11}	U_{22}	U_{33}	U_{23}	U_{13}	U_{12}
C8	25.8(11)	20.6(11)	14.4(10)	-0.3(9)	2.2(8)	0.1(8)
C12	30.1(11)	22.0(11)	14.3(10)	-3.4(9)	0.1(8)	-0.6(8)
C13	23.7(11)	20.8(11)	25.8(11)	-3.6(9)	-3.4(9)	-2.1(9)
C16	24.0(10)	19.5(10)	16.3(10)	1.8(8)	0.1(8)	-1.3(8)
C17	27.6(11)	20.8(11)	17.1(10)	2.6(9)	1.5(9)	-1.4(9)
C15	45.6(15)	25.8(12)	21.3(11)	-11.0(11)	-1.7(10)	-0.7(10)

Table 3: Bond Lengths in Å for **IW0506902**.

Atom	Atom	Length/Å
O2	C11	1.445(3)
O2	C12	1.361(3)
O3	C12	1.210(3)
O1	C1	1.446(3)
O1	C16	1.343(3)
O4	C16	1.204(3)
C11	C9	1.501(3)
C14	C4	1.540(3)
C9	C10	1.502(3)
C9	C8	1.344(3)
C10	C1	1.532(3)
C10	C5	1.566(3)

Atom	Atom	Length/Å
C10	C13	1.543(3)
C1	C2	1.518(3)
C2	C3	1.514(3)
C3	C4	1.537(3)
C4	C5	1.568(3)
C4	C15	1.538(3)
C5	C6	1.544(3)
C6	C7	1.543(3)
C7	C8	1.496(3)
C8	C12	1.460(3)
C16	C17	1.499(3)

Table 4: Bond Angles in ° for **IW0506902**.

Atom	Atom	Atom	Angle/°
C12	O2	C11	109.33(17)
C16	O1	C1	119.11(16)
C9	C11	O2	104.79(18)
C10	C9	C11	127.94(19)
C8	C9	C11	108.08(19)
C8	C9	C10	123.60(19)
C1	C10	C9	114.09(17)
C5	C10	C9	109.53(17)
C5	C10	C1	110.02(18)
C13	C10	C9	107.14(17)
C13	C10	C1	106.45(18)
C13	C10	C5	109.47(17)
C10	C1	O1	108.41(17)
C2	C1	O1	108.29(17)
C2	C1	C10	114.40(18)
C3	C2	C1	108.39(18)
C4	C3	C2	113.01(19)
C3	C4	C14	106.78(19)
C5	C4	C14	108.5(2)
C5	C4	C3	109.45(19)
C15	C4	C14	107.3(2)
C15	C4	C3	109.5(2)
C15	C4	C5	114.93(19)
C4	C5	C10	116.35(18)
C6	C5	C10	110.73(19)
C6	C5	C4	113.54(18)
C7	C6	C5	115.96(18)
C8	C7	C6	111.30(18)
C7	C8	C9	126.1(2)
C12	C8	C9	109.0(2)
C12	C8	C7	124.8(2)
O3	C12	O2	121.6(2)
C8	C12	O2	108.62(18)
C8	C12	O3	129.8(2)
O4	C16	O1	124.2(2)
C17	C16	O1	110.50(18)
C17	C16	O4	125.3(2)

Table 5: Torsion Angles in ° for **IW0506902**.

Atom	Atom	Atom	Atom	Angle/°
O2	C11	C9	C10	176.64(15)
O2	C11	C9	C8	3.5(2)
O2	C12	C8	C9	2.4(2)
O2	C12	C8	C7	-178.30(17)
O3	C12	C8	C9	-177.5(3)
O3	C12	C8	C7	1.7(3)
O1	C1	C10	C9	-48.05(19)
O1	C1	C10	C5	-171.60(16)
O1	C1	C10	C13	69.89(18)
O1	C1	C2	C3	-178.92(17)
C11	C9	C10	C1	37.6(3)
C11	C9	C10	C5	161.4(2)
C11	C9	C10	C13	-80.0(2)
C11	C9	C8	C7	177.09(18)
C11	C9	C8	C12	-3.6(2)
C14	C4	C3	C2	171.8(2)
C14	C4	C5	C10	-161.73(18)
C14	C4	C5	C6	67.98(19)
C9	C10	C1	C2	72.9(2)
C9	C10	C5	C4	-82.59(17)
C9	C10	C5	C6	49.02(18)
C9	C8	C7	C6	-4.2(3)
C10	C1	C2	C3	60.07(19)
C10	C5	C4	C3	-45.6(2)

Atom	**Atom**	**Atom**	**Atom**	**Angle/°**
C10	C5	C4	C15	78.1(2)
C10	C5	C6	C7	-53.6(2)
C1	C2	C3	C4	-61.9(2)
C2	C3	C4	C5	54.6(2)
C2	C3	C4	C15	-72.3(2)
C3	C4	C5	C6	-175.86(17)
C4	C5	C6	C7	79.5(2)
C5	C6	C7	C8	29.8(2)
C6	C7	C8	C12	176.63(18)

Table 6: Hydrogen Fractional Atomic Coordinates (×10^4) and Equivalent Isotropic Displacement Parameters (Å^2×10^3) for **IW0506902**. U_{eq} is defined as 1/3 of the trace of the orthogonalised U_{ij}.

Atom	**x**	**y**	**z**	U_{eq}
H16a	6555(7)	2159(4)	4383.9(18)	55.4(9)
H16b	4700(6)	757(6)	4287.1(14)	55.4(9)
H16c	6334(7)	1282(4)	3774(2)	55.4(9)
H1a	-470(30)	6590(40)	3305(12)	55.4(9)
H1b	1300(50)	7937(15)	3145(14)	55.4(9)
H4	3646(10)	6197(3)	4514(3)	29.5(7)
H5a	448(6)	4858(3)	4682(2)	30.4(6)
H5b	257(7)	4385(3)	4021(2)	30.4(6)

Atom	x	y	z	U_{eq}
H6a	3770(8)	3564(3)	4734(2)	31.7(6)
H6b	1800(7)	2356(7)	4543.7(12)	31.7(6)
H8	6344(11)	4461(3)	4025(3)	32.4(7)
H9a	7524(9)	4796(6)	3189.1(10)	39.0(8)
H9b	7040(6)	2884(8)	3249.6(10)	39.0(8)
H10a	5971(7)	4370(4)	2403(2)	39.7(8)
H10b	4465(5)	2905(8)	2637.7(11)	39.7(8)
H13a	6412(6)	7048(3)	4029(2)	35.1(7)
H13b	6376(6)	6999(3)	3338(2)	35.1(7)
H13c	4578(6)	8125(6)	3680.5(9)	35.1(7)
H15a	-1992(8)	8940(3)	4531.7(12)	32.8(7)
H15b	-173(4)	10403(6)	4546.9(12)	32.8(7)
H15c	-670(4)	9449(3)	3959(2)	32.8(7)
H17a	3416(6)	1666(4)	3224.8(19)	46.4(9)
H17b	1637(6)	1259(6)	3725.2(13)	46.4(9)
H17c	1475(7)	2972(5)	3383.2(12)	46.4(9)

Table 7: Selected Bond Lengths in Å for **IW0506902**.

Atom	Atom	Length/Å	Atom	Atom	Length/Å
C11	H1a	1.087(8)	C14	H16a	1.081(6)
C11	H1b	1.090(8)	C14	H16b	1.081(6)

Atom	Atom	Length/Å
C14	H16c	1.081(6)
C1	H4	1.082(10)
C2	H5a	1.087(6)
C2	H5b	1.087(6)
C3	H6a	1.086(7)
C3	H6b	1.086(7)
C5	H8	1.100(10)
C6	H9a	1.087(7)
C6	H9b	1.087(7)
C7	H10a	1.082(7)

Atom	Atom	Length/Å
C7	H10b	1.082(7)
C13	H13a	1.093(6)
C13	H13b	1.093(6)
C13	H13c	1.093(6)
C17	H15a	1.085(6)
C17	H15b	1.085(6)
C17	H15c	1.085(6)
C15	H17a	1.087(6)
C15	H17b	1.087(6)
C15	H17c	1.087(6)

Table 8: Selected Bond Angles in ° for **IW0506902**.

Atom	Atom	Atom	Angle/°
H1a	C11	O2	107.1(19)
H1b	C11	O2	114(2)
H1b	C11	H1a	104.4(16)
C9	C11	H1a	116.7(19)
C9	C11	H1b	110.0(19)
H16b	C14	H16a	109.5
H16c	C14	H16a	109.5
H16c	C14	H16b	109.5

Atom	Atom	Atom	Angle/°
C4	C14	H16a	109.5
C4	C14	H16b	109.5
C4	C14	H16c	109.5
H4	C1	O1	108.54(10)
H4	C1	C10	108.54(11)
C2	C1	H4	108.54(12)
H5a	C2	C1	110.02(12)
H5b	C2	C1	110.02(12)

Atom	Atom	Atom	Angle/°
H5b	C2	H5a	108.4
C3	C2	H5a	110.02(12)
C3	C2	H5b	110.02(13)
H6a	C3	C2	108.98(13)
H6b	C3	C2	108.98(13)
H6b	C3	H6a	107.8
C4	C3	H6a	108.98(13)
C4	C3	H6b	108.98(13)
H8	C5	C10	105.00(11)
H8	C5	C4	105.00(12)
C6	C5	H8	105.00(12)
H9a	C6	C5	108.29(13)
H9b	C6	C5	108.29(12)
H9b	C6	H9a	107.4
C7	C6	H9a	108.29(13)
C7	C6	H9b	108.29(12)
H10a	C7	C6	109.37(13)
H10b	C7	C6	109.37(13)
H10b	C7	H10a	108.0
C8	C7	H10a	109.37(12)
C8	C7	H10b	109.37(13)
H13a	C13	C10	109.5
H13b	C13	C10	109.5
H13b	C13	H13a	109.5

Atom	Atom	Atom	Angle/°
H13c	C13	C10	109.5
H13c	C13	H13a	109.5
H13c	C13	H13b	109.5
H15a	C17	C16	109.5
H15b	C17	C16	109.5
H15b	C17	H15a	109.5
H15c	C17	C16	109.5
H15c	C17	H15a	109.5
H15c	C17	H15b	109.5
H17a	C15	C4	109.5
H17b	C15	C4	109.5
H17b	C15	H17a	109.5
H17c	C15	C4	109.5
H17c	C15	H17a	109.5
H17c	C15	H17b	109.5

Single crystal citations

CrysAlisPro (Rigaku, V1.171.41.116a, 2021)

CrysAlisPro (ROD), Rigaku Oxford Diffraction, Poland.

L.J. Bourhis and O.V. Dolomanov and R.J. Gildea and J.A.K. Howard and H. Puschmann, The Anatomy of a Comprehensive Constrained, Restrained, Refinement Program for the Modern Computing Environment - Olex2 Disected, *Acta Cryst. A*, (2015), **A71**, 59-71.

O.V. Dolomanov and L.J. Bourhis and R.J. Gildea and J.A.K. Howard and H. Puschmann, Olex2: A complete structure solution, refinement and analysis program, *J. Appl. Cryst.*, (2009), **42**, 339-341.

Sheldrick, G.M., ShelXT-Integrated space-group and crystal-structure determination, *Acta Cryst.*, (2015), **A71**, 3-8.

6.7 SI References

1. Coffinier, R.; El Assal, M.; Peixoto, P. A.; Bosset, C.; Miqueu, K.; Sotiropoulos, J. M.; Pouysegu, L.; Quideau, S., Total Synthesis of (-)-Bacchopetiolone via an Asymmetric Hydroxylative Phenol Dearomatization/[4+2]-Dimerization Cascade Promoted by a Novel Salen-Type Chiral Iodane. *Org. Lett.* **2016,** *18* (5), 1120-3.
2. Fletcher, C. J.; Blair, D. J.; Wheelhouse, K. M. P.; Aggarwal, V. K., The total synthesis of (−)-aplysin via a lithiation–borylation–propenylation sequence. *Tetrahedron* **2012,** *68* (37), 7598-7604.
3. Nave, S.; Sonawane, R. P.; Elford, T. G.; Aggarwal, V. K., Protodeboronation of Tertiary Boronic Esters: Asymmetric Synthesis of Tertiary Alkyl Stereogenic Centers. *J. Am. Chem. Soc.* **2010,** *132* (48), 17096-17098.
4. Coffinier, R.; Assal, M. E.; Peixoto, P. A.; Bosset, C.; Miqueu, K.; Sotiropoulos, J.-M.; Pouységu, L.; Quideau, S., Total Synthesis of (−)-Bacchopetiolone via an Asymmetric Hydroxylative Phenol Dearomatization/[4+2]-Dimerization Cascade Promoted by a Novel Salen-Type Chiral Iodane. *Org. Lett.* **2016,** *18* (5), 1120-1123.
5. Montiel, L. E.; Zepeda, L. G.; Tamariz, J., Efficient Total Synthesis of Racemic Bisabolane Sesquiterpenes Curcuphenol and Xanthorrhizol Starting from Substituted Acetophenones. *Helv. Chim.* **2010,** *93* (7), 1261-1273.
6. Bieszczad, B.; Gilheany, D. G., Asymmetric Grignard Synthesis of Tertiary Alcohols through Rational Ligand Design. *Angew. Chem. Int. Ed.* **2017,** *56* (15), 4272-4276.
7. Mikula, H.; Skrinjar, P.; Sohr, B.; Ellmer, D.; Hametner, C.; Fröhlich, J., Total synthesis of masked Alternaria mycotoxins—sulfates and glucosides of alternariol (AOH) and alternariol-9-methyl ether (AME). *Tetrahedron* **2013,** *69* (48), 10322-10330.
8. O'Brien, P.; Warren, S., Synthesis of (R)- or (S)-diphenylphosphinoyl hydroxy aldehydes and 1,2-diols using Mukaiyama's bicyclic aminal methodology and Sharpless asymmetric dihydroxylation. *J. Chem. Soc. Perkin. Trans. I* **1996,** (17), 2129-2138.
9. Zhang, C.; Ito, S.; Hosoda, N.; Asami, M., First asymmetric total synthesis of (+)-curcutetraol. *Tetrahedron Lett.* **2008,** *49* (16), 2552-2554.

10. Huang, X.; He, W.; Peng, L.; Tang, L.; Wang, L.; Bai, Q. Preparation method of Venetoclax intermediate and product. CN109320516 (A), 2019/02/12/, 2019.

11. Gibbons, P.; Lai, K. W.; Nilewski, C.; Pastor, R. M.; Staben, S. T.; Stivala, C.; Zhu, B.-Y.; Chen, H. Sulfonimidamide Compounds as Nlrp3 Modulators. WO2021150574 (A1), 2021/07/29/, 2021.

12. Li, X. D.; Li, X. M.; Xu, G. M.; Zhang, P.; Wang, B. G., Antimicrobial Phenolic Bisabolanes and Related Derivatives from Penicillium aculeatum SD-321, a Deep Sea Sediment-Derived Fungus. *J. Nat. Prod.* **2015,** *78* (4), 844-9.

13. Yadav, S.; Taylor, C. M., Synthesis of orthogonally protected (2S)-2-amino-adipic acid (alpha-AAA) and (2S,4R)-2-amino-4-hydroxyadipic acid (Ahad). *J. Org. Chem.* **2013,** *78* (11), 5401-9.

14. Harrington, P. M.; Singh, B. K.; Szamosi, I. T.; Birk, J. H., Synthesis and Herbicidal Activity of Cyperin. *J. Agric. Food Chem.* **1995,** *43* (3), 804-808.

15. Kanematsu, K.; Nagashima, S., An efficient synthesis of a key intermediate of forskolin. *J. Chem. Soc., Chem. Commun.* **1989,** (15), 1028-1029.

16. Nanjo, T.; Kato, N.; Takemoto, Y., Oxidative Decarboxylation Enables Chemoselective, Racemization-Free Esterification: Coupling of alpha-Ketoacids and Alcohols Mediated by Hypervalent Iodine(III). *Org. Lett.* **2018,** *20* (18), 5766-5769.

17. Thuaud, F.; Rohrbacher, F.; Zwicky, A.; Bode, J. W., Incorporation of Acid-Labile Masking Groups for the Traceless Synthesis of C-Terminal Peptide α-Ketoacids. *Org. Lett.* **2016,** *18* (15), 3670-3673.

18. Huang, R.-Z.; Zhang, B.; Huang, X.-C.; Liang, G.-B.; Qin, J.-M.; Pan, Y.-M.; Liao, Z.-X.; Wang, H.-S., Synthesis and biological evaluation of terminal functionalized thiourea-containing dipeptides as antitumor agents. *RSC Adv.* **2017,** *7* (15), 8866-8878.

7.1. Appendix chapter 2

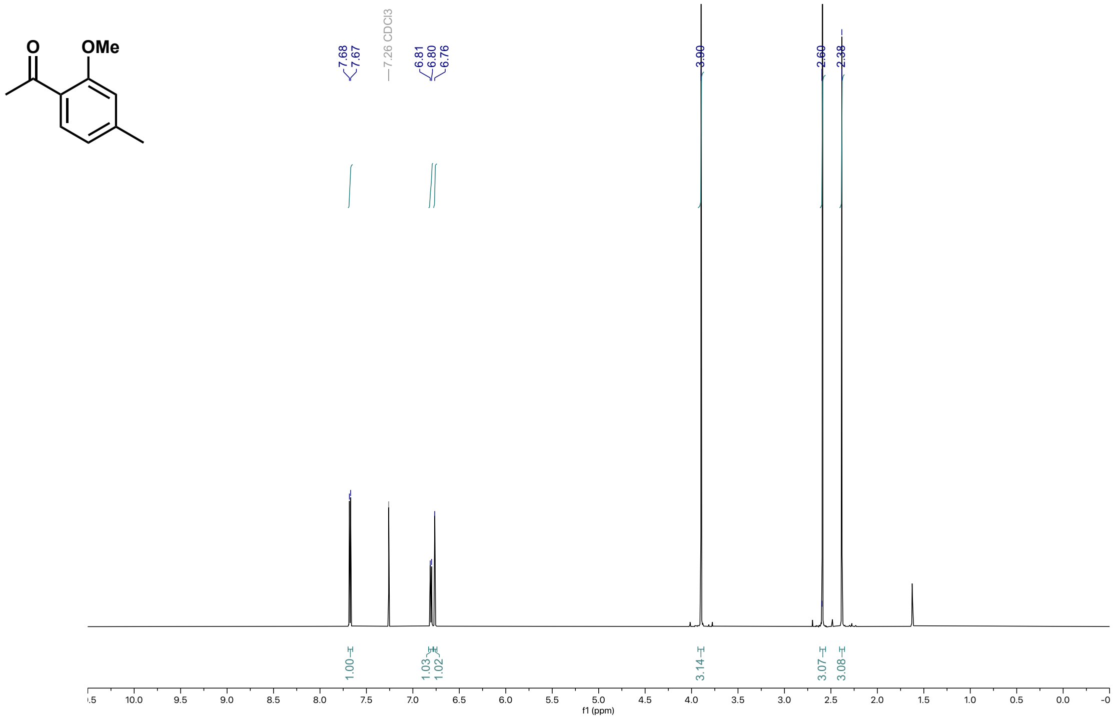

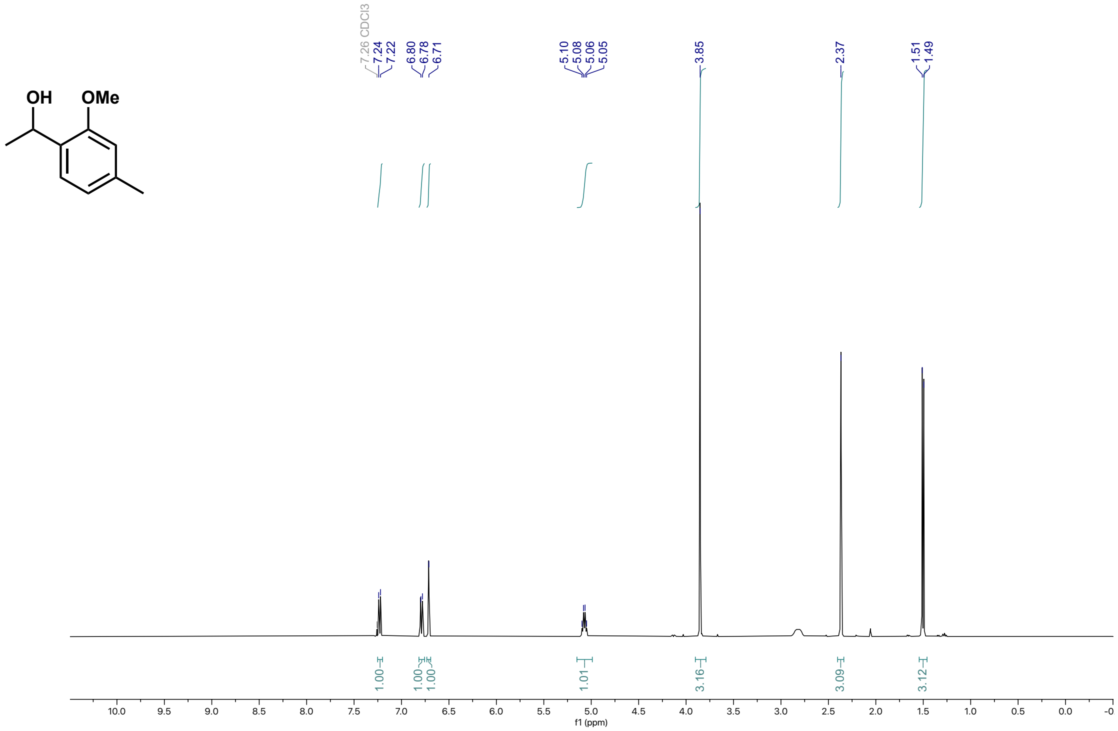

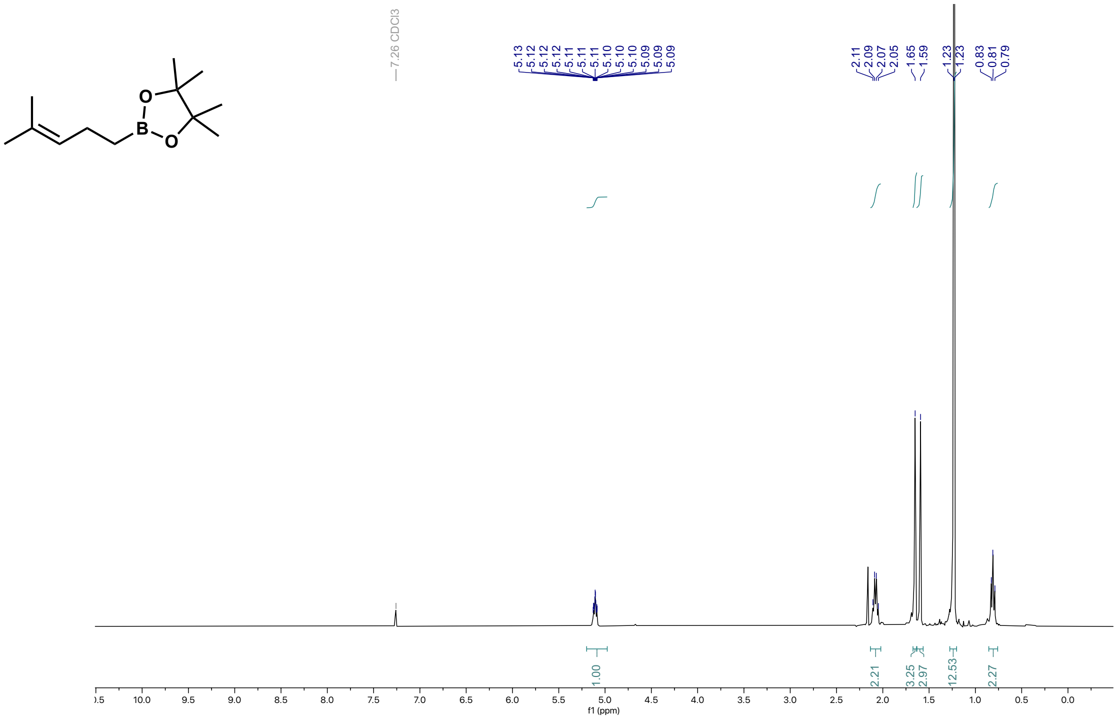
7.26 CDCl3
5.13
5.12
5.12
5.11
5.11
5.11
5.10
5.10
5.09
5.09
2.11
2.09
2.07
2.05
1.65
1.59
1.23
1.23
0.83
0.81
0.79
1.00
2.21
3.25
2.97
12.53
2.27
f1 (ppm)

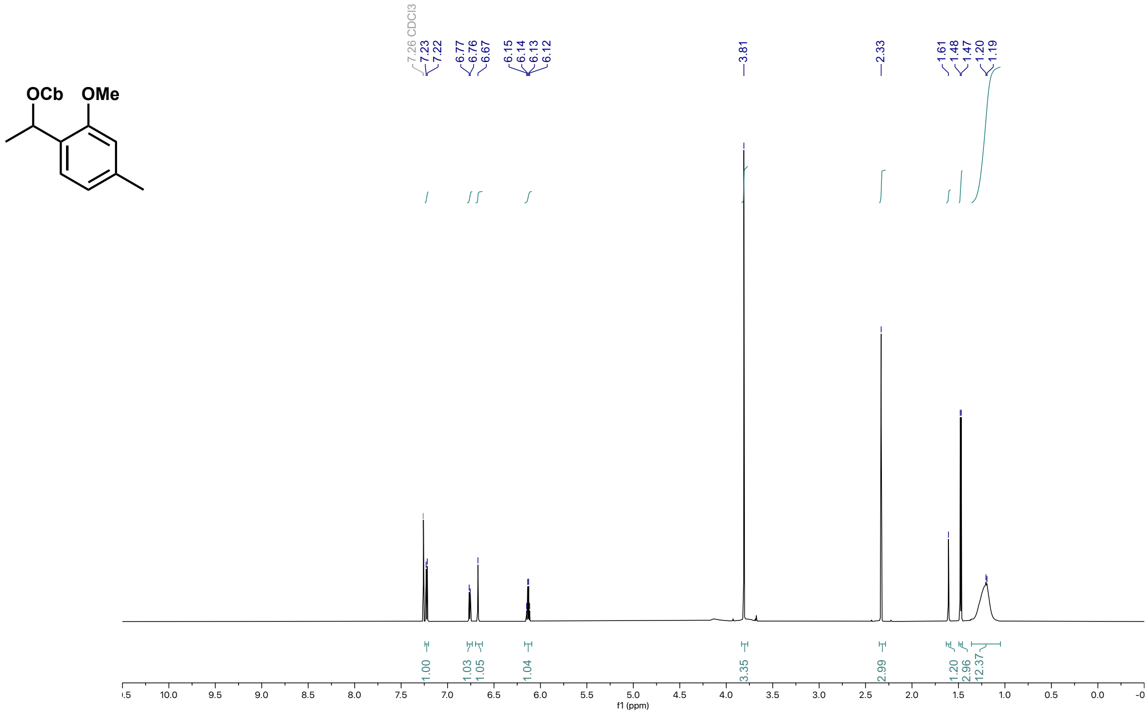
OCb
OMe
7.26 CDCl3
7.23
7.22
6.77
6.76
6.67
6.15
6.14
6.13
6.12
3.81
2.33
1.61
1.48
1.47
1.20
1.19
1.00
1.03
1.05
1.04
3.35
2.99
1.20
2.96
12.37
f1 (ppm)

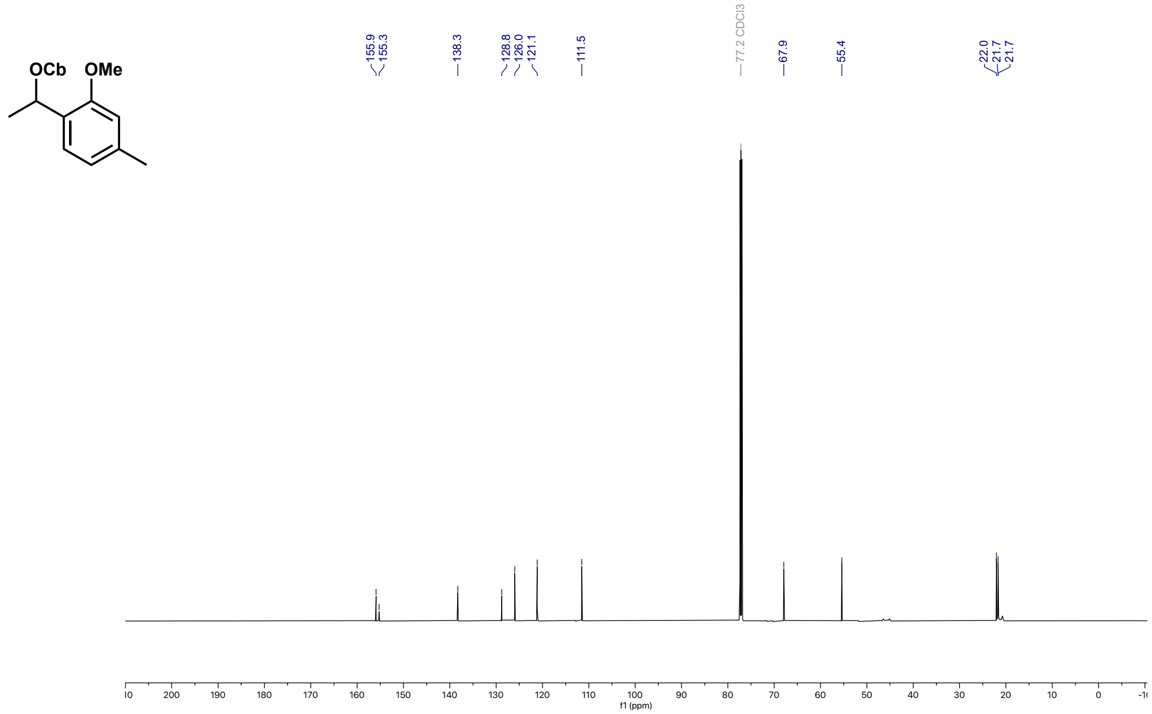
OCb
OMe
155.9
155.3
138.3
128.8
126.0
121.1
111.5
77.2 CDCl3
67.9
55.4
22.0
21.7
21.7
200
190
180
170
160
150
140
130
120
110
100
90
80
70
60
50
40
30
20
10
0
f1 (ppm)

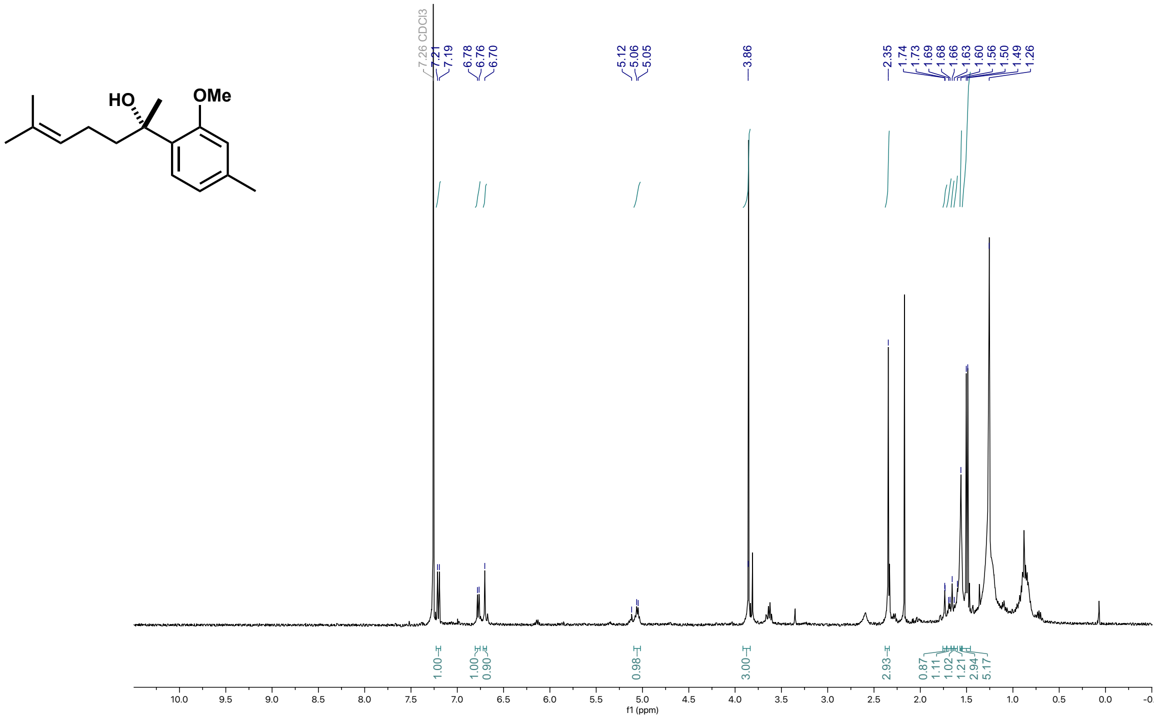
HO
OMe
7.26 CDCl3
7.21
7.19
6.78
6.76
6.70
5.12
5.06
5.05
3.86
2.35
1.74
1.73
1.69
1.68
1.66
1.63
1.60
1.56
1.50
1.49
1.26
1.00
1.00
0.90
0.98
3.00
2.93
0.87
1.11
1.02
1.21
2.94
5.17
10.0
9.5
9.0
8.5
8.0
7.5
7.0
6.5
6.0
5.5
5.0
4.5
4.0
3.5
3.0
2.5
2.0
1.5
1.0
0.5
0.0
f1 (ppm)

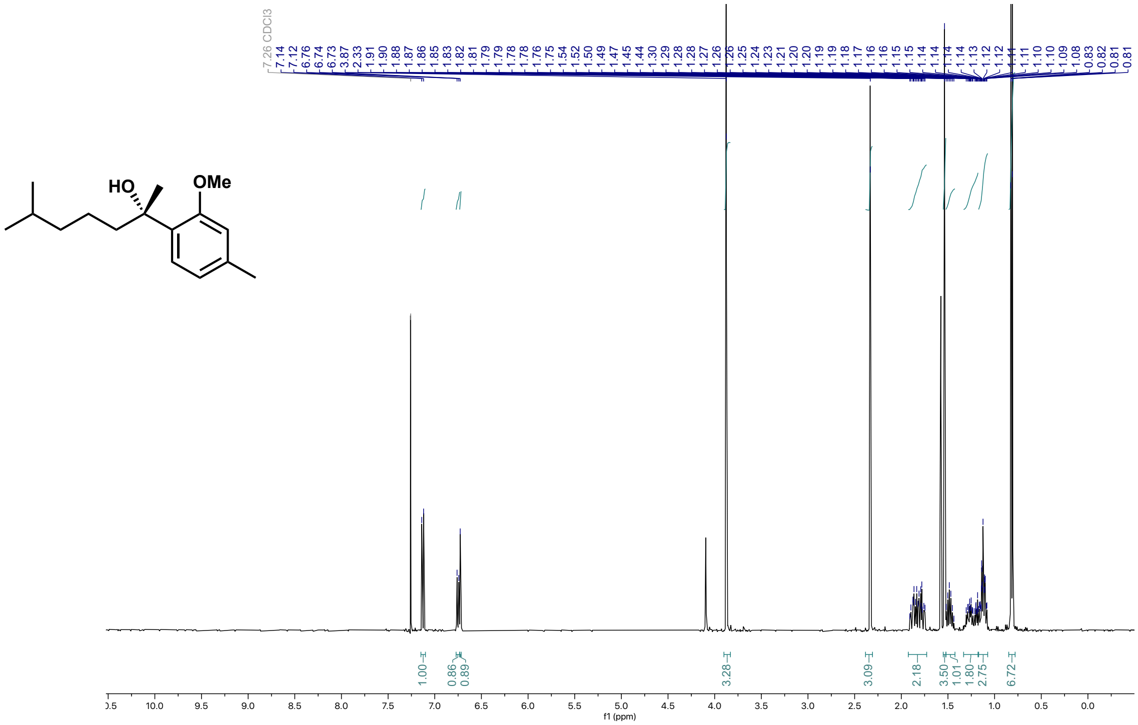
7.26 CDCl3
7.14
7.12
6.76
6.74
6.73
3.87
2.33
1.91
1.90
1.88
1.87
1.86
1.85
1.83
1.82
1.81
1.79
1.79
1.78
1.78
1.76
1.75
1.54
1.52
1.50
1.49
1.47
1.45
1.44
1.30
1.29
1.28
1.28
1.27
1.26
1.26
1.25
1.24
1.23
1.21
1.20
1.20
1.19
1.19
1.18
1.17
1.16
1.16
1.15
1.15
1.14
1.14
1.14
1.14
1.13
1.12
1.12
1.11
1.11
1.10
1.10
1.09
1.08
0.83
0.82
0.81
0.81
HO
OMe
1.00
0.86
0.89
3.28
3.09
2.18
3.50
1.01
1.80
2.75
6.72
10.5
10.0
9.5
9.0
8.5
8.0
7.5
7.0
6.5
6.0
5.5
5.0
4.5
4.0
3.5
3.0
2.5
2.0
1.5
1.0
0.5
0.0
f1 (ppm)

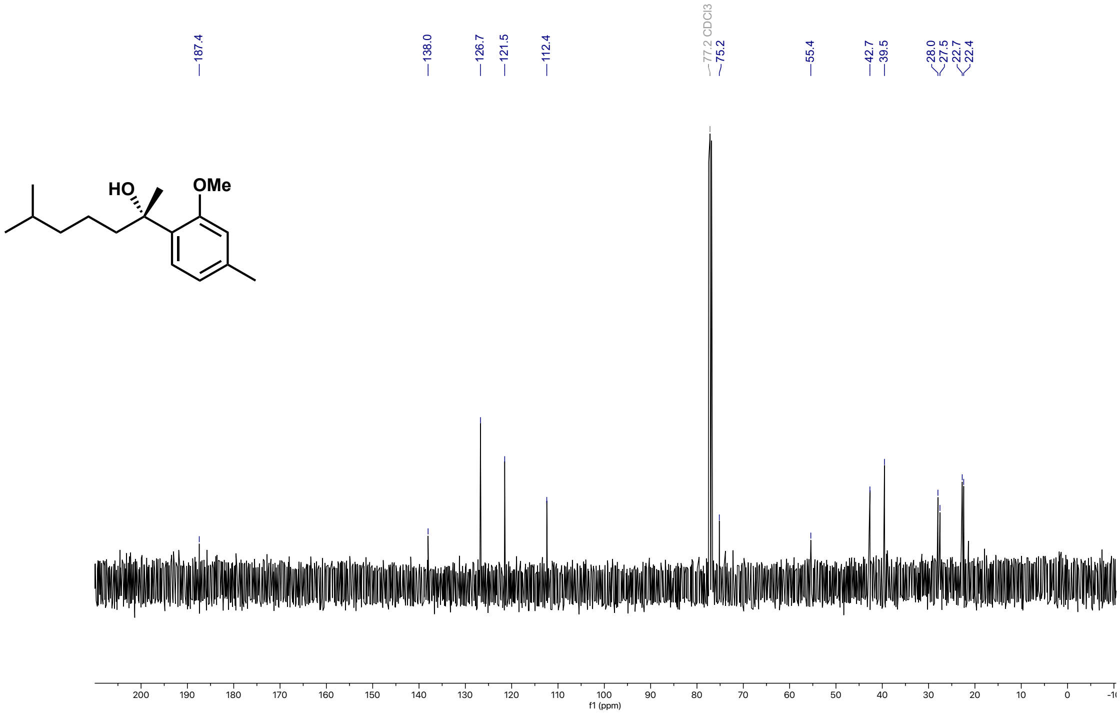
187.4
138.0
126.7
121.5
112.4
77.2 CDCl3
75.2
55.4
42.7
39.5
28.0
27.5
22.7
22.4
HO
OMe
200
190
180
170
160
150
140
130
120
110
100
90
80
70
60
50
40
30
20
10
0
-10
f1 (ppm)

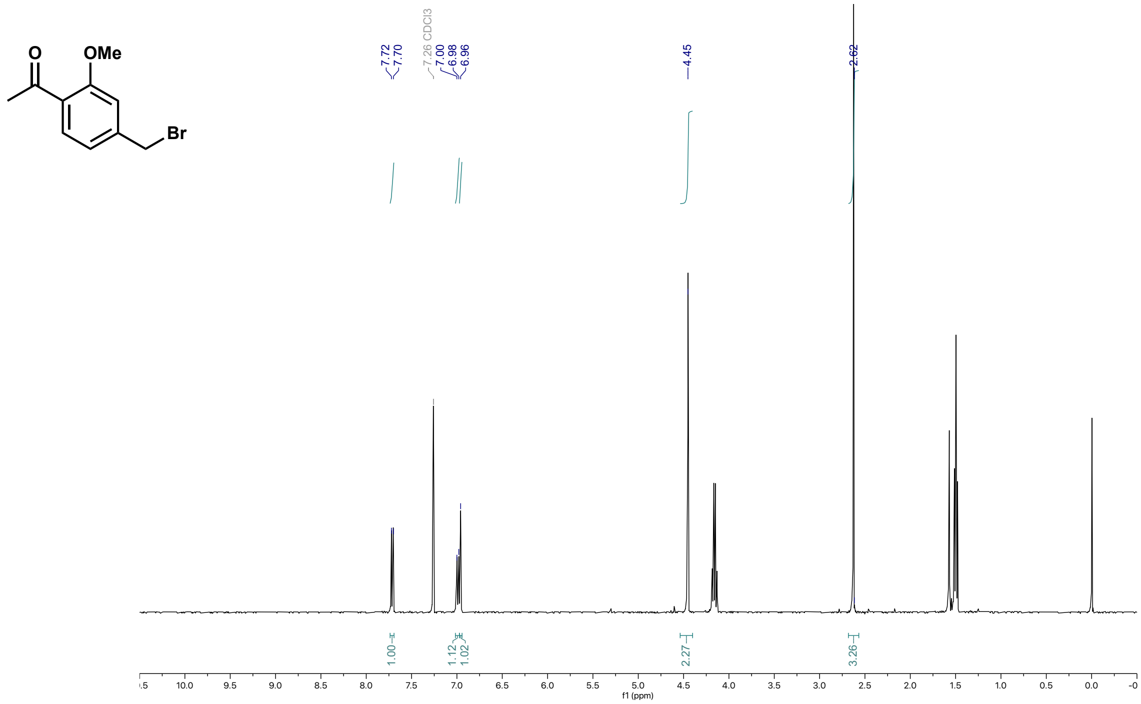
O
OMe
Br
7.72
7.70
7.26 CDCl3
7.00
6.98
6.96
4.45
2.62
1.00
1.12
1.02
2.27
3.26
10.5
10.0
9.5
9.0
8.5
8.0
7.5
7.0
6.5
6.0
5.5
5.0
4.5
4.0
3.5
3.0
2.5
2.0
1.5
1.0
0.5
0.0
-0.5
f1 (ppm)

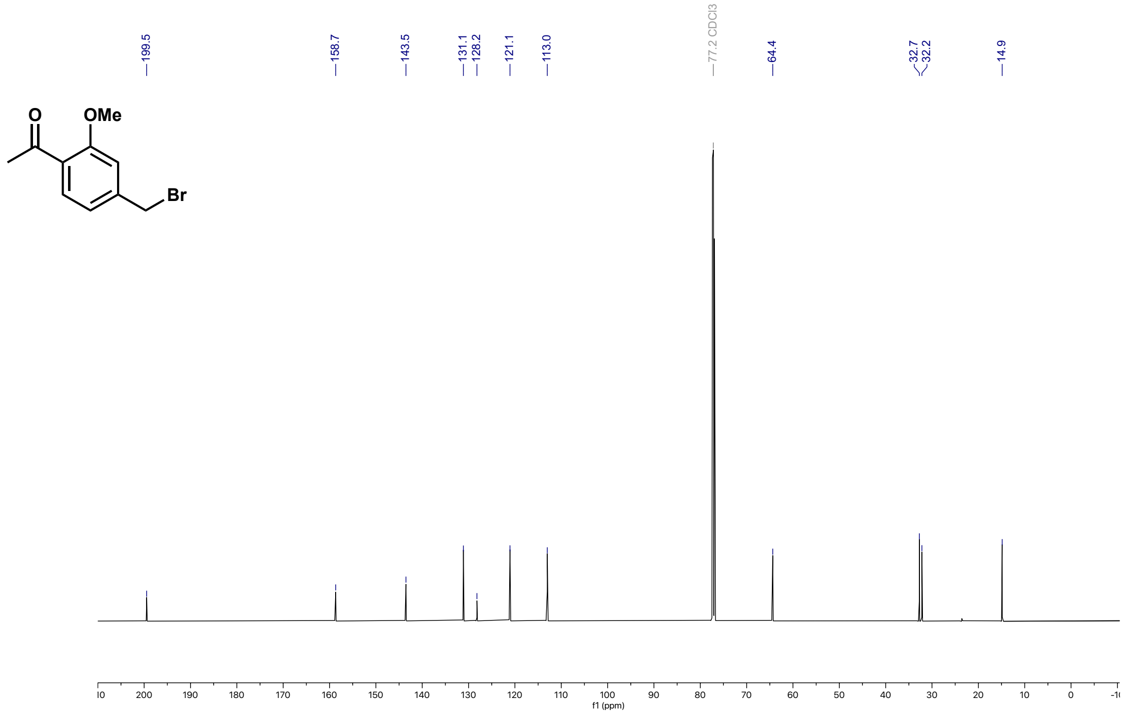
199.5
158.7
143.5
131.1
128.2
121.1
113.0
77.2 CDCl3
64.4
32.7
32.2
14.9
O
OMe
Br
210
200
190
180
170
160
150
140
130
120
110
100
90
80
70
60
50
40
30
20
10
0
-10
f1 (ppm)

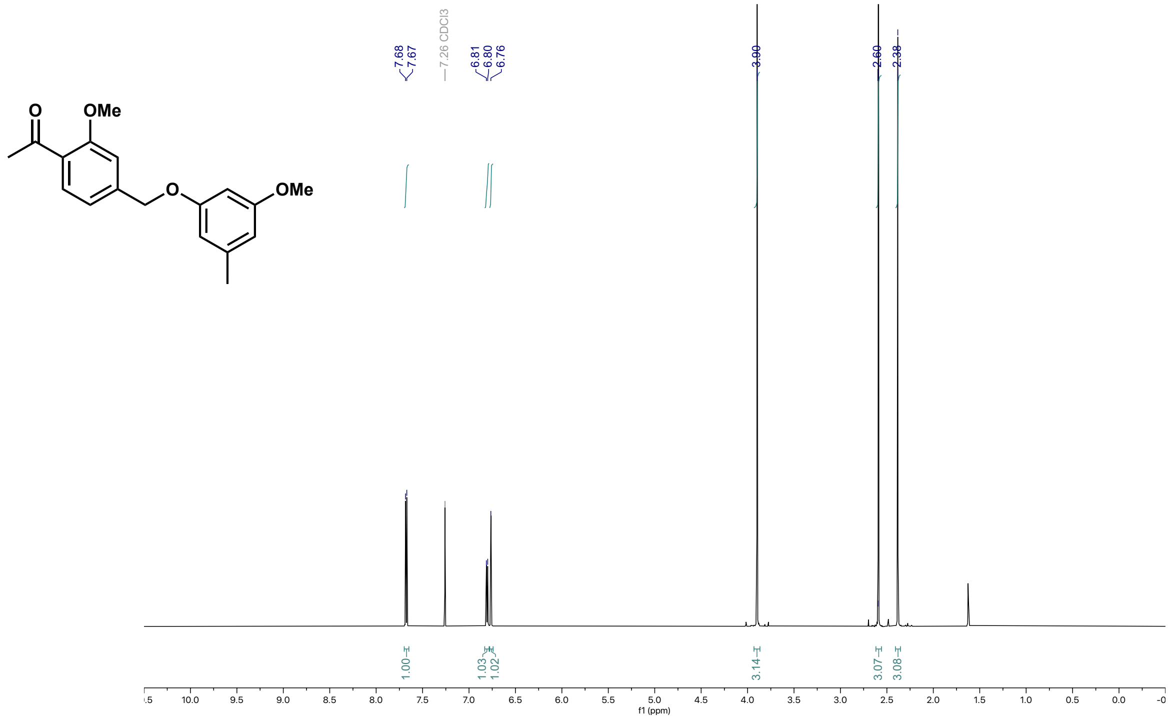
O
OMe
O
OMe
7.68
7.67
7.26 CDCl3
6.81
6.80
6.76
3.90
2.60
2.38
1.00
1.03
1.02
3.14
3.07
3.08
10.0
9.5
9.0
8.5
8.0
7.5
7.0
6.5
6.0
5.5
5.0
4.5
4.0
3.5
3.0
2.5
2.0
1.5
1.0
0.5
0.0
f1 (ppm)

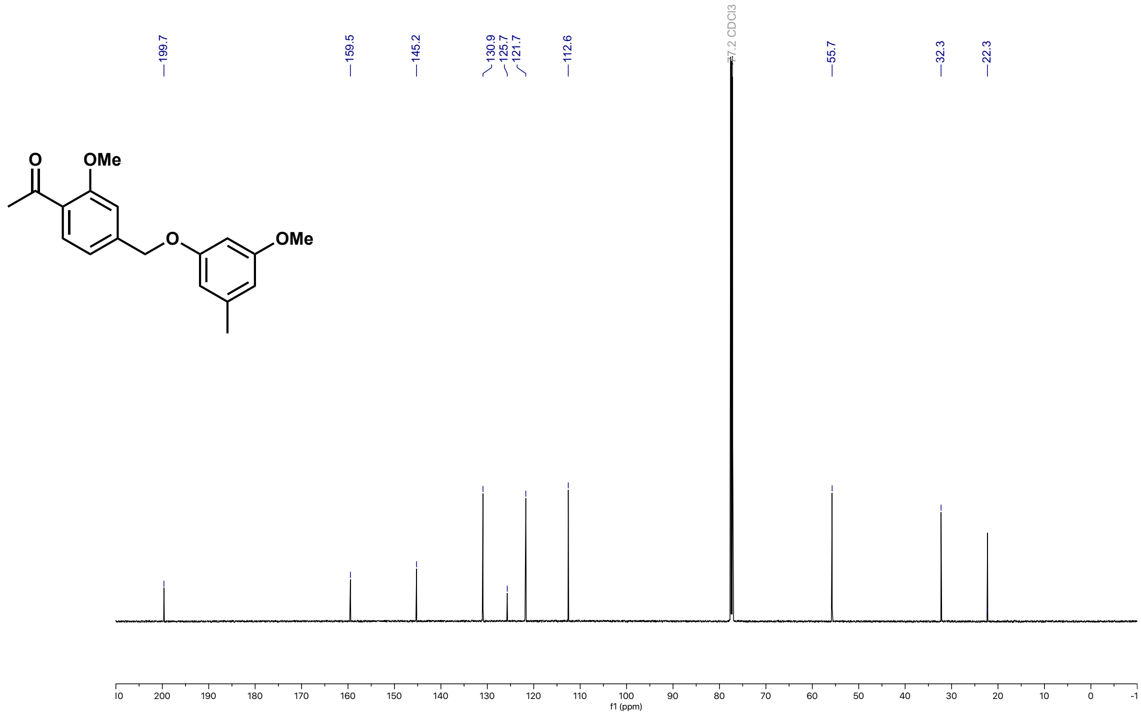
199.7
159.5
145.2
130.9
125.7
121.7
112.6
77.2 CDCl3
55.7
32.3
22.3
O
OMe
O
OMe
200
190
180
170
160
150
140
130
120
110
100
90
80
70
60
50
40
30
20
10
0
f1 (ppm)

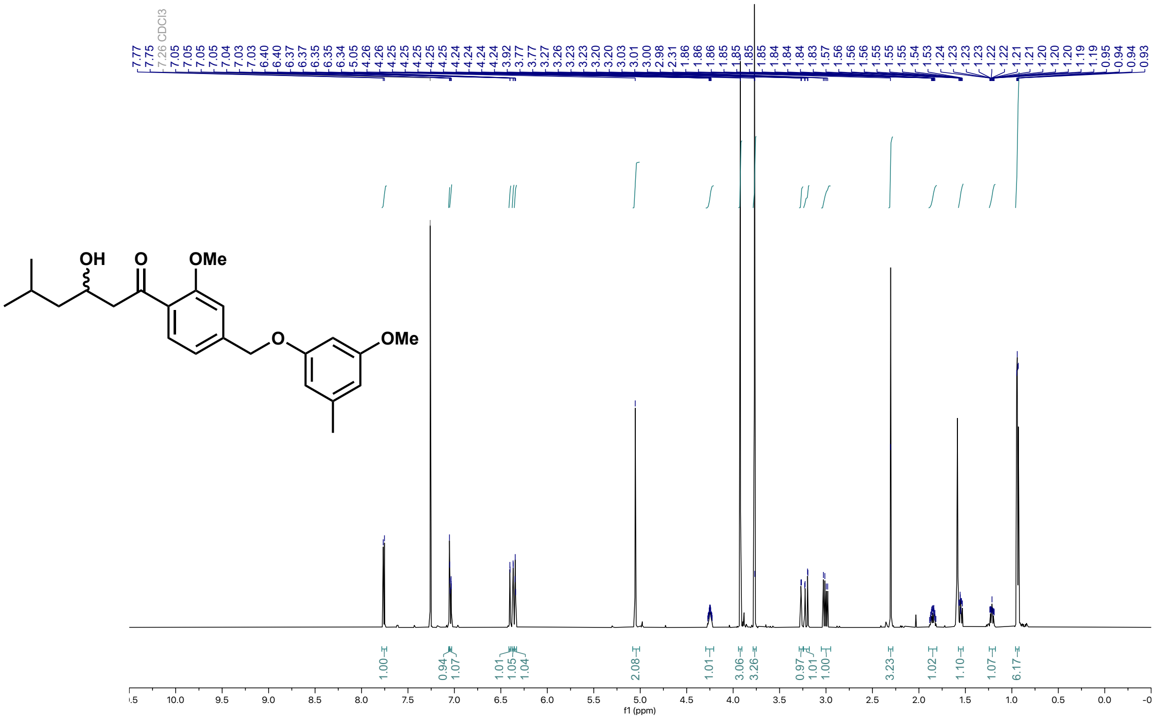
7.77
7.75
7.26 CDCl3
7.05
7.05
7.05
7.05
7.04
7.03
7.03
6.40
6.37
6.37
6.35
6.35
6.34
5.05
4.26
4.25
4.25
4.25
4.25
4.24
4.24
4.24
4.24
3.92
3.77
3.77
3.27
3.26
3.23
3.23
3.20
3.20
3.03
3.01
3.00
2.98
2.31
1.86
1.86
1.86
1.85
1.85
1.85
1.85
1.84
1.84
1.84
1.83
1.57
1.56
1.56
1.56
1.55
1.55
1.55
1.54
1.53
1.24
1.23
1.23
1.23
1.22
1.22
1.21
1.21
1.20
1.20
1.19
0.95
0.94
0.94
0.93
OH
O
OMe
O
OMe
1.00
0.94
1.07
1.01
1.05
1.04
2.08
1.01
3.06
3.26
0.97
1.01
1.00
3.23
1.02
1.10
1.07
6.17
10.5
10.0
9.5
9.0
8.5
8.0
7.5
7.0
6.5
6.0
5.5
5.0
4.5
4.0
3.5
3.0
2.5
2.0
1.5
1.0
0.5
0.0
-0.5
f1 (ppm)

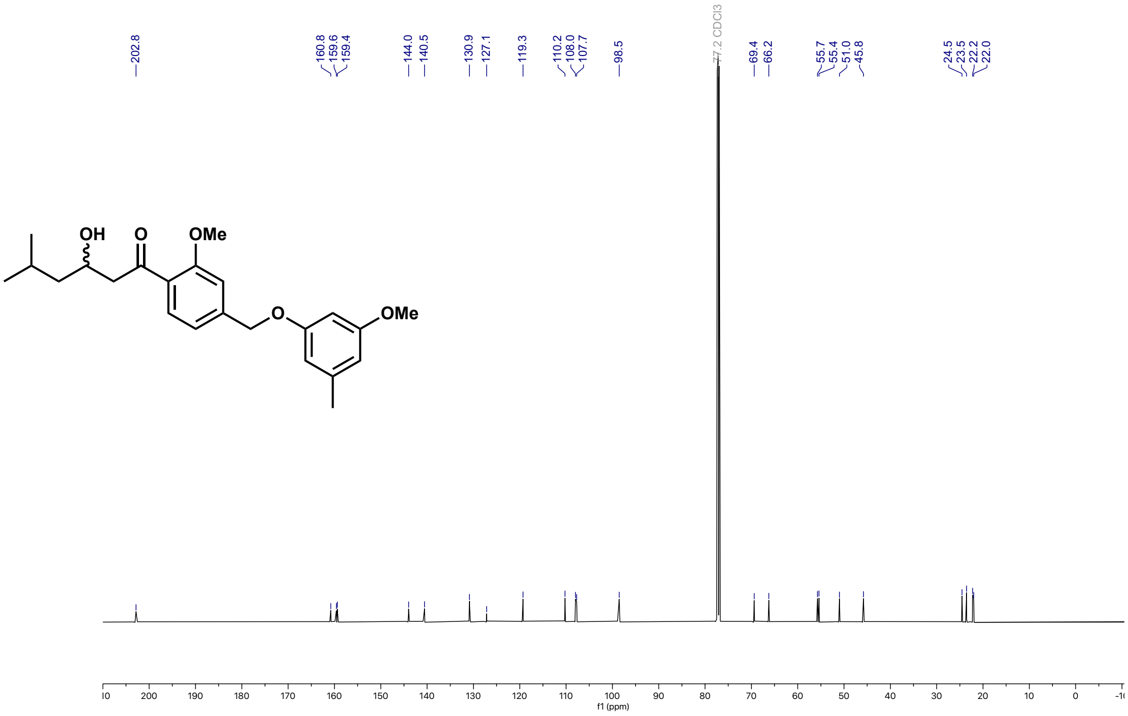
202.8
160.8
159.6
159.4
144.0
140.5
130.9
127.1
119.3
110.2
108.0
107.7
98.5
77.2 CDCl3
69.4
66.2
55.7
55.4
51.0
45.8
24.5
23.5
22.2
22.0
OH
O
OMe
O
OMe
210
200
190
180
170
160
150
140
130
120
110
100
90
80
70
60
50
40
30
20
10
0
-10
f1 (ppm)

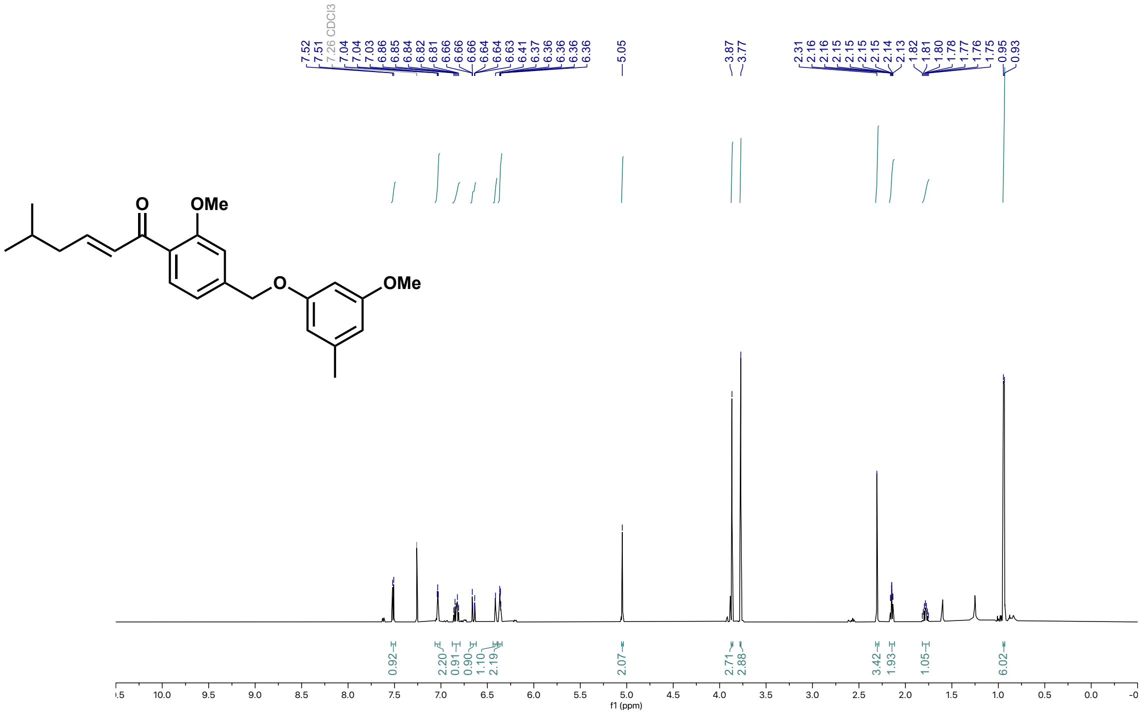
7.52
7.51
7.26 CDCl3
7.04
7.04
7.03
6.86
6.85
6.84
6.82
6.81
6.66
6.66
6.66
6.64
6.64
6.63
6.41
6.37
6.36
6.36
6.36
6.36
5.05
3.87
3.77
2.31
2.16
2.16
2.15
2.15
2.15
2.14
2.13
1.82
1.81
1.80
1.78
1.77
1.76
1.75
0.95
0.93
O
OMe
O
OMe
0.92
2.20
0.91
0.90
1.10
2.19
2.07
2.71
2.88
3.42
1.93
1.05
6.02
f1 (ppm)

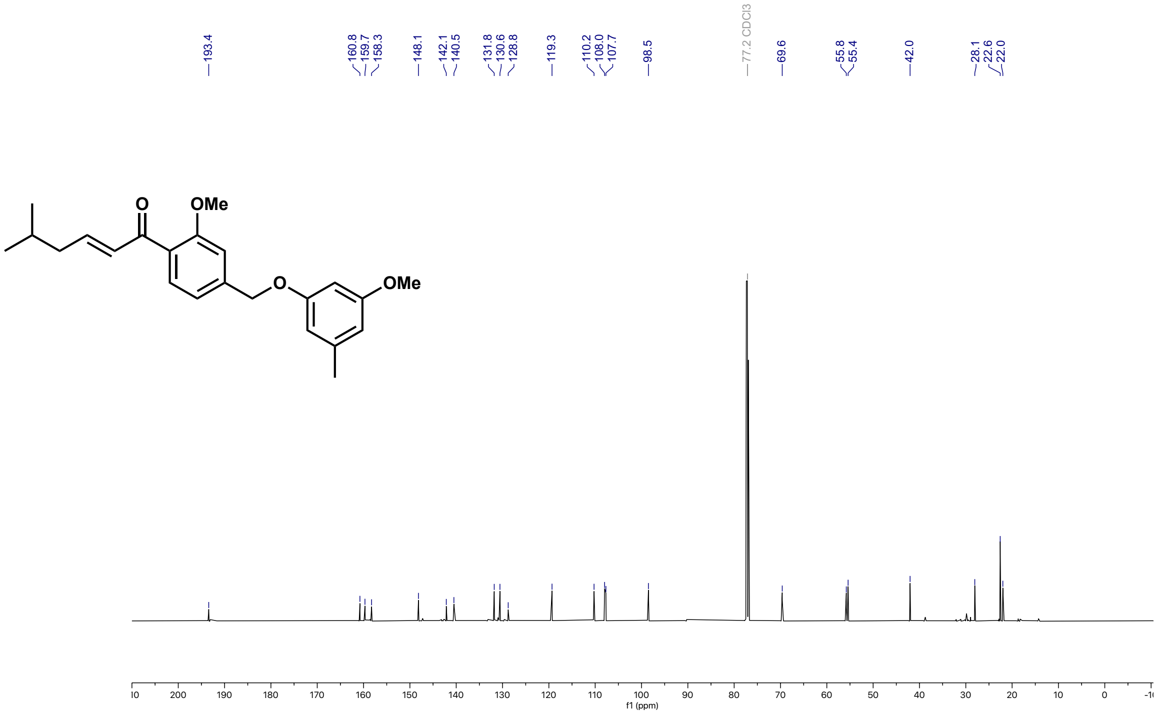
193.4
160.8
159.7
158.3
148.1
142.1
140.5
131.8
130.6
128.8
119.3
110.2
108.0
107.7
98.5
77.2 CDCl3
69.6
55.8
55.4
42.0
28.1
22.6
22.0
O
OMe
O
OMe
f1 (ppm)

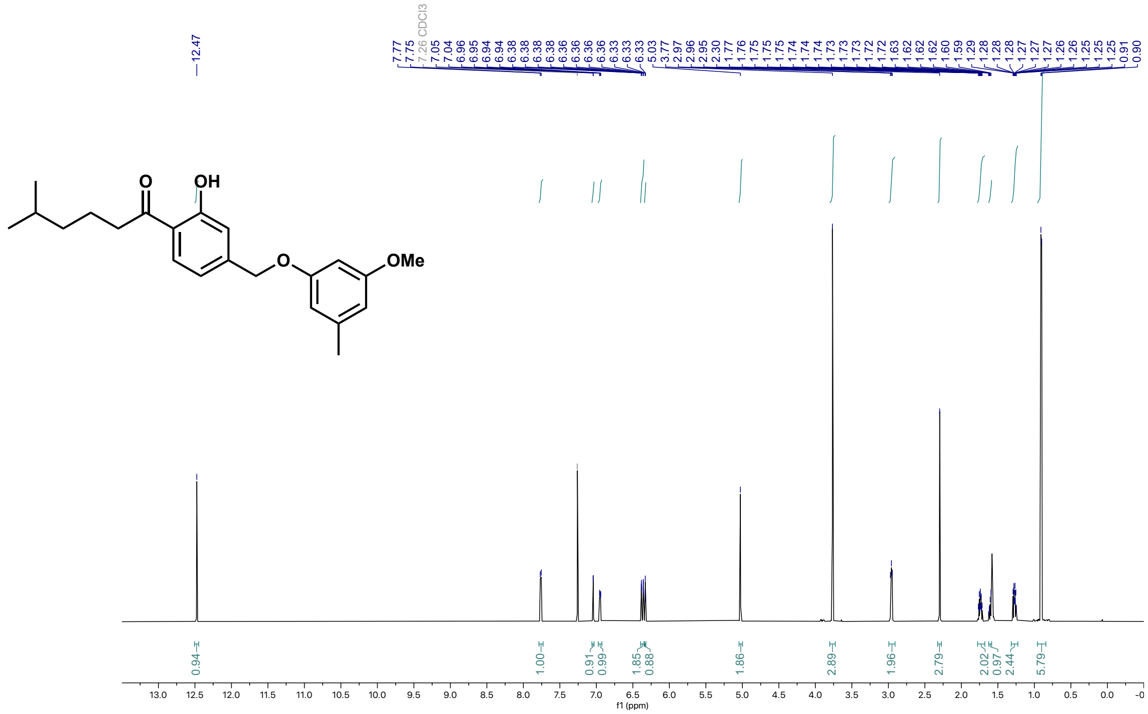
12.47
7.77
7.75
7.26 CDCl3
7.05
7.04
6.96
6.95
6.94
6.94
6.38
6.38
6.38
6.38
6.36
6.36
6.36
6.36
6.33
6.33
6.33
5.03
3.77
2.97
2.96
2.95
2.30
1.77
1.76
1.75
1.75
1.74
1.74
1.74
1.73
1.73
1.73
1.72
1.72
1.63
1.62
1.62
1.62
1.60
1.59
1.29
1.28
1.28
1.27
1.27
1.26
1.26
1.25
1.25
1.25
0.91
0.90
O
OH
O
OMe
0.94
1.00
0.91
0.99
1.85
0.88
1.86
2.89
1.96
2.79
2.02
0.97
2.44
5.79
13.0
12.5
12.0
11.5
11.0
10.5
10.0
9.5
9.0
8.5
8.0
7.5
7.0
6.5
6.0
5.5
5.0
4.5
4.0
3.5
3.0
2.5
2.0
1.5
1.0
0.5
0.0
-0
f1 (ppm)

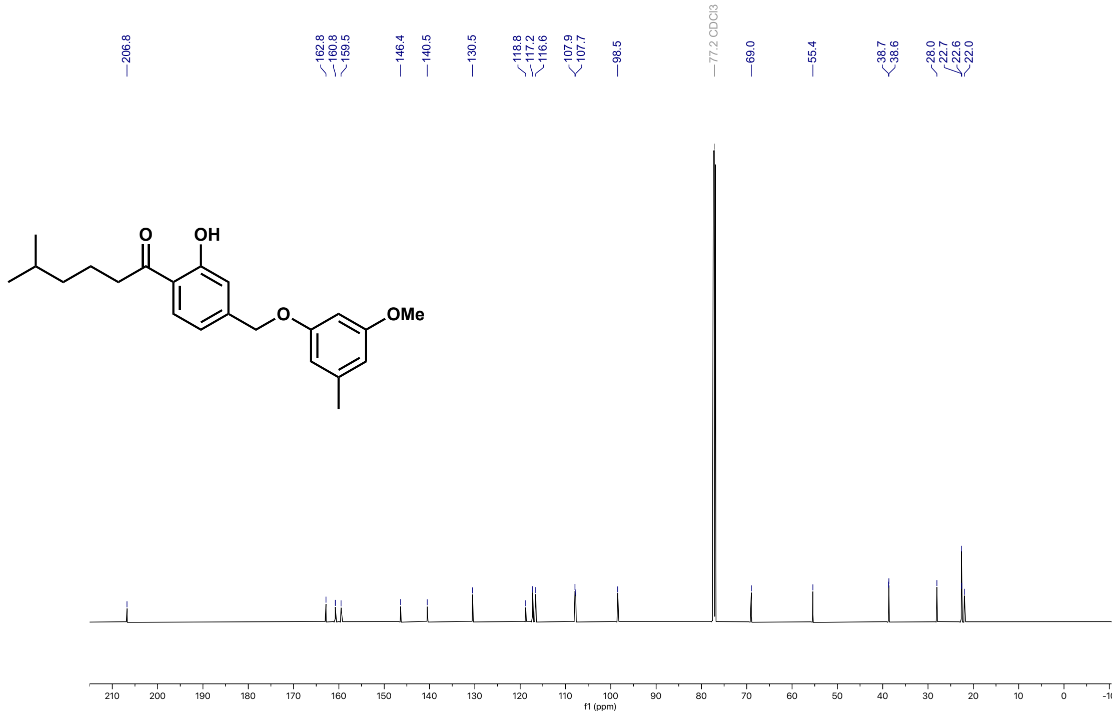
206.8
162.8
160.8
159.5
146.4
140.5
130.5
118.8
117.2
116.6
107.9
107.7
98.5
77.2 CDCl3
69.0
55.4
38.7
38.6
28.0
22.7
22.6
22.0
O
OH
O
OMe
210
200
190
180
170
160
150
140
130
120
110
100
90
80
70
60
50
40
30
20
10
0
-1
f1 (ppm)

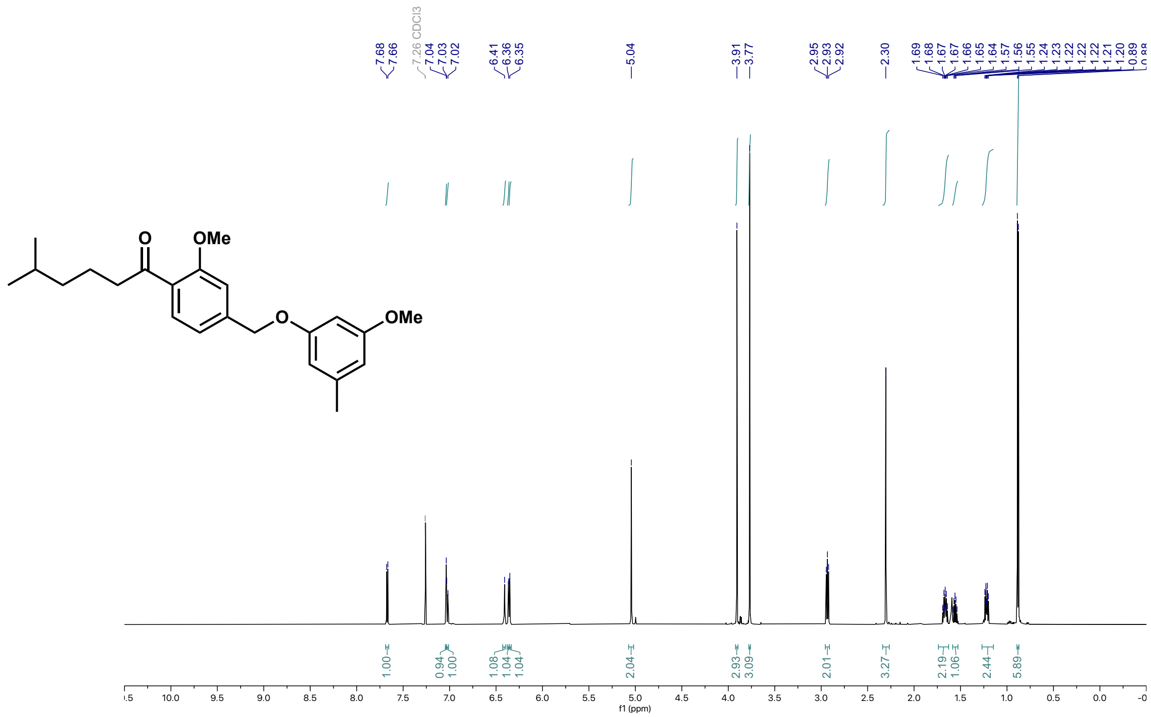
7.68
7.66
7.26 CDCl3
7.04
7.03
7.02
6.41
6.36
6.35
5.04
3.91
3.77
2.95
2.93
2.92
2.30
1.69
1.68
1.67
1.66
1.65
1.64
1.57
1.56
1.55
1.24
1.23
1.22
1.22
1.21
1.20
0.89
O
OMe
O
OMe
1.00
0.94
1.00
1.08
1.04
1.04
2.04
2.93
3.09
2.01
3.27
2.19
1.06
2.44
5.89
10.0
9.5
9.0
8.5
8.0
7.5
7.0
6.5
6.0
5.5
5.0
4.5
4.0
3.5
3.0
2.5
2.0
1.5
1.0
0.5
0.0
f1 (ppm)

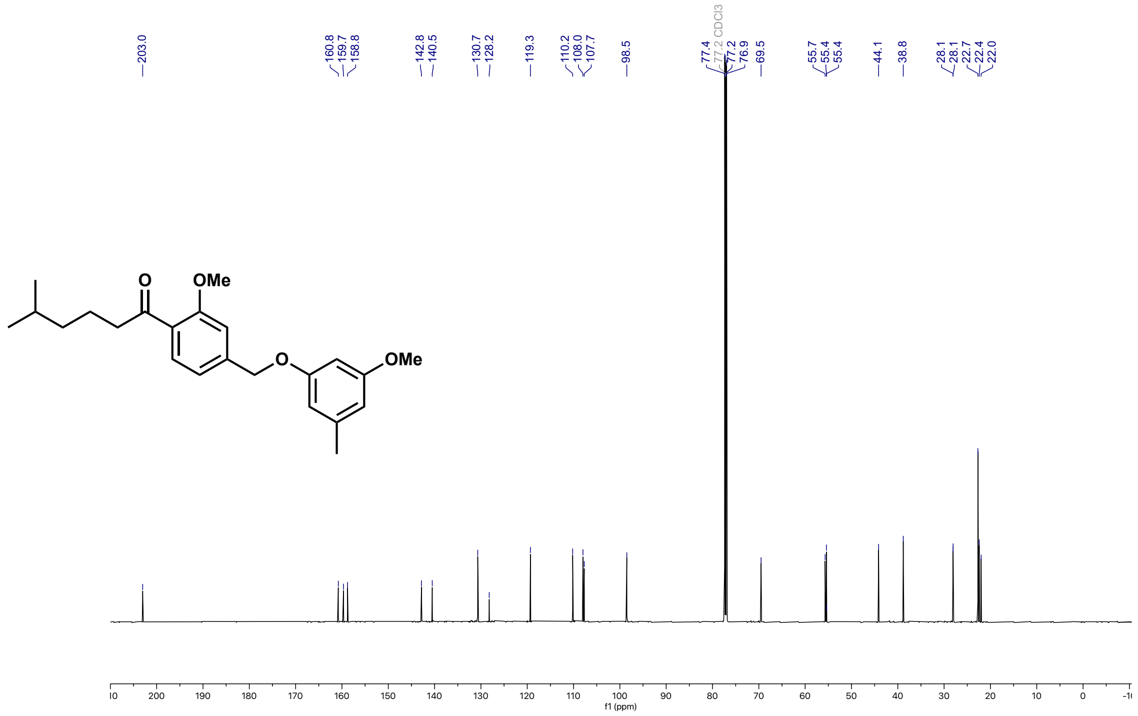
203.0
160.8
159.7
158.8
142.8
140.5
130.7
128.2
119.3
110.2
108.0
107.7
98.5
77.4
77.2 CDCl3
76.9
69.5
55.7
55.4
55.4
44.1
38.8
28.1
28.1
22.7
22.4
22.0
O
OMe
O
OMe
200
190
180
170
160
150
140
130
120
110
100
90
80
70
60
50
40
30
20
10
0
f1 (ppm)

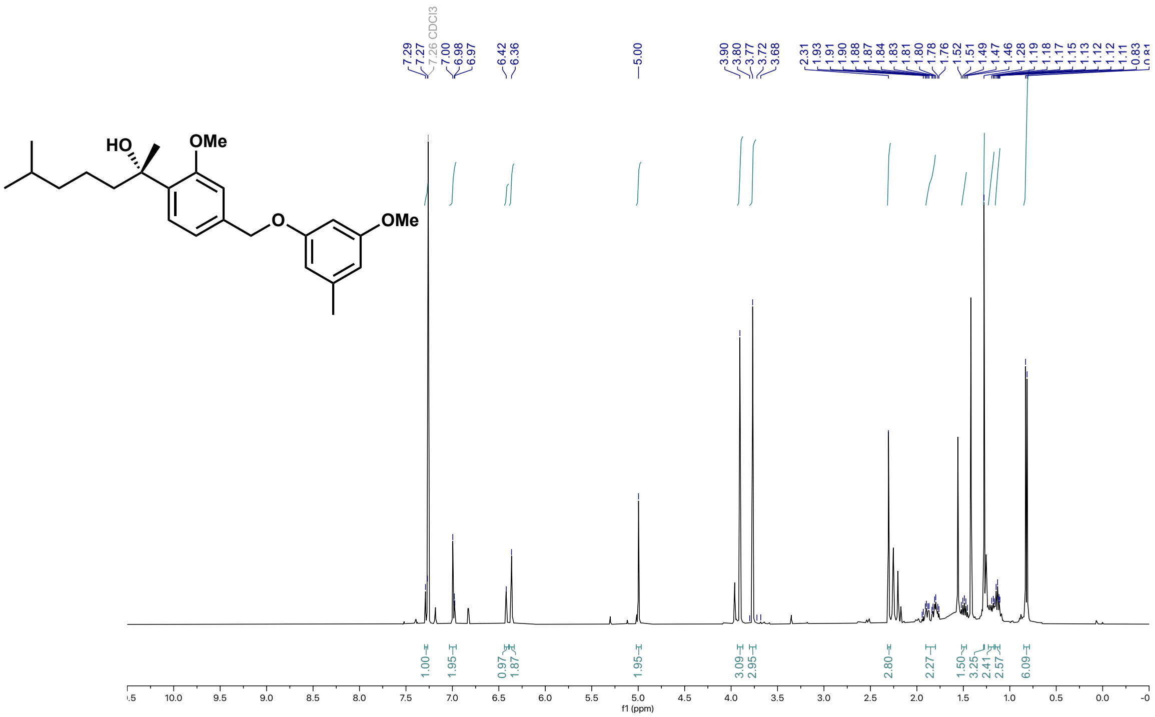
HO
OMe
O
OMe
7.29
7.27
7.26 CDCl3
7.00
6.98
6.97
6.42
6.36
5.00
3.90
3.80
3.77
3.72
3.68
2.31
1.93
1.91
1.90
1.88
1.87
1.84
1.83
1.81
1.80
1.78
1.76
1.52
1.51
1.49
1.47
1.46
1.28
1.19
1.18
1.17
1.15
1.13
1.12
1.12
1.11
0.83
0.81
1.00
1.95
0.97
1.87
1.95
3.09
2.95
2.80
2.27
1.50
3.25
2.41
2.57
6.09
10.0
9.5
9.0
8.5
8.0
7.5
7.0
6.5
6.0
5.5
5.0
4.5
4.0
3.5
3.0
2.5
2.0
1.5
1.0
0.5
0.0
f1 (ppm)

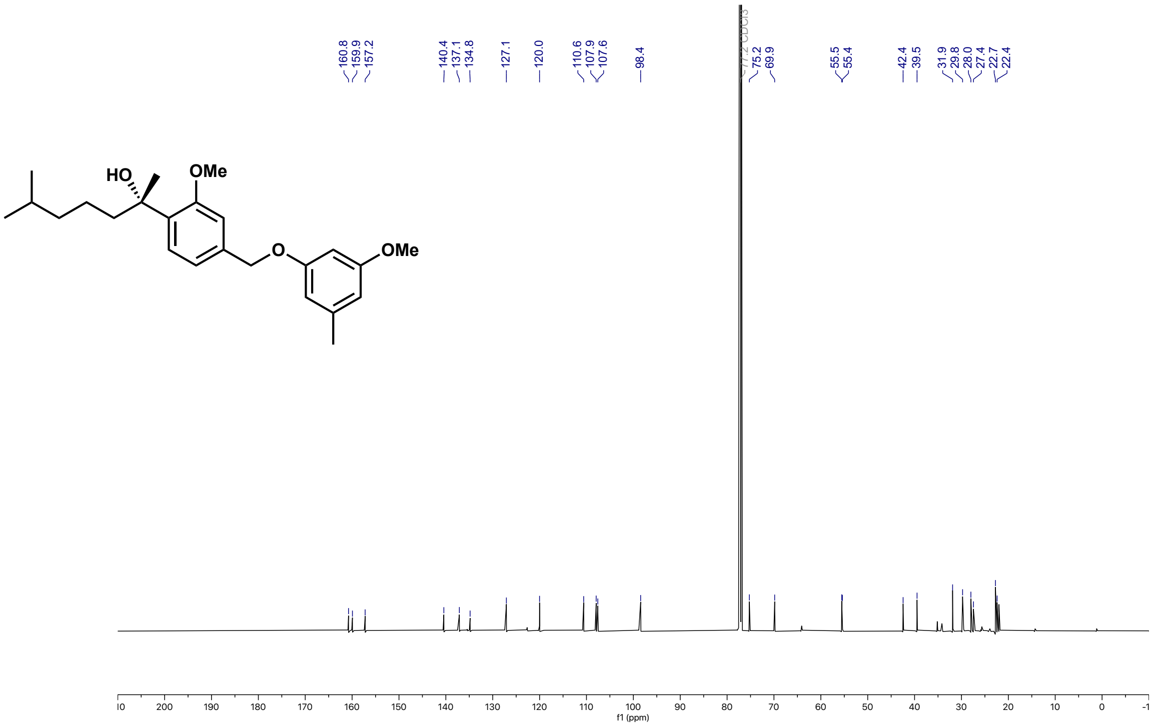
HO
OMe
O
OMe
160.8
159.9
157.2
140.4
137.1
134.8
127.1
120.0
110.6
107.9
107.6
98.4
77.2 CDCl3
75.2
69.9
55.5
55.4
42.4
39.5
31.9
29.8
28.0
27.4
22.7
22.4
200
190
180
170
160
150
140
130
120
110
100
90
80
70
60
50
40
30
20
10
0
f1 (ppm)

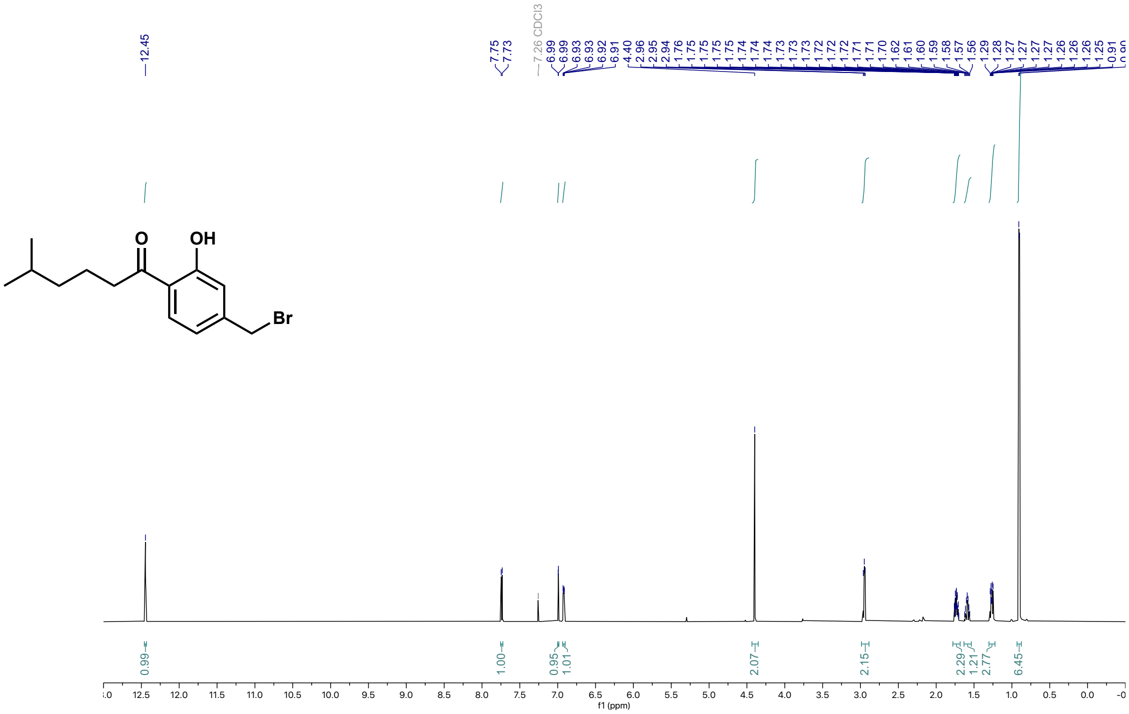
12.45
7.75
7.73
7.26 CDCl3
6.99
6.99
6.93
6.93
6.92
6.91
4.40
2.96
2.95
2.94
1.76
1.75
1.75
1.75
1.75
1.74
1.74
1.74
1.73
1.73
1.73
1.72
1.72
1.71
1.71
1.70
1.62
1.61
1.60
1.59
1.58
1.57
1.56
1.29
1.28
1.27
1.27
1.27
1.27
1.26
1.26
1.25
0.91
O
OH
Br
0.99
1.00
0.95
1.01
2.07
2.15
2.29
1.21
2.77
6.45
12.5
12.0
11.5
11.0
10.5
10.0
9.5
9.0
8.5
8.0
7.5
7.0
6.5
6.0
5.5
5.0
4.5
4.0
3.5
3.0
2.5
2.0
1.5
1.0
0.5
0.0
f1 (ppm)

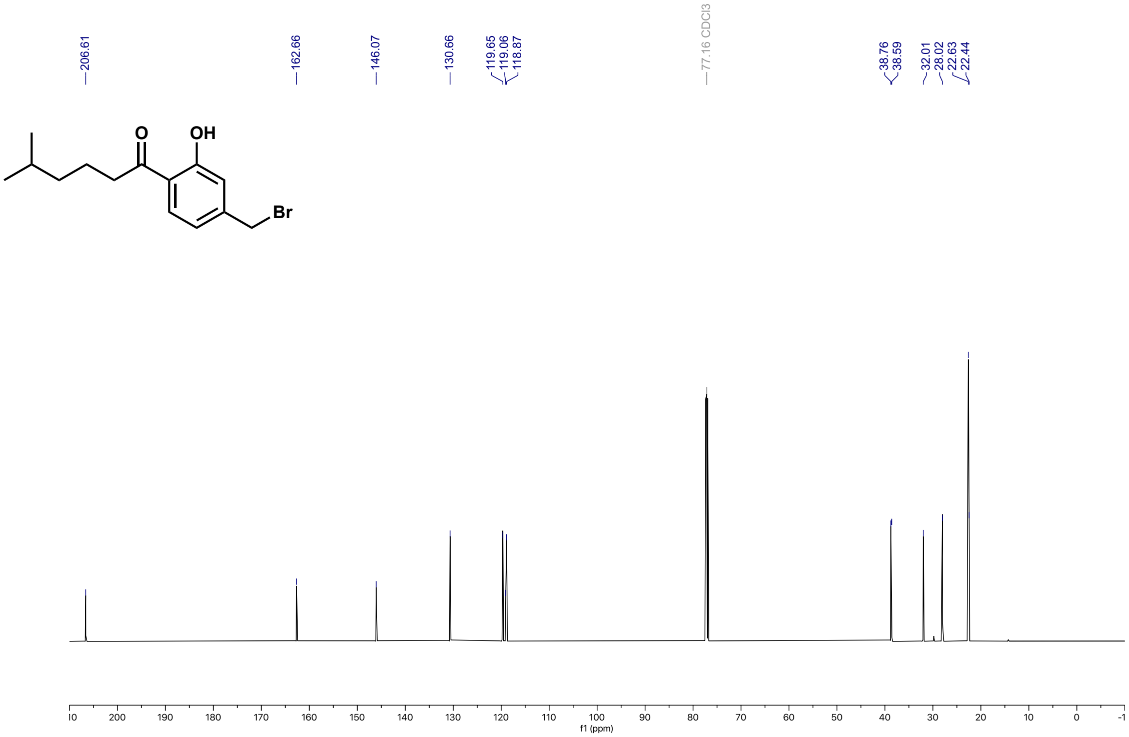
206.61
162.66
146.07
130.66
119.65
119.06
118.87
77.16 CDCl3
38.76
38.59
32.01
28.02
22.63
22.44
O
OH
Br
200
190
180
170
160
150
140
130
120
110
100
90
80
70
60
50
40
30
20
10
0
f1 (ppm)

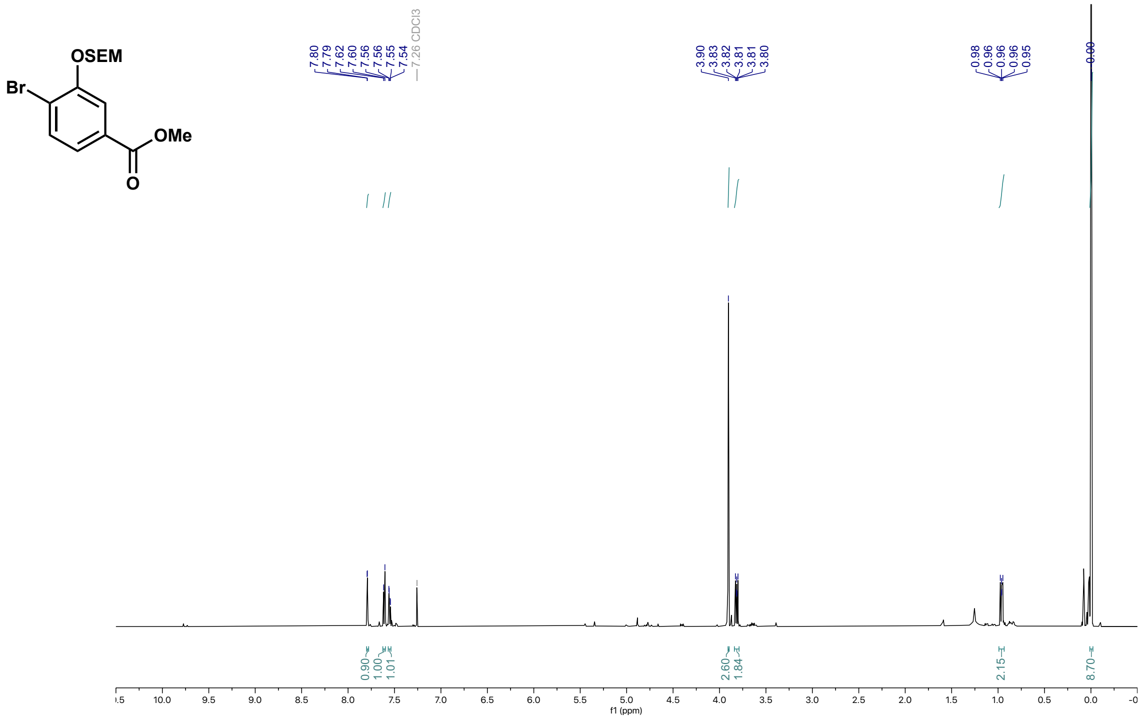
OSEM
Br
OMe
O
7.80
7.79
7.62
7.60
7.56
7.56
7.55
7.54
7.26 CDCl3
3.90
3.83
3.82
3.81
3.81
3.80
0.98
0.96
0.96
0.96
0.95
0.00
0.90
1.00
1.01
2.60
1.84
2.15
8.70
10.0
9.5
9.0
8.5
8.0
7.5
7.0
6.5
6.0
5.5
5.0
4.5
4.0
3.5
3.0
2.5
2.0
1.5
1.0
0.5
0.0
f1 (ppm)

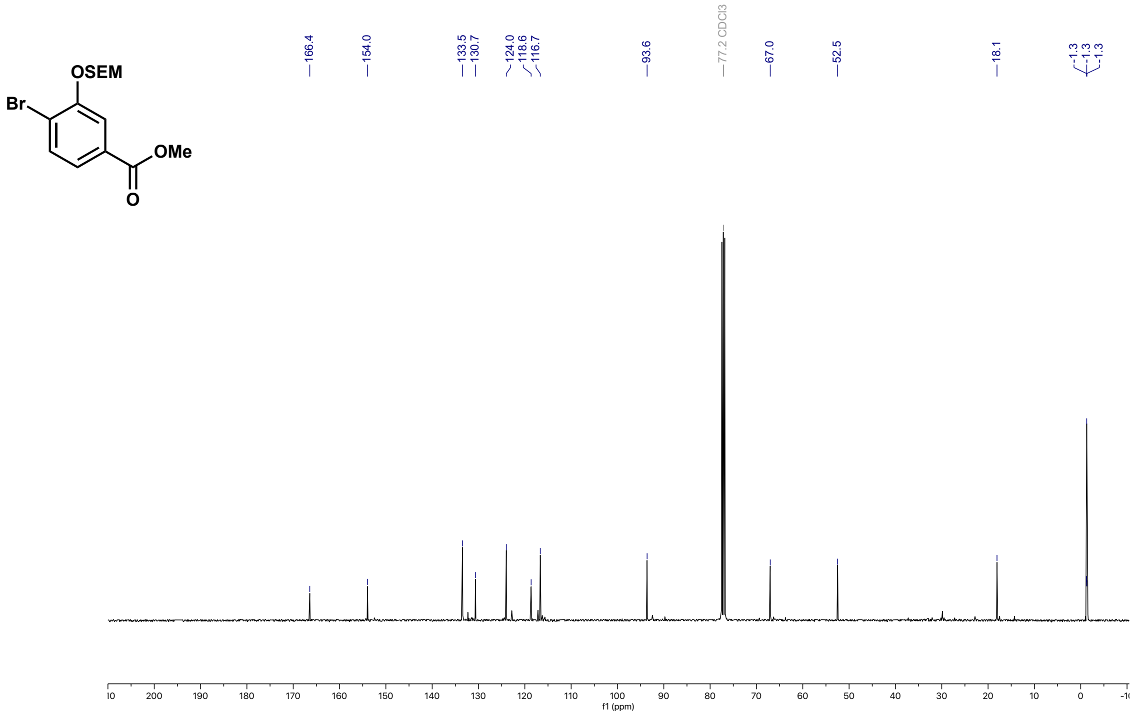
OSEM
Br
OMe
O
166.4
154.0
133.5
130.7
124.0
118.6
116.7
93.6
77.2 CDCl3
67.0
52.5
18.1
-1.3
-1.3
-1.3
200
190
180
170
160
150
140
130
120
110
100
90
80
70
60
50
40
30
20
10
0
f1 (ppm)

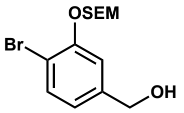
OSEM
Br
OH

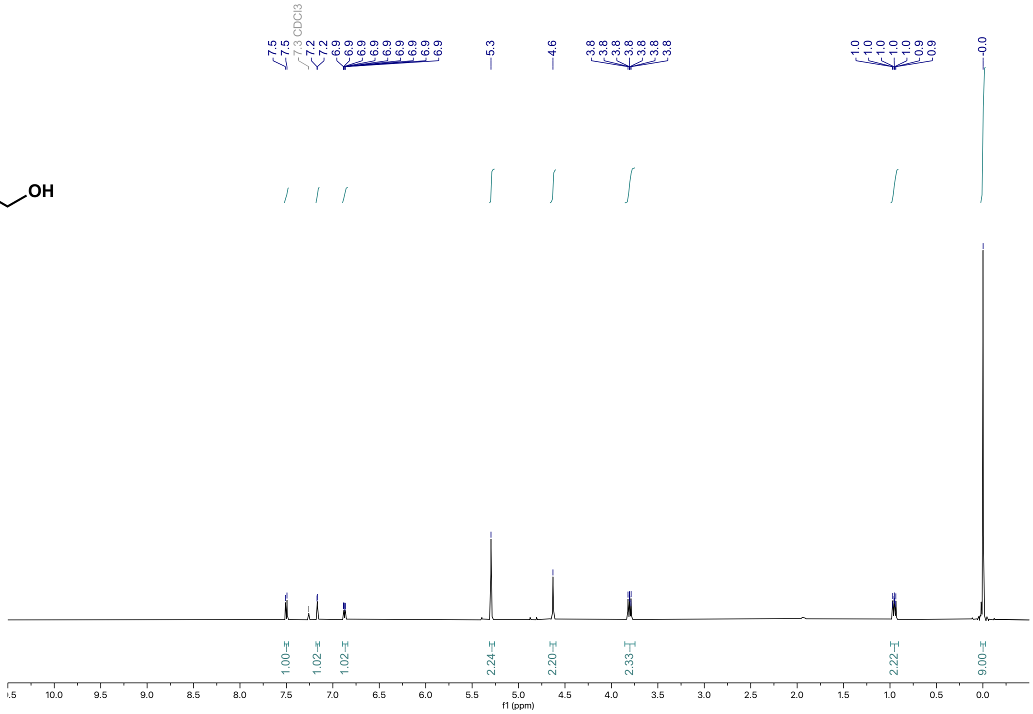
7.5
7.5
7.3 CDCl3
7.2
7.2
6.9
6.9
6.9
6.9
6.9
6.9
6.9
6.9
6.9
5.3
4.6
3.8
3.8
3.8
3.8
3.8
3.8
3.8
1.0
1.0
1.0
1.0
1.0
0.9
0.9
-0.0
1.00
1.02
1.02
2.24
2.20
2.33
2.22
9.00
10.0
9.5
9.0
8.5
8.0
7.5
7.0
6.5
6.0
5.5
5.0
4.5
4.0
3.5
3.0
2.5
2.0
1.5
1.0
0.5
0.0
f1 (ppm)

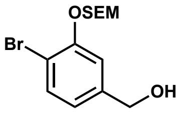
OSEM
Br
OH

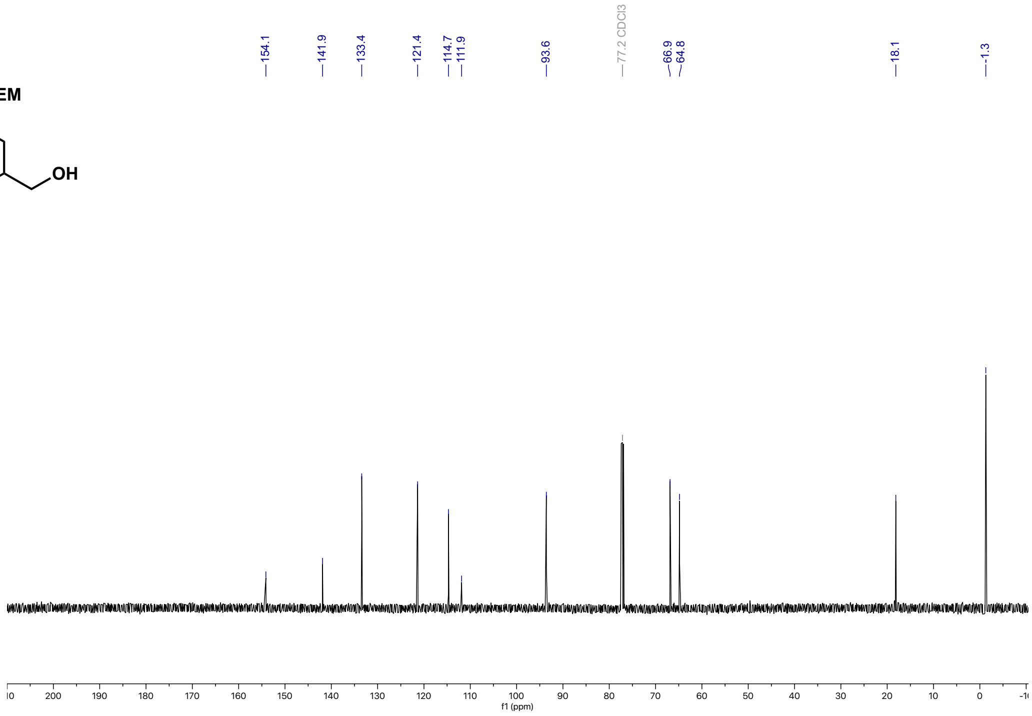
154.1
141.9
133.4
121.4
114.7
111.9
93.6
77.2 CDCl3
66.9
64.8
18.1
-1.3
200
190
180
170
160
150
140
130
120
110
100
90
80
70
60
50
40
30
20
10
0
f1 (ppm)

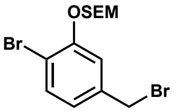
OSEM
Br
Br

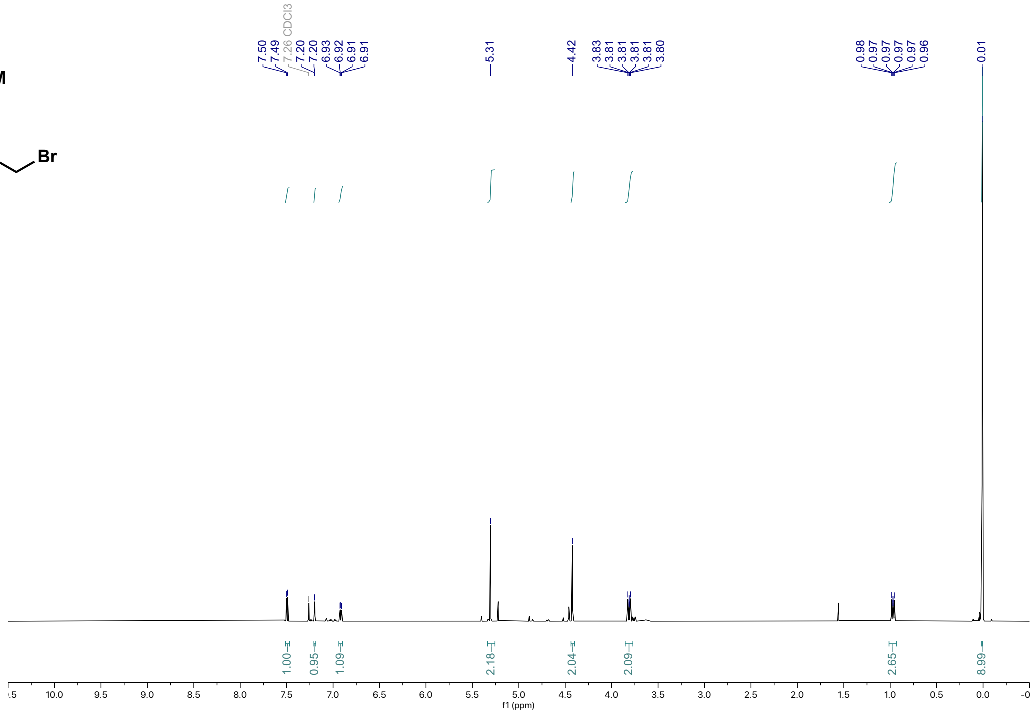
7.50
7.49
7.26 CDCl3
7.20
7.20
6.93
6.92
6.91
6.91
5.31
4.42
3.83
3.81
3.81
3.81
3.81
3.80
0.98
0.97
0.97
0.97
0.97
0.96
0.01
1.00
0.95
1.09
2.18
2.04
2.09
2.65
8.99
10.0
9.5
9.0
8.5
8.0
7.5
7.0
6.5
6.0
5.5
5.0
4.5
4.0
3.5
3.0
2.5
2.0
1.5
1.0
0.5
0.0
f1 (ppm)

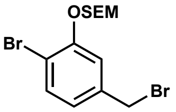
OSEM
Br
Br

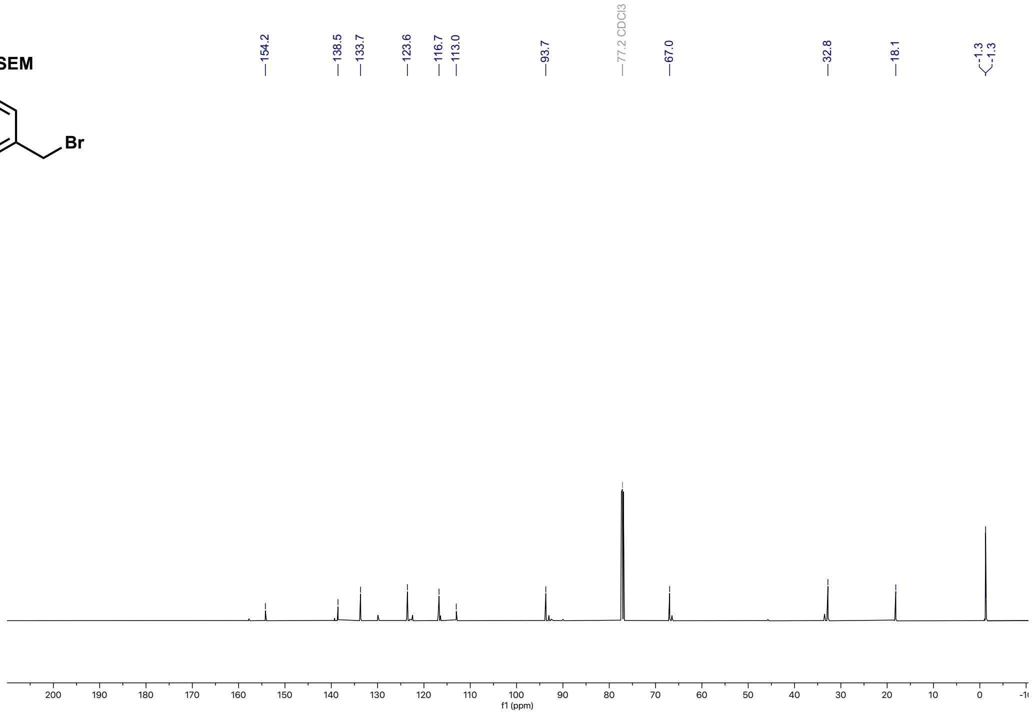
154.2
138.5
133.7
123.6
116.7
113.0
93.7
77.2 CDCl3
67.0
32.8
18.1
-1.3
-1.3
200
190
180
170
160
150
140
130
120
110
100
90
80
70
60
50
40
30
20
10
0
f1 (ppm)

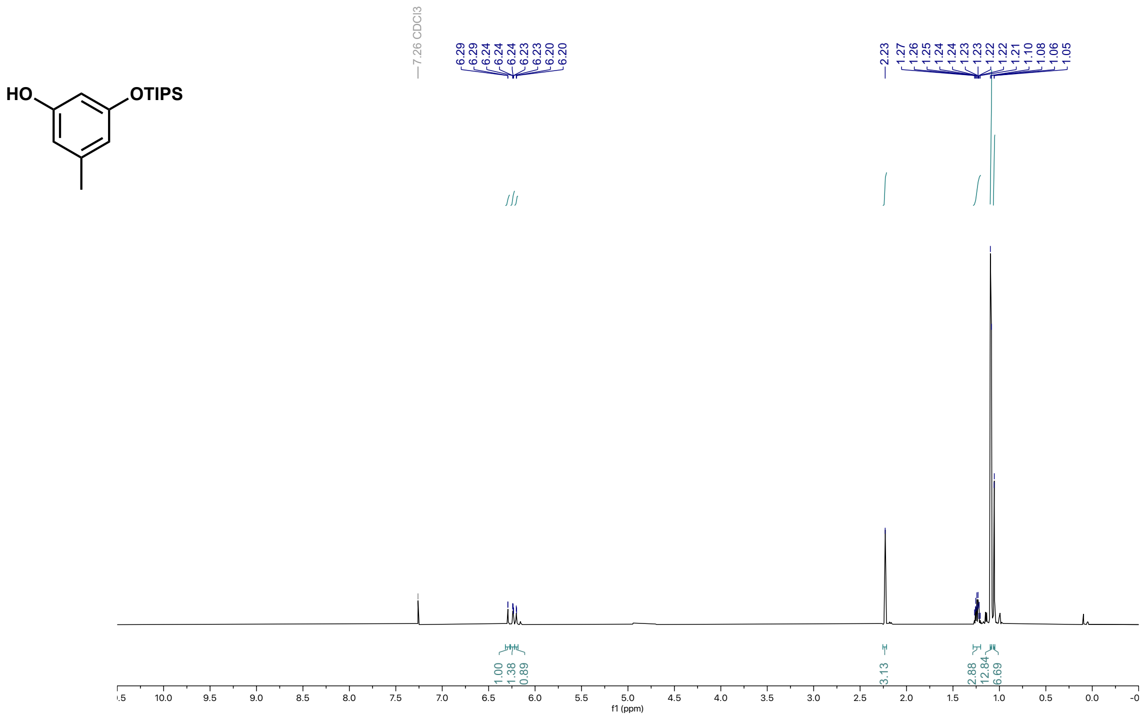
HO
OTIPS
7.26 CDCl3
6.29
6.29
6.24
6.24
6.24
6.23
6.23
6.20
6.20
2.23
1.27
1.26
1.25
1.24
1.24
1.23
1.23
1.22
1.22
1.21
1.10
1.08
1.06
1.05
1.00
1.38
0.89
3.13
2.88
12.84
6.69
f1 (ppm)

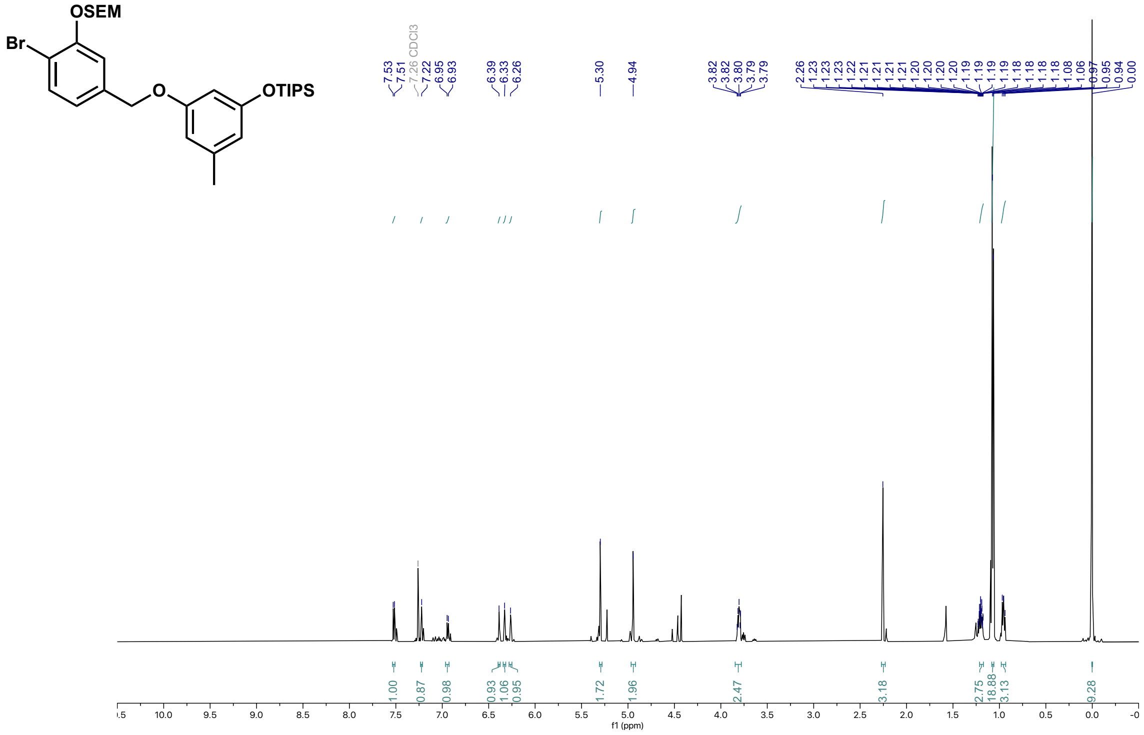
OSEM
Br
O
OTIPS
7.53
7.51
7.26 CDCl3
7.22
6.95
6.93
6.39
6.33
6.26
5.30
4.94
3.82
3.82
3.80
3.79
3.79
2.26
1.00
0.87
0.98
0.93
1.06
0.95
1.72
1.96
2.47
3.18
2.75
18.88
3.13
9.28
0.97
0.95
0.94
0.00
f1 (ppm)

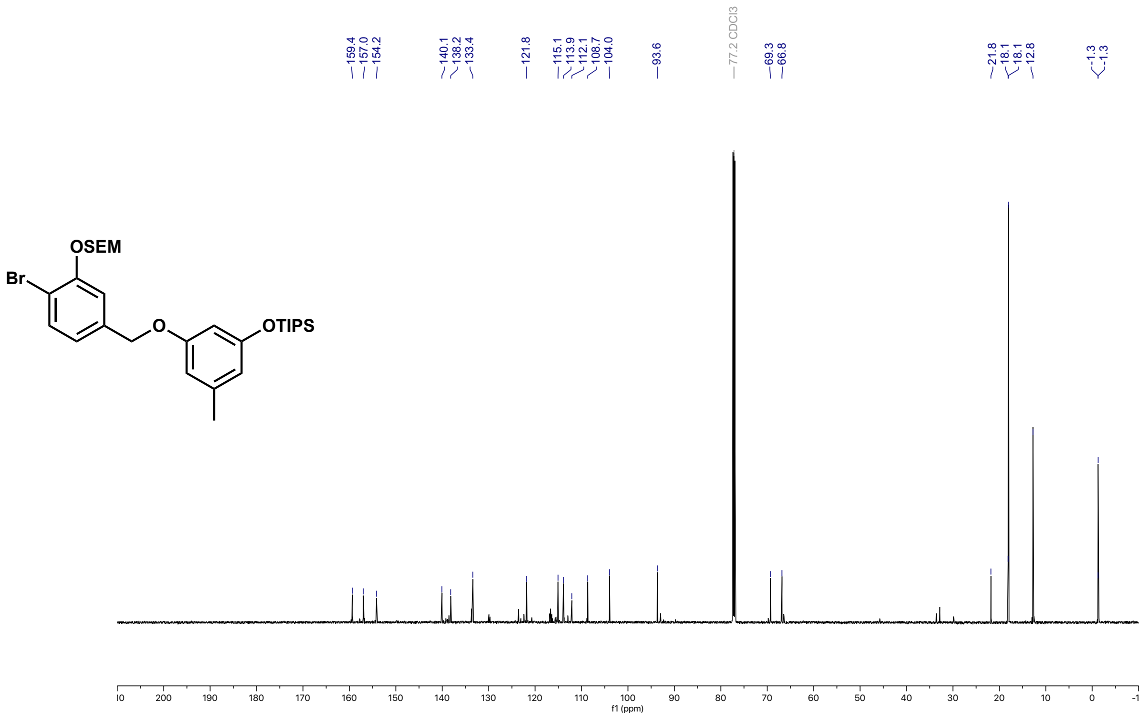
159.4
157.0
154.2
140.1
138.2
133.4
121.8
115.1
113.9
112.1
108.7
104.0
93.6
77.2 CDCl3
69.3
66.8
21.8
18.1
18.1
12.8
-1.3
-1.3
OSEM
Br
O
OTIPS
f1 (ppm)

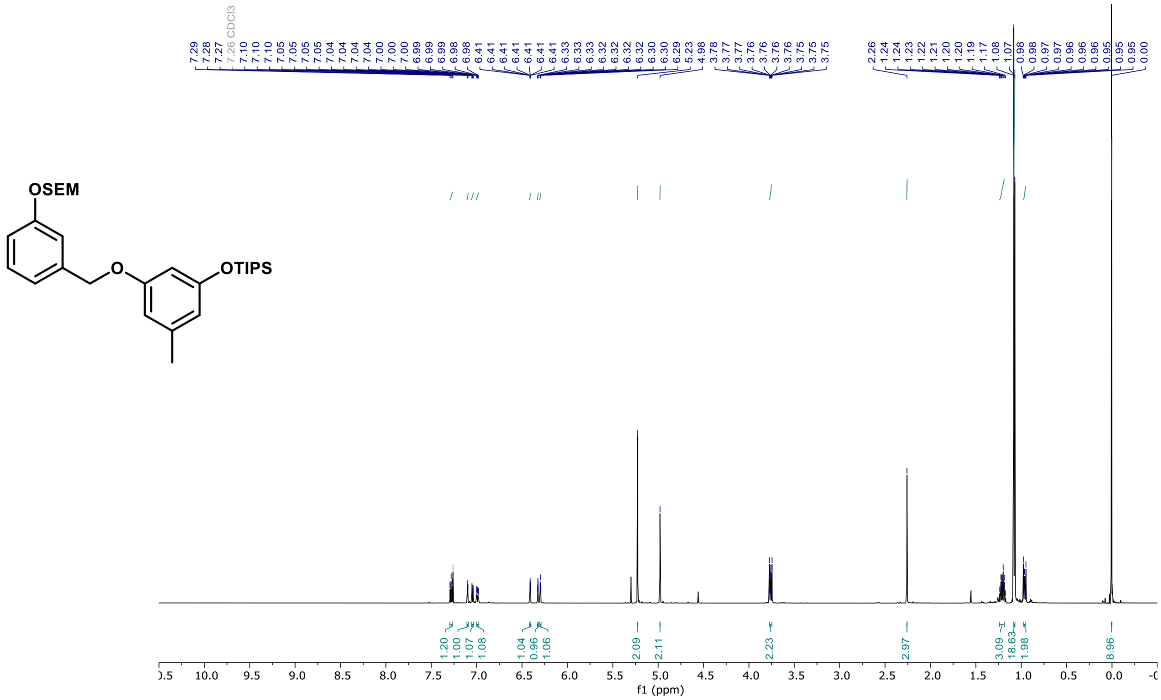
7.29 7.28 7.27 7.26 CDCl3 7.10 7.10 7.05 7.05 7.05 7.04 7.04 7.04 7.00 7.00 6.99 6.99 6.99 6.98 6.98 6.41 6.41 6.41 6.41 6.41 6.41 6.33 6.33 6.32 6.32 6.32 6.30 6.30 6.29 5.23 4.98 3.78 3.77 3.76 3.76 3.76 3.75 3.75 3.75 2.26 1.24 1.23 1.22 1.21 1.20 1.20 1.19 1.17 1.08 1.07 0.98 0.98 0.97 0.97 0.96 0.96 0.95 0.95 0.95 0.00
1.20 1.00 1.07 1.08 1.04 0.96 1.06 2.09 2.11 2.23 2.97 3.09 18.63 1.98 8.96
OSEM
O
OTIPS
f1 (ppm)

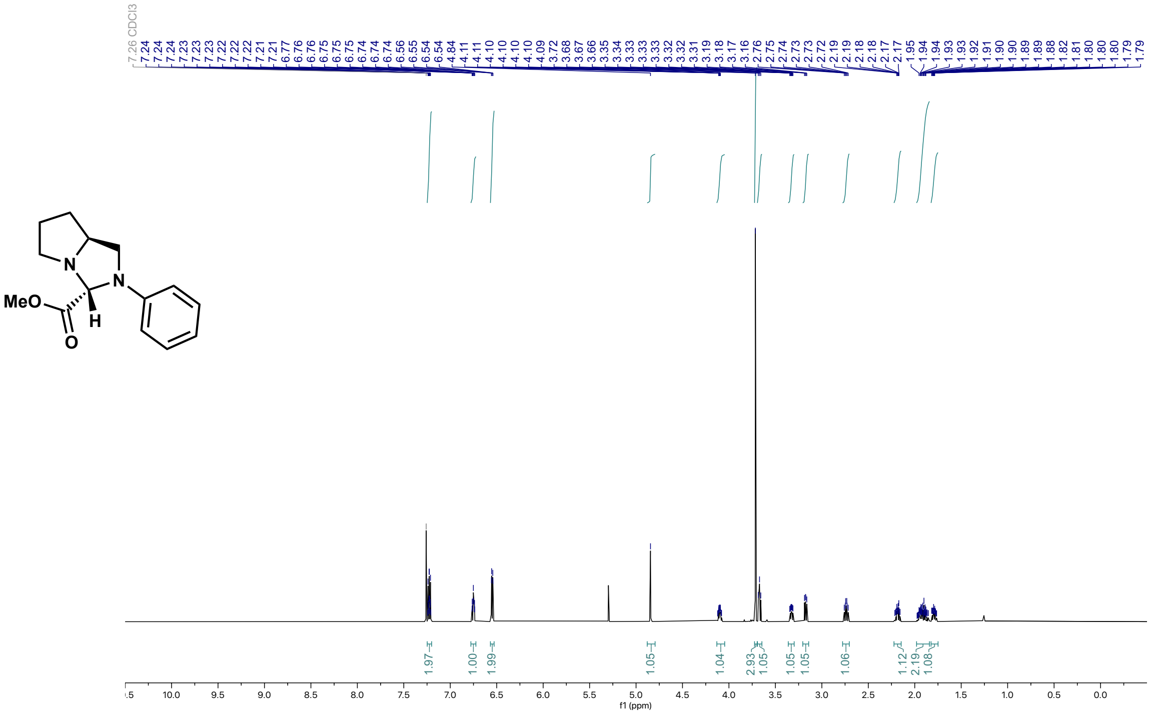
MeO
O
N
N
H
7.26 CDCl3
7.24 7.24 7.24 7.23 7.23 7.22 7.22 7.22 7.21 7.21 6.77 6.76 6.76 6.75 6.75 6.74 6.74 6.74 6.56 6.55 6.54 6.54 4.84 4.11 4.10 4.10 4.10 4.10 4.09 3.72 3.68 3.67 3.66 3.35 3.34 3.33 3.33 3.33 3.32 3.32 3.31 3.19 3.18 3.17 3.16 2.76 2.75 2.74 2.73 2.73 2.72 2.19 2.19 2.18 2.18 2.17 2.17 1.95 1.94 1.94 1.93 1.93 1.92 1.91 1.90 1.90 1.89 1.89 1.88 1.82 1.81 1.80 1.80 1.80 1.79 1.79
1.97
1.00
1.99
1.05
1.04
2.93
1.05
1.05
1.05
1.06
1.12
2.19
1.08
10.0 9.5 9.0 8.5 8.0 7.5 7.0 6.5 6.0 5.5 5.0 4.5 4.0 3.5 3.0 2.5 2.0 1.5 1.0 0.5 0.0
f1 (ppm)

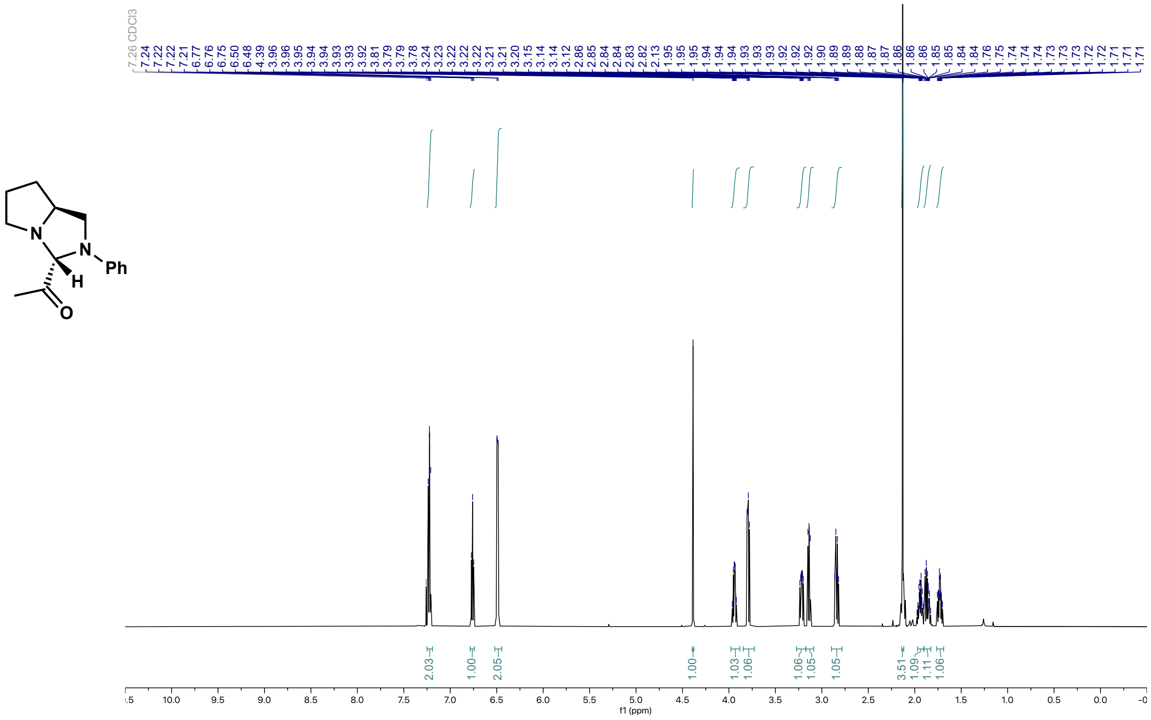
N
N
Ph
H
O
7.26 CDCl3
7.24 7.22 7.22 7.21 6.77 6.76 6.76 6.75 6.50 6.48 4.39 3.96 3.95 3.94 3.93 3.93 3.92 3.81 3.79 3.79 3.78 3.24 3.23 3.22 3.22 3.21 3.21 3.20 3.15 3.14 3.12 2.86 2.85 2.84 2.84 2.83 2.82 2.13 1.95 1.95 1.94 1.94 1.93 1.93 1.92 1.92 1.92 1.90 1.89 1.88 1.87 1.87 1.86 1.86 1.86 1.85 1.85 1.84 1.76 1.75 1.74 1.74 1.74 1.73 1.73 1.72 1.72 1.71 1.71 1.71
2.03
1.00
2.05
1.00
1.03
1.06
1.06
1.05
1.05
3.51
1.09
1.11
1.06
10.0 9.5 9.0 8.5 8.0 7.5 7.0 6.5 6.0 5.5 5.0 4.5 4.0 3.5 3.0 2.5 2.0 1.5 1.0 0.5 0.0
f1 (ppm)

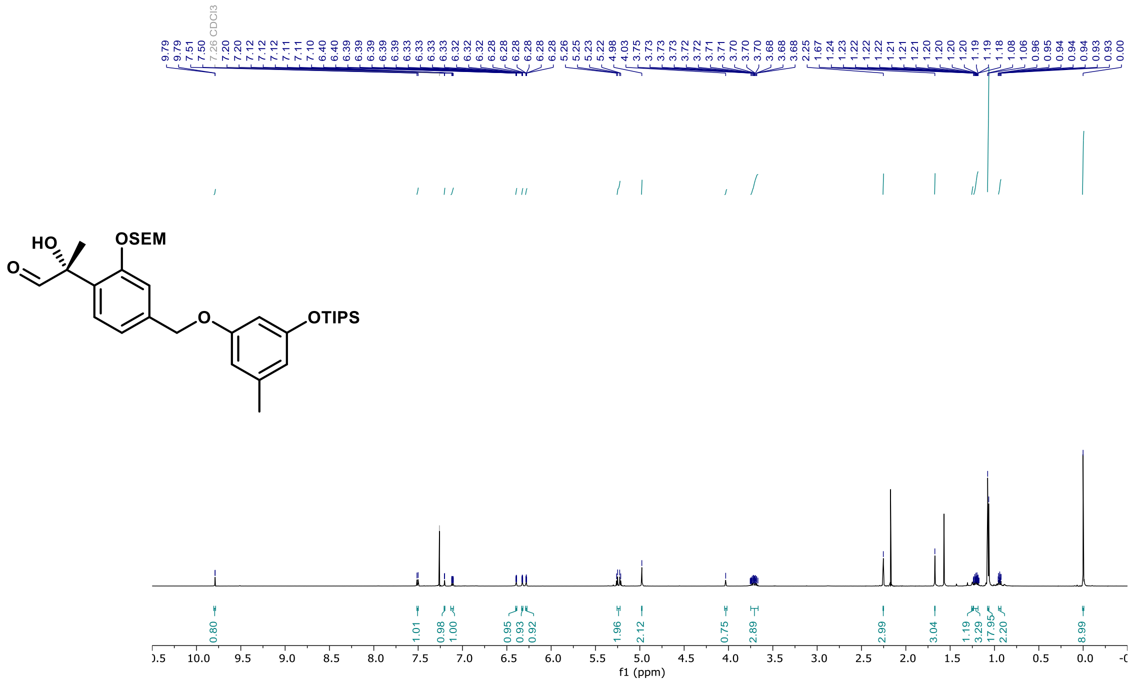
9.79
9.79
7.51
7.50
7.26 CDCl3
7.20
7.20
7.12
7.12
7.12
7.11
7.11
7.10
6.40
6.40
6.39
6.39
6.39
6.39
6.39
6.33
6.33
6.33
6.33
6.32
6.32
6.32
6.28
6.28
6.28
6.28
6.28
6.28
5.26
5.25
5.23
5.22
4.98
4.03
3.75
3.73
3.73
3.73
3.72
3.72
3.71
3.71
3.70
3.70
3.70
3.68
3.68
3.68
2.25
1.67
1.24
1.23
1.22
1.22
1.22
1.21
1.21
1.21
1.20
1.20
1.20
1.19
1.19
1.18
1.08
1.06
0.96
0.95
0.94
0.94
0.94
0.93
0.93
0.00
HO
OSEM
O
O
OTIPS
0.80
1.01
0.98
1.00
0.95
0.93
0.92
1.96
2.12
0.75
2.89
2.99
3.04
1.19
3.29
17.95
2.20
8.99
).5
10.0
9.5
9.0
8.5
8.0
7.5
7.0
6.5
6.0
5.5
5.0
4.5
4.0
3.5
3.0
2.5
2.0
1.5
1.0
0.5
0.0
-(
f1 (ppm)

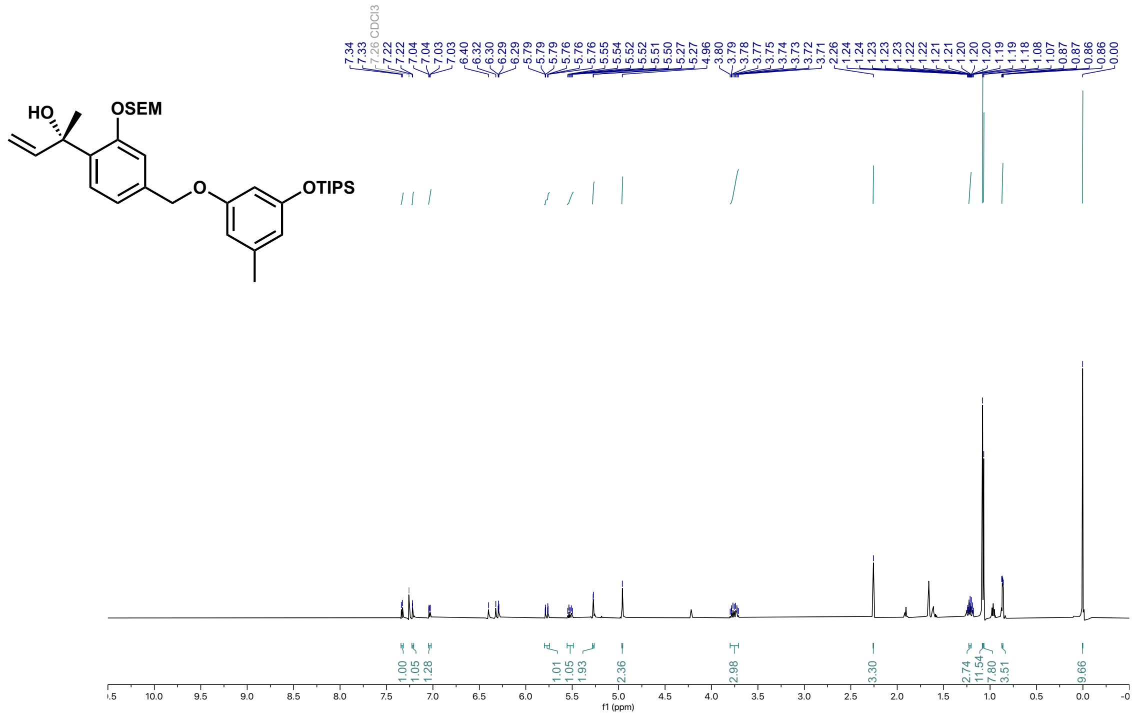
7.34
7.33
7.26 CDCl3
7.22
7.22
7.04
7.04
7.03
7.03
6.40
6.32
6.30
6.29
6.29
5.79
5.79
5.79
5.76
5.76
5.76
5.55
5.54
5.52
5.52
5.51
5.50
5.27
5.27
4.96
3.80
3.79
3.78
3.77
3.75
3.74
3.73
3.72
3.71
2.26
1.24
1.24
1.23
1.23
1.22
1.22
1.21
1.21
1.20
1.20
1.20
1.19
1.19
1.18
1.08
1.07
0.87
0.87
0.86
0.86
0.00
HO
OSEM
O
OTIPS
1.00
1.05
1.28
1.01
1.05
1.93
2.36
2.98
3.30
2.74
11.54
7.80
3.51
9.66
.5
10.0
9.5
9.0
8.5
8.0
7.5
7.0
6.5
6.0
5.5
5.0
4.5
4.0
3.5
3.0
2.5
2.0
1.5
1.0
0.5
0.0
-(
f1 (ppm)

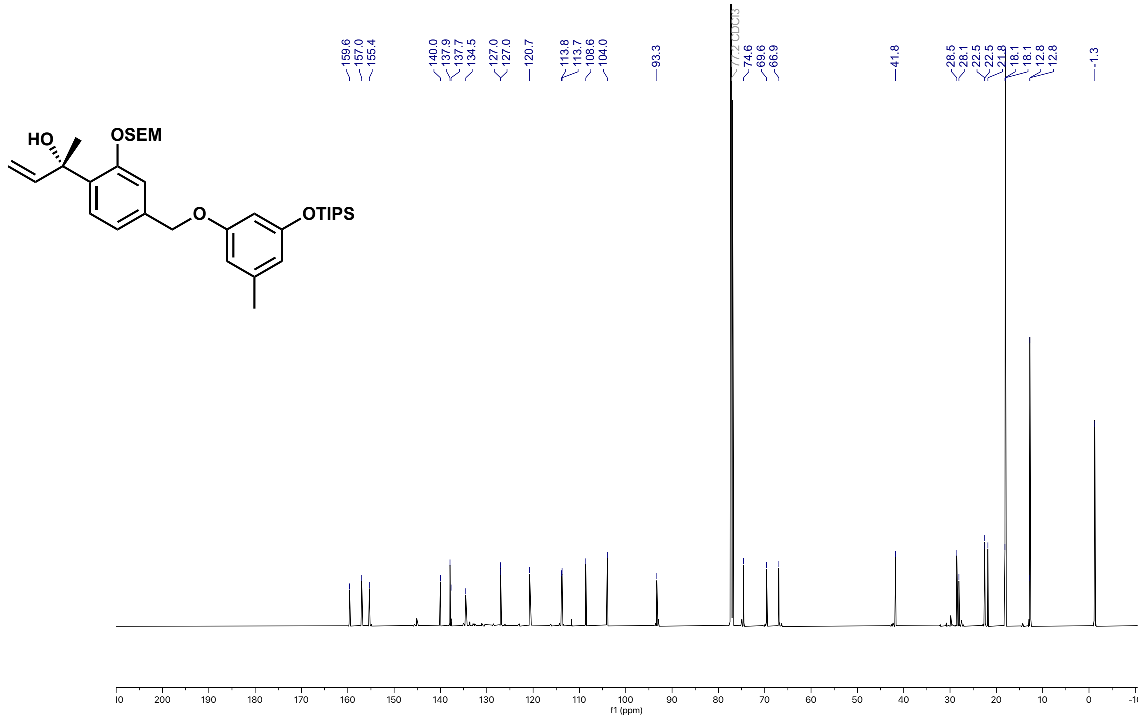
HO
OSEM
O
OTIPS
159.6
157.0
155.4
140.0
137.9
137.7
134.5
127.0
127.0
120.7
113.8
113.7
108.6
104.0
93.3
77.2 CDCl3
74.6
69.6
66.9
41.8
28.5
28.1
22.5
22.5
21.8
18.1
18.1
12.8
12.8
-1.3
210
200
190
180
170
160
150
140
130
120
110
100
90
80
70
60
50
40
30
20
10
0
-10
f1 (ppm)

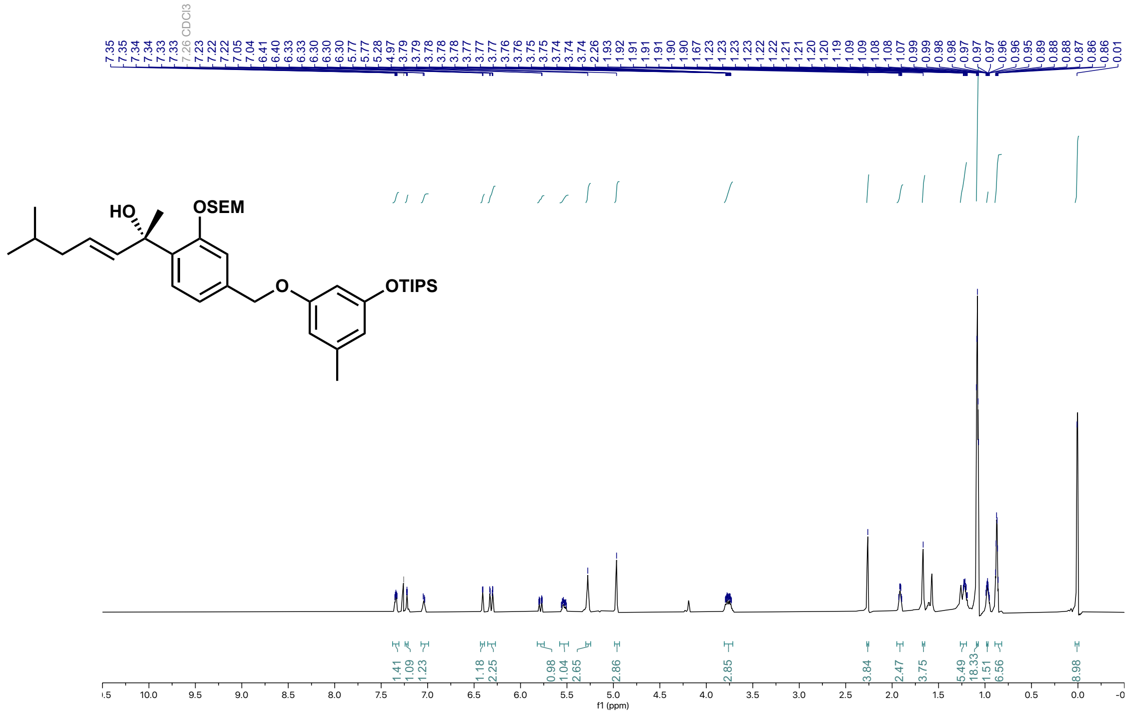
HO
OSEM
O
OTIPS
7.35
7.35
7.34
7.34
7.33
7.33
7.26 CDCl3
7.23
7.23
7.22
7.22
7.05
7.04
6.41
6.40
6.33
6.33
6.30
6.30
5.77
5.77
5.28
4.97
3.79
3.79
3.78
3.78
3.77
3.77
3.76
3.75
3.74
3.74
2.26
1.93
1.92
1.91
1.91
1.91
1.90
1.67
1.23
1.23
1.23
1.22
1.22
1.21
1.21
1.20
1.20
1.19
1.09
1.09
1.08
1.08
1.07
0.99
0.99
0.98
0.98
0.97
0.97
0.96
0.96
0.95
0.89
0.88
0.88
0.87
0.86
0.86
0.01
1.41
1.09
1.23
1.18
2.25
0.98
1.04
2.65
2.86
2.85
3.84
2.47
3.75
5.49
18.33
1.51
6.56
8.98
10.5
10.0
9.5
9.0
8.5
8.0
7.5
7.0
6.5
6.0
5.5
5.0
4.5
4.0
3.5
3.0
2.5
2.0
1.5
1.0
0.5
0.0
-0.5
f1 (ppm)

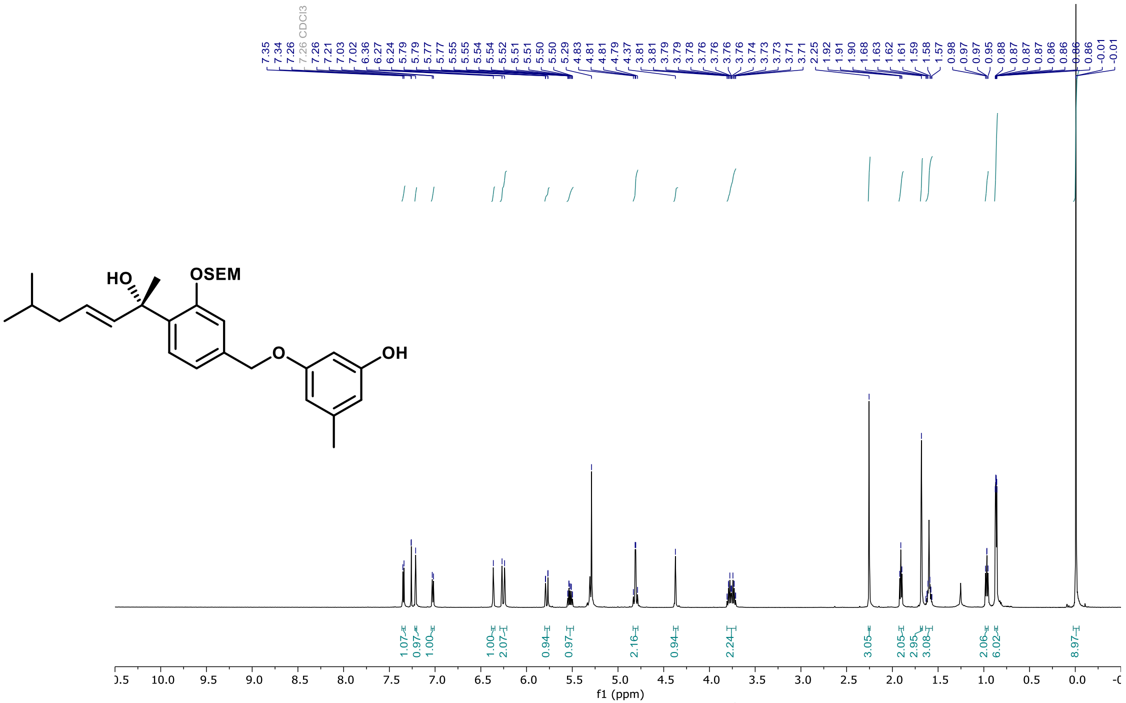
7.35
7.34
7.26
7.26 CDCl3
7.26
7.21
7.03
7.02
6.36
6.27
6.24
5.79
5.79
5.77
5.77
5.55
5.55
5.54
5.54
5.52
5.51
5.51
5.50
5.50
5.29
4.83
4.81
4.79
4.37
3.81
3.81
3.79
3.79
3.78
3.76
3.76
3.76
3.74
3.73
3.73
3.71
3.71
2.25
1.92
1.91
1.90
1.68
1.63
1.62
1.61
1.59
1.58
1.57
0.98
0.97
0.97
0.95
0.88
0.87
0.87
0.87
0.86
0.86
0.86
0.86
-0.01
-0.01
HO
OSEM
O
OH
1.07
0.97
1.00
1.00
2.07
0.94
0.97
2.16
0.94
2.24
3.05
2.05
2.95
3.08
2.06
6.02
8.97
f1 (ppm)

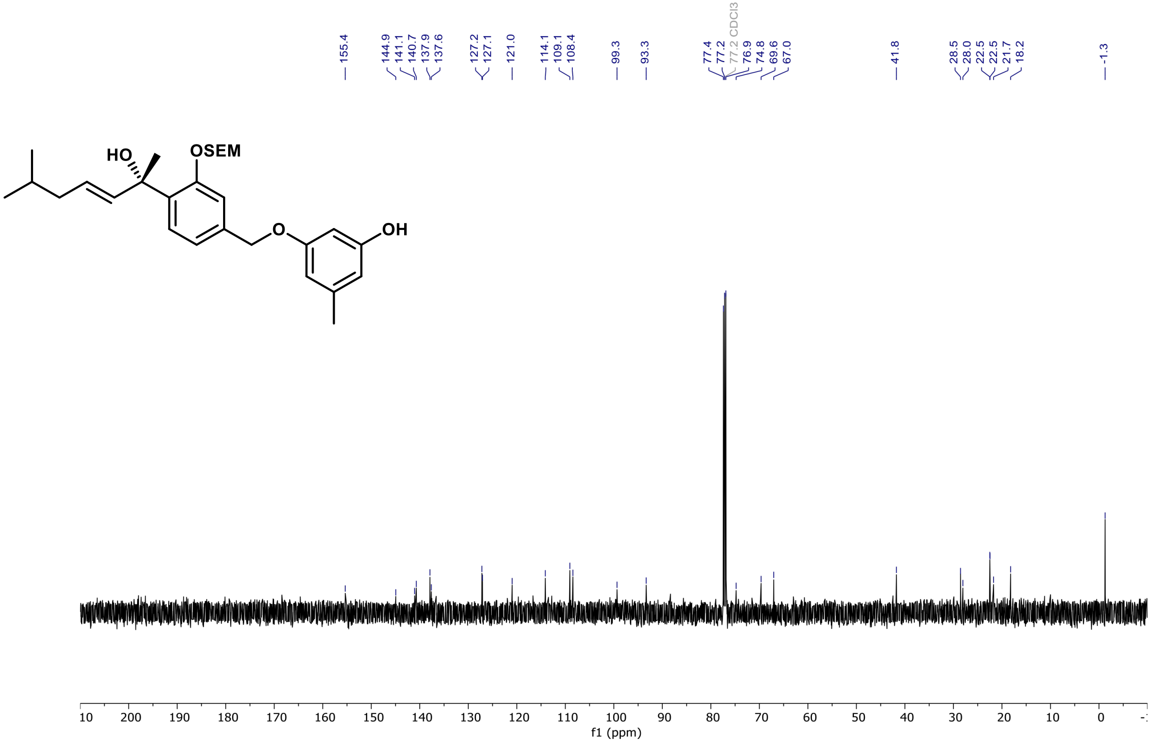
155.4
144.9
141.1
140.7
137.9
137.6
127.2
127.1
121.0
114.1
109.1
108.4
99.3
93.3
77.4
77.2
77.2 CDCl3
76.9
74.8
69.6
67.0
41.8
28.5
28.0
22.5
22.5
21.7
18.2
-1.3
HO
OSEM
O
OH
f1 (ppm)

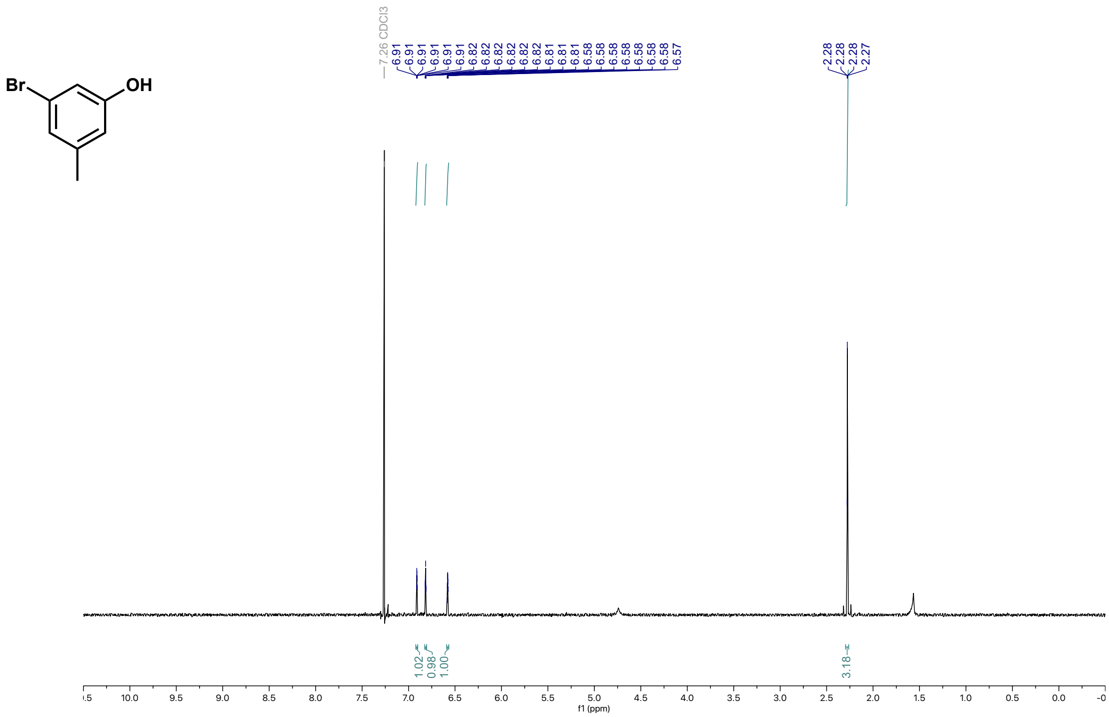
Br
OH
7.26 CDCl3
6.91
6.91
6.91
6.91
6.91
6.82
6.82
6.82
6.82
6.82
6.81
6.81
6.58
6.58
6.58
6.58
6.58
6.58
6.57
2.28
2.28
2.28
2.27
1.02
0.98
1.00
3.18
10.0 9.5 9.0 8.5 8.0 7.5 7.0 6.5 6.0 5.5 5.0 4.5 4.0 3.5 3.0 2.5 2.0 1.5 1.0 0.5 0.0
f1 (ppm)

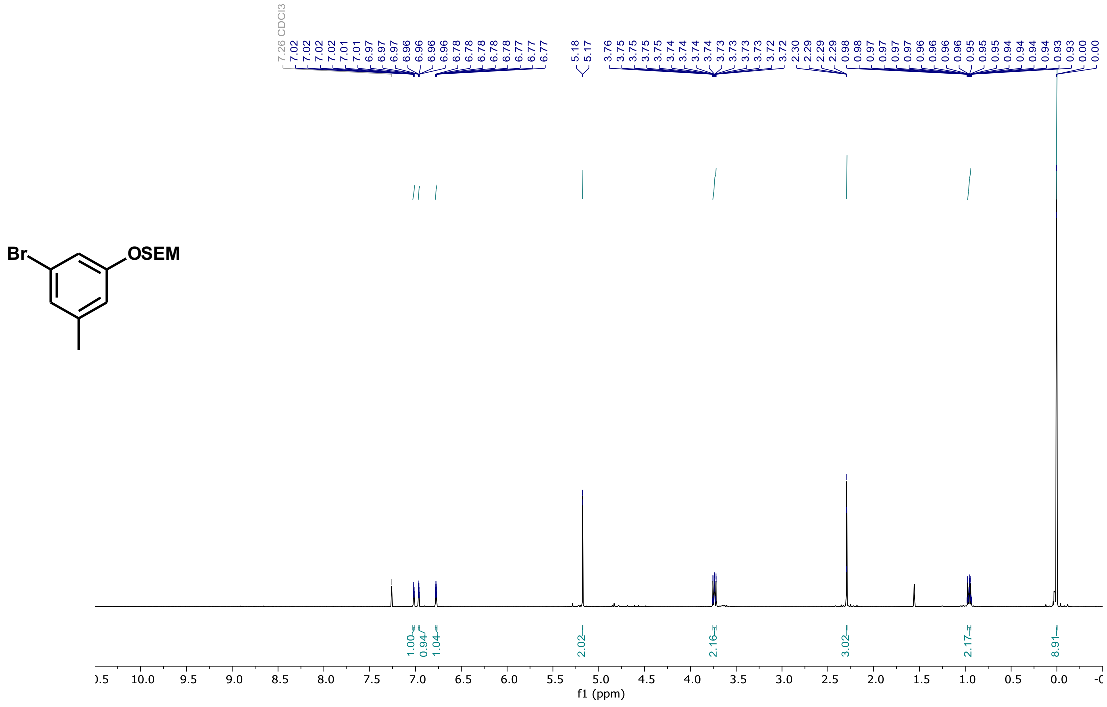
Br
OSEM
7.26 CDCl3
7.02
7.02
7.02
7.01
7.01
6.97
6.97
6.96
6.96
6.96
6.78
6.78
6.78
6.78
6.77
6.77
5.18
5.17
3.76
3.75
3.75
3.75
3.74
3.74
3.74
3.73
3.73
3.73
3.72
2.30
2.29
2.29
0.98
0.97
0.97
0.97
0.96
0.96
0.96
0.95
0.95
0.94
0.94
0.94
0.93
0.93
0.00
0.00
1.00
0.94
1.04
2.02
2.16
3.02
2.17
8.91
10.0 9.5 9.0 8.5 8.0 7.5 7.0 6.5 6.0 5.5 5.0 4.5 4.0 3.5 3.0 2.5 2.0 1.5 1.0 0.5 0.0
f1 (ppm)

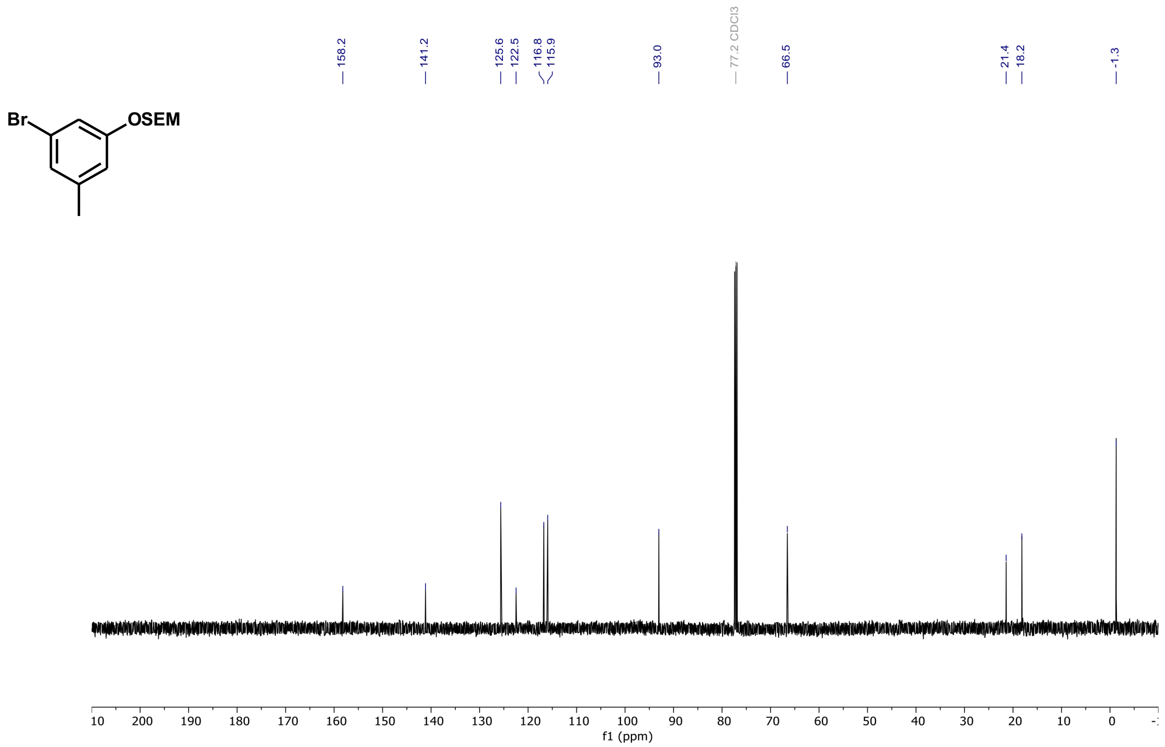
Br
OSEM
158.2
141.2
125.6
122.5
116.8
115.9
93.0
77.2 CDCl3
66.5
21.4
18.2
-1.3
10 200 190 180 170 160 150 140 130 120 110 100 90 80 70 60 50 40 30 20 10 0
f1 (ppm)

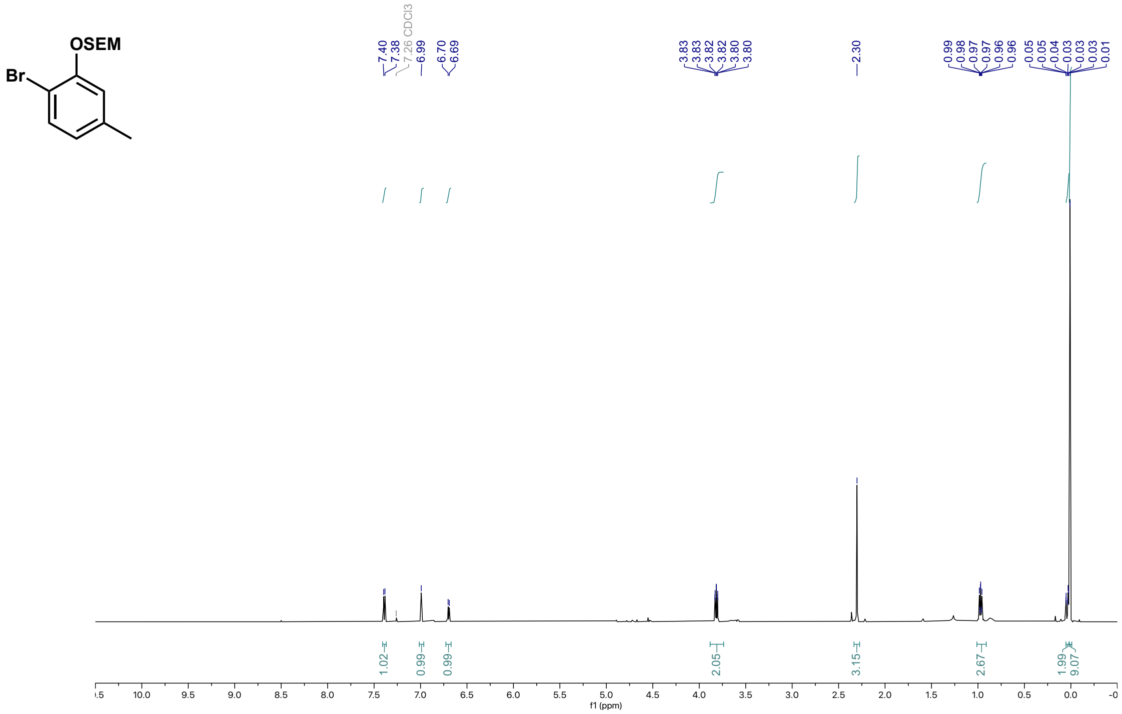
OSEM
Br
7.40
7.38
7.26 CDCl3
6.99
6.70
6.69
3.83
3.83
3.82
3.82
3.80
3.80
2.30
0.99
0.98
0.97
0.97
0.96
0.96
0.05
0.05
0.04
0.03
0.03
0.03
0.01
1.02
0.99
0.99
2.05
3.15
2.67
1.99
9.07
10.0 9.5 9.0 8.5 8.0 7.5 7.0 6.5 6.0 5.5 5.0 4.5 4.0 3.5 3.0 2.5 2.0 1.5 1.0 0.5 0.0
f1 (ppm)

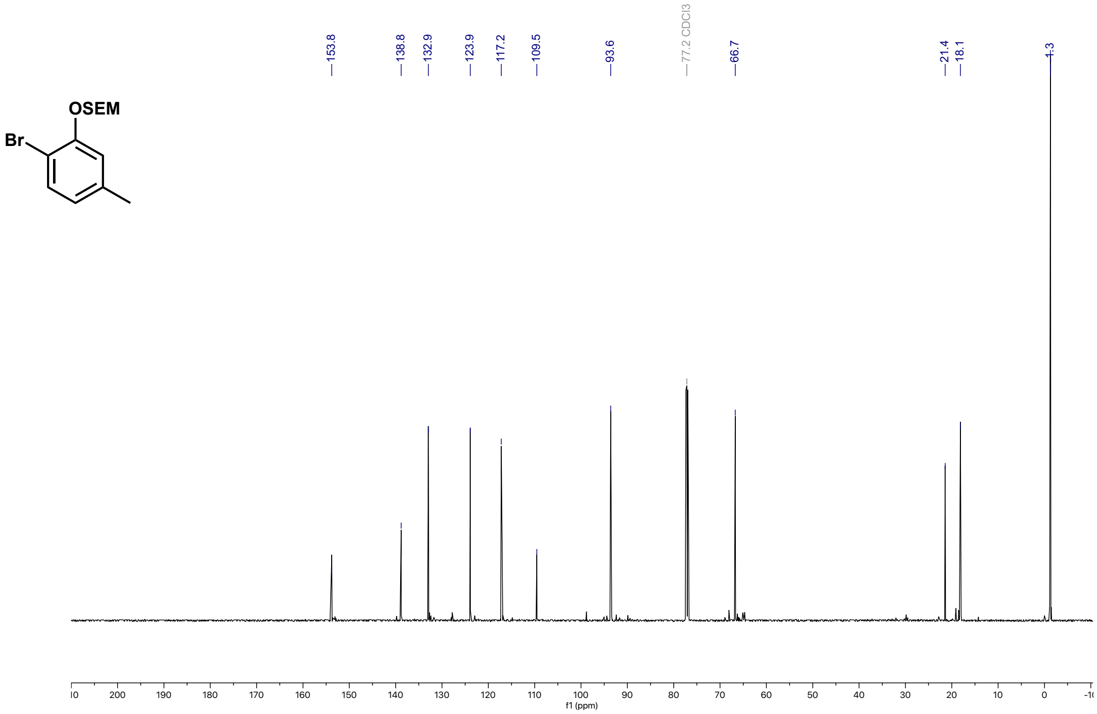
OSEM
Br
153.8
138.8
132.9
123.9
117.2
109.5
93.6
77.2 CDCl3
66.7
21.4
18.1
-1.3
200 190 180 170 160 150 140 130 120 110 100 90 80 70 60 50 40 30 20 10 0
f1 (ppm)

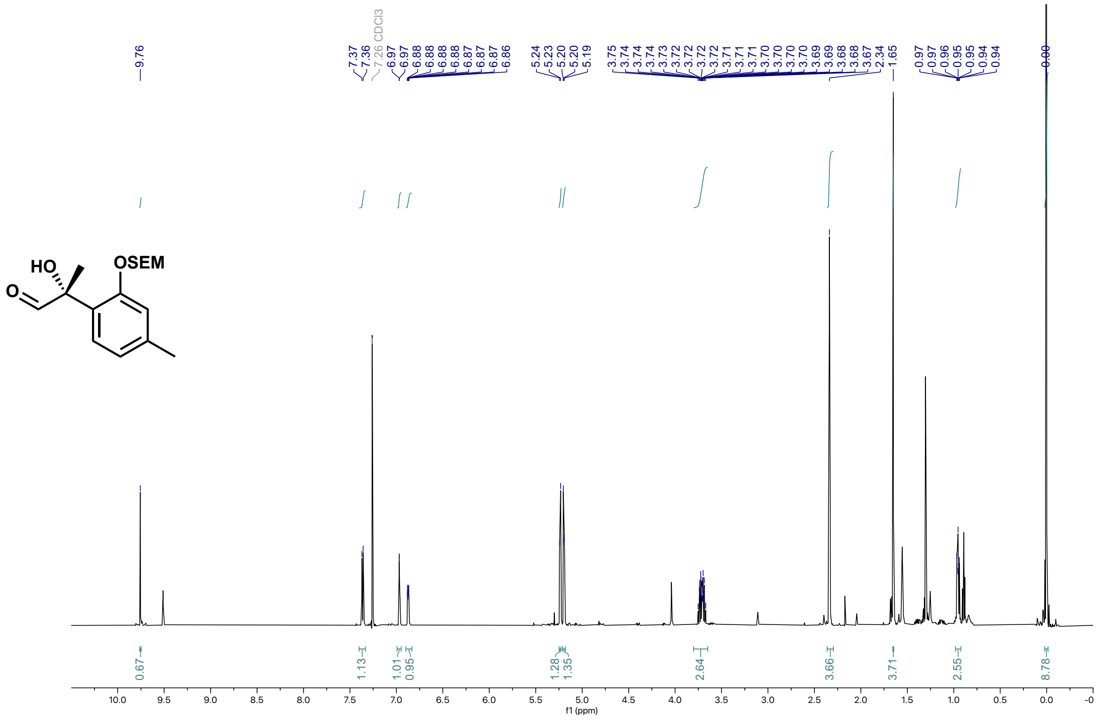
HO
O
OSEM
9.76
7.37
7.36
7.26 CDCl3
6.97
6.97
6.88
6.88
6.88
6.88
6.87
6.87
6.87
6.86
5.24
5.23
5.20
5.20
5.19
3.75
3.74
3.74
3.74
3.73
3.72
3.72
3.72
3.72
3.71
3.71
3.70
3.70
3.70
3.69
3.69
3.68
3.68
3.67
2.34
1.65
0.97
0.97
0.96
0.95
0.95
0.94
0.94
0.00
0.67
1.13
1.01
0.95
1.28
1.35
2.64
3.66
3.71
2.55
8.78
10.0 9.5 9.0 8.5 8.0 7.5 7.0 6.5 6.0 5.5 5.0 4.5 4.0 3.5 3.0 2.5 2.0 1.5 1.0 0.5 0.0
f1 (ppm)

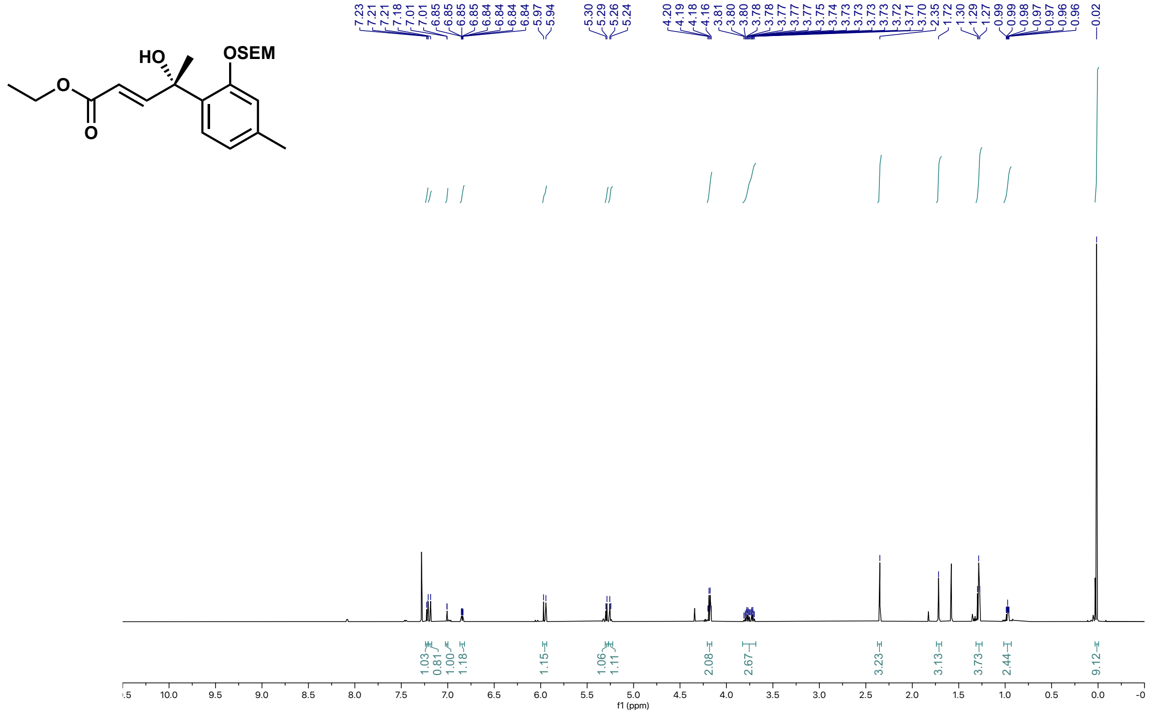
HO
OSEM
O
O
7.23
7.21
7.21
7.18
7.01
7.01
6.85
6.85
6.85
6.85
6.84
6.84
6.84
6.84
5.97
5.94
5.30
5.29
5.26
5.24
4.20
4.19
4.18
4.16
3.81
3.80
3.78
3.78
3.77
3.77
3.77
3.75
3.74
3.73
3.73
3.73
3.73
3.72
3.71
3.70
2.35
1.72
1.30
1.29
1.27
0.99
0.99
0.98
0.97
0.97
0.96
0.96
0.02
1.03
0.81
1.00
1.18
1.15
1.06
1.11
2.08
2.67
3.23
3.13
3.73
2.44
9.12
10.0
9.5
9.0
8.5
8.0
7.5
7.0
6.5
6.0
5.5
5.0
4.5
4.0
3.5
3.0
2.5
2.0
1.5
1.0
0.5
0.0
f1 (ppm)

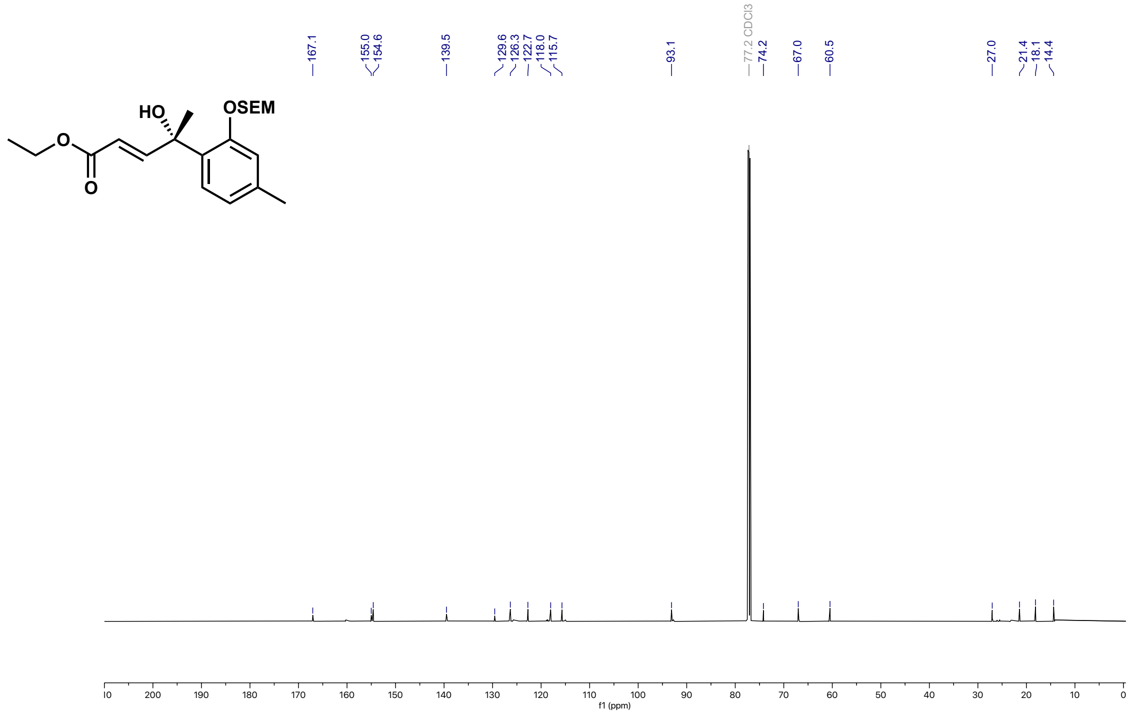
HO
OSEM
O
O
167.1
155.0
154.6
139.5
129.6
126.3
122.7
118.0
115.7
93.1
77.2 CDCl3
74.2
67.0
60.5
27.0
21.4
18.1
14.4
200
190
180
170
160
150
140
130
120
110
100
90
80
70
60
50
40
30
20
10
0
f1 (ppm)

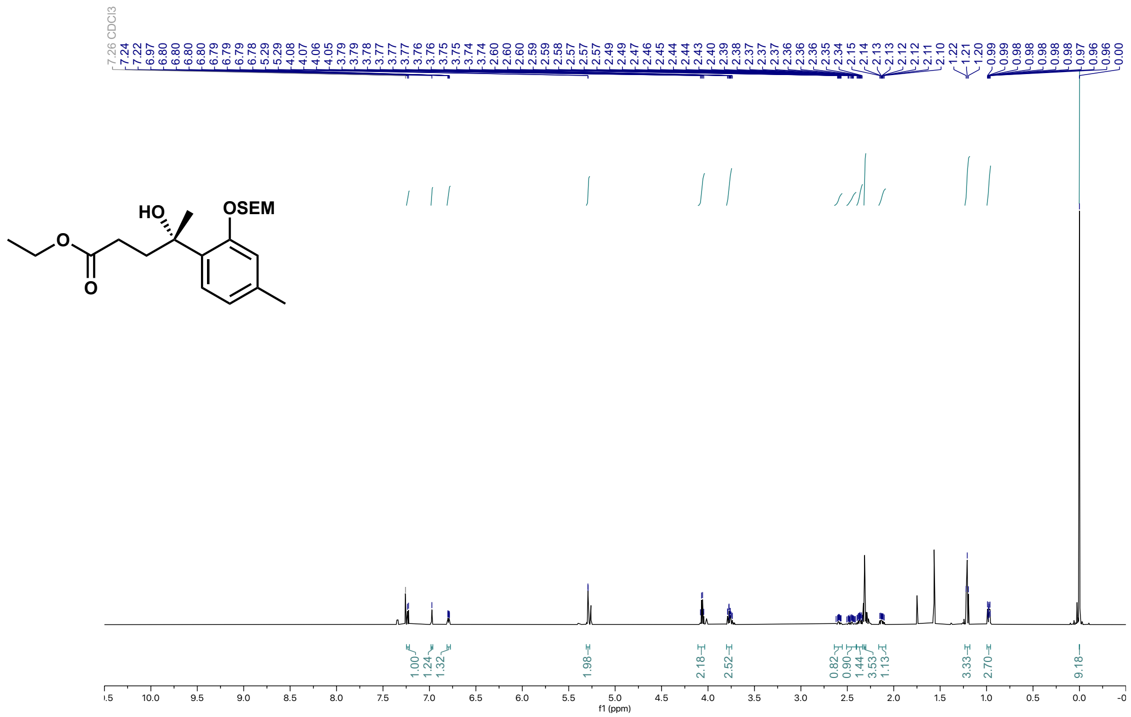
7.26 CDCl3
7.24
7.22
6.97
6.80
6.80
6.80
6.80
6.79
6.79
6.78
5.29
5.29
4.08
4.07
4.06
4.05
3.79
3.79
3.78
3.77
3.77
3.76
3.76
3.75
3.75
3.74
3.74
2.60
2.60
2.59
2.59
2.58
2.57
2.57
2.49
2.49
2.47
2.46
2.45
2.44
2.44
2.43
2.40
2.39
2.38
2.37
2.37
2.37
2.36
2.36
2.35
2.34
2.15
2.14
2.13
2.13
2.12
2.12
2.11
2.10
1.22
1.21
1.20
0.99
0.99
0.98
0.98
0.98
0.98
0.98
0.97
0.96
0.96
0.00
HO
OSEM
O
O
1.00
1.24
1.32
1.98
2.18
2.52
0.82
0.90
1.44
3.53
1.13
3.33
2.70
9.18
10.0
9.5
9.0
8.5
8.0
7.5
7.0
6.5
6.0
5.5
5.0
4.5
4.0
3.5
3.0
2.5
2.0
1.5
1.0
0.5
0.0
f1 (ppm)

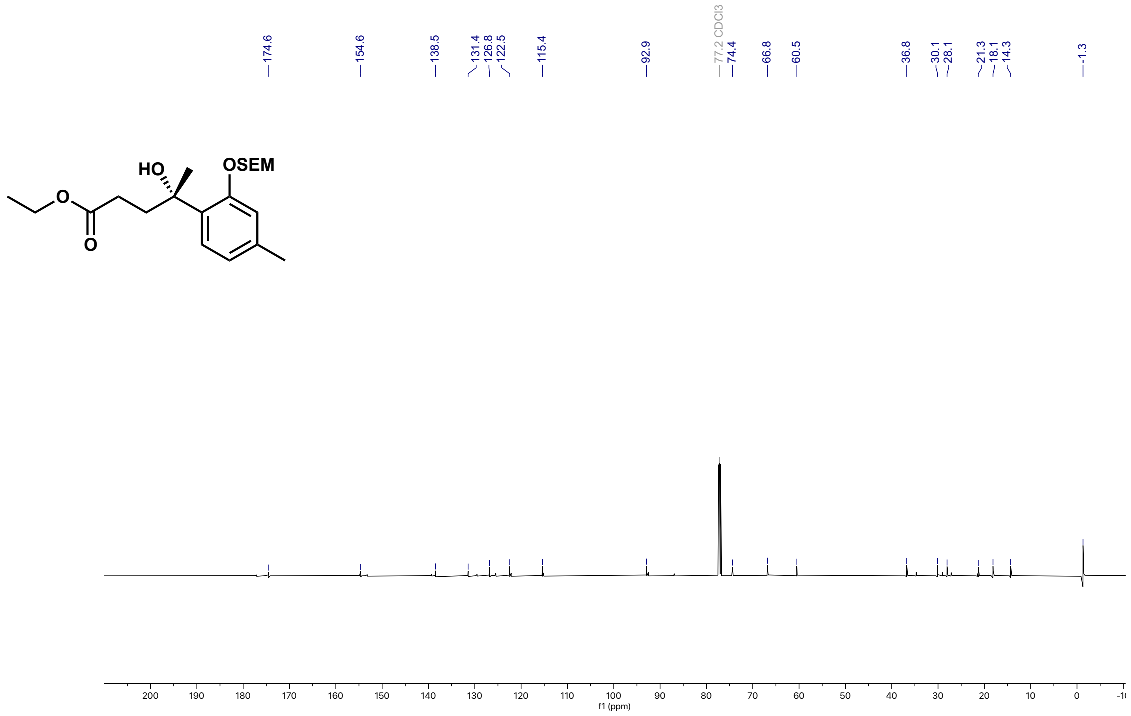
174.6
154.6
138.5
131.4
126.8
122.5
115.4
92.9
77.2 CDCl3
74.4
66.8
60.5
36.8
30.1
28.1
21.3
18.1
14.3
-1.3
HO
OSEM
O
O
200
190
180
170
160
150
140
130
120
110
100
90
80
70
60
50
40
30
20
10
0
f1 (ppm)

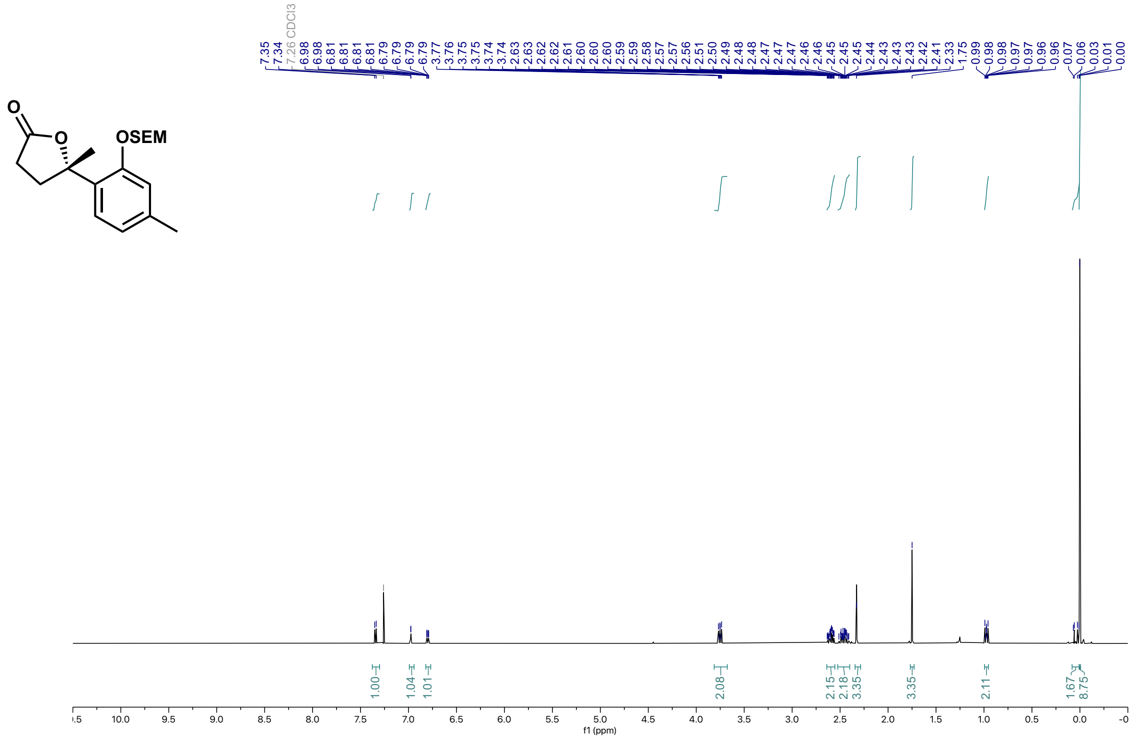
OSEM
O
O
7.35
7.34
7.26 CDCl3
6.98
6.98
6.81
6.81
6.81
6.81
6.79
6.79
6.79
6.79
3.77
3.76
3.75
3.75
3.74
3.74
2.63
2.63
2.62
2.62
2.61
2.60
2.60
2.60
2.59
2.59
2.58
2.57
2.57
2.56
2.51
2.50
2.49
2.48
2.48
2.47
2.47
2.47
2.46
2.46
2.45
2.45
2.45
2.44
2.43
2.43
2.43
2.42
2.41
2.33
1.75
0.99
0.98
0.98
0.97
0.97
0.96
0.96
0.07
0.06
0.03
0.01
0.00
1.00
1.04
1.01
2.08
2.15
2.18
3.35
3.35
2.11
1.67
8.75
10.0
9.5
9.0
8.5
8.0
7.5
7.0
6.5
6.0
5.5
5.0
4.5
4.0
3.5
3.0
2.5
2.0
1.5
1.0
0.5
0.0
f1 (ppm)

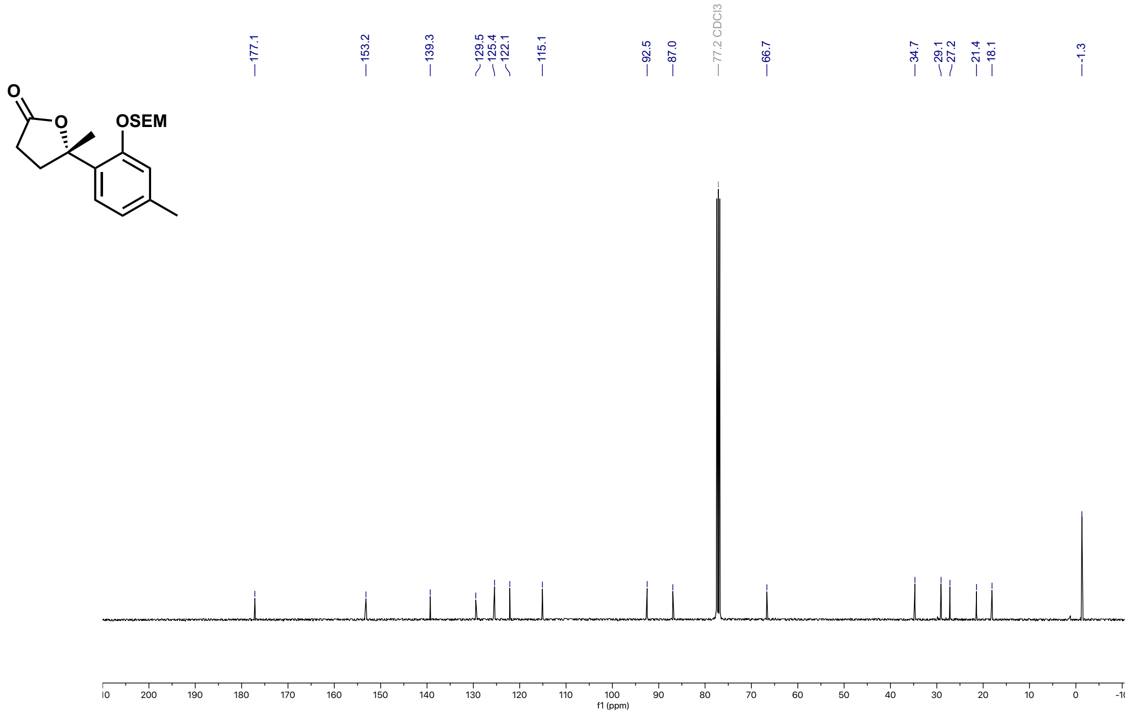
OSEM
O
O
177.1
153.2
139.3
129.5
125.4
122.1
115.1
92.5
87.0
77.2 CDCl3
66.7
34.7
29.1
27.2
21.4
18.1
-1.3
200
190
180
170
160
150
140
130
120
110
100
90
80
70
60
50
40
30
20
10
0
f1 (ppm)

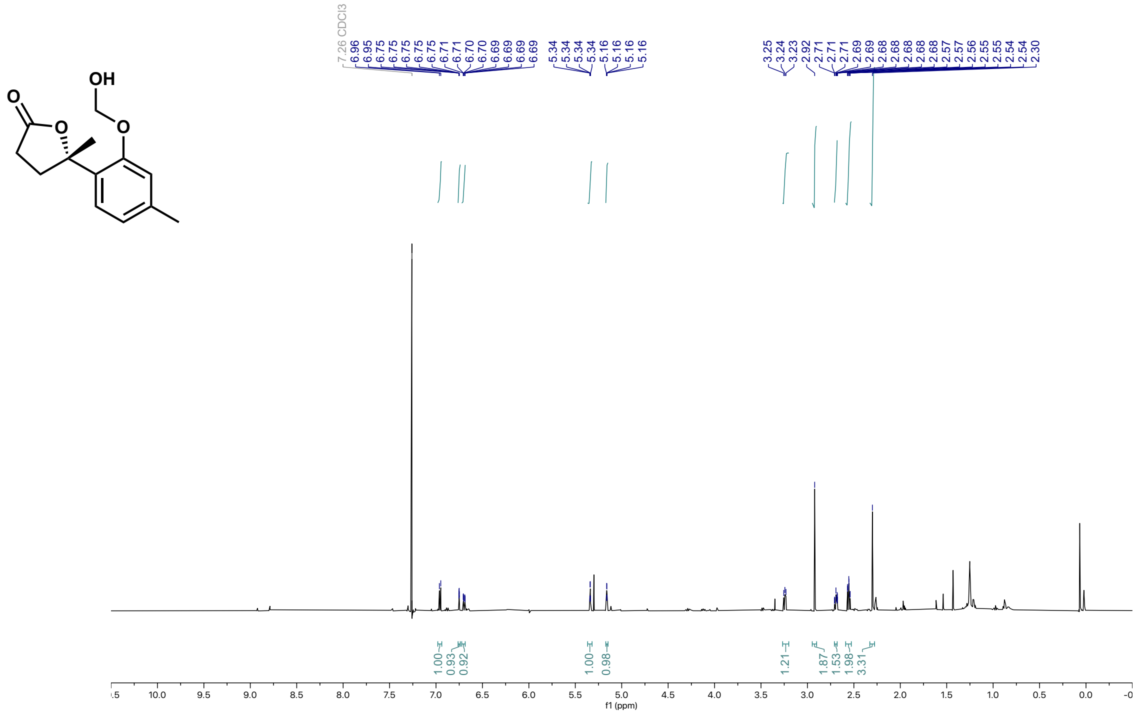
OH
O
O
O
7.26 CDCl3
6.96
6.95
6.75
6.75
6.75
6.75
6.75
6.71
6.71
6.70
6.70
6.69
6.69
6.69
6.69
5.34
5.34
5.34
5.34
5.16
5.16
5.16
5.16
3.25
3.24
3.23
2.92
2.71
2.71
2.71
2.69
2.69
2.68
2.68
2.68
2.68
2.68
2.57
2.57
2.56
2.55
2.54
2.54
2.30
1.00
0.93
0.92
1.00
0.98
1.21
1.87
1.53
1.98
3.31
10.0
9.5
9.0
8.5
8.0
7.5
7.0
6.5
6.0
5.5
5.0
4.5
4.0
3.5
3.0
2.5
2.0
1.5
1.0
0.5
0.0
f1 (ppm)

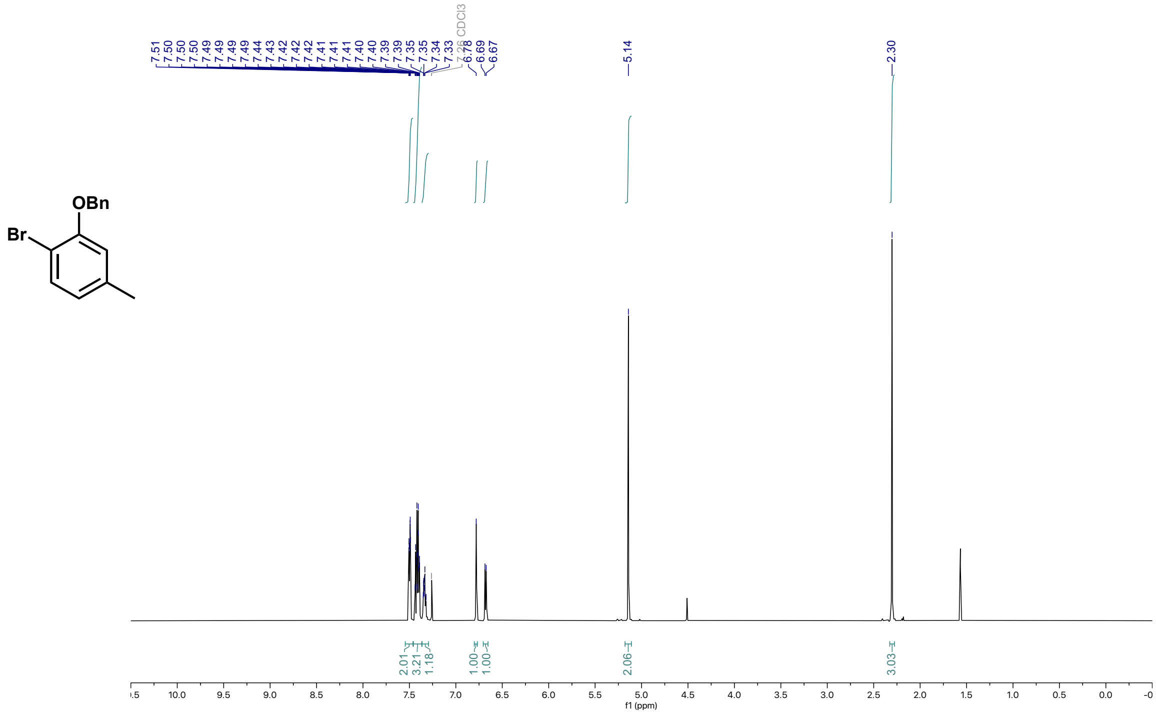
OBn
Br
7.51
7.50
7.50
7.49
7.49
7.49
7.44
7.43
7.42
7.42
7.42
7.41
7.41
7.41
7.40
7.40
7.39
7.35
7.35
7.34
7.33
7.26 CDCl3
6.78
6.69
6.67
5.14
2.30
2.01
3.21
1.18
1.00
1.00
2.06
3.03
10.0
9.5
9.0
8.5
8.0
7.5
7.0
6.5
6.0
5.5
5.0
4.5
4.0
3.5
3.0
2.5
2.0
1.5
1.0
0.5
0.0
f1 (ppm)

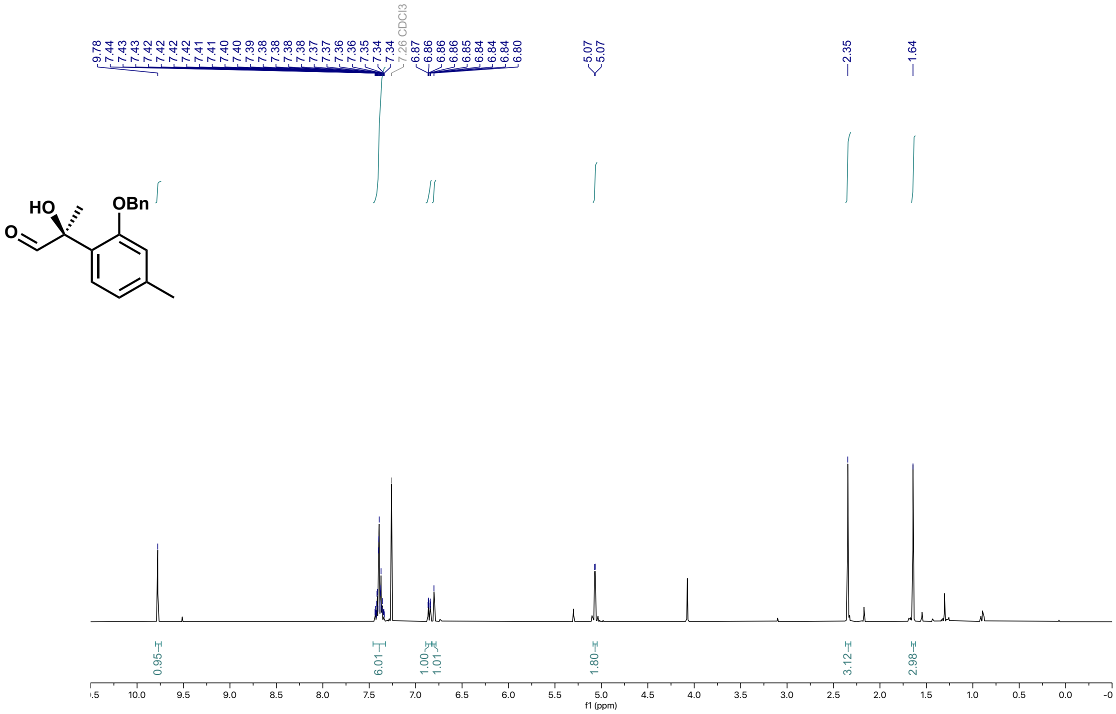
9.78
7.44
7.43
7.43
7.42
7.42
7.42
7.41
7.40
7.39
7.38
7.38
7.38
7.38
7.37
7.37
7.36
7.36
7.35
7.34
7.34
7.26 CDCl3
6.87
6.86
6.86
6.86
6.85
6.84
6.84
6.84
6.80
5.07
5.07
2.35
1.64
HO
OBn
O
0.95
6.01
1.00
1.01
1.80
3.12
2.98
10.0
9.5
9.0
8.5
8.0
7.5
7.0
6.5
6.0
5.5
5.0
4.5
4.0
3.5
3.0
2.5
2.0
1.5
1.0
0.5
0.0
f1 (ppm)

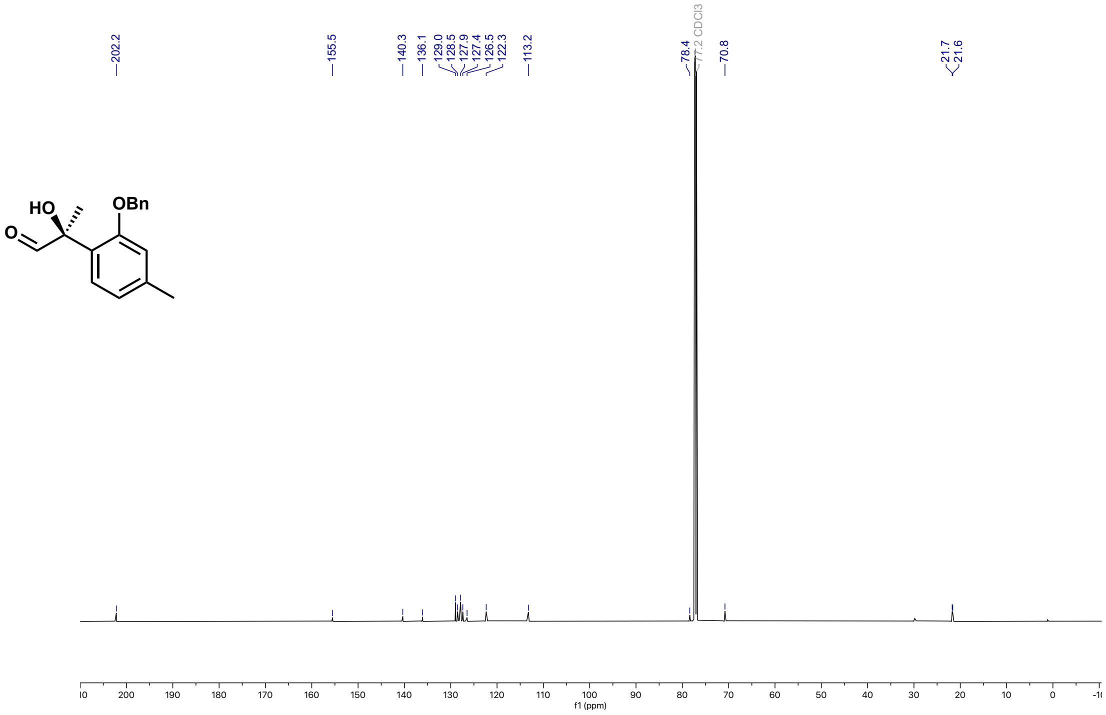
202.2
155.5
140.3
136.1
129.0
128.5
127.9
127.4
126.5
122.3
113.2
78.4
77.2 CDCl3
70.8
21.7
21.6
HO
OBn
O
200
190
180
170
160
150
140
130
120
110
100
90
80
70
60
50
40
30
20
10
0
f1 (ppm)

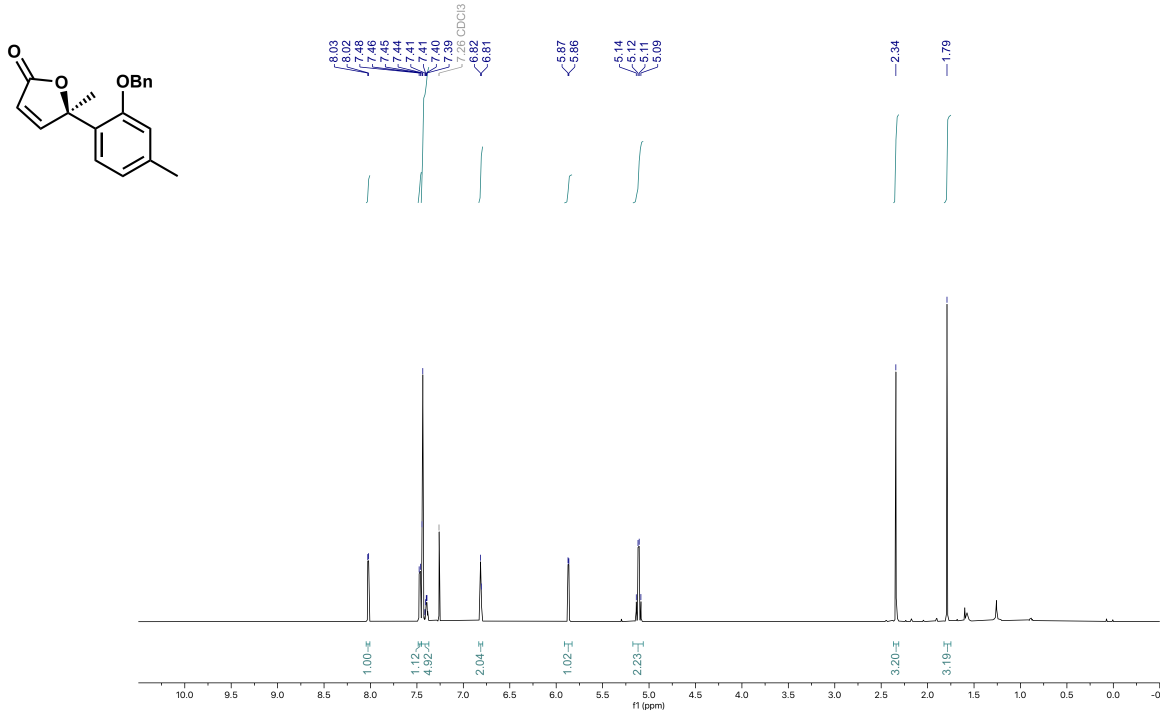
O
O
OBn
8.03
8.02
7.48
7.46
7.45
7.44
7.41
7.41
7.40
7.39
7.26 CDCl3
6.82
6.81
5.87
5.86
5.14
5.12
5.11
5.09
2.34
1.79
1.00
1.12
4.92
2.04
1.02
2.23
3.20
3.19
10.0
9.5
9.0
8.5
8.0
7.5
7.0
6.5
6.0
5.5
5.0
4.5
4.0
3.5
3.0
2.5
2.0
1.5
1.0
0.5
0.0
f1 (ppm)

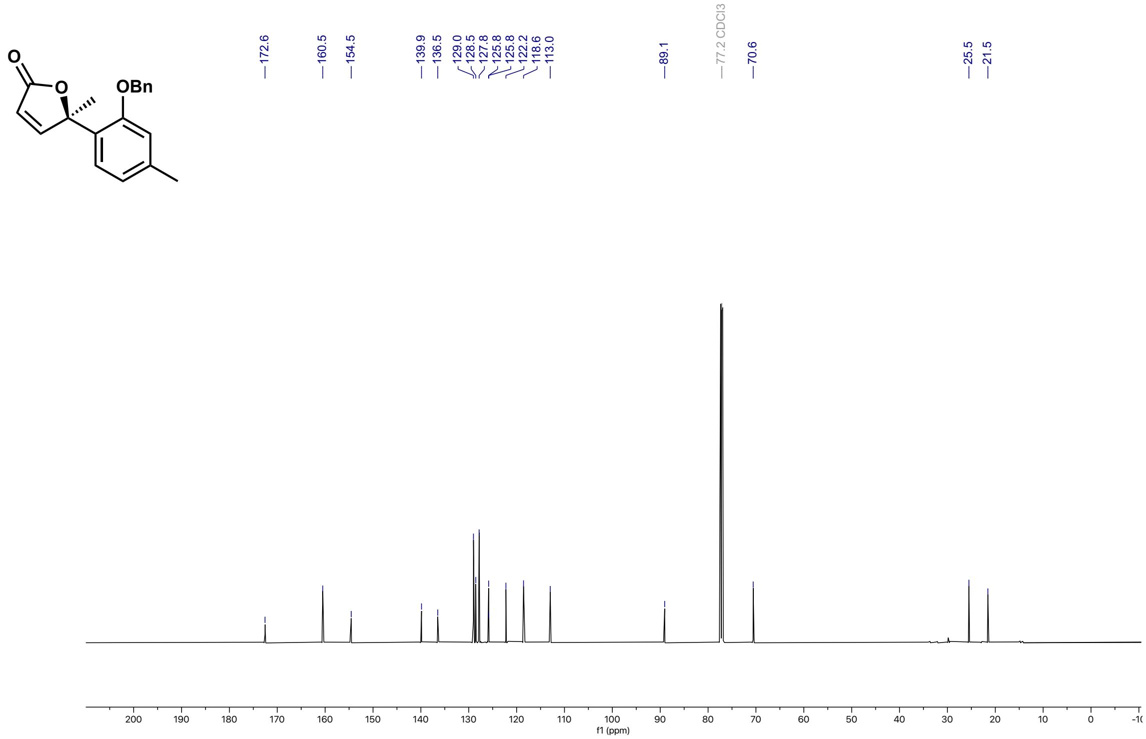
O
O
OBn
172.6
160.5
154.5
139.9
136.5
129.0
128.5
127.8
125.8
125.8
122.2
118.6
113.0
89.1
77.2 CDCl3
70.6
25.5
21.5
200
190
180
170
160
150
140
130
120
110
100
90
80
70
60
50
40
30
20
10
0
f1 (ppm)

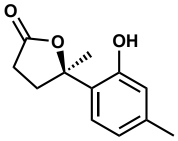
O
O
OH

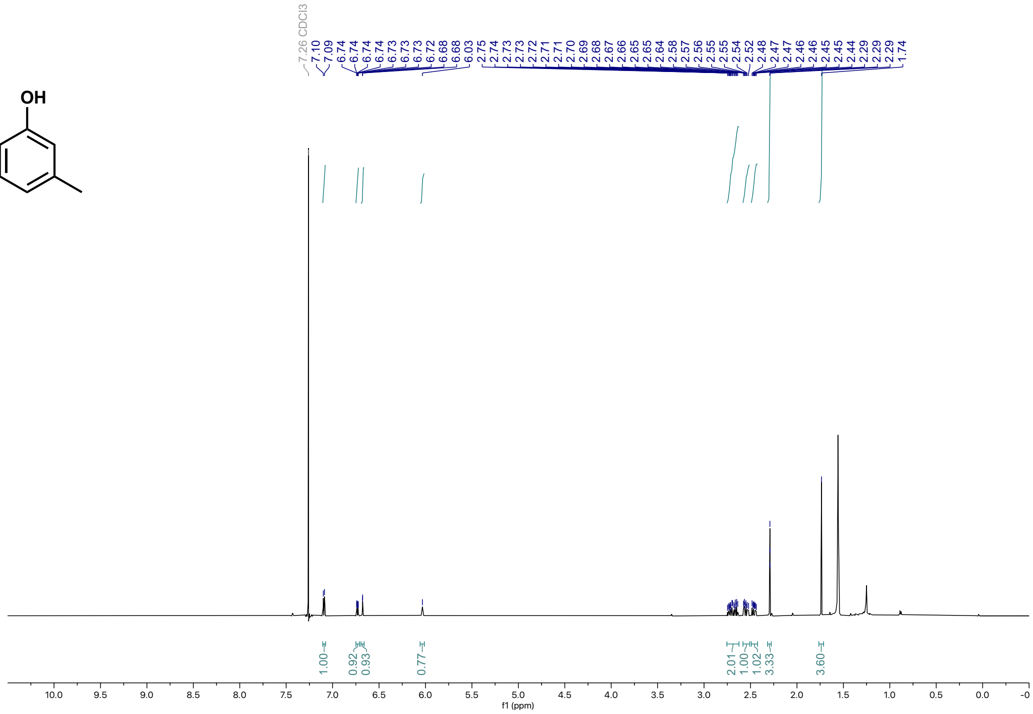
7.26 CDCl3
7.10
7.09
6.74
6.74
6.74
6.74
6.73
6.73
6.73
6.72
6.68
6.03
2.75
2.74
2.73
2.73
2.72
2.71
2.71
2.70
2.69
2.68
2.67
2.66
2.65
2.65
2.64
2.58
2.57
2.56
2.55
2.55
2.54
2.52
2.48
2.47
2.47
2.46
2.46
2.45
2.45
2.44
2.29
2.29
2.29
1.74
1.00
0.92
0.93
0.77
2.01
1.00
1.02
3.33
3.60
10.0
9.5
9.0
8.5
8.0
7.5
7.0
6.5
6.0
5.5
5.0
4.5
4.0
3.5
3.0
2.5
2.0
1.5
1.0
0.5
0.0
-0
f1 (ppm)

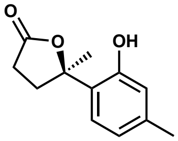
O
O
OH

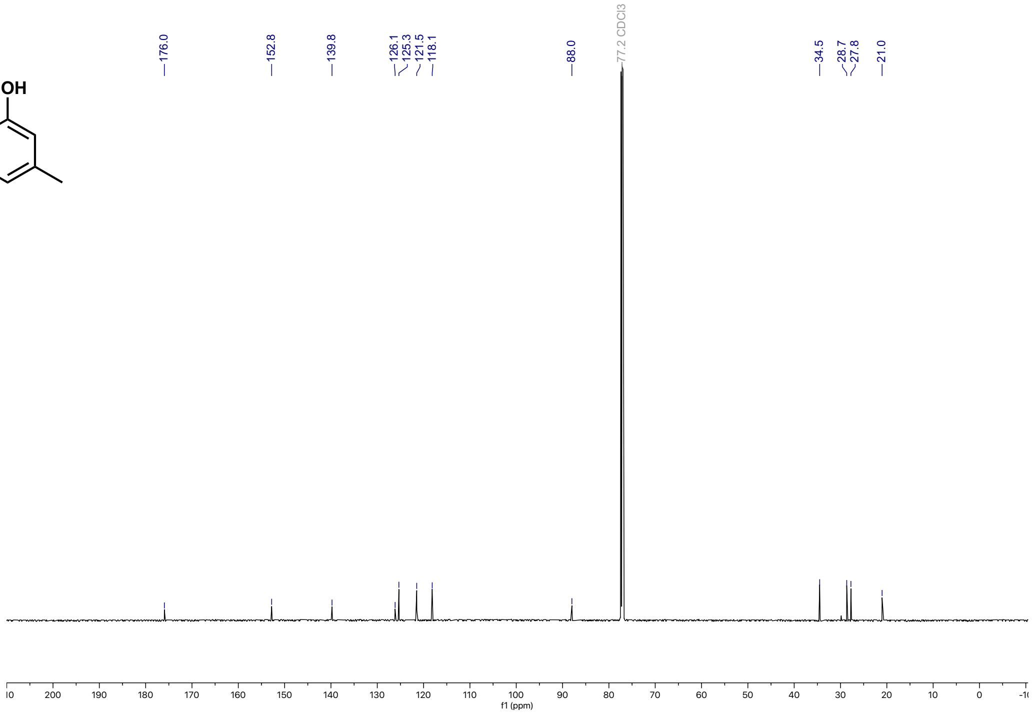
176.0
152.8
139.8
126.1
125.3
121.5
118.1
88.0
77.2 CDCl3
34.5
28.7
27.8
21.0
10
200
190
180
170
160
150
140
130
120
110
100
90
80
70
60
50
40
30
20
10
0
-1
f1 (ppm)

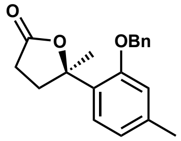
O
O
OBn

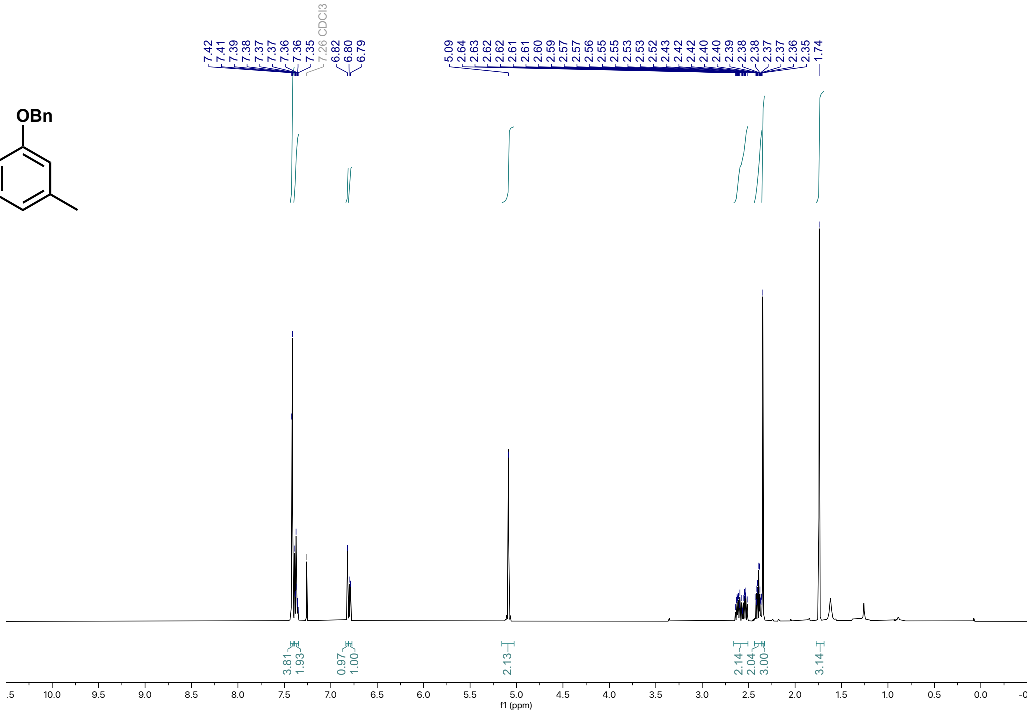
7.42
7.41
7.39
7.38
7.37
7.37
7.36
7.36
7.35
7.26 CDCl3
6.82
6.80
6.79
5.09
2.64
2.63
2.62
2.62
2.61
2.61
2.60
2.59
2.57
2.56
2.55
2.55
2.53
2.53
2.52
2.43
2.42
2.42
2.40
2.39
2.39
2.38
2.38
2.37
2.37
2.36
2.35
1.74
3.81
1.93
0.97
1.00
2.13
2.14
2.04
3.00
3.14
10.0
9.5
9.0
8.5
8.0
7.5
7.0
6.5
6.0
5.5
5.0
4.5
4.0
3.5
3.0
2.5
2.0
1.5
1.0
0.5
0.0
f1 (ppm)

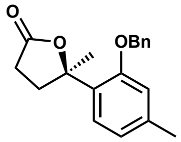
O
O
OBn

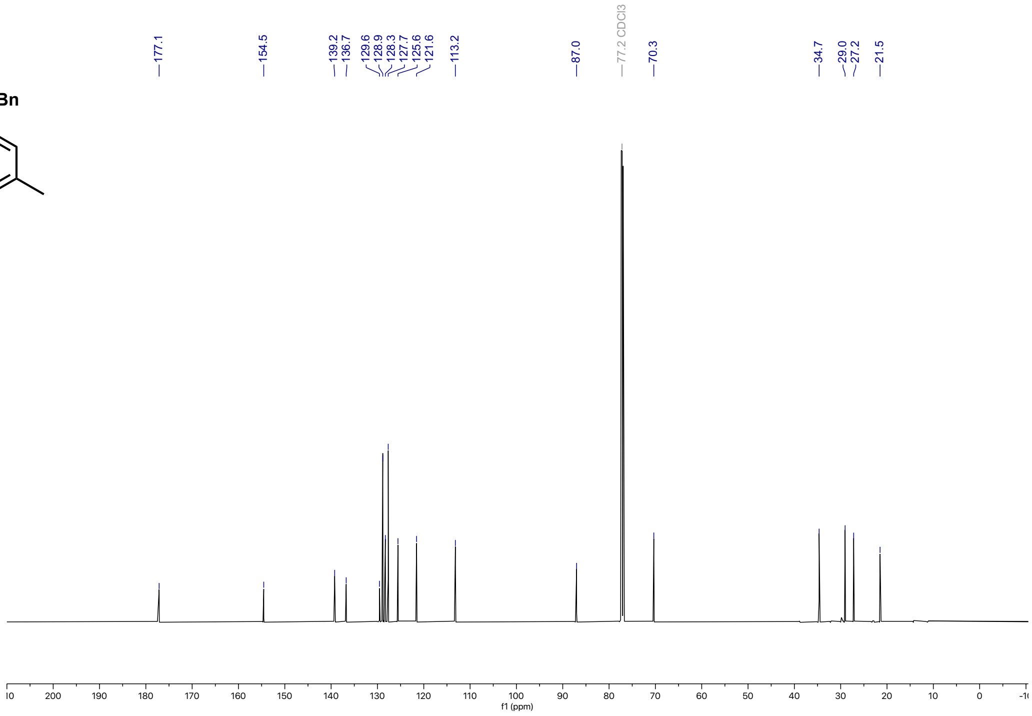
177.1
154.5
139.2
136.7
129.6
128.9
128.3
127.7
125.6
121.6
113.2
87.0
77.2 CDCl3
70.3
34.7
29.0
27.2
21.5
200
190
180
170
160
150
140
130
120
110
100
90
80
70
60
50
40
30
20
10
0
f1 (ppm)

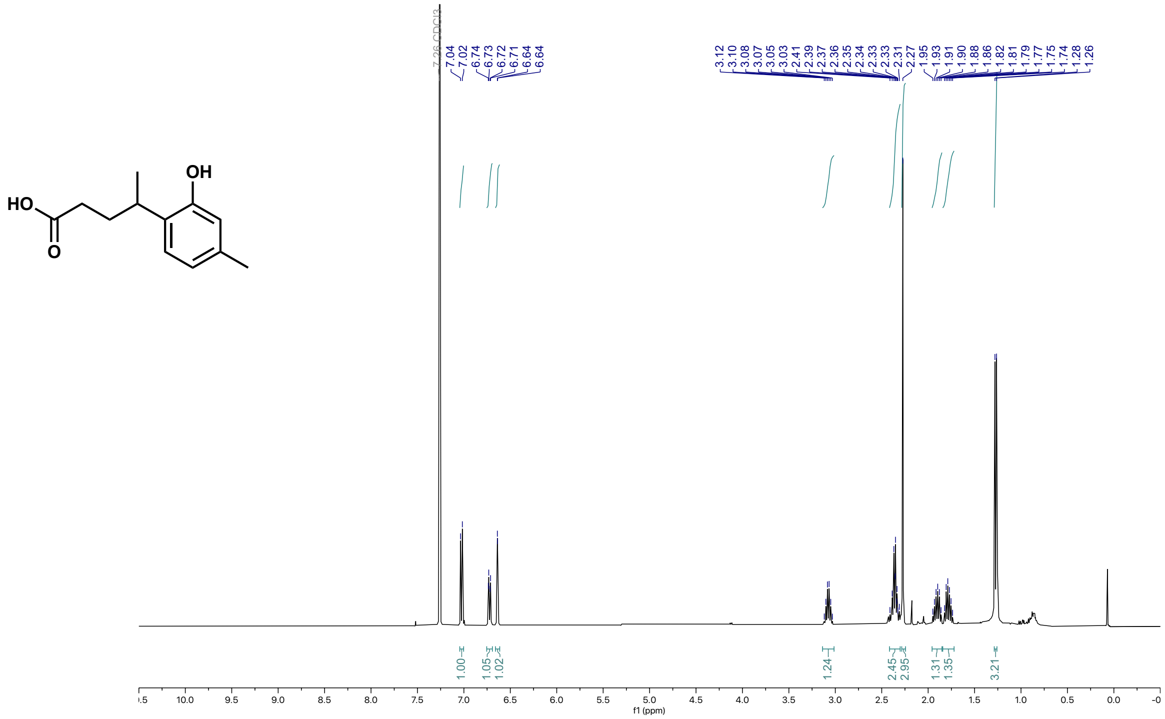
OH
HO
O
7.26 CDCl3
7.04
7.02
6.74
6.73
6.72
6.71
6.64
6.64
3.12
3.10
3.08
3.07
3.05
3.03
2.41
2.39
2.37
2.36
2.35
2.34
2.33
2.33
2.31
2.27
1.95
1.93
1.91
1.90
1.88
1.86
1.82
1.81
1.79
1.77
1.75
1.74
1.28
1.26
1.00
1.05
1.02
1.24
2.45
2.95
1.31
1.35
3.21
10.0
9.5
9.0
8.5
8.0
7.5
7.0
6.5
6.0
5.5
5.0
4.5
4.0
3.5
3.0
2.5
2.0
1.5
1.0
0.5
0.0
f1 (ppm)

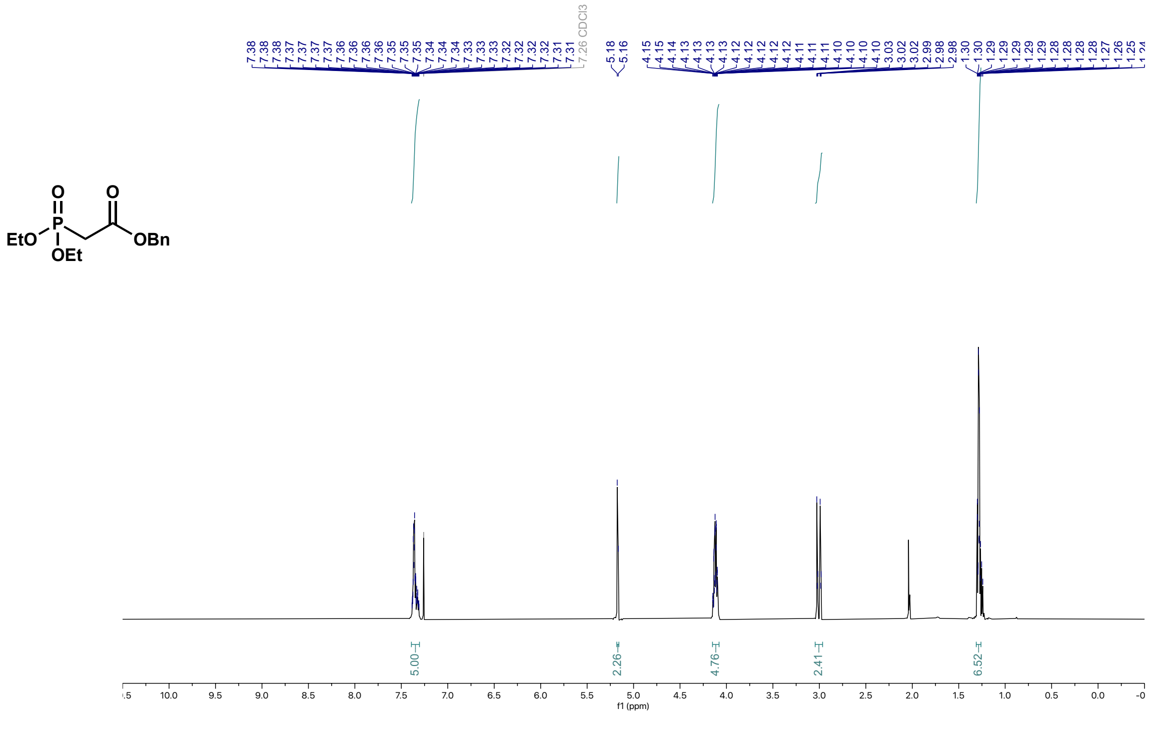
O
O
P
EtO
OEt
OBn
7.38
7.38
7.38
7.37
7.37
7.37
7.36
7.36
7.36
7.35
7.35
7.35
7.34
7.34
7.34
7.33
7.33
7.33
7.32
7.32
7.32
7.32
7.31
7.31
7.26 CDCl3
5.18
5.16
4.15
4.15
4.14
4.13
4.13
4.13
4.13
4.12
4.12
4.12
4.12
4.11
4.11
4.11
4.10
4.10
4.10
4.10
3.03
3.02
3.02
2.99
2.98
2.98
1.30
1.30
1.29
1.29
1.29
1.29
1.28
1.28
1.28
1.27
1.26
1.25
5.00
2.26
4.76
2.41
6.52
10.0
9.5
9.0
8.5
8.0
7.5
7.0
6.5
6.0
5.5
5.0
4.5
4.0
3.5
3.0
2.5
2.0
1.5
1.0
0.5
0.0
f1 (ppm)

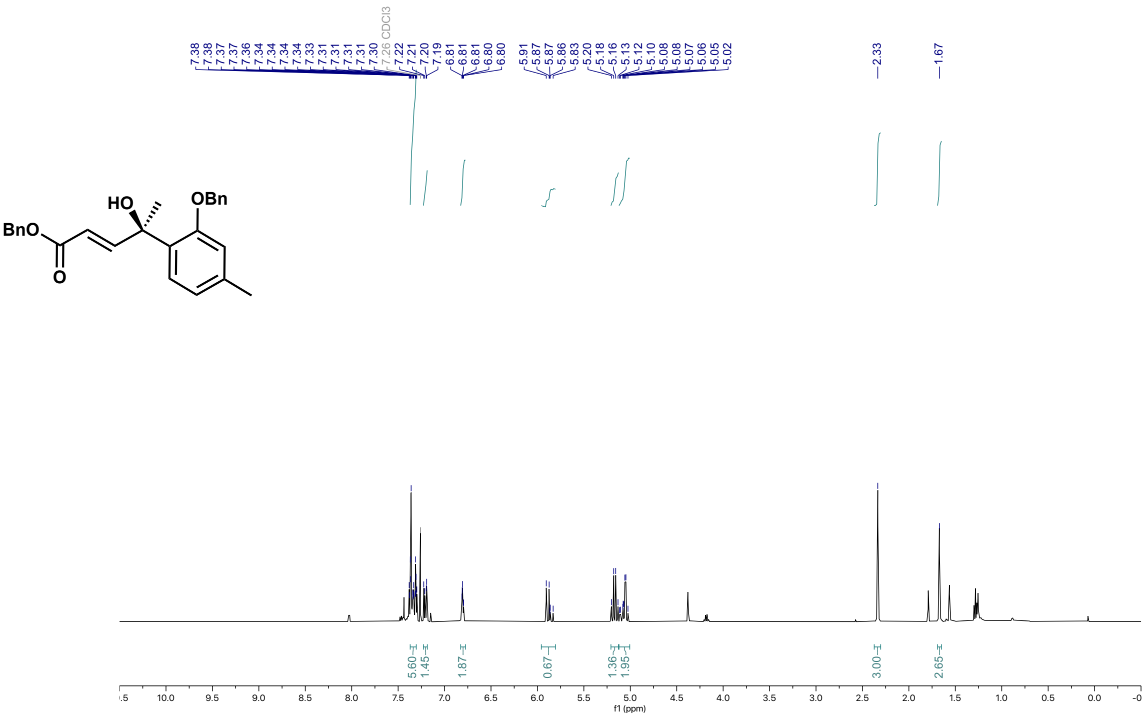
BnO
O
HO
OBn
7.38
7.38
7.37
7.37
7.36
7.34
7.34
7.34
7.34
7.33
7.31
7.31
7.31
7.31
7.30
7.26 CDCl3
7.22
7.21
7.20
7.19
6.81
6.81
6.81
6.80
6.80
5.91
5.87
5.87
5.86
5.83
5.20
5.16
5.13
5.12
5.10
5.08
5.08
5.07
5.06
5.05
5.02
2.33
1.67
5.60
1.45
1.87
0.67
1.36
1.95
3.00
2.65
10.5
10.0
9.5
9.0
8.5
8.0
7.5
7.0
6.5
6.0
5.5
5.0
4.5
4.0
3.5
3.0
2.5
2.0
1.5
1.0
0.5
0.0
-0
f1 (ppm)

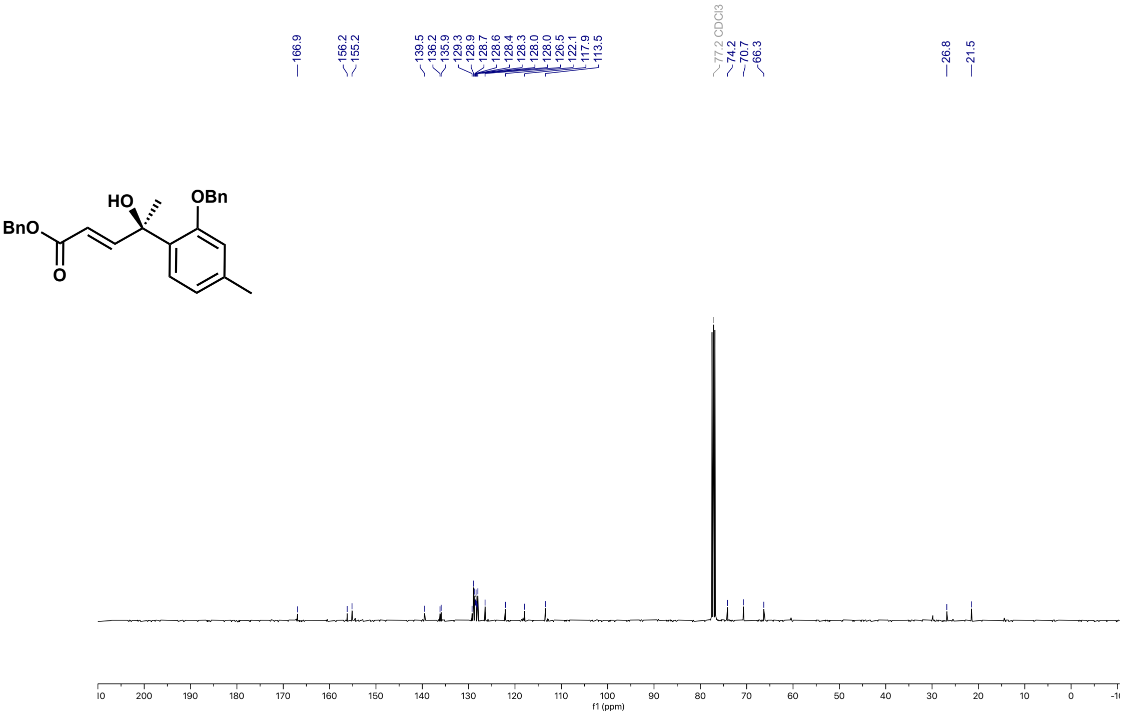
BnO
O
HO
OBn
166.9
156.2
155.2
139.5
136.2
135.9
129.3
128.9
128.7
128.6
128.4
128.3
128.0
128.0
126.5
122.1
117.9
113.5
77.2 CDCl3
74.2
70.7
66.3
26.8
21.5
210
200
190
180
170
160
150
140
130
120
110
100
90
80
70
60
50
40
30
20
10
0
-10
f1 (ppm)

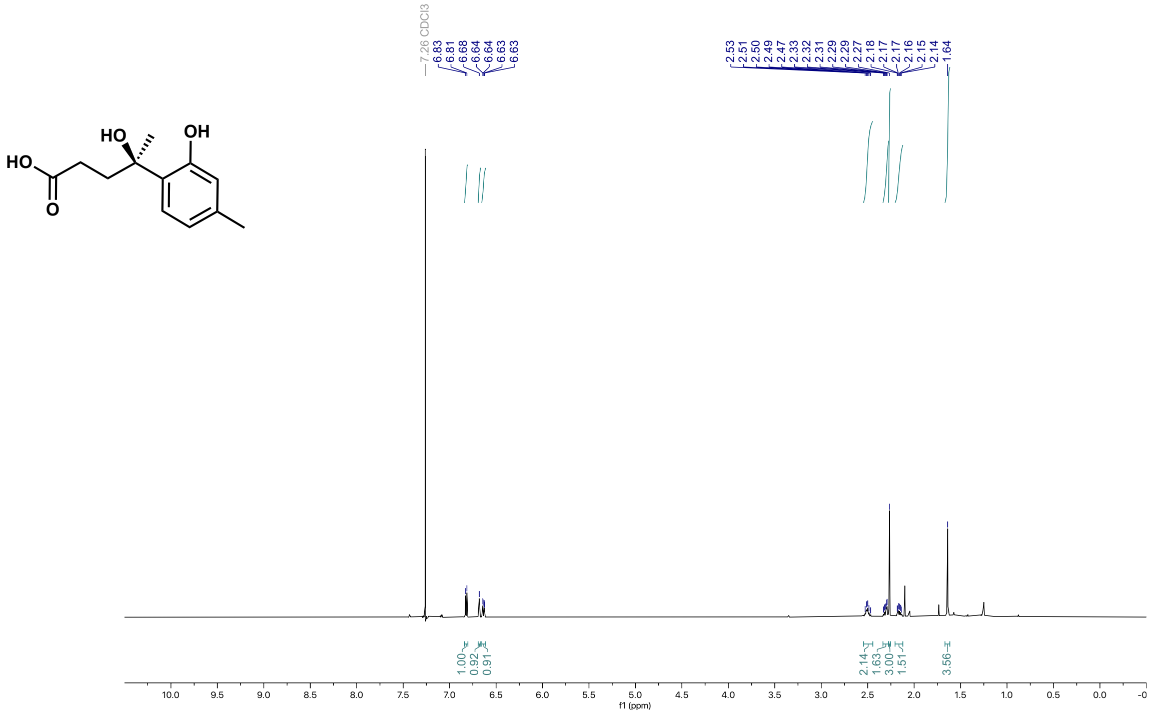
HO
HO
OH
O
7.26 CDCl3
6.83
6.81
6.68
6.64
6.64
6.63
6.63
2.53
2.51
2.50
2.49
2.47
2.33
2.32
2.31
2.29
2.29
2.27
2.18
2.17
2.17
2.16
2.15
2.14
1.64
1.00
0.92
0.91
2.14
1.63
3.00
1.51
3.56
10.0
9.5
9.0
8.5
8.0
7.5
7.0
6.5
6.0
5.5
5.0
4.5
4.0
3.5
3.0
2.5
2.0
1.5
1.0
0.5
0.0
-0
f1 (ppm)

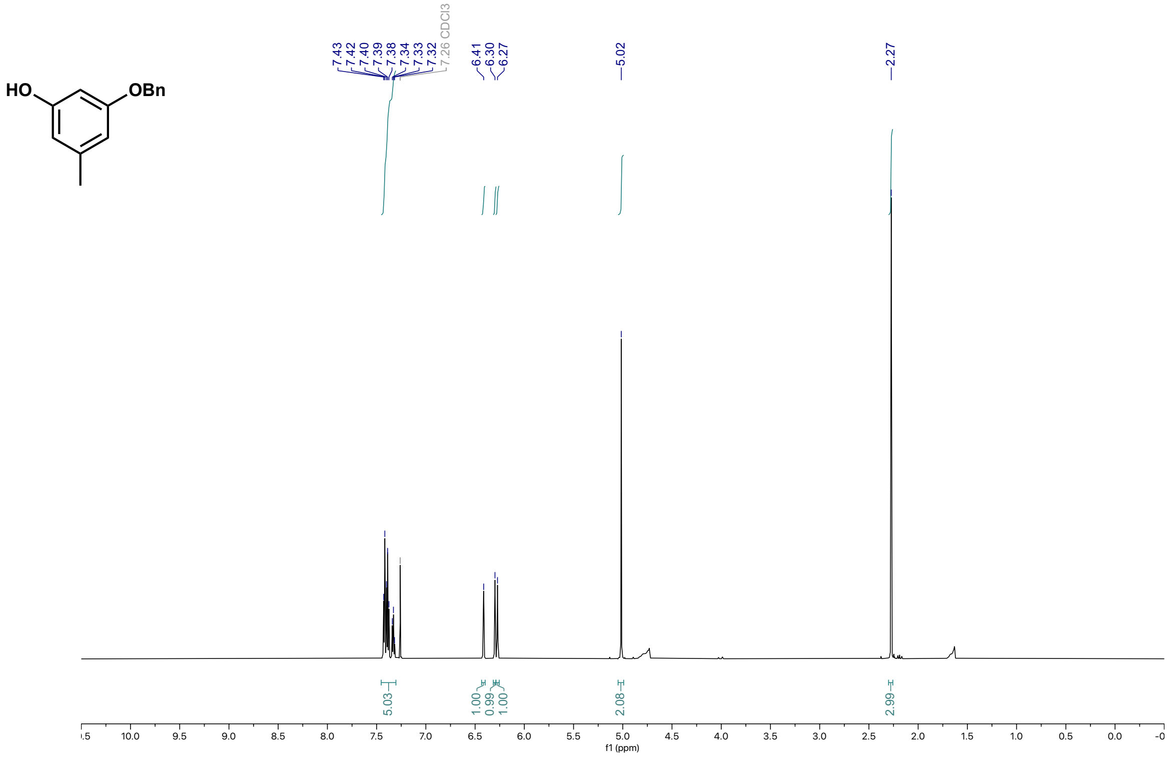
HO
OBn
7.43
7.42
7.40
7.39
7.38
7.34
7.33
7.32
7.26 CDCl3
6.41
6.30
6.27
5.02
2.27
5.03
1.00
0.99
1.00
2.08
2.99
10.5
10.0
9.5
9.0
8.5
8.0
7.5
7.0
6.5
6.0
5.5
5.0
4.5
4.0
3.5
3.0
2.5
2.0
1.5
1.0
0.5
0.0
-0
f1 (ppm)

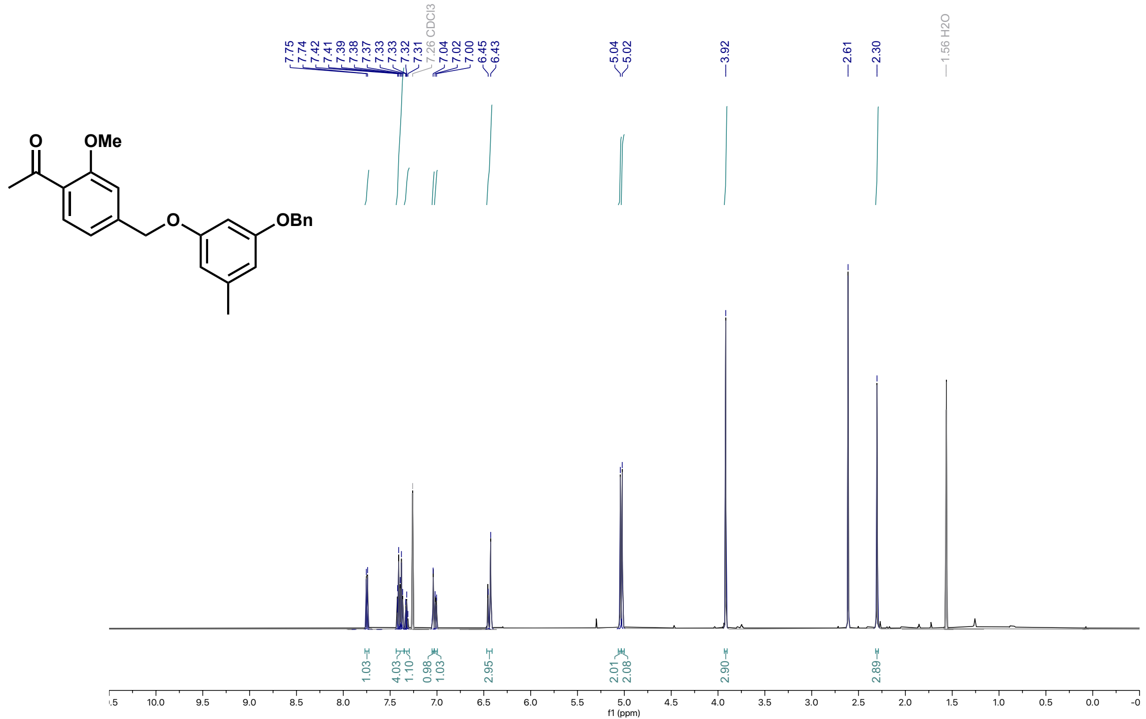
7.75
7.74
7.42
7.41
7.39
7.38
7.37
7.33
7.33
7.32
7.31
7.26 CDCl3
7.04
7.02
7.00
6.45
6.43
5.04
5.02
3.92
2.61
2.30
1.56 H2O
O
OMe
O
OBn
1.03
4.03
1.10
0.98
1.03
2.95
2.01
2.08
2.90
2.89
f1 (ppm)

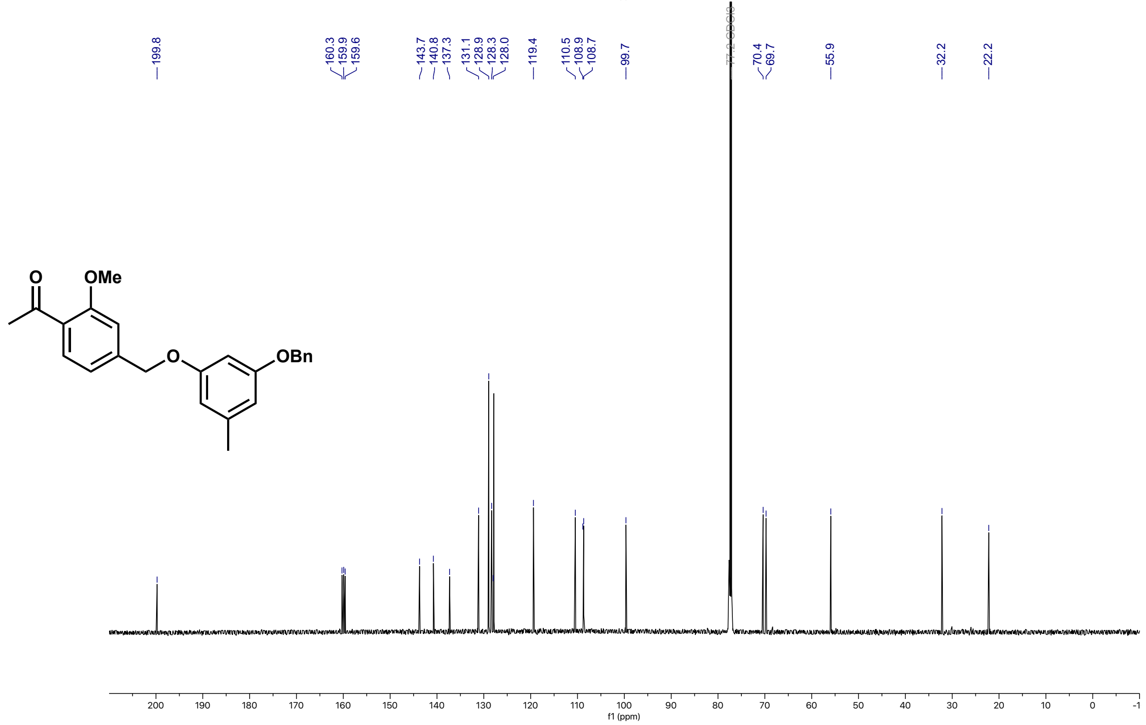
199.8
160.3
159.9
159.6
143.7
140.8
137.3
131.1
128.9
128.3
128.0
119.4
110.5
108.9
108.7
99.7
77.2 CDCl3
70.4
69.7
55.9
32.2
22.2
O
OMe
O
OBn
f1 (ppm)

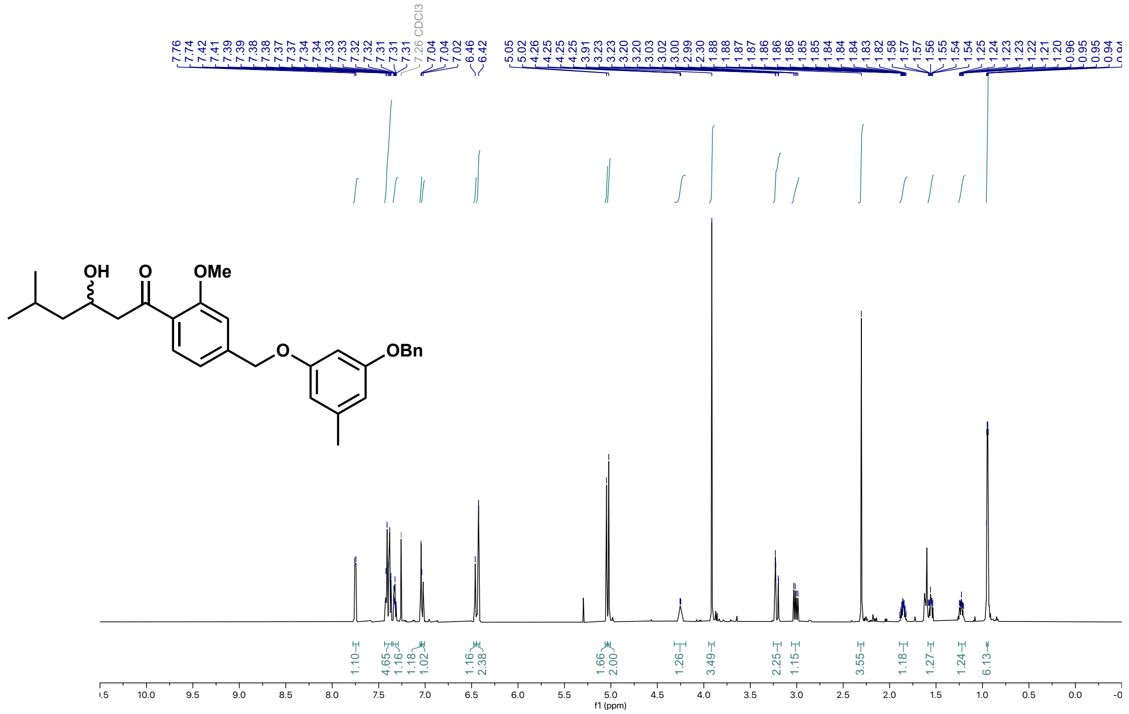
7.76
7.74
7.42
7.41
7.39
7.39
7.38
7.38
7.37
7.37
7.34
7.34
7.33
7.33
7.32
7.32
7.31
7.31
7.31
7.26 CDCl3
7.04
7.04
7.02
6.46
6.42
5.05
5.02
4.26
4.25
4.25
4.25
3.91
3.23
3.23
3.20
3.20
3.03
3.02
3.00
2.99
2.30
1.88
1.88
1.87
1.87
1.86
1.86
1.86
1.85
1.85
1.84
1.84
1.84
1.83
1.82
1.58
1.57
1.57
1.56
1.55
1.54
1.54
1.25
1.24
1.23
1.23
1.22
1.21
1.20
0.96
0.95
0.95
0.94
OH
O
OMe
O
OBn
1.10
4.65
1.16
1.18
1.02
1.16
2.38
1.66
2.00
1.26
3.49
2.25
1.15
3.55
1.18
1.27
1.24
6.13
10.0
9.5
9.0
8.5
8.0
7.5
7.0
6.5
6.0
5.5
5.0
4.5
4.0
3.5
3.0
2.5
2.0
1.5
1.0
0.5
0.0
f1 (ppm)

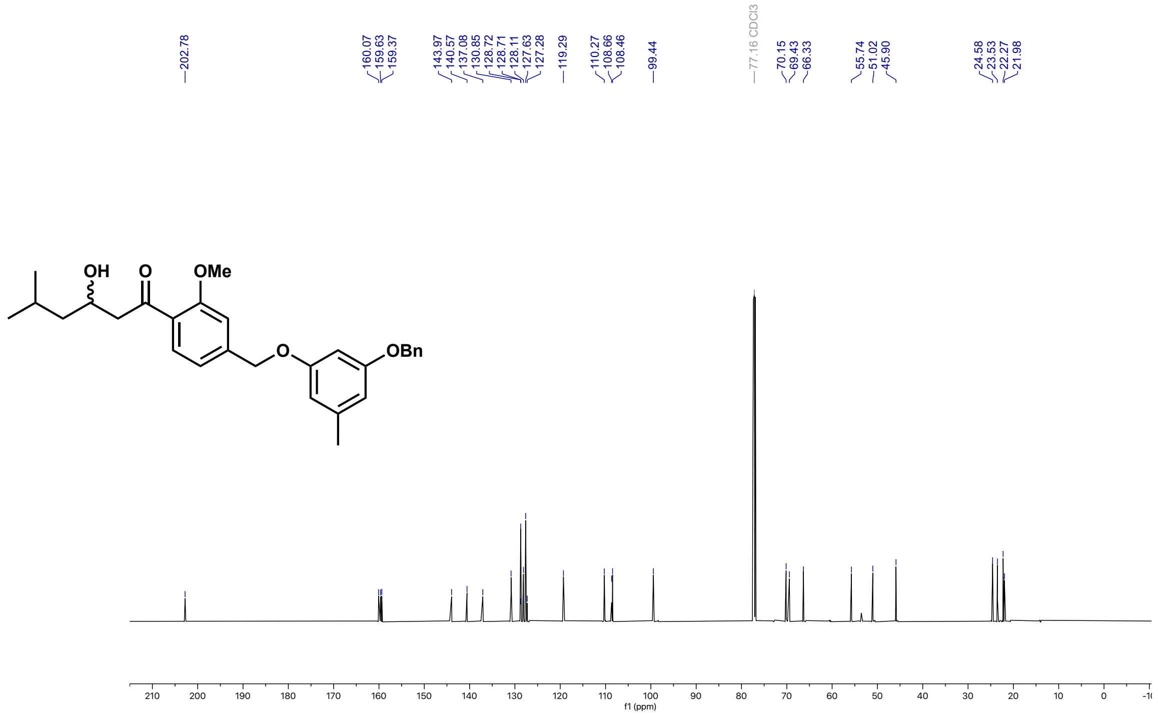
202.78
160.07
159.63
159.37
143.97
140.57
137.08
130.85
128.72
128.71
128.11
127.63
127.28
119.29
110.27
108.66
108.46
99.44
77.16 CDCl3
70.15
69.43
66.33
55.74
51.02
45.90
24.58
23.53
22.27
21.98
OH
O
OMe
O
OBn
210
200
190
180
170
160
150
140
130
120
110
100
90
80
70
60
50
40
30
20
10
0
f1 (ppm)

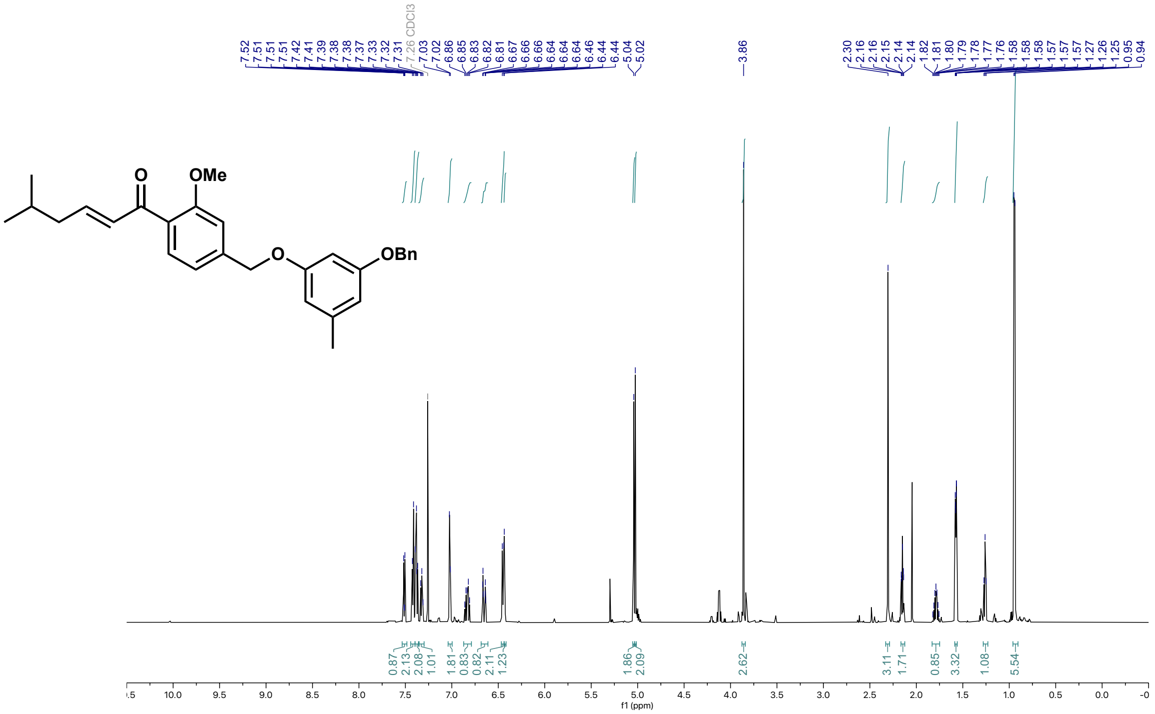
O
OMe
O
OBn
7.52
7.51
7.51
7.51
7.42
7.41
7.39
7.38
7.38
7.37
7.33
7.32
7.31
7.26 CDCl3
7.03
7.02
6.86
6.85
6.83
6.82
6.81
6.67
6.66
6.66
6.64
6.64
6.64
6.46
6.44
6.44
5.04
5.02
3.86
2.30
2.16
2.16
2.15
2.14
2.14
1.82
1.81
1.80
1.79
1.78
1.77
1.76
1.58
1.58
1.58
1.57
1.57
1.57
1.27
1.26
1.25
0.95
0.94
0.87
2.13
2.08
1.01
1.81
0.83
0.82
2.11
1.23
1.86
2.09
2.62
3.11
1.71
0.85
3.32
1.08
5.54
10.0
9.5
9.0
8.5
8.0
7.5
7.0
6.5
6.0
5.5
5.0
4.5
4.0
3.5
3.0
2.5
2.0
1.5
1.0
0.5
0.0
f1 (ppm)

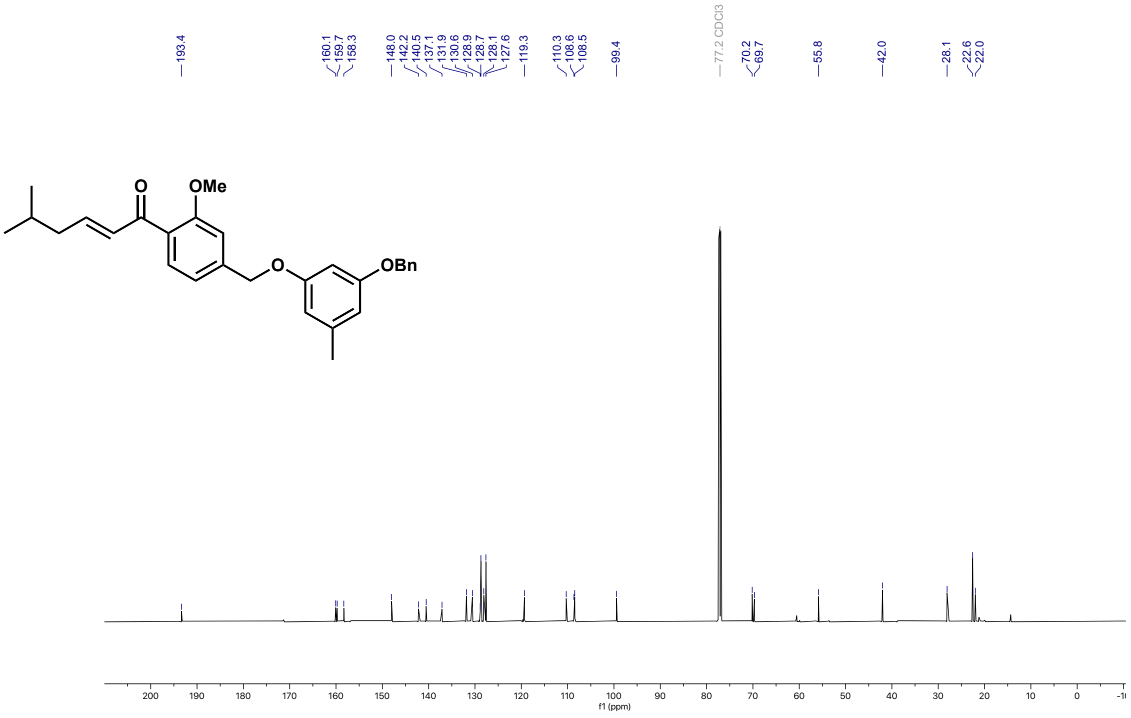
193.4
160.1
159.7
158.3
148.0
142.2
140.5
137.1
131.9
130.6
128.9
128.7
128.1
127.6
119.3
110.3
108.6
108.5
99.4
77.2 CDCl3
70.2
69.7
55.8
42.0
28.1
22.6
22.0
O
OMe
O
OBn
200
190
180
170
160
150
140
130
120
110
100
90
80
70
60
50
40
30
20
10
0
f1 (ppm)

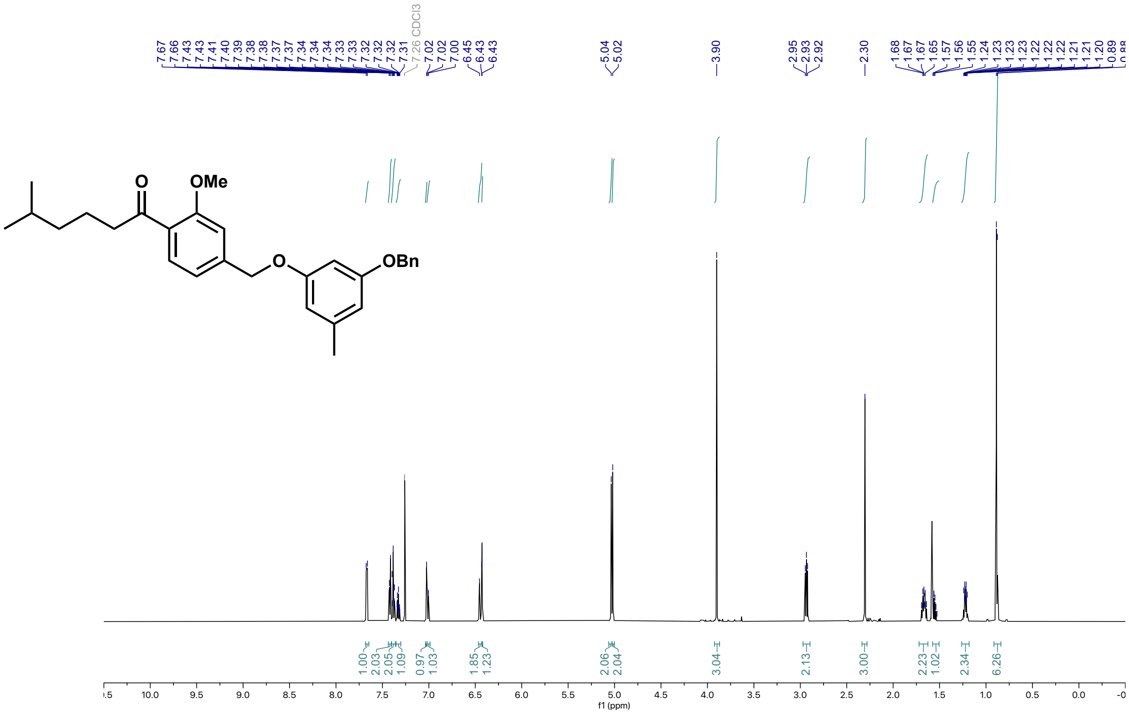
O
OMe
O
OBn
7.67
7.66
7.43
7.43
7.41
7.40
7.39
7.38
7.38
7.37
7.37
7.34
7.34
7.34
7.33
7.33
7.32
7.32
7.32
7.31
7.26 CDCl3
7.02
7.02
7.00
6.45
6.43
6.43
5.04
5.02
3.90
2.95
2.93
2.92
2.30
1.68
1.67
1.65
1.57
1.56
1.55
1.24
1.23
1.23
1.22
1.22
1.22
1.21
1.21
1.20
0.89
0.88
1.00
2.03
2.05
1.09
0.97
1.03
1.85
1.23
2.06
2.04
3.04
2.13
3.00
2.23
1.02
2.34
6.26
10.0
9.5
9.0
8.5
8.0
7.5
7.0
6.5
6.0
5.5
5.0
4.5
4.0
3.5
3.0
2.5
2.0
1.5
1.0
0.5
0.0
f1 (ppm)

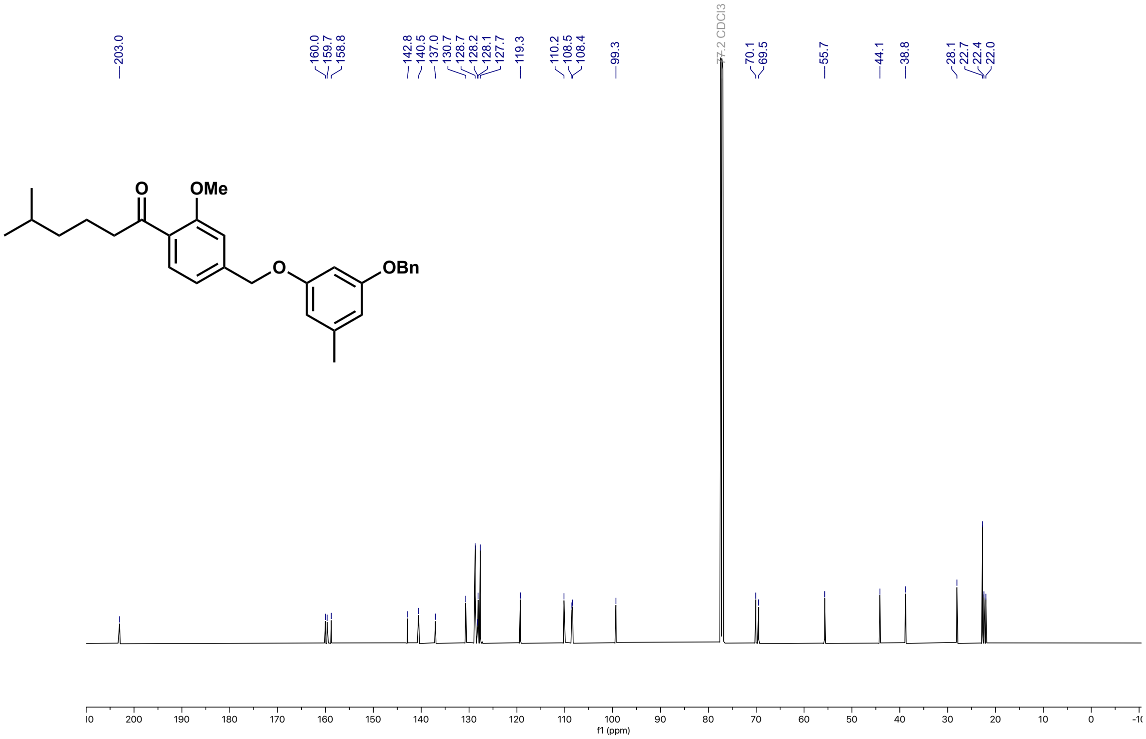
O
OMe
O
OBn
203.0
160.0
159.7
158.8
142.8
140.5
137.0
130.7
128.7
128.2
128.1
127.7
119.3
110.2
108.5
108.4
99.3
77.2 CDCl3
70.1
69.5
55.7
44.1
38.8
28.1
22.7
22.4
22.0
200
190
180
170
160
150
140
130
120
110
100
90
80
70
60
50
40
30
20
10
0
f1 (ppm)

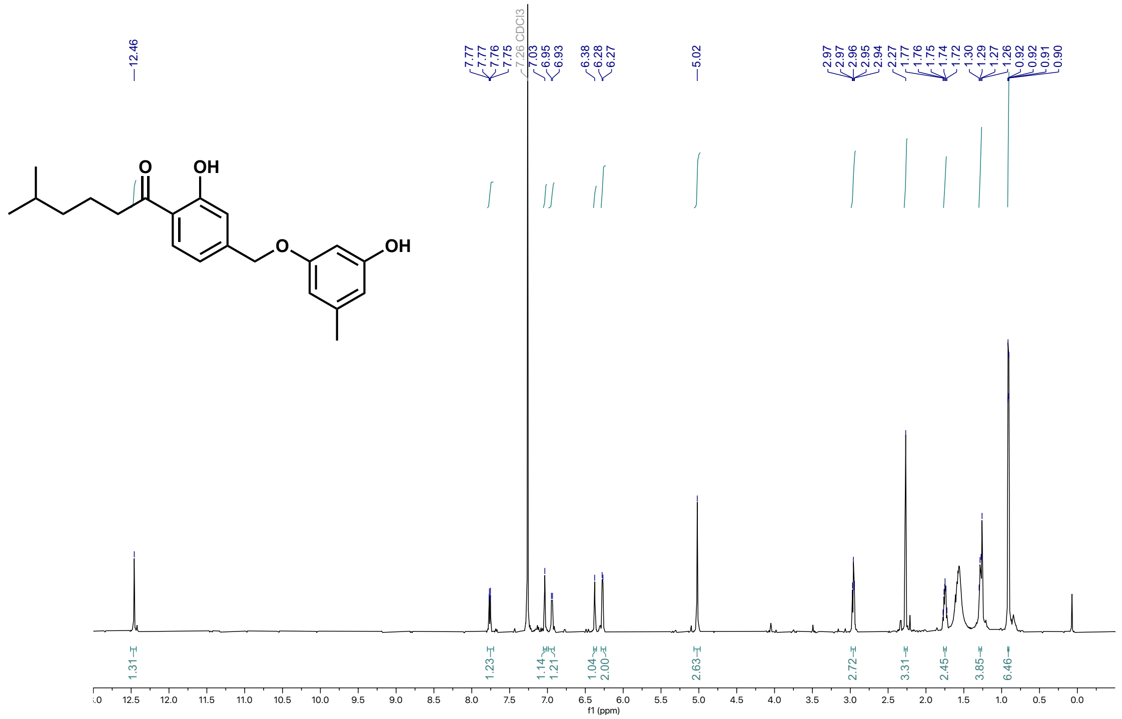
O
OH
O
OH
12.46
7.77
7.77
7.76
7.75
7.26 CDCl3
7.03
6.95
6.93
6.38
6.28
6.27
5.02
2.97
2.97
2.96
2.95
2.94
2.27
1.77
1.76
1.75
1.74
1.72
1.30
1.29
1.27
1.26
0.92
0.92
0.91
0.90
1.31
1.23
1.14
1.21
1.04
2.00
2.63
2.72
3.31
2.45
3.85
6.46
f1 (ppm)

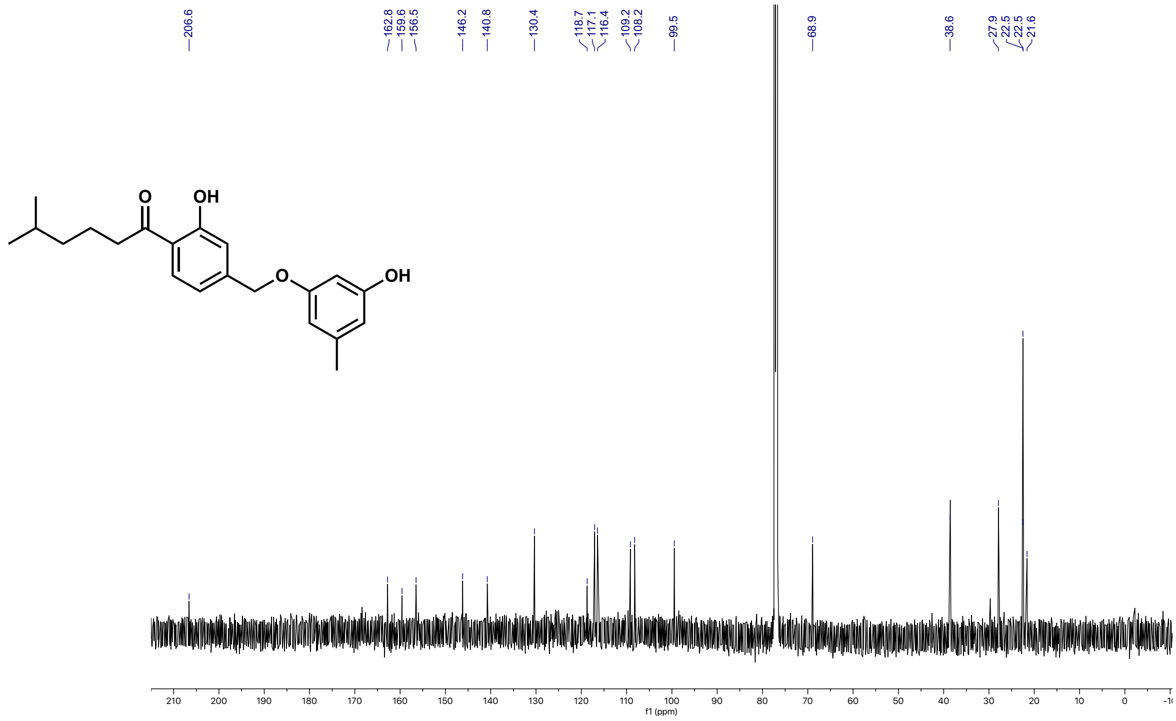
O
OH
O
OH
206.6
162.8
159.6
156.5
146.2
140.8
130.4
118.7
117.1
116.4
109.2
108.2
99.5
68.9
38.6
27.9
22.5
22.5
21.6
f1 (ppm)

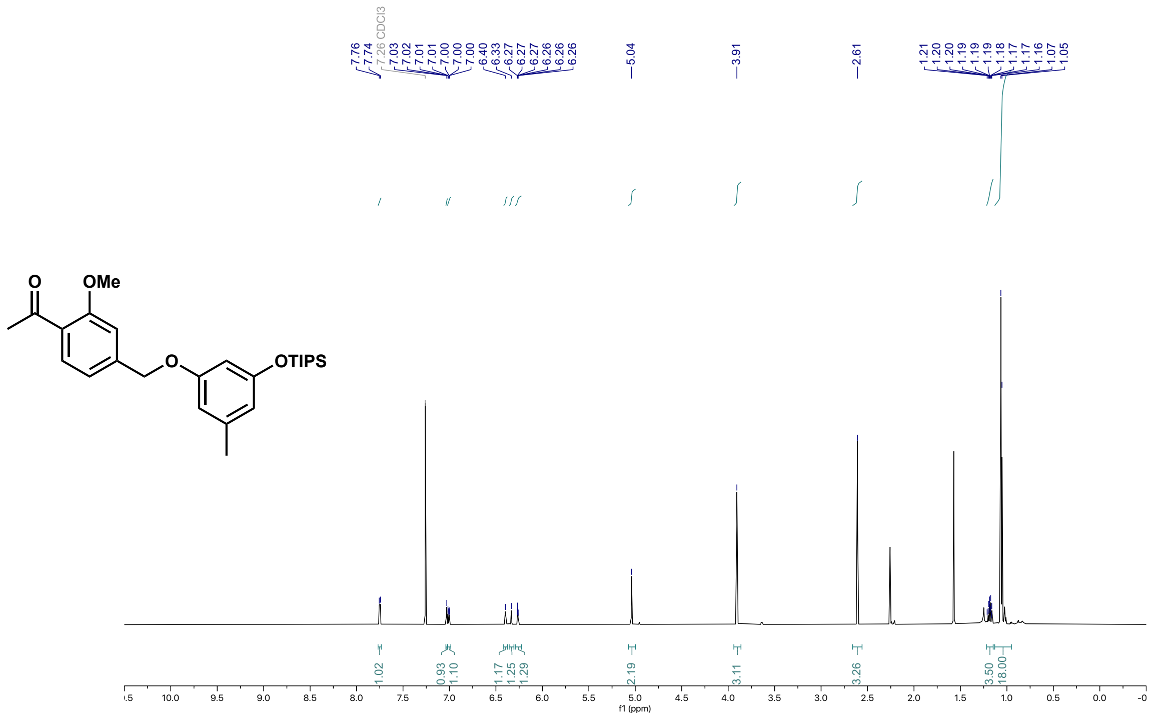
7.76
7.74
7.26 CDCl3
7.03
7.02
7.01
7.01
7.00
7.00
7.00
6.40
6.33
6.27
6.27
6.27
6.26
6.26
6.26
5.04
3.91
2.61
1.21
1.20
1.20
1.19
1.19
1.19
1.18
1.17
1.17
1.16
1.07
1.05
O
OMe
O
OTIPS
1.02
0.93
1.10
1.17
1.25
1.29
2.19
3.11
3.26
3.50
18.00
10.0
9.5
9.0
8.5
8.0
7.5
7.0
6.5
6.0
5.5
5.0
4.5
4.0
3.5
3.0
2.5
2.0
1.5
1.0
0.5
0.0
f1 (ppm)

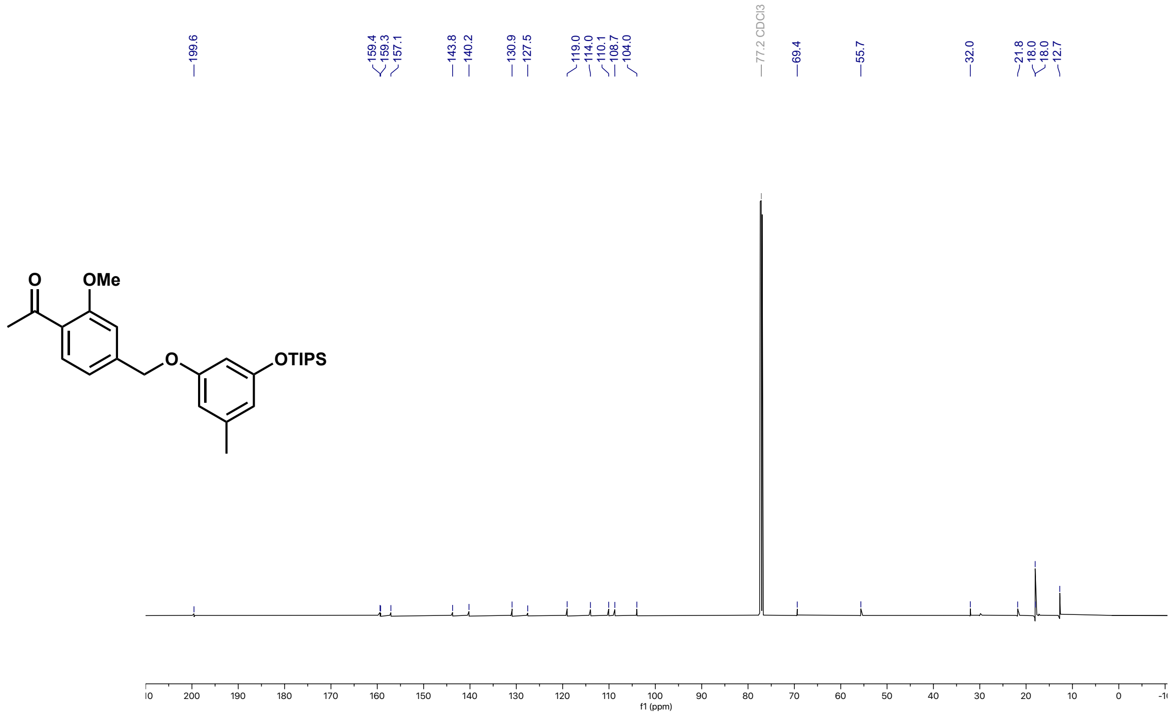
199.6
159.4
159.3
157.1
143.8
140.2
130.9
127.5
119.0
114.0
110.1
108.7
104.0
77.2 CDCl3
69.4
55.7
32.0
21.8
18.0
12.7
O
OMe
O
OTIPS
200
190
180
170
160
150
140
130
120
110
100
90
80
70
60
50
40
30
20
10
0
f1 (ppm)

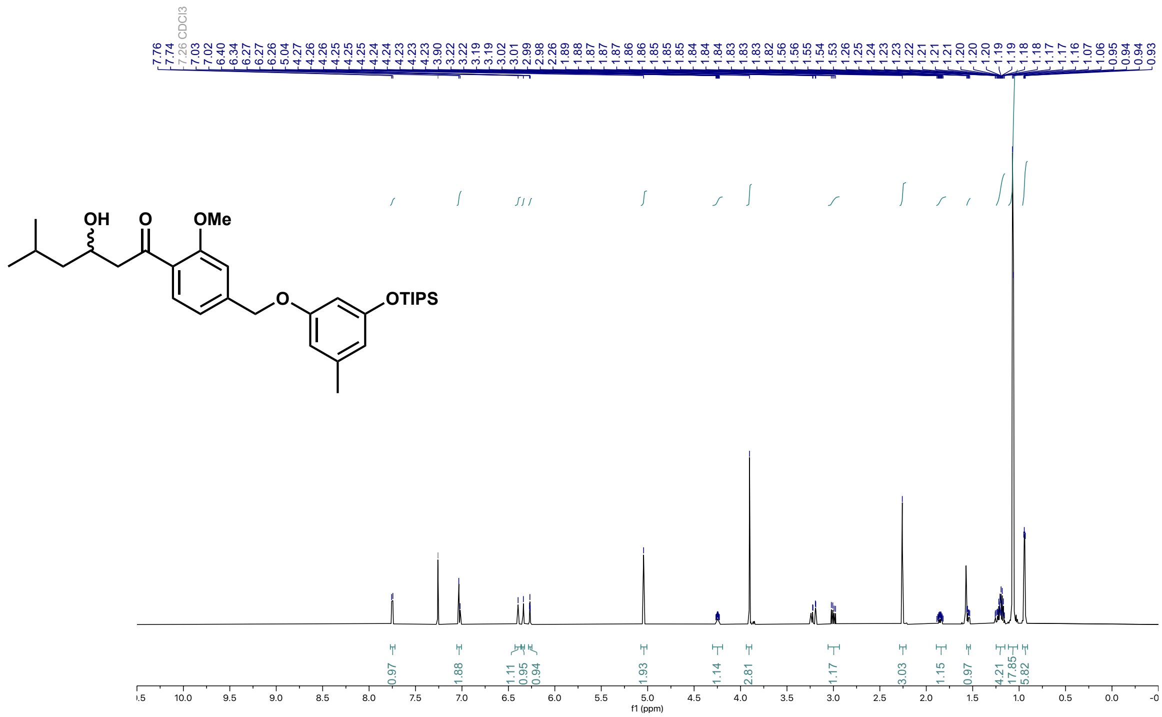
7.76
7.74
7.26 CDCl3
7.03
7.02
6.40
6.34
6.27
6.26
5.04
4.27
4.26
4.26
4.25
4.25
4.24
4.24
4.23
4.23
4.23
3.90
3.22
3.22
3.19
3.19
3.02
3.01
2.99
2.98
2.26
1.89
1.88
1.87
1.87
1.86
1.86
1.85
1.85
1.85
1.84
1.84
1.84
1.83
1.83
1.83
1.82
1.56
1.56
1.55
1.54
1.53
1.26
1.25
1.24
1.23
1.23
1.22
1.21
1.21
1.21
1.20
1.20
1.20
1.19
1.19
1.18
1.18
1.17
1.16
1.07
1.06
0.95
0.94
0.94
0.93
OH
O
OMe
O
OTIPS
0.97
1.88
1.11
0.95
0.94
1.93
1.14
2.81
1.17
3.03
1.15
0.97
4.21
17.85
5.82
10.0
9.5
9.0
8.5
8.0
7.5
7.0
6.5
6.0
5.5
5.0
4.5
4.0
3.5
3.0
2.5
2.0
1.5
1.0
0.5
0.0
f1 (ppm)

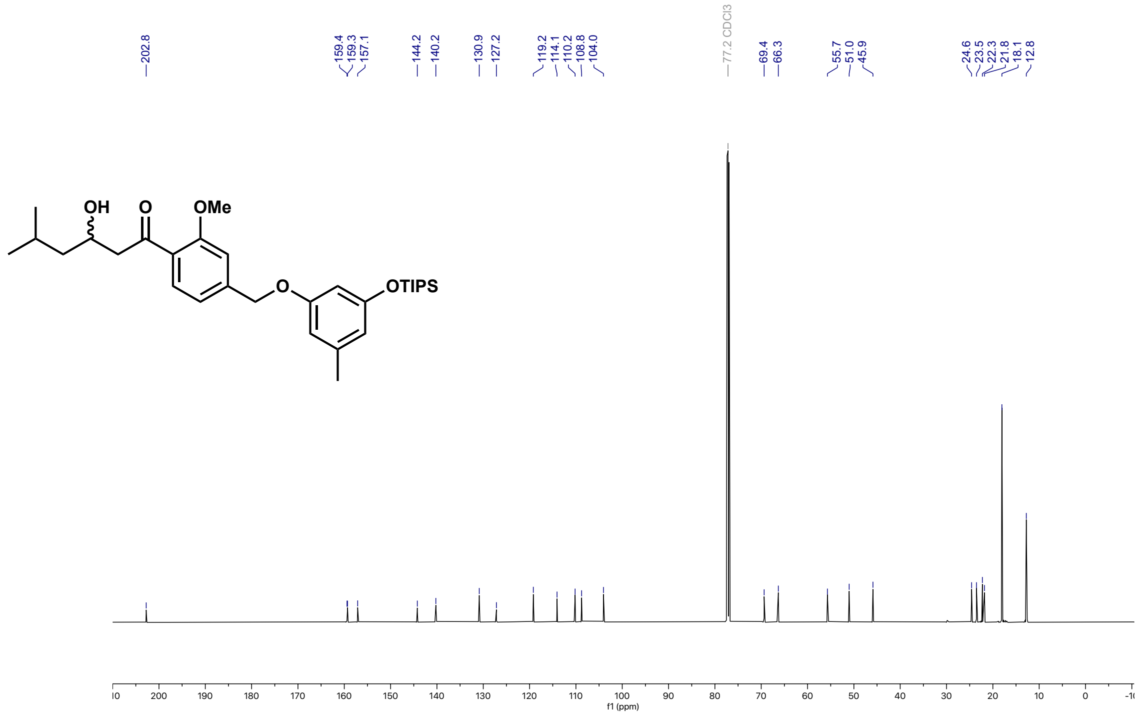
202.8
159.4
159.3
157.1
144.2
140.2
130.9
127.2
119.2
114.1
110.2
108.8
104.0
77.2 CDCl3
69.4
66.3
55.7
51.0
45.9
24.6
23.5
22.3
21.8
18.1
12.8
OH
O
OMe
O
OTIPS
200
190
180
170
160
150
140
130
120
110
100
90
80
70
60
50
40
30
20
10
0
f1 (ppm)

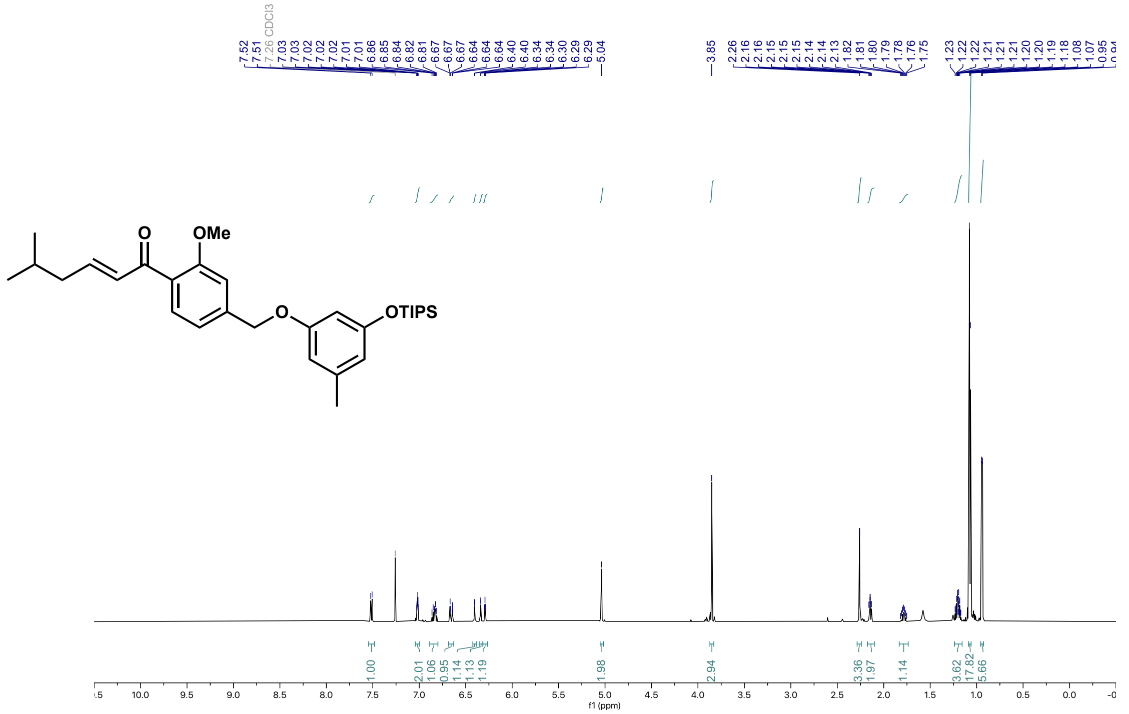
7.52
7.51
7.26 CDCl3
7.03
7.03
7.02
7.02
7.02
7.01
7.01
6.86
6.85
6.84
6.82
6.81
6.67
6.67
6.67
6.64
6.64
6.64
6.40
6.40
6.34
6.34
6.30
6.29
6.29
5.04
3.85
2.26
2.16
2.16
2.15
2.15
2.15
2.15
2.14
2.14
2.13
1.82
1.81
1.80
1.79
1.78
1.76
1.75
1.23
1.22
1.22
1.21
1.21
1.21
1.20
1.19
1.18
1.08
1.07
0.95
O
OMe
O
OTIPS
1.00
2.01
1.06
0.95
1.14
1.13
1.19
1.98
2.94
3.36
1.97
1.14
3.62
17.82
5.66
10.0
9.5
9.0
8.5
8.0
7.5
7.0
6.5
6.0
5.5
5.0
4.5
4.0
3.5
3.0
2.5
2.0
1.5
1.0
0.5
0.0
f1 (ppm)

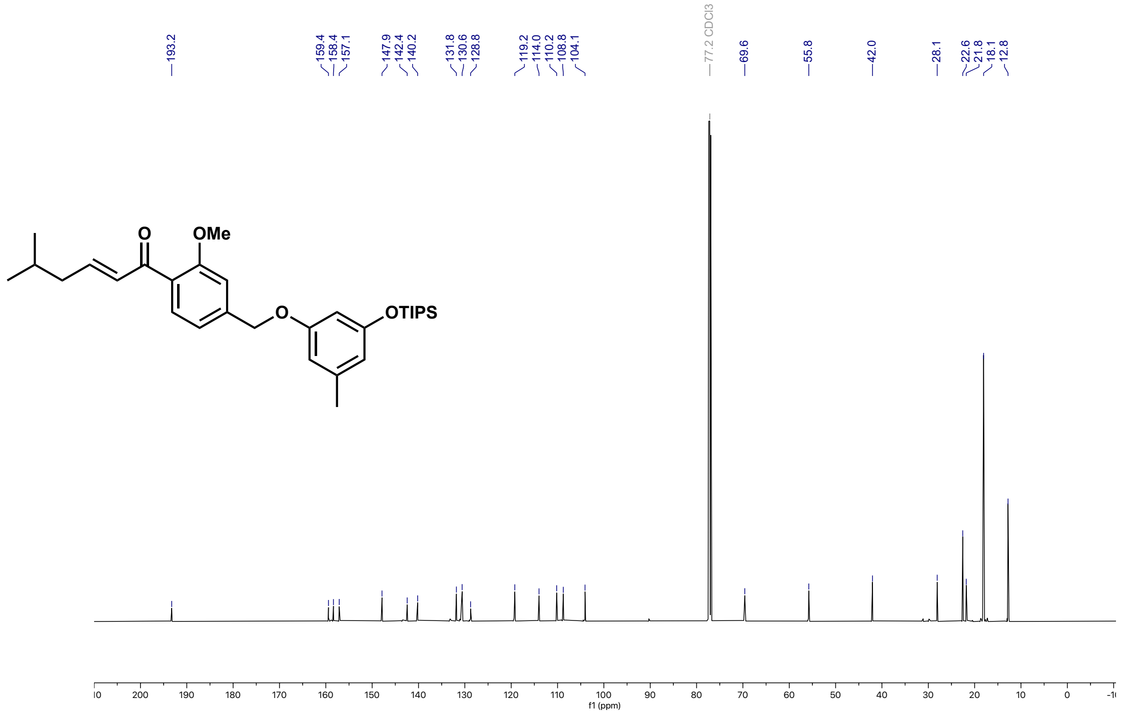
193.2
159.4
158.4
157.1
147.9
142.4
140.2
131.8
130.6
128.8
119.2
114.0
110.2
108.8
104.1
77.2 CDCl3
69.6
55.8
42.0
28.1
22.6
21.8
18.1
12.8
O
OMe
O
OTIPS
200
190
180
170
160
150
140
130
120
110
100
90
80
70
60
50
40
30
20
10
0
f1 (ppm)

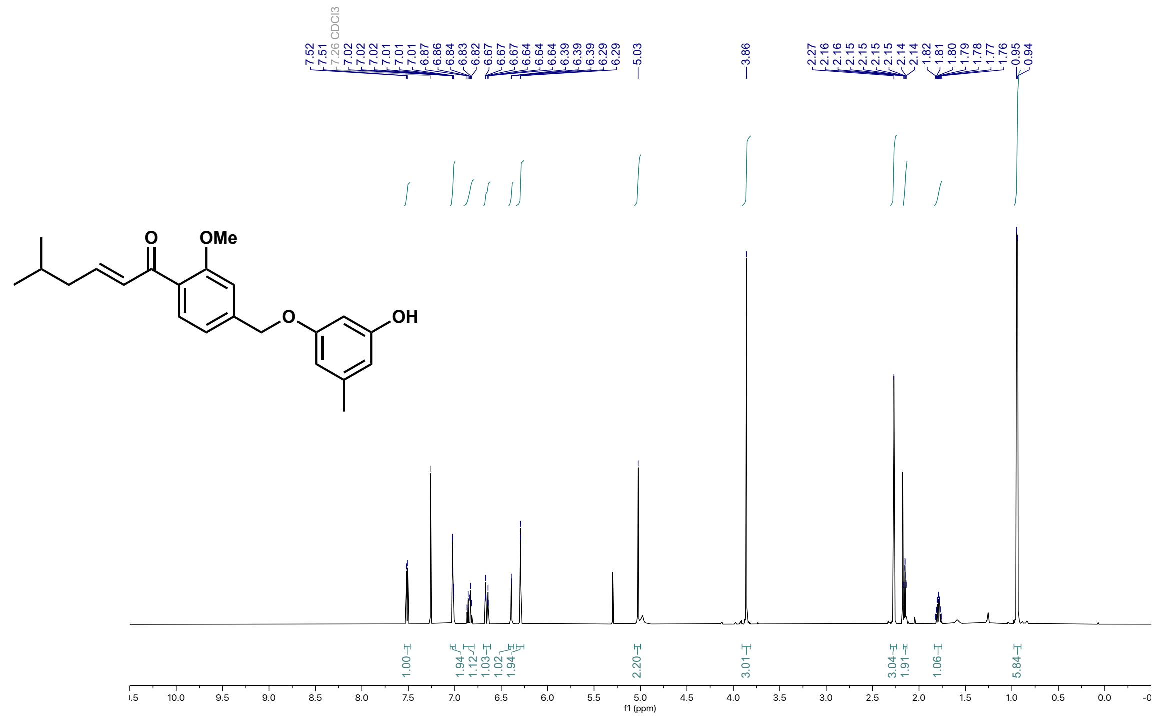
7.52
7.51
7.26 CDCl3
7.02
7.02
7.02
7.01
7.01
7.01
6.87
6.86
6.84
6.83
6.82
6.67
6.67
6.67
6.64
6.64
6.64
6.39
6.39
6.39
6.29
6.29
5.03
3.86
2.27
2.16
2.16
2.15
2.15
2.15
2.15
2.14
1.82
1.81
1.80
1.79
1.78
1.77
1.76
0.95
0.94
O
OMe
O
OH
1.00
1.94
1.12
1.03
1.02
1.94
2.20
3.01
3.04
1.91
1.06
5.84
10.0
9.5
9.0
8.5
8.0
7.5
7.0
6.5
6.0
5.5
5.0
4.5
4.0
3.5
3.0
2.5
2.0
1.5
1.0
0.5
0.0
f1 (ppm)

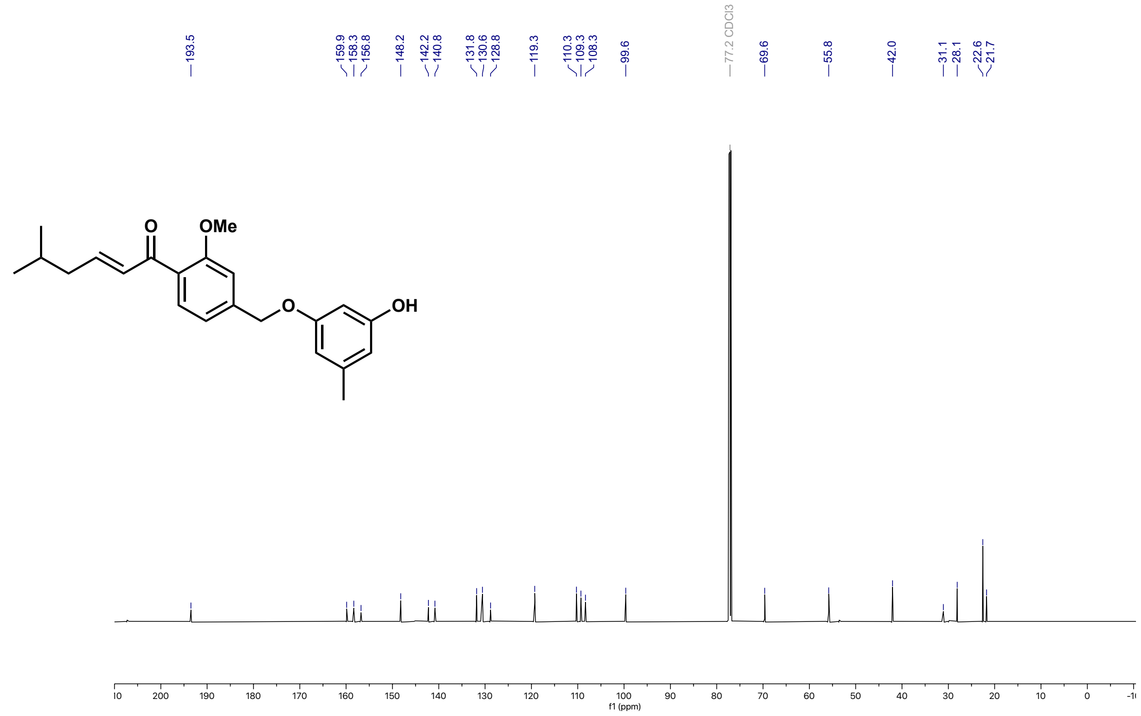
193.5
159.9
158.3
156.8
148.2
142.2
140.8
131.8
130.6
128.8
119.3
110.3
109.3
108.3
99.6
77.2 CDCl3
69.6
55.8
42.0
31.1
28.1
22.6
21.7
O
OMe
O
OH
200
190
180
170
160
150
140
130
120
110
100
90
80
70
60
50
40
30
20
10
0
f1 (ppm)

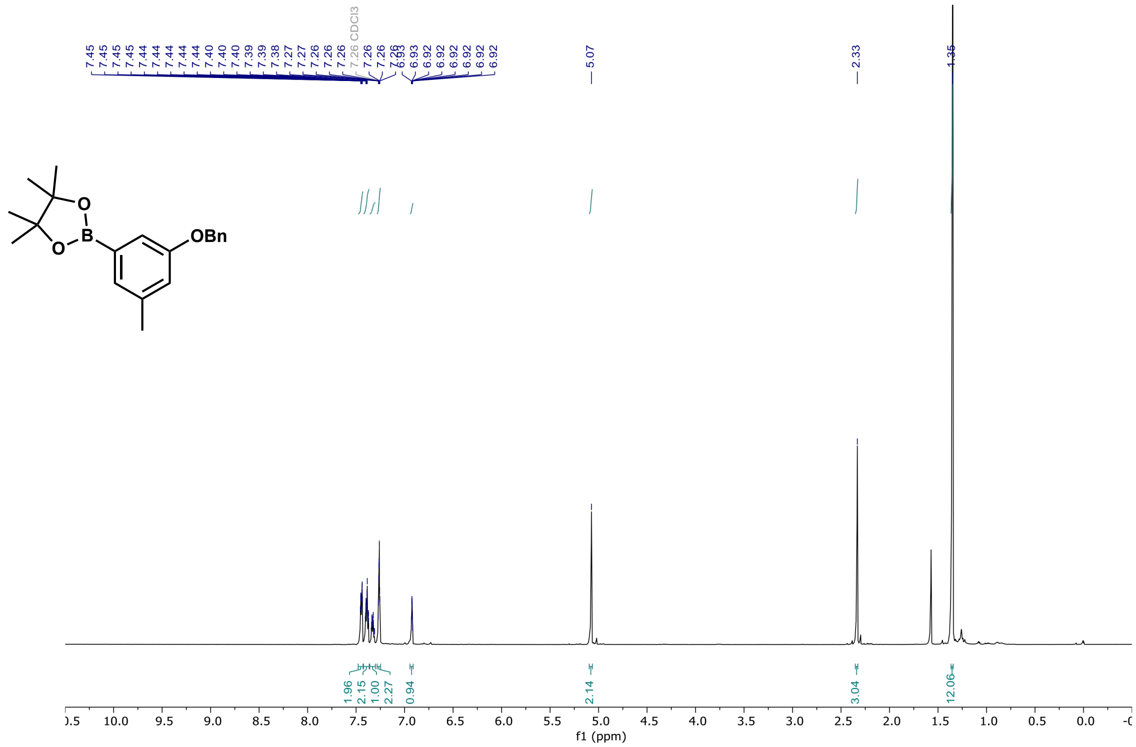
7.45
7.26 CDCl3
6.93
6.92
5.07
2.33
1.35
1.96
2.15
1.00
2.27
0.94
2.14
3.04
12.06
OBn
O
B
f1 (ppm)

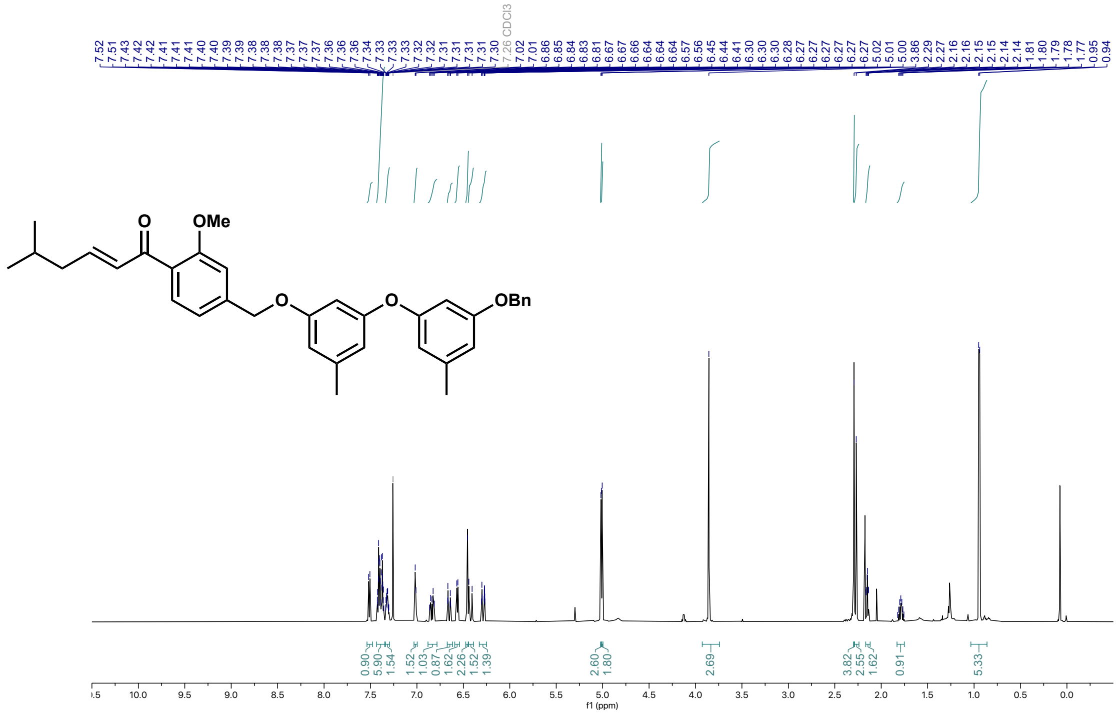
7.52
7.26 CDCl3
7.02
6.86
6.45
5.02
3.86
2.29
2.16
1.81
0.95
0.94
0.90
5.90
1.54
1.52
1.03
0.87
1.62
2.26
1.52
1.39
2.60
1.80
2.69
3.82
2.55
1.62
0.91
5.33
O
OMe
OBn
f1 (ppm)

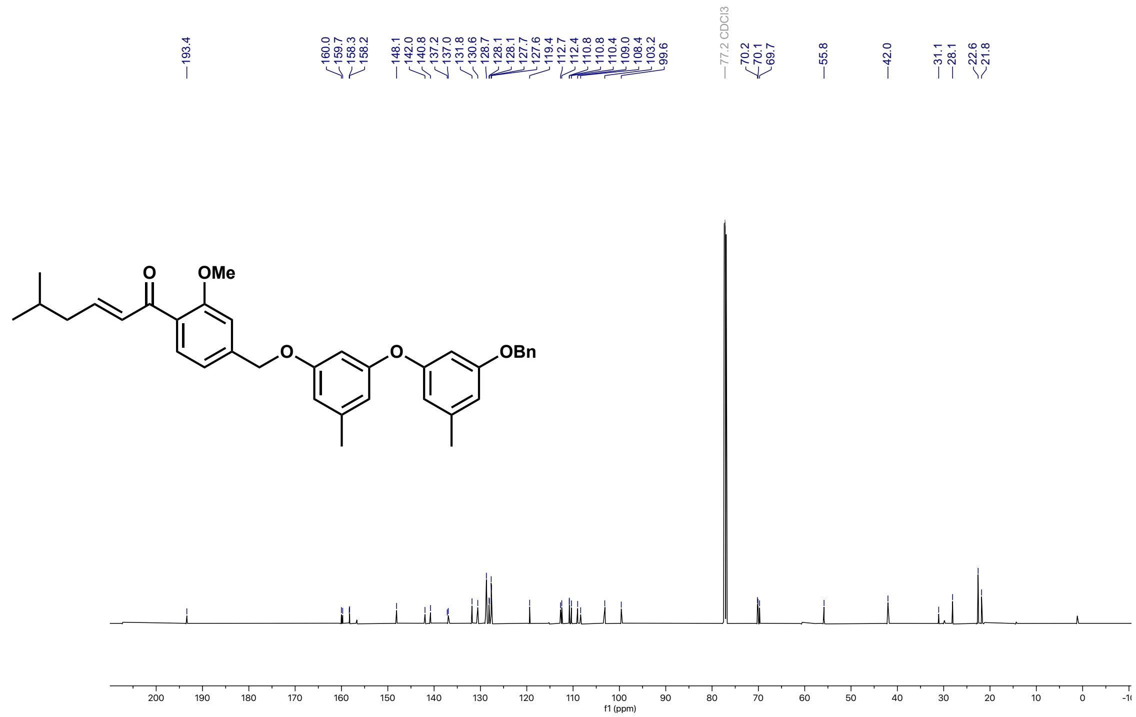
193.4
160.0
159.7
158.3
158.2
148.1
142.0
140.8
137.2
137.0
131.8
130.6
128.7
128.1
128.1
127.7
127.6
119.4
112.7
112.4
110.8
110.8
110.4
109.0
108.4
103.2
99.6
77.2 CDCl3
70.2
70.1
69.7
55.8
42.0
31.1
28.1
22.6
21.8
O
OMe
O
O
OBn
200
190
180
170
160
150
140
130
120
110
100
90
80
70
60
50
40
30
20
10
0
f1 (ppm)

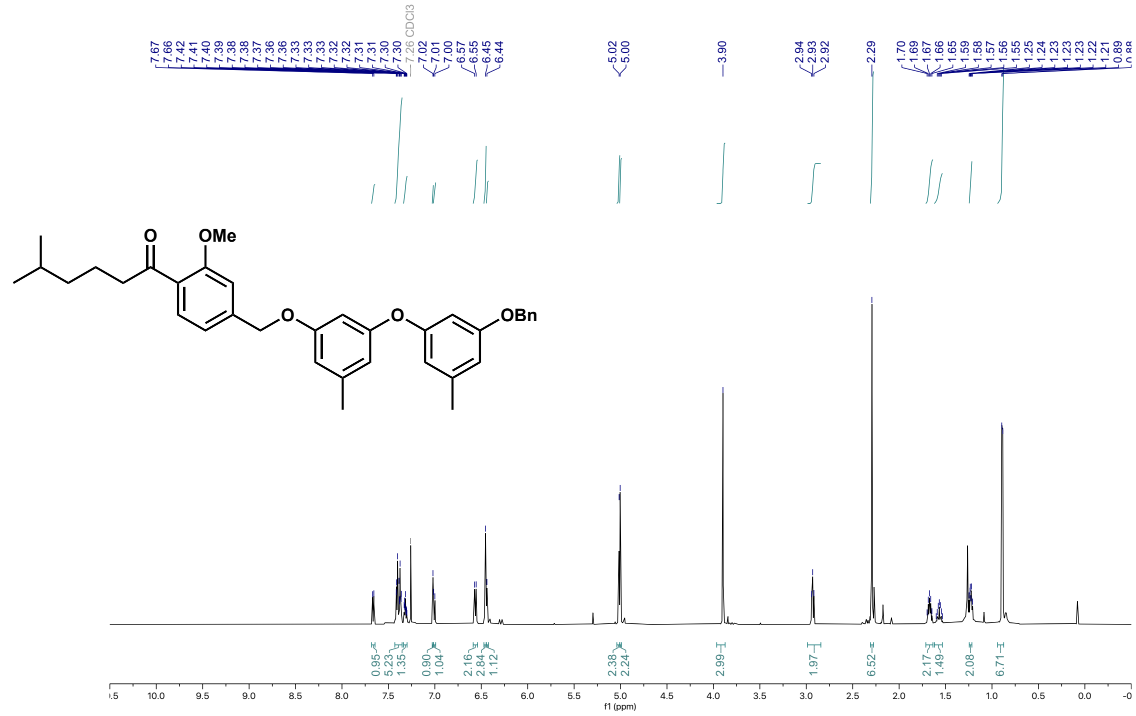
7.67
7.66
7.42
7.41
7.40
7.39
7.38
7.38
7.37
7.36
7.36
7.33
7.33
7.33
7.32
7.32
7.31
7.31
7.30
7.30
7.26 CDCl3
7.02
7.01
7.00
6.57
6.55
6.45
6.44
5.02
5.00
3.90
2.94
2.93
2.92
2.29
1.70
1.69
1.67
1.66
1.65
1.59
1.58
1.57
1.56
1.55
1.25
1.24
1.23
1.23
1.23
1.22
1.21
0.89
O
OMe
O
O
OBn
0.95
5.23
1.35
0.90
1.04
2.16
2.84
1.12
2.38
2.24
2.99
1.97
6.52
2.17
1.49
2.08
6.71
10.0
9.5
9.0
8.5
8.0
7.5
7.0
6.5
6.0
5.5
5.0
4.5
4.0
3.5
3.0
2.5
2.0
1.5
1.0
0.5
0.0
f1 (ppm)

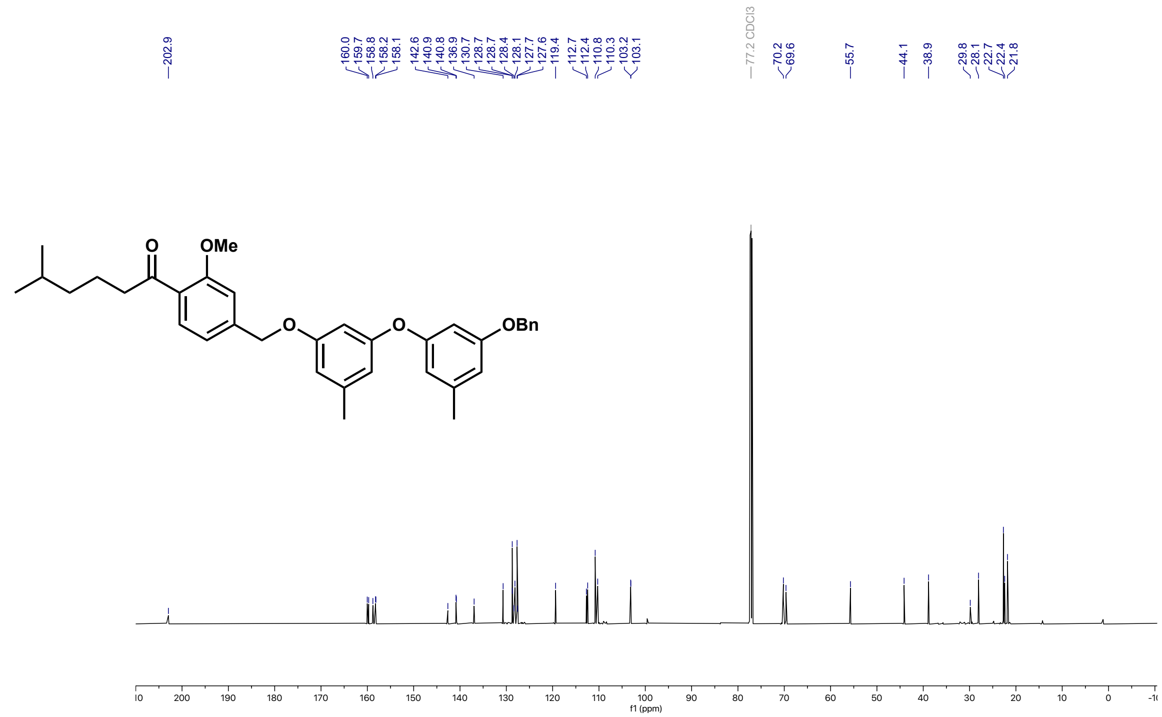
202.9
160.0
159.7
158.8
158.2
158.1
142.6
140.9
140.8
136.9
130.7
128.7
128.7
128.4
128.1
127.7
127.6
119.4
112.7
112.4
110.8
110.3
103.2
103.1
77.2 CDCl3
70.2
69.6
55.7
44.1
38.9
29.8
28.1
22.7
22.4
21.8
O
OMe
O
O
OBn
200
190
180
170
160
150
140
130
120
110
100
90
80
70
60
50
40
30
20
10
0
f1 (ppm)

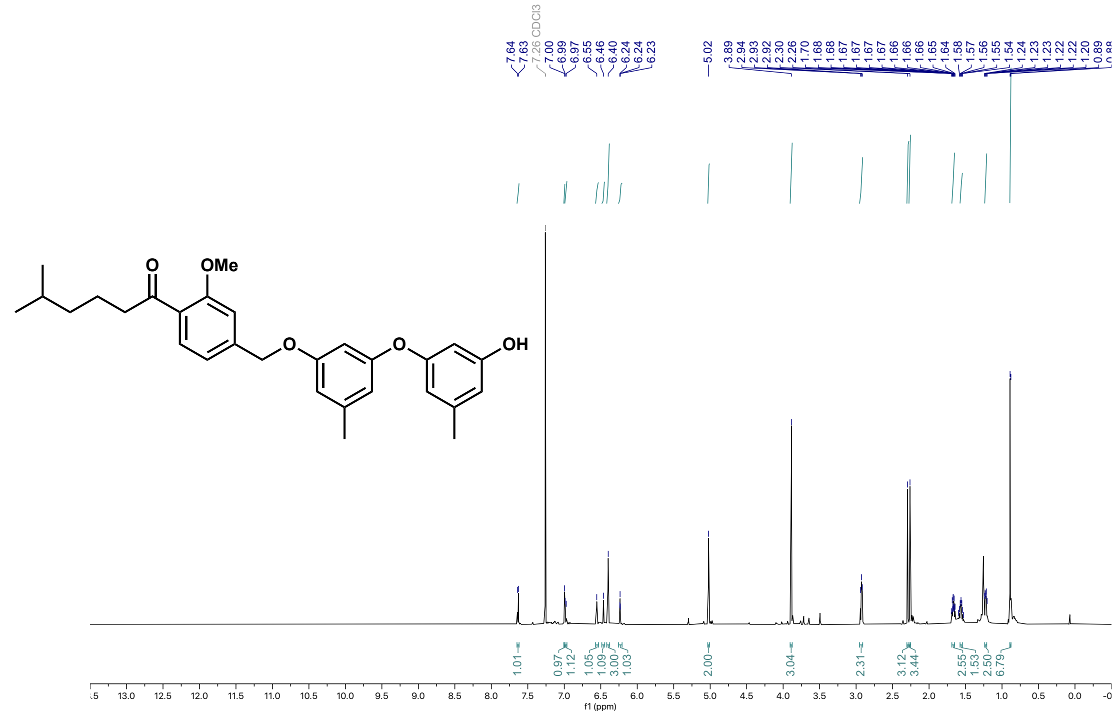
7.64
7.63
7.26 CDCl3
7.00
6.99
6.97
6.55
6.46
6.40
6.24
6.23
5.02
3.89
2.94
2.93
2.92
2.30
2.26
1.70
1.68
1.68
1.67
1.67
1.67
1.66
1.66
1.65
1.64
1.58
1.57
1.56
1.55
1.54
1.24
1.24
1.23
1.23
1.22
1.22
1.20
0.89
0.88
O
OMe
O
O
OH
1.01
0.97
1.12
1.05
1.09
3.00
1.03
2.00
3.04
2.31
3.12
3.44
2.55
1.53
2.50
6.79
13.0
12.5
12.0
11.5
11.0
10.5
10.0
9.5
9.0
8.5
8.0
7.5
7.0
6.5
6.0
5.5
5.0
4.5
4.0
3.5
3.0
2.5
2.0
1.5
1.0
0.5
0.0
f1 (ppm)

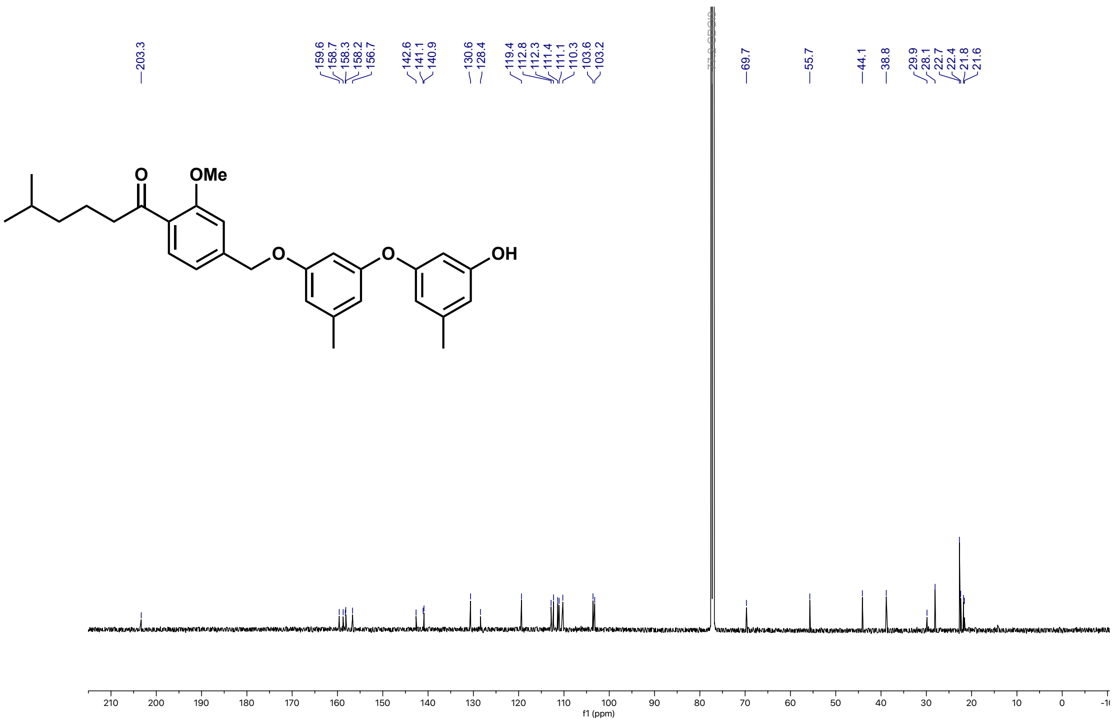
203.3
159.6
158.7
158.3
158.2
156.7
142.6
141.1
140.9
130.6
128.4
119.4
112.8
112.3
111.4
111.1
110.3
103.6
103.2
77.0 CDCl3
69.7
55.7
44.1
38.8
29.9
28.1
22.7
22.4
21.8
21.6
O
OMe
O
O
OH
210 200 190 180 170 160 150 140 130 120 110 100 90 80 70 60 50 40 30 20 10 0
f1 (ppm)

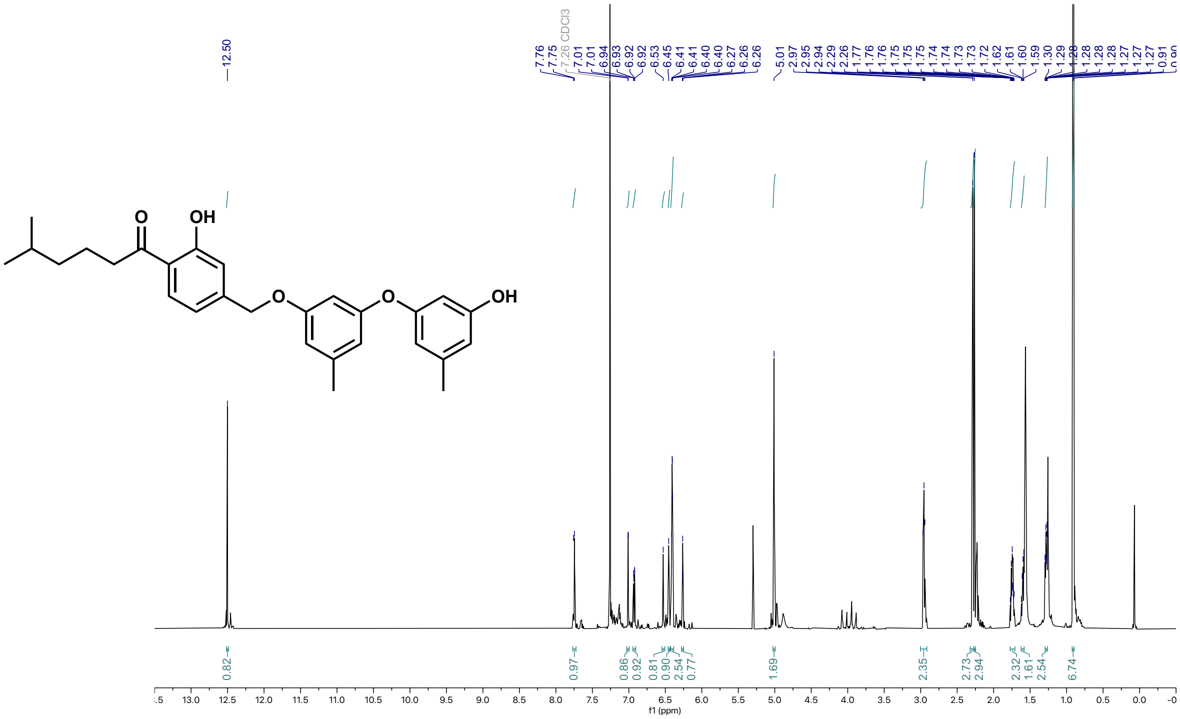
12.50
7.76
7.75
7.26 CDCl3
7.01
7.01
6.94
6.93
6.92
6.92
6.53
6.45
6.41
6.41
6.40
6.40
6.27
6.26
6.26
5.01
2.97
2.95
2.94
2.29
2.26
1.77
1.76
1.76
1.75
1.75
1.75
1.74
1.74
1.73
1.73
1.72
1.62
1.61
1.60
1.59
1.30
1.29
1.28
1.28
1.28
1.28
1.27
1.27
1.27
0.91
O
OH
O
O
OH
0.82
0.97
0.86
0.92
0.81
0.90
2.54
0.77
1.69
2.35
2.73
2.94
2.32
1.61
2.54
6.74
13.0 12.5 12.0 11.5 11.0 10.5 10.0 9.5 9.0 8.5 8.0 7.5 7.0 6.5 6.0 5.5 5.0 4.5 4.0 3.5 3.0 2.5 2.0 1.5 1.0 0.5 0.0
f1 (ppm)

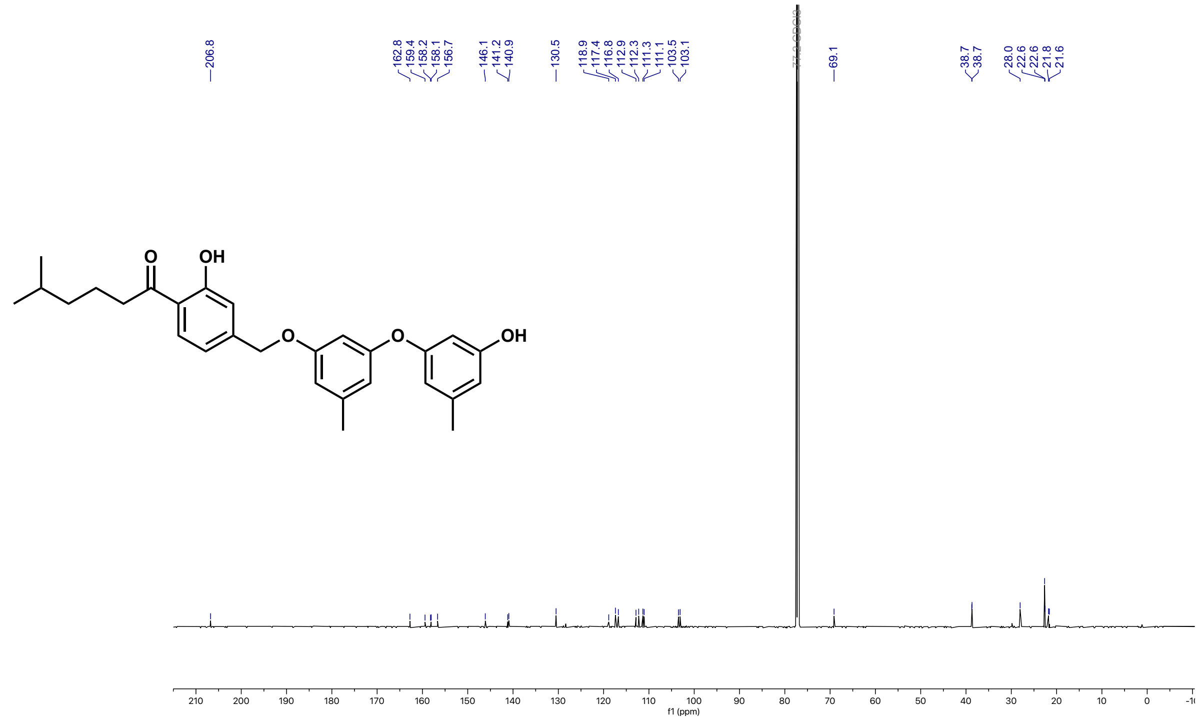

7.2. Appendix chapter 3

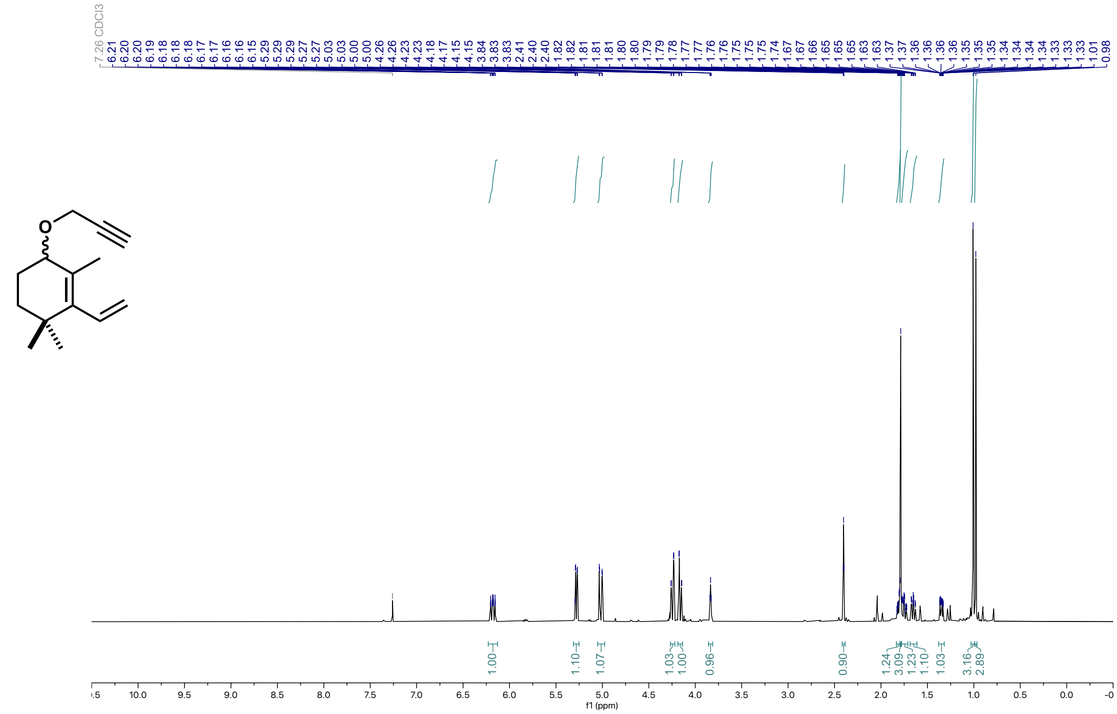
7.26 CDCl3
6.21
6.20
6.20
6.19
6.18
6.18
6.17
6.16
6.16
6.15
5.29
5.29
5.29
5.27
5.03
5.03
5.00
5.00
4.26
4.23
4.23
4.18
4.17
4.15
4.15
3.84
3.83
3.83
2.41
2.40
2.40
1.82
1.81
1.81
1.81
1.80
1.80
1.79
1.79
1.78
1.77
1.77
1.76
1.75
1.75
1.74
1.67
1.67
1.66
1.65
1.65
1.63
1.63
1.37
1.36
1.36
1.36
1.35
1.35
1.35
1.34
1.34
1.34
1.34
1.33
1.33
1.01
0.98
O
1.00
1.10
1.07
1.03
1.00
0.96
0.90
1.24
3.09
1.23
1.10
1.03
3.16
2.89
.5
10.0
9.5
9.0
8.5
8.0
7.5
7.0
6.5
6.0
5.5
5.0
4.5
4.0
3.5
3.0
2.5
2.0
1.5
1.0
0.5
0.0
-0
f1 (ppm)

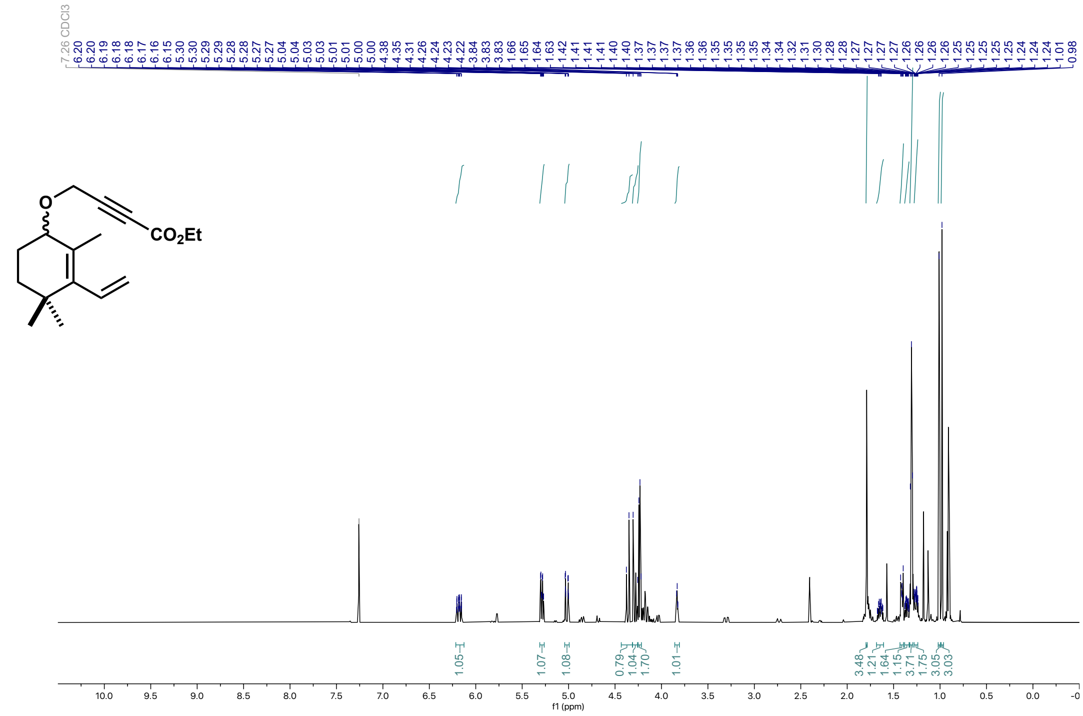
7.26 CDCl3
6.20
6.20
6.19
6.18
6.18
6.17
6.16
6.15
5.30
5.30
5.29
5.29
5.28
5.27
5.27
5.04
5.04
5.03
5.03
5.01
5.00
4.38
4.35
4.31
4.26
4.24
4.23
4.22
3.84
3.83
3.83
1.66
1.65
1.64
1.63
1.42
1.42
1.41
1.41
1.40
1.40
1.37
1.37
1.37
1.36
1.35
1.35
1.35
1.35
1.34
1.32
1.31
1.30
1.28
1.28
1.27
1.27
1.27
1.26
1.26
1.26
1.25
1.25
1.25
1.25
1.24
1.24
1.24
1.01
0.98
O
CO2Et
1.05
1.07
1.08
0.79
1.04
1.70
1.01
3.48
1.21
1.64
1.15
3.71
1.75
3.05
3.03
10.0
9.5
9.0
8.5
8.0
7.5
7.0
6.5
6.0
5.5
5.0
4.5
4.0
3.5
3.0
2.5
2.0
1.5
1.0
0.5
0.0
-0
f1 (ppm)

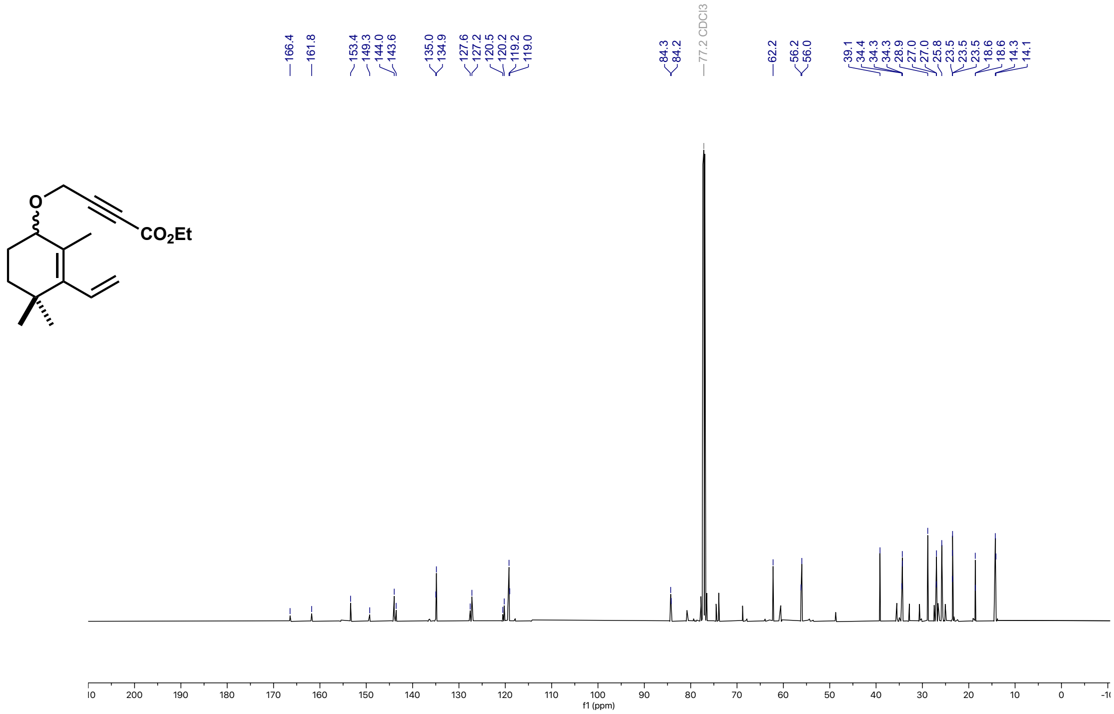
166.4
161.8
153.4
149.3
144.0
143.6
135.0
134.9
127.6
127.2
120.5
120.2
119.2
119.0
84.3
84.2
77.2 CDCl3
62.2
56.2
56.0
39.1
34.4
34.3
34.3
28.9
27.0
27.0
25.8
23.5
23.5
23.5
18.6
18.6
14.3
14.1
O
CO2Et
0
200
190
180
170
160
150
140
130
120
110
100
90
80
70
60
50
40
30
20
10
0
-1
f1 (ppm)

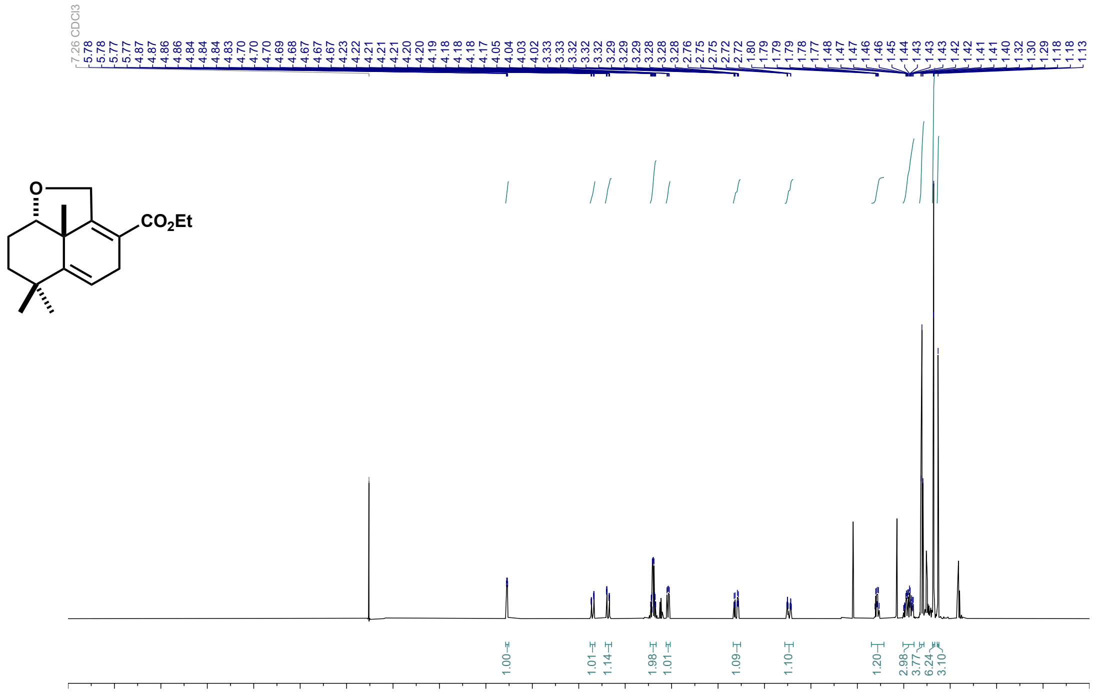
7.26 CDCl3
5.78
5.78
5.77
4.87
4.86
4.86
4.84
4.84
4.83
4.70
4.70
4.69
4.68
4.67
4.67
4.23
4.22
4.21
4.21
4.20
4.19
4.18
4.18
4.18
4.17
4.05
4.04
4.03
4.02
3.33
3.33
3.32
3.32
3.29
3.29
3.28
3.28
2.76
2.75
2.75
2.72
1.80
1.79
1.79
1.78
1.77
1.48
1.47
1.47
1.46
1.45
1.44
1.43
1.43
1.43
1.42
1.42
1.41
1.40
1.32
1.30
1.29
1.18
1.18
1.13
O
CO2Et
1.00
1.01
1.14
1.98
1.01
1.09
1.10
1.20
2.98
3.77
6.24
3.10
.5
10.0
9.5
9.0
8.5
8.0
7.5
7.0
6.5
6.0
5.5
5.0
4.5
4.0
3.5
3.0
2.5
2.0
1.5
1.0
0.5
0.0
-0
f1 (ppm)

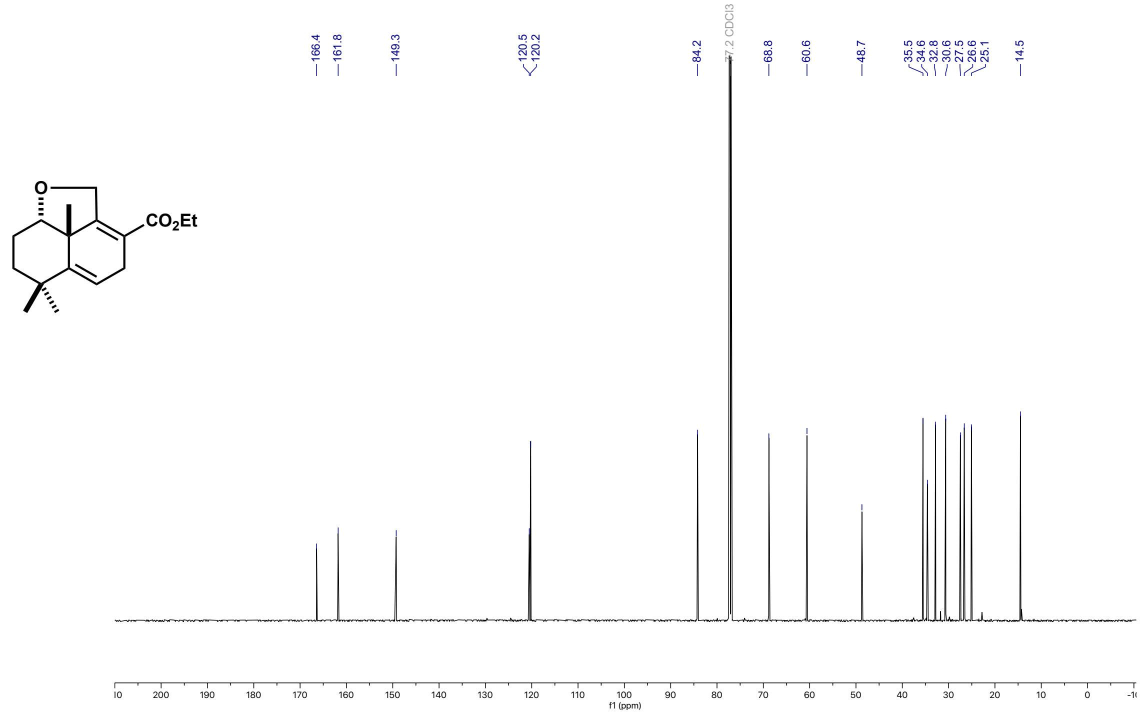

O
CO2Et
166.4
161.8
149.3
120.5
120.2
84.2
77.2 CDCl3
68.8
60.6
48.7
35.5
34.6
32.8
30.6
27.5
26.6
25.1
14.5
200 190 180 170 160 150 140 130 120 110 100 90 80 70 60 50 40 30 20 10 0
f1 (ppm)

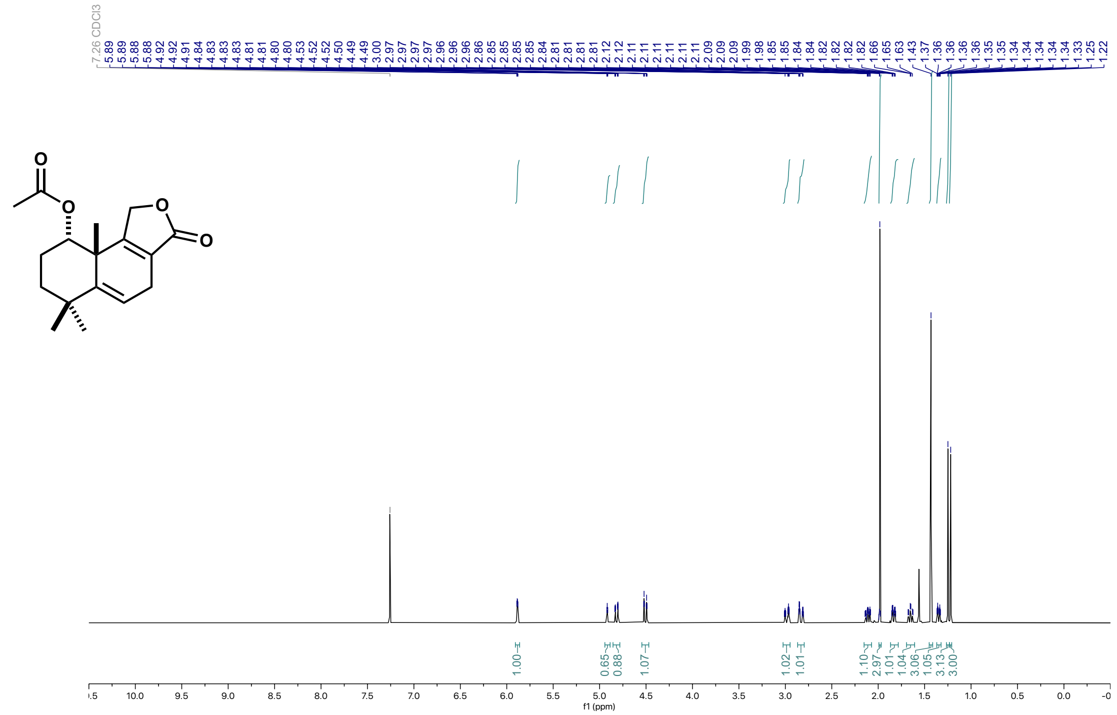

O
O
O
O
7.26 CDCl3
5.89 5.89 5.88 5.88 4.92 4.92 4.91 4.84 4.83 4.83 4.81 4.80 4.80 4.53 4.52 4.52 4.50 4.49 4.49 3.00 2.97 2.97 2.97 2.96 2.96 2.96 2.86 2.85 2.85 2.85 2.84 2.81 2.81 2.81 2.81 2.12 2.12 2.11 2.11 2.11 2.11 2.11 2.11 2.09 2.09 2.09 1.99 1.98 1.85 1.85 1.84 1.84 1.82 1.82 1.82 1.82 1.66 1.65 1.63 1.43 1.37 1.36 1.36 1.36 1.35 1.35 1.34 1.34 1.34 1.34 1.34 1.33 1.25 1.22
1.00
0.65
0.88
1.07
1.02
1.01
1.10
2.97
1.01
1.04
3.06
1.05
3.13
3.00
10.0 9.5 9.0 8.5 8.0 7.5 7.0 6.5 6.0 5.5 5.0 4.5 4.0 3.5 3.0 2.5 2.0 1.5 1.0 0.5 0.0
f1 (ppm)

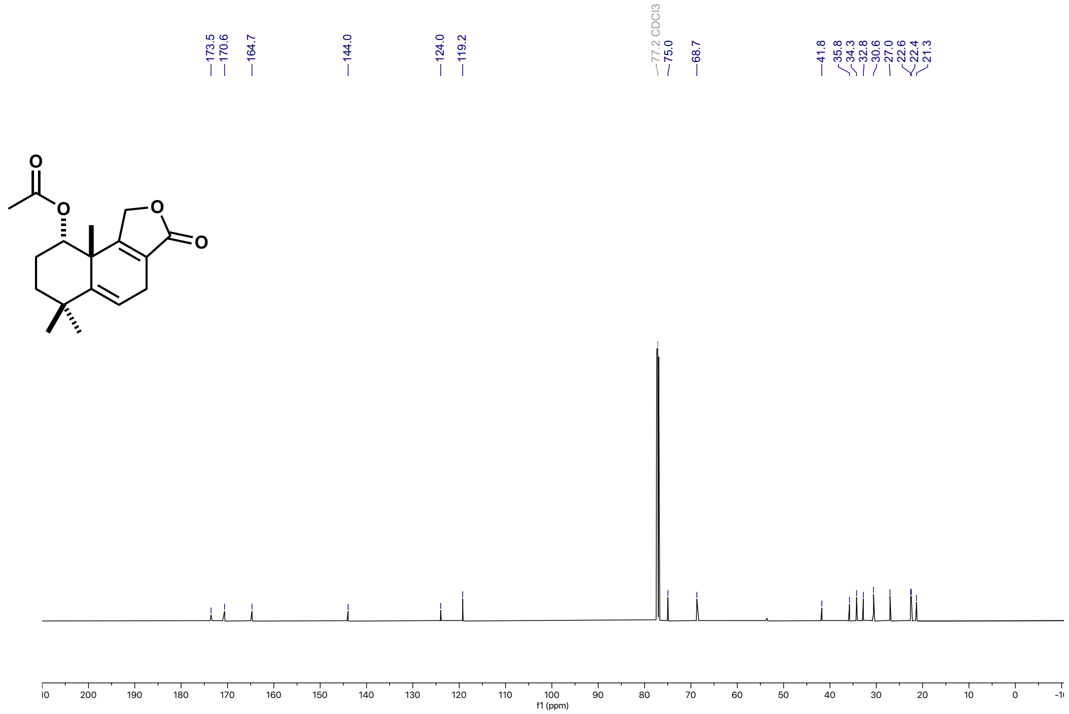
O
O
O
O
173.5
170.6
164.7
144.0
124.0
119.2
77.2 CDCl3
75.0
68.7
41.8
35.8
34.3
32.8
30.6
27.0
22.6
22.4
21.3
200
190
180
170
160
150
140
130
120
110
100
90
80
70
60
50
40
30
20
10
0
f1 (ppm)

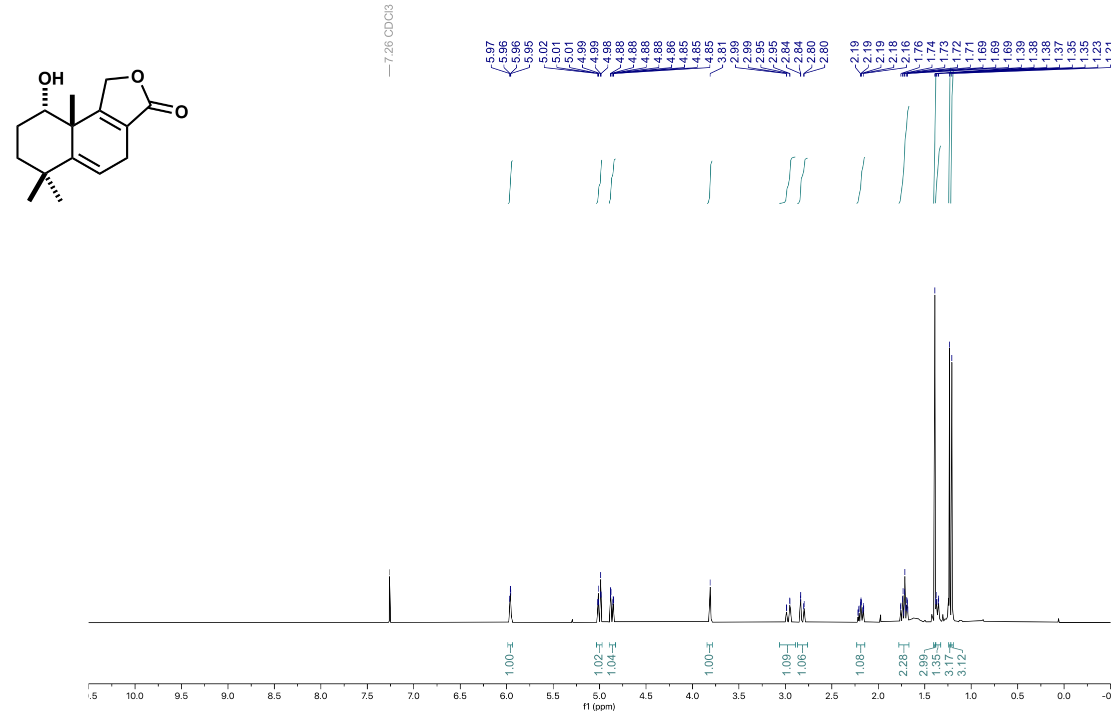
OH
O
O
7.26 CDCl3
5.97
5.96
5.96
5.95
5.02
5.01
4.99
4.99
4.98
4.88
4.88
4.88
4.86
4.85
4.85
3.81
2.99
2.99
2.95
2.95
2.84
2.84
2.80
2.80
2.19
2.19
2.19
2.18
2.16
1.76
1.74
1.73
1.72
1.71
1.69
1.69
1.39
1.38
1.38
1.37
1.35
1.23
1.00
1.02
1.04
1.00
1.09
1.06
1.08
2.28
2.99
1.35
3.17
3.12
10.0
9.5
9.0
8.5
8.0
7.5
7.0
6.5
6.0
5.5
5.0
4.5
4.0
3.5
3.0
2.5
2.0
1.5
1.0
0.5
0.0
f1 (ppm)

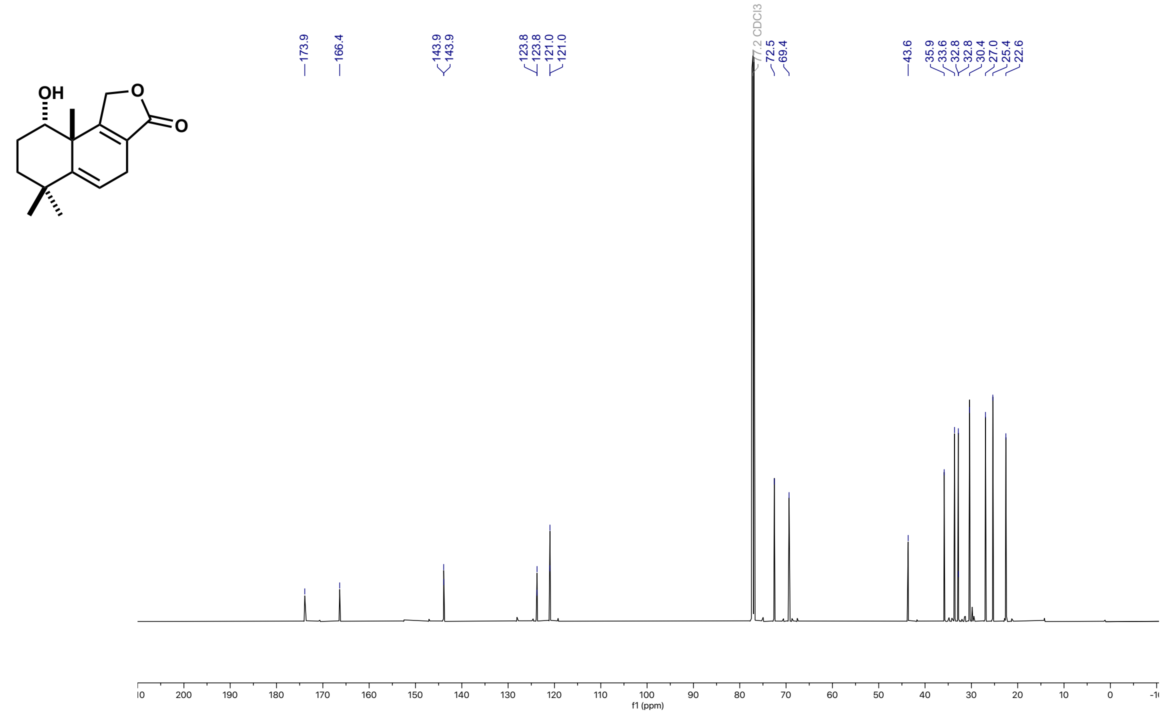
OH
O
O
173.9
166.4
143.9
143.9
123.8
123.8
121.0
121.0
77.2 CDCl3
72.5
69.4
43.6
35.9
33.6
32.8
32.8
30.4
27.0
25.4
22.6
200
190
180
170
160
150
140
130
120
110
100
90
80
70
60
50
40
30
20
10
0
f1 (ppm)

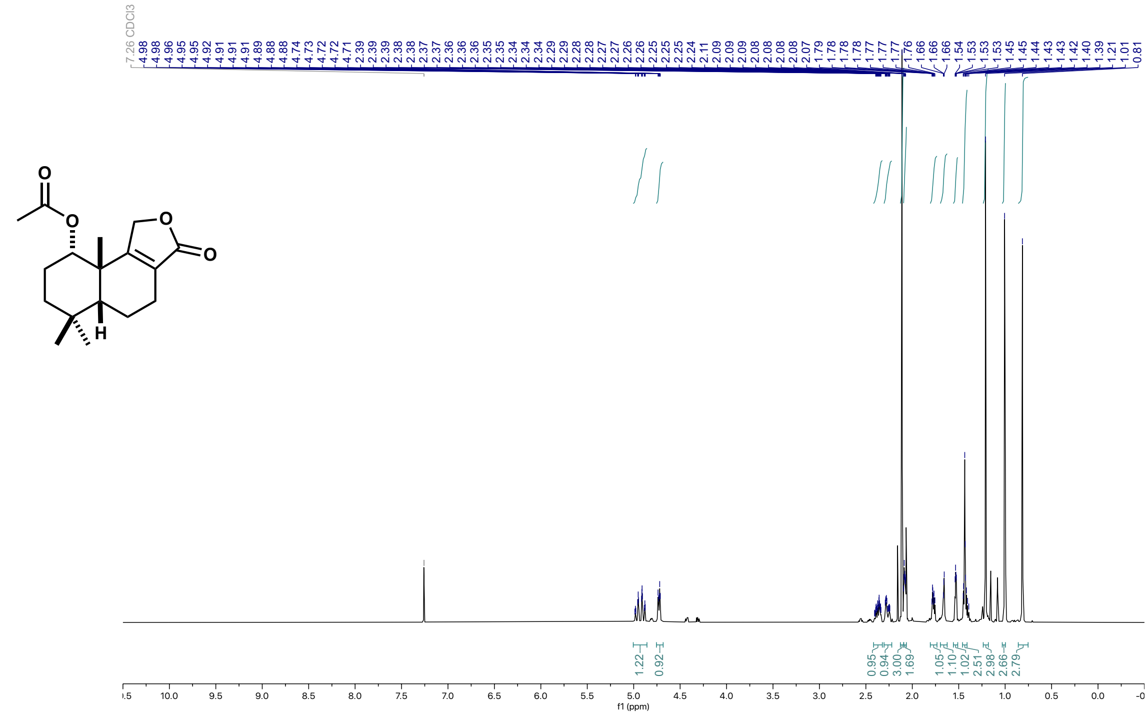
O
O
O
O
H
7.26 CDCl3
4.98
4.98
4.96
4.95
4.95
4.92
4.91
4.91
4.91
4.89
4.88
4.88
4.74
4.73
4.72
4.72
4.71
2.39
2.39
2.39
2.38
2.38
2.37
2.37
2.36
2.36
2.36
2.35
2.34
2.34
2.34
2.29
2.29
2.28
2.28
2.27
2.27
2.26
2.26
2.25
2.25
2.25
2.24
2.11
2.09
2.09
2.09
2.08
2.08
2.08
2.07
1.79
1.78
1.78
1.78
1.77
1.77
1.77
1.76
1.66
1.66
1.54
1.53
1.53
1.53
1.45
1.45
1.44
1.43
1.43
1.42
1.40
1.39
1.21
1.01
0.81
1.22
0.92
0.95
0.94
3.00
1.69
1.05
1.10
1.02
2.51
2.98
2.66
2.79
10.0
9.5
9.0
8.5
8.0
7.5
7.0
6.5
6.0
5.5
5.0
4.5
4.0
3.5
3.0
2.5
2.0
1.5
1.0
0.5
0.0
f1 (ppm)

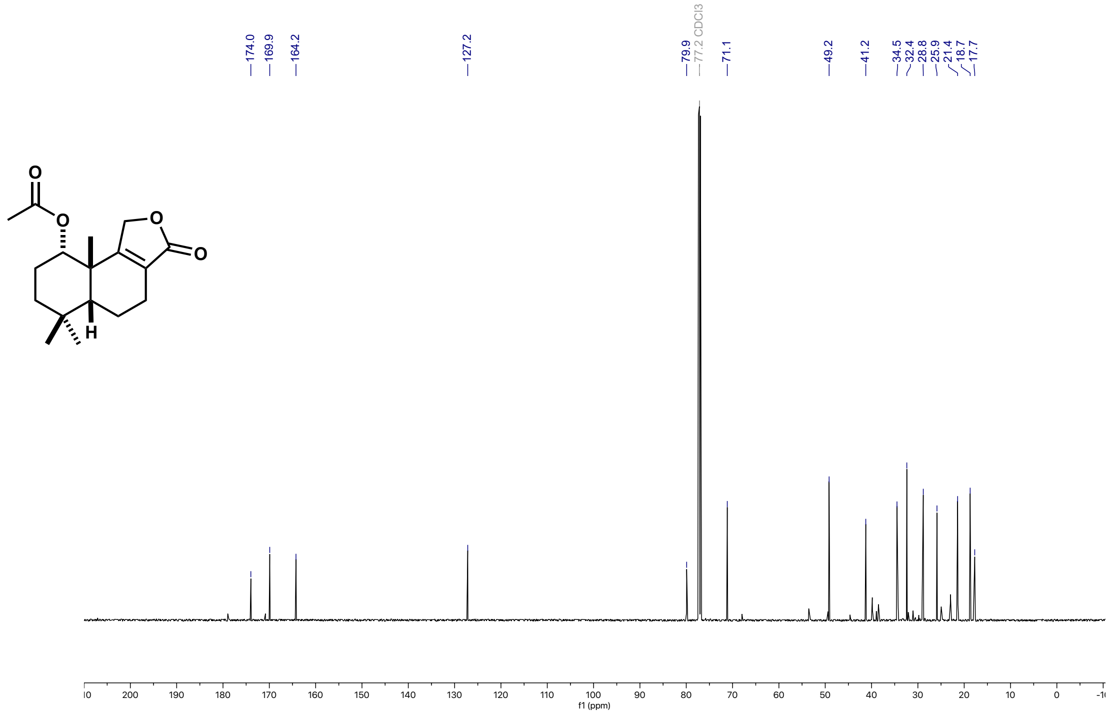
174.0
169.9
164.2
127.2
79.9
77.2 CDCl3
71.1
49.2
41.2
34.5
32.4
28.8
25.9
21.4
18.7
17.7
O
O
O
O
H
200
190
180
170
160
150
140
130
120
110
100
90
80
70
60
50
40
30
20
10
0
f1 (ppm)

NOESY

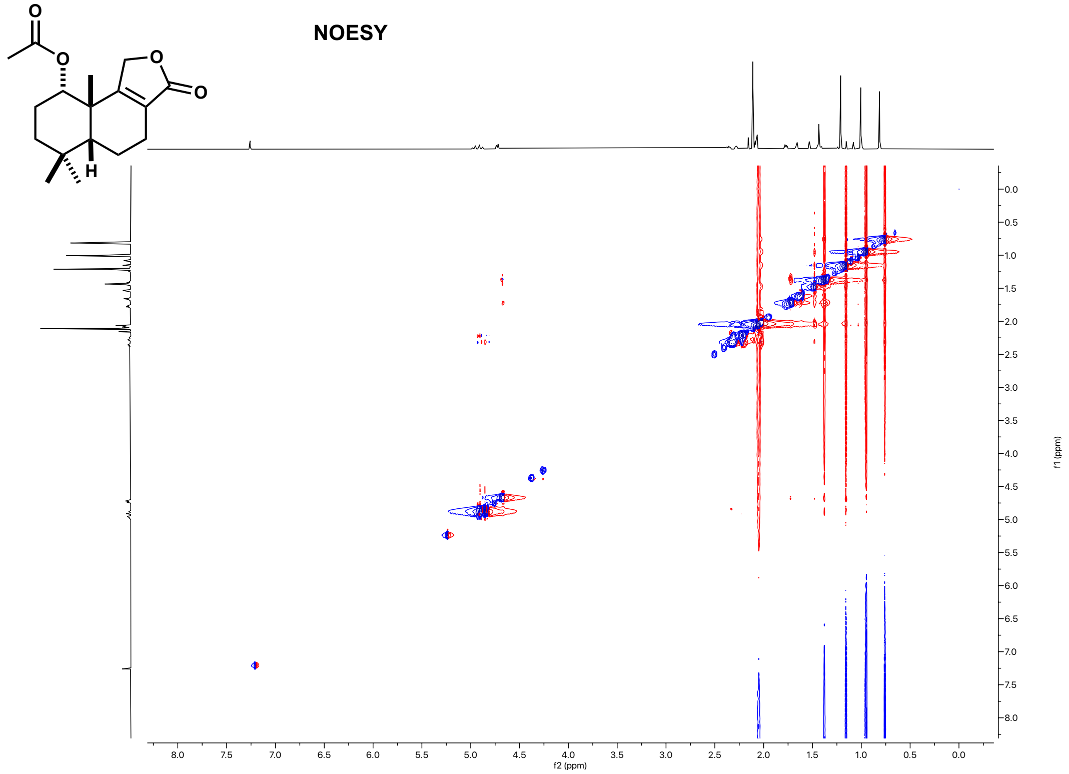
O
O
O
O
H
8.0
7.5
7.0
6.5
6.0
5.5
5.0
4.5
4.0
3.5
3.0
2.5
2.0
1.5
1.0
0.5
0.0
f2 (ppm)
f1 (ppm)

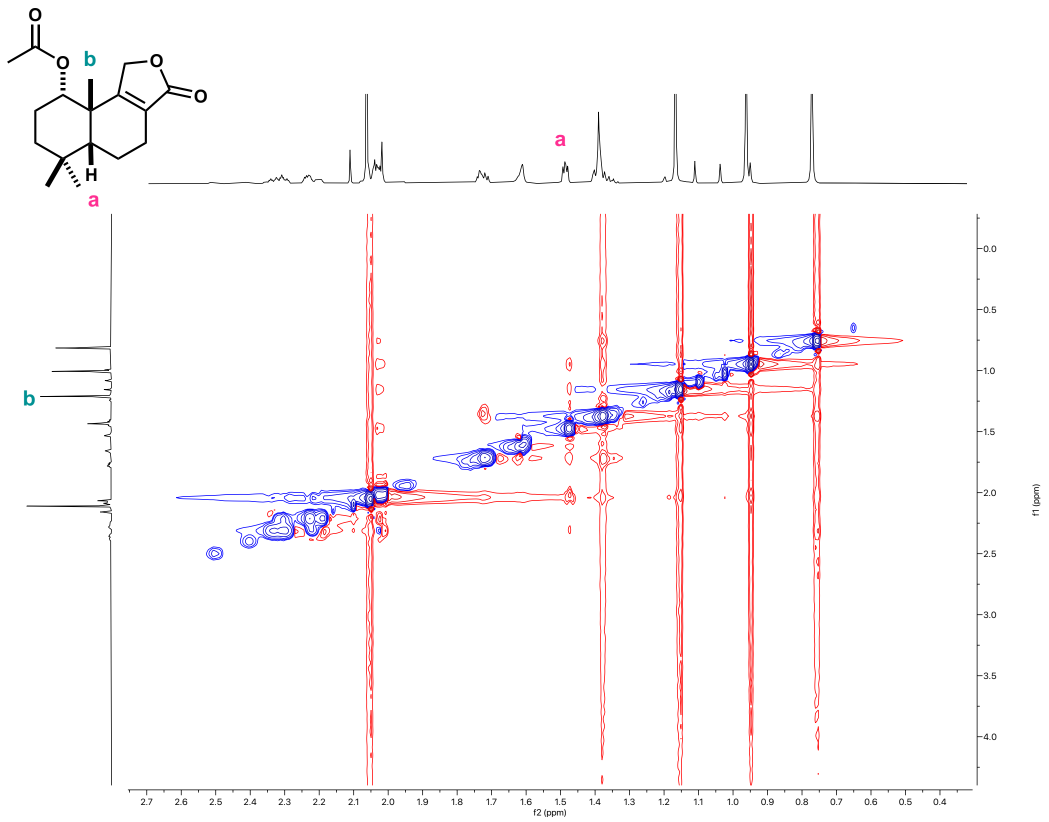
b
a
a
b
f2 (ppm)
f1 (ppm)
2.7 2.6 2.5 2.4 2.3 2.2 2.1 2.0 1.9 1.8 1.7 1.6 1.5 1.4 1.3 1.2 1.1 1.0 0.9 0.8 0.7 0.6 0.5 0.4
0.0 0.5 1.0 1.5 2.0 2.5 3.0 3.5 4.0

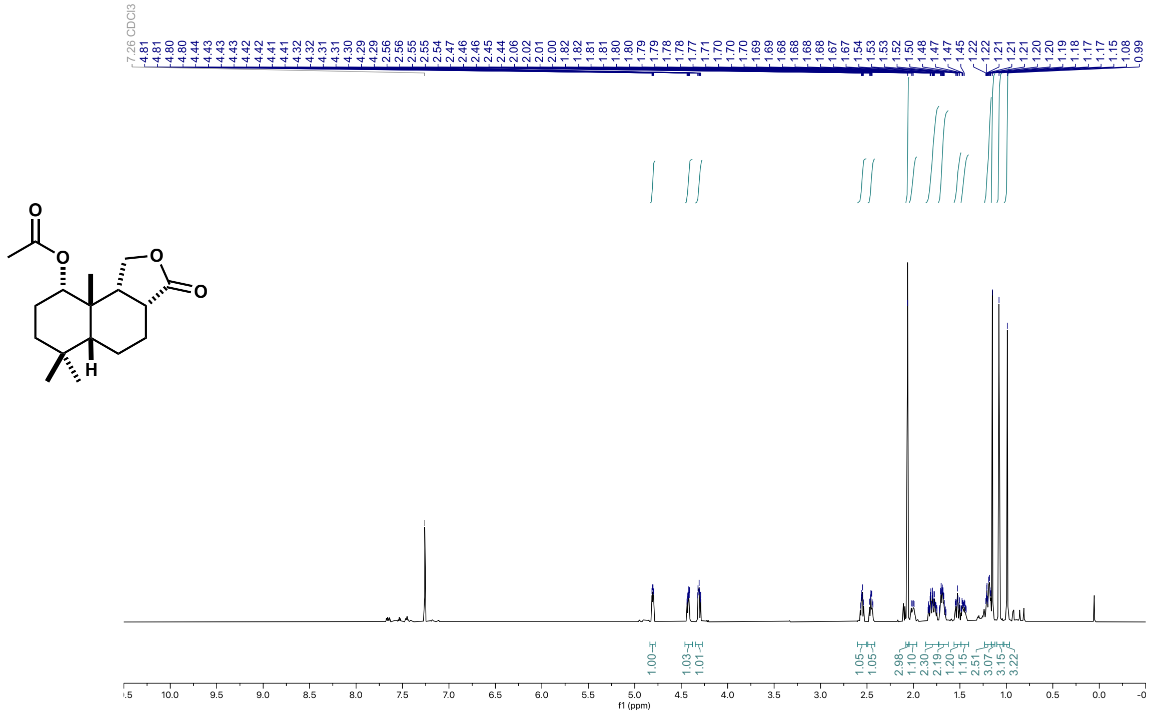
7.26 CDCl3
4.81 4.81 4.80 4.80 4.44 4.43 4.43 4.43 4.42 4.42 4.41 4.41 4.32 4.32 4.31 4.31 4.30 4.29 2.56 2.56 2.55 2.55 2.54 2.47 2.46 2.46 2.45 2.44 2.06 2.02 2.01 2.00 1.82 1.82 1.81 1.81 1.80 1.80 1.79 1.79 1.78 1.78 1.77 1.71 1.70 1.70 1.70 1.69 1.69 1.68 1.68 1.68 1.68 1.67 1.67 1.54 1.53 1.53 1.52 1.50 1.48 1.47 1.47 1.45 1.22 1.22 1.21 1.21 1.21 1.20 1.20 1.19 1.18 1.17 1.17 1.15 1.08 0.99
1.00 1.03 1.01 1.05 1.05 2.98 1.10 2.30 2.19 1.20 1.15 2.51 3.07 3.15 3.22
10.0 9.5 9.0 8.5 8.0 7.5 7.0 6.5 6.0 5.5 5.0 4.5 4.0 3.5 3.0 2.5 2.0 1.5 1.0 0.5 0.0
f1 (ppm)

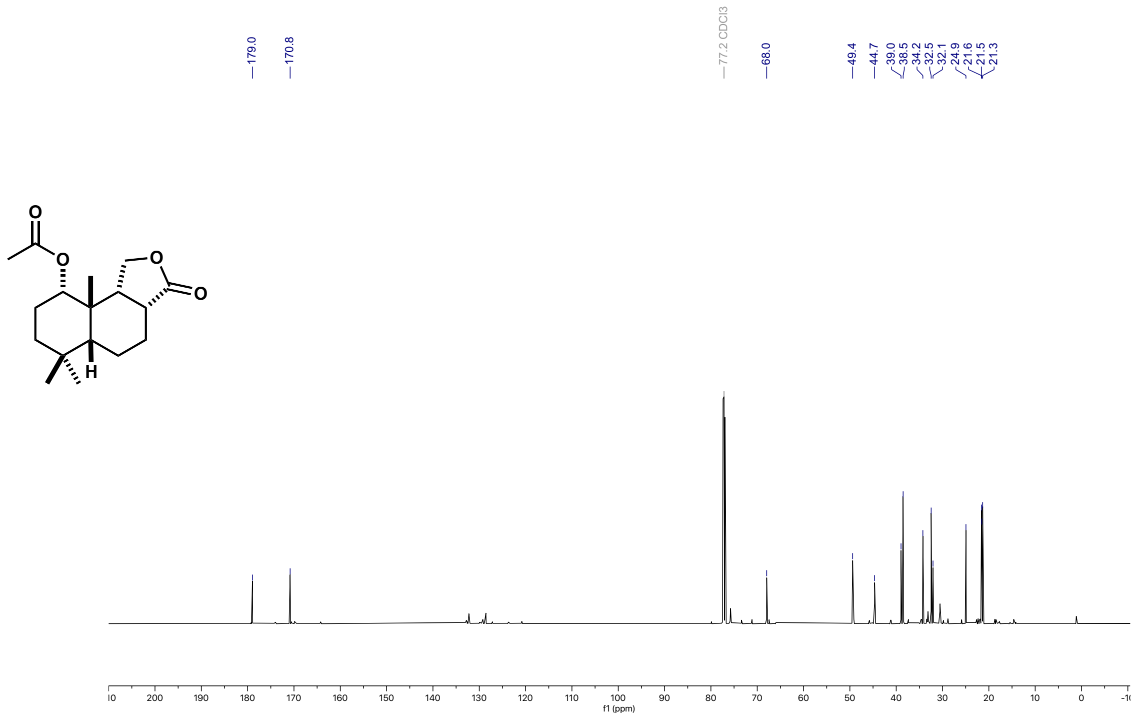
179.0
170.8
77.2 CDCl3
68.0
49.4
44.7
39.0
38.5
34.2
32.5
32.1
24.9
21.6
21.5
21.3
O
O
O
O
H
200
190
180
170
160
150
140
130
120
110
100
90
80
70
60
50
40
30
20
10
0
f1 (ppm)

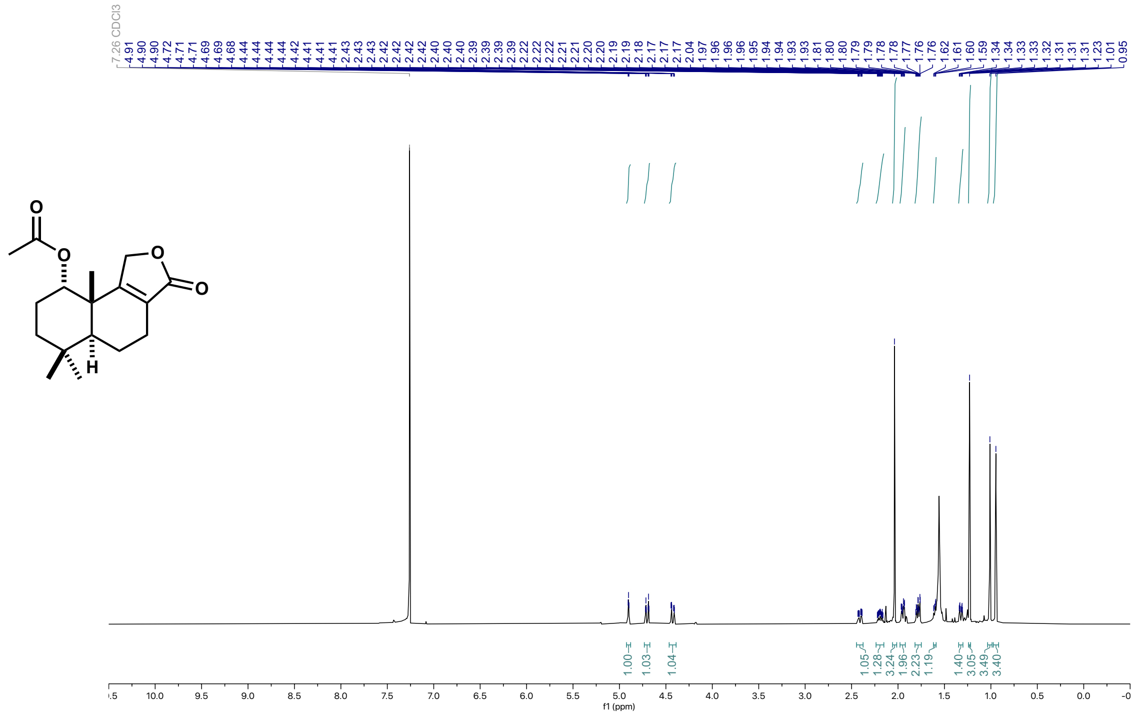
7.26 CDCl3
4.91
4.90
4.90
4.72
4.71
4.71
4.69
4.68
4.44
4.44
4.44
4.44
4.42
4.41
4.41
4.41
2.43
2.43
2.43
2.42
2.42
2.42
2.42
2.40
2.40
2.40
2.39
2.39
2.39
2.22
2.22
2.22
2.21
2.21
2.20
2.20
2.19
2.19
2.18
2.17
2.17
2.17
2.04
1.97
1.96
1.96
1.95
1.94
1.94
1.93
1.93
1.81
1.80
1.80
1.79
1.79
1.78
1.78
1.77
1.76
1.62
1.61
1.60
1.59
1.34
1.34
1.33
1.33
1.32
1.31
1.31
1.31
1.23
1.01
0.95
O
O
O
O
H
1.00
1.03
1.04
1.05
1.28
3.24
1.96
2.23
1.19
1.40
3.05
3.49
3.40
10.0
9.5
9.0
8.5
8.0
7.5
7.0
6.5
6.0
5.5
5.0
4.5
4.0
3.5
3.0
2.5
2.0
1.5
1.0
0.5
0.0
f1 (ppm)

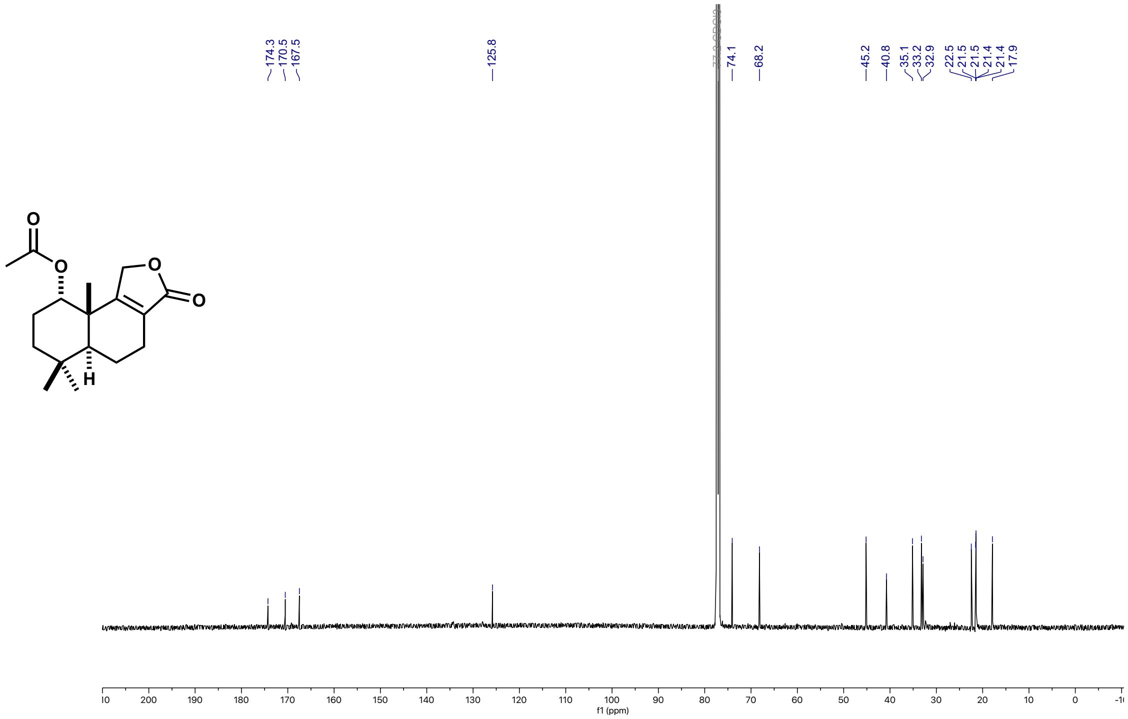
O
O
O
O
H

174.3
170.5
167.5
125.8
77.0 CDCl3
74.1
68.2
45.2
40.8
35.1
33.2
32.9
22.5
21.5
21.5
21.4
21.4
17.9
f1 (ppm)

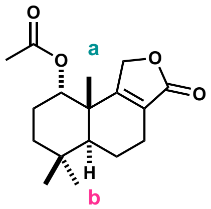
O
O
a
O
O
H
b

NOESY

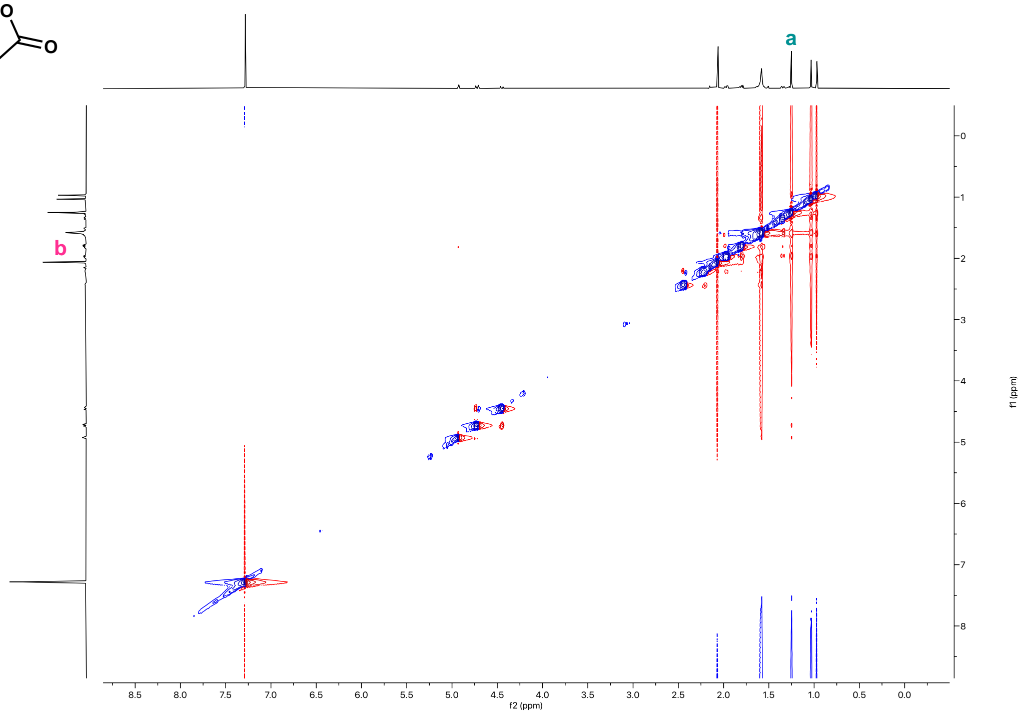
a
b
f2 (ppm)
f1 (ppm)

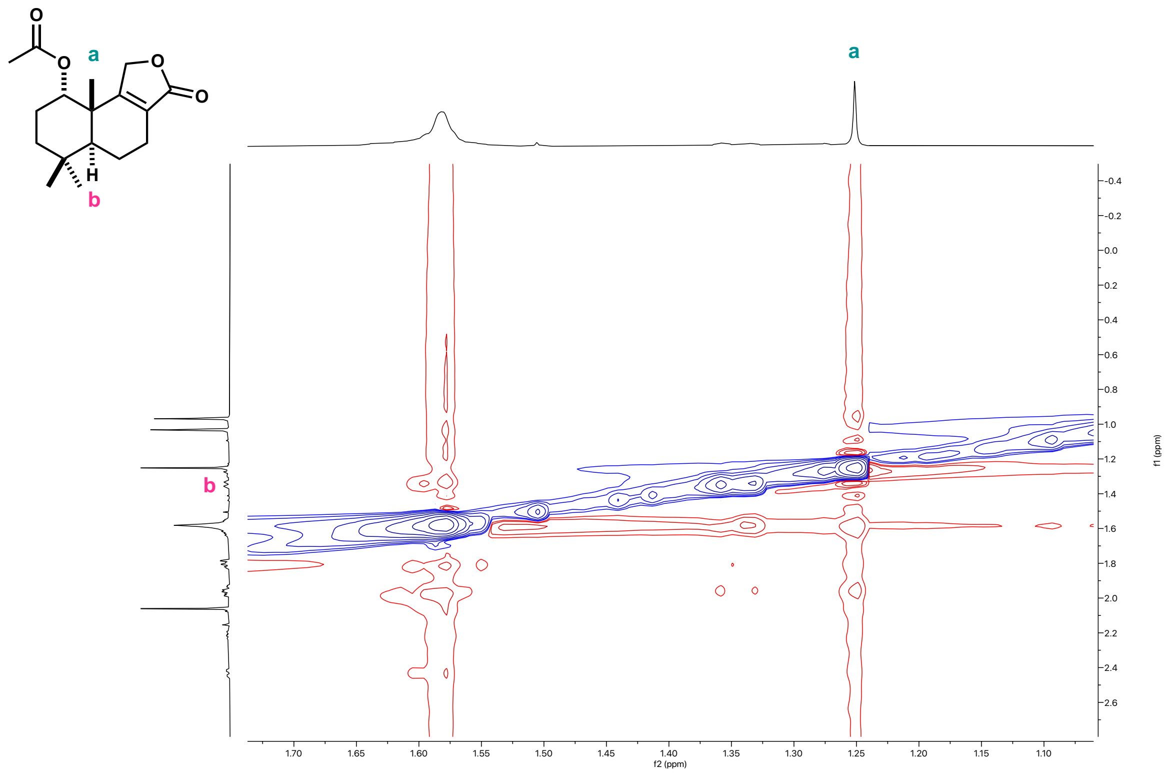
a
b
a
b
O
O
O
O
H
f2 (ppm)
f1 (ppm)
1.70
1.65
1.60
1.55
1.50
1.45
1.40
1.35
1.30
1.25
1.20
1.15
1.10
-0.4
-0.2
0.0
0.2
0.4
0.6
0.8
1.0
1.2
1.4
1.6
1.8
2.0
2.2
2.4
2.6

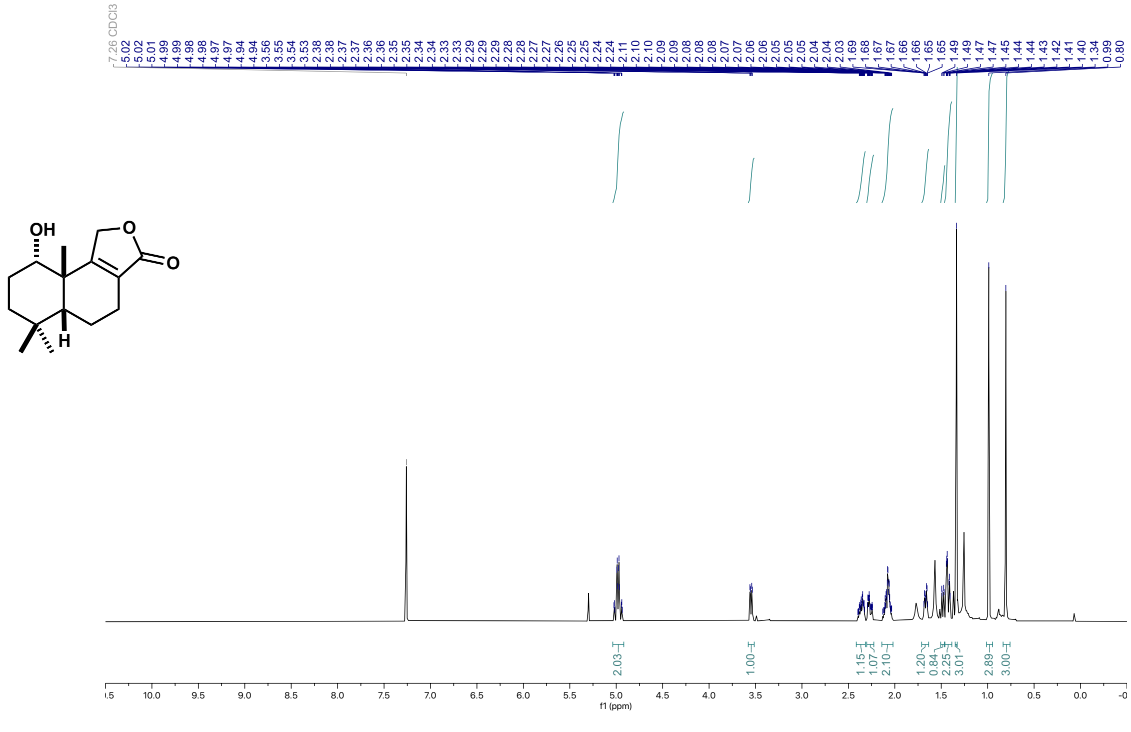
OH
O
O
H
7.26 CDCl3
5.02
5.02
5.01
4.99
4.99
4.98
4.98
4.97
4.97
4.94
3.56
3.55
3.54
3.53
2.38
2.38
2.37
2.37
2.36
2.36
2.35
2.35
2.34
2.34
2.33
2.33
2.29
2.29
2.28
2.28
2.27
2.27
2.26
2.25
2.25
2.24
2.24
2.11
2.10
2.10
2.09
2.09
2.08
2.08
2.08
2.07
2.07
2.06
2.06
2.05
2.05
2.05
2.04
2.04
2.03
2.03
1.69
1.68
1.67
1.66
1.66
1.65
1.65
1.49
1.49
1.47
1.47
1.45
1.45
1.44
1.44
1.43
1.42
1.41
1.40
1.34
0.99
0.80
2.03
1.00
1.15
1.07
2.10
1.20
0.84
2.25
3.01
2.89
3.00
f1 (ppm)
10.0
9.5
9.0
8.5
8.0
7.5
7.0
6.5
6.0
5.5
5.0
4.5
4.0
3.5
3.0
2.5
2.0
1.5
1.0
0.5
0.0

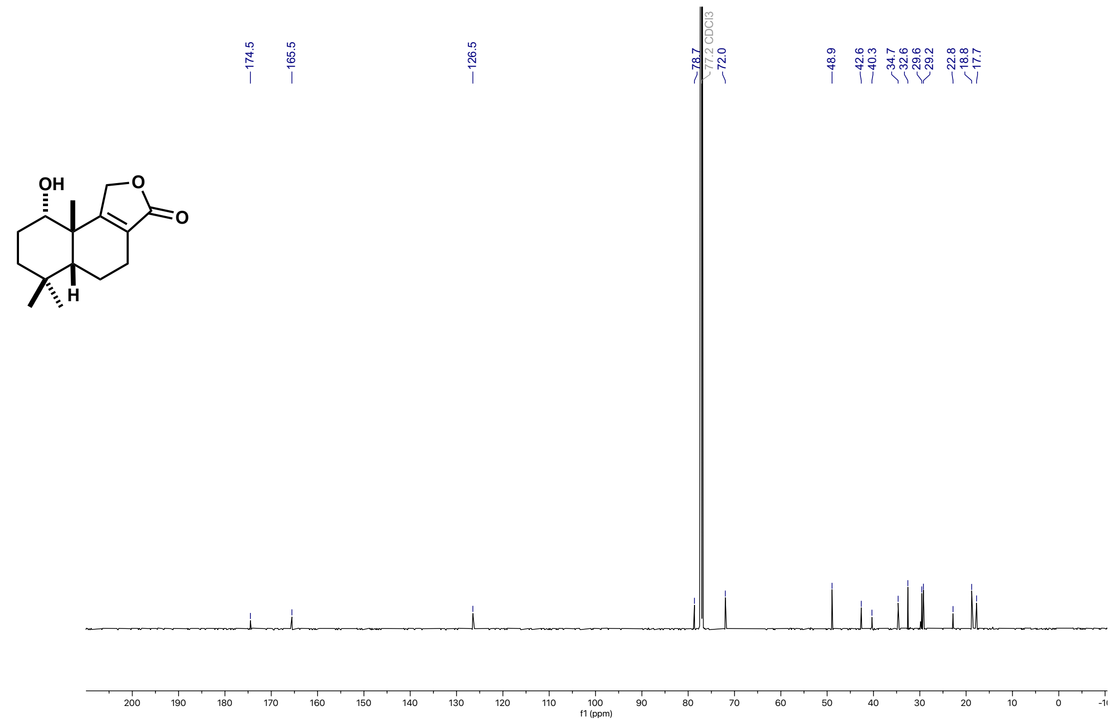
OH
O
O
H

174.5
165.5
126.5
78.7
77.2 CDCl3
72.0
48.9
42.6
40.3
34.7
32.6
29.6
29.2
22.8
18.8
17.7
200
190
180
170
160
150
140
130
120
110
100
90
80
70
60
50
40
30
20
10
0
f1 (ppm)

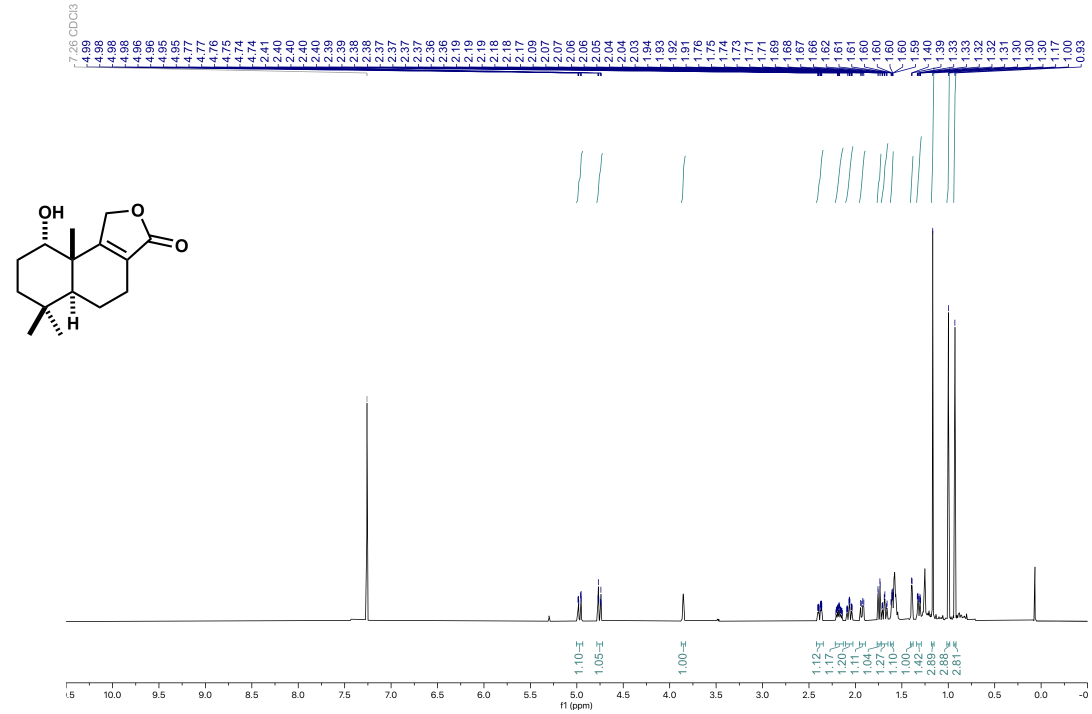
OH
O
O
H

7.26 CDCl3
4.99
4.98
4.98
4.98
4.96
4.96
4.95
4.95
4.77
4.77
4.76
4.75
4.74
4.74
2.41
2.40
2.40
2.40
2.40
2.39
2.39
2.38
2.38
2.37
2.37
2.37
2.37
2.36
2.36
2.19
2.19
2.19
2.18
2.18
2.17
2.09
2.07
2.07
2.06
2.06
2.05
2.04
2.04
2.03
1.94
1.93
1.92
1.91
1.76
1.75
1.74
1.73
1.71
1.71
1.69
1.68
1.67
1.66
1.62
1.61
1.61
1.60
1.60
1.60
1.60
1.59
1.40
1.39
1.33
1.33
1.32
1.32
1.31
1.30
1.30
1.30
1.17
1.00
0.93
1.10
1.05
1.00
1.12
1.17
1.20
1.11
1.04
1.27
1.10
1.00
1.42
2.89
2.88
2.81
10.0
9.5
9.0
8.5
8.0
7.5
7.0
6.5
6.0
5.5
5.0
4.5
4.0
3.5
3.0
2.5
2.0
1.5
1.0
0.5
0.0
f1 (ppm)

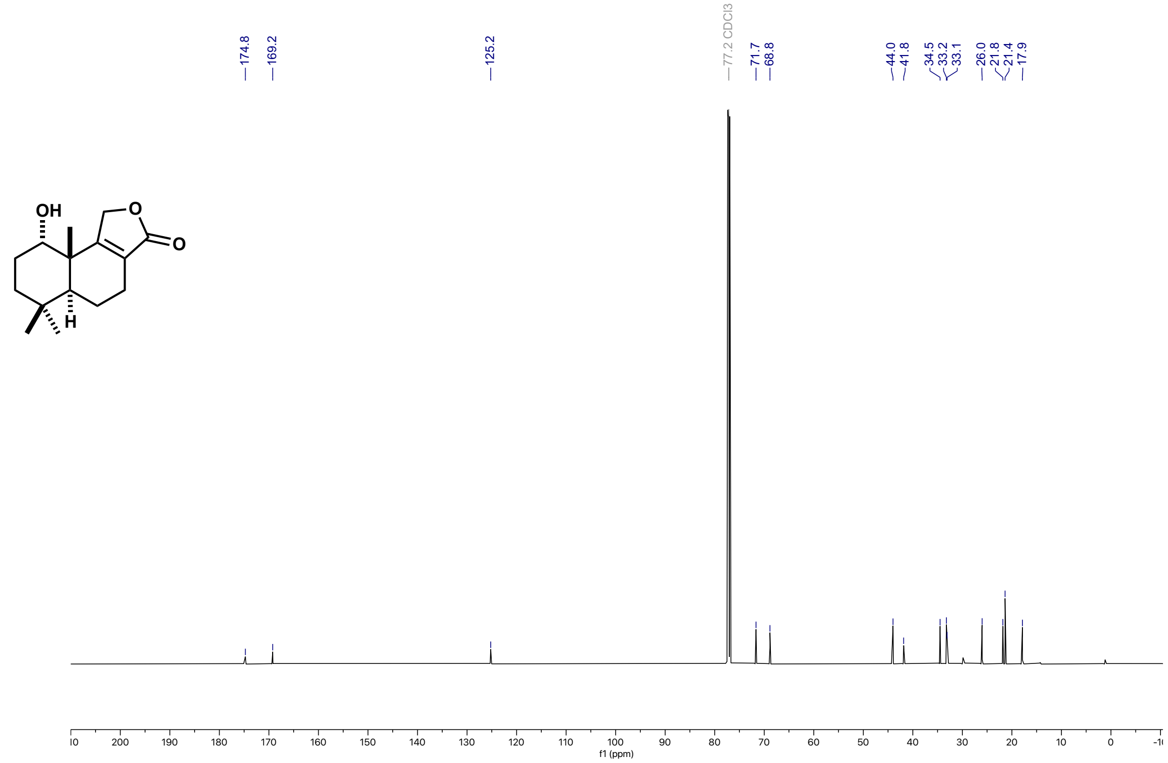

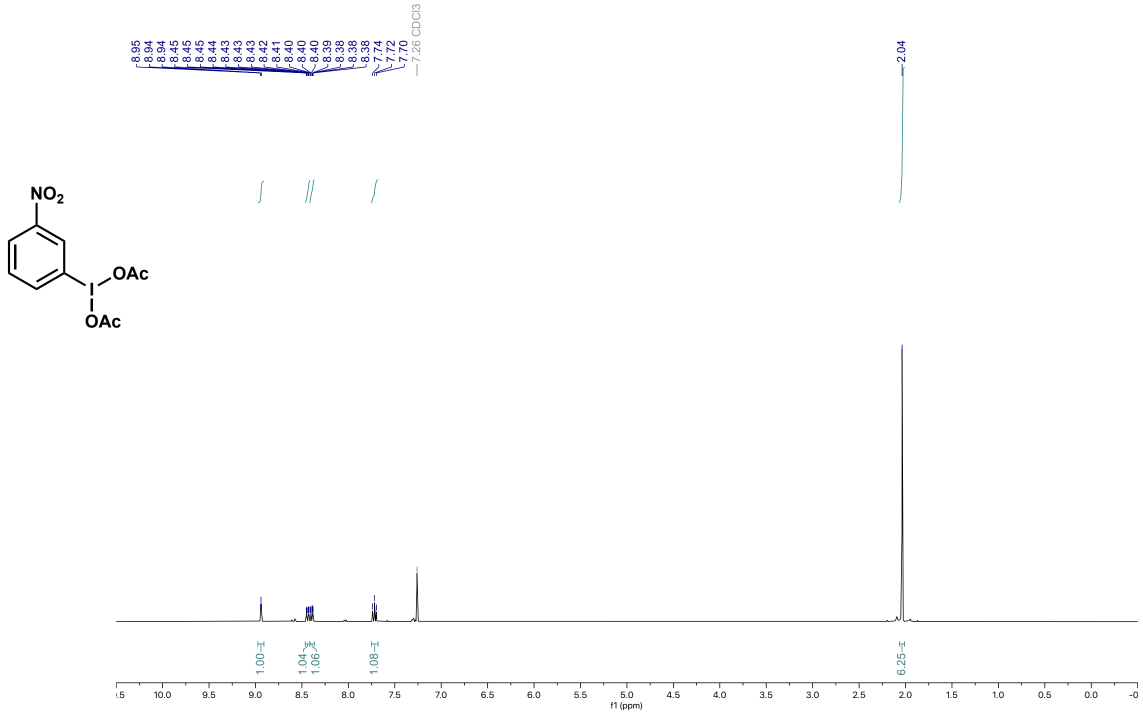

7.3. Appendix chapter 4

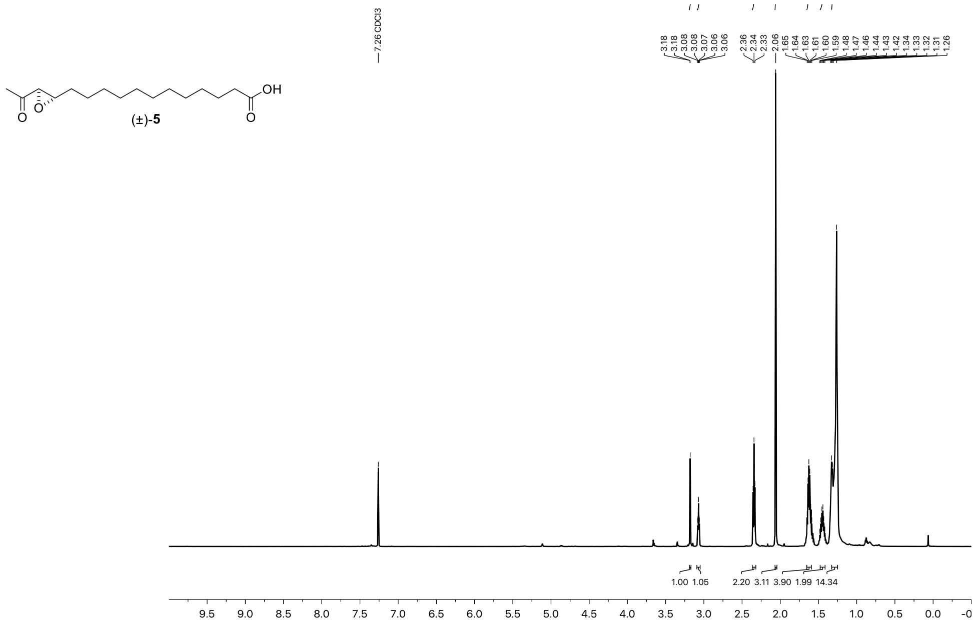
(±)-5
OH
O
O
O
7.26 CDCl3
3.18
3.18
3.08
3.08
3.07
3.06
3.06
2.36
2.34
2.33
2.06
1.65
1.64
1.63
1.61
1.60
1.59
1.48
1.47
1.46
1.44
1.43
1.42
1.34
1.33
1.32
1.31
1.26
1.00
1.05
2.20
3.11
3.90
1.99
14.34
9.5
9.0
8.5
8.0
7.5
7.0
6.5
6.0
5.5
5.0
4.5
4.0
3.5
3.0
2.5
2.0
1.5
1.0
0.5
0.0

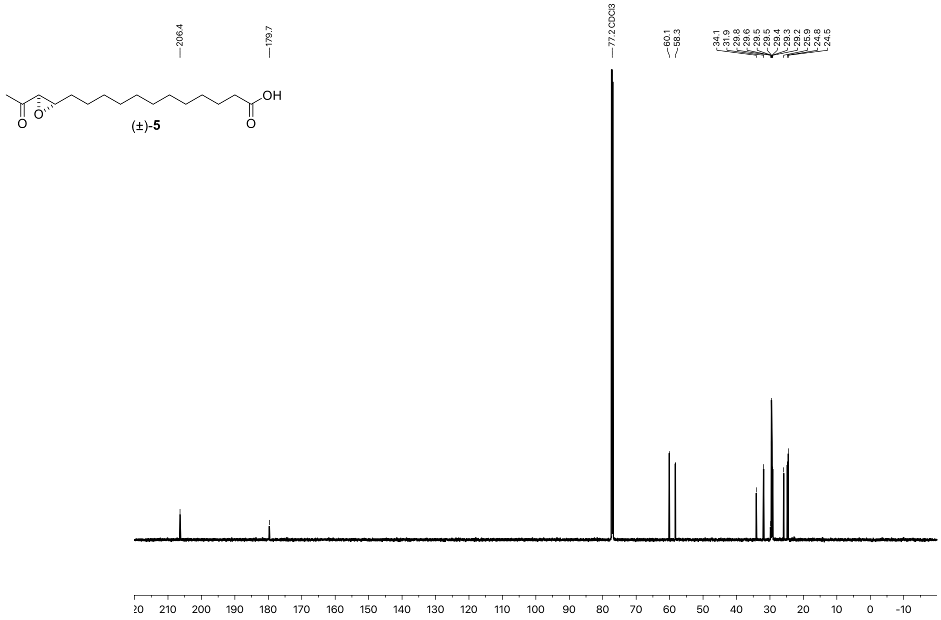
(±)-5
OH
O
O
O
206.4
179.7
77.2 CDCl3
60.1
58.3
34.1
31.9
29.8
29.6
29.5
29.5
29.4
29.3
29.2
25.9
24.8
24.5
210
200
190
180
170
160
150
140
130
120
110
100
90
80
70
60
50
40
30
20
10
0
-10

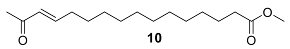

10

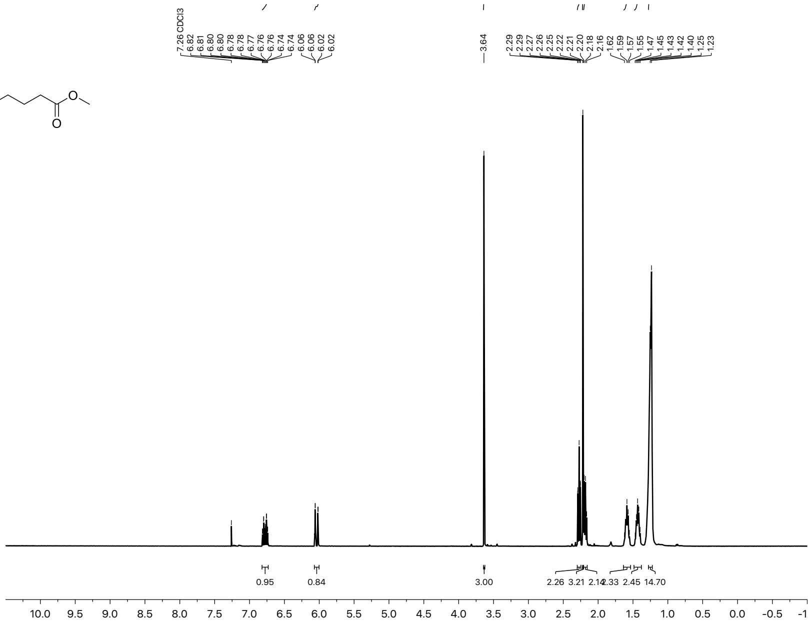
7.26 CDCl3
6.82
6.81
6.80
6.80
6.78
6.78
6.77
6.76
6.76
6.74
6.74
6.06
6.06
6.02
6.02
3.64
2.29
2.29
2.27
2.26
2.25
2.22
2.21
2.20
2.18
2.16
1.62
1.59
1.57
1.55
1.47
1.45
1.43
1.42
1.40
1.25
1.23
0.95
0.84
3.00
2.26
3.21
2.14
2.33
2.45
14.70
10.0
9.5
9.0
8.5
8.0
7.5
7.0
6.5
6.0
5.5
5.0
4.5
4.0
3.5
3.0
2.5
2.0
1.5
1.0
0.5
0.0
-0.5
-1

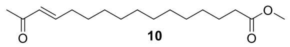

10

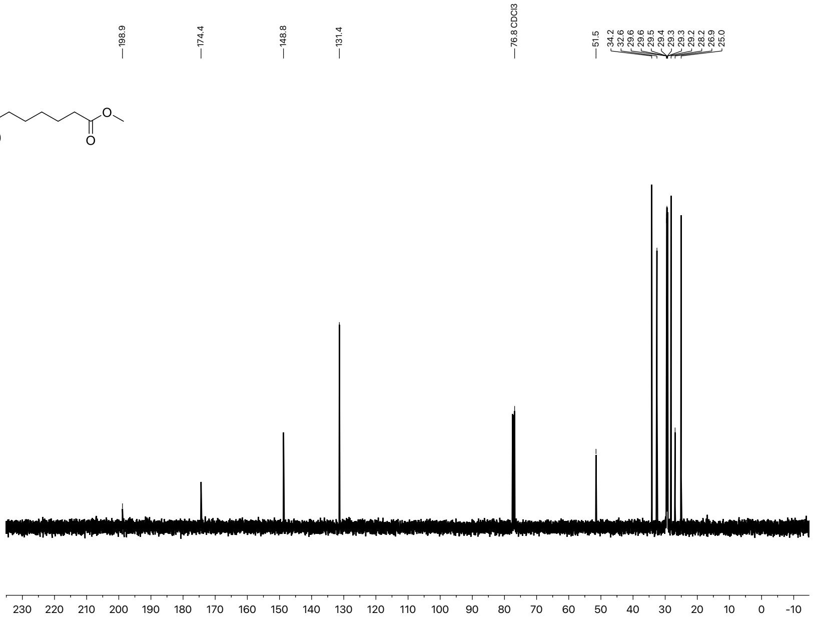
198.9
174.4
148.8
131.4
76.8 CDCl3
51.5
34.2
32.6
29.6
29.6
29.5
29.4
29.3
29.3
29.2
28.2
26.9
25.0
230
220
210
200
190
180
170
160
150
140
130
120
110
100
90
80
70
60
50
40
30
20
10
0
-10

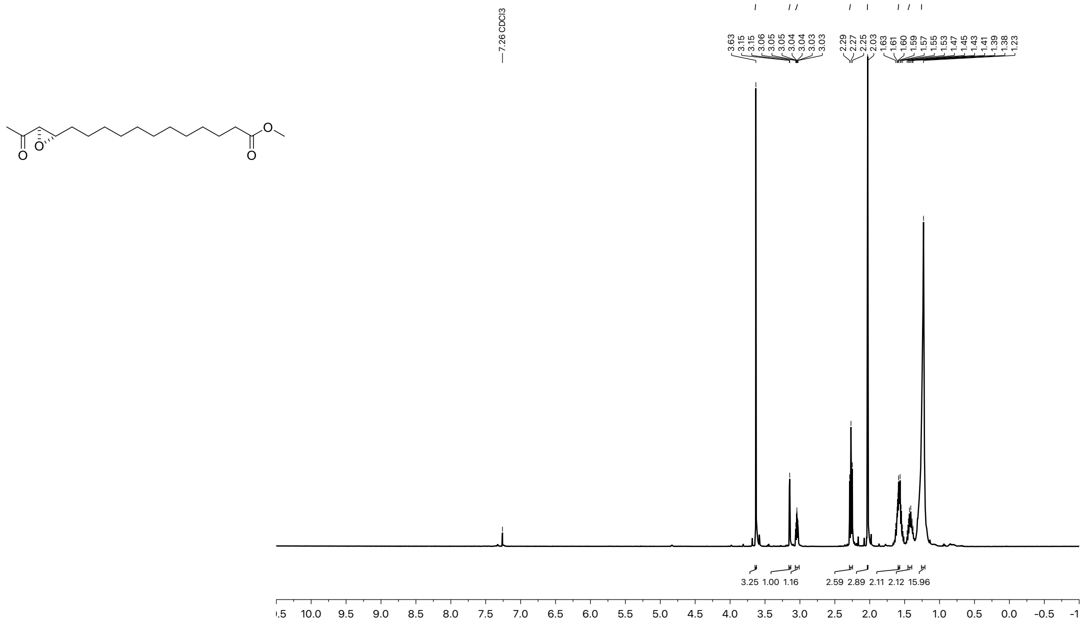

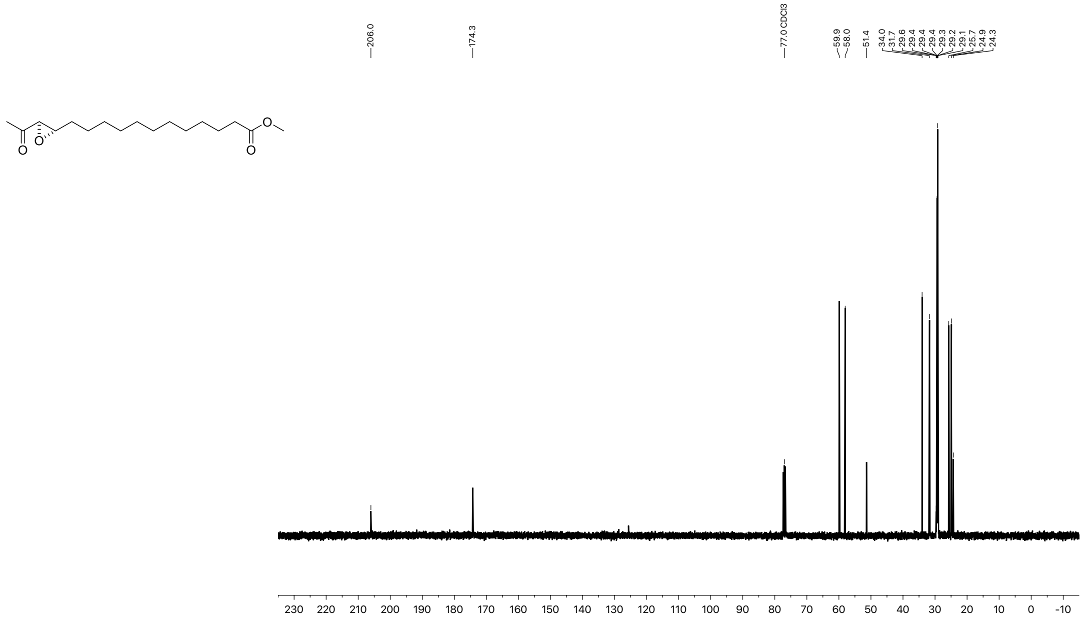

7.4. Appendix chapter 5

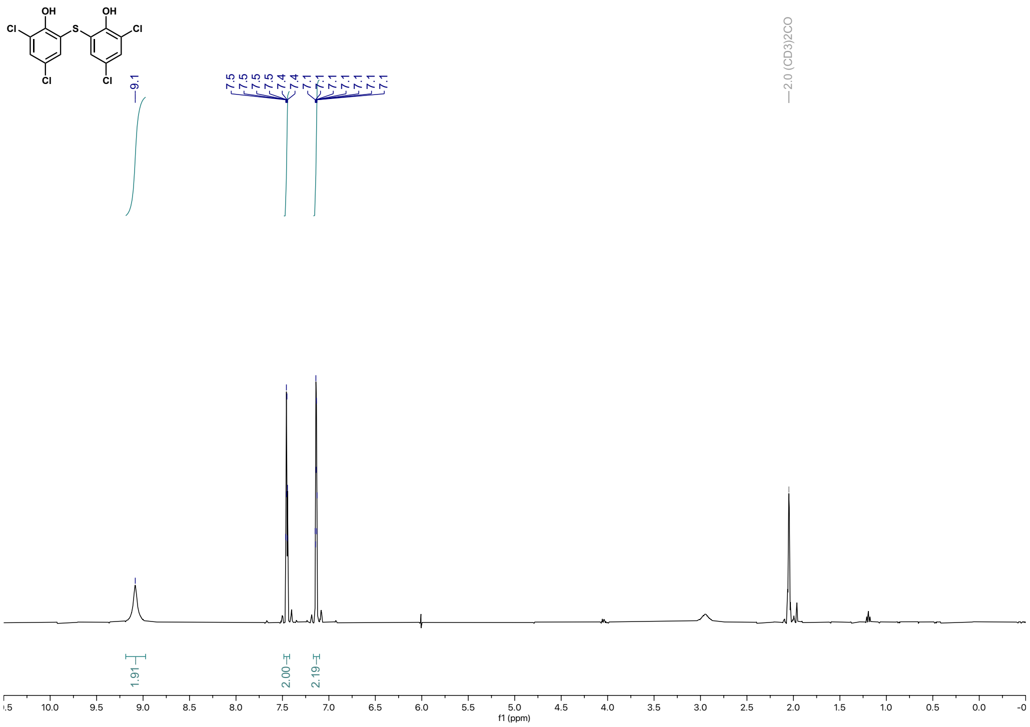
OH
OH
Cl
S
Cl
Cl
Cl
9.1
7.5
7.5
7.5
7.5
7.4
7.4
7.1
7.1
7.1
7.1
7.1
7.1
7.1
2.0 (CD3)2CO
1.91
2.00
2.19
.5
10.0
9.5
9.0
8.5
8.0
7.5
7.0
6.5
6.0
5.5
5.0
4.5
4.0
3.5
3.0
2.5
2.0
1.5
1.0
0.5
0.0
-0
f1 (ppm)

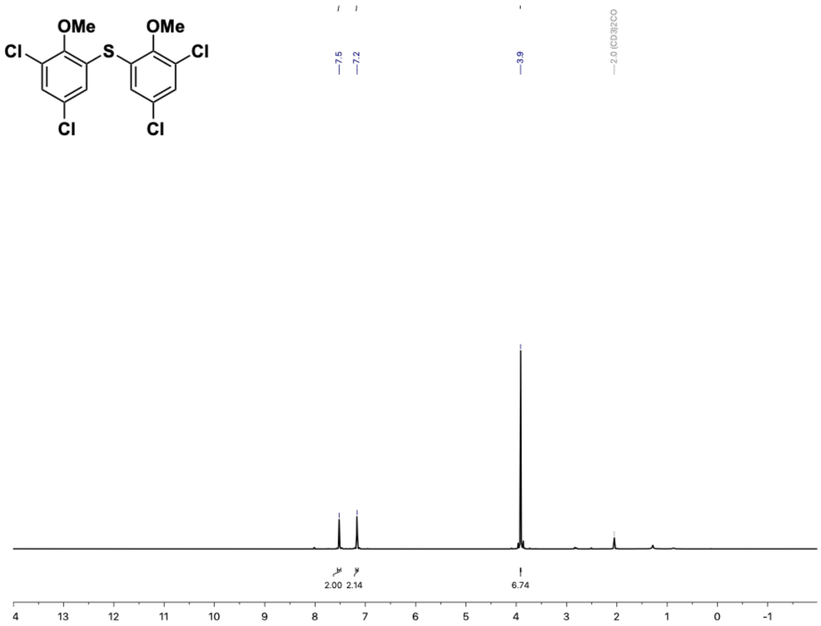
OMe
OMe
Cl
S
Cl
Cl
Cl
7.5
7.2
3.9
2.0 (CD3)2CO
2.00
2.14
6.74
4
13
12
11
10
9
8
7
6
5
4
3
2
1
0
-1

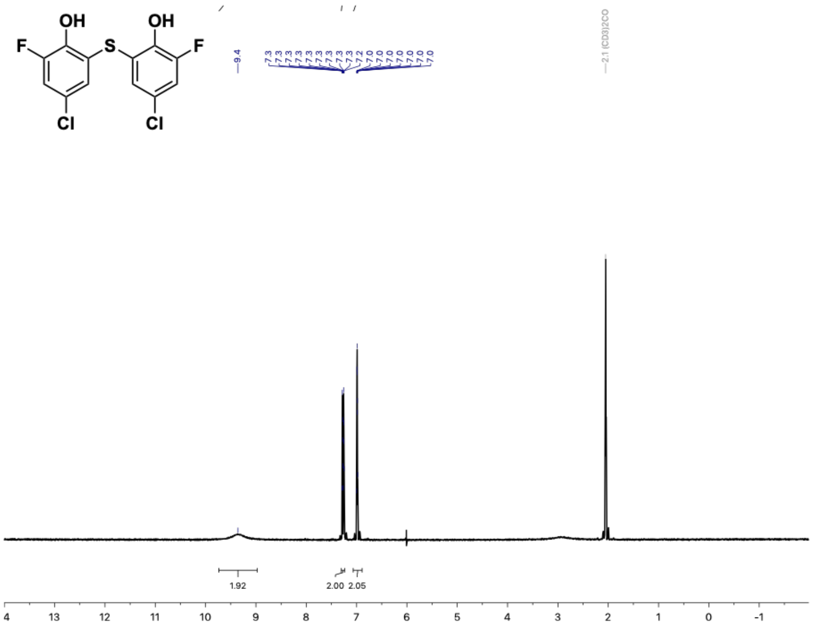
OH
OH
F
S
F
Cl
Cl
9.4
7.3
7.3
7.3
7.3
7.3
7.3
7.3
7.3
7.3
7.2
7.0
7.0
7.0
7.0
7.0
7.0
7.0
2.1 (CD3)2CO
1.92
2.00
2.05
4
13
12
11
10
9
8
7
6
5
4
3
2
1
0
-1

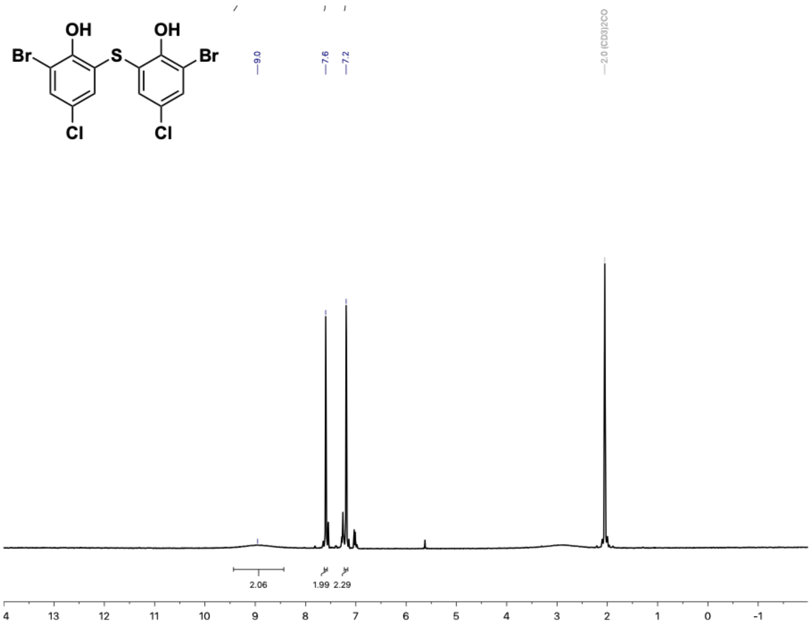
OH
OH
Br
S
Br
Cl
Cl
9.0
7.6
7.2
2.0 (CD3)2CO
2.06
1.99
2.29
4
13
12
11
10
9
8
7
6
5
4
3
2
1
0
-1

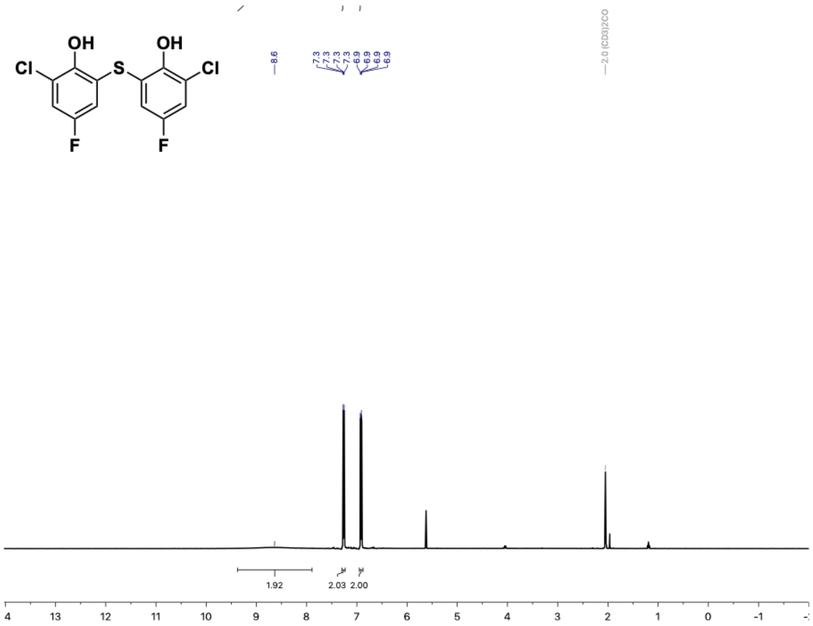
OH
OH
Cl
S
Cl
F
F
8.6
7.3
7.3
7.3
7.3
6.9
6.9
6.9
6.9
2.0 (CD3)2CO
1.92
2.03
2.00
4
13
12
11
10
9
8
7
6
5
4
3
2
1
0
-1

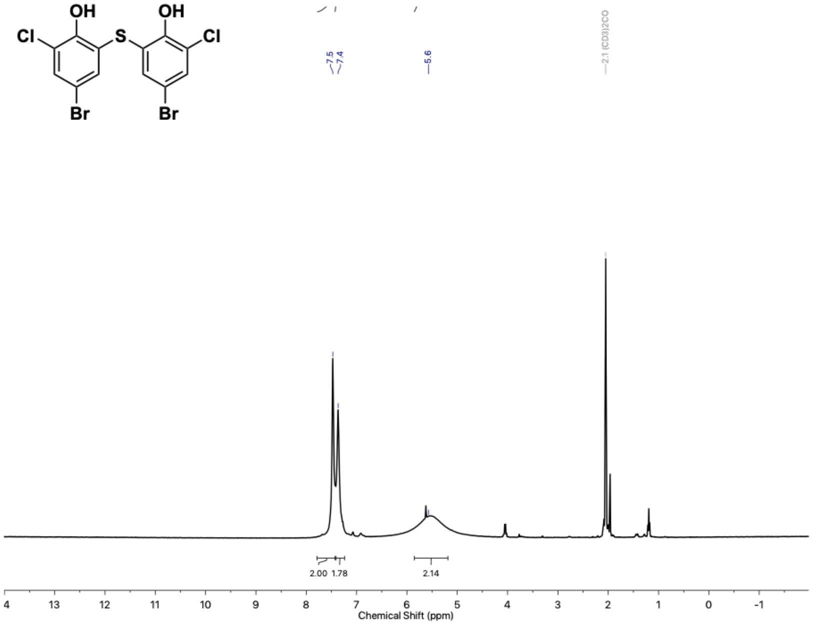
OH
OH
Cl
S
Cl
Br
Br
7.5
7.4
5.6
2.1 (CD3)2CO
2.00
1.78
2.14
4
13
12
11
10
9
8
7
6
5
4
3
2
1
0
-1
Chemical Shift (ppm)

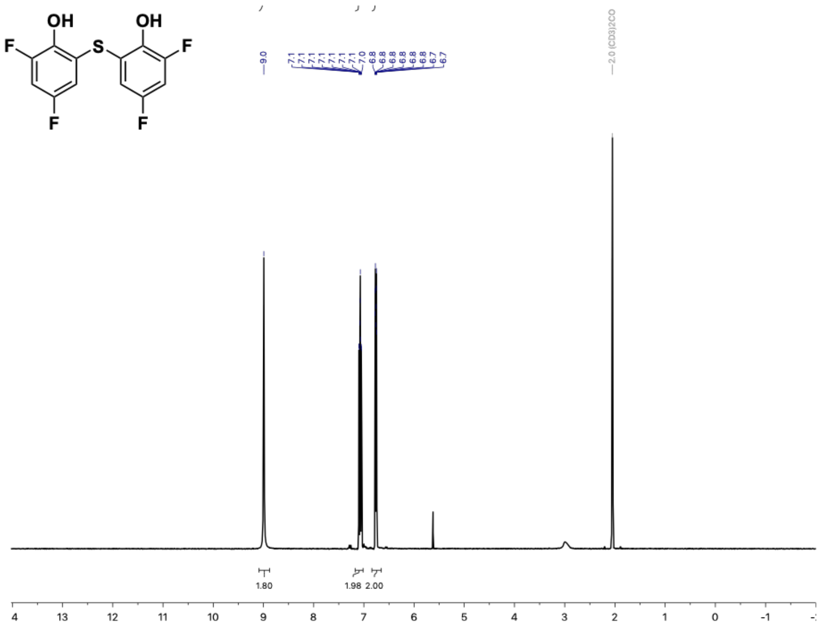
OH
OH
F
S
F
F
F
9.0
7.1
7.1
7.1
7.1
7.1
7.1
7.1
7.0
6.8
6.8
6.8
6.8
6.8
6.8
6.8
6.7
6.7
2.0 (CD3)2CO
1.80
1.98
2.00
14
13
12
11
10
9
8
7
6
5
4
3
2
1
0
-1
-2

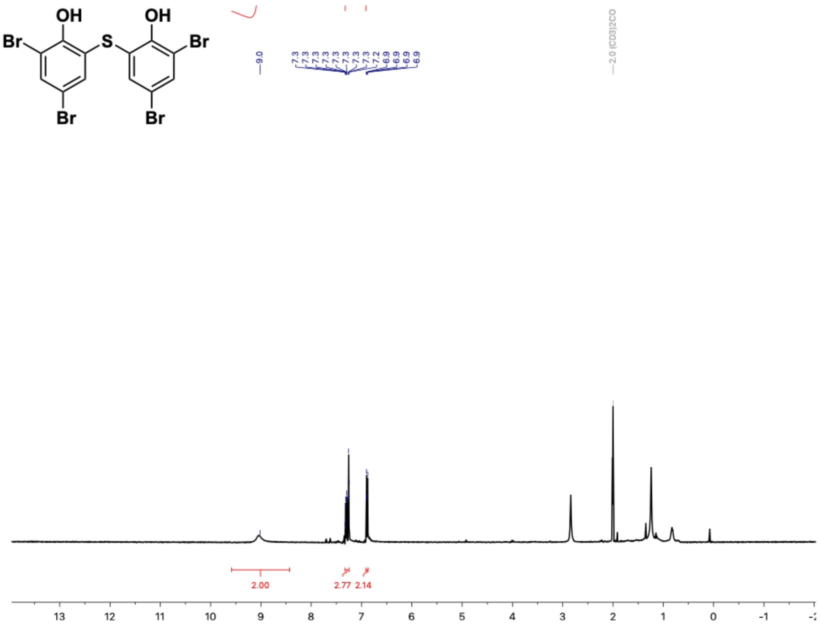
OH
OH
Br
S
Br
Br
Br
9.0
7.3
7.3
7.3
7.3
7.3
7.3
7.3
7.3
7.2
6.9
6.9
6.9
6.9
2.0 (CD3)2CO
2.00
2.77
2.14
13
12
11
10
9
8
7
6
5
4
3
2
1
0
-1
-2